NSSDC
WDC-A-R&S
National Space Science Data Center/
World Data Center A For Rockets and Satellites

80-09

Coordinated Ionospheric and Magnetospheric Observations from the ISIS 2 Satellite by the ISIS 2 Experimenters

(NASA-TM-82283) COORDINATED IONOSPHERIC AND MAGNETOSPHERIC OBSERVATIONS FROM THE ISIS 2 SATELLITE BY THE ISIS 2 EXPERIMENTERS. VOLUME 2: AURORAL OPTICAL EMISSIONS MAGNETIC FIELD PERTURBATIONS, AND PLASMA

N81-23743

Unclas
G3/46 42386

Volume 2

Auroral Optical Emissions, Magnetic Field Perturbations, and Plasma Characteristics, Measured Simultaneously on the Same Magnetic Field Line

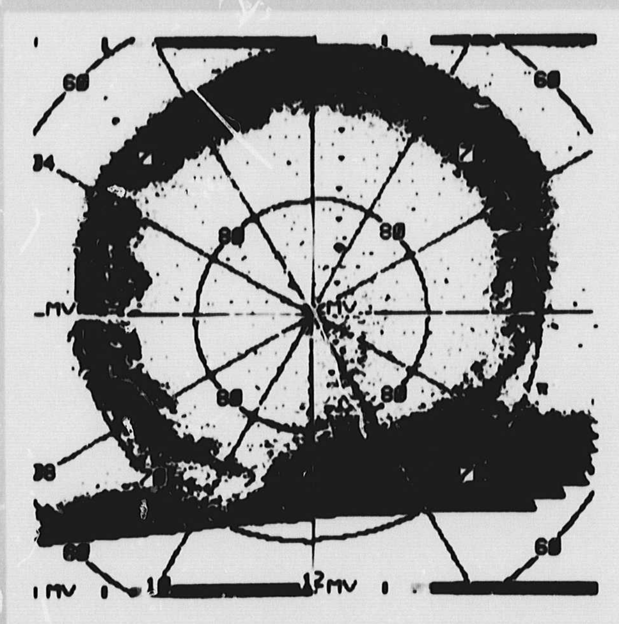

December 1980

COORDINATED IONOSPHERIC AND MAGNETOSPHERIC OBSERVATIONS FROM THE ISIS 2 SATELLITE BY THE ISIS 2 EXPERIMENTERS

Volume 2

AURORAL OPTICAL EMISSIONS, MAGNETIC FIELD PERTURBATIONS, AND PLASMA CHARACTERISTICS, MEASURED SIMULTANEOUSLY ON THE SAME MAGNETIC FIELD LINE

Coordinator: G.G. Shepherd
York University, Toronto, Canada

December 1980

The Experimenters are grateful to the National Space Data Center, Greenbelt, Maryland, for making this publication possible.

This Data Book is dedicated

to the memory of John H. Chapman,

through whose efforts the Alouette-ISIS

satellite program became a reality.

TABLE OF CONTENTS

I. INTRODUCTION

ISIS 2 is the fourth and final satellite launched in the Alouette/ISIS series. In this International Satellites for Ionospheric Studies program, Canada provided the spacecraft, data acquisition, and satellite control. The USA provided the launch capability, tracking, and data acquisition. Satellite instruments and data processing support were provided by both countries. During the course of the program these countries contributed telemetry support and collaborative data analysis: Australia, Finland, France, India, Japan, New Zealand, Norway, and the United Kingdom.

Alouette 1 won recognition mainly through the success of the topside sounder, but subsequent evolution led to a highly coordinated ISIS 2 satellite, having the capability for both direct measurements and remote sensing. Launched on April 1, 1971, into a near-circular near-polar orbit at 1400 km, it was essentially an observatory-type satellite with the potential of making fundamental measurements of both the ionosphere and magnetosphere, thereby yielding important information on the coupling processes between these regions.

At the time the program was planned, no provision was made for the generation or presentation of uniform and coordinated data sets, as this concept did not emerge until much later. This work has been done, for a selected number of passes, by the ISIS Experimenters Committee, and this publication is the result of their coordinated efforts.

The purpose of this work is to provide at the end of the data acquisition phase of the ISIS program, a representative set of data from ISIS 2 covering a range of operating modes and geophysical conditions. The data presented here show the typical values and range of ionospheric and magnetospheric characteristics, as viewed from 1400 km with the ISIS 2 instruments. For any scientist using ISIS data, this book should give a useful background and helpful perspective as to what is available. For others, this publication should be helpful in providing typical and extreme values of ionospheric and magnetospheric parameters, or may even provide research material. Anyone making serious quantitative use of these data may wish to contact the experimenters themselves. Original data from the instruments have been deposited in the National Space Science Data Center (NSSDC), NASA/GSFC, Greenbelt, Maryland 20771.

The overall publication comprises seven data sets in four volumes. The definition of each data set depends partly on geophysical parameters and partly on satellite operating mode. Preceding the data set is a description of the organizational parameters and a review of the objectives and general characteristics of the data set. The data are shown as a selection from 12 different data formats. Each data set has a different selection of formats, but uniformity of a given format selection is preserved throughout each data set. A description of how to interpret each format is given in the introductory sections. Most of the data that are plotted linearly in time are on one of two possible scales, corresponding to either 12 min/page or 20 min/page. Thus easy comparison of data is made possible. To summarize, each data set consists of a selected number of passes, each comprising a format combination that is most appropriate for the particular data set. Following this introduction is a list of ISIS 2 experimenters, with addresses and telephone numbers, then a brief description of the ISIS 2 satellite, followed by more detailed instrument descriptions, format descriptions, data set descriptions, and the data themselves. At the end of Volume 1 is a bibliography of ISIS 2 published papers. This bibliography was produced from a computerized technical reference file at the National Space Science Data Center. Comprehensive bibliographies for the other satellites of the Alouette-ISIS program also are available from NSSDC.

II. LIST OF ISIS 2 EXPERIMENTERS (as of 1980)

Communications Research Centre - Department of Communications P.O. Box 11490, Station "H", Ottawa, Ontario, Canada K2H 8S2

- H. G. James - Topside sounder, VLF, Cosmic Noise (613-596-9279)
- D. Muldrew - Topside sounder (613-596-9101)
- J. H. Whitteker - " " "
- J.D.R. Boulding - Satellite controller (613-596-9539)

Goddard Space Flight Center, Greenbelt, MD, USA 20771

- L. H. Brace - Cylindrical electrostatic probe, Code 961 (301-344-8575)
- E. J. Maier - Retarding potential analyzer, Code 963 (301-344-8912)
- C. Freeman - Data analyst (301-344-6374)

National Research Council - Herzberg Institute of Astrophysics, Ottawa, Ontario, Canada K1A OR6 (613-992-2734)

- I. B. McDiarmid, J. R. Burrows, D. D. Wallis, M. D. Wilson } Energetic Particle Detector and Fluxgate Magnetometer

University of Calgary, Physics Department, Calgary, Alberta, Canada T2N 1N4 (403-284-6340)

- C. D. Anger, L. L. Cogger, J. S. Murphree } Auroral Scanning Photometer

University of Texas at Dallas, Center for Space Sciences, MS F02.2, P.O. Box 688, Richardson, TX, USA 75080

- W. J. Heikkila, J. D. Winningham, D. M. Klumpar } Soft Particle Spectrometer (214-690-2835)

- J. H. Hoffman - Ion Mass Spectrometer (214-690-2840)
- W. H. Dodson - " " " "

York University, Centre for Research in Experimental Space Science, 4700 Keele Street, Downsview (Toronto), Ontario, Canada M3J 1P3 (416-667-3221)

G. G. Shepherd - Red Line Photometer
F. W. Thirkettle - Data Analyst

III. SATELLITE DESCRIPTION

ISIS 2 (Figure 1) was launched from the Western Test Range, California on April 1, 1971 (Franklin and Maclean, 1969; Daniels, 1971). The orbital parameters are: apogee 1423 km, perigee 1356 km, inclination 88.16°, and period 113.55 min. ISIS 2 carries 12 instruments (Figure 2), 10 of which are described in detail below. The other two are the Beacon experiment for measuring ionospheric irregularities and the Cosmic Noise experiment for measuring the cosmic or natural background noise level.

The satellite is an approximate oblate spheroid with a height of 119 cm, a diameter of 127 cm, and a weight of 260 kg. Its attitude is controlled by torquing coils and is measured by a 6-probe fluxgate magnetometer and a solar aspect sensor. The spin rate varies between about 2.5 and 3.5 rpm and can be changed by about 0.10 - 0.15 rpm/orbit. The spin axis is normally kept in the orbital plane (orbit-aligned) or at right angles to the orbital plane (cartwheel). For the orbit-aligned configuration the attitude can be changed by 2.0° - 2.5°/orbit and in the cartwheel configuration, by about 0.5°/orbit. The spacecraft contains about 11,000 solar cells and 3 Ni-Cd batteries. It was capable of operating for about 9 hours/day at launch and presently (1980) is capable of operating for about 2.5 hours/day. It has 3 telemetry transmitters at 136.08, 136.59, and 401.75 MHz and a tracking beacon at 136.41 MHz. Data are telemetered to several ground stations situated around the world. The spacecraft has a tape recorder and clock, but these failed in 1971 and 1974, respectively.

IV. INSTRUMENT DESCRIPTION AND DATA PROCESSING

AURORAL SCANNING PHOTOMETER (ASP)

The ISIS 2 dual wavelength auroral scanning photometer (Anger et al, 1973) is designed to map the distribution of auroral and airglow emissions at 5577Å and 3914Å over the portion of the dark Earth visible to the spacecraft.

Franklin, C. A., and M. A. Maclean, The design of swept-frequency topside sounders, Proc. IEEE, 57, 897-929, June 1969.

Daniels, F., The ISIS-II spacecraft, Communications Research Centre Report No. 1218, Department of Communications, Ottawa, March 1971.

Anger, C. D., T. Fancott, J. McNally, and H. S. Kerr, ISIS 2 scanning auroral photometer, App. Optics, 12, 1753-1766, Aug. 1973.

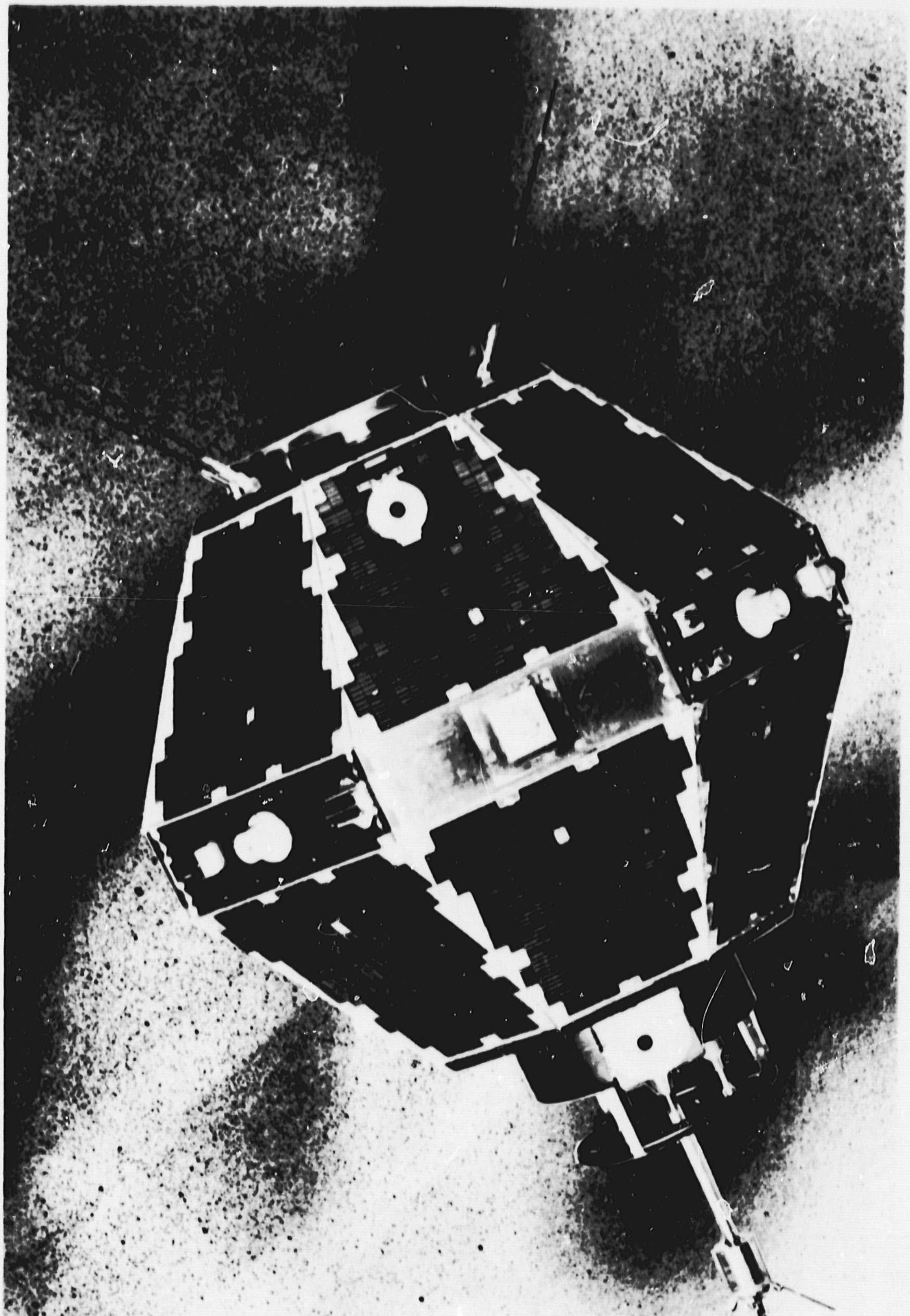

Figure 1. ISIS 2 Spacecraft.

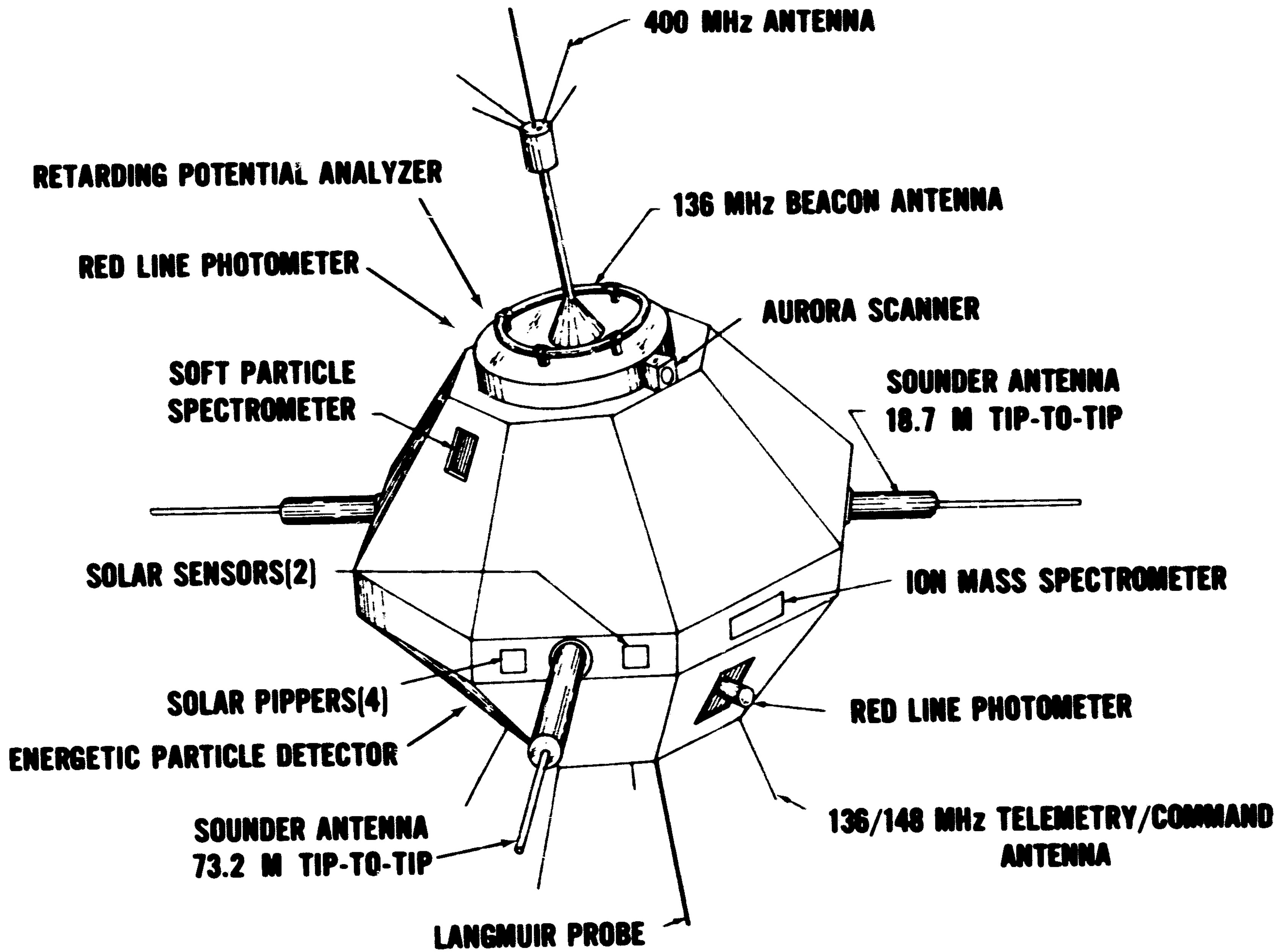

Figure 2. ISIS 2 Instrumentation.

Meaningful optical observations are possible at angles between the viewing direction of the instrument and the Sun direction of >60° and <120° due to a two-stage baffle system which shields the optics. The optical system consists of two separate barrels which are 180° apart so that only one barrel can look at the Earth at a time. The light from each of the barrels passes through its own interference filter (5581 ± 9Å or 3914 ± 13Å), lens, and mirror, and then is focused at a common point on a single-image dissector photomultiplier tube. This tube is similar to an ordinary photomultiplier tube except that an electrostatic imaging system and aperture are interposed between the cathode and first dynode. At any instant, only those photoelectrons from a small region of the cathode can pass through the aperture and be multiplied. This region is scanned across the photocathode by a magnetic scanning coil, thus generating a 13-element linear scan which is oriented at 90° to the direction of motion produced by rotational motion of the spacecraft (see Figure 3). The instantaneous field of view of each of these elements is 0.4° x 0.4°, resulting in an average output of one photoelectron pulse for ~250 rayleighs (R) from each point viewed, and hence a signal to noise ratio of one. The spatial resolution at 100 km directly under the spacecraft is ~8 km for each element.

Each photoelectron passing through the imaging electron optics and aperture of the image dissector tube is multiplied by about 10^7 by the dynode chain. The resulting output pulse is amplified by a pulse preamplifier, which produces standard pulses suitable for driving high-speed digital logic. Pulses from the preamplifier are accumulated in a digital logarithmic accumulator, the seven-bit output of which is transferred to a buffer and shifted out in standard PCM format at 630 words per second. As one frame of data consists of the 13 elements in a scan plus a frame synchronization word, there are 45 frames of data output per second.

The photometer scans the Earth by a combination of the rotational and translational motions of the spacecraft together with the internal electronic scanning performed by the image dissector (see Figure 3). The spacecraft spin axis and orbital plane remain essentially fixed in space as the spacecraft orbits the Earth, and, therefore, each rotation of the spacecraft results in the scanning of a strip, which, for the orbit-aligned mode of the spacecraft, is at right angles to the orbital plane. The width of the strip (5°) is chosen so that it will just join onto the strip scanned during the previous rotation. The image dissector repetitively scans at high speed across the narrow dimension of each strip, dividing it into 13 separately resolved regions (0.4° x 0.4°). Similar strips are scanned at each of the two wavelengths, although they differ in time by half the rotation period.

RED LINE PHOTOMETER (RLP)

The RLP (<u>Shepherd et al</u>, 1973) was designed to measure the emission of 6300Å aurora and airglow from the F-region of the Earth's ionosphere. It has two optical inputs, 180° apart and at 90° to the satellite spin axis. One input is characterized by a 10Å bandwidth filter and the other by an 88Å bandpass. They have roughly equal responses to white light, but the responses to

---

Shepherd, G. G., T. Fancott, J. McNally, and H. S. Kerr, The ISIS-II atomic oxygen red line photometer, <u>Appl. Opt. 12</u>, 1767 (1973).

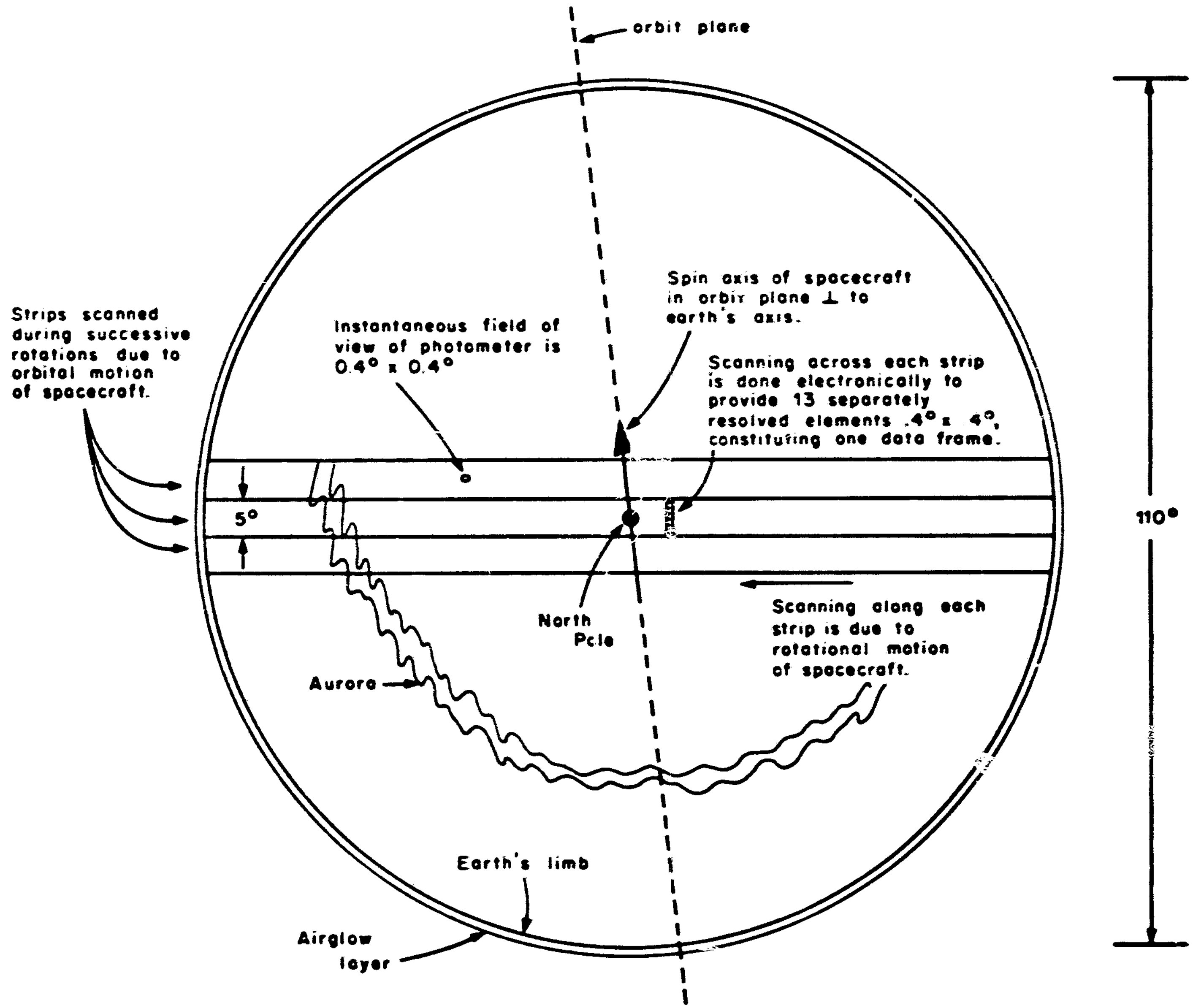

Figure 3. The Earth as it would appear from the spacecraft 1400 km above the pole, with scanning pattern of photometer superimposed.

6300Å emission are in the ratio of 9:1. The field of view of both is 2.5° in diameter. These optical inputs enter the same telescope system, and the intensities are summed onto one photomultiplier detector. As one input views the Earth the other views the dark sky, allowing the signals to be separated. Corrections for the starlight background intensity are made in data analysis. Intensities are measured at a rate of 30 samples/sec.

With the satellite spin axis in the plane of the orbit, the Earth scans caused by satellite rotation (19-second period, normally) form a raster-like scan pattern, generating two pictures per orbit; one as seen through the 10Å filter, the other by the 88Å filter. These pictures are combined to eliminate the white light background, leaving the 6300Å intensities. These intensity values are contoured in "spin coordinates," and then transformed to magnetic invariant coordinates using the method of Boyd (1977) . The details are described under Format 8.

When the spin axis is perpendicular to the orbit plane (cartwheel configuration), the RLP scans repeatedly along the satellite track. The output in this case is presented as intensity along the spacecraft track as a function of spacecraft time. The details are described under Format 1.

SWEPT-FREQUENCY SOUNDER

The sounder is essentially a radar, operating between 0.1 and 20 MHz, which transmits pulses approximately 100 μs in duration, and then listens for reflected signals. The pulses are repeated at the rate of 45 per second, as the frequency is gradually swept through its range. The received signal is displayed in the form of an ionogram, in which the density of the display at any point depends on the signal level.

An ionogram is shown in Figure 4. In a well-behaved (horizontally stratified) ionosphere, there will be at most two echoes for a given frequency. For each echo, the time delay is determined by the electron density (N) as a function of altitude (h). The delay-time scale is marked in units of distance (apparent range), corresponding to a signal propagating at the speed of light. In a plasma, the signal travels more slowly than this, and the delay time depends on an integral of group refractive index along the path. The ionogram provides apparent range as a function of frequency, and with this information, the integral can be inverted to give the vertical electron density profile N(h). A procedure for this inversion is described by Jackson (1969).

The trace in the lower portion of the ionogram represents the automatic gain control (AGC) voltage. Zero voltage is given by the horizontal line that is designated 2800 km apparent range, and the maximum AGC voltage of 5 volts is shown by the 2400 km apparent range marker. The AGC voltage can be used as a measure of the background noise level at the satellite.

Boyd, J. S., Invariant geomagnetic coordinates for epoch 1977.25, Planet. Space Sci. 25, 411 (1977).

Jackson, J. E., The reduction of topside ionograms to electron-density profiles. Proc. IEEE, 57, 960-976, June 1969.

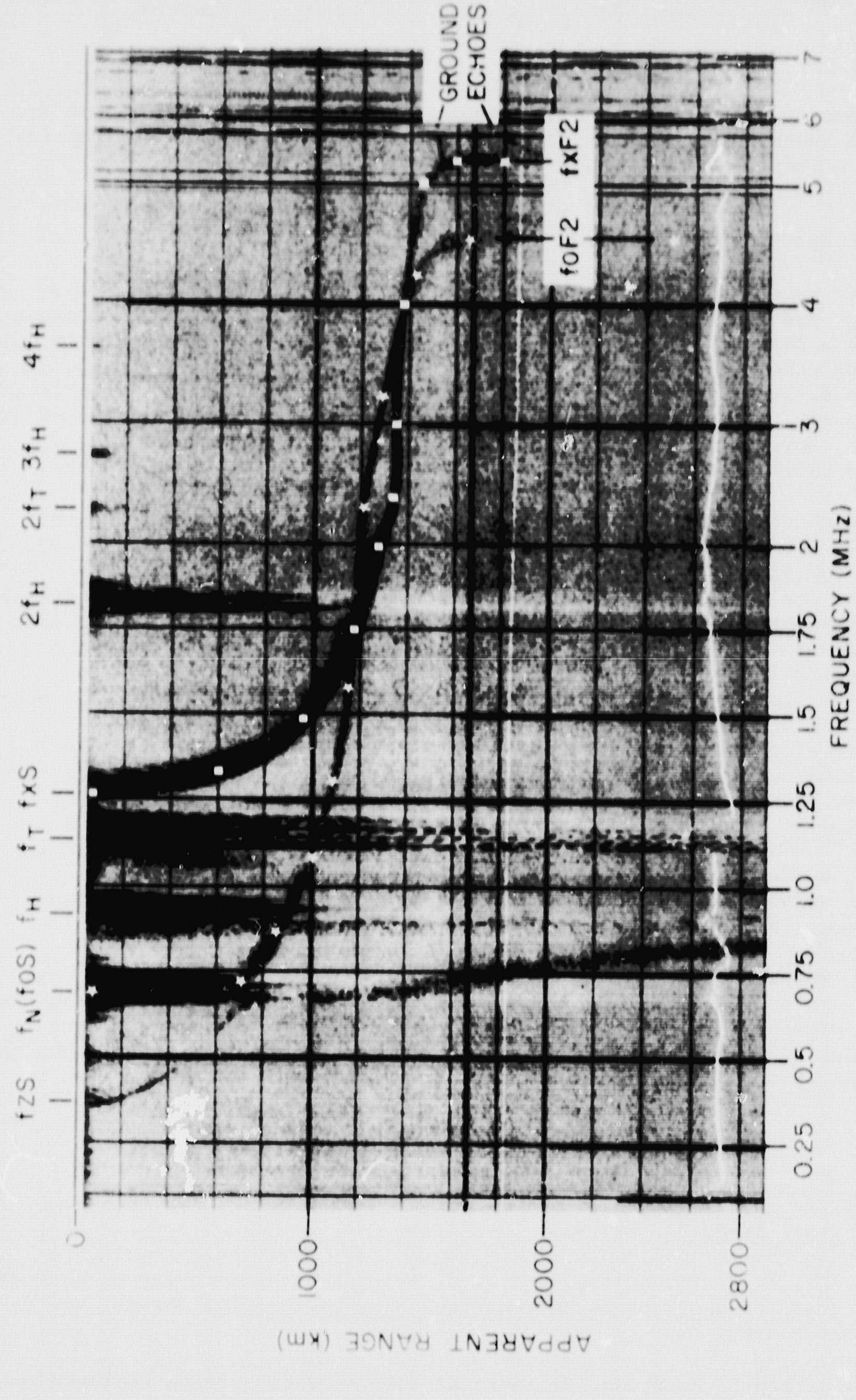

Figure 4. ISIS 2 Ionogram.

ORIGINAL PAGE IS
OF POOR QUALITY

The sounder is described in more detail by Franklin and Maclean (1969). In the same issue of Proc. IEEE, there are several other articles on topside sounding. A short review on topside sounding is given by Jackson et al (1980).

CYLINDRICAL ELECTROSTATIC PROBE (CEP)

The CEP is a Langmuir probe instrument which measures the electron density (N_e) and temperature (T_e) of the ionospheric plasma. The instrument consists of a pair of thin wire collectors projecting from the spacecraft spin axis at both ends. The two collectors are operated independently in a time-shared fashion by a common electronic unit which applies an appropriate voltage waveform and measures the resulting volt-ampere characteristics of the collectors. Details of similar instruments used on the Alouette 2 and Explorer 31 satellites are discussed elsewhere (Findlay and Brace, 1969).

A typical CEP plot of N_e and T_e is shown in Figure 5. The plot format reflects the details of the instrument design. Points are shown at 6-second intervals, reflecting the repetition rate of the sweep voltage waveform. Each collector is assigned to the electronics during alternate 30-second intervals, thus alternate groups of five measurements are derived from different probes. Owing to damage of one of the probes at launch, which introduced a spin modulated error in its N_e measurement, only one probe is employed for N_e measurements. Both probes are capable of good T_e measurements, although wake effects on one or the other may cause slight disagreement in their T_e measurements at certain points in the orbit. This will be evident as an offset in alternate groups of five T_e points in the plots. The T_e values are given either by solid points or by question marks (?) in the case of poor curves caused by ionospheric irregularities, as discussed later.

The N_e measurements are made in the range of about 10^2 to $10^5/cm^3$. The lower limit arises from electrostatic shielding by the spacecraft sheath which grows out over the collectors at very low densities.

The T_e measurements can be made when N_e exceeds about $200/cm^3$ when the collectors are not in sunlight. When in sunlight, photoelectrons leaving the collectors prevent a proper ion current reference to be established until N_e exceeds about $10^3/cm^3$. T_e may be resolved between 500°K and 15,000°K when the above N_e conditions are attained.

Franklin, C. A. and M. A. Maclean, The design of swept-frequency topside sounders, Proc. IEEE, 57, 897-929, June 1969.

Jackson, J. E., E. R. Schmerling, and J. H. Whitteker, Mini-review on topside sounding, IEEE Transactions on Antennas and Propagation, Vol. AP-28, No. 2, 284-288, March 1980.

Findlay, J. A. and L. H. Brace, Cylindrical electrostatic probes employed on Alouette 2 and Explorer 31 satellites, Proc. IEEE, 57, 1054-1056, June 1969.

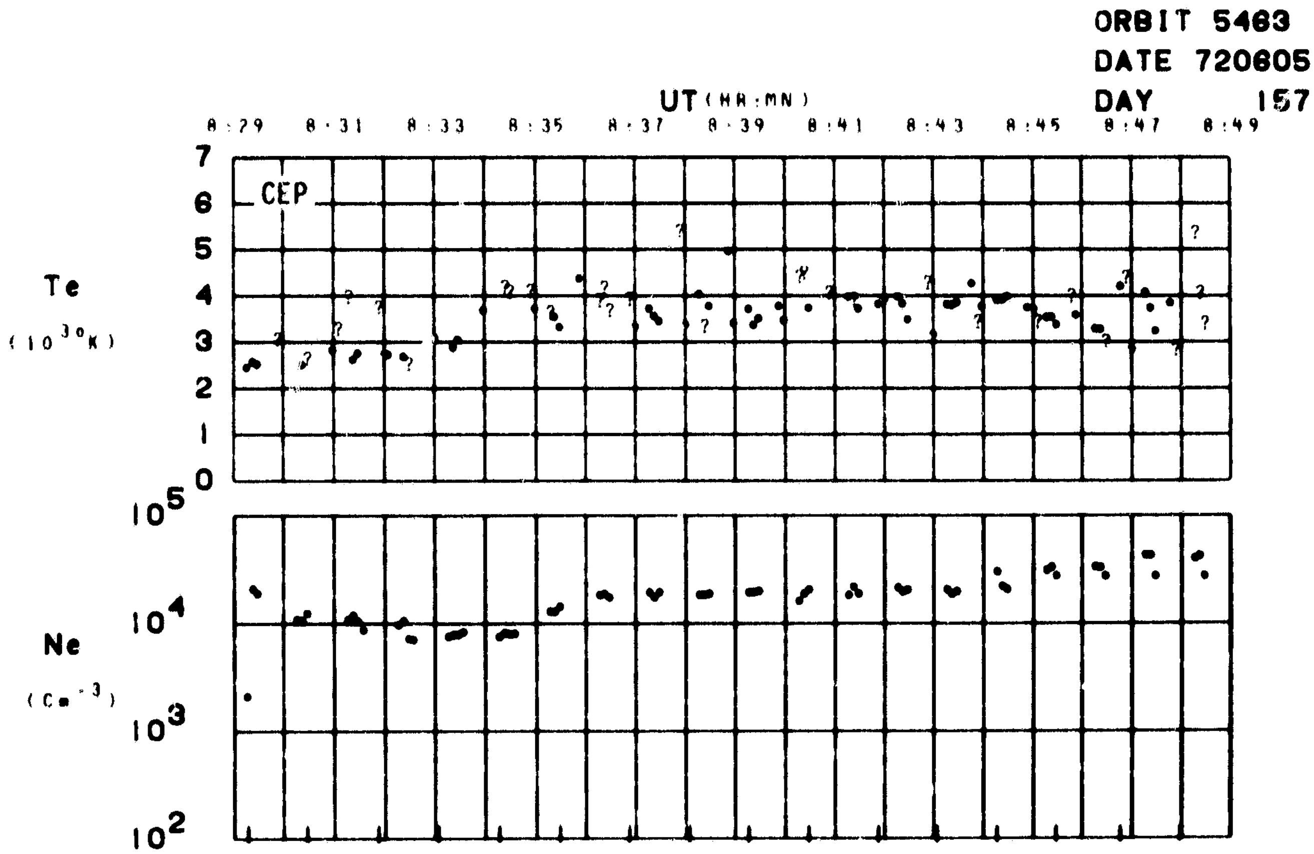

LAT	42	45	50	54	57	61	66	69	73	77	81	85	87	86	82	78
LONG	-155	-155	-155	-155	-155	-154	-154	-154	-153	-151	-147	-136	-84	-7	5	9
LT	22:10	22:11	22:12	22:13	22:15	22:17	22:20	22:23	22:28	22:36	22:54	23:37	3:07	8:17	9:09	9:27
DIP	73	75	77	78	80	81	83	84	85	86	88	88	88	88	86	85
DIPLAT	59	62	66	68	71	74	77	79	81	84	86	88	88	86	84	82
L	2.1	2.4	2.8	3.3	4.0	4.9	6.7	9.1	13.1	20.3	37.5	64.3	80.9	59.8	32.7	19.6
INVLAT	46	49	53	56	59	63	67	70	73	77	80	82	83	82	79	76
ZA	110	107	103	100	96	93	89	86	82	70	75	72	68	65	61	58

Figure 5. Example of CEP data.

The main sources of error in N_e are wake effects and inadequacies of the theory for the conversion of electron current to density. Comparisons with the sounder and the other direct measurements on ISIS 2 show that the errors seldom exceed a factor of two, even when wake effects are ignored. Thus we have not eliminated N_e data on the basis of spacecraft orientation.

The main source of error in T_e arises from the irregular structure of the high-latitude ionosphere which introduces distortions in the volt-ampere characteristics. When a solid point is employed to plot T_e, the error is probably less than 10 percent. Larger errors may be expected when question marks are used. No T_e value is plotted if the plasma is so structured as to distort the curve beyond recognition to the curve fitting program. In general, question mark symbols should be used only when solid T_e points are not available, and then only as an estimate of T_e.

ENERGETIC PARTICLE DETECTOR (EPD)

The EPD instrument was designed to provide directional flux measurements of electrons (from 0.15 keV to 2 MeV) and positive ions (from 2 keV to 20 MeV with some gaps). A diversity of sensors are used. A stepped electrostatic analyzer provides an 8-point electron spectrum ($0.15 < E < 10$ keV) and an 8-point positive ion spectrum ($2.0 < E < 26$ keV), each once per second. However, only three of these electron differential channels are displayed in the normal EPD format. Geiger counters and solid state detectors provide integral flux measurement at 12 different threshold energies starting at $E >$ 22 keV for electrons and $E >$ 150 keV for protons. Only three of these integral channels are included in Format 3, averaged to one second time resolution. The instrumental time resolution is ~1/4 second. The energy bandpass ($\Delta E/E$) of the electrostatic analyzer is 30 percent for electrons and 15 percent for positive ions.

All of the sensors but one have the axis of their fields of view fixed in the same direction in the plane perpendicular to the spacecraft's spin axis. One geiger counter axis is along the spin axis. The fields of view of the integral detectors are conical. The electrostatic analyzer differential spectrometer has a rectangular field of view defined by a collimator with half angles 1.5° x 1.7°.

The electron differential channels are unaffected by positive ion fluxes but do give spurious counts due to solar ultraviolet light when viewing the Sun. The integral channels respond to both electrons and protons in general at different threshold energies. In Format 3, channel I(210) has had the positive ion flux removed. The $I_{\parallel}(40)$ channel includes both electron ($E >$ 40 keV) and positive ions ($E >$ 150 keV) fluxes. The latter flux is negligible except during solar proton events. Both I(40) and $I_{\parallel}(40)$ also sometimes have spurious Sun counts.

The gain of the differential spectrometers' channeltron detector decreased quickly between April and October 1974 and should be regarded as quantitatively inaccurate after April 1974. The geiger counter, $I_{\parallel}(40)$, failed in June 1973.

The instrumentation and detector characteristics are more fully described by Venkatarangan et al, 1975. Some relevant EPD detector characteristics are tabulated below.

Detector	Type	Energy Threshold keV	Geometric Factor cm^2 ster	Collimator Half-Angle
I(210)	solid state	e^- 210	8.15×10^{-3}	7.0°
I(40)	solid state	e^- 40 p^+ 150	7.84×10^{-3}	6.8°
$I_{\parallel}(40)$	geiger	e^- 40 p^+ 600	1.03×10^{-3}	5.6°
I(22)	geiger	e^- 22 p^+ 240	8.83×10^{-4}	5.5°
Ip(750)	solid state	$750<p^+<4000$	4.9×10^{-2}	11.3°

ION MASS SPECTROMETER (IMS)

The ion mass spectrometer (Hoffman et al, 1974) is a magnetic sector type mass spectrometer with two electron multiplier detectors located on two different radii within the sector. The incoming ions are accelerated by a potential that makes a complete sweep in 1 second such that the mass range 1 to 9 AMU is sampled on one channel and, simultaneously, the mass range 8 to 64 AMU is sampled on the other channel. Thus the mass spectrum from 1 to 64 AMU is sampled each second. The output current from the electron multipliers is then converted to an ion concentration using conversion constants determined by in-flight calibration using the electron density obtained from the topside sounder also located on the ISIS satellite.

The ion concentration is given in number of ions per cubic centimeter of the five dominant ions found at 1400 km, each plotted as a function of time in 20-minute segments. Each data point has been obtained by curve fitting the spacecraft spin-modulated cartwheel data and determining the maxima and time of maxima of the fitted curve. Thus the absence of data for a given ion may indicate that a good curve fit was not possible; this generally occurs at concentrations less than 10 ions/cm^3.

Venkatarangan, P., J. R. Burrows, and I. B. McDiarmid, On the angular distributions of electrons in 'inverted V' substructures, J. Geophys. Res. 80, 66-72, Jan. 1975.

Hoffman, J. H., W. H. Dodson, C. R. Lippincott, and H. D. Hammack, Initial ion composition results from the ISIS 2 satellite, J. Geophys. Res. 79, 4246, 1974.

RETARDING POTENTIAL ANALYZER (RPA)

The retarding potential analyzer (Kayser et al, 1978) is a planar multigrid instrument designed to measure ionospheric density and temperature parameters over the range 10 to 10^6 ions/cm^3 and 500-10,000°K, respectively. This is accomplished by performing an electrostatic retardation of the ions flowing into the instrument at the spacecraft velocity when the instrument is oriented in the nearly forward direction. The instrument is mounted in the equatorial plane of the spacecraft, with the sensor normal directed radially outward. Thus the viewing angle scans a variety of directions as the spacecraft rotates at the nominal 3-rpm spin rate. In the cartwheel mode, in which the spacecraft spin axis is perpendicular to the orbit plane, the sensor scans the full angle range 0° to 360° between the sensor normal and the velocity vector every (nominally) 20 seconds. In the orbit aligned mode, in which the spacecraft spin axis is in the orbit plane, the sensor cannot scan the forward direction at all latitudes. In particular, at high latitudes, the sensor normal is almost perpendicular to the velocity vector, thus precluding data collection when the optical instruments are obtaining "spin scan" images. Thus only the cartwheel data sets contain results from the RPA.

Plasma analysis is performed by applying programmed voltages to the various grids within the ion trap and measuring the current transmitted to the collector as a function of the applied potentials (Moss and Hyman, 1968). The resulting current voltage (I-V) response is fitted to a predicted response to provide the estimates of the ambient parameters. Results presented in this data book are based on the assumptions that the ions present in significant concentrations (>1 percent of the total) may be H^+, He^+, and O^+, all assumed to be at a common temperature T. Useful data are obtained only when the sensor normal is within 35° of the spacecraft velocity vector. The combination of the 3-second instrument program cycle and the 20-second spacecraft spin period yields a limit of 1 or 2 plasma analyses per 20-second interval. This nominal rate of 3 per minute may not be attained for several reasons. (1) Operation of the sounder transmitter sometimes perturbs the local plasma, yielding non-geophysical results. (2) Photoemission effects within the instrument sometimes preclude analysis of the I-V curve when the Sun is within the field of view of the instrument. This is most significant in regions of low plasma density. (3) Highly structured plasma often cannot be analyzed if the local plasma variations are fast on the 1-second time scale on the instrument. This is usually the reason for the apparent data gaps in the auroral zone. (4) Extreme spacecraft potentials are sometimes encountered, exceeding the range of the applied sweep voltages. For all of these cases, appropriate tests are used to delete, or correct, data points before analysis and to select results based on the quality of their fit to the theoretical I-V curve.

Kayser, S. E., E. J. Maier, and L. H. Brace, Quiet time plasma irregularities at 1400 km in the cleft region, J. Geophys. Res. 83, 2533, 1978.

Moss, S. J., and E. Hyman, Minimum variance technique for the analysis of ionospheric data acquired in satellite retarding potential analyzer experiments, J. Geophys. Res. 73, 4315, 1968.

SOFT PARTICLE SPECTROMETER (SPS)

The ISIS 2 Soft Particle Spectrometers measure the fluxes and energy spectra of electrons and positive ions over the energy range from 5 eV to approximately 15 keV.

There are two independent electrostatic analyzers (SPS's) on the ISIS 2 satellite, each of which is capable of measuring electrons and/or positive ions in either an energy step dwell mode or a spectral sweep mode. Each of the spectrometers, referred to as "top beam" and "bottom beam," are mounted looking in identical directions perpendicular to the satellite spin axis. The top detector is normally operated in an electron sweep mode and as such has a geometric factor of 4.95×10^{-4} cm^2 ster and an energy bandpass ($\Delta E/E$) of 24.7 percent with center energies from 13.15 keV to 5.5 eV in 38 levels. The bottom detector is normally operated in a positive ion sweep mode and in this mode has a geometric factor of 1.27×10^{-3} cm^2 ster and an energy bandpass ($\Delta E/E$) of 35.5 percent with center energies from 14.675 keV to 5.0 eV in 39 levels. Both spectrometers have rectangular fields of view with a full width of 5 degrees by 25 degrees for the top beam (electron mode) and 10 degrees by 25 degrees for the top beam (ion mode) and the bottom beam in both electron and ion modes. In both cases the long dimension of the field of view is parallel to the spin axis and the short dimension is in the equatorial plane. A similar instrument flown on ISIS 1 is described by Heikkila et al (1970).

VERY LOW FREQUENCY RECEIVER (VLF)

The center of the VLF instrument is a broadband receiver covering the frequency range from 50 Hz to 30 kHz (Franklin et al, 1960). A receiving antenna connects to the receiver through a protective low pass filter. Normally, the antenna is the 73.2-m dipole shared with the topside sounder. Also, the receiver input can be connected instead to the spacecraft torquing coils used for attitude adjustment; however, the torquing coils have not produced meaningful data. VLF emissions are observed over a wide amplitude range and consequently the receiver has been designed with a dynamic range of 68 dB, most of which is achieved by use of automatic gain control (AGC).

Output from the receiver directly modulates an FM telemetry transmitter and has a dynamic range of 3 dB above the AGC threshold. The AGC is sampled 60 times per second and telemetered to ground via the PCM data channel. The receiver threshold is 20 μV across an input impedance of 16 kΩ.

On ISIS 2 the VLF experiment also includes an exciter connected to the short (18.7 m) sounder dipole. It sweeps logarithmically from 15 to 0.05 kHz

---

Heikkila, W. J., J. B. Smith, J. Tarstrup, and J. D. Winningham, The soft particle spectrometer in the ISIS 1 satellite, Rev. Sci. Instr. 41, 1393, 1970.

Franklin, C. A., T. Nishizaki, and W. E. Mather, A wideband VLF Receiver for the Alouette II and ISIS-A satellites, DRTE Technical Memorandum 522, Department of National Defence, Ottawa, Canada, May 1960.

once every 5 or 10 seconds. In addition, the short-dipole impedance can be measured by recording the amplitude and phase of the current drawn by the dipole in response to the VLF exciter. These data are telemetered via the PCM system.

TRIAXIAL FLUXGATE MAGNETOMETER

The orthogonal set of magnetometers (McDiarmid et al, 1978) is mounted in the body of the spacecraft with one component oriented along the spin axis (designated the z-magnetometer) and the other two in the plane perpendicular to the spin axis (designated x-y plane). The x-and z-magnetometers each have two ranges, ± 60,000 nT (± 600 milligauss) and ± 20,000 nT. The former range has digitization steps of 480 nT while the latter has 160 nT. The y-magnetometer has only the ± 60,000 nT range. All components are sampled at the rate of 1 sample/sec. There is no in-flight calibration capability. There is an induced field due to the surrounding spacecraft mass and wiring harness which is of the order of 1 percent of the external field. This field and some other periodic sources of interference from spacecraft equipment are removed in the data processing.

In this data book, only data from the axial (z) component are presented since its processing is more straightforward than for the spinning components. Only data sets in which the spin axis is nearly perpendicular to the orbit plane (i.e., cartwheel) have magnetometer measurements included, since it is desirable to use the higher sensitivity (± 20,000 nT) range. In cartwheel, the axial component is aligned approximately in the East-West direction when crossing the auroral ovals.

V. DATA FORMAT DESCRIPTIONS

The data most appropriate, and available, for a particular study are presented in formats selected from the following list. A format may contain data from a single instrument or from several instruments. A description of the information provided by each instrument is provided in this section. The following table specifies what instrument and quantities are plotted in each format. Unless otherwise specified all quantities plotted are profiles along the spacecraft track.

McDiarmid, I. B., J. R. Burrows, and M. D. Wilson, Comparison of magnetic field perturbation at high latitudes with charged particle and IMF measurements, J. Geophys. Res. 83, 681, 1978.

Format Number	Instrument	Quantity Plotted
1	Auroral Scanning Photometer	5577Å, 3914Å intensity
	Red Line Photometer	6300Å intensity
	Soft Particle Spectrometer	Electron energy flux
2	Topside Sounder	Electron density contours at different altitudes
	Magnetometer	Magnetic field deviation
3	Energetic Particle Detector	Electron and proton flux/energy
4	Cylindrical Electrostatic Probe	Electron density and temperature
	Ion Mass Spectrometer	Concentration of H^+, He^+, O^{++}, N^+, O^+
5	Retarding Potential Analyzer	Concentration of H^+, O^+, He^+ and ion temperature
6	Soft Particle Spectrometer	Electron and positive ion spectrograms
7	Auroral Scanning Photometer	Grey-scale two dimension co-ordinate transform of 5577Å, 3914Å intensities and the 5577Å/3914Å ratio
8	Red Line Photometer	Contour plot of 6300Å intensity
9	Auroral Scanning Photometer	5577Å E and F region latitude profiles
	Red Line Photometer	6300Å latitude profile
10	Cylindrical Electrostatic Probe	Electron density and temperature
	Topside Sounder	Electron density contours at different altitudes
11	VLF	VLF spectra
12	Auroral Scanning Photometer	Height profiles of 5577Å slant intensity

FORMAT 1 (ASP, RLP and SPS)

The sample of Format 1 shown in Figure 6 has been retouched for clarity, but it corresponds to the direct computer plot reproduced in the ISIS 2 data book. This format contains a combination of Soft Particle Spectrometer (SPS) electron data and optical data from the Auroral Scanning Photometer (ASP) and Red Line Photometer (RLP). A minimum-time-delay algorithm is used, in which the time delay between the satellite crossing of a particular field line and the optical viewing of the emission from the foot of the field line is minimized. This delay can be kept to within one-half of a spin period, by selecting optical data from the most appropriate spin for a given latitude range, and splicing it together to form a continuous sequence. For this data set the satellite has its spin axis perpendicular to the orbit plane and the optical scans are repeatedly along the spacecraft track. Thus, there is adequate redundancy for the above procedure.

The electron data and optical data are then plotted as a function of Universal Time, corresponding to the time of the spacecraft motion (the time of the SPS measurement), which will be somewhat different from the optical viewing time as described above. The start time is shown at the lower left and minute values are given on the horizontal axis. The atomic oxygen 6300Å emission intensity from the RLP and the atomic oxygen 5577Å and N_2^+ 3914Å emission intensities from the ASP are plotted in kR on a logarithmic scale at the bottom. These intensities have not been corrected for airglow background or albedo. The SPS electron energy fluxes have been integrated over four energy bands as shown on Figure 6: 5 -60 eV, 60 -300 eV, .3 -1. keV, 1 -15 keV and plotted on vertically separated scales, with the ordinate labeled in units of the logarithm of the energy flux in erg cm^{-2} sr^{-1} sec^{-1}.

The modulation that appears on these fluxes results from the rotation of the spacecraft. The detectors look outward in the equatorial planes, sweeping through a pitch angle coverage shown by the sawtooth at the top of the plot. A downward sawtooth corresponds to downward-going particles.

At the top of Figure 6 the following geophysical quantities are indicated along the horizontal axis: INVL - invariant latitude, INVT - invariant time, SDEP - local solar depression angle at the location of the viewed emission, CDEP - solar depression angle at the magnetic conjugate point to the viewed emission.

The 5577Å and 3914Å data plotted are derived from the slow-speed PCM data link, the same as used for the 6300Å data, but not the same as the high speed data link employed for the high-resolution ASP photos. To achieve this reduced data rate the intensity across a 13-element scan is averaged into essentially a single value by filtering. Because of this, the PCM data should be used with caution when accurate intensities are desired. Optical observations from satellites (and rockets) include in addition to the real emission intensity, a variable contribution from ground scattering. In principle this contamination can be quantitatively removed using the method of Hays and Anger (1978) assuming

---

Hays, P. B. and C. D. Anger, Influence of ground scattering or satellite auroral observations, Appl. Opt. 17, 1898-1904, June, 1978.

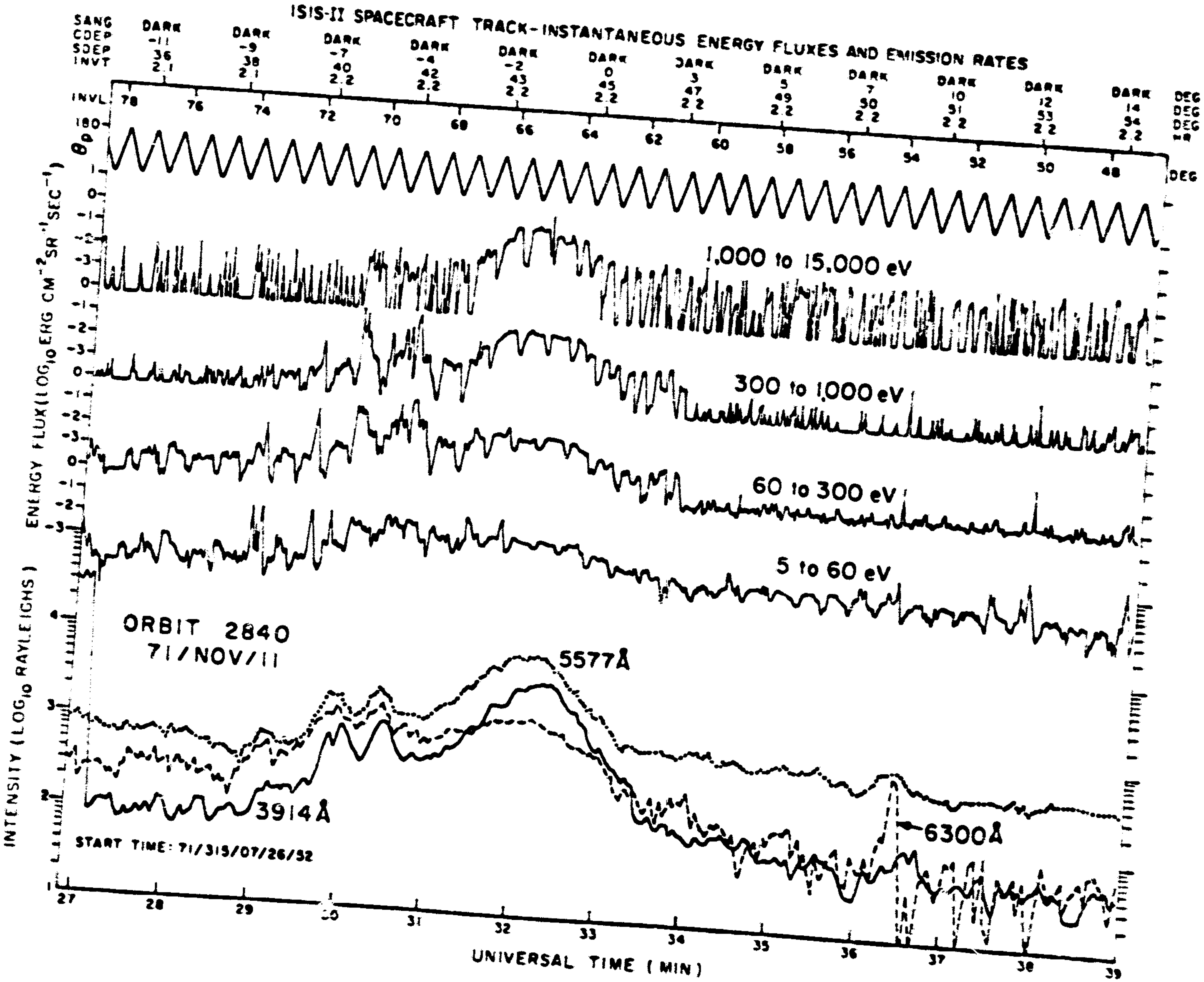

Figure 6. Example of Format 1 (Optical data and SPS).

the altitude of the emission and the spectral albedo of the surface are known. Practical experience has shown that the factor by which to divide an observed intensity (5577Å or 3914Å) varies from 2 for a large-scale, reasonably uniform region to 1 (i.e., no correction) for thin discrete arcs (Murphree et al, 1978). This correction factor is not as serious for the 6300Å emission because of its higher altitude and consequently lower susceptibility to contamination.

FORMAT 2, TOP (MAGNETOMETER)

The axial magnetometer plot is Format 2, combined on the same page with the sounder isodensity height profile plot. They have a common abscissa labeled in minutes of Universal Time. The orbit number and Universal Time at the beginning of the plot appear at the bottom. The ordinate is in units of nanoteslas (nT). The quantity plotted is the residual deviation of the filtered axial component from the GSFC 06/74* model field computed in the direction of the inferred spacecraft spin axis orientation. The residual baseline is offset from zero by an amount of the order of 400 to 1000 nT, in different orbits, depending on field contributions from electrical subsystems in the spacecraft. The offset from these sources remains unchanged for the duration of any plot. The data are low pass filtered with a 9-point filter and plotted at 1 point/sec. The principal source of noise is the digitization step size. After filtering, the typical RMS noise from this source is ~40 nT. Where deviations exceed the statistical fluctuations, negative-trending deviations correspond to Birkeland currents flowing into the ionosphere and positive-trending deviations correspond to Birkeland currents flowing out of the ionosphere.

FORMAT 2, BOTTOM (SOUNDER)

For each chosen value of electron density, the altitude at which that density was observed to occur is plotted as a function of UT. The values chosen for these plots are powers p of 10 such that 4p is integral, e.g., p= 3.0, 3.25, 3.5, 3.75, 4.0, etc. Units are cm^{-3}. Data points are indicated by * symbols on the contours for integral powers of 10, and by + symbols on the others. All the symbols in a vertical line represent the density information obtained from one ionogram.

The broken line at the top of the plot represents the position of the spacecraft (for ISIS 2 this line is straight and horizontal). The broken line at the bottom represents the lowest altitude from which density information was obtained. In favorable cases, this will be close to the peak of the F layer, but it can be any distance above the peak.

The altitudes are obtained under the assumption that the radio propagation from the topside sounder was vertical. At high latitudes, the propagation is more likely to be along the magnetic field. When this occurs, the altitudes shown are too low. At very high latitudes, the difference is small, but close to 60° magnetic latitude, it can amount to 50 km.

Murphree, J. S., I. W. H. Robertson, C. D. Anger, and L. L. Cogger, Rocket observations of auroral albedo over snow, Appl. Opt. 17, 1849-1850, June 1978.

*Cain, J. C., private communication, 1974.

The usual sampling rate for the topside sounder is about 4 per minute. On many passes, two consecutive samples are taken, then two missed. This mode was chosen on most cartwheel passes to provide the ion probes with interference-free intervals. Where data points are missing at irregular intervals, it is because some ionogram traces were too weak or too irregular to be scaled properly.

FORMAT 3 (EPD)

With two exceptions, the traces represent electron fluxes as a function of time. Those labeled D are differential channels while those labeled I are integral channels. The number in parentheses indicates the detected energy (keV) for the differential channels or the threshold energy for the integral detectors. Units are designated by R for 'counts per second' and I for 'electrons cm^{-2} sec^{-1} $ster^{-1}$ keV^{-1}'.

All of the above vertical scales are logarithmic.

The bottom trace, $\bar{E}$, indicates the average energy (keV) computed from the complete electrostatic analyzer energy range (0.15 to 9.6 keV); it does not include the integral detectors. The vertical scale is linear.

The top trace, I(22)/I(40), shows the ratio of geiger counter flux (electrons E > 22 keV and protons E > 240 keV) to the solid state detector flux (electrons E > 40 keV and protons E > 150 keV). Since the electron fluxes are normally greater than the positive ion fluxes, the ratio normally exceeds unity. However, when the proton flux between 150 and 240 keV predominates, the ratio is less than unity.

Shown across the bottom of each plot are the Universal Time (minutes), Invariant Latitude (degrees), magnetic local time (hours), B - the intensity of the magnetic field measured at the spacecraft (gauss), and Theta z - the angle between the spacecraft spin axis and the local magnetic field vector (degrees). Theta z (θ_z) is defined to be zero in both hemispheres for downward-coming field-aligned particles.

Detector $I_{\parallel}$(40) thus looks at θ_z to the local magnetic field while all other detectors execute pitch angle scans from $90°-\theta_z$ to $90°+\theta_z$. Consequently, fluxes are often modulated at twice the spin frequency for anisotropic fluxes or at the spin frequency in regions of isotropic precipitation. The nominal spacecraft spin frequency is 3 rpm.

The integral channels record a small component of background counts due to penetrating electron flux (e.g., outer zone electrons near invariant latitude of 60°) or due to penetrating proton flux in the inner zone and during solar flare events, over the polar cap. At other places, the penetrating background counts are negligible relative to the directional flux entering the collimator.

FORMAT 4, TOP (CEP)

CEP measurements of electron density, N_e, and temperature, T_e, are plotted independently. T_e is plotted either as a point or a question mark (?) depending upon the quality of fit of the exponential portion of the volt-ampere characteristic, as described in the CEP instrument description. T_e measurements of highest reliability are plotted as points, and those of lower reliability are plotted with question marks. If the plasma is highly structured or too low in density, no T_e measurement will be made.

The values of N_e are plotted as solid points. The points come in groups of five during alternate 30-second intervals as discussed in the instrument description.

Universal Time is given at 2-minute intervals and is represented by vertical lines at 1-minute intervals.

FORMAT 4, BOTTOM (IMS)

The date and time of the start of the frame are given in the upper left hand corner. The date is given in day, month, year, and Julian day in brackets. The time is given in hours, minutes, seconds, and second of day. The orbit number is given in the upper right hand corner and is the orbit number of the start of the data frame. The orbit is incremented on the north-bound crossing of the geographic equator. The orbital data at the bottom of the plot has been interpolated to an even 2-minute point on the plot. The description and units of the orbital data are given below:

	Description	Units
UT	Universal Time	HH:MM
LAST	Local apparent solar time	HH:MM
MLT	Magnetic local time	HH:MM
DLAT	Dip latitude	Degrees
INVL	Invariant latitude	Degrees
GLAT	Geodetic latitude	Degrees
GLNG	Geodetic longitude	Degrees
SZEN	Solar Zenith Angle	Degrees
ALT	Height above the geoid	Kilometers

The ion species are identified as follows:

Symbol	Species	Mass	Units
H	H^+	1	cm^{-3}
+	He^+	4	cm^{-3}
Δ	O^{++}	8	cm^{-3}
N	N^+	14	cm^{-3}
O	O^+	16	cm^{-3}

FORMAT 5 (RPA)

Geophysical parameters deduced from the RPA as described in the instrument section are plotted on two graphs using the standard 20-min. abscissa. The lower frame shows the H^+ (symbol H) and O^+ (symbol O) densities plotted against a logarithmic ordinate scale. The density grid shown is usually over the range 10 to 10^5 cm^{-3}, but occasionally is truncated if there are no data to allow more space for an extended scale on the second plot. The upper frame shows the ion temperature on a linear scale (symbol T) and the He^+ density (symbol 4) on a logarithmic scale. The temperature scale is usually 0° to 5000°K, but occasionally may be truncated at the lower limit (if no data are present) to permit extension of the upper limit. The scale factor in the plot (degrees/cm) is constant, regardless of scale truncation.

Universal Time is used for the standard 20-min. long linear abscissa, with a vertical line every 2 minutes. Additional abscissa values are shown to identify the local time, magnetic local time, dip latitude, invariant latitude, geodetic latitude, geodetic longitude, solar zenith angle, and altitude of the spacecraft as defined under Format 4, IMS.

FORMAT 6 (SPS)

Data from these instruments are displayed as energy versus time grey-shaded spectrograms where the plotted grey-scale intensity is proportional to the log of the instrument count rate at each energy level. Due to the operational characteristics of the instrument, the count rate at a particular energy, and thus the grey-scale intensity, is an indicator of the directional energy flux per unit energy at the measured energy. In the mode of operation for data presented here, one complete electron spectrum and one complete positive ion spectrum are obtained each second.

The upper and center panels of the plot contain the electron and positive ion spectrograms, respectively. The vertical scales are logarithmic in energy from 1 eV to over 10^4 eV. The lower panel contains pitch angle information and average energies. The pitch angle denotes the instrument look direction such that 0° refers to downward-moving particles, 90° to locally mirroring particles, and 180° refers to particles coming from below the spacecraft. Note that the range of pitch angles sampled by the detectors, which look radial to the spacecraft spin axis, depends upon the angle between the spacecraft spin axis and the local magnetic field. This angle is denoted by θ_z and appears along the upper edge of the electron spectrogram. For θ_z=90° the spin axis is perpendicular to the magnetic field, and all pitch angles from 0° to 180° are sampled each half spin period. The average energies in the lower panel are computed once each second for electrons and for positive ions and represent the average energy per particle over the range 5 eV to approximately 15 keV. The horizontal axis is time ordered with the beginning Universal Time printed at the lower left hand corner. Each succeeding minute of Universal Time is indicated along each horizontal axis. Geographic latitude, geographic longitude, and local time are given at the bottom of the plots for the first and last data points. The quantities called "ECAL" are calibration indicators for internal use. The spacecraft location in Magnetic Local Time and Invariant Latitude at 1-minute intervals appears along the top horizontal axis. Orbit number and satellite altitude also are shown above the plots.

FORMAT 7 (ASP)

Because of the large dynamic range of the Auroral Scanning Photometer (ASP), it is necessary to use a grey-scale representation and a sequence of varying upper and lower intensity limits to display the data. An example of the plotted data is shown in Figure 7. The data are plotted on an electrostatic dot matrix plotter and arranged in three independent rows with the leftmost picture in each row containing the coordinate system. There is, in addition, header information at the top of the page giving basic information about the pass and how the data were transformed. In all cases, the coordinates are corrected geomagnetic latitude (CGL) (Hakura, 1965) and time (see Murphree and Anger, 1980, for a description of the transform procedure). This magnetic coordinate system is denoted by the "M" in the lower left-hand corner of each coordinate picture. The accompanying "V" indicates that the intensity data have been corrected for look direction, i.e., van Rhijn effect. However, the data are not corrected for ground scattering and thus real intensity levels will be less depending on the spectral albedo of the surface under the auroral emissions. Latitudes are labeled in general every 10° and the Magnetic Local Time (MLT) every 6 hours. The geomagnetic pole is represented by a " + ".

The spacecraft track projected down to 100 km along magnetic field lines is given by the sequence of triangles, the approximate orbital motion being defined as the direction of the apex of the triangle. The triangles represent the position of the spacecraft exactly on the minute, the particular minute being derivable from the sequence of triangle shapes as follows. The basic shape

---

Hakura, Y., Tables and maps of geomagnetic coordinates corrected by the higher order spherical harmonic terms, Rep. Ionosph. Space Res., Japan, 19, 121, 1965.

Murphree, J. S., and C. D. Anger, An observation of the instantaneous optical auroral distribution, Can. J. Phys., 58, No. 2, 214-223, Feb. 1980.

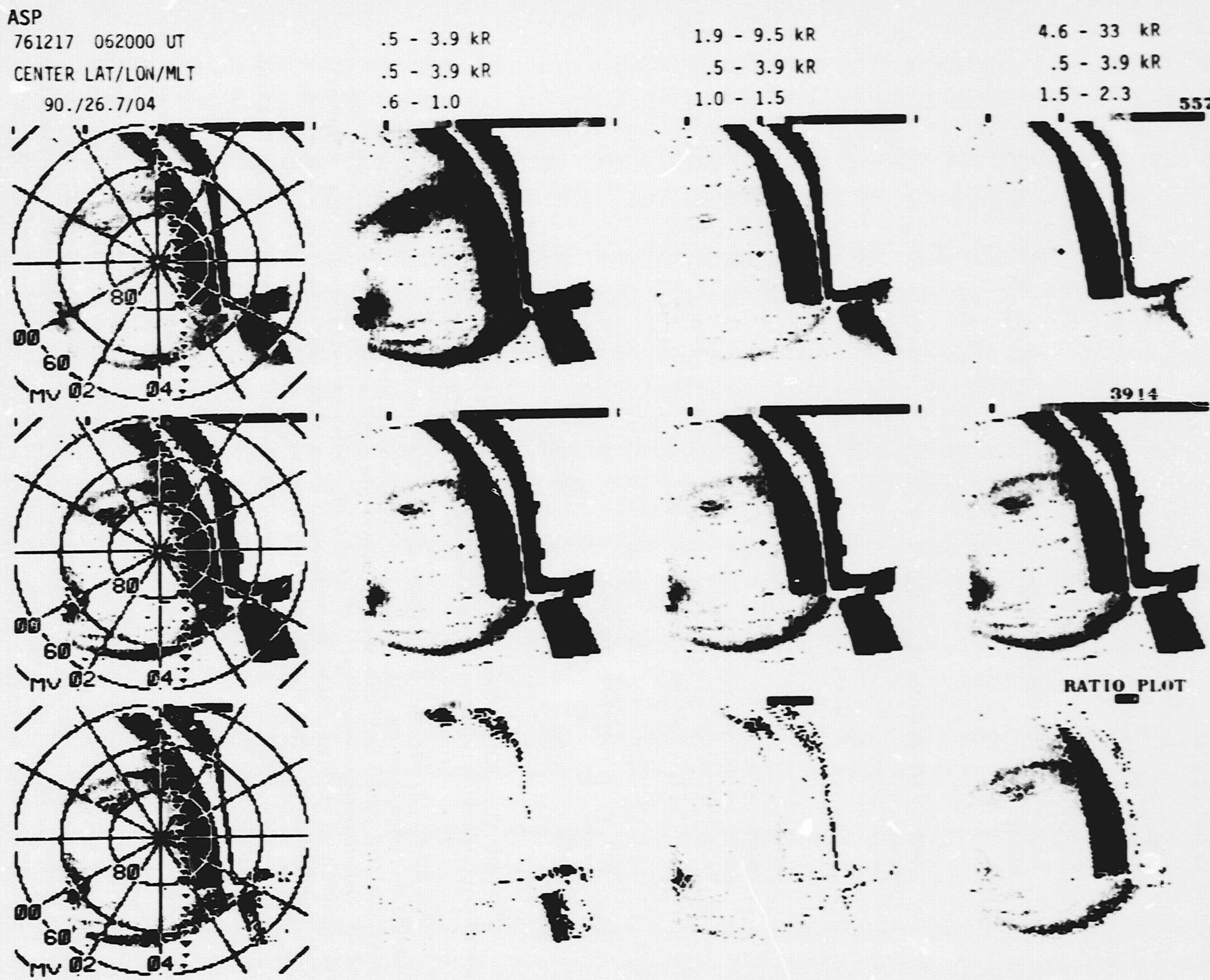

Figure 7. Example of Format 7 (ASP).

consists of filled (or a blank, depending on the surrounding background) blocks denoted below by "x":

```
  x
 xxx - represents any minute not specified in the following


  x
 xxx - one of the following:  5, 15, 25, 35, 45, 55 UT minute
xxxxx


  x
 xxx  - UT minute 10 or 50
xxxxx
  x


  x
 xxx
xxxxx  - UT minute 20 or 40
 xxx


  x
 xxx  - UT minute 0 or 30
xxxxx
xxxxx
```

The actual time values can be obtained by noting the start time in the header and identifying the first time symbol in the coordinate picture.

The start and/or end of a pass may or may not be apparent in the given transform, depending on the range (in degrees) to which it was desired to transform the data, but the spacecraft track indication will continue to the end of the coordinate system. If start or end does occur within the range of the transform, the data will be truncated in a straight line. In contrast to this, the limit of optical observations at 90° to the spacecraft track (its limbs) will form a pair of irregular lines parallel to and equidistant from the spacecraft track.

The data appearing in each picture in each row are a grey-scale representation of the intensity for the appropriate wavelength. Each picture element is represented by a 3 x 3 square matrix of dots and anywhere from 0 (at or below the bottom of the desired intensity range) to 9 (at or above the top of the range) of the dots are blackened so as to provide a grey scale. For example, if the picture is labeled .6 - .95 (the numbers representing kR for intensities and ratio values for ratio plots), then any points with intensities less than or equal to .6 kR will be white while any elements greater than or equal to .95 kR will be black. The three rows of pictures represent 5577Å intensity, 3914Å intensity and the ratio I(5577Å)/I(3914Å), respectively. In general, the 5577Å data are displayed in the three rightmost pictures of the first row with three different intensity ranges (in kR), e.g., .5 - 3.9, 1.9 - 9.5, 4.6 - 33, while 3914Å uses a single range for all three pictures, this range being the same as that for the lowest 5577Å range. The picture onto which the coordinate system is overlayed has a range equal to the entire range of intensities covered by all of the pictures in the row. For example, in the above 5577Å ranges, the coordinate picture would contain .5 - 33 as the kR range.

In the pass shown in Figure 7, the 5577Å and 3914Å data illustrate the northern hemisphere polar cap on 761217 at 0620 UT. The satellite track is basically from 16 MLT to 5 MLT as the data show well-defined auroral emissions in the evening (16 - 21 MLT) and morning (00 - 07 MLT) sectors. The midnight sector of the auroral emissions was beyond the limb on this pass as indicated by the irregular boundary of the data in that MLT sector. The dayside is contaminated by scattered sunlight as is illustrated by the high intensity, regular feature in both wavelengths. This is a common feature because of the difficulty in combining the correct satellite altitude with both time of year and UT to optimize dayside viewing conditions. Such features are usually easily distinguished from auroral emissions because they are aligned with the spacecraft track rather than with the magnetic coordinate system.

Because of contrast problems, it is necessary to approach the ratio in a different manner. Each of the three pictures in the ratio plot row represents different ratio ranges which are always chosen to be: 0.6 - 1.0, 1.0 - 1.5, 1.5 - 2.3. The ratio for each element (i.e., position in the coordinate system) in each picture is calculated. If it falls within the specified range as given above, then the 3914Å intensity at the point is plotted based upon the 3914Å intensity thresholds in the same column of the previous row (this is why all 3914Å thresholds are identical). The result is three pictures which show where 3914Å emissions are observed (and their intensity) for the three ratio ranges. The composite (i.e., the leftmost picture with the superimposed coordinate grid) then should be similar to the composite 3914Å given in the previous row. Any missing points in the composite picture will correspond to ratio values outside the range 0.6 - 2.3.

FORMAT 8 (RLP)

In this format the isointensity contours of atomic oxygen 6300Å emission are shown, obtained with the Red Line Photometer (RLP) and plotted in a polar invariant projection. The perimeter corresponds to 50° invariant, and dashed circles indicate 60°, 70°, and 80° invariant. Invariant noon is at the top and morning (06 h) on the right. The intensities corresponding to the contours selected are listed on the upper right, and the contours themselves are labeled in units of tens of rayleighs (25 = 250R). The orbit number, date, day number, and Universal Time for the first and last spins of the pass are given on the upper left. The hatched line shows the track of the spacecraft traced down to the 250 km level, the height assumed for the altitude of emission; each hatch mark indicates one rotation (spin) of the spacecraft, and every tenth spin is labeled. The spin axis is nearly parallel to the orbit plane. The Universal Times that correspond to each spin number are given on the far right-hand side.

The intensities given are not corrected for albedo and so over regions of widespread emission they may be too large by a factor of two. If the label at the top reads "6300 angstrom intensity" then a correction for white light background has been applied. If it reads "10 angstrom bandpass intensity" then there has been difficulty with white light subtraction in part of the picture and the 10Å channel data are shown uncorrected. The intensities shown for these cases will be less accurate than for the others.

The example shown in Figure 8 illustrates some aspects of the data and some of the peculiarities. The features discussed below correspond to contours that have been labeled, A → G.

A. These contours arise from sunlight scattered from the Earth. They can be recognized by their proximity to noon and by their steep gradient.

B. These linear contours are caused by scattering in the RLP baffle system, and the steep gradient is caused by one critical baffle element. When the solar illumination leaves this element the baffle scattering falls rapidly and the auroral contours become visible.

C. These linear contours, having a steep gradient, are generated by the passage of the spacecraft from sunlight into darkness, with the cessation of baffle scattering. These contours are perpendicular to the spacecraft track, and the rectangular pattern of B/C normally can be recognized readily.

D. Dayside auroral contours. The morning extension of the dayside auroral contours are evident here, extending from the region of baffle scattering. When baffle scattering is not present this pattern is normally roughly symmetric about noon.

E. Night auroral contours. These contours define the region of brighter nightside aurora.

F. Equatorward auroral boundary. These contours define the equatorward boundary of 6300Å aurora. The termination after midnight is caused by the scans reaching the "edge" of the Earth; i.e., the limb.

G. Poleward auroral boundary. These contours define the poleward auroral boundary and normally form a near-circular region in the polar cap.

FORMAT 9 (ASP AND RLP)

This format provides latitude profiles of airglow emission rate at 5577Å and 6300Å obtained from the ASP and RLP. In the cartwheel mode of operation, the fields of view of the photometer sweep along the path of the orbit to provide data over a large range of latitudes but a very small range of longitudes. Pole-to-pole coverage can be achieved in a time interval of about 30 minutes.

The latitude profiles are based on airglow limb data which result in a measurement at the leading and trailing limb for each limb. This ensures that the data are free from cloud and ground albedo effects and contamination by other sources of light. It also permits the separation of the 5577Å airglow into the E- and F-region components (see Format 12), both of which are plotted. The maximum of the E region airglow is defined to occur at 95 km for the 5577Å data and the F region is then referenced to that level. The emission rates given correspond to what would be observed in the zenith from below at the location of the airglow limbs. The plots therefore represent the vertical

ORBIT 3598 (72/JAN/10)
DAY 10 OF YEAR 1972

FIRST SPIN U.T. $3^{H}21^{M}$
LAST SPIN U.T. $3^{H}42^{M}$

6300 ANGSTROM INTENSITY

DATE PROCESSED: 79/OCT/18
INVARIANT COORDINATES (250 KM.)

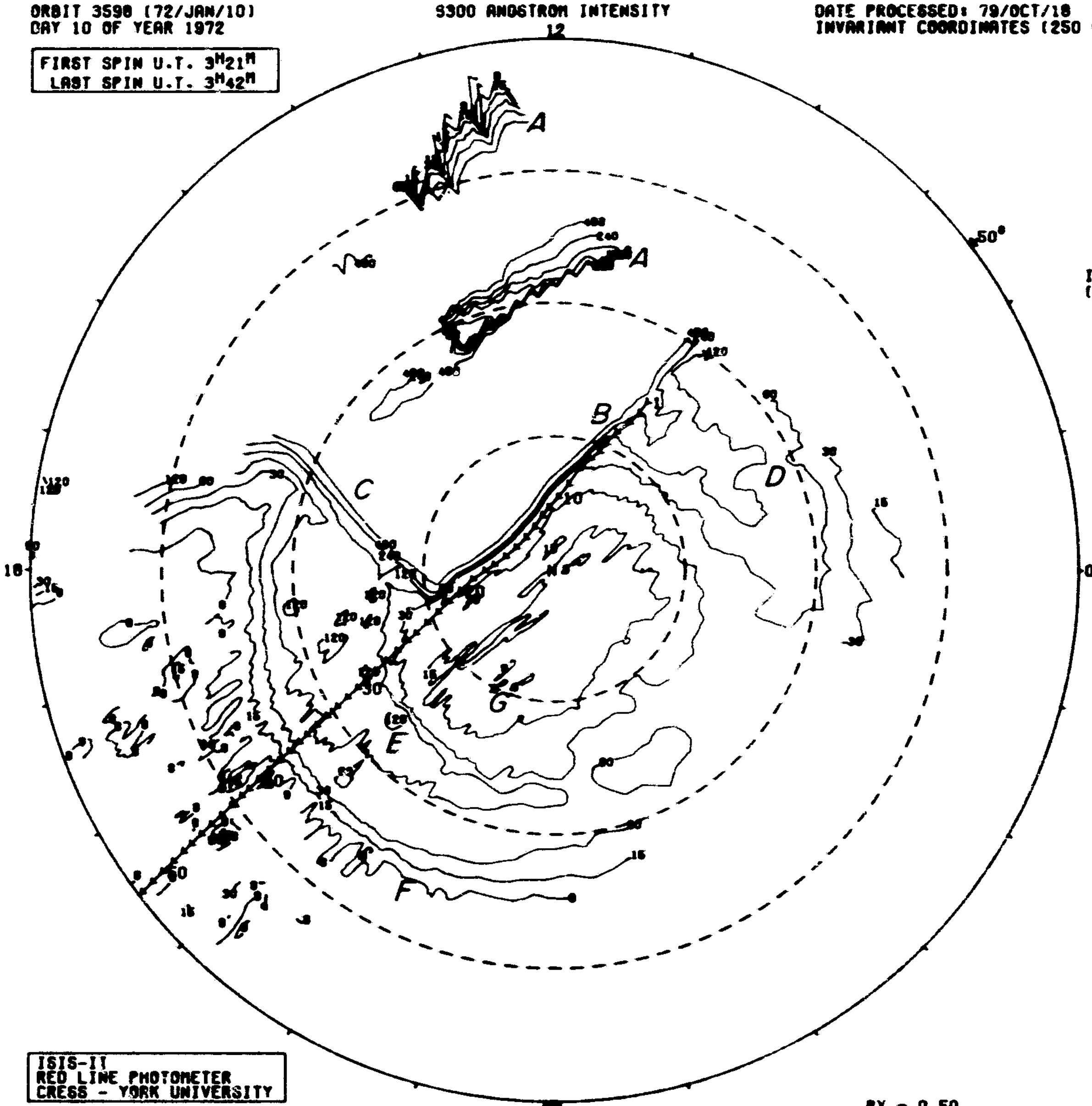

CONTOURS PLOTTED

80
150
300
600
1200
2400
4800
ZENITHAL INTENSITIES (RAYLEIGHS)

SPACECRAFT INFORMATION

SPIN NUMBER	ORBIT TIME (HRMMSC)	INVARIANT LATITUDE (DEGREES)
1	032159	76.3
2	032223	77.3
3	032247	78.3
4	032311	79.3
5	032335	80.2
6	032359	80.9
7	032417	82.0
8	032441	82.9
9	032505	83.6
10	032529	84.0
11	032553	84.2
12	032611	84.3
13	032635	84.3
14	032659	84.3
15	032723	84.3
16	032747	84.3
17	032811	84.2
18	032829	83.9
19	032853	83.5
20	032917	82.8
21	032941	81.9
22	033005	80.8
23	033029	79.8
24	033053	78.8
25	033111	78.1
26	033135	77.1
27	033159	76.0
28	033223	75.0
29	033247	73.9
30	033305	73.1
31	033329	72.1
32	033353	71.0
33	033417	69.9
34	033441	68.8
35	033505	67.7
36	033523	66.9
37	033547	65.8
38	033611	64.7
39	033635	63.6
40	033659	62.5
41	033723	61.3
42	033741	60.5
43	033805	59.4
44	033829	58.3
45	033853	57.2
46	033917	56.0
47	033941	54.9
48	033959	54.1
49	034023	53.0
50	034047	51.9
51	034111	50.8
52	034135	49.7
53	034159	48.6
54	034217	47.7
55	034241	46.7

ISIS-II
RED LINE PHOTOMETER
CRESS - YORK UNIVERSITY

MRT Y00254
FILE 37

SPACECRAFT TRACK TRACED DOWN TO 250 KM. (NUMBERS DENOTE SPINS)

RX = 0.50
DATA FILTERED
ZERO SUBTRACTION NOT PERFORMED

Figure 8. Example of Format 8 (RLP) with the events A through G.

emission rate in rayleighs as a function of geographic latitude. The points are not independent due to the fact that the optical viewing path in the atmosphere is longer than the spatial sample interval which is determined by the orbital speed of the satellite. As a consequence the plots correspond to a running mean of the emission rate.

In practice, the latitude range is restricted to low and mid-latitudes due to the presence of aurora at higher latitudes. The difference between leading and trailing limb values when they overlap in the plot is due either to the small difference in longitude or to temporal variation in the airglow.

FORMAT 10, TOP (CEP)

See Format 4 (Top) description. The latitude, longitude, local time, dip angle, dip latitude, L value, invariant latitude, and solar zenith angle are given below the graphs.

FORMAT 10, BOTTOM (SOUNDER)

See Format 2 (Bottom) description.

FORMAT 11 (VLF)

VLF data published herewith are presented in the conventional amplitude-frequency-time display wherein signal corresponds to the dark parts of the display. These data are from routine 35-mm records having the frequency axis across the film and the time along the film. This data book has room only for interesting excerpts of the receiver film record. In data set C of Volume 4 the VLF film has been printed at 2X magnification to illustrate the details of a variety of typical phenomena observed by ISIS 2. In the other data sets, film is printed at 1X magnification. The VLF receiver was off during the majority of the passes. Excerpts of the VLF record for receiver-on passes have been chosen to show the highlights of those passes. In many cases, the VLF exciter was on and its periodic frequency downsweeps can be seen.

The example of the data format given in Figure 9 shows the frequency axis running linearly from 0 to 21 kHz, and the Universal Time axis running linearly from 06:41:10 to 06:41:39 (hours:minutes:seconds). Both the frequency and time limits are to be associated with the extremes of the film. In the example given, the broad diffuse patches are a natural emission, VLF hiss. The record also contains four instances of the received exciter signal. Two of these are on the fast duty cycle, at 06:41:15 and 06:41:21, and two on the slow cycle, at 06:41:23 and 06:41:34.

FORMAT 12 (ASP)

This format provides examples of the 5577Å airglow limb profiles obtained during a pass. The selection was made to demonstrate the variation of the two components of the airglow. The vertical axis gives the tangential height. In all cases the reference height of 95 km has been arbitrarily assigned to the maximum of the E- region airglow response. The slant intensity in kilorayleighs (kR) is plotted along the horizontal axis. The profiles, obviously broadened by the finite field of view of the instrument, do not give information about the detailed vertical distribution; they merely demonstrate the resolution of the main components.

71/299/0639

Excerpts of VLF Spectral film for the period 0641 - 0642

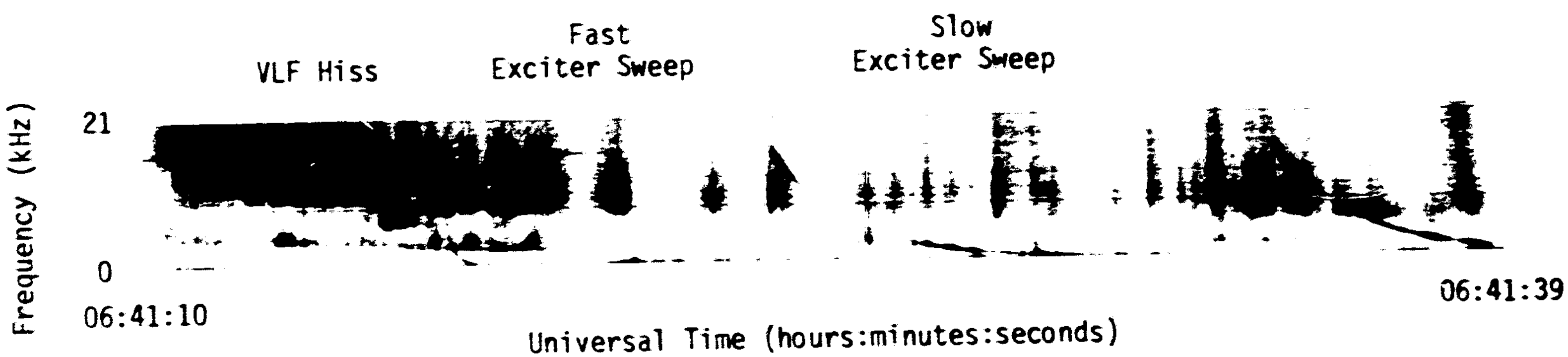

Figure 9. Example of Format 11 (VLF).

VI. GEOPHYSICAL DATA SET: AURORAL OPTICAL EMISSIONS, MAGNETIC FIELD PERTURBATIONS, AND PLASMA CHARACTERISTICS, MEASURED SIMULTANEOUSLY ON THE SAME MAGNETIC FIELD LINE

DATA SET DESCRIPTION

The objective of this data set is to provide a series of cross-sectional profiles across the auroral oval, covering the full range of local times. For each profile, the ionospheric optical emission intensities are plotted, along with the direct measurements made at the 1400 km level of the satellite, and the topside profile of electron density between the satellite and the height of maximum density. For these measurements, the satellite was in a cartwheel configuration, with the spin axis perpendicular to the orbit plane. This mode provides good plasma data, because the full range of pitch and ram angles is covered. It also provides good magnetic field perturbation data. For the optical data, it provides the redundancy of repeated scans along the spacecraft track, which allows the selection of optical data that are simultaneous, to within about 10 seconds of the direct measurements made on the same magnetic field line (Shepherd et al, 1980). The details of this are provided under the Format 1 description.

The formats composing this data set are as follows, in order of their presentation:

1.	Format 1	Optical intensities and soft electron fluxes from RLP, ASP, and SPS.
2.	Format 6	Soft electron and proton spectrograms from SPS.
3.	Format 3	Energetic particle fluxes from EPD.
4.	Format 2	Electron density contours from the topside sounder, and magnetic field perturbations.
5.	Format 4	Electron density and temperature from CEP and ion densities from IMS.
6.	Format 5	Ion densities and temperatures from RPA.
7.	Format 11	VLF data - available for only a few passes.

The passes (Table 1) are presented in groups corresponding to 3-hour intervals of local magnetic time. Within each group they are ordered by increasing value of 3 hr Kp. The data are selected from the period October 13, 1971, to November 24, 1971, for the Northern Hemisphere and the period June 5, 1972, to August 2, 1972, for the Southern Hemisphere. These are the only available periods of darkness with cartwheel configuration, when all experiments were functioning well. Unfortunately no good data were available for the magnetic local time intervals of 6-9 and 9-12 hours. The detailed pass list is given on page 34. The passes for which VLF data exist are identified in the list.

G.G. Shepherd, J.D. Winningham, F.E. Bunn and F.W. Thirkettle, An empirical determination of the production efficiency for auroral 6300 Å emission by energetic electrons. J. Geophys. Res. 85, 715-721, 1980.

Each instrument has its own peculiarities and susceptibilities, and it is not possible to eradicate them all in the data processing. We draw attention to some of them here. In Set 1, Format 1, there is solar contamination from 07:22 UT until 07:24, when the spacecraft enters the Earth's shadow as indicated by the "DARK" entry for sun angle ("SANG") given at the top of the page. In this interval, sun pulses are evident in the SPS channels while the sawtooth behavior in the optical B channel results from the solar protection circuit turning on and off. The downward step in the R channel at 07:24 results from cessation of baffle-scattered sunlight. In Set 8, Formats 1 and 6, sounder interference is present from about 06:55 UT to 07:00 in the SPS channels.

In terms of geophysical responses, comparison of the different data sets reveals a consistent behavior pattern, at least for some features. For these nighttime passes some quantities, such as the magnetic field perturbation, show marked responses only for enhanced disturbance levels. While no data set is really typical, data set 8 provides an example of disturbed conditions that displays most of the features. In Format 1, the optical peaks from 06:48:40 to 06:50:00 correspond to discrete aurora while the emission from 06:50 to 06:55 arises from diffuse aurora, which itself is divided at 06:52:30 into two parts. Each part probably corresponds to different earlier substorms. Format 6 shows the spectrogram presentation of these different aurora regions; it also shows proton precipitation near the location dividing the diffuse aurora into two parts. Format 3 shows that while both diffuse regions have relatively isotropic populations below 10 keV, there are marked differences in the anisotropy in the two regions for the 40 keV electrons. The onset of durable trapping at lower latitudes is evident in these data. In Format 2, the magnetometer deviation shows the existence of strong field-aligned currents through most of the precipitation region. The sounder electron density contours below show clearly the electron trough, and enhanced electron density in regions of precipitation. In Format 4, the low-altitude plasmapause is clearly shown in the electron density (above), along with a characteristic increase in electron temperature in the same region. In the ion mass spectrometer data shown below, the transition from an oxygen-dominant auroral ionosphere to a hydrogen-dominant plasmasphere is apparent. In Format 5, the RPA ion composition is consistent with that of Format 4, while the ion temperatures show elevated values inside the plasmasphere.

Table 1 Data Set Pass List

MLT RANGE	DATE	DAY NO.	TIME (UT)	KP	VLF	PAGE	DATA SET
0-3	Nov. 17/71	321	0722	0	-	35	1
	Nov. 16/71	320	0644	0+	-	41	2
	Nov. 18/71	322	0605	2-	-	47	3
	Nov. 11/71	315	0727	2	-	53	4
	Nov. 18/71	322	0413	3+	-	59	5
	Nov. 22/71	326	0452	4	-	65	6
	Nov. 24/71	328	0607	4+	-	71	7
	Nov. 22/71	326	0648	5-	-	77	8
3-6	Oct. 23/71	296	0842	1-	YES	83	9
	Oct. 24/71	297	0725	3-	-	89	10
	Oct. 13/71	286	0811	3	-	94	11
	Oct. 13/71	286	0959	3	-	99	12
	Oct. 29/71	302	0650	3+	-	103	13
	Oct. 22/71	295	0807	4-	-	109	14
	Oct. 30/71	303	0727	4-	-	114	15
6-9	No data						
9-12	No data						
12-15	Nov. 17/71	321	0524	0	-	120	16
	Nov. 20/71	324	0523	2-	YES	126	17
	Nov. 18/71	322	0600	3+	-	134	18
	Nov. 22/71	326	0445	4	-	140	19
15-18	Nov. 17/71	321	0718	0	-	146	20
	Oct. 19/71	292	0759	1-	-	152	21
	Oct. 23/71	296	0642	1-	YES	157	22
	Oct. 23/71	296	0836	1-	-	163	23
18-21	July 13/72	195	0712	0+	-	167	24
	July 14/72	196	0749	1-	-	173	25
	July 15/72	197	0634	1+	-	179	26
	Aug. 02/72	215	0631	2-	-	185	27
	July 16/72	198	0711	2	-	191	28
	July 11/72	193	0750	2+	-	197	29
21-24	June 13/72	165	0909	0+	-	203	30
	June 11/72	163	0948	1-	-	209	31
	June 15/72	167	1025	2-	-	215	32
	July 10/72	192	0712	2-	-	221	33
	June 05/72	157	0948	3	-	227	34
	July 08/72	190	0750	3+	-	233	35
	June 18/72	170	0126	8+	-	239	36

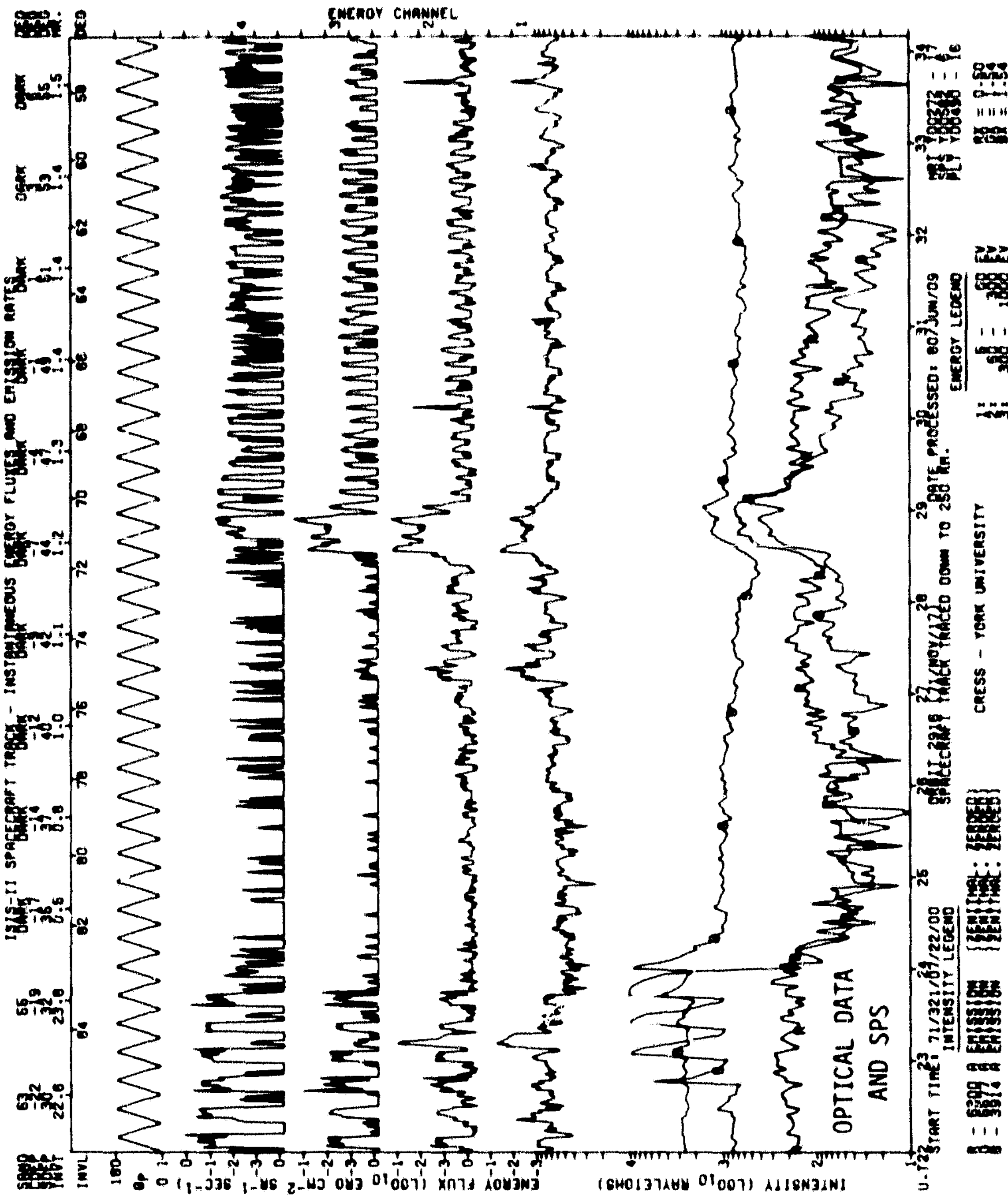

SET 1, FORMAT 1

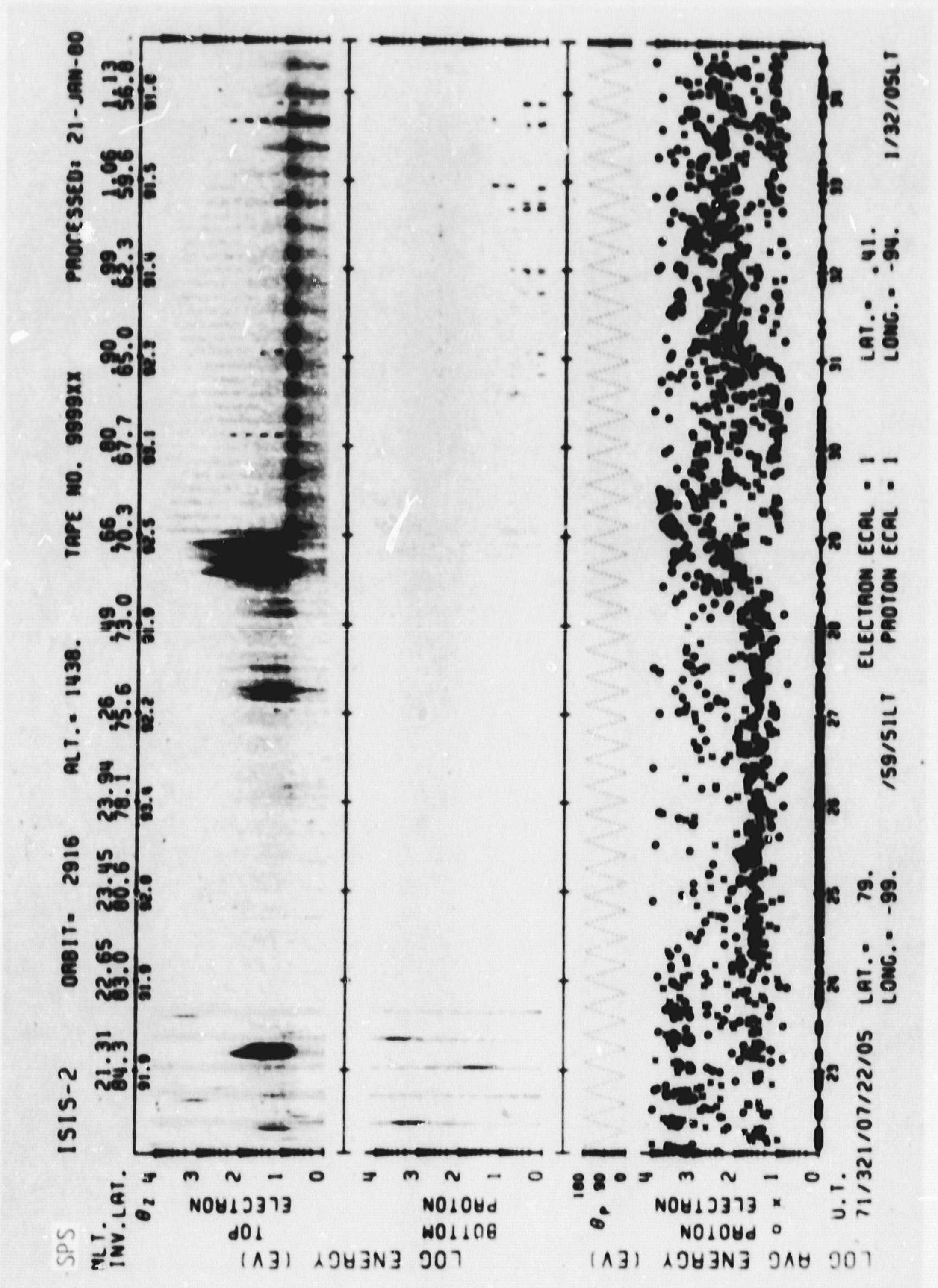

SET 1, FORMAT 6

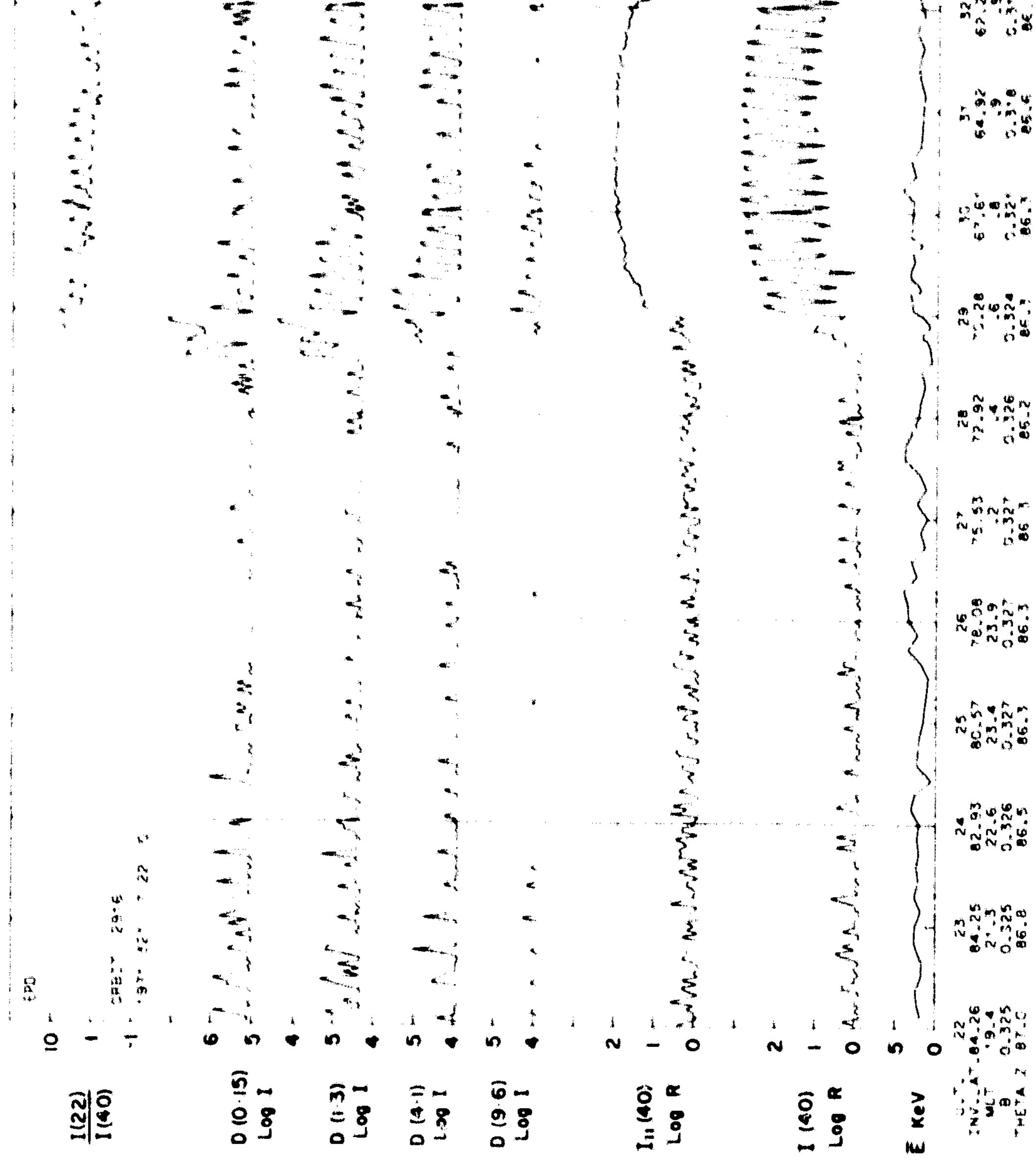

SET 1, FORMAT 3

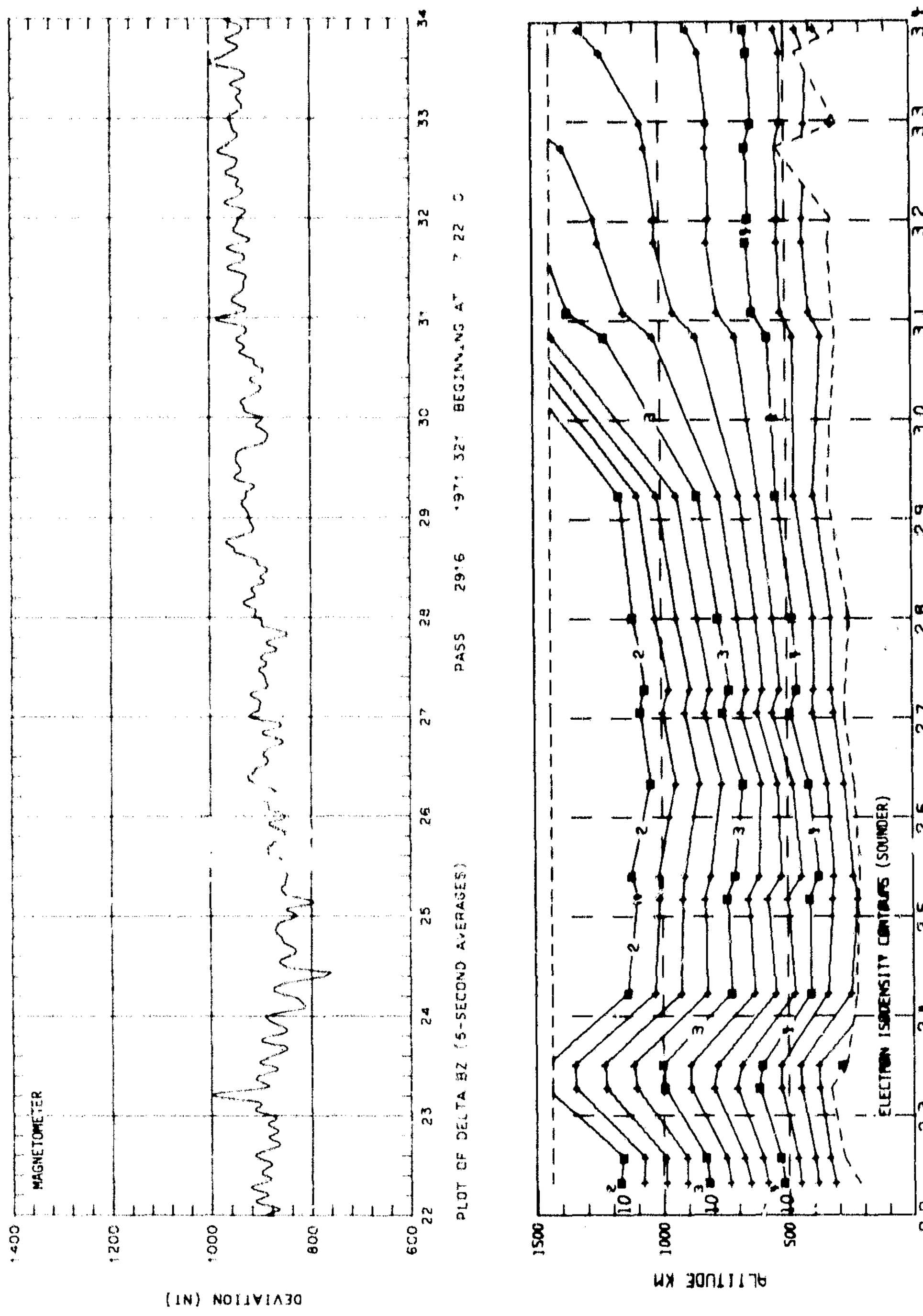

SET 1, FORMAT 2

ORBIT 2916
DATE 711117
DAY 321

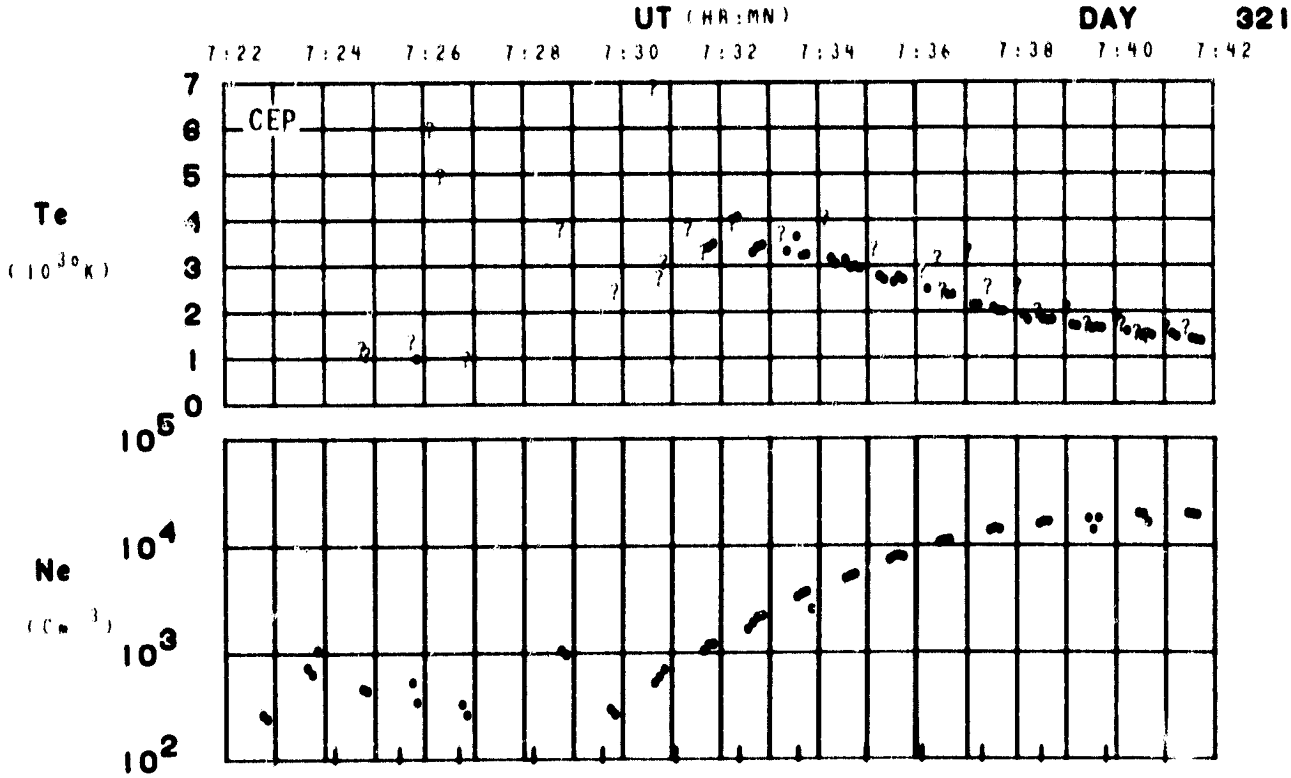

17 NOV 1971 (321) ISIS-II IMS
7:22:10 26530 ORBIT 2916

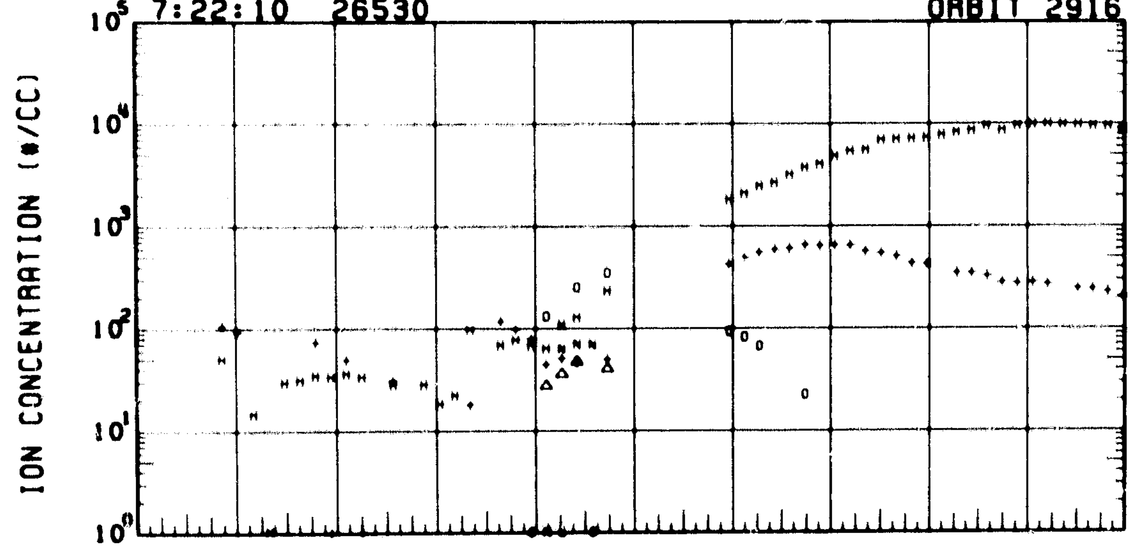

1 - H	UT	7:24	7:26	7:28	7:30	7:34	7:36	7:38	7:40
4 - +	LAST	1:14	1:21	1:25	1:28	1:32	1:33	1:34	1:35
8 - △	MLT	22:40	15:14	0:30	0:48	1:08	1:14	1:19	1:23
14 - N	DLAT	85	80	75	68	55	48	40	33
16 - O	INVL	83	78	73	68	57	51	46	41
	GLAT	73	67	61	54	42	36	29	23
	GLNG	-95	-94	-93	-93	-93	-94	-94	-94
	SZEN	125	130	136	141	150	154	156	157
	ALT	1437	1437	1435	1433	1428	1425	1421	1418

SET 1, FORMAT 4

Note different temperature scale

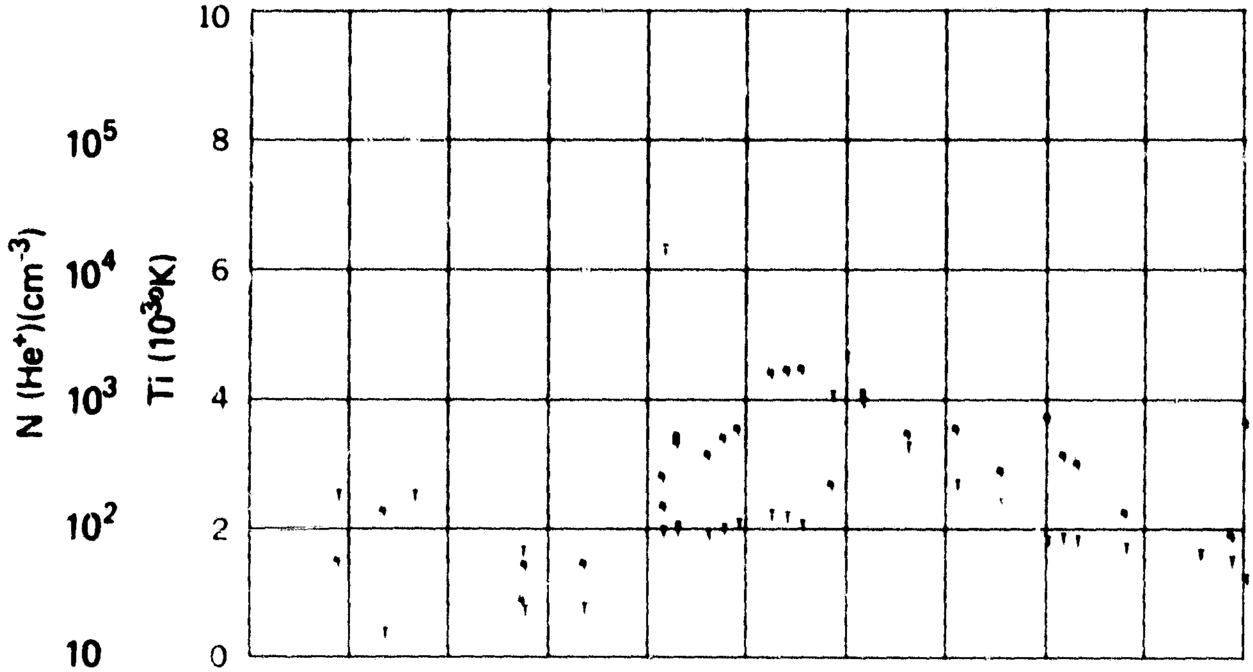

UT	7:24	7:26	7:28	7:30	7:34	7:36	7:38	7:40
LAST	1:14	1:21	1:25	1:28	1:32	1:33	1:34	1:35
MLT	22:40	15:14	0:30	0:48	1:08	1:14	1:19	1:23
DLAT	85	80	75	68	55	48	40	33
INVL	83	78	73	68	57	51	46	41
GLAT	73	67	61	54	42	36	29	23
GLNG	-95	-94	-93	-93	93	-94	94	-94
SZEN	125	130	136	141	150	154	156	157
ALT	1437	1437	1435	1433	1428	1425	1421	1418

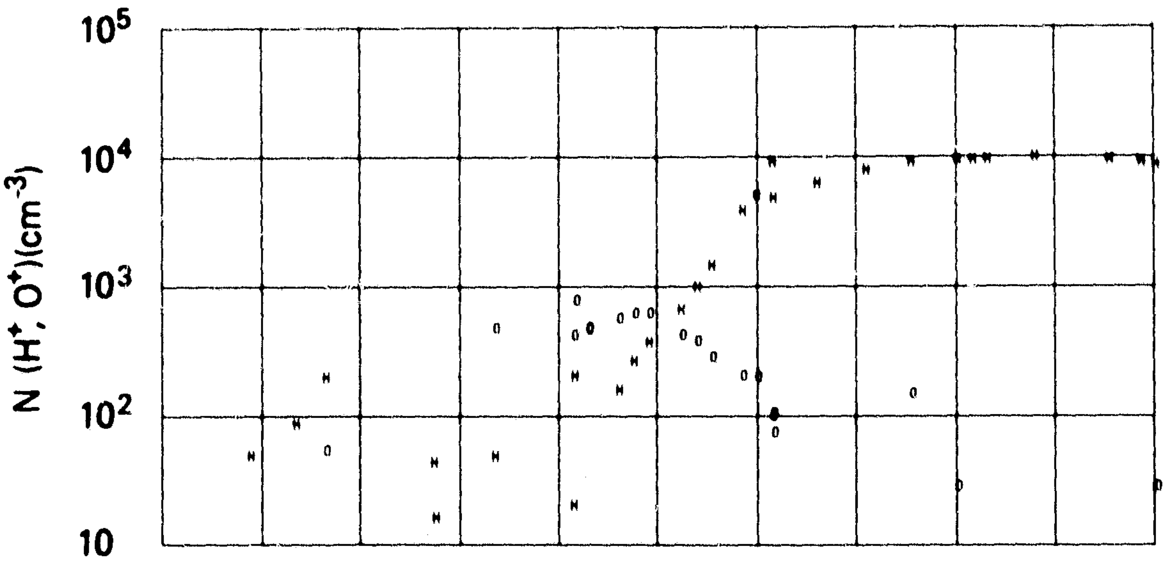

SET 1, FORMAT 5

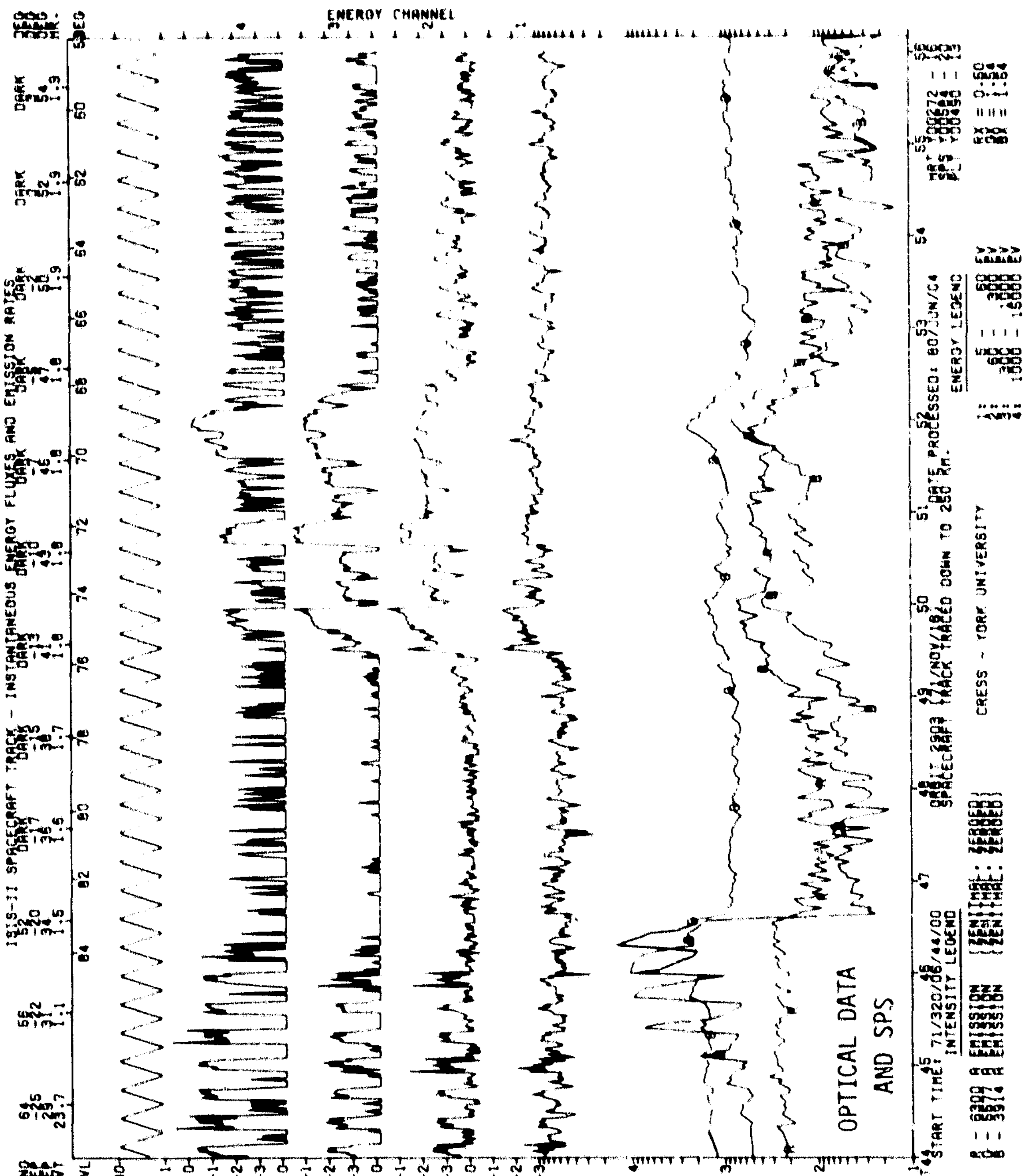

SET 2, FORMAT 1

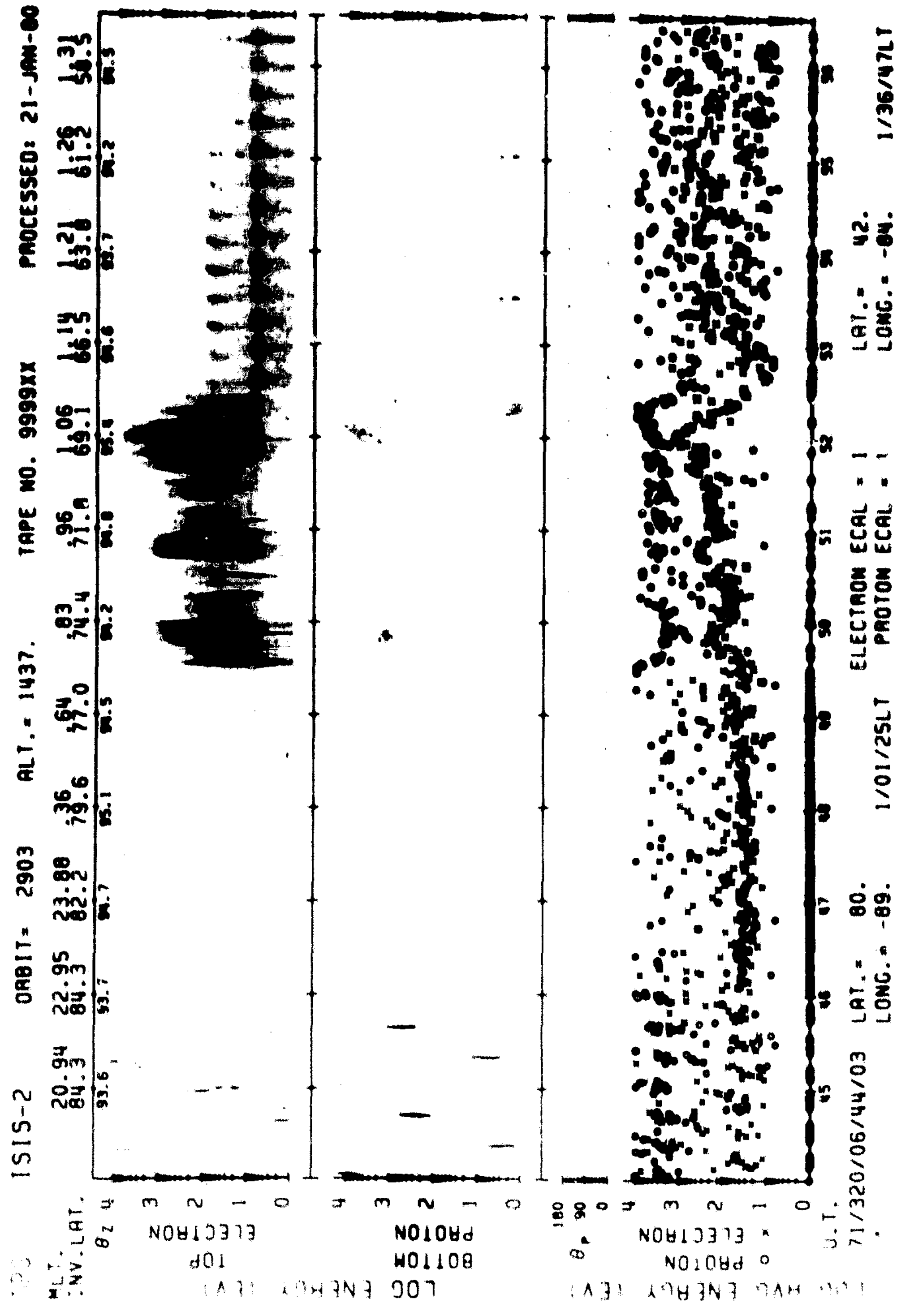

SET 2, FORMAT 6

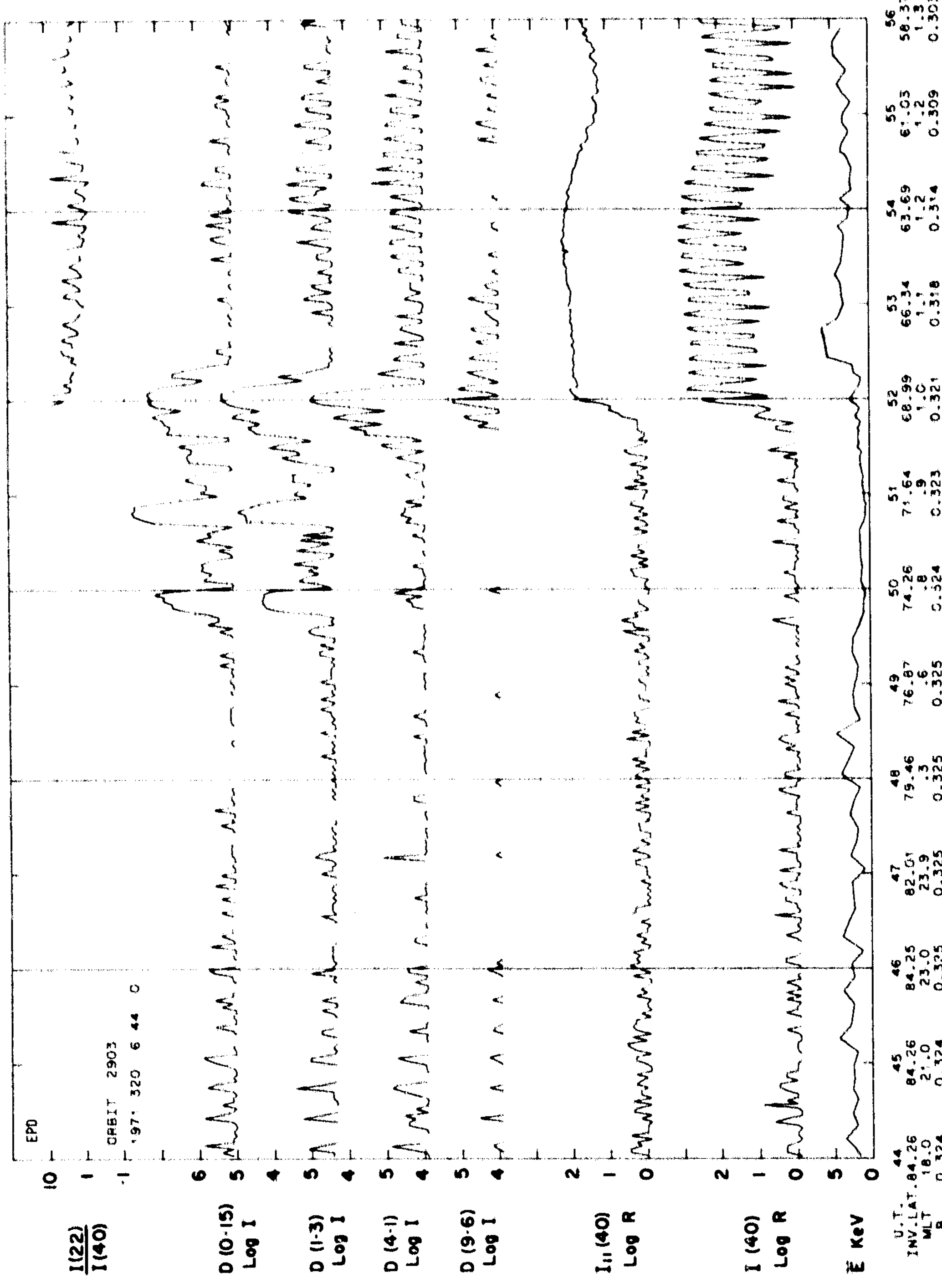

SET 2, FORMAT 3

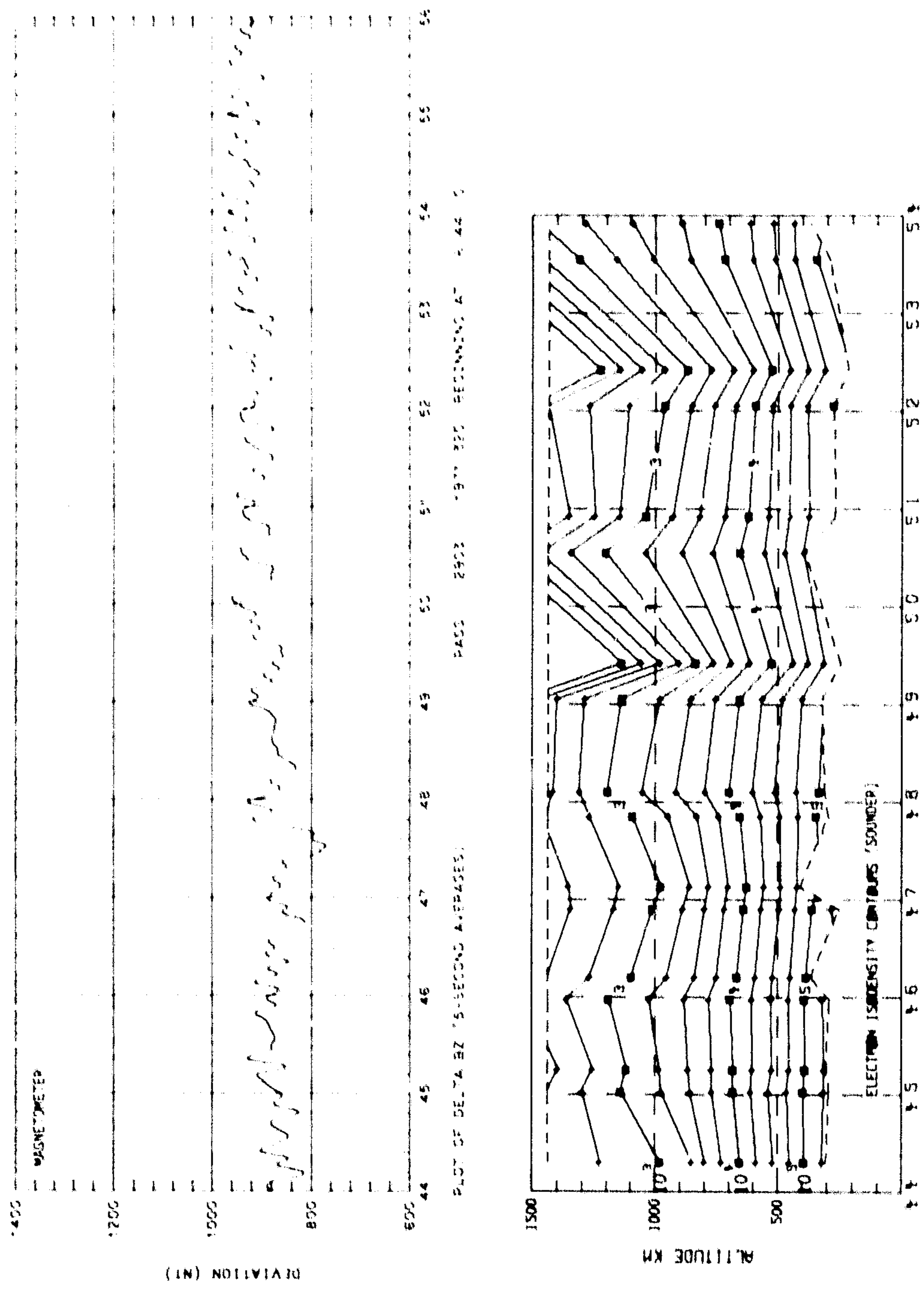

SET 2, FORMAT 2

ORBIT 2903
DATE 711116
DAY 320

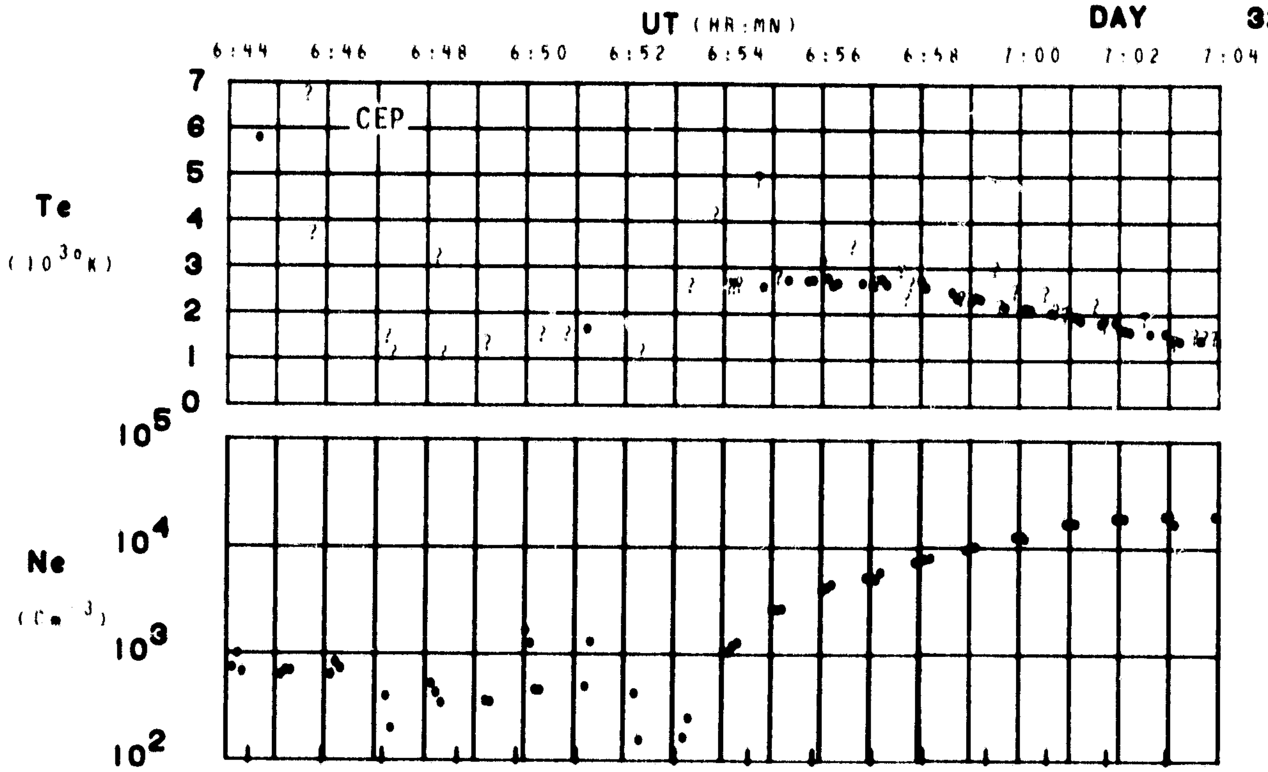

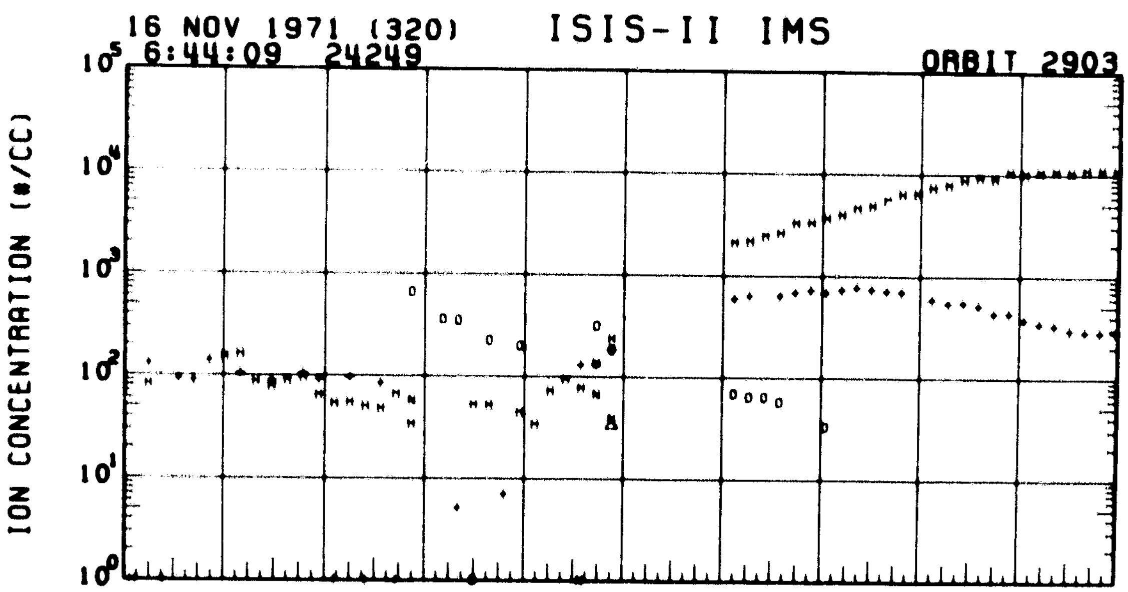

1 H	UT	6:46	6:48	6:50	6:52	6:56	6:58	6:60	7:02
4 +	LAST	1:17	1:25	1:30	1:33	1:36	1:38	1:39	1:40
8 Δ	MLT	23:00	0:22	0:50	1:04	1:19	1:23	1:27	1:30
14 N	DLAT	85	81	76	70	56	50	43	36
16 O	INVL	84	79	74	69	58	53	48	43
	GLAT	74	68	62	55	43	36	30	24
	GLNG	-85	-83	-83	-83	-83	-83	-83	-83
	SZEN	124	129	134	139	148	152	155	156
	ALT	1437	1437	1435	1434	1429	1426	1423	1420

SET 2, FORMAT 4

RPA

711116

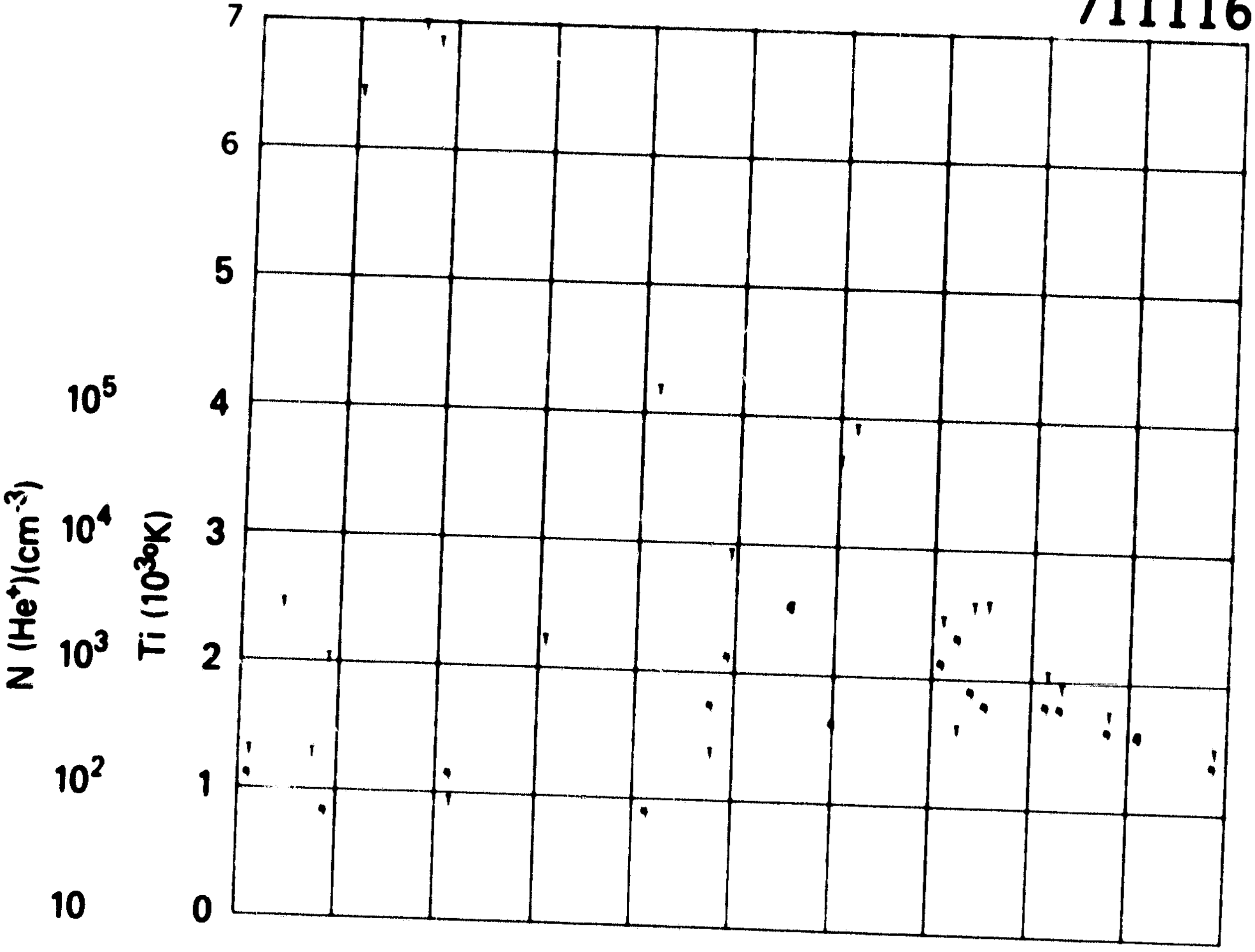

UT	6:46	6:48	6:50	6:52	6:56	6:58	6:60	7:02
LAST	1:17	1:25	1:30	1:33	1:36	1:38	1:39	1:40
MLT	23:00	0:22	0:50	1:04	1:19	1:23	1:27	1:30
DLAT	85	81	76	70	56	50	43	36
INVL	84	79	74	69	58	53	48	43
GLAT	74	68	62	55	43	38	30	24
GLNG	-85	-83	-83	-83	-83	-83	-83	-83
SZEN	124	129	134	139	148	152	155	156
ALT	1437	1437	1435	1434	1429	1426	1423	1420

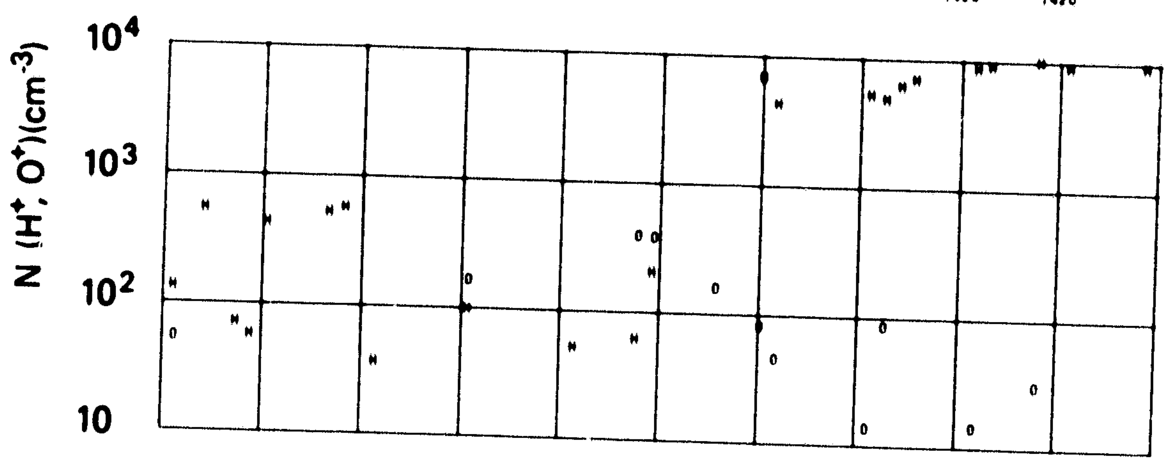

SET 2, FORMAT 5

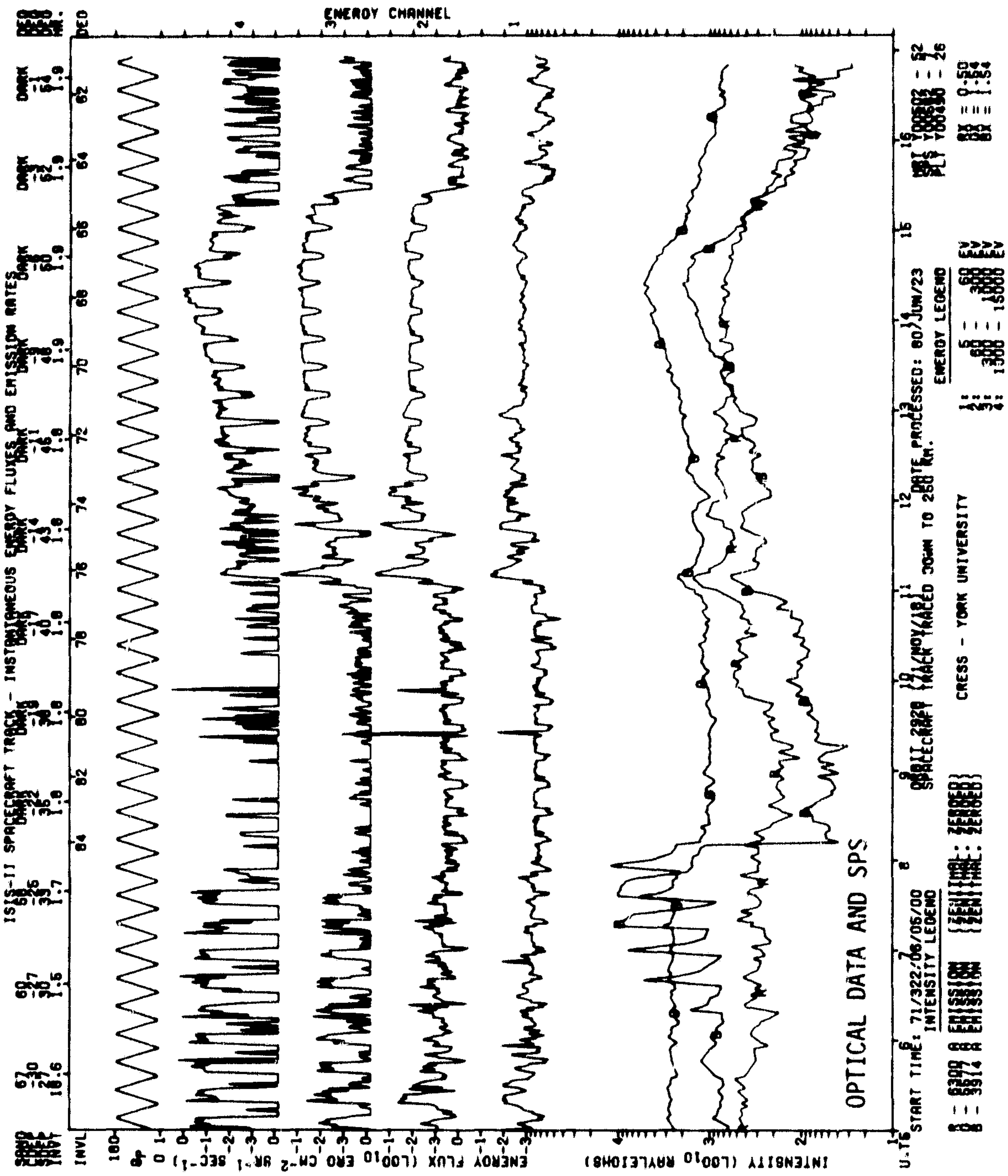

SET 3, FORMAT 1

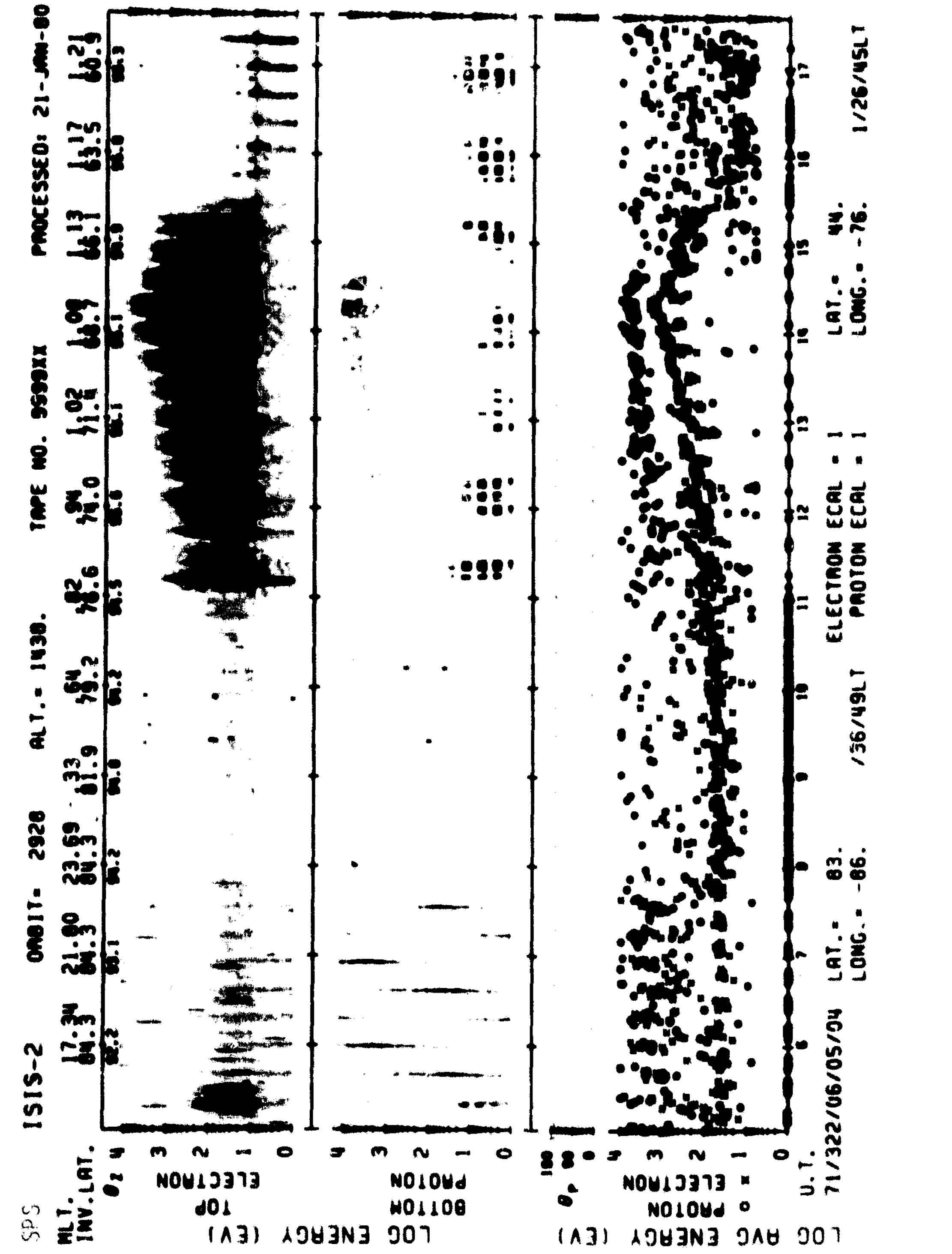

SET 3, FORMAT 6

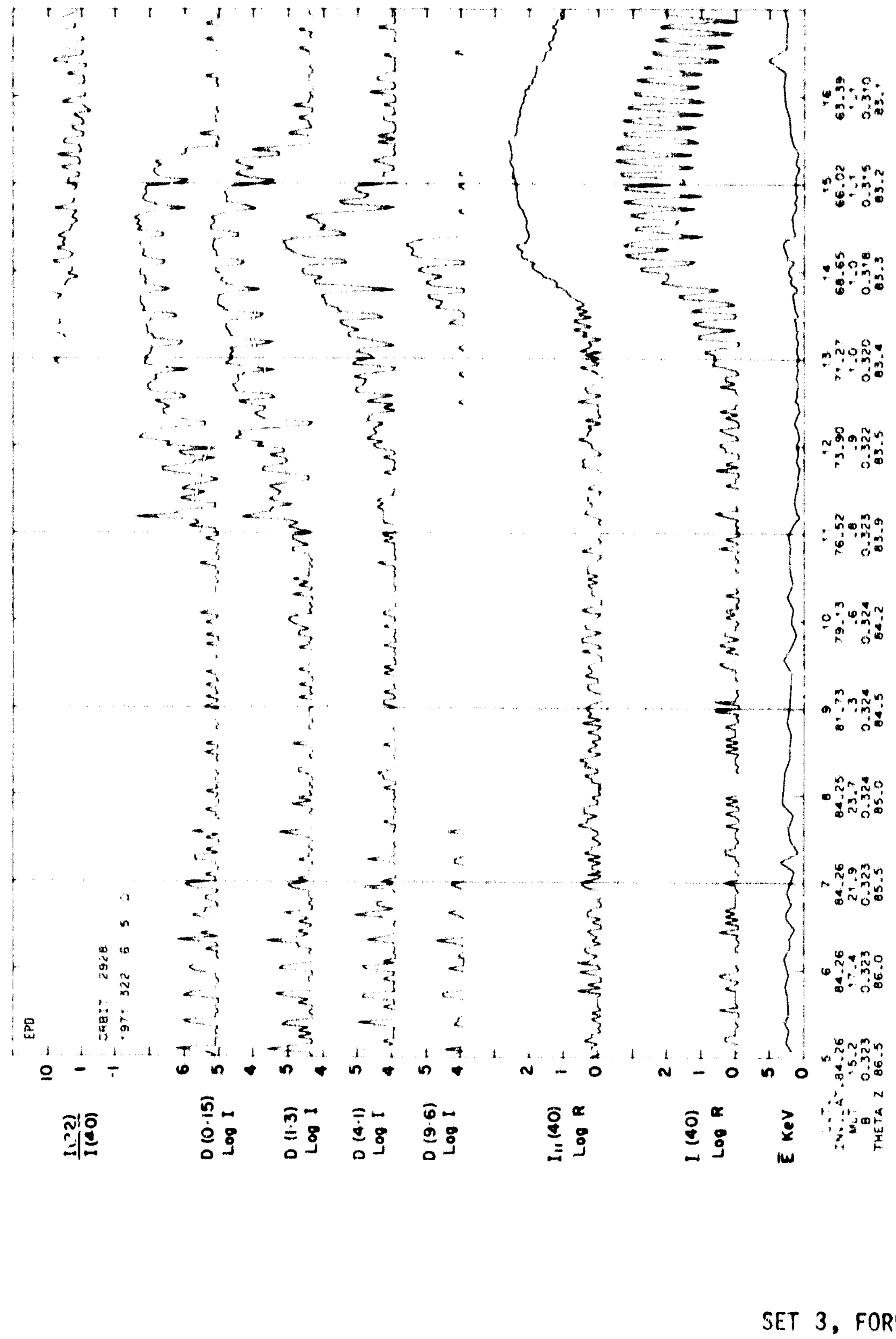

SET 3, FORMAT 3

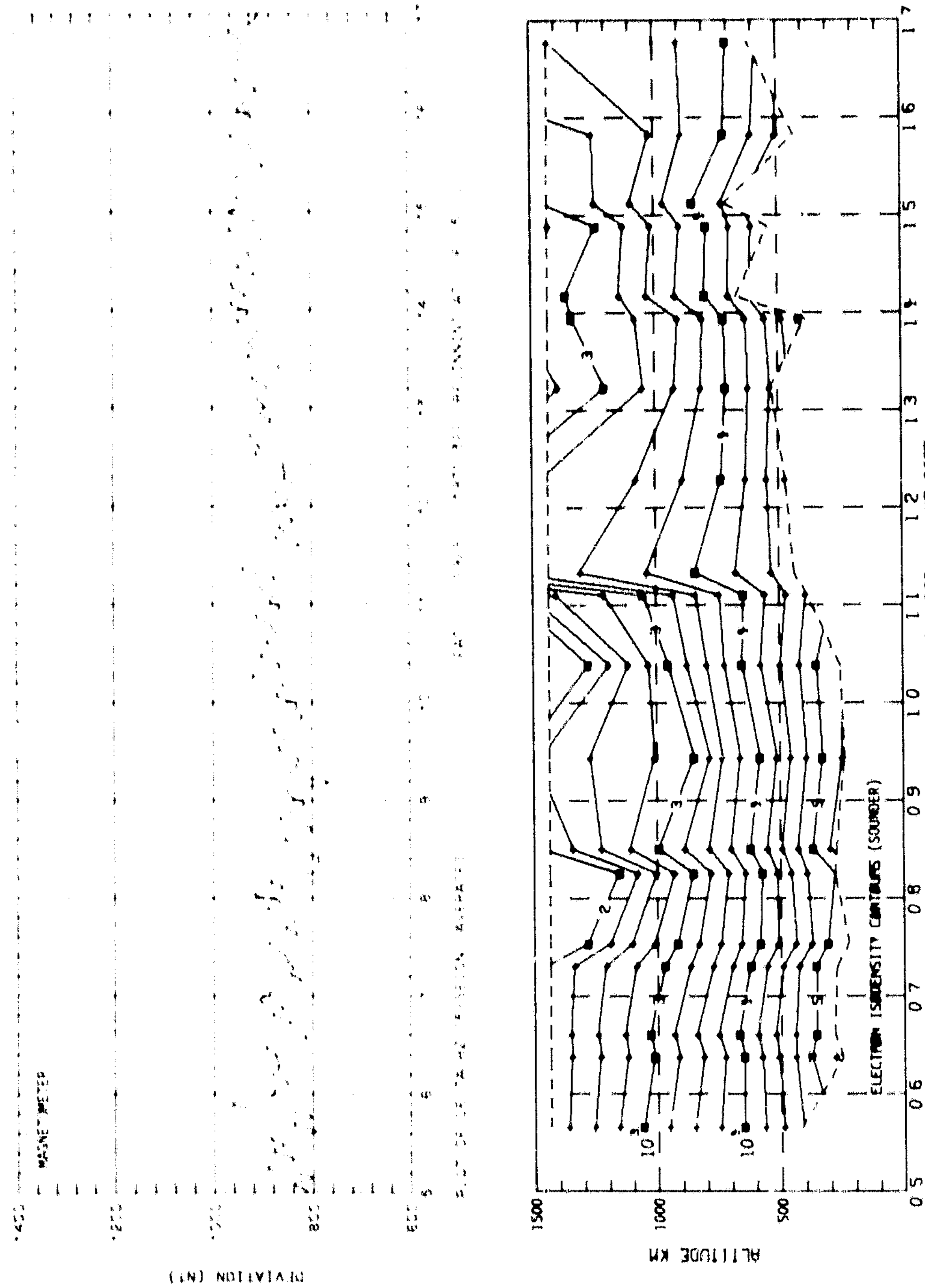

SET 3, FORMAT 2

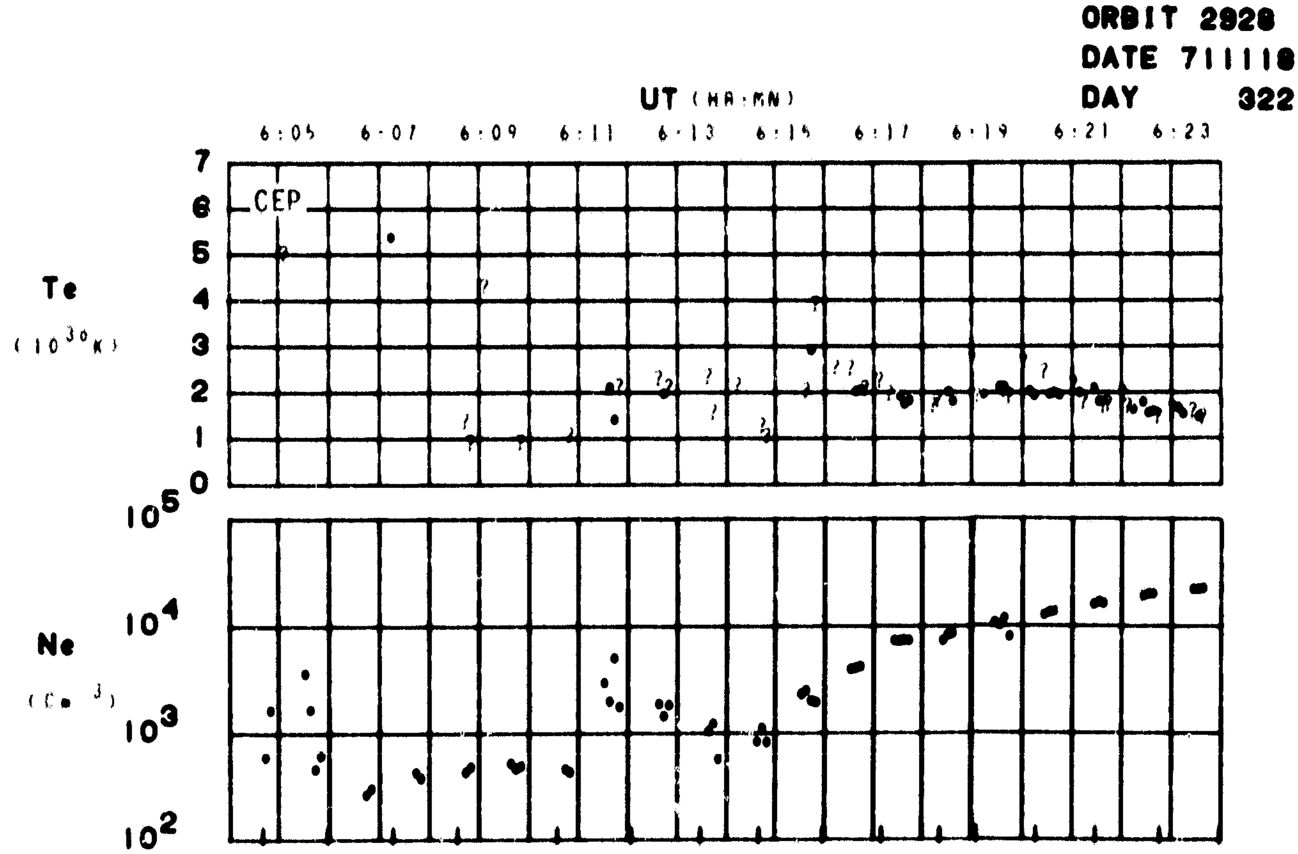

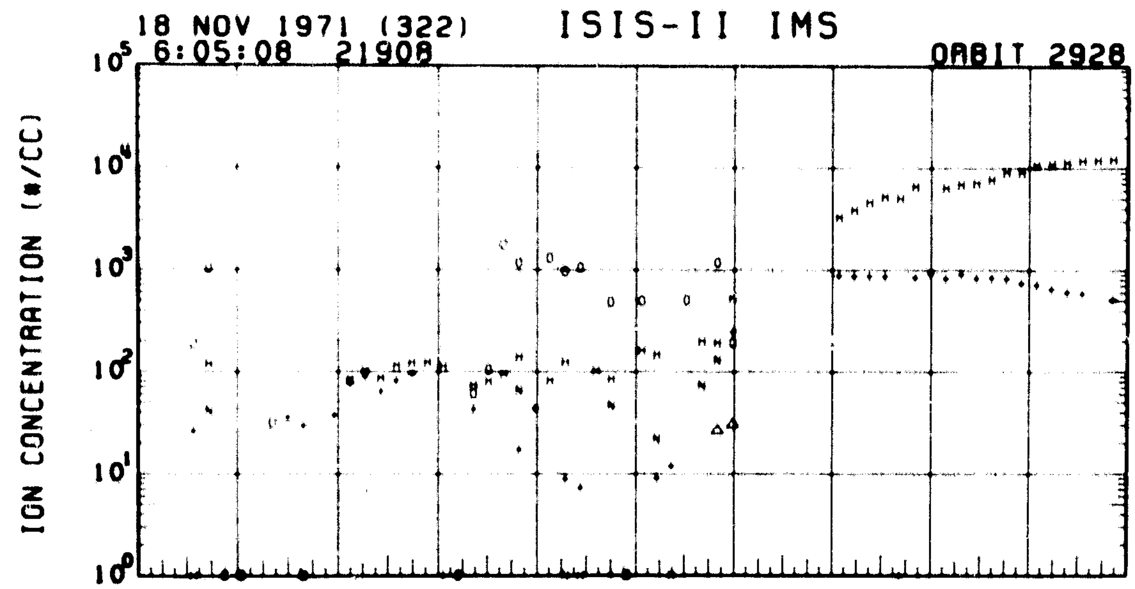

1 H		UT	6:06	6:08	6:10	6:12	6:14	6:18	6:20	6:22	6:24
4 +		LAST	0:52	1:09	1:16	1:21	1:23	1:27	1:29	1:30	1:31
8 △		MLT	17:29	23:43	0:39	0:56	1:05	1:14	1:17	1:20	1:22
14 N		DLAT	87	84	79	74	68	56	48	42	36
16 O		INVL	84	84	79	74	69	58	53	48	43
		GLAT	80	74	67	61	55	42	36	30	24
		GLNG	81	77	-76	-78	-75	-75	-76	-76	-76
		SZEN	119	125	130	136	141	150	154	157	158
		ALT	1438	1438	1437	1435	1433	1427	1424	1421	1417

SET 3, FORMAT 4

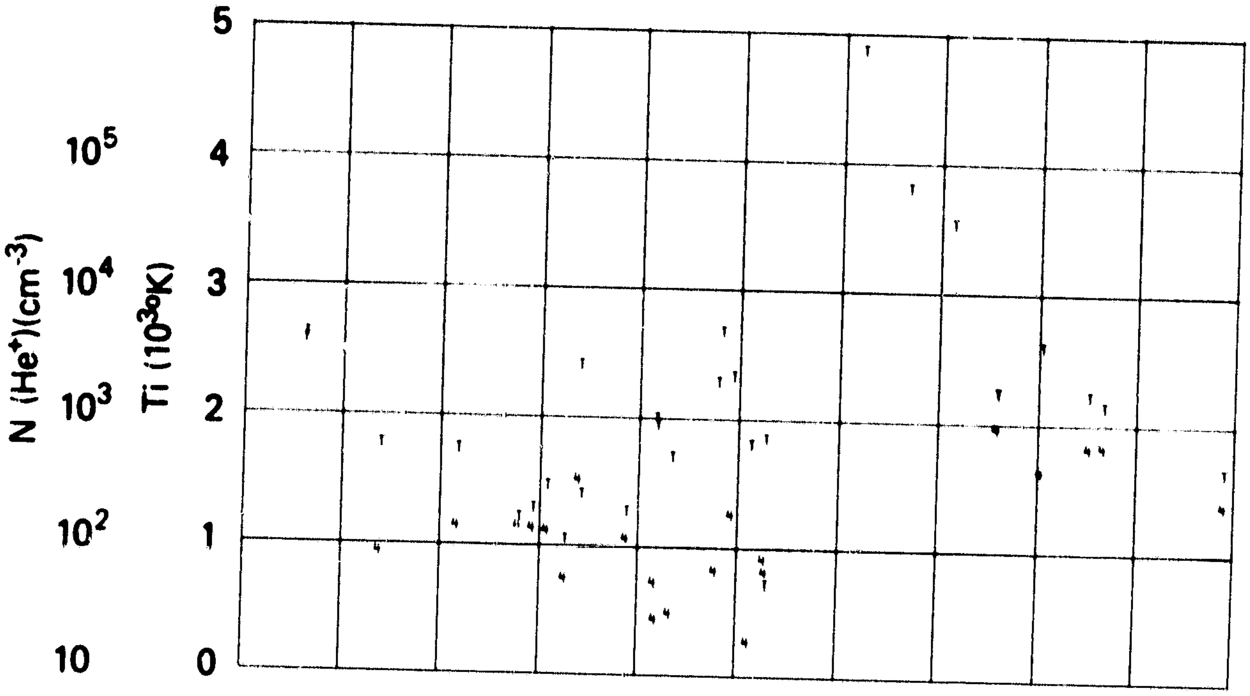

UT	6:06	6:08	6:10	6:12	6:14	6:18	6:20	6:22	6:24
LAST	0:52	1:09	1:16	1:21	1:23	1:27	1:29	1:30	1:31
MLT	17:29	23:43	0:39	0:56	1:05	1:14	1:17	1:20	1:22
OLAT	87	84	79	74	[illegible]	56	49	42	36
INVL	[illegible]	84	79	74	69	58	53	48	43
GLAT	80	74	67	61	55	42	36	30	23
GLNG	-81	-77	-76	-76	-75	-75	-76	-76	-76
SZEN	119	125	130	136	141	150	154	157	158
ALT	1438	1438	1437	1435	1433	1427	1424	1421	1417

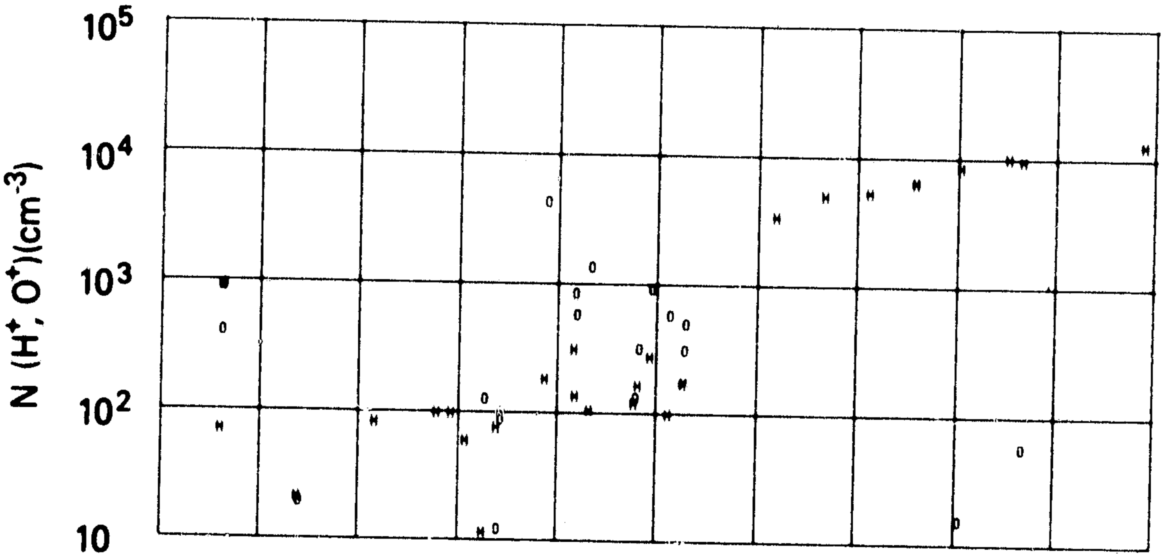

SET 3, FORMAT 5

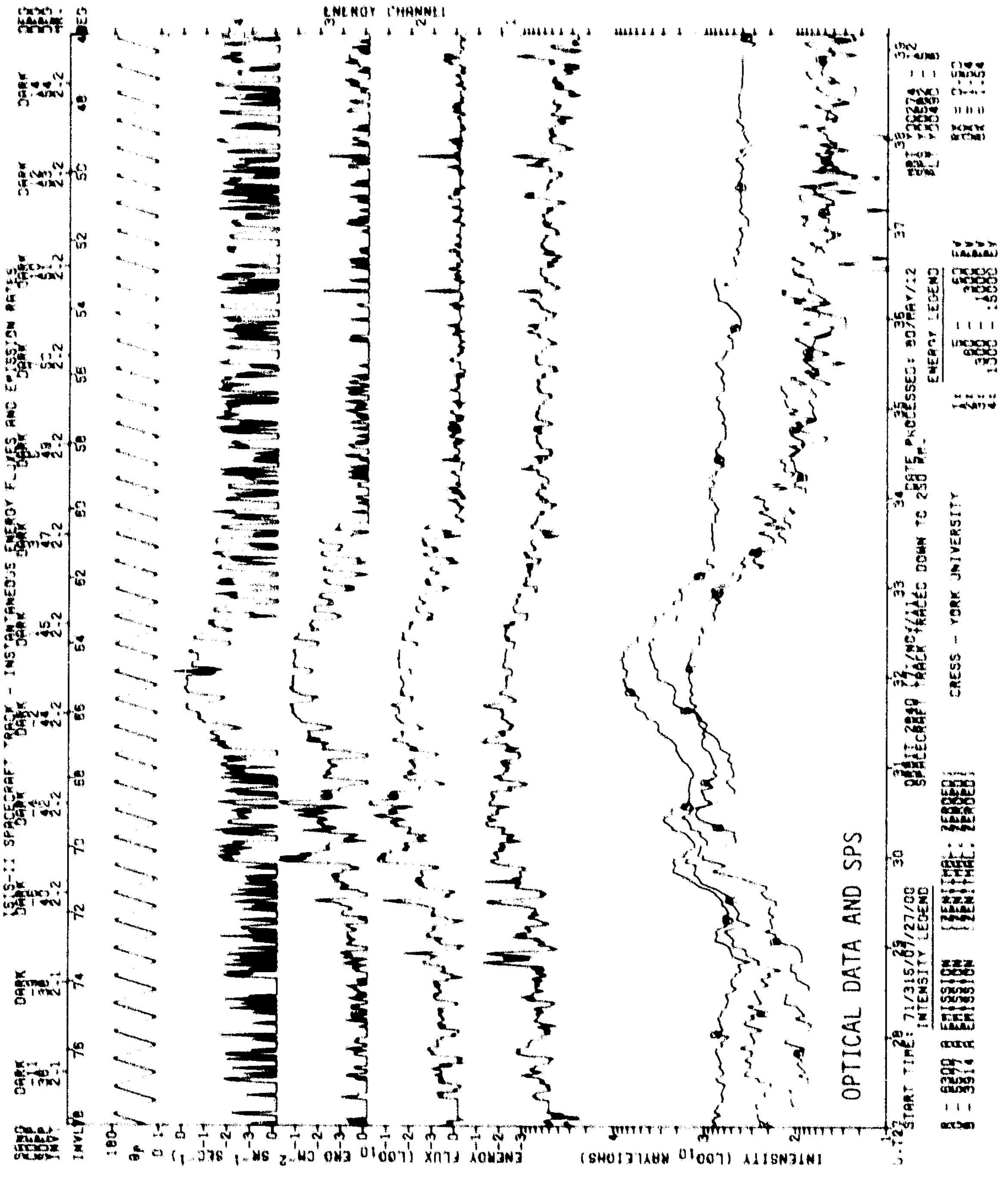

SET 4, FORMAT 1

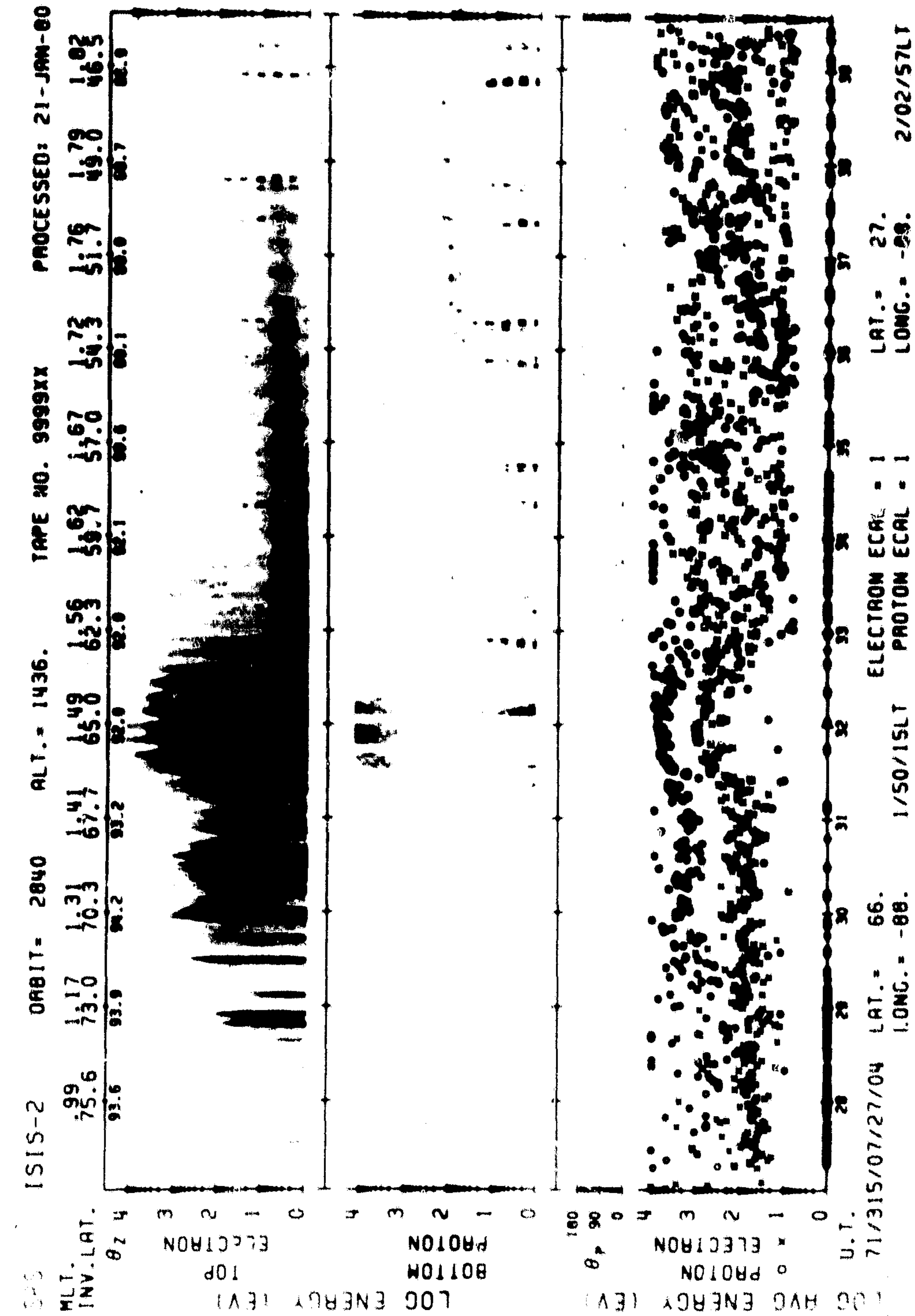

SET 4, FORMAT 6

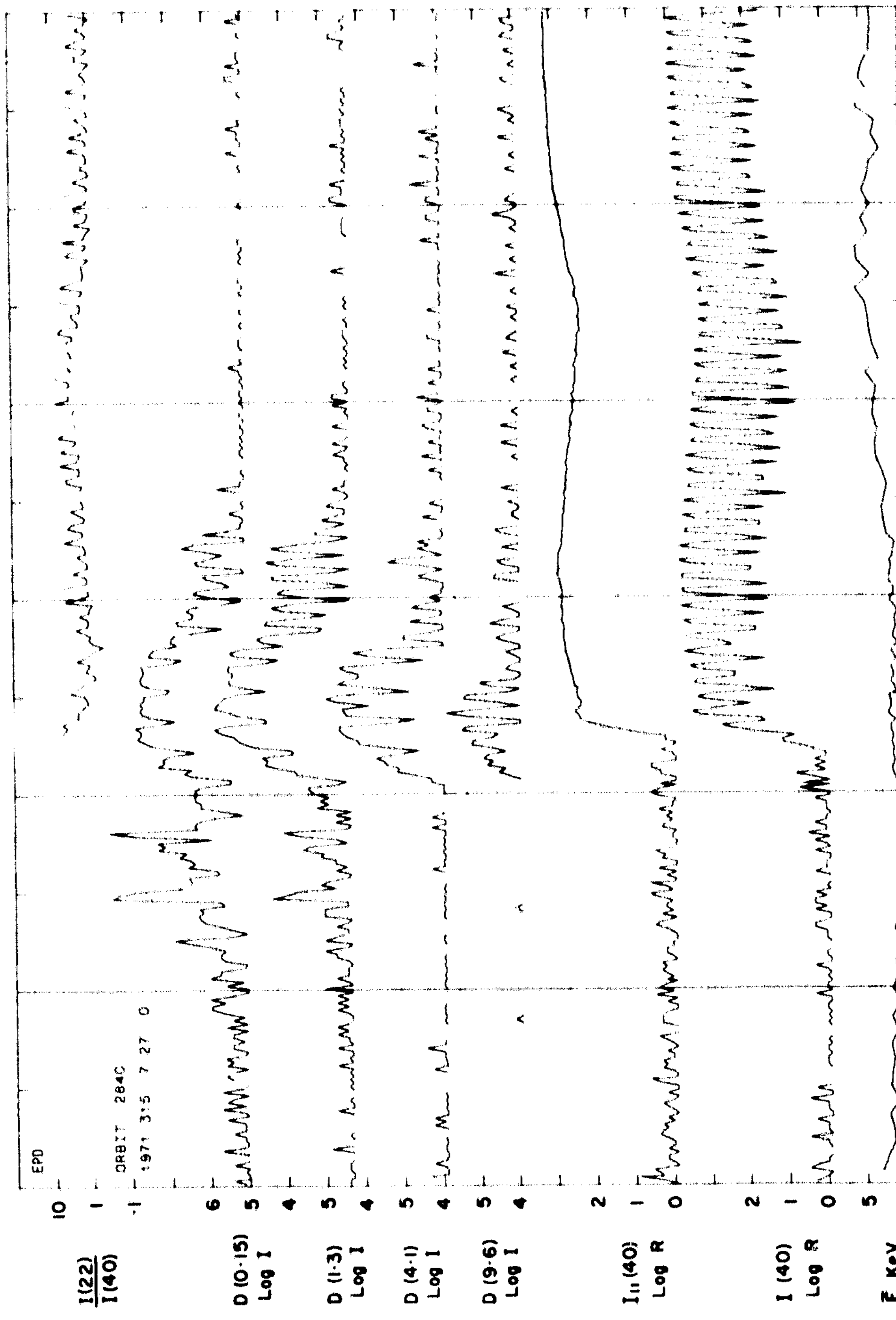

SET 4, FORMAT 3

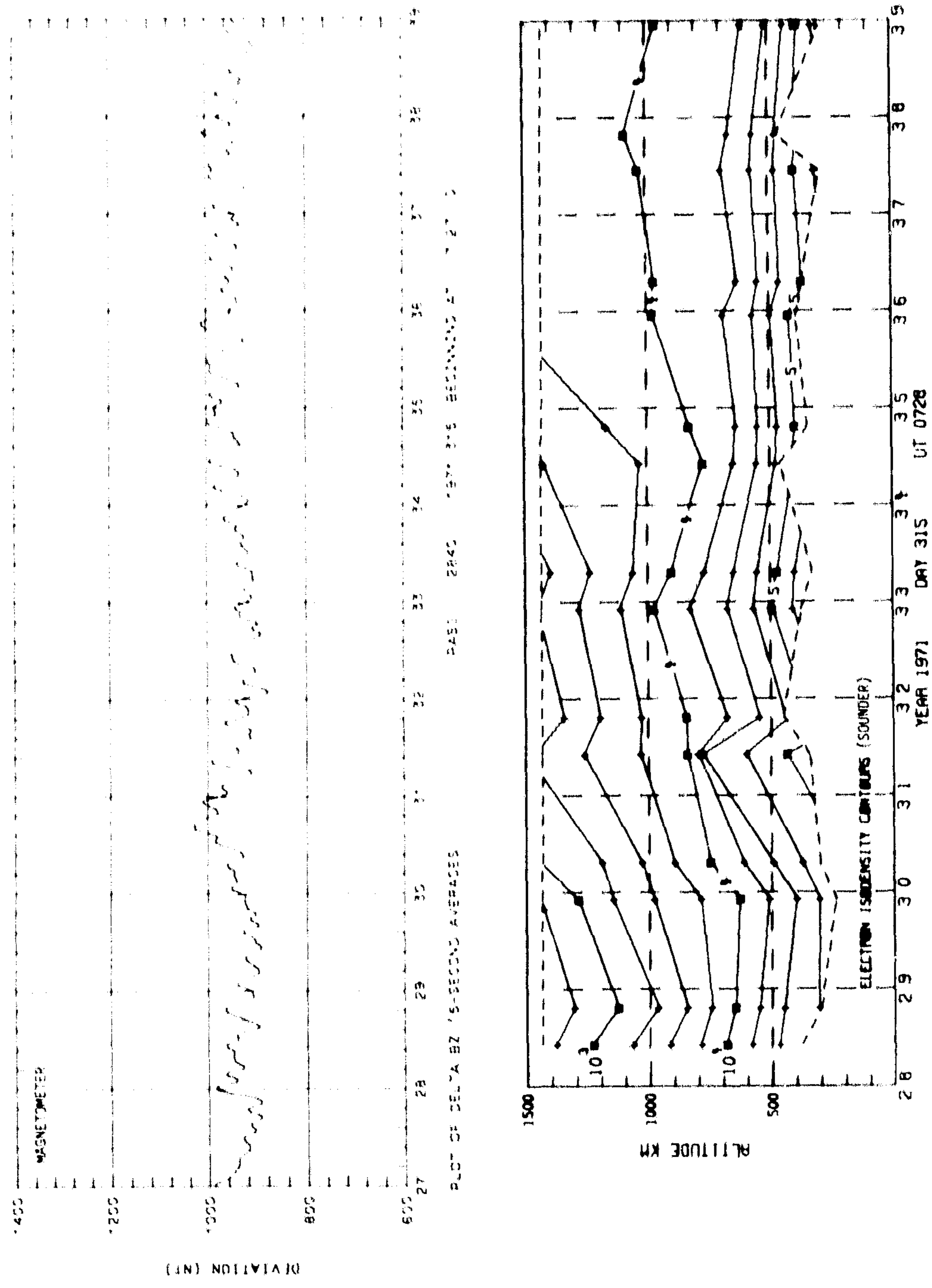

SET 4, FORMAT 2

ORBIT 2840
DATE 711111
DAY 315

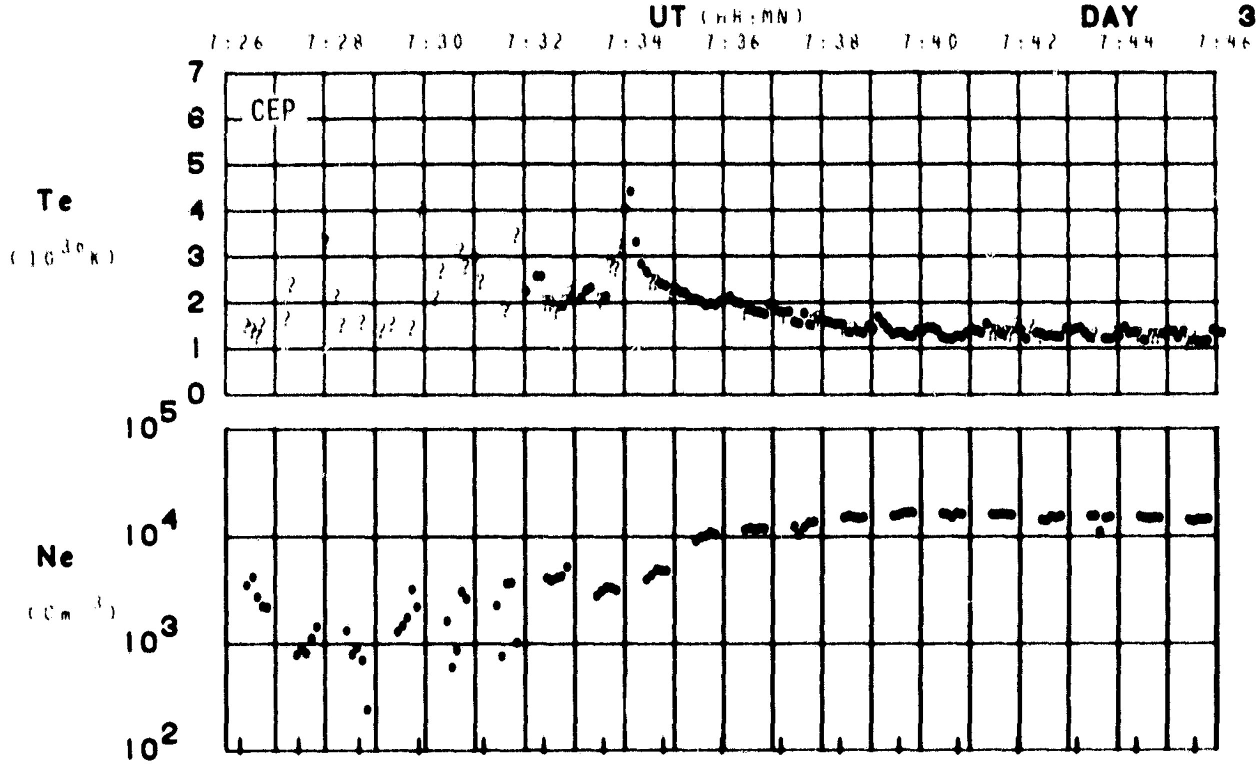

LAT	68	64	61	57	53	49	45	41	38	34	30	26	23	19	15	11	7
LONG	-88	-88	-87	-87	-87	-87	-87	-87	-87	-87	-87	-88	-88	-88	-88	-88	-88
LT	1:48	1:51	1:53	1:55	1:56	1:58	1:59	2:00	2:01	2:01	2:02	2:03	2:03	2:04	2:04	2:05	2:05
DIP	85	84	82	80	78	76	73	71	68	65	61	57	53	49	44	39	33
DIPLAT	82	79	75	72	68	64	60	56	51	47	43	39	35	30	26	22	19
L	32.5	19.5	12.8	9.1	6.6	5.2	4.2	3.5	2.9	2.5	2.2	2.0	1.8	1.7	1.5	1.5	1.4
INVLAT	79	76	73	70	67	63	60	57	54	51	48	44	41	39	36	33	31
ZA	126	128	131	134	137	140	142	144	146	147	149	150	150	150	150	149	147

SET 4, FORMAT 4

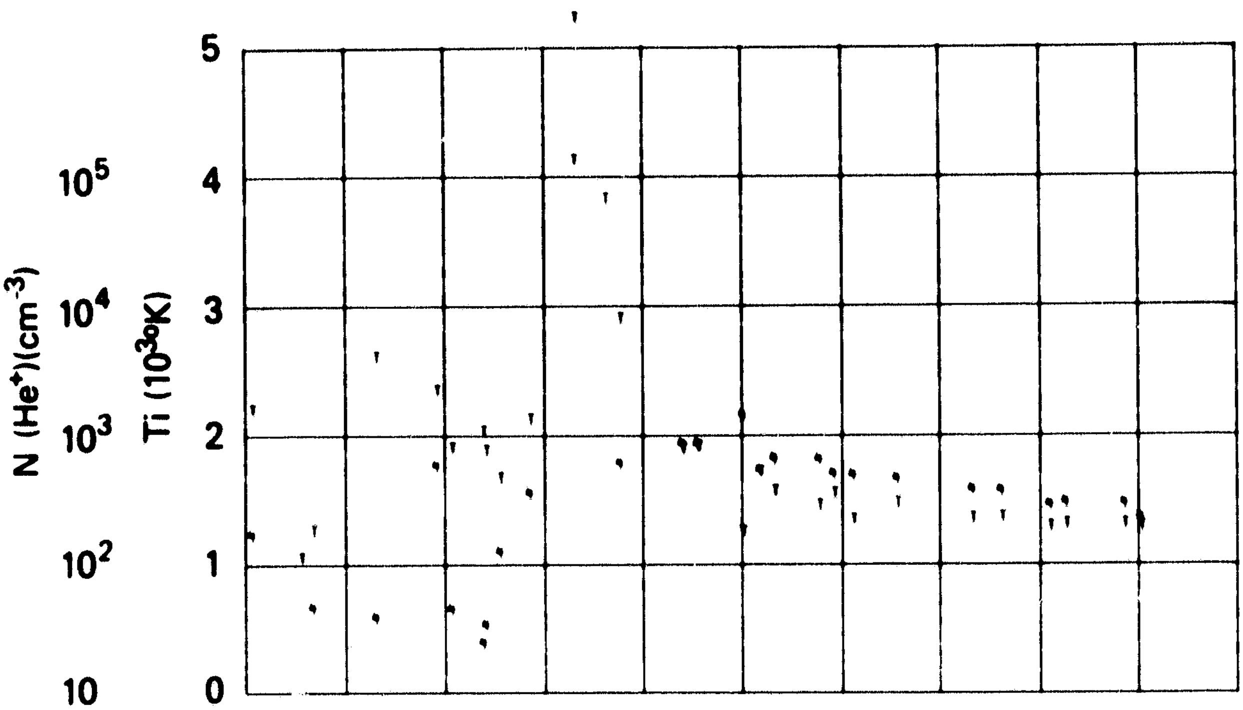

UT	07:28	07:30	07:32	07:34	07:36	07:38	07:40	07:42	07:44
LAST									
MLT									
DLAT									
INVL	76	71	65	60	55	49	44	40	35
GLAT	63	57	51	45	38	32	26	20	13
GLNG	-88	-88	-88	-88	-88	-88	-88	-88	-89
SZEN									
ALT	1435	1434	1433	1431	1430	1427	1424	1422	1419

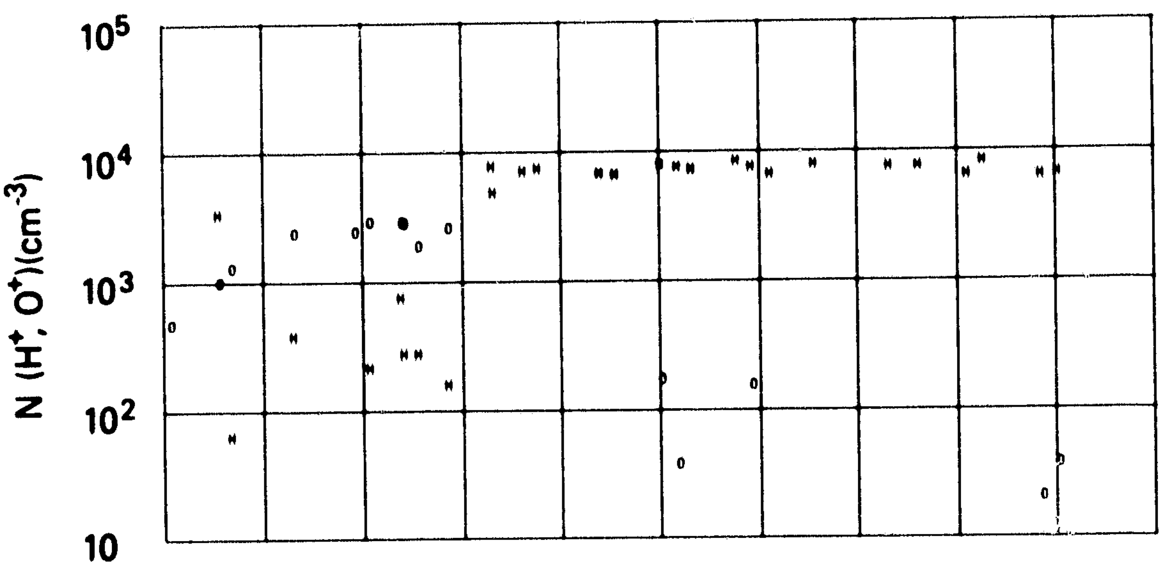

SET 4, FORMAT 5

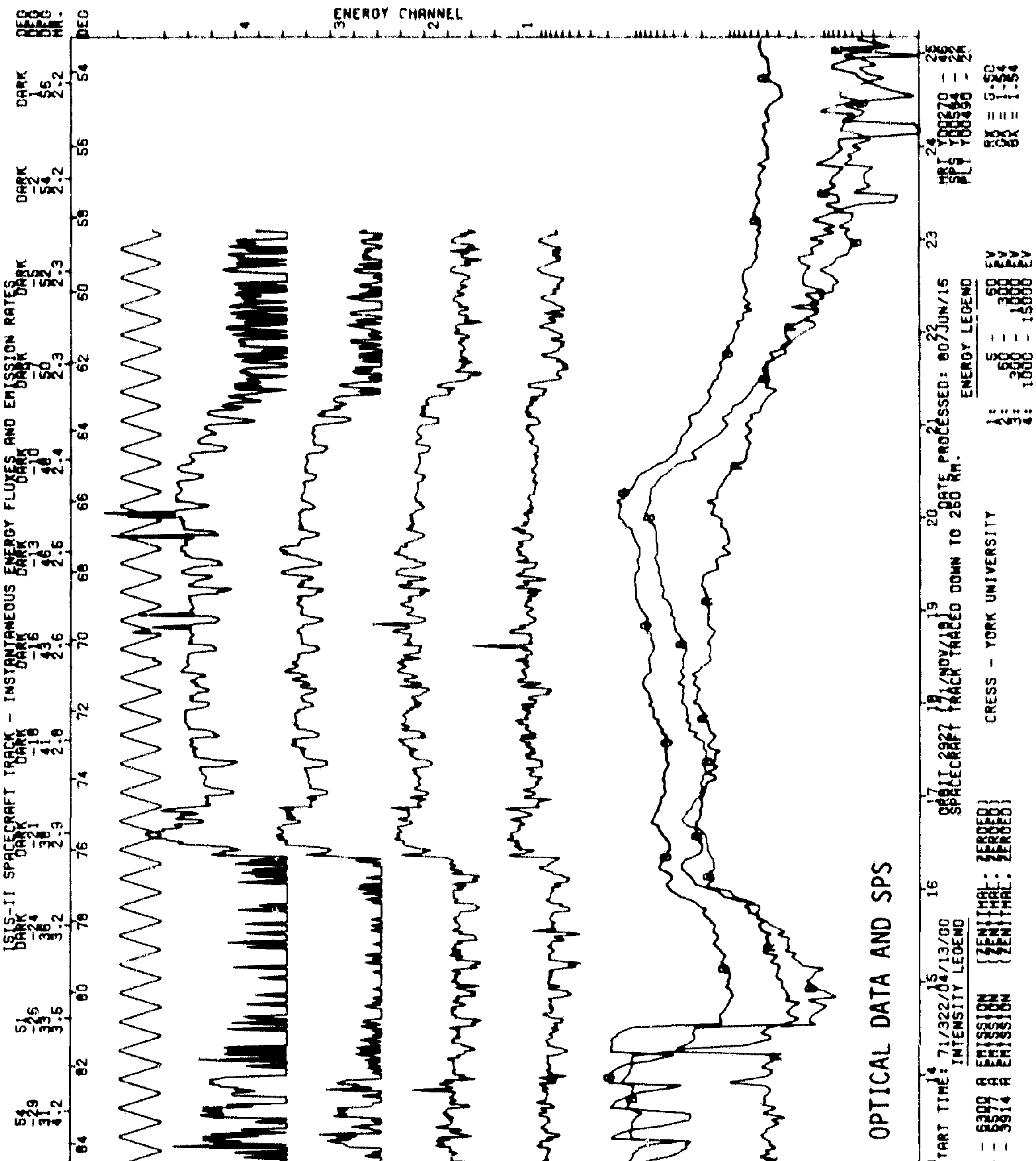

SET 5, FORMAT 1

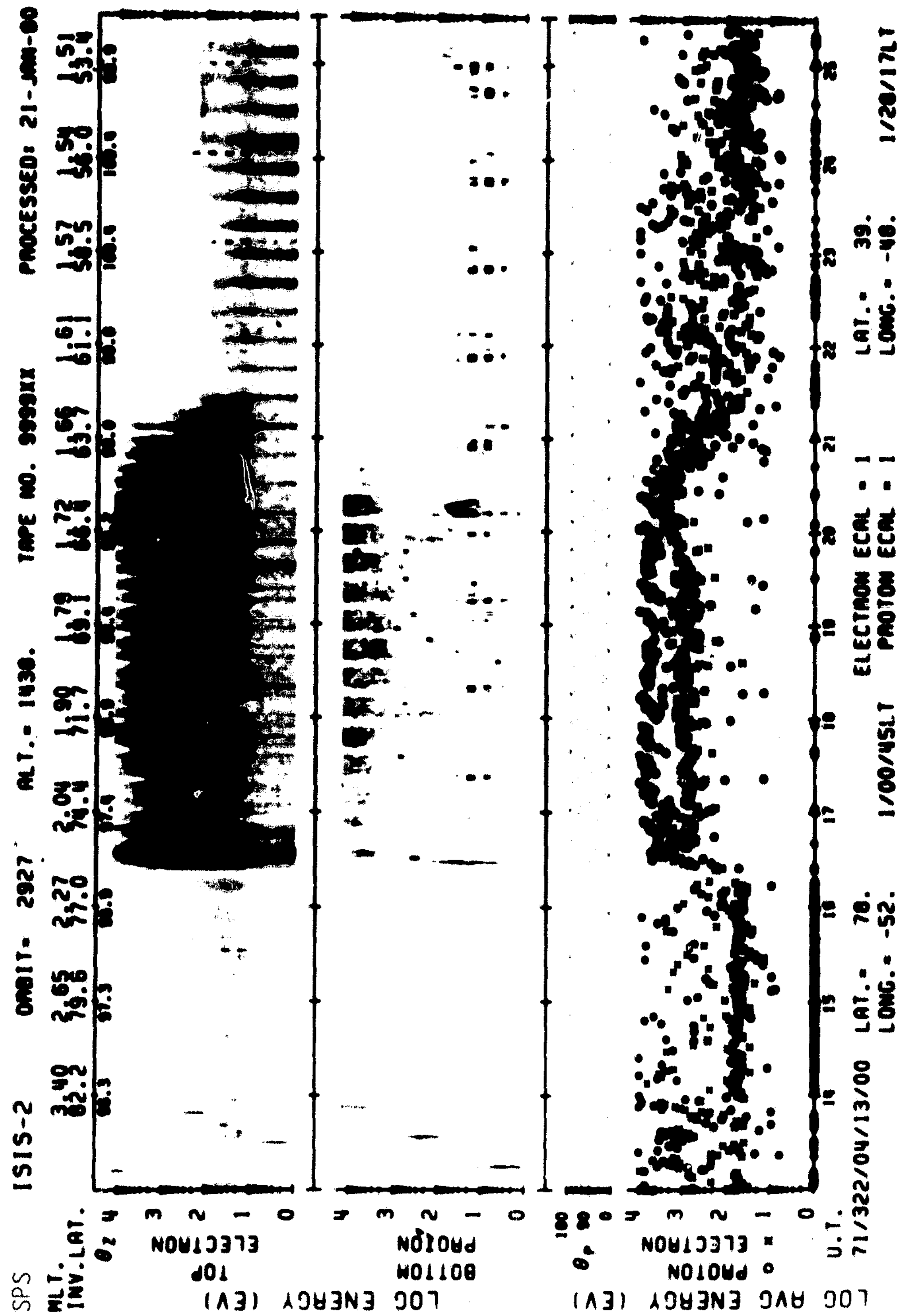

SET 5, FORMAT 6

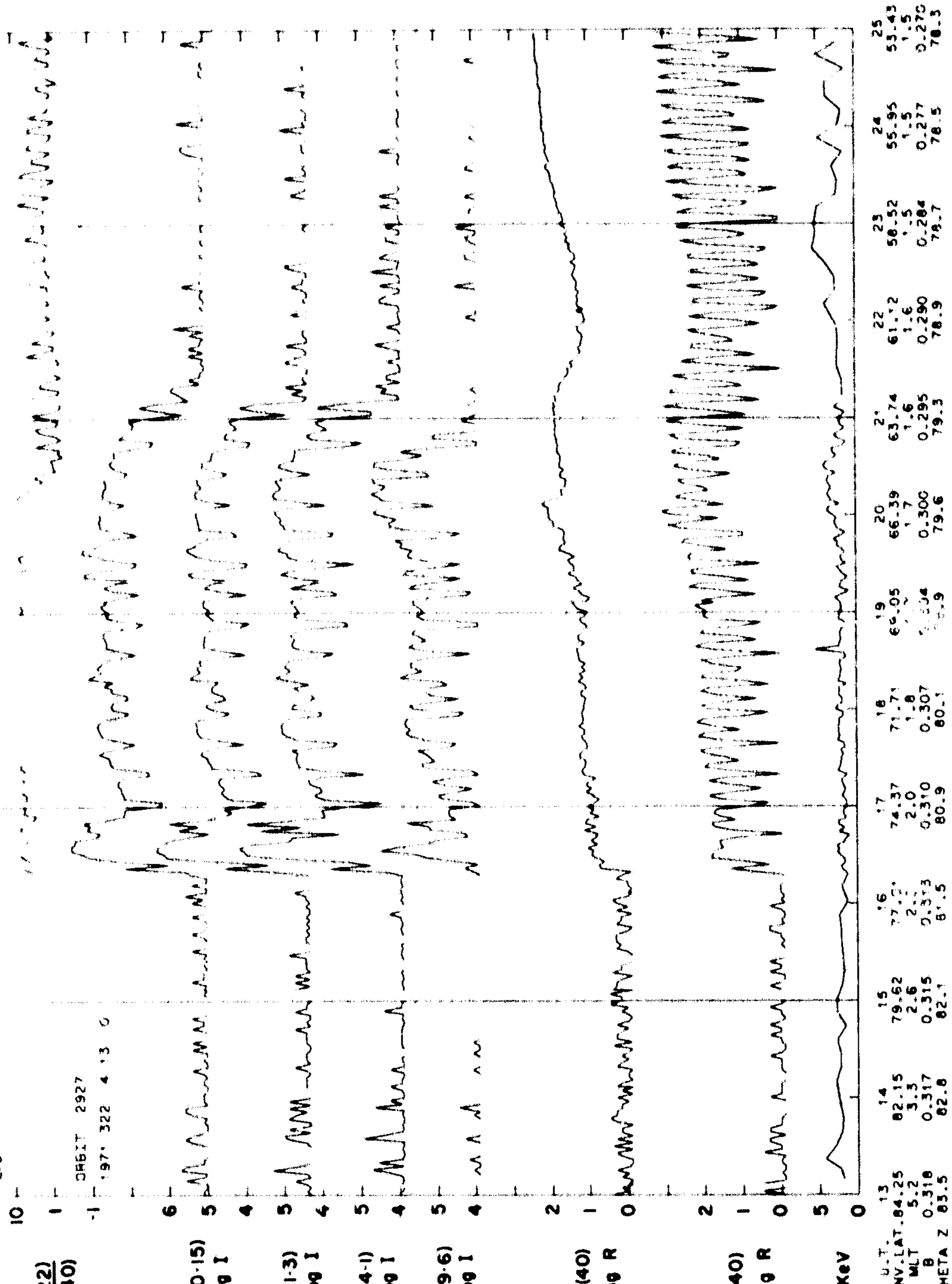

SET 5, FORMAT 3

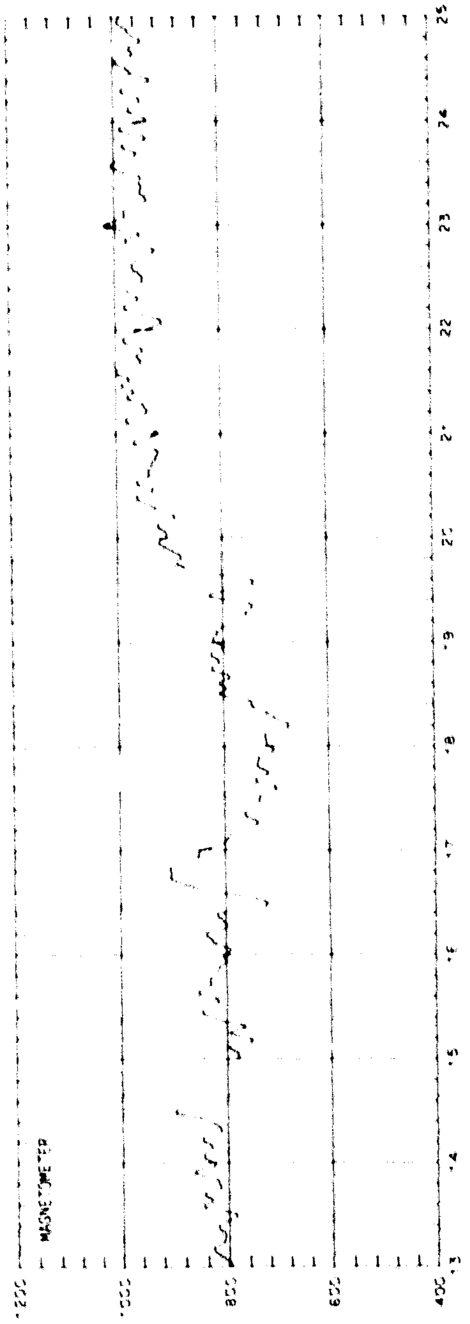

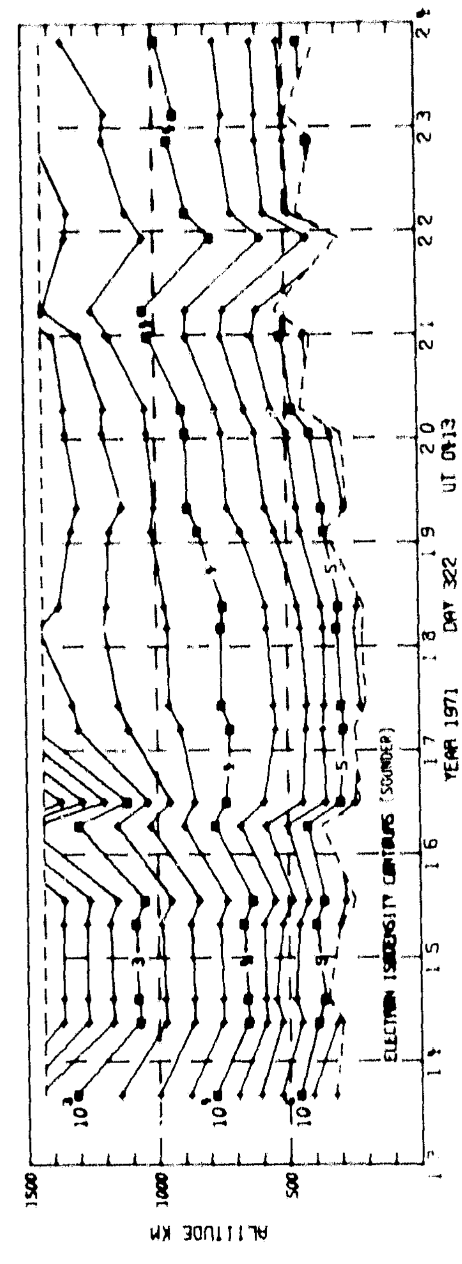

SET 5, FORMAT 2

ORBIT 2927
DATE 711118
DAY 322

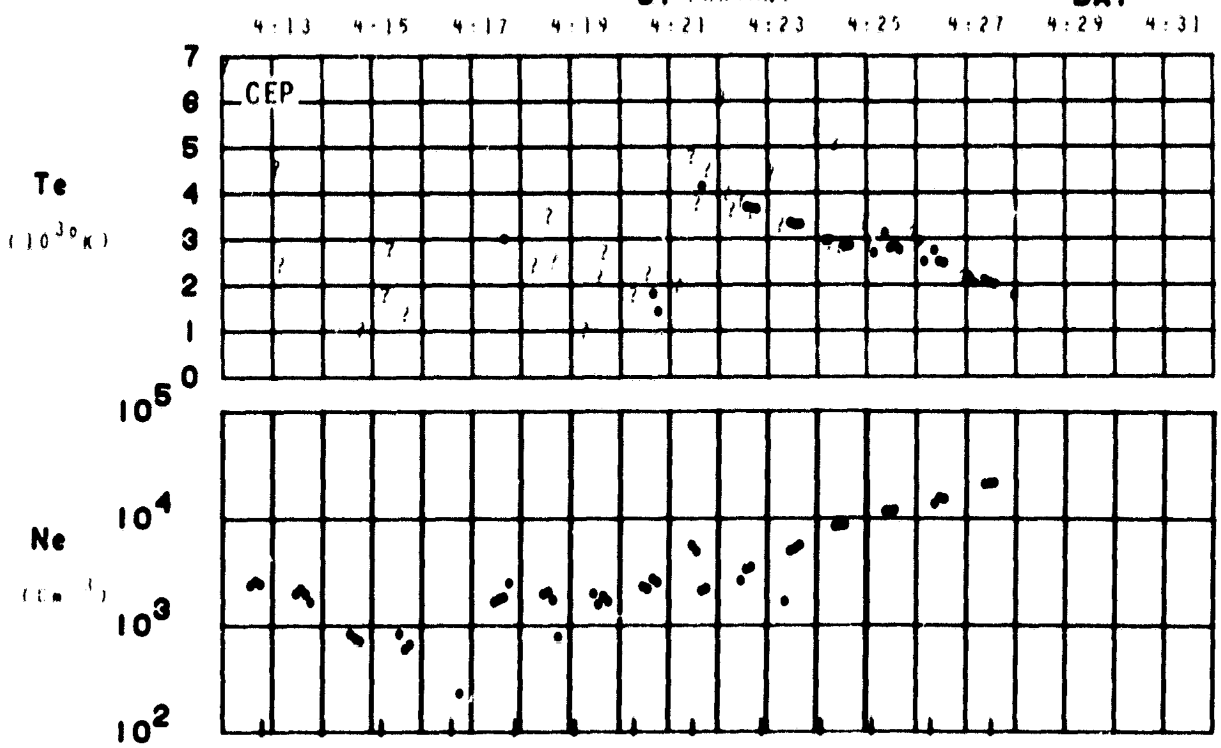

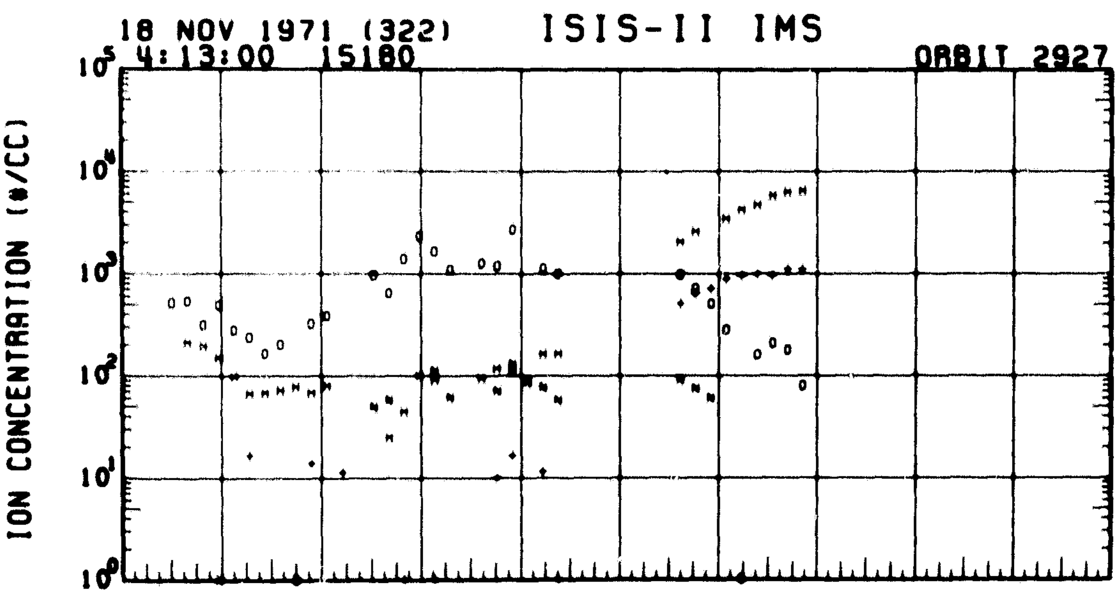

		UT	4:14	4:16	4:18	4:20	4:24
1 - H		LAST	1:07	1:18	1:20	1:23	1:27
4 - +		MLT	3:25	2:16	1:54	1:43	1:32
8 - Δ		DLAT	78	73	68	62	50
14 - N		INVL	82	77	72	66	56
16 - O		GLAT	75	68	62	56	43
		GLNG	-49	-48	-47	-47	-47
		SZEN	124	128	135	140	150
		ALT	1438	1437	1435	1433	1428

SET 5, FORMAT 4

RPA 711118

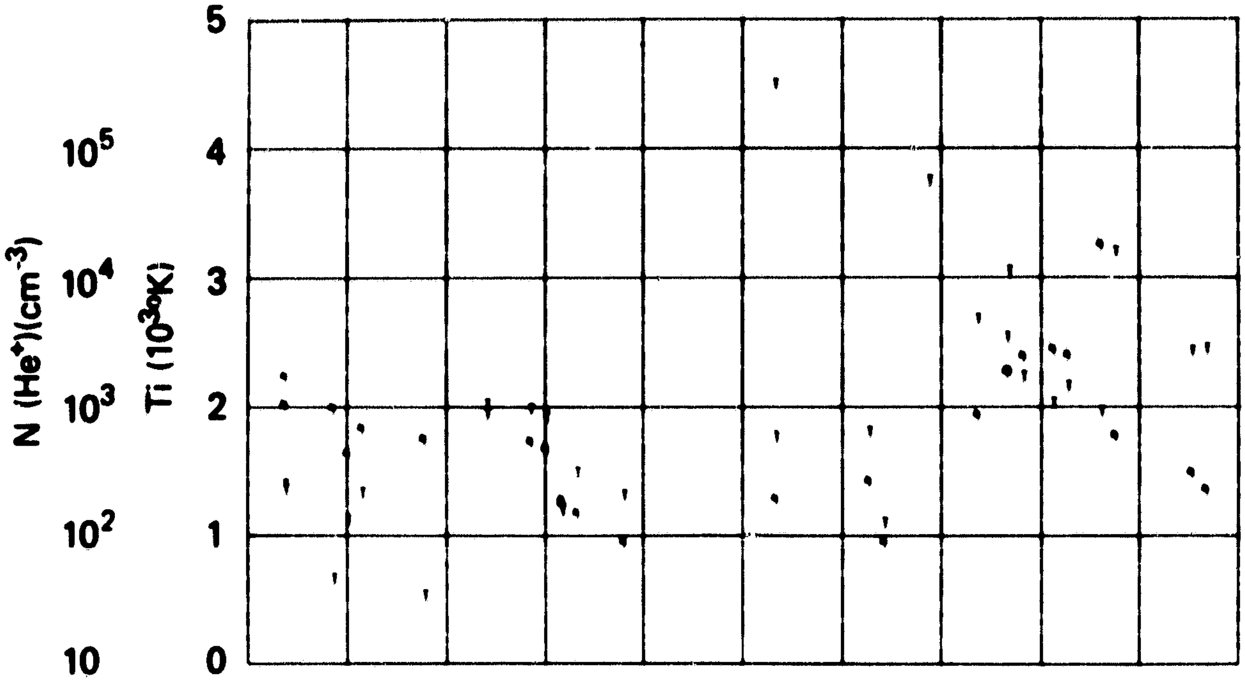

UT	4:14	4:16	4:18	4:20	4:24
LAST	1:07	1:16	1:20	1:23	1:27
MLT	3:25	2:16	1:54	1:43	1:32
MLAT	70	73	80	82	50
INVL	82	77	72	66	56
GLAT	75	80	82	58	43
GLNG	-48	-48	-47	-47	-47
SZEN	124	128	135	140	150
ALT	1438	1437	1435	1433	1428

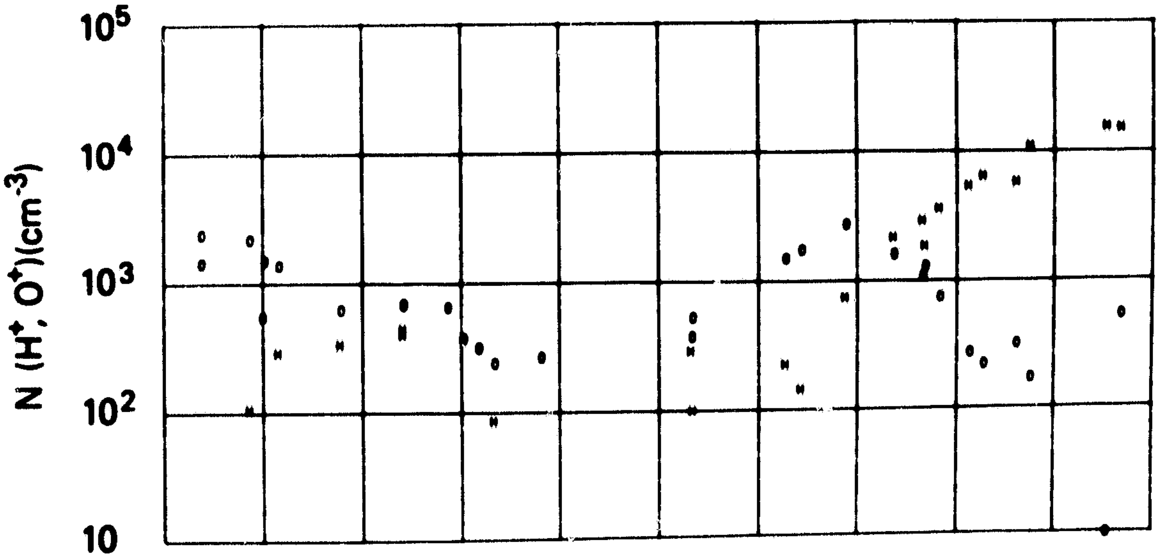

SET 5, FORMAT 5

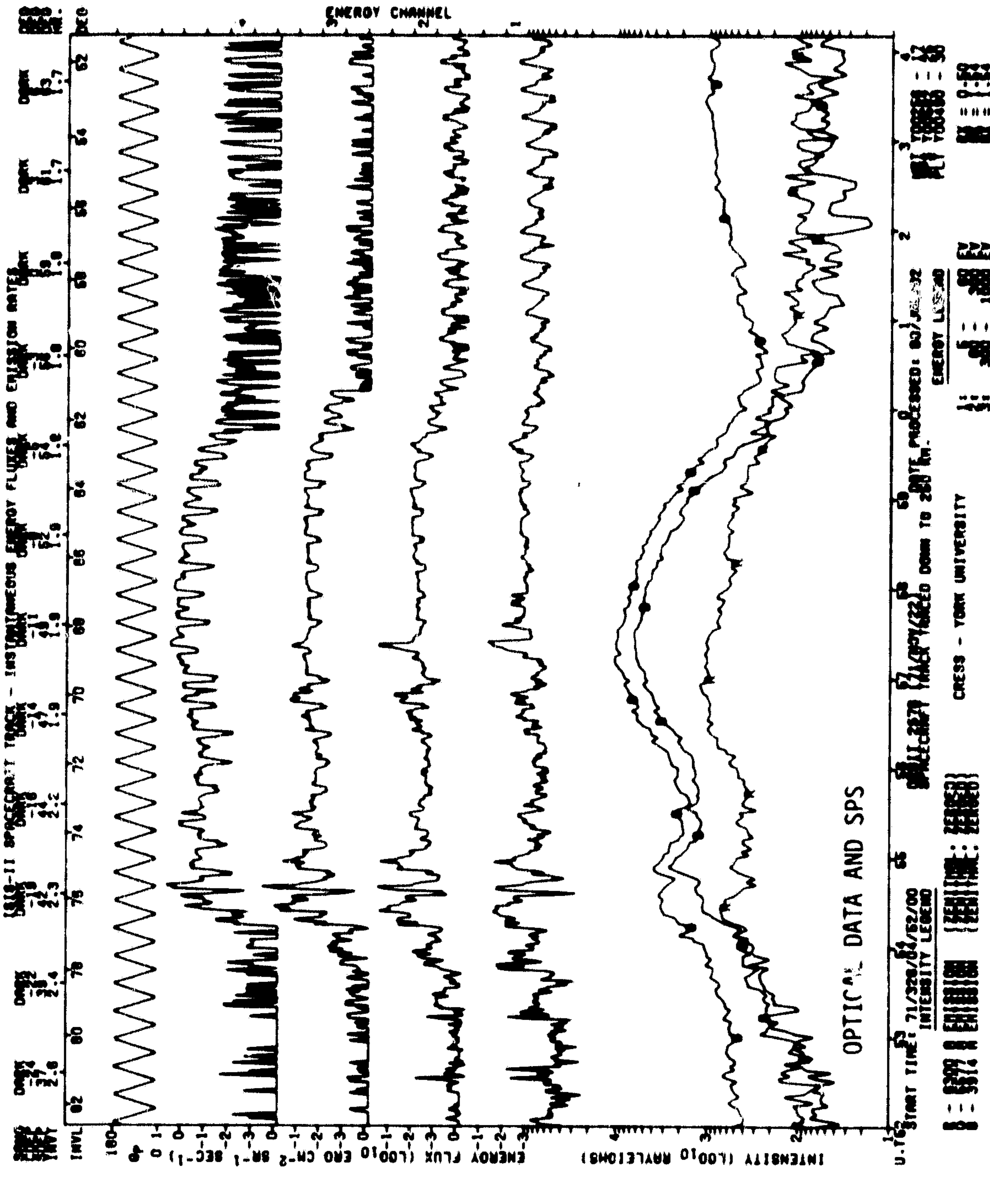

SET 6, FORMAT 1

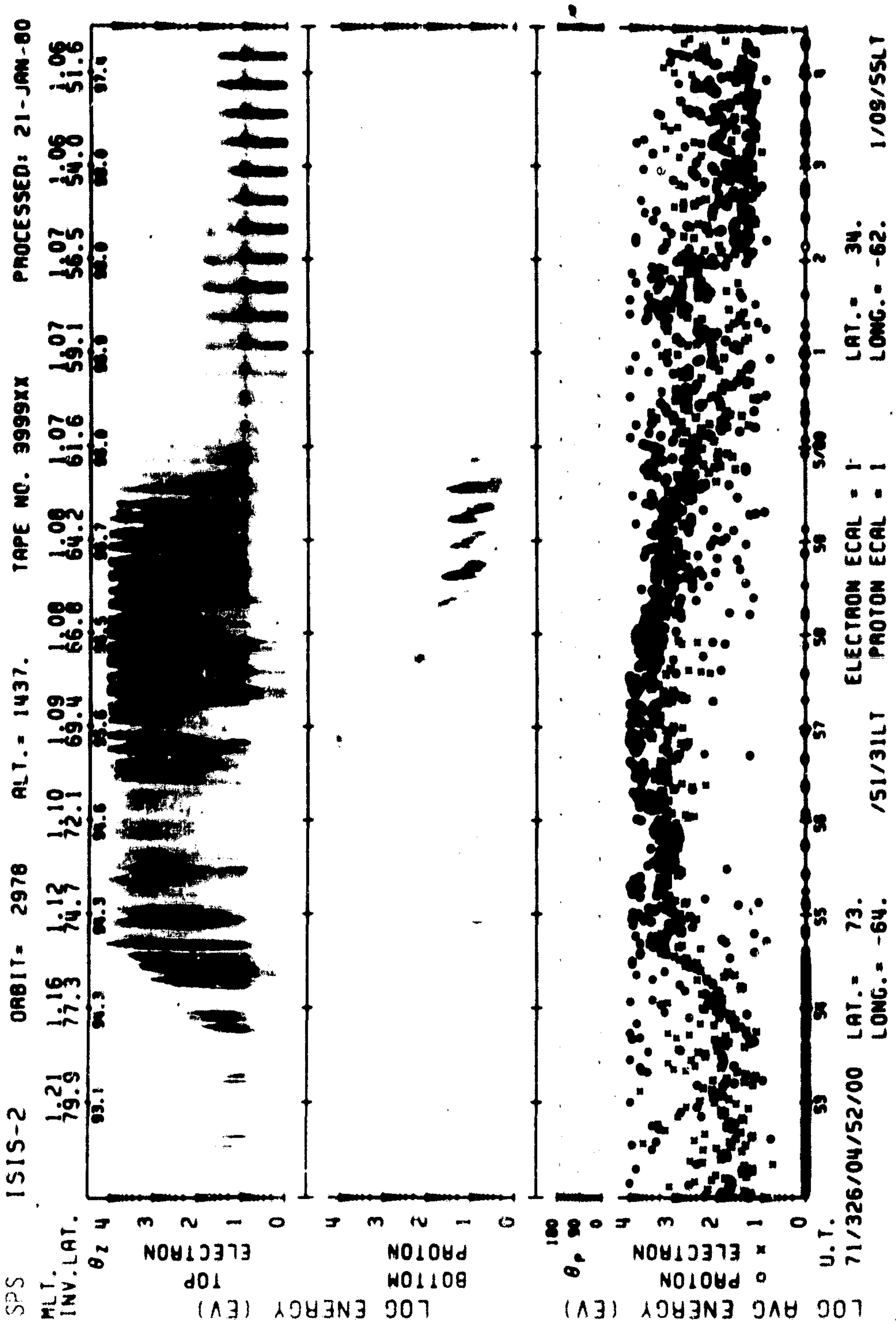

SET 6, FORMAT 6

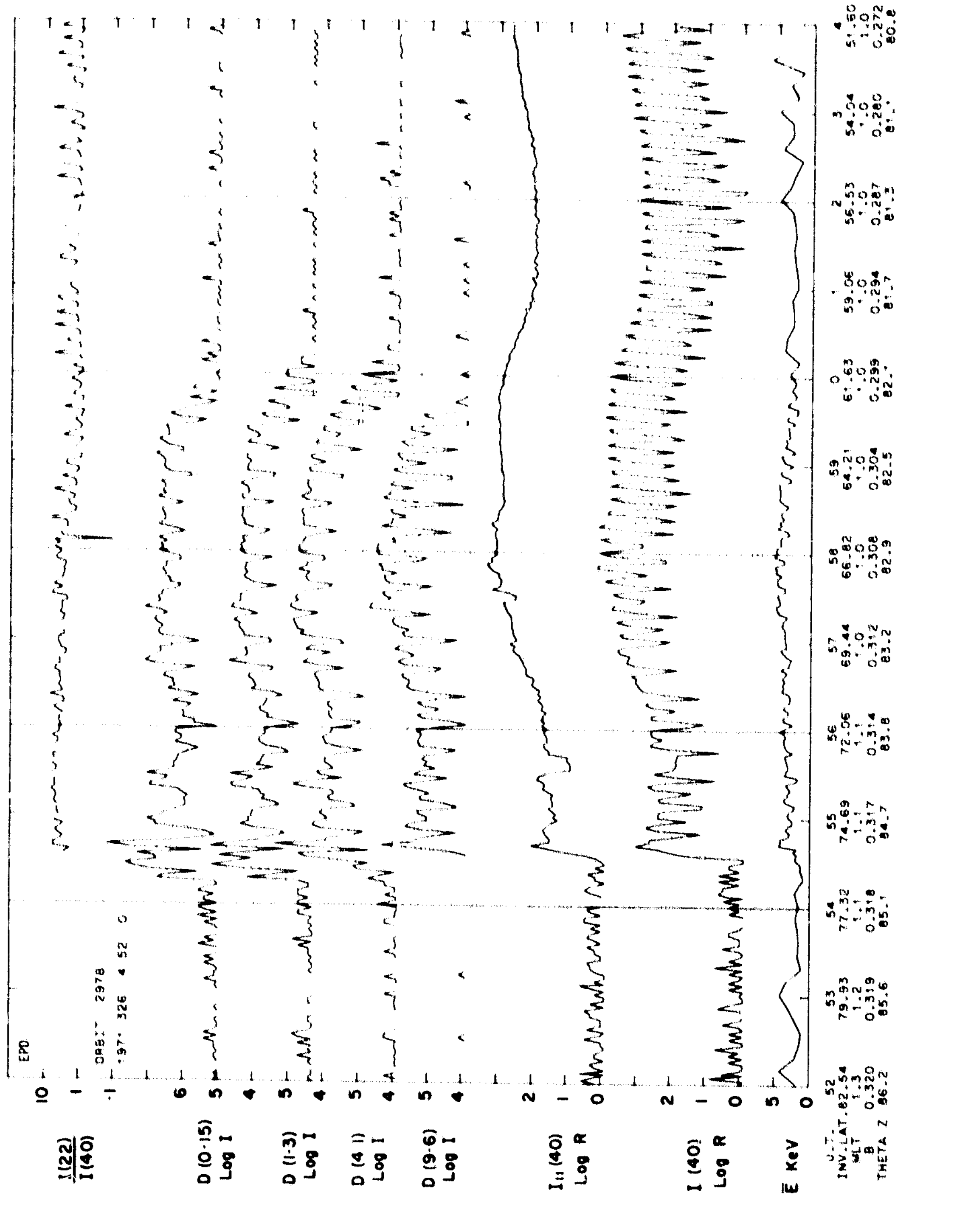

SET 6, FORMAT 3

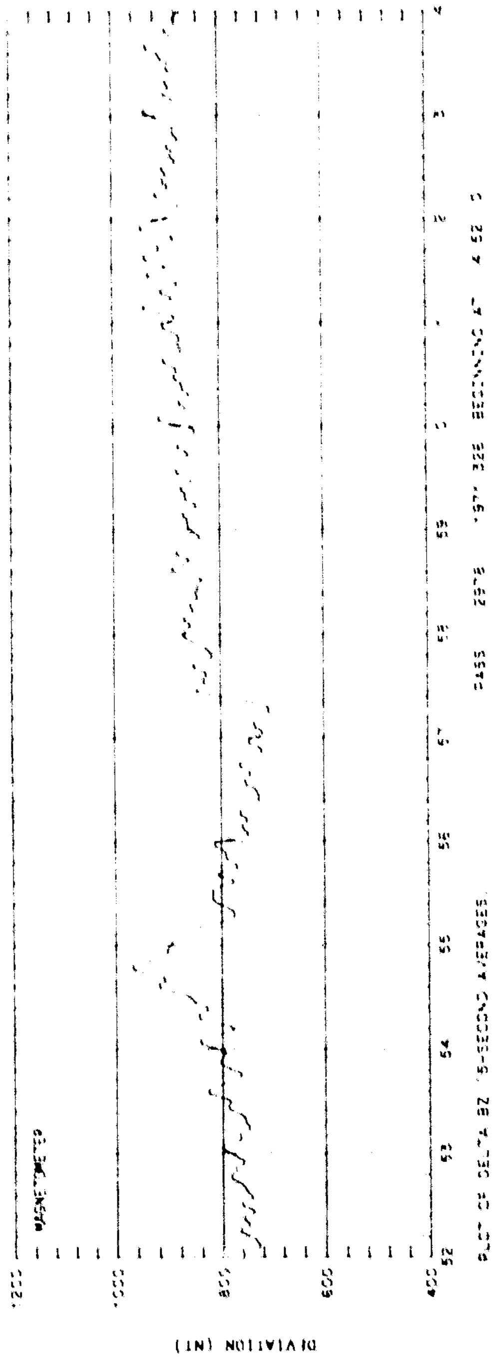

SET 6, FORMAT 2

ORBIT 2978
DATE 711122
DAY 326

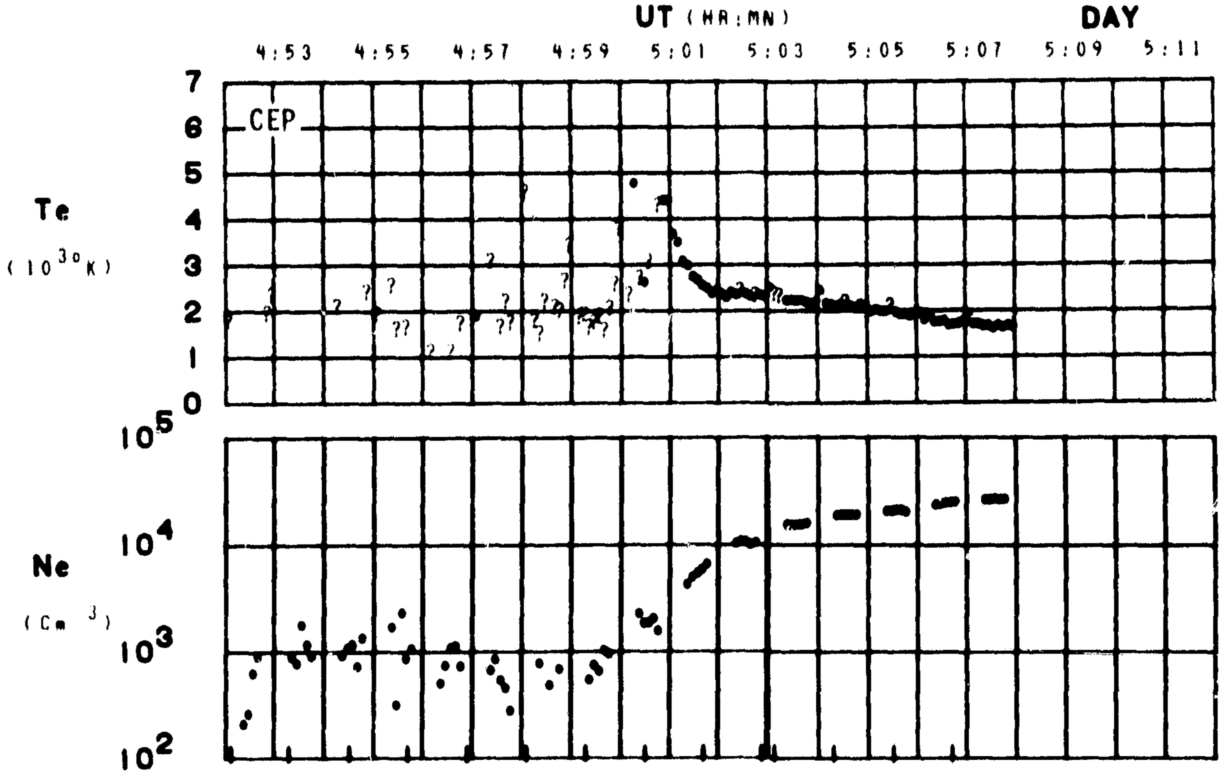

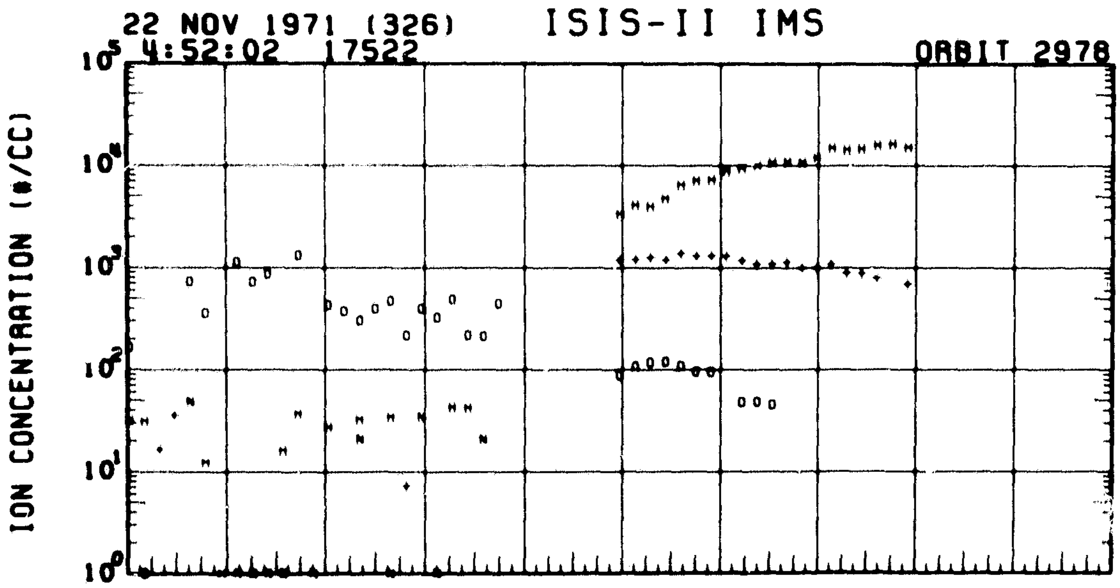

1 - H	UT	4:54	4:56	4:58	5:02	5:04	5:06
4 - +	LAST	0:58	1:02	1:05	1:08	1:10	1:11
8 - Δ	MLT	1:09	1:06	1:05	1:04	1:04	1:04
14 - N	DLAT	75	70	64	52	46	40
16 - O	INVL	77	72	67	57	52	47
	GLAT	66	60	54	41	35	29
	GLNG	-81	-81	-81	-81	-81	-81
	SZEN	133	139	144	154	159	162
	ALT	1436	1433	1430	1424	1420	1416

SET 6, FORMAT 4

RPA

711122

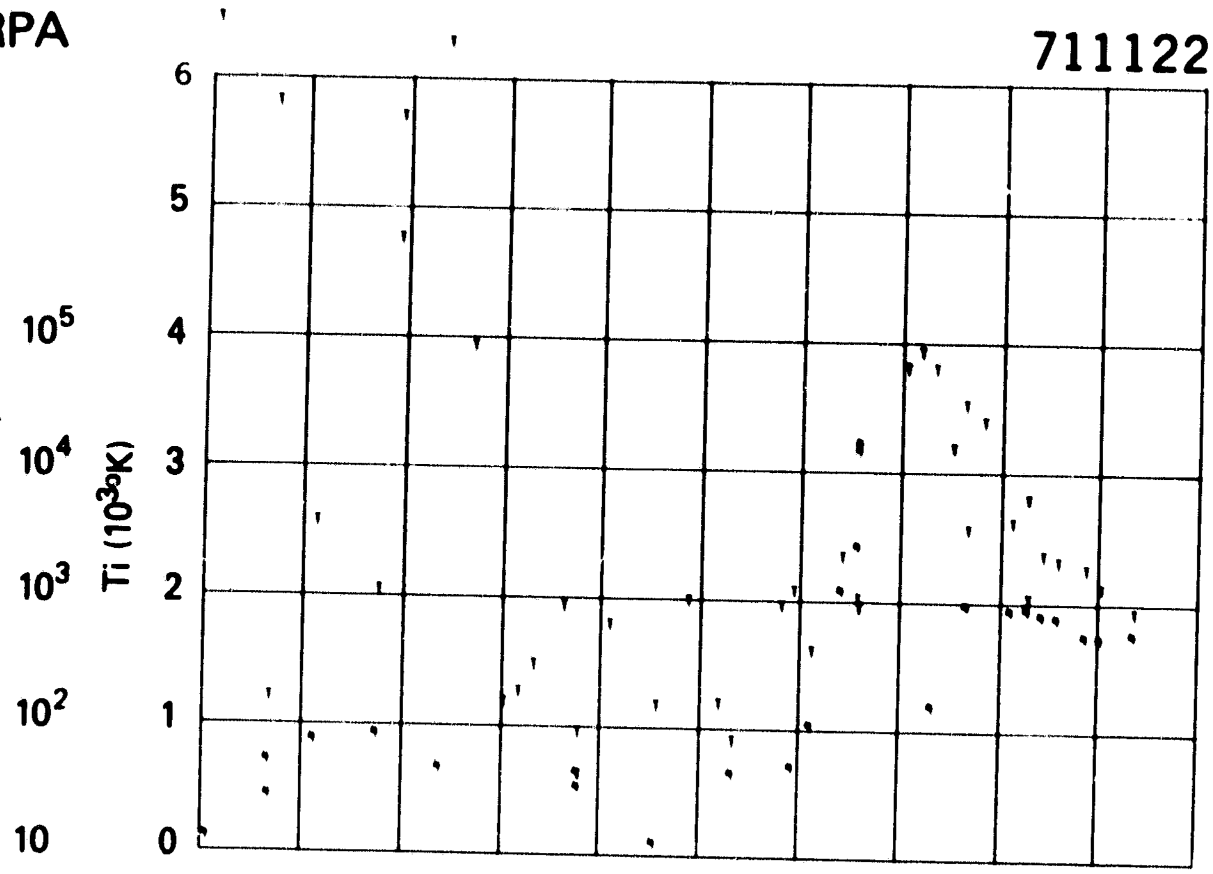

UT	4:48	4:50	4:52	:54	4:56	4:58	5:02	5:04	5:06
LAST	23:51	0:37	0:51	:58	1:02	1:05	1:08	1:10	1:11
MLT	12:41	7:56	1:19	1:09	1:06	1:05	1:04	1:04	1:04
DLAT	87	84	80	75	70	64	52	46	40
INVL	84	84	83	77	72	67	57	52	47
GLAT	85	79	73	66	60	54	41	35	29
GLNG	-77	-66	-63	-61	-61	-61	-61	-61	-61
SZEN	115	121	127	133	139	144	154	159	162
ALT	1439	1438	1437	1436	1433	1430	1424	1420	1416

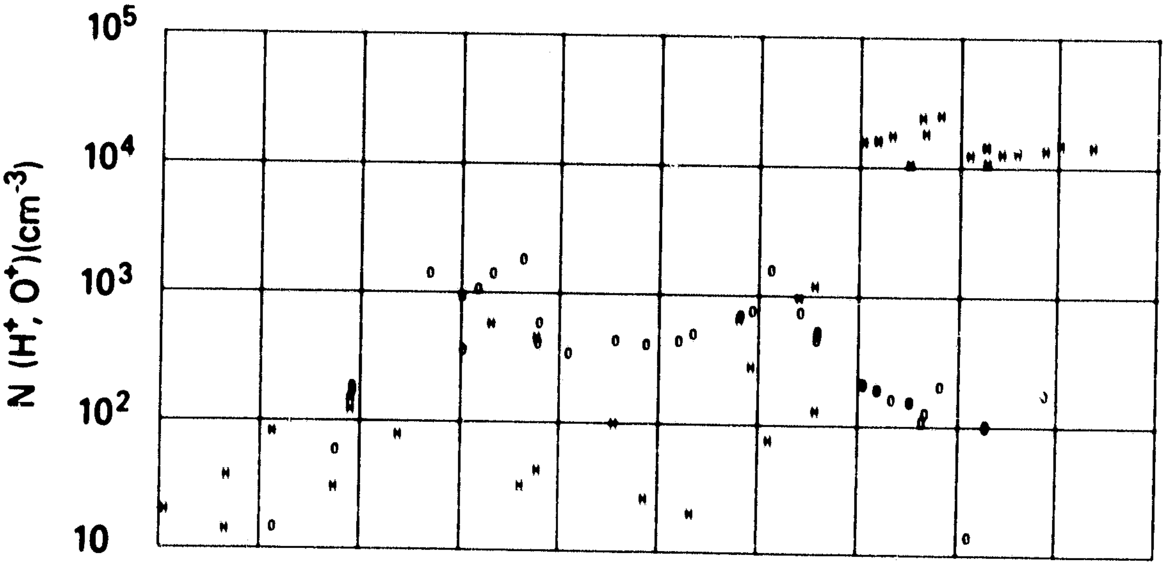

SET 6, FORMAT 5

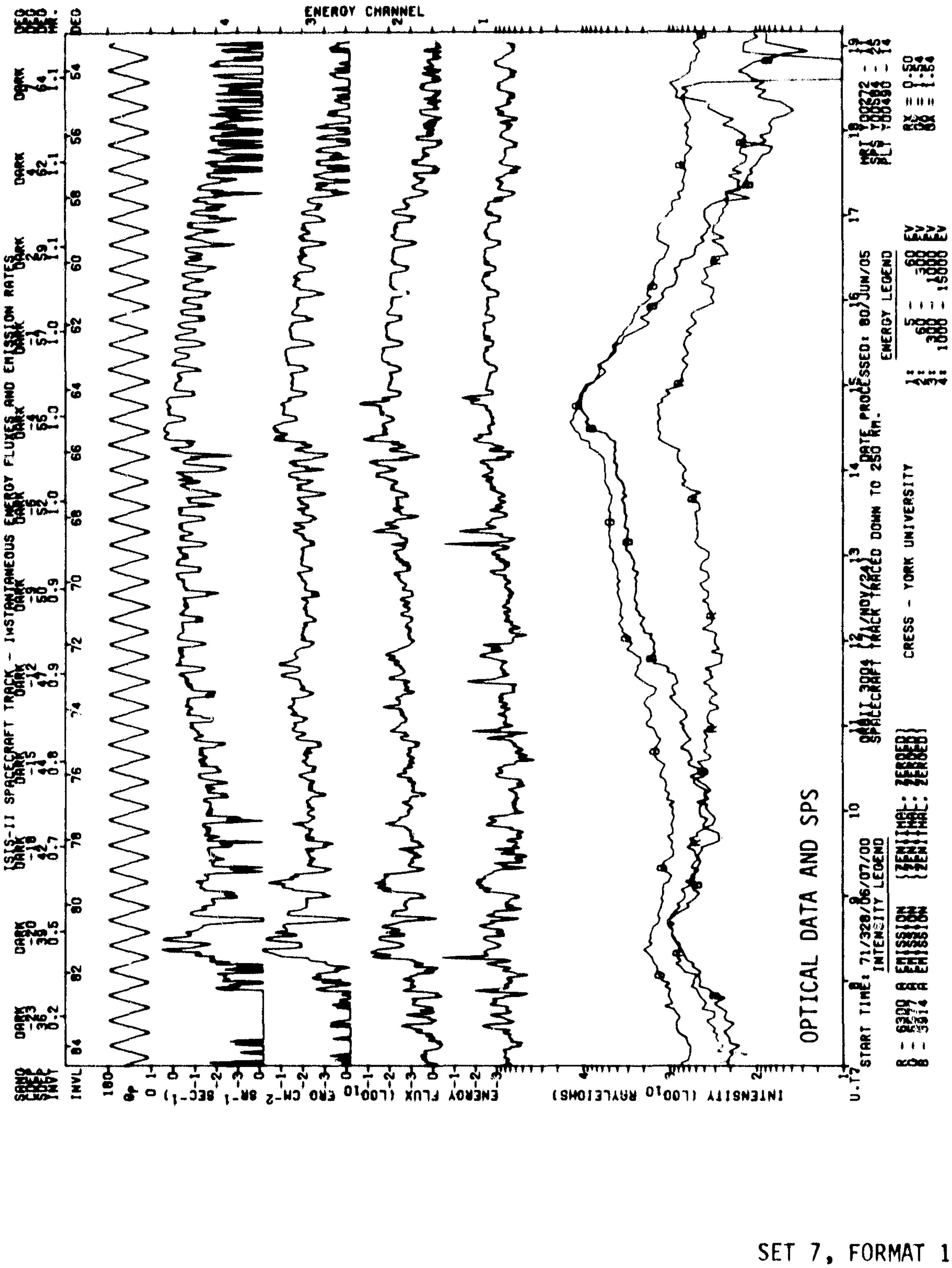

SET 7, FORMAT 1

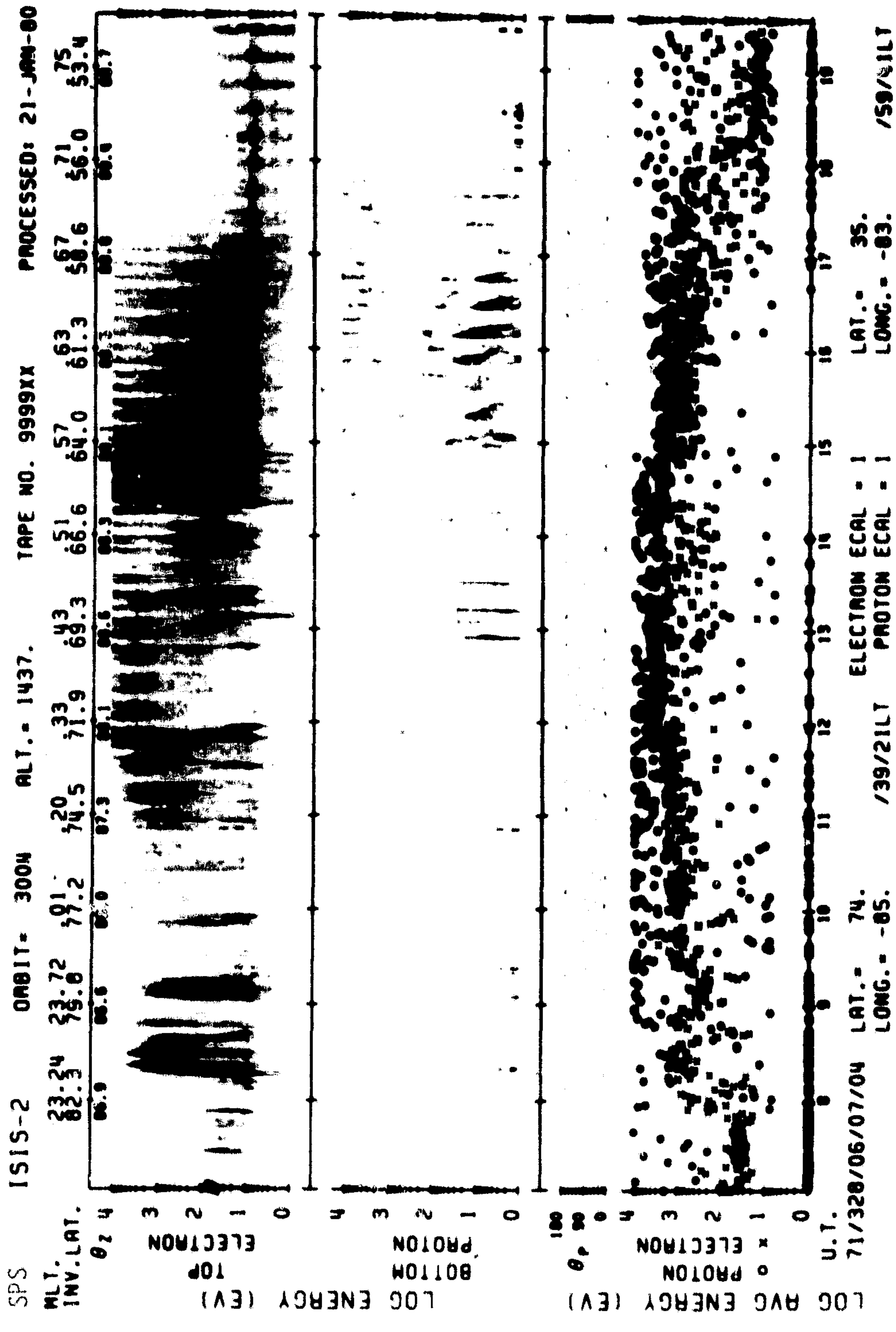

SET 7, FORMAT 6

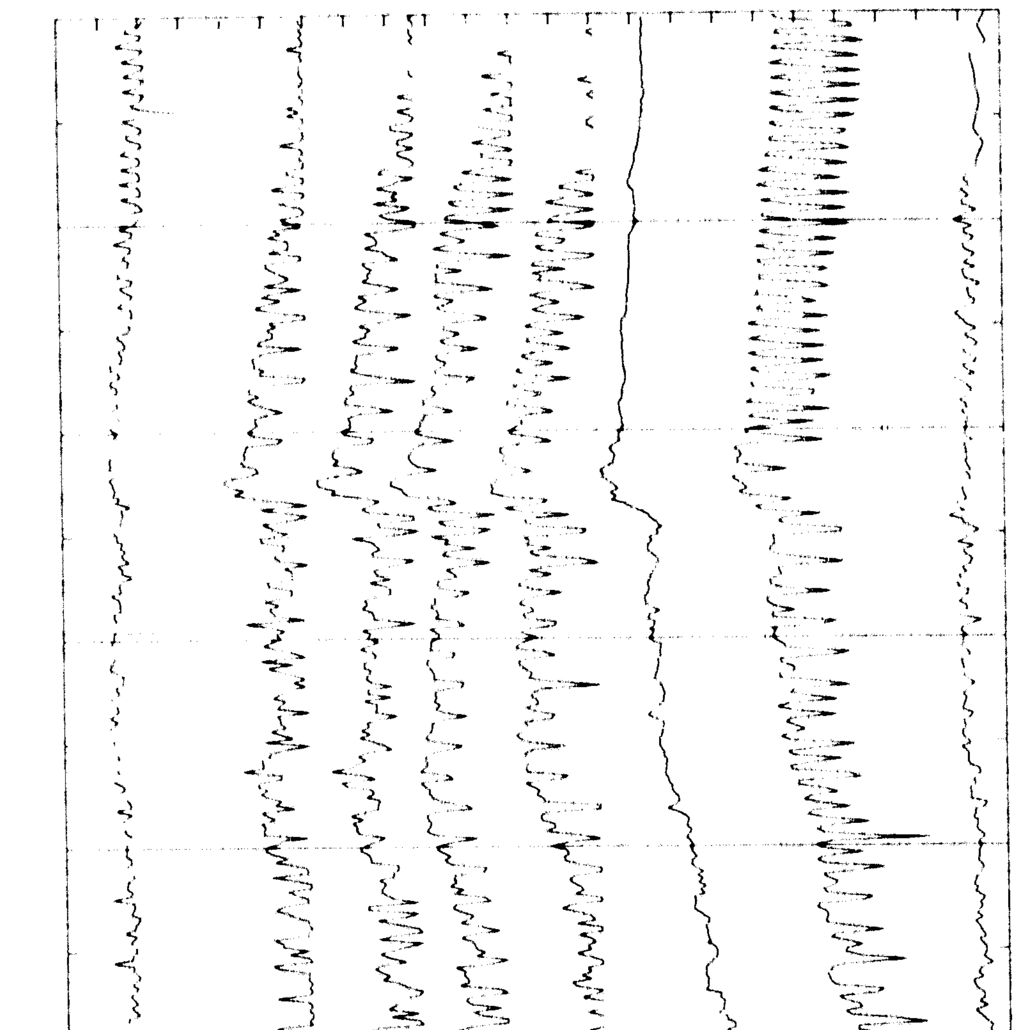

SET 7, FORMAT 3

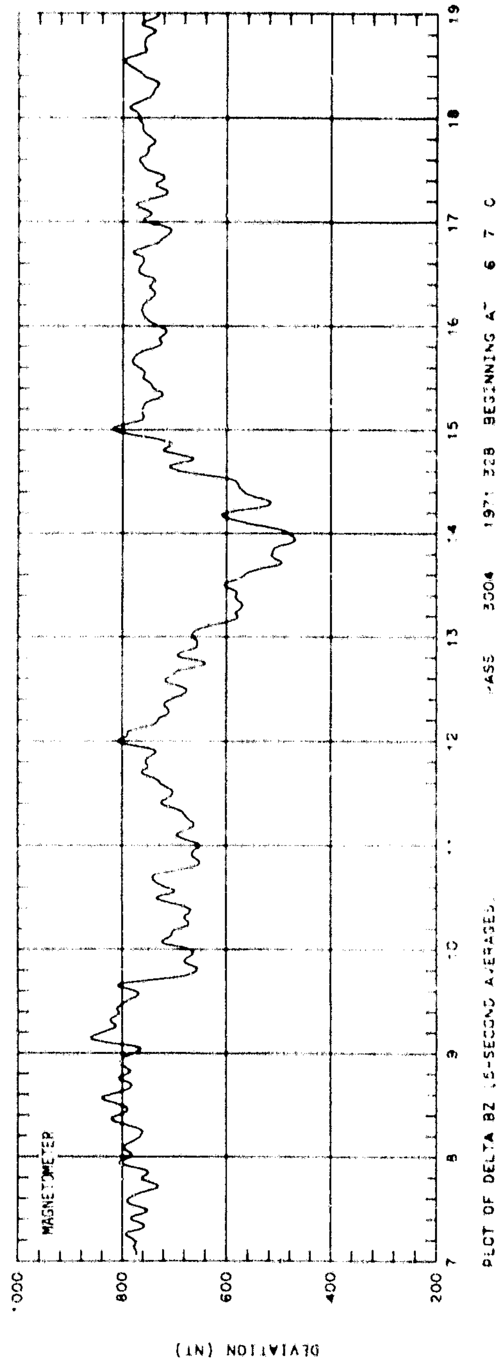

SET 7, FORMAT 2

ORBIT 3004
DATE 711124
DAY 328

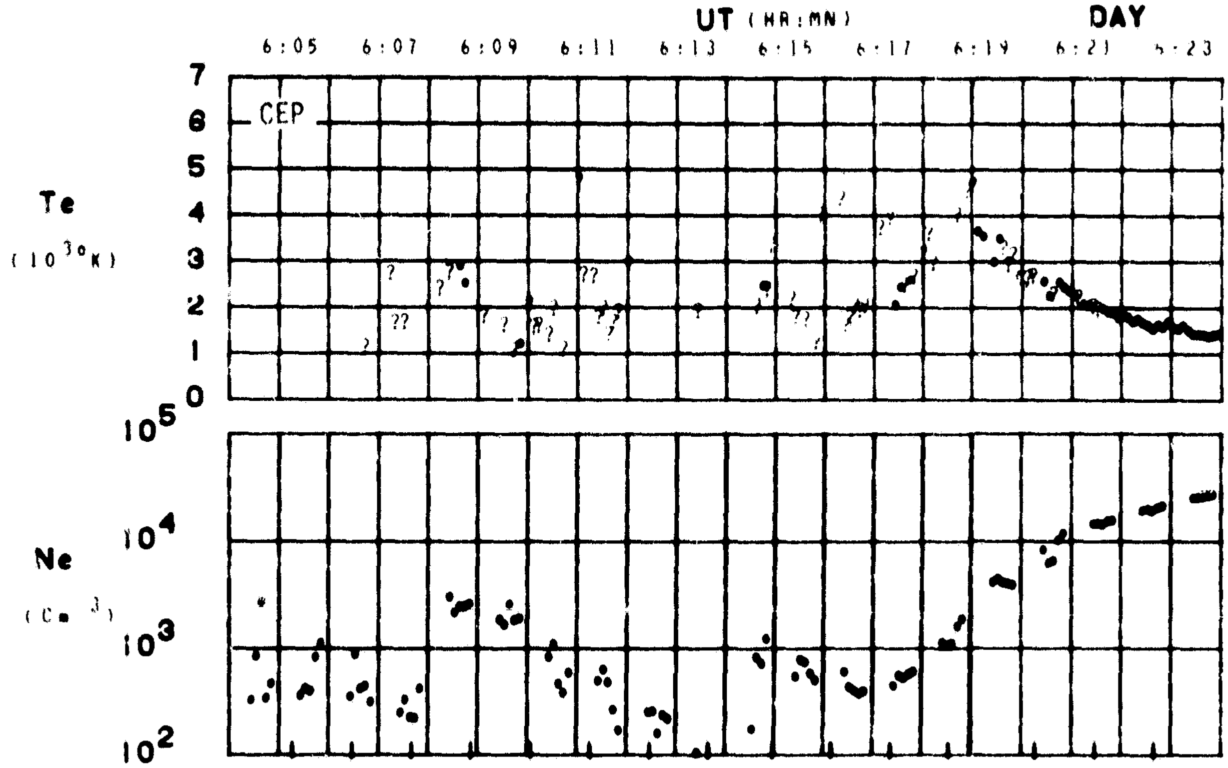

LAT	79	76	72	68	64	60	57	53	49	45	41	37	32	28	24
LONG	-88	-86	-84	-83	-83	-83	-83	-83	-83	-83	-83	-83	-83	83	-83
LT	0:24	0:35	0:42	0:46	0:49	0:51	0:53	0:55	0:56	0:57	0:58	0:59	1:00	1:00	1:01
DIP	89	88	86	85	84	82	80	78	76	73	71	68	63	60	56
DIPLAT	88	36	84	81	78	75	71	68	64	60	55	51	45	41	37
L	99.6	103.5	70.8	33.3	19.5	12.8	9.1	6.8	5.2	4.2	3.5	3.0	2.4	2.1	1.9
INVLAT	84	84	83	80	76	73	70	67	63	60	57	54	49	46	43
ZA	120	124	128	131	135	138	142	145	149	152	155	158	161	163	165

SET 7, FORMAT 4

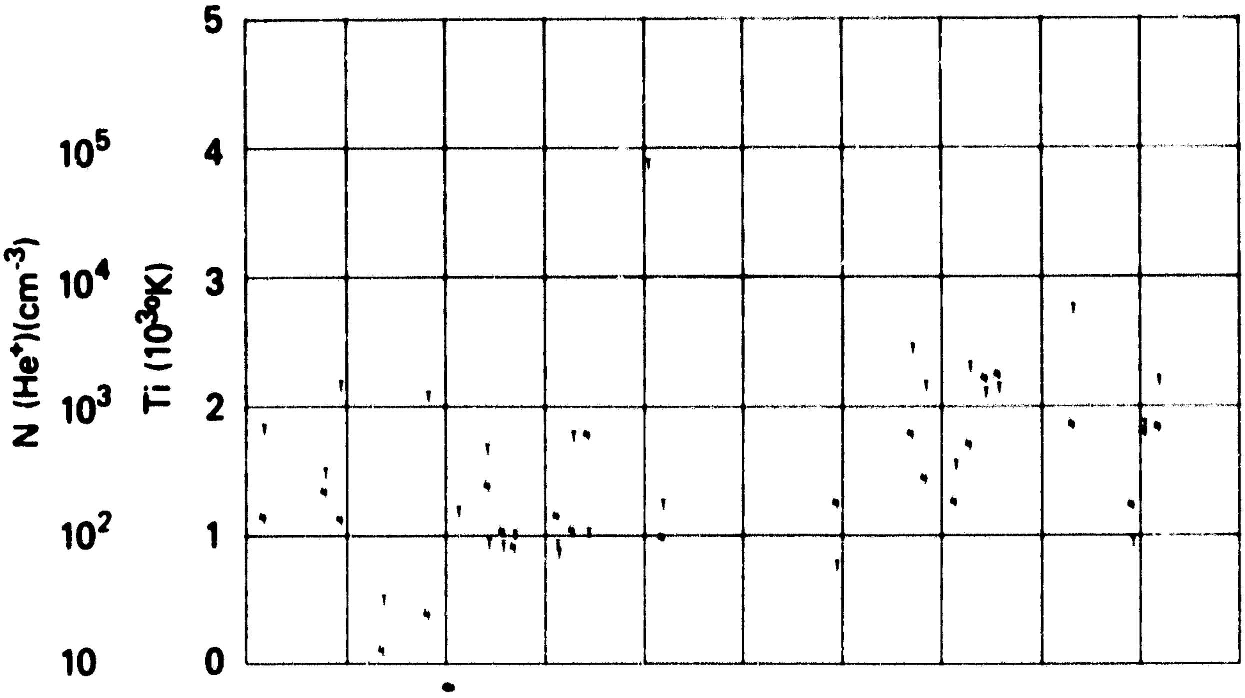

UT	06:06	06:08	06:10	06:12	06:14	06:16	06:18	06:20	06:22
LAST	00:32	00:43	00:49	00:53	00:55	00:57	00:59	01:00	01:01
MLT									
DLAT									
INVL	84	82	77	71	66	61	55	50	45
GLAT	77	71	65	59	52	46	40	33	27
GLNG	-87	-85	-84	-83	-83	-83	-83	-83	-84
SZEN	122	128	134	140	146	151	156	161	164
ALT	1437	1436	1434	1431	1428	1424	1420	1416	1412

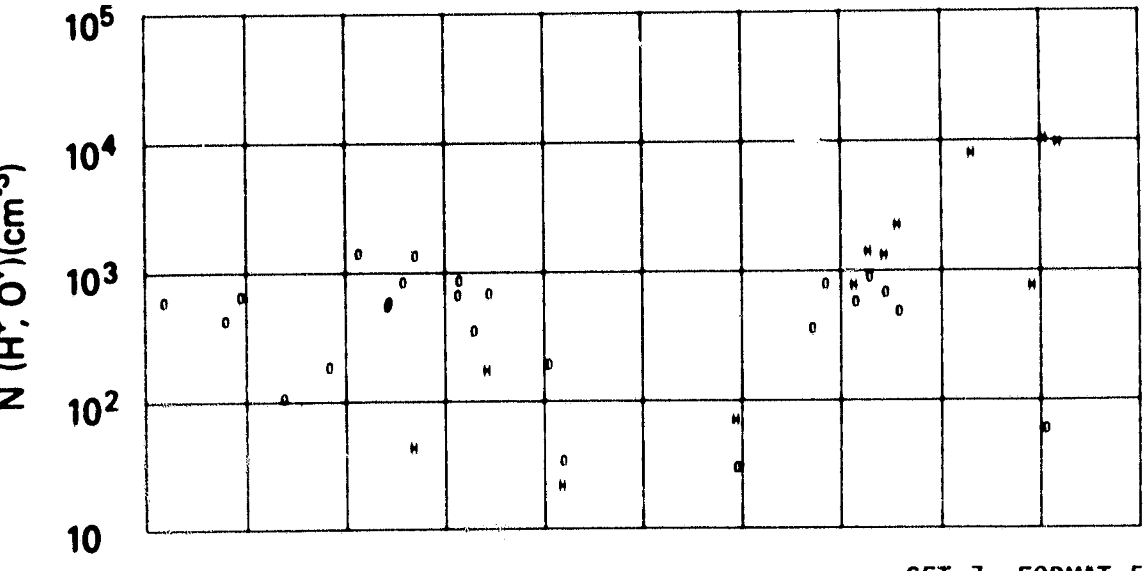

SET 7, FORMAT 5

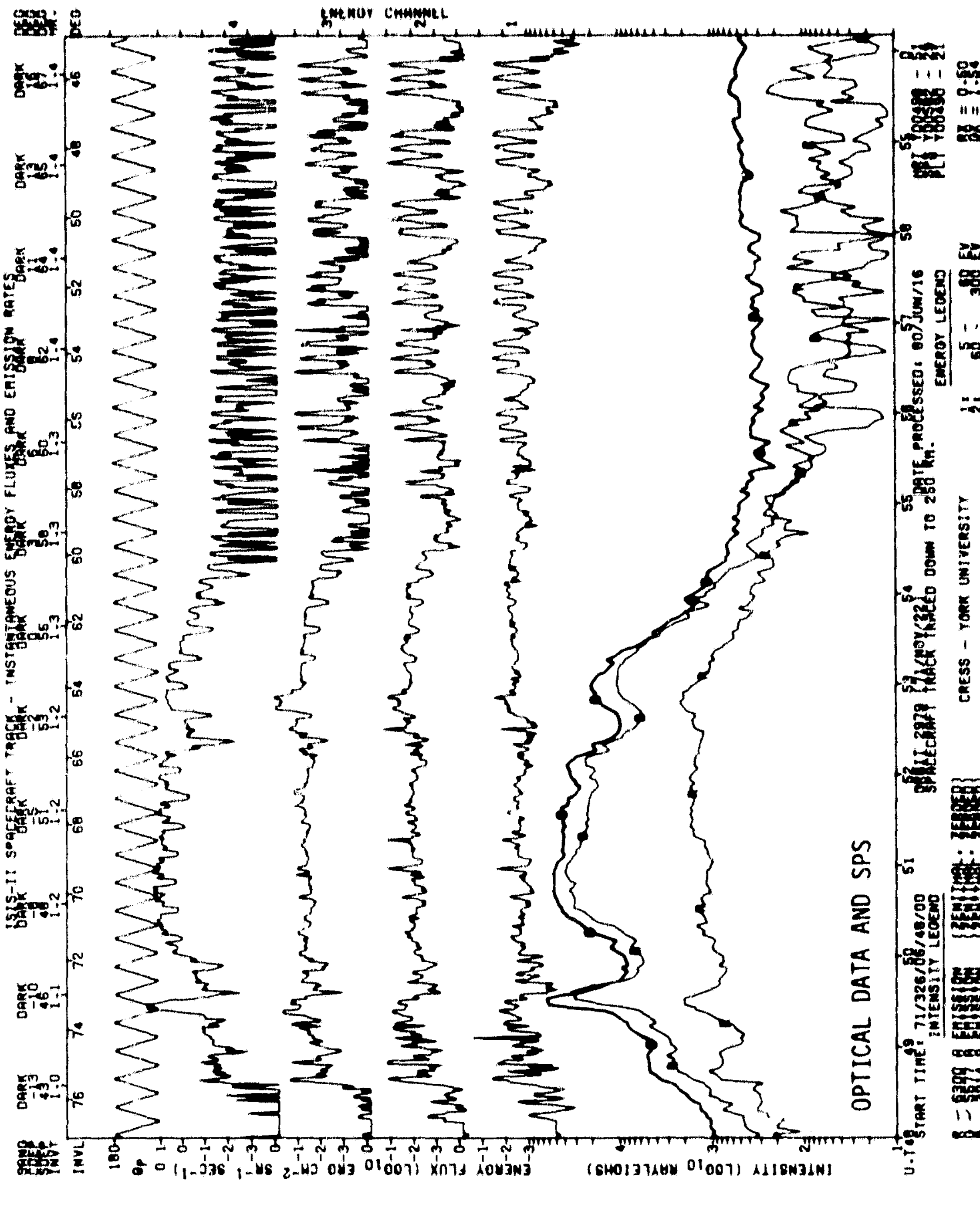

SET 8, FORMAT 1

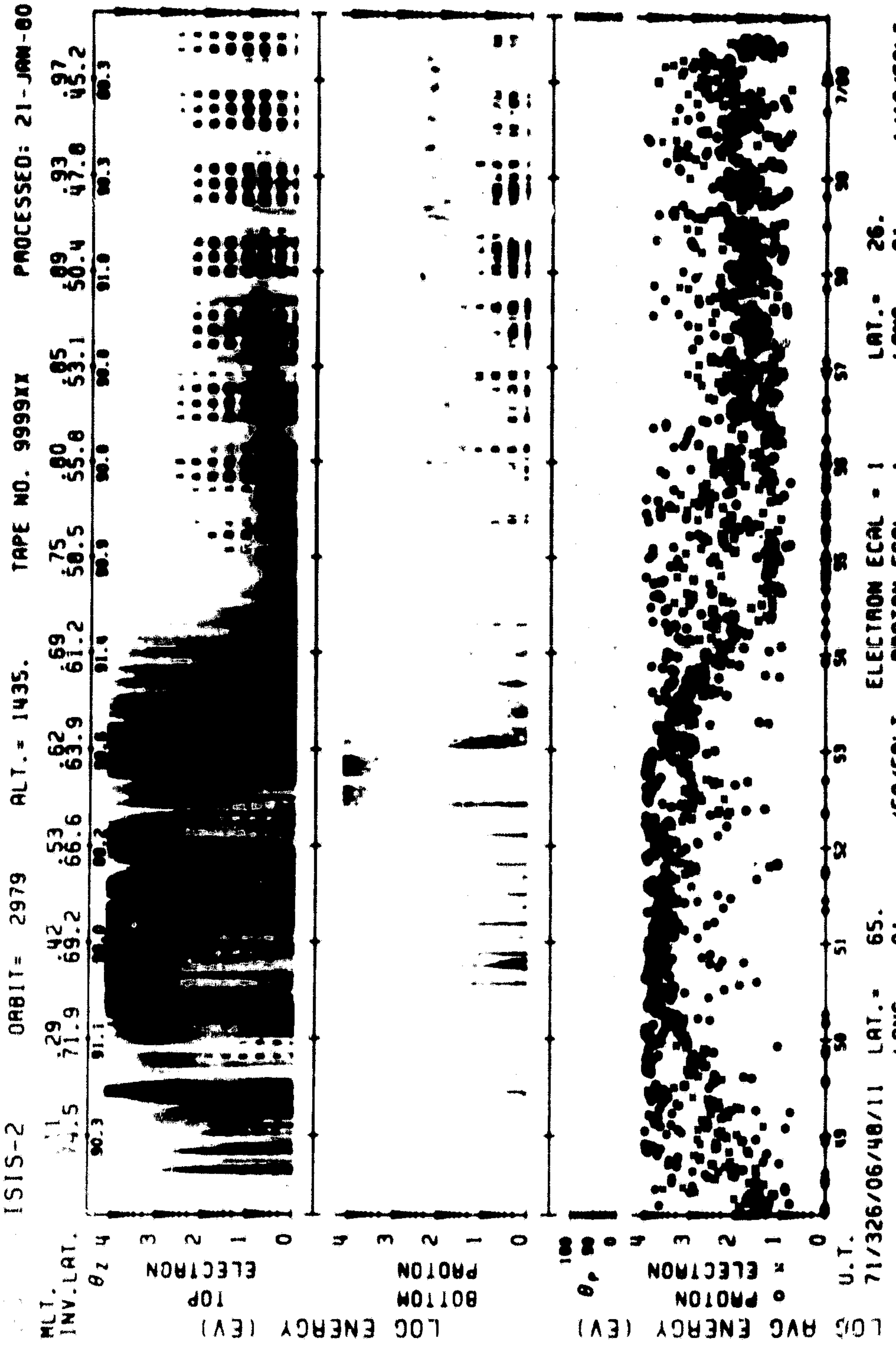

SET 8, FORMAT 6

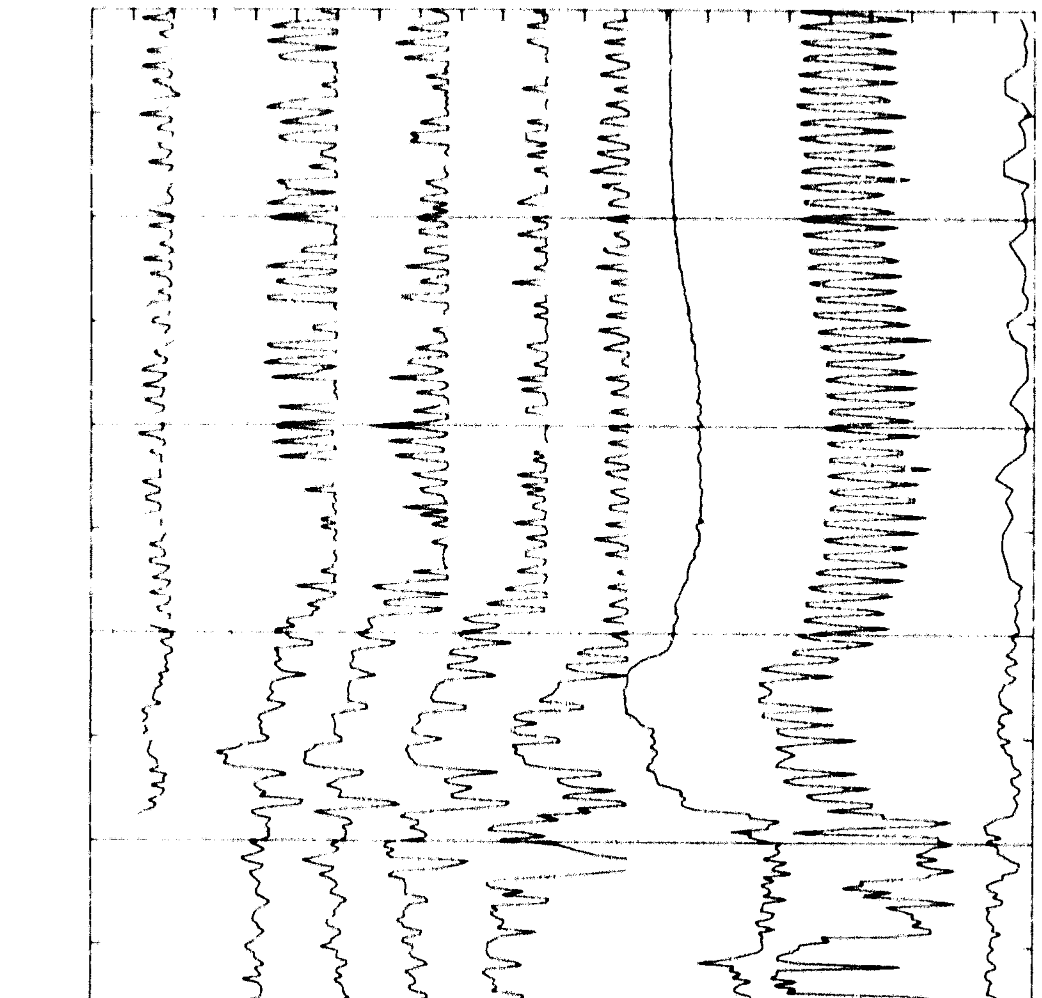

SET 8, FORMAT 3

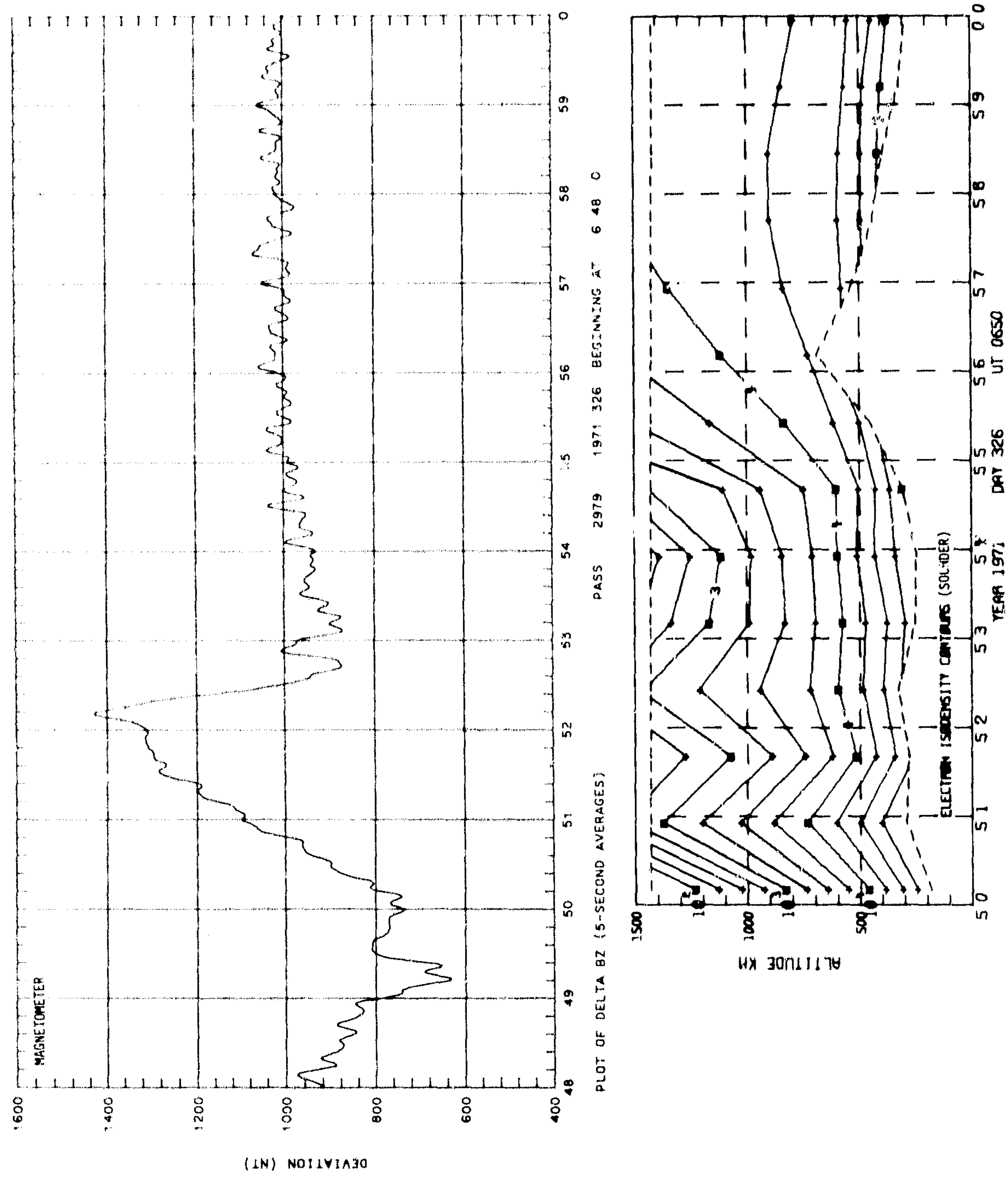

SET 8, FORMAT 2

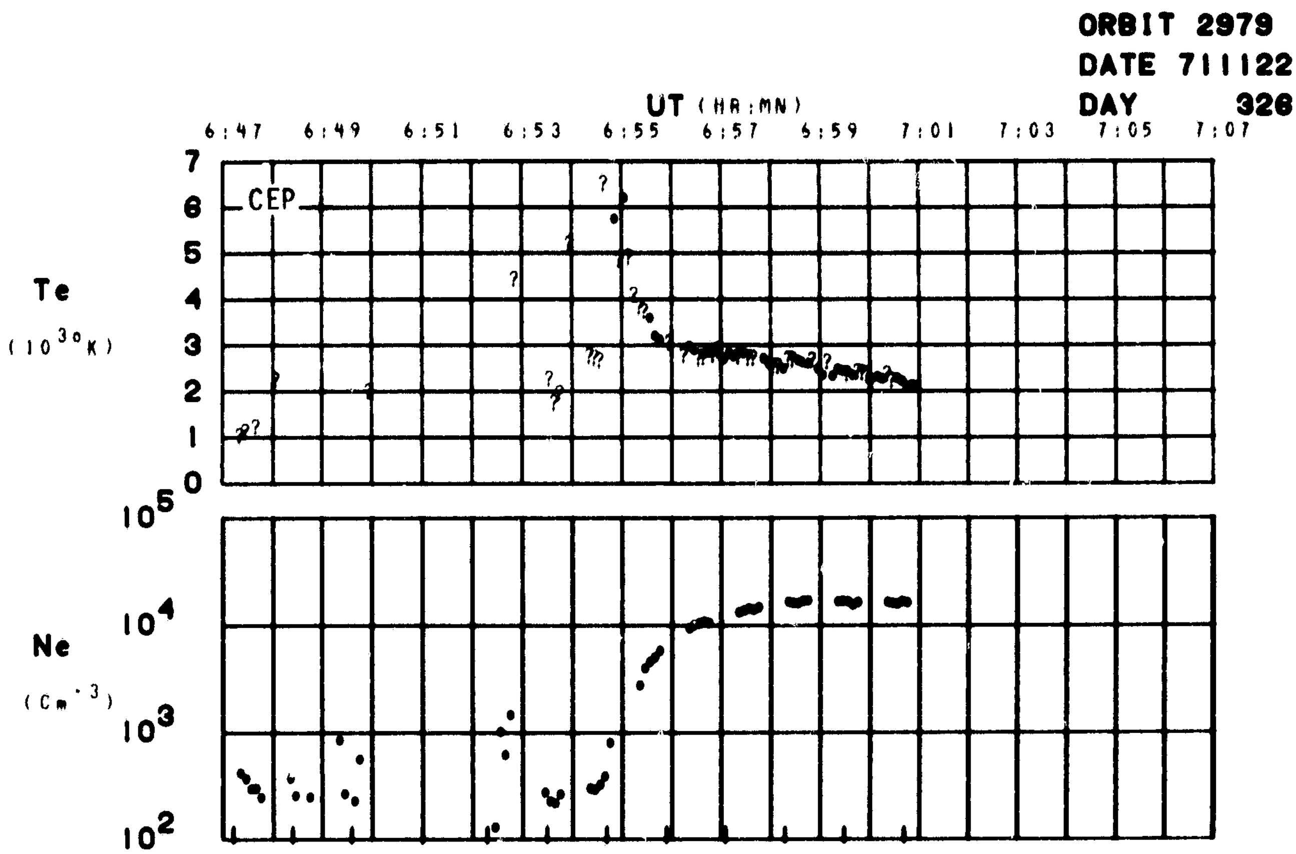

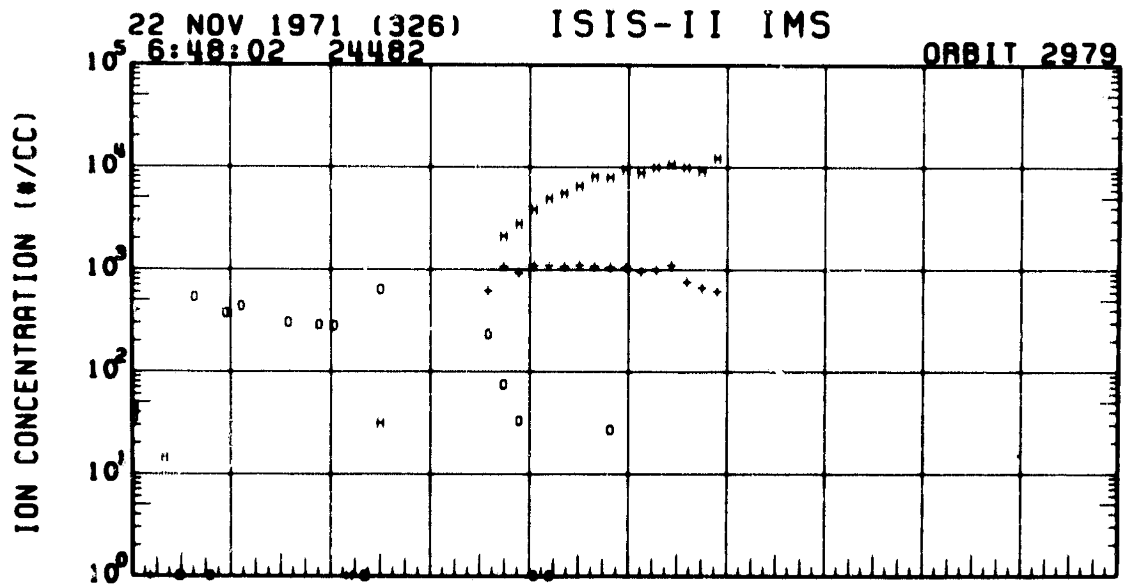

1 - H	UT	6:50	6:52	6:56	6:58
4 - +	LAST	1:02	1:05	1:08	1:10
8 - Δ	MLT	0:17	0:32	0:48	0:54
14 - N	DLAT	73	67	53	46
16 - O	INVL	72	67	56	50
	GLAT	59	53	40	34
	GLNG	-89	-89	-89	-90
	SZEN	139	145	155	159
	ALT	1433	1430	1423	1419

SET 8, FORMAT 4

RPA

711122

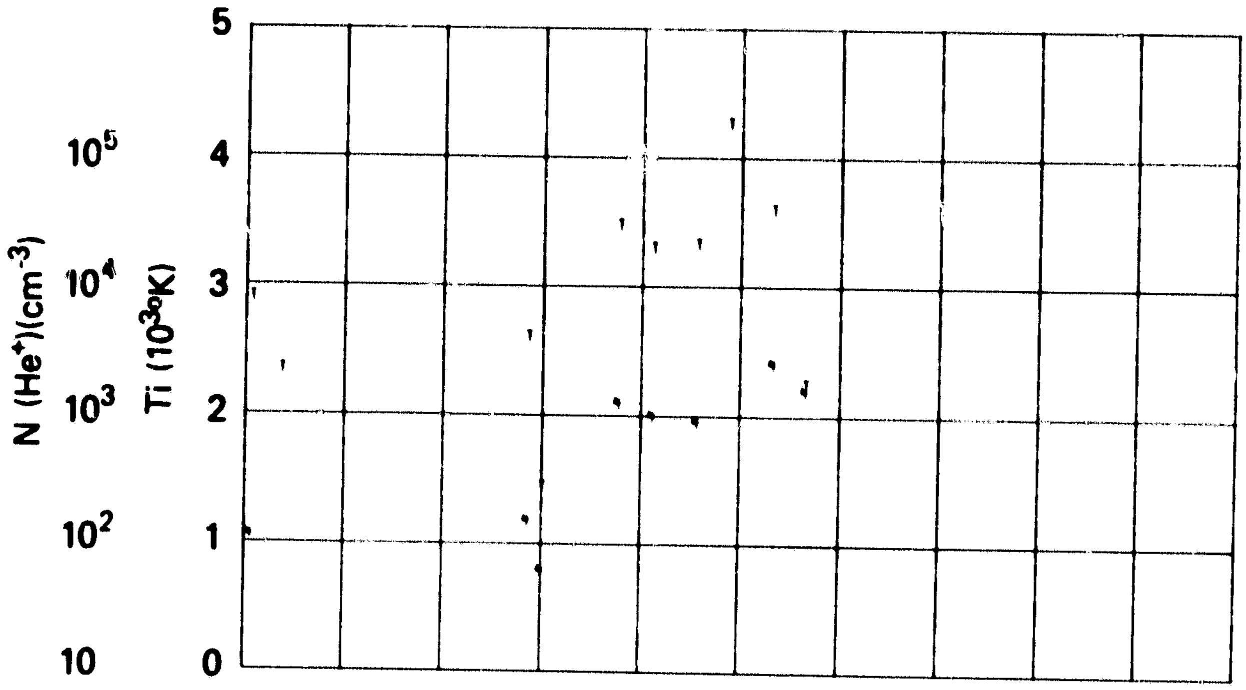

UT	6:50	6:52	6:56	6:58
LAST	1:02	1:05	1:08	1:10
MLT	0:17	0:32	0:48	0:54
DLAT	73	67	53	46
INVL	72	67	56	50
GLAT	59	53	40	34
GLNG	89	-89	-89	-90
SZEN	139	145	155	159
ALT	1433	1430	1423	1419

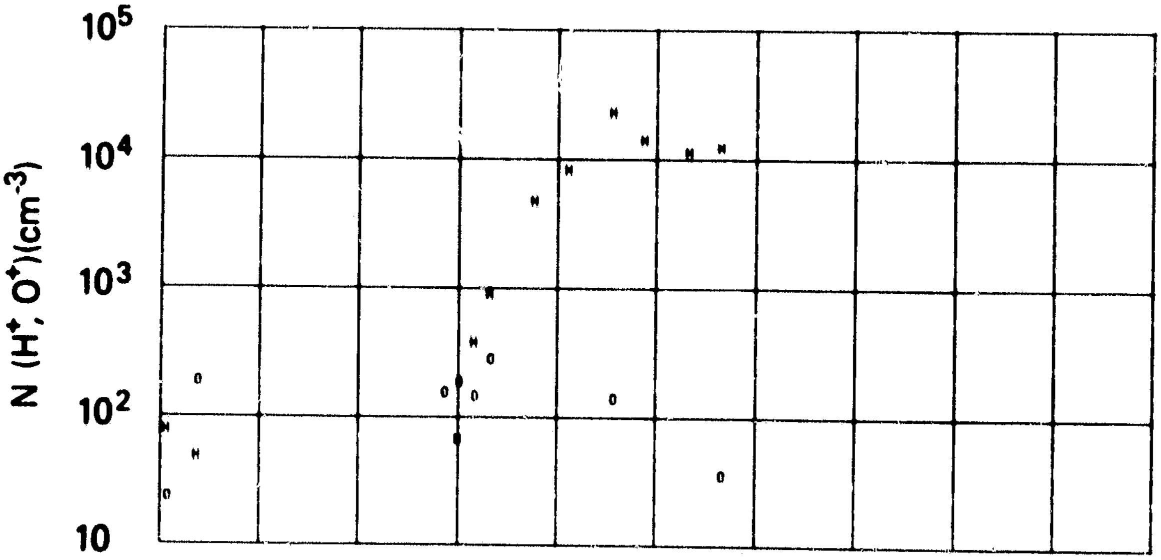

SET 8, FORMAT 5

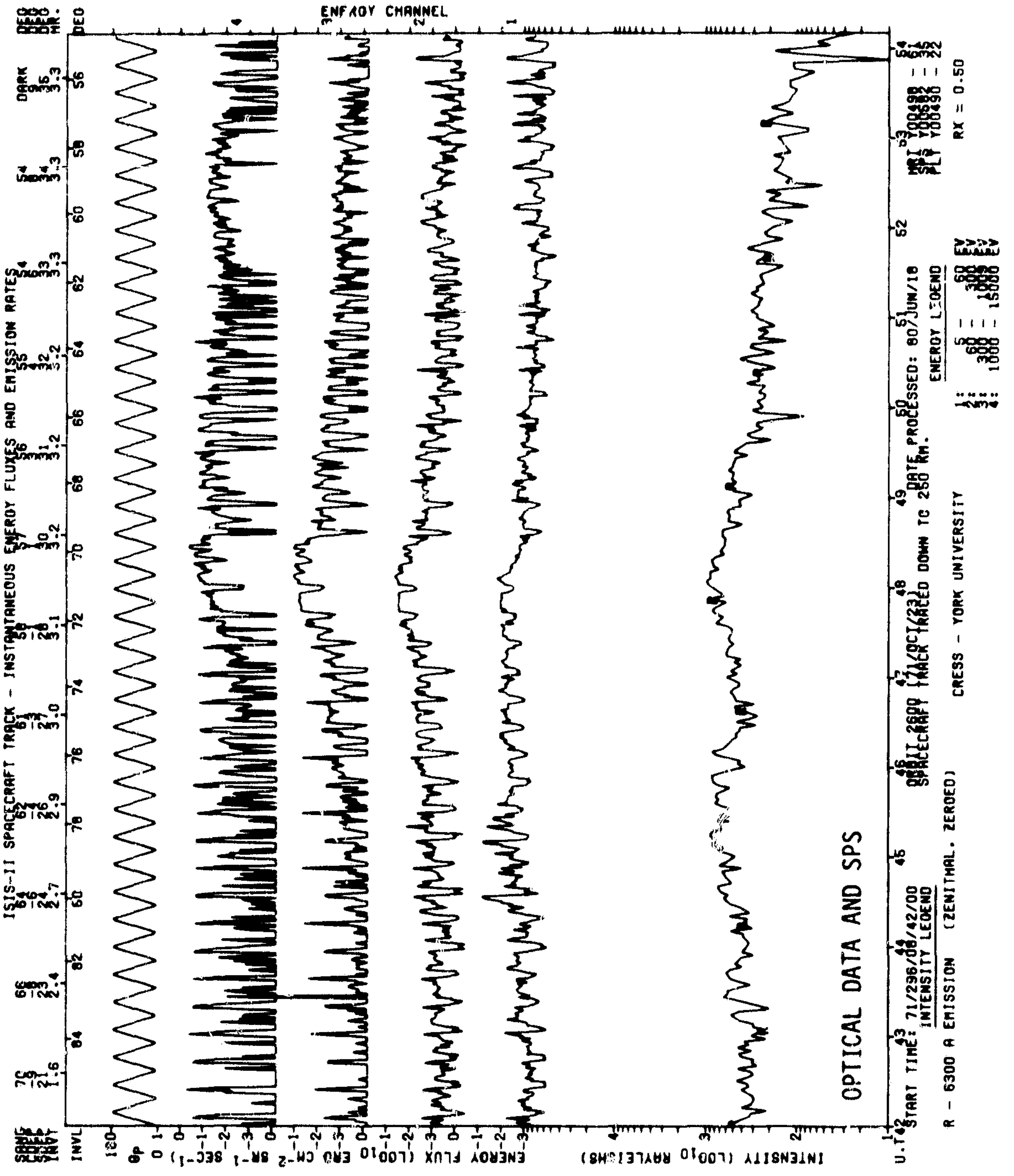

SET 9, FORMAT 1

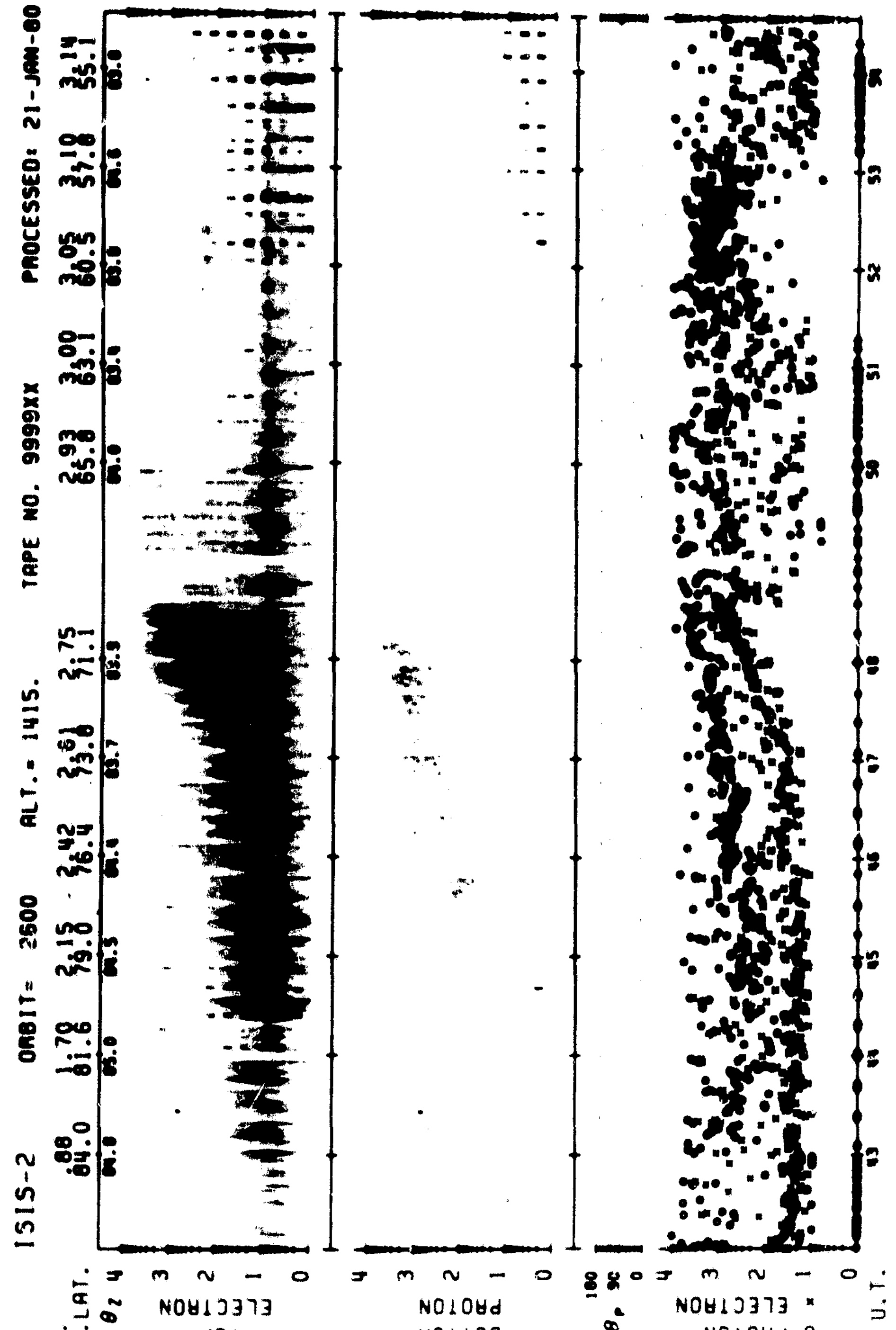

SET 9, FORMAT 6

ORBIT 2600
DATE 711023
DAY 296

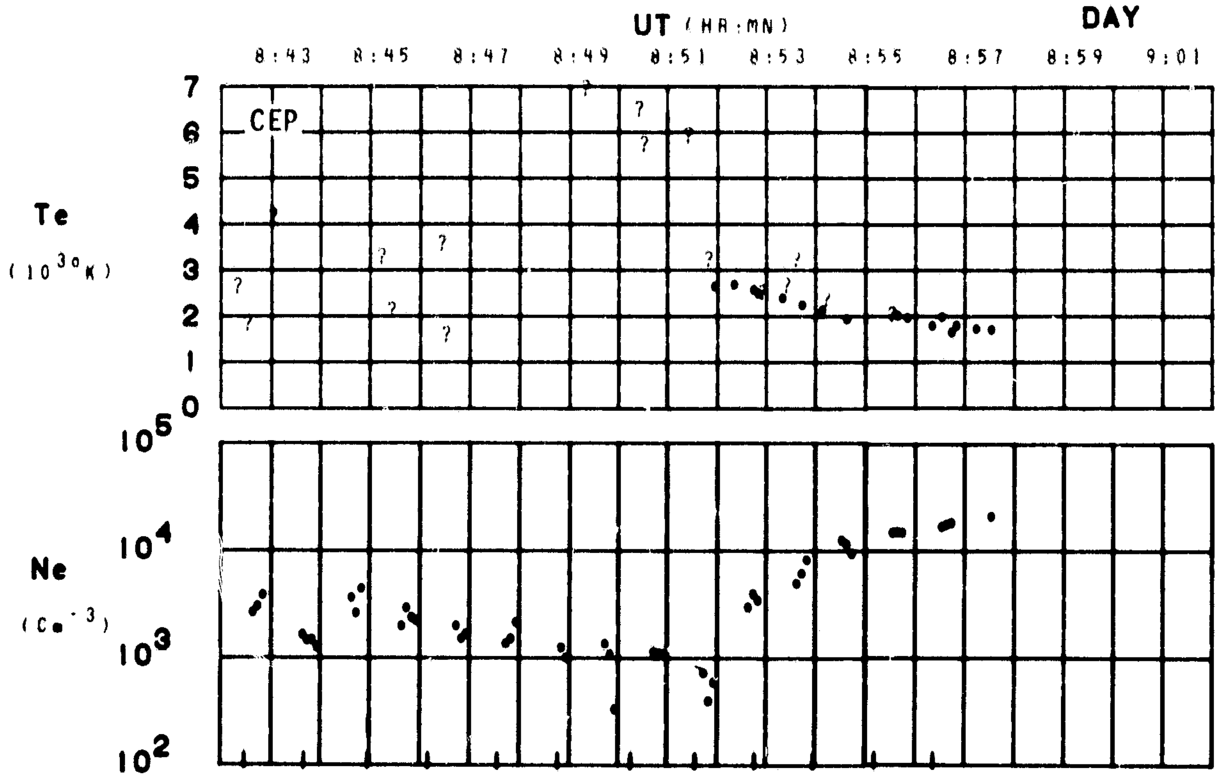

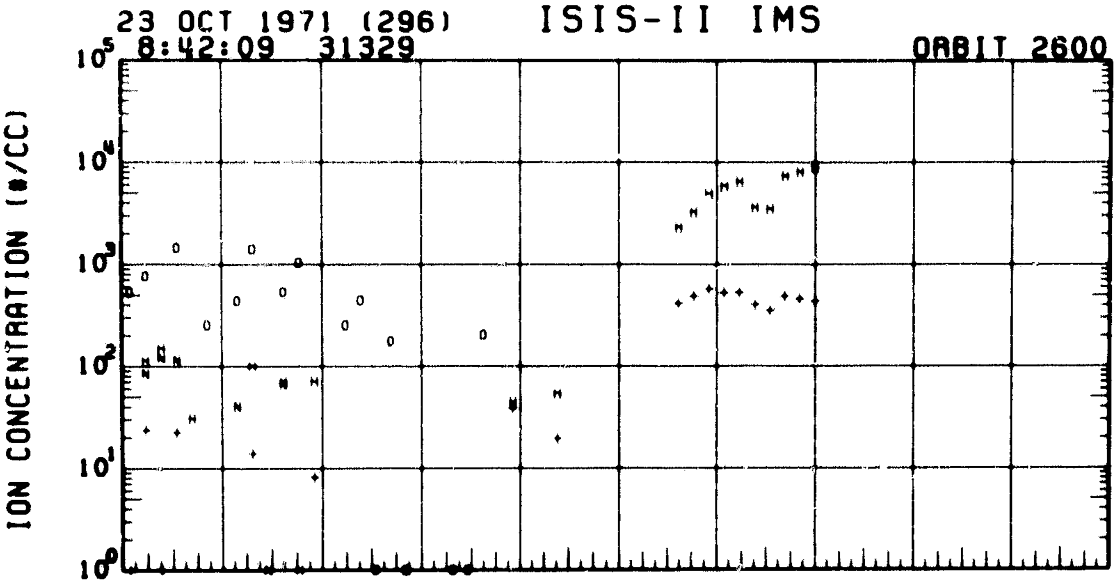

1 - H	UT	8:44	8:46	8:48	8:50	8:54
4 - +	LAST	3:13	3:18	3:22	3:24	3:27
8 - Δ	MLT	1:43	2:26	2:45	2:56	3:08
14 - N	DLAT	83	78	72	66	52
16 - O	INVL	81	76	[illegible]	66	55
	GLAT	70	64	58	51	38
	GLNG	-86	-85	-85	-84	-85
	SZEN	114	117	120	123	127
	ALT	1419	1420	1422	1423	1425

SET 9, FORMAT 4

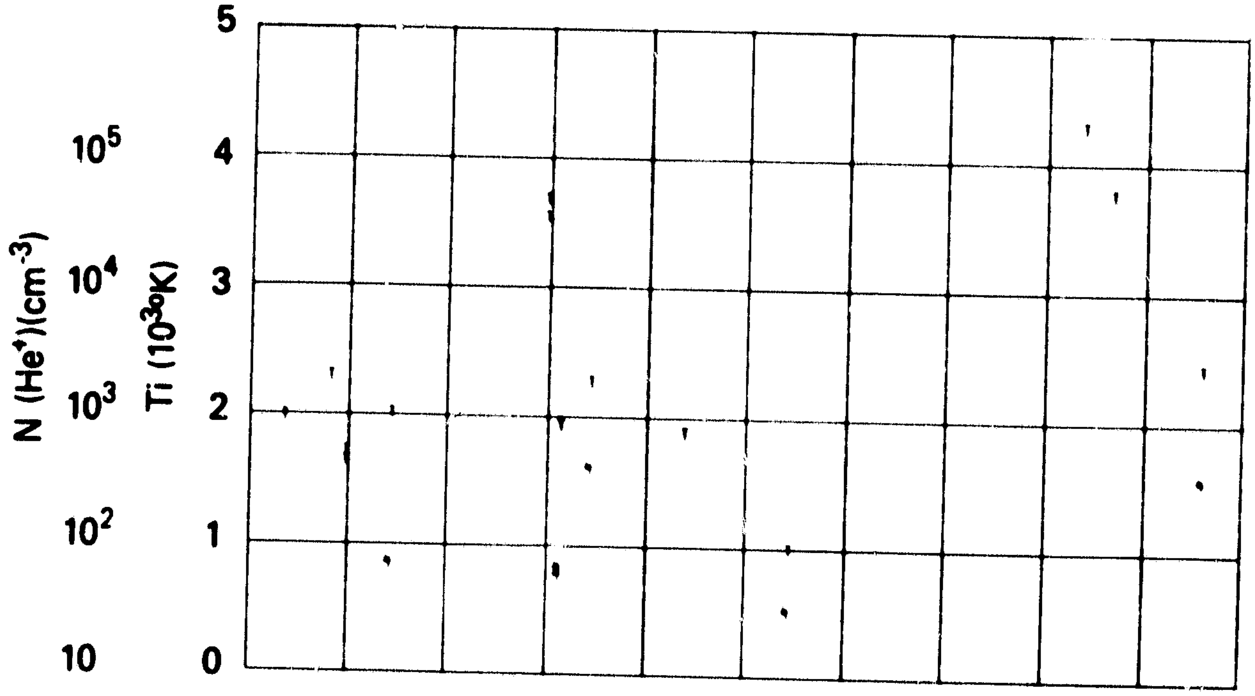

UT	8:38	8:40	8:42	8:44	8:46	8:48	8:50	8:54
LAST	22:34	2:34	3:02	3:13	3:18	3:22	3:24	3:27
MLT	16:53	18:26	23:14	1:43	2:26	2:45	2:56	3:08
DLAT	87	89	87	83	78	72	66	52
INVL	82	84	84	81	76	71	66	55
GLAT	88	83	77	70	64	58	51	39
GLNG	-148	-94	-88	-86	-85	-85	-84	-85
SZEN	103	107	110	114	117	120	123	127
ALT	1409	1412	1415	1418	1420	1422	1423	1425

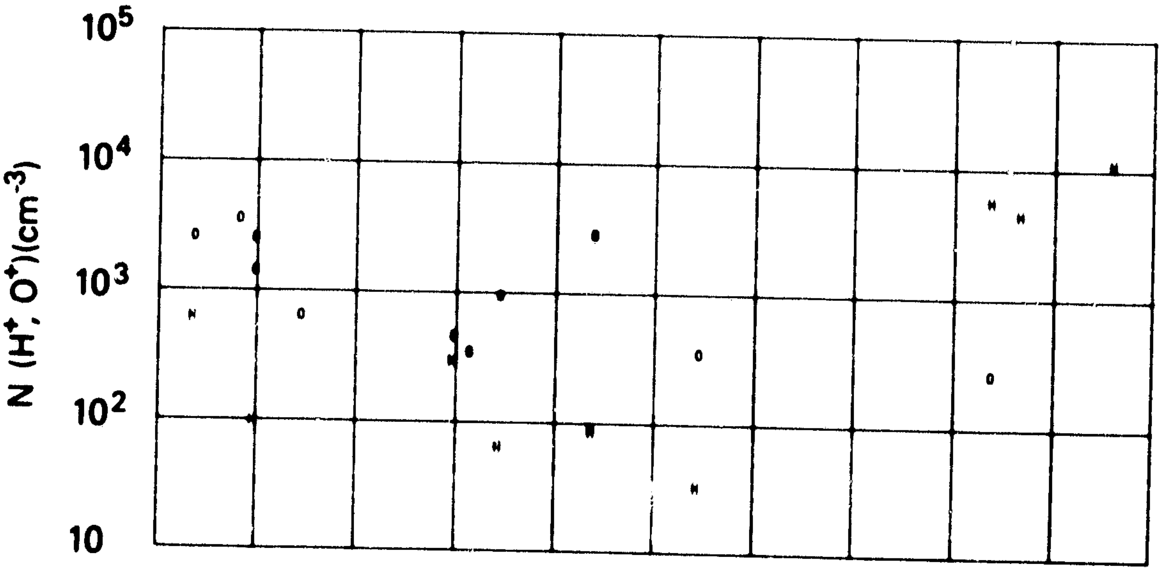

SET 9, FORMAT 5

71/296/0842

Excerpts of VLF Spectral film for the period 0845 - 0854

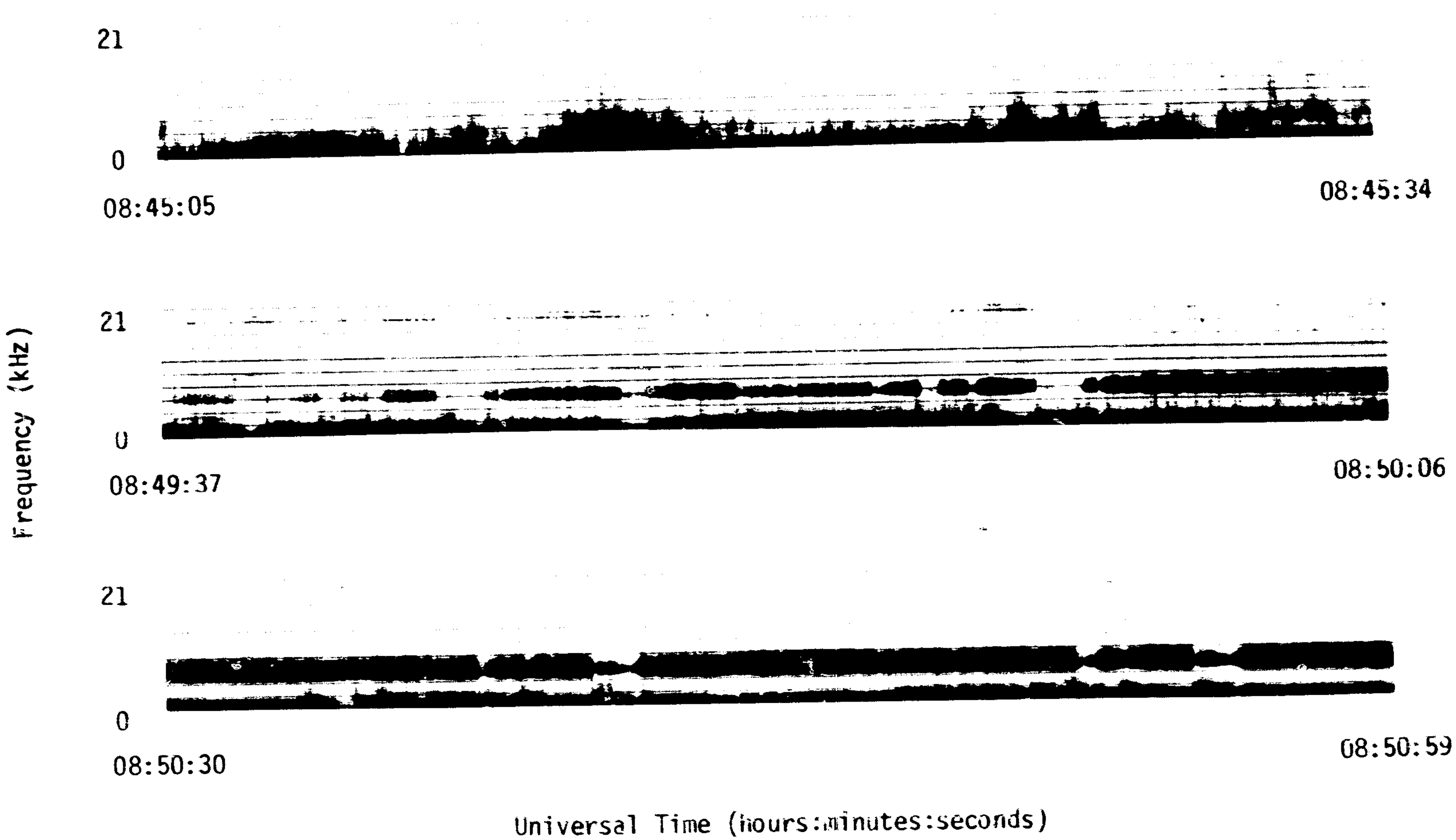

SET 9, FORMAT 11

71/296/0842

Excerpts of VLF Spectral film for the period 0845 - 0854

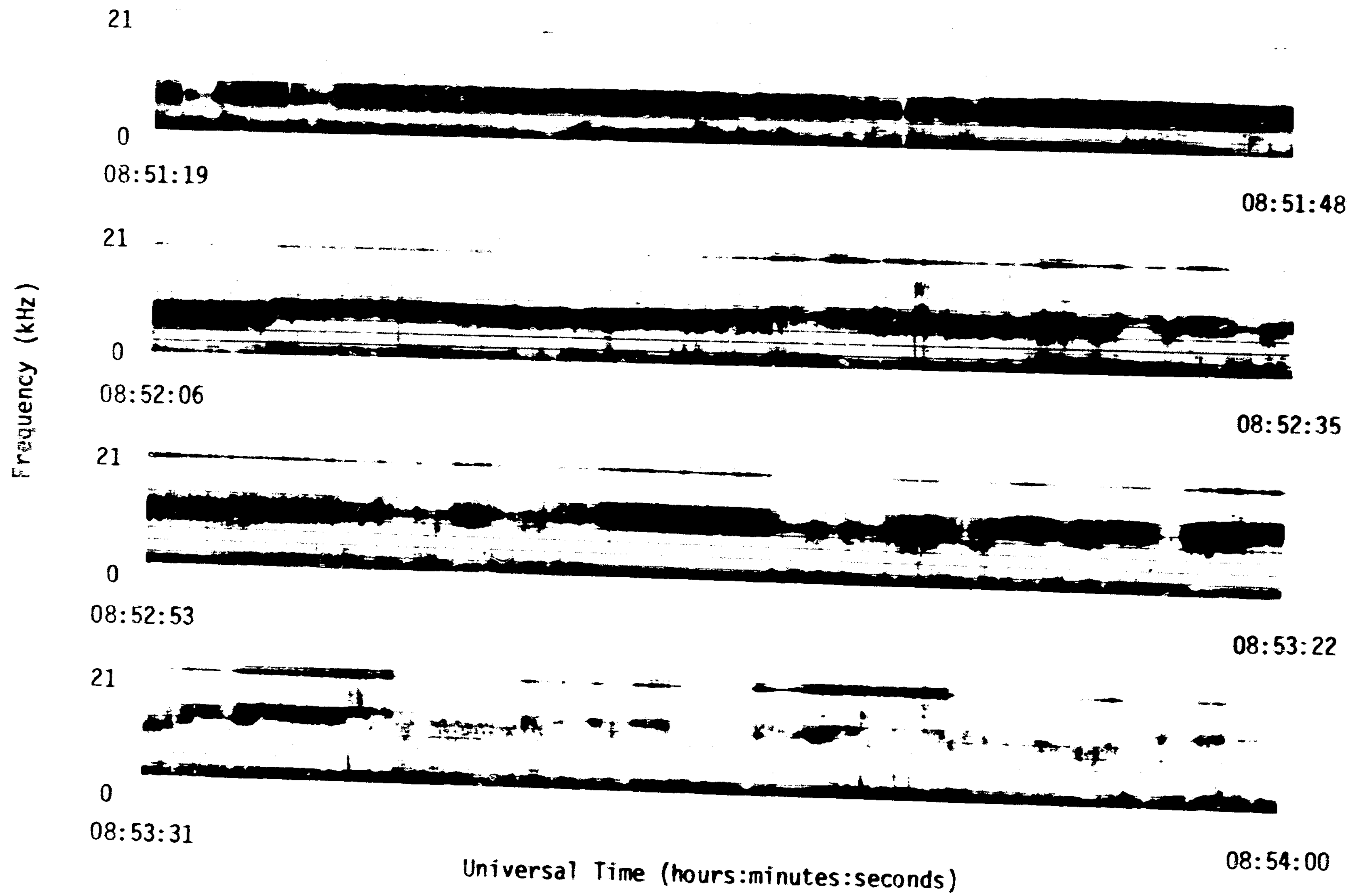

SET 9, FORMAT 11

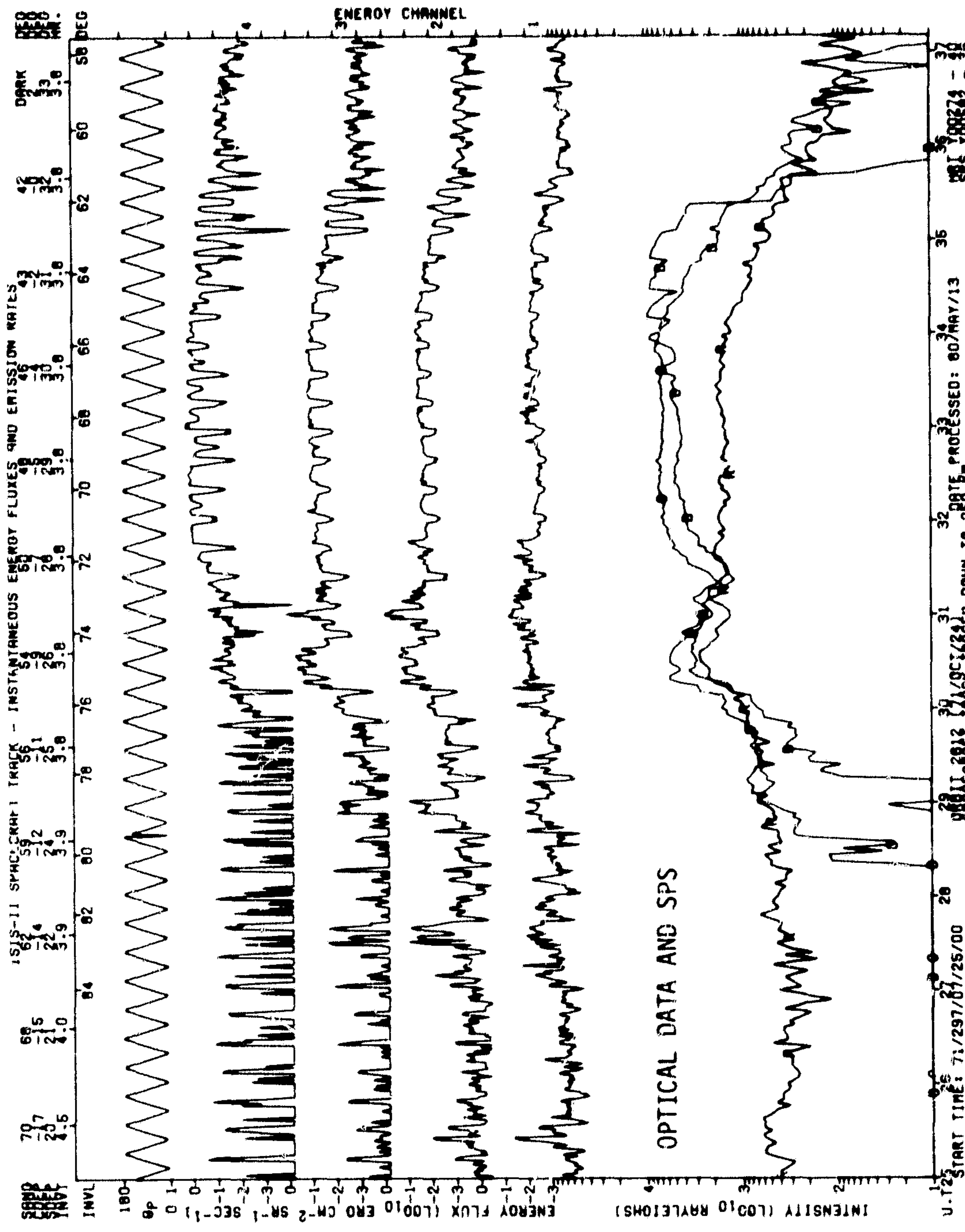

SET 10, FORMAT 1

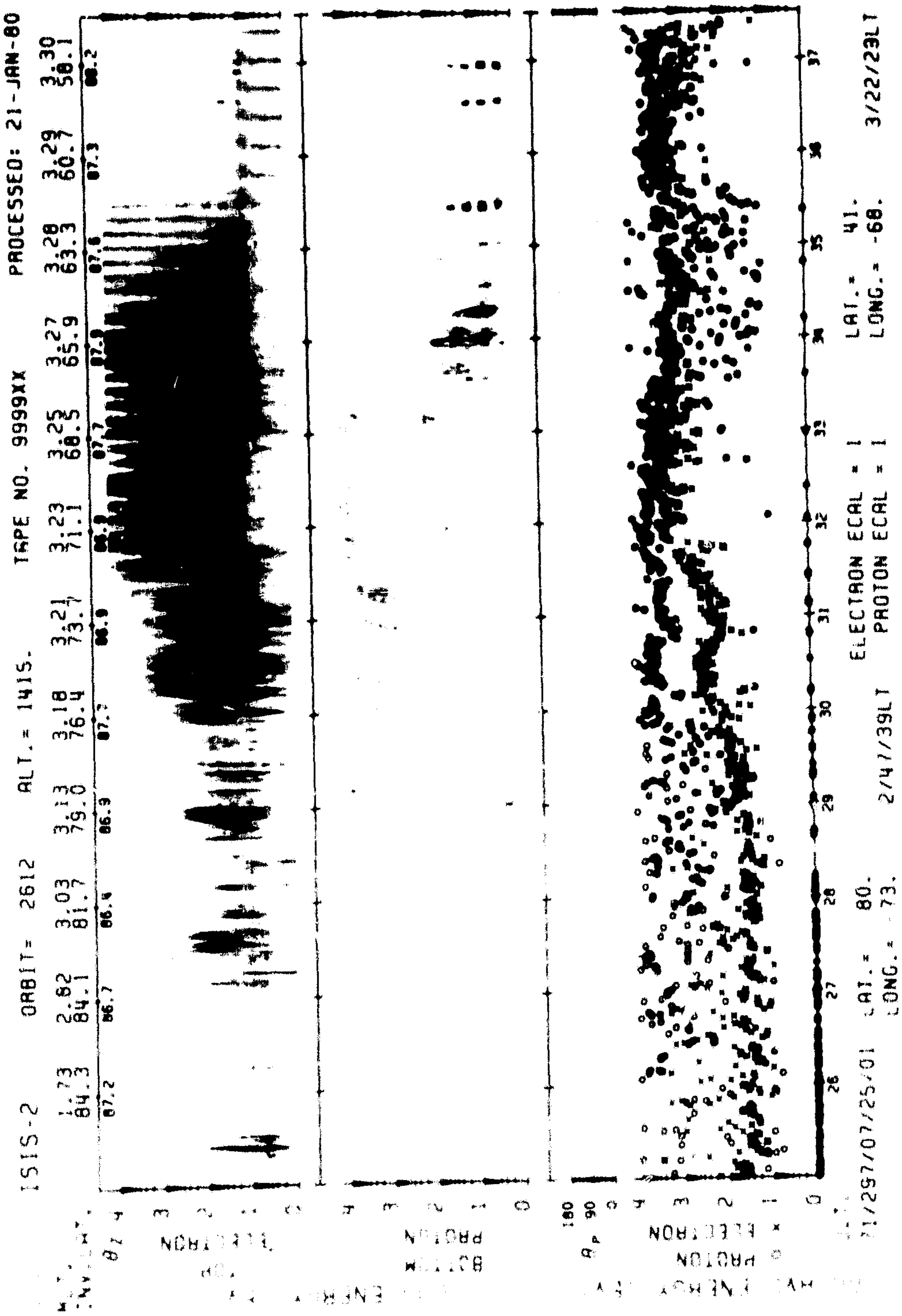

SET 10, FORMAT 6

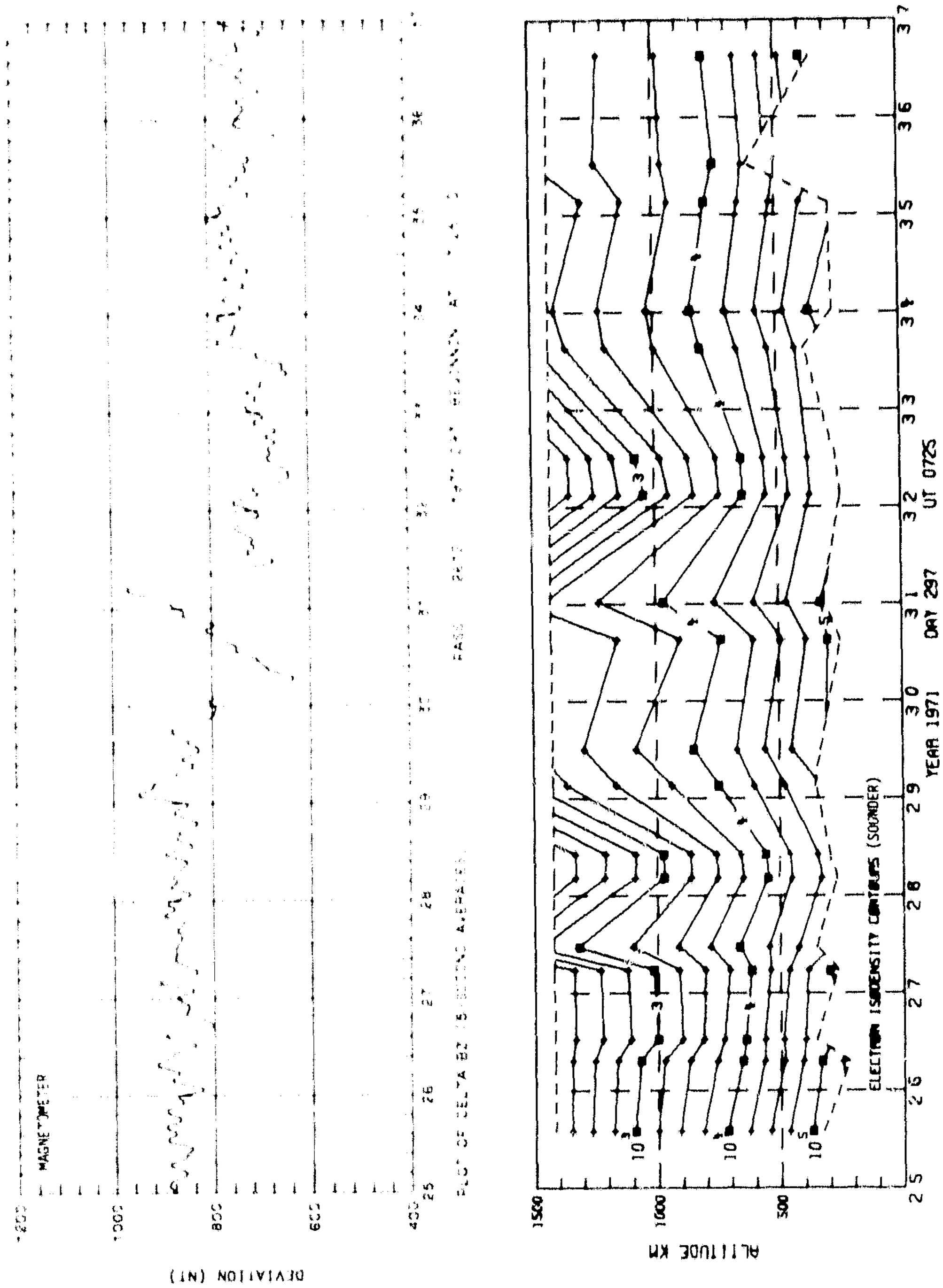

SET 10, FORMAT 2

ORBIT 2612
DATE 711024
DAY 297

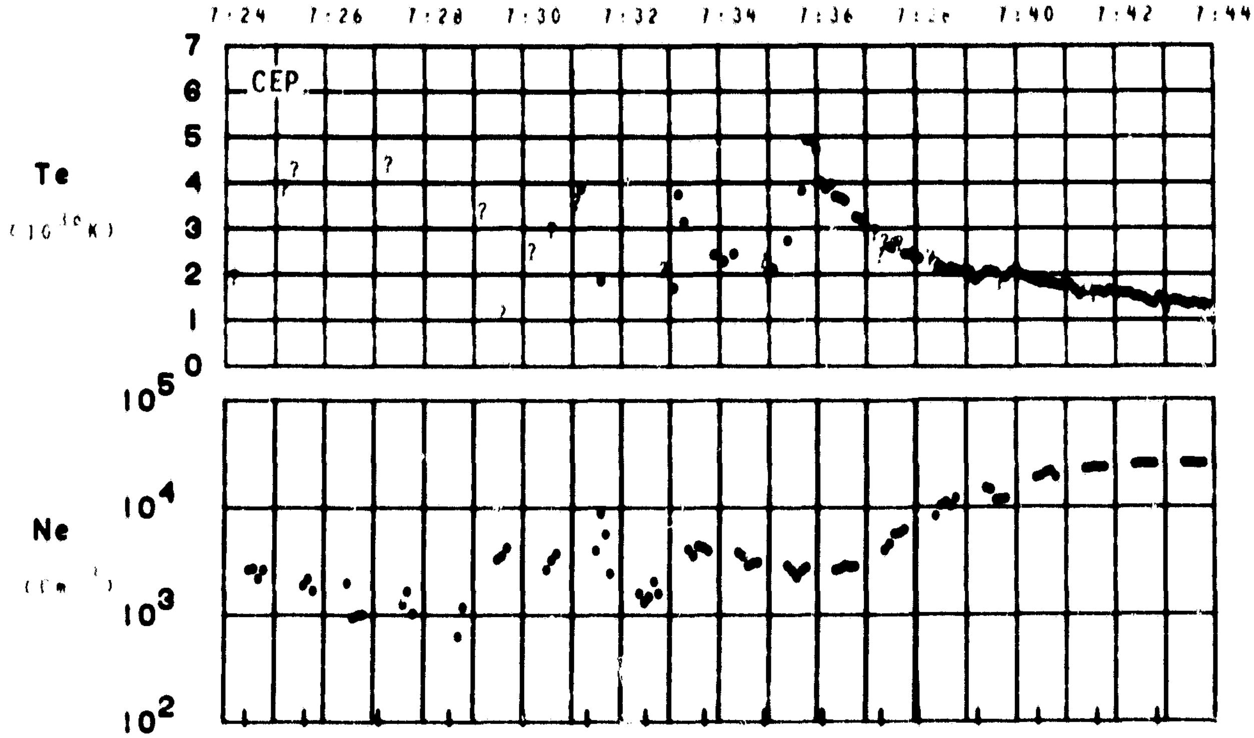

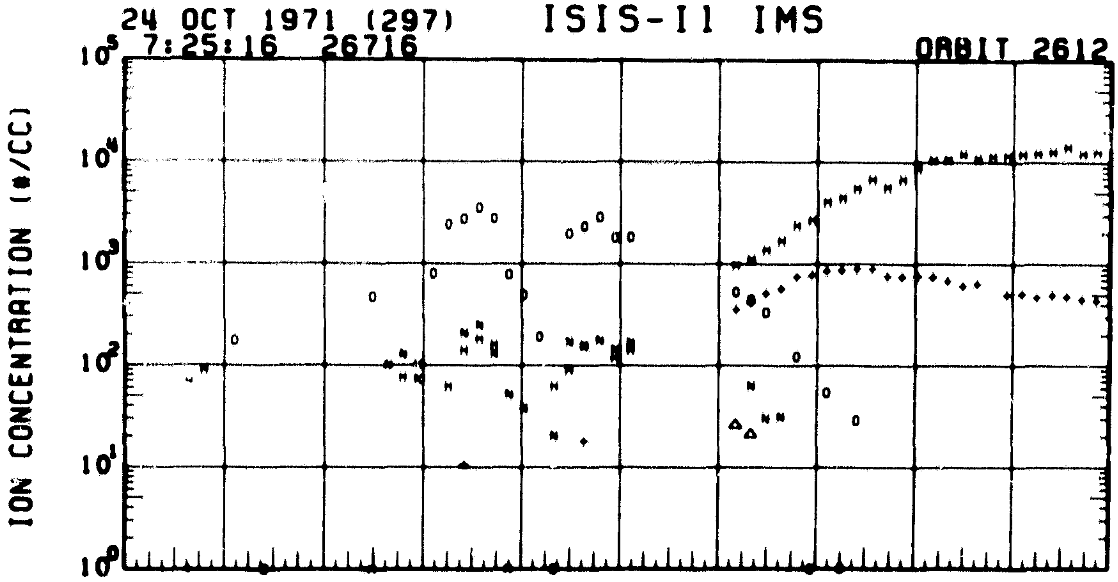

1 - H	UT	7:26	7:28	7:30	7:32	7:34	7:36	7:38	7:40	7:42
4 - +	LAST	2:57	3:08	3:14	3:17	3:20	3:21	3:23	3:24	3:25
8 - △	ALT	1:52	3:03	3:11	3:14	3:16	3:17	3:18	3:19	3:20
14 - N	DLAT	84	80	75	70	64	58	51	45	38
16 - O	INVL	84	81	76	71	66	60	55	50	46
	GLAT	77	71	64	58	52	45	38	33	27
	GLNG	-70	-88	-87	-87	-87	-87	-87	-87	-87
	SZEN	111	114	118	121	123	126	127	128	130
	ALT	1417	1419	1421	1423	1424	1425	1426	1427	1427

SET 10, FORMAT 4

RPA

711024

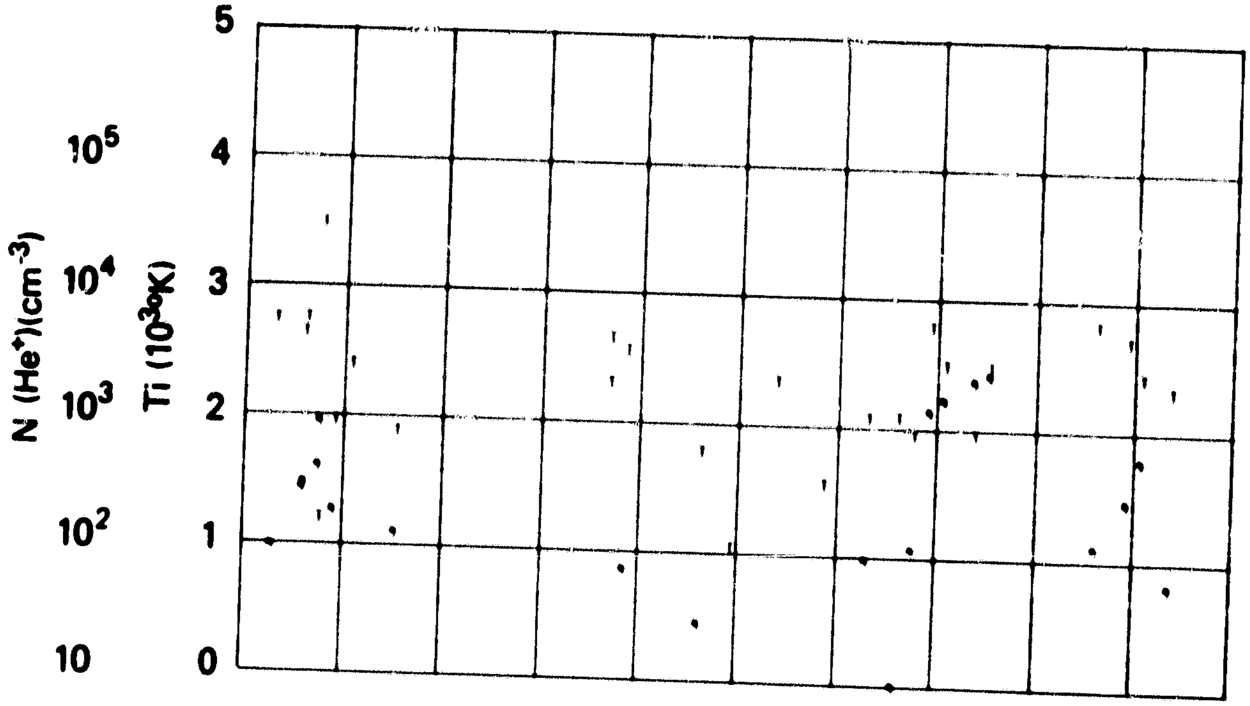

UT	7:26	7:28	7:30	7:32	7:34	7:36	7:38	7:40	7:42
LAST	2:57	3:00	3:14	3:17	3:20	3:21	3:23	3:24	3:25
MLT	1:52	3:03	3:11	3:14	3:16	3:17	3:18	3:18	3:20
DLAT	84	80	75	70	64	58	51	45	38
INVL	84	81	76	71	66	60	55	50	46
GLAT	77	71	64	58	52	45	38	33	27
GLNG	-70	-68	-67	-67	67	-67	-67	-67	67
SZEN	111	114	118	121	123	126	127	128	130
ALT	1417	1419	1421	1423	1424	1425	1426	1427	1427

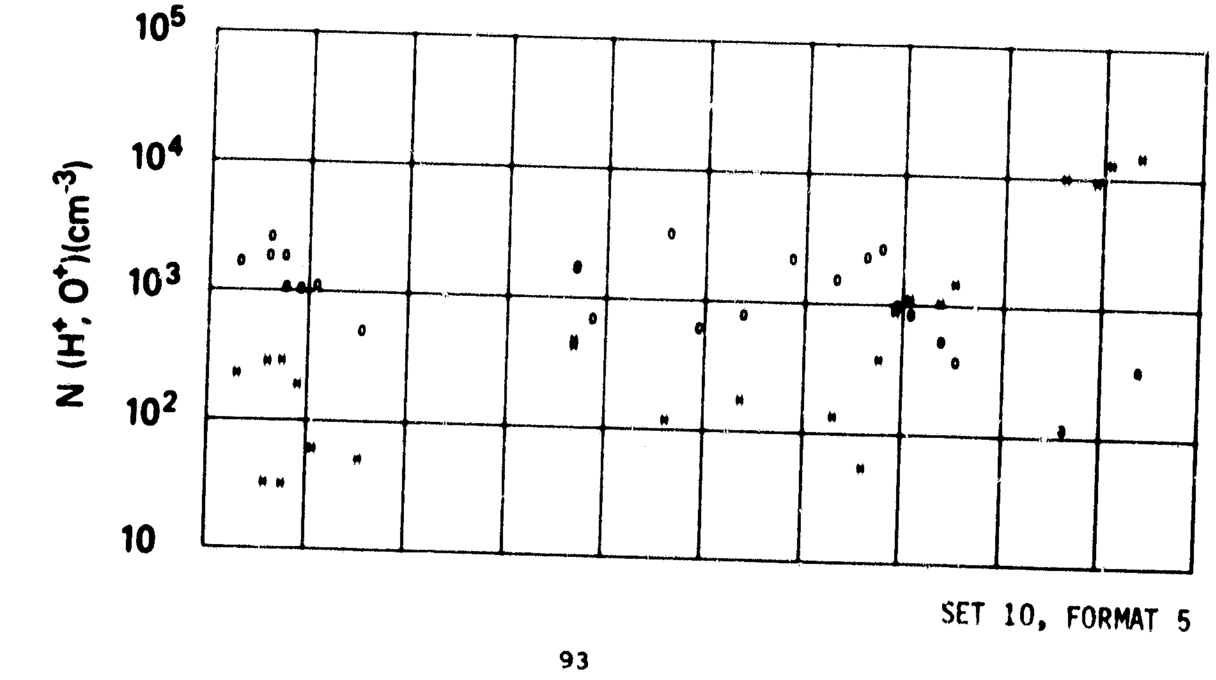

SET 10, FORMAT 5

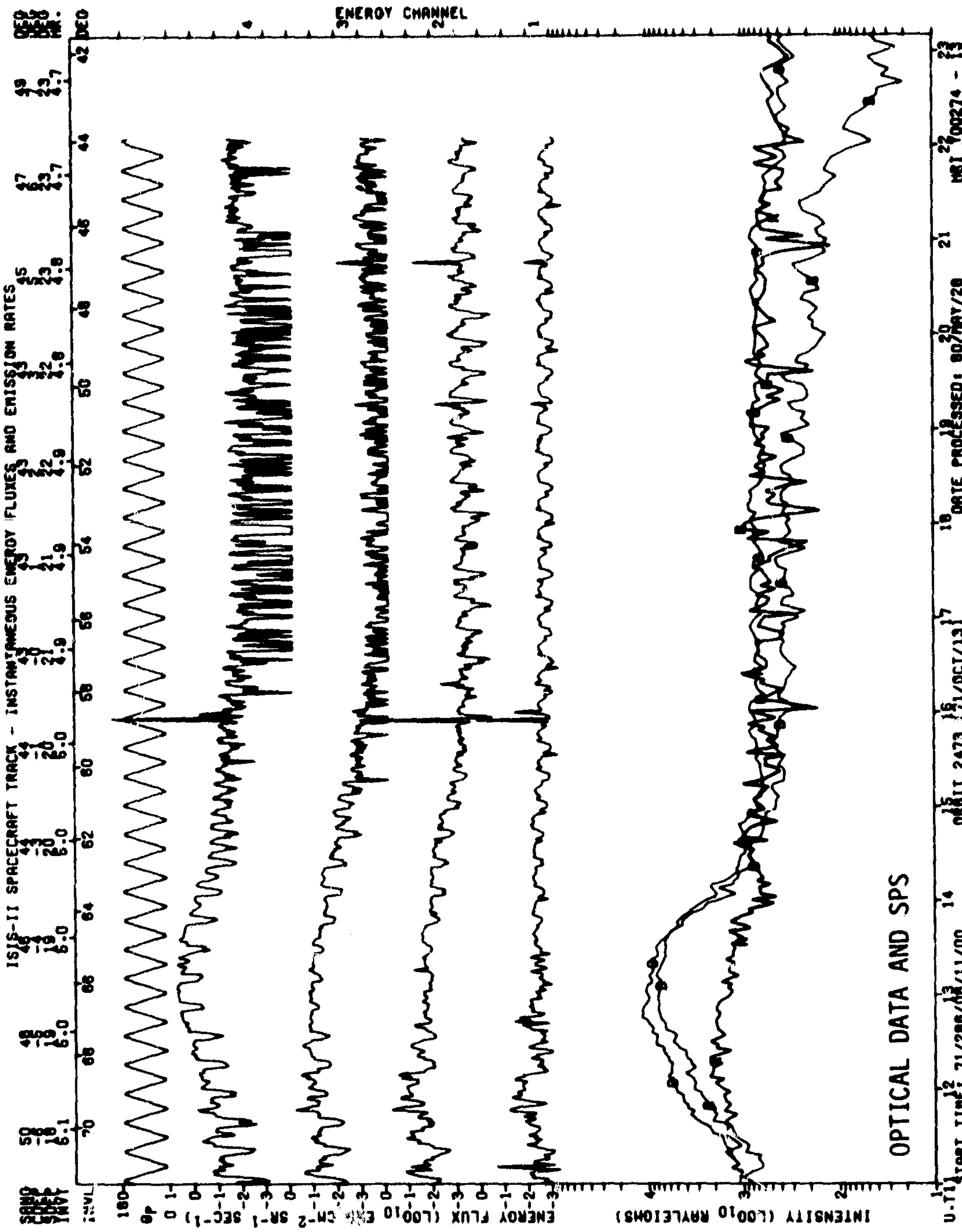

SET 11, FORMAT 1

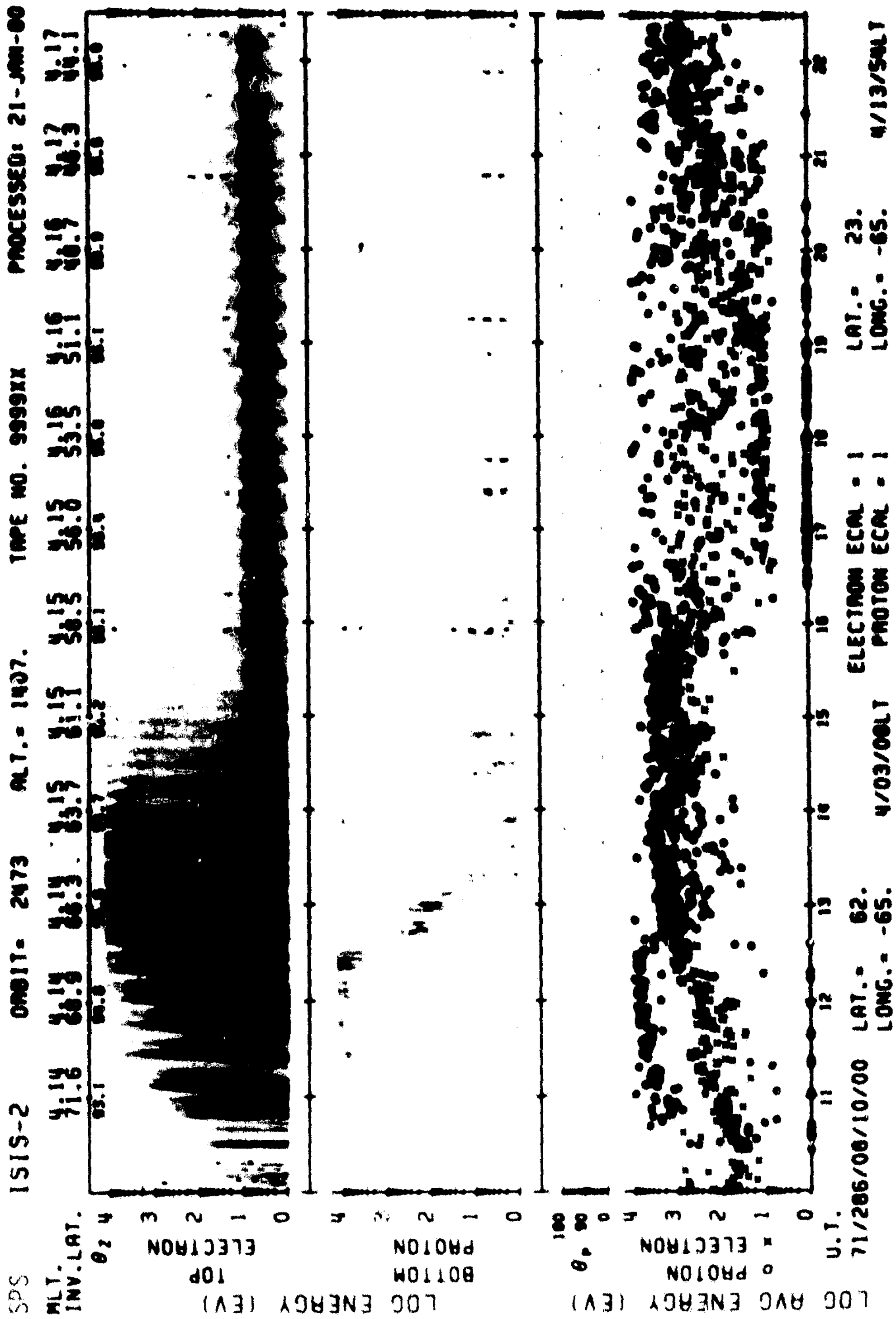

SET 11, FORMAT 6

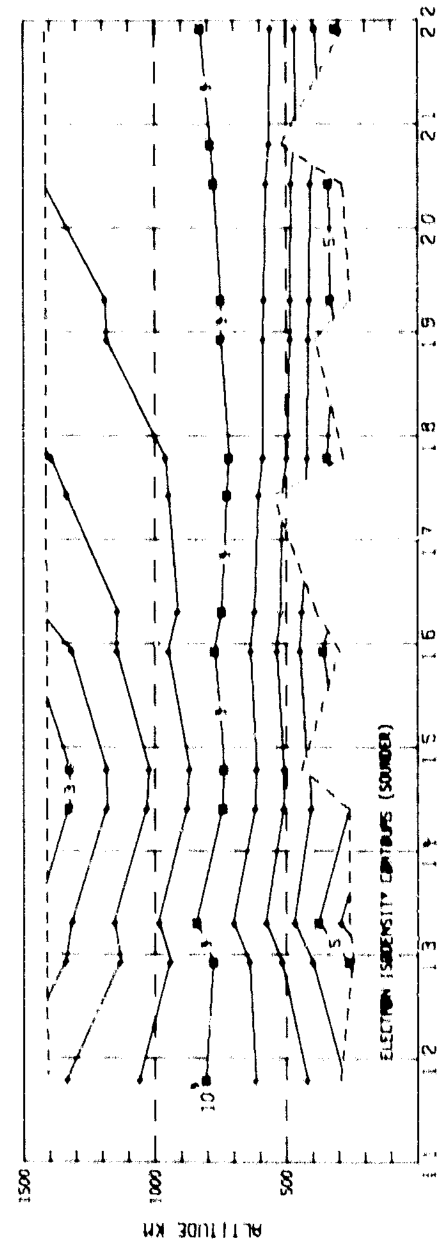

SET 11, FORMAT 2

ORBIT 2473
DATE 711013
DAY 286

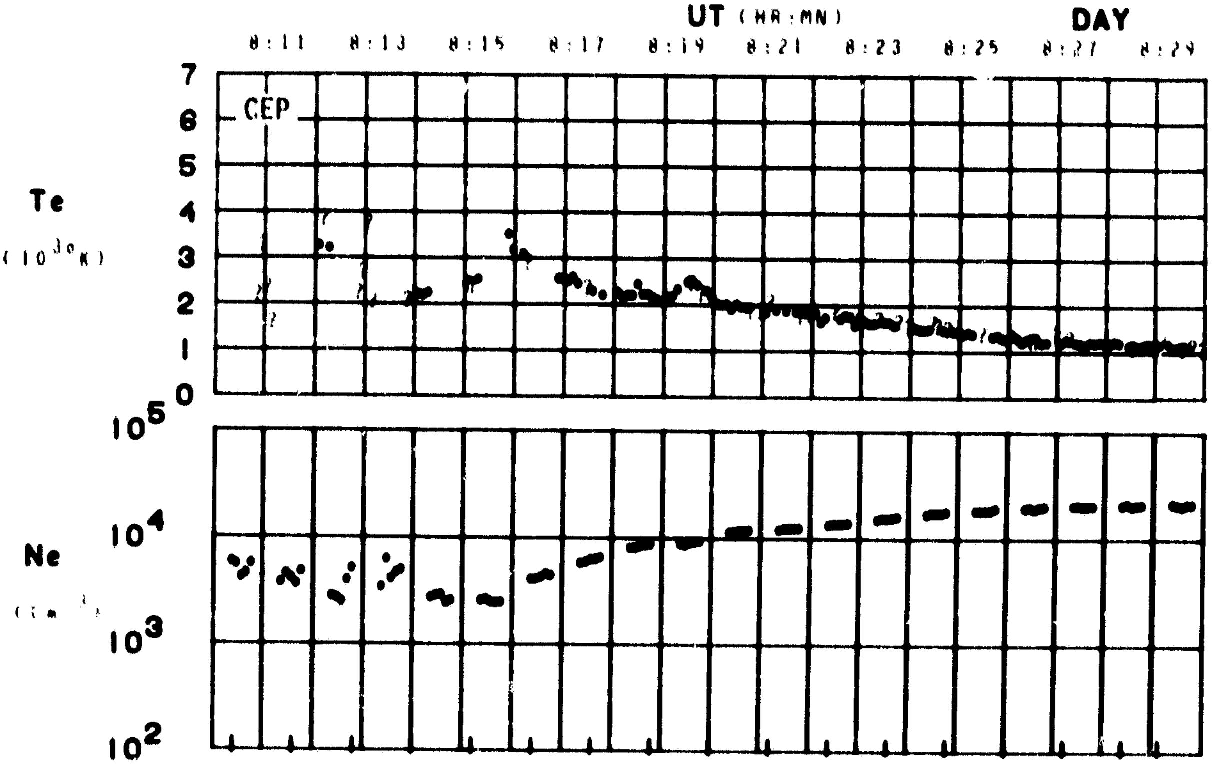

LAT	61	57	53	49	45	42	38	34	30	26	23	19	15	11	7	4	1
LONG	-65	-64	-64	-64	-64	-64	-64	-65	-65	-65	-65	-65	-65	-66	-66	-66	-66
LT	4:03	4:05	4:07	4:08	4:09	4:10	4:11	4:12	4:12	4:13	4:13	4:14	4:15	4:15	4:16	4:16	4:16
DIP	80	78	76	74	72	69	67	64	61	57	54	50	45	41	35	30	26
DIPLAT	72	68	65	61	57	54	50	46	42	38	35	31	27	24	20	16	14
L	11.9	8.5	6.4	5.1	4.1	3.5	3.0	2.6	2.3	2.1	1.9	1.7	1.6	1.5	1.5	1.4	1.4
INVLAT	73	69	66	63	60	57	54	51	48	45	43	40	38	36	34	32	31
ZA	110	111	112	113	114	115	115	116	116	117	117	117	117	116	116	116	115

SET 11, FORMAT 4

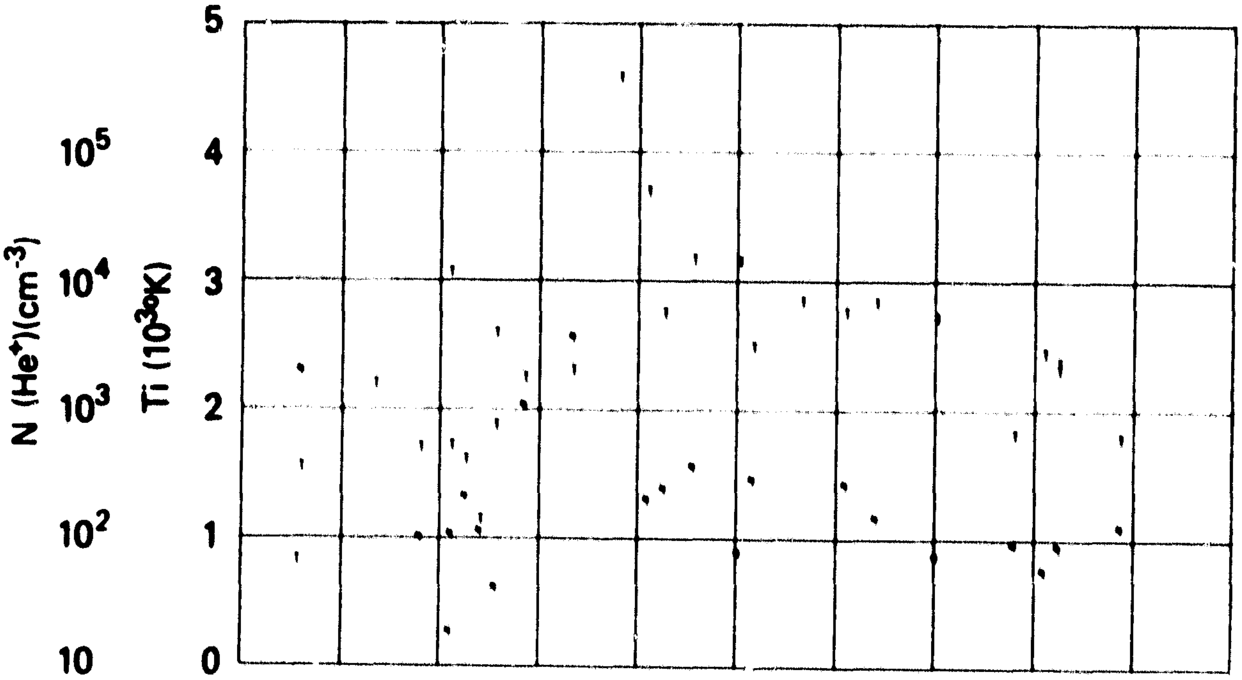

UT	08:12	08:14	08:16	08:18	08:20	08:22	08:24	08:26	08:28
LAST	04:06	04:08	04:10	04:12	04:13	04:14	04:15	04:16	04:16
MLT									
DLAT									
INVL	68	63	58	53	48	44	39	36	32
GLAT	56	50	43	37	31	24	18	12	5
GLNG	-65	-65	-65	-65	-65	-66	-66	-66	-66
SZEN	111	113	115	116	116	117	117	116	116
ALT	1409	1411	1413	1415	1417	1419	1421	1423	1425

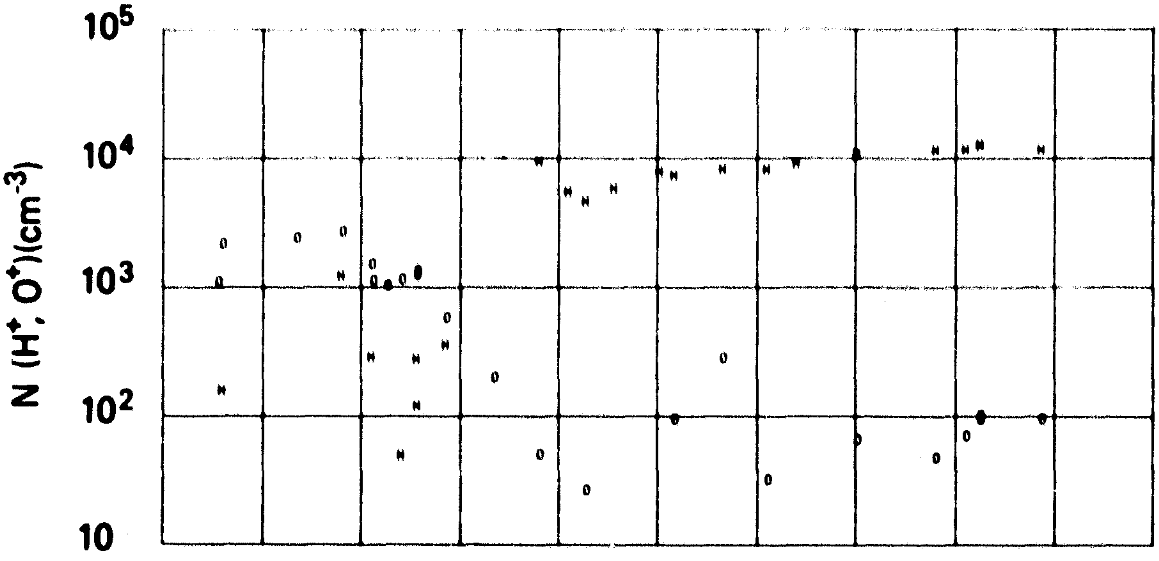

SET 11, FORMAT 5

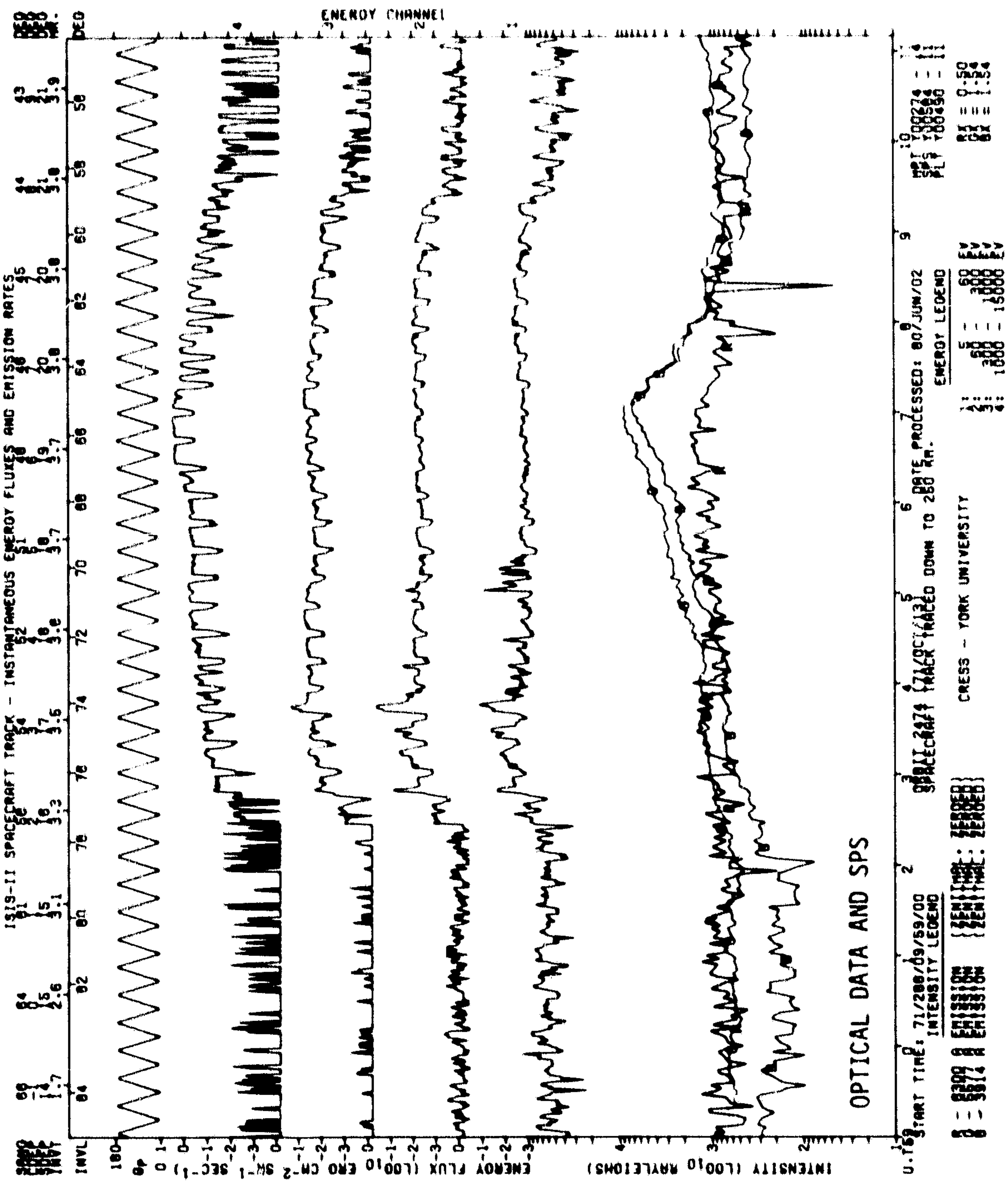

SET 12, FORMAT 1

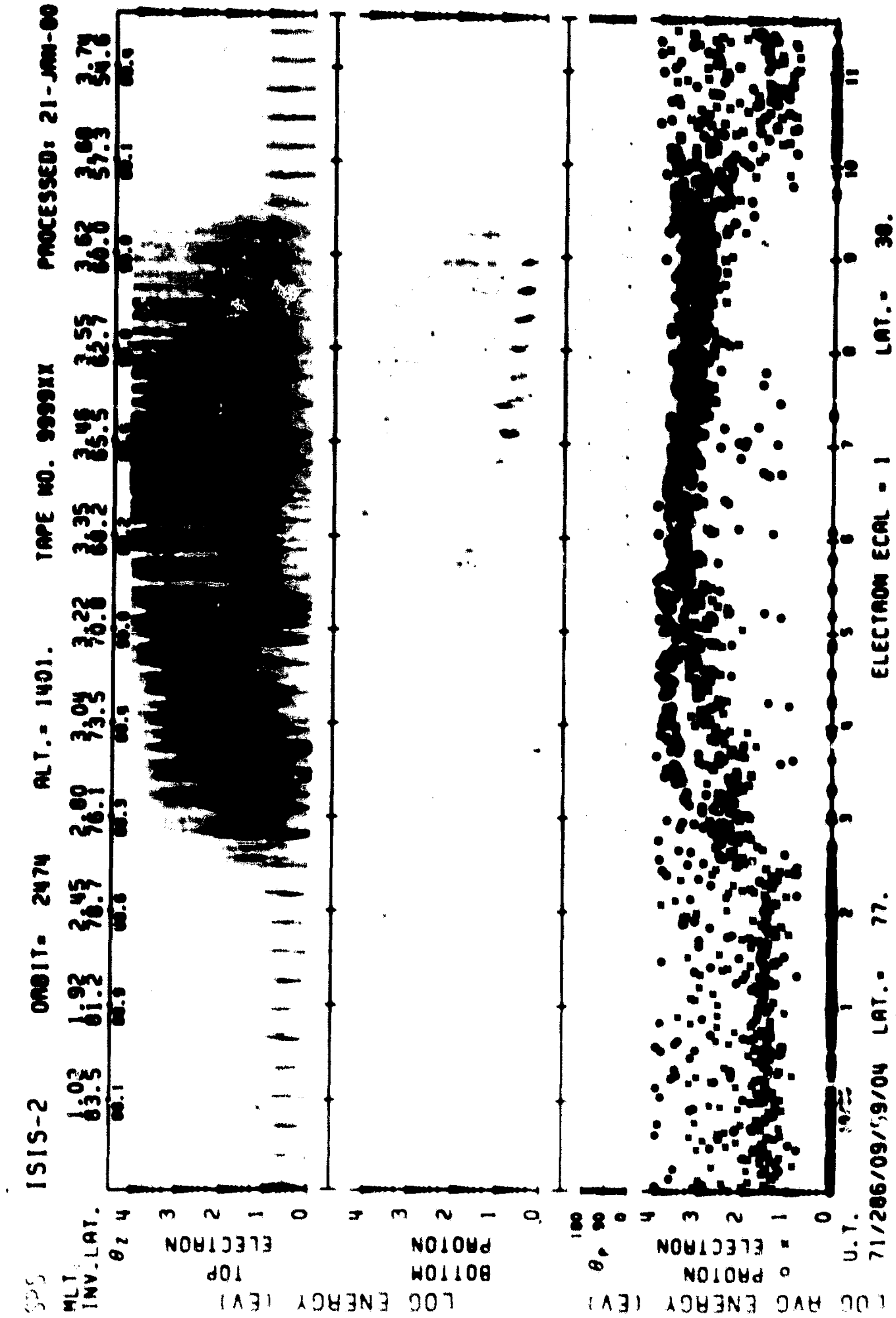

SET 12, FORMAT 6

ORBIT 2474
DATE 711013
DAY 286

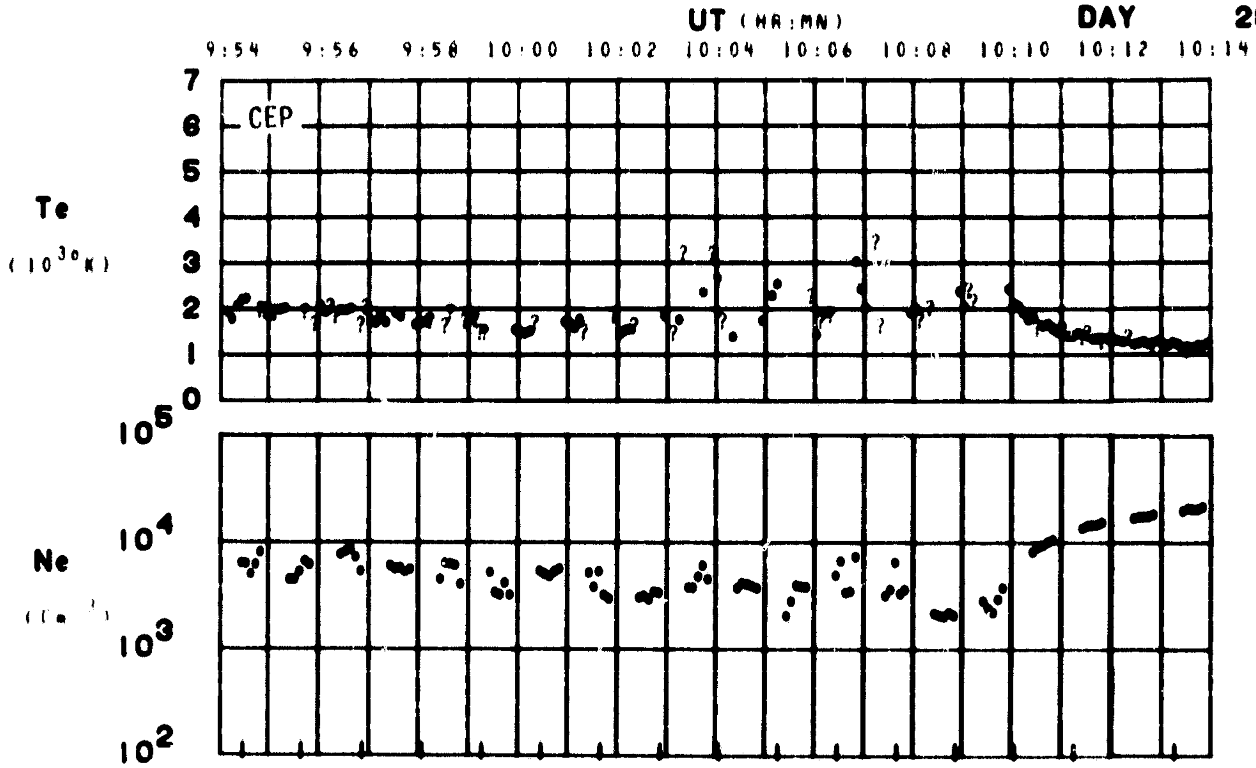

LAT	87	87	83	79	76	72	68	64	61	57	53	49	45	42	38	31
LONG	151	-130	-104	-99	-96	-95	-94	-93	-93	-93	-93	-93	-93	-93	-93	-93
LT	20:15	1:29	3:11	3:35	3:46	3:53	3:58	4:01	4:03	4:05	4:06	4:08	4:09	4:10	4:10	4:12
DIP	87	88	89	89	88	87	85	84	82	80	78	75	73	70	67	62
DIPLAT	85	87	89	89	87	84	82	78	75	71	67	63	59	55	51	44
L	35.6	90.0	97.9	100.1	96.2	60.1	29.7	18.0	12.0	8.6	6.4	5.0	4.1	3.4	2.9	2.3
INVLAT	80	83	84	84	84	82	79	76	73	70	66	63	60	57	53	48
ZA	98	100	101	103	105	106	107	109	110	111	112	113	114	115	116	116

SET 12, FORMAT 4

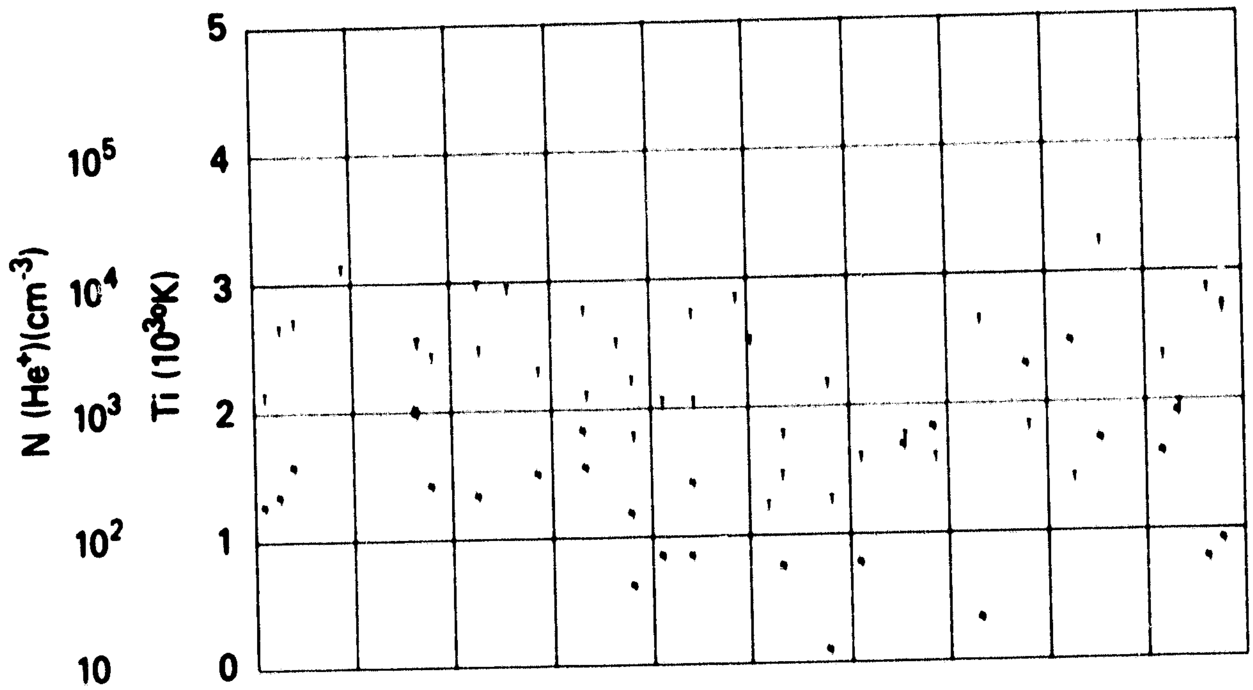

UT	09:56	09:58	10:00	10:02	10:04	10:06	10:08	10:10	10:12
LAST	02:20	03:34	03:51	03:59	04:03	04:06	04:08	04:10	04:11
MLT									
DLAT									
INVL	84	84	83	78	73	68	62	57	51
GLAT	[illegible]	80	74	68	61	55	49	42	36
GLNG	-117	-99	-96	-94	-94	-93	-93	-93	-94
SZEN	100	103	105	[illegible]	110	112	113	115	116
ALT	1395	1399	1402	1405	1407	1409	1412	1414	1416

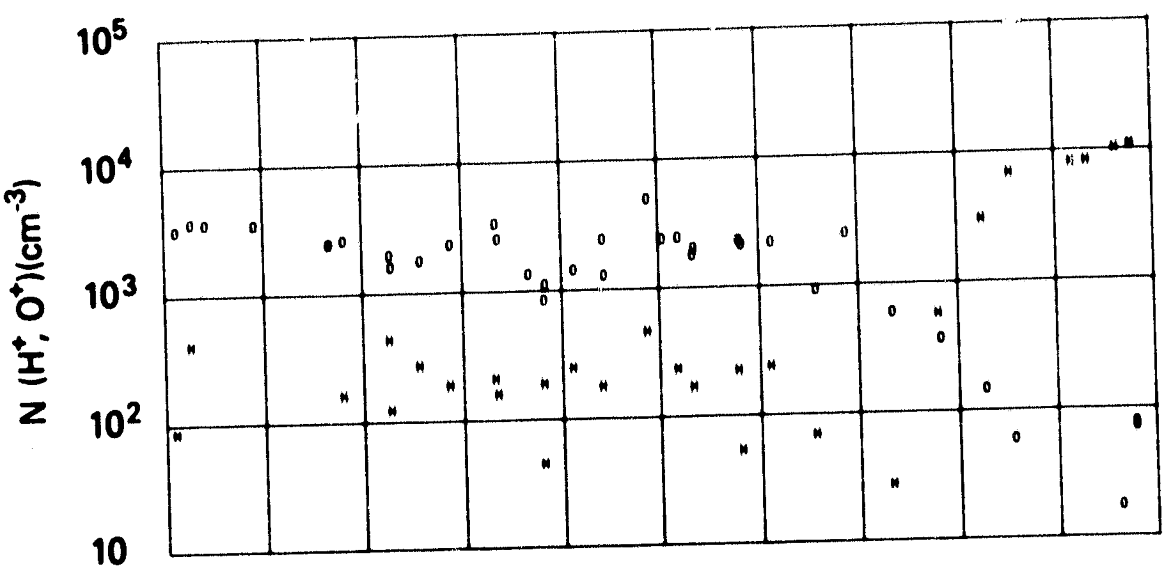

SET 12, FORMAT 5

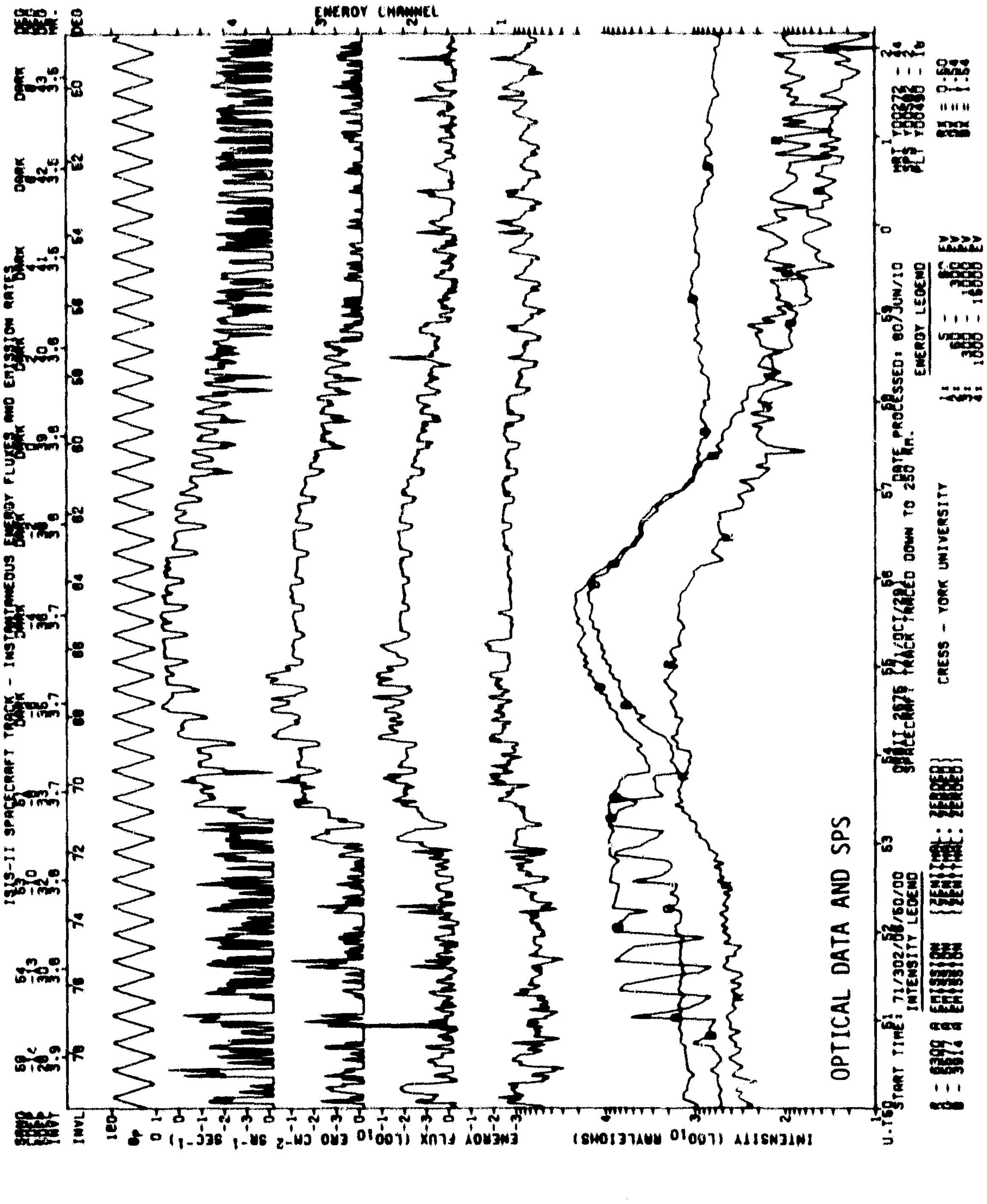

SET 13, FORMAT 1

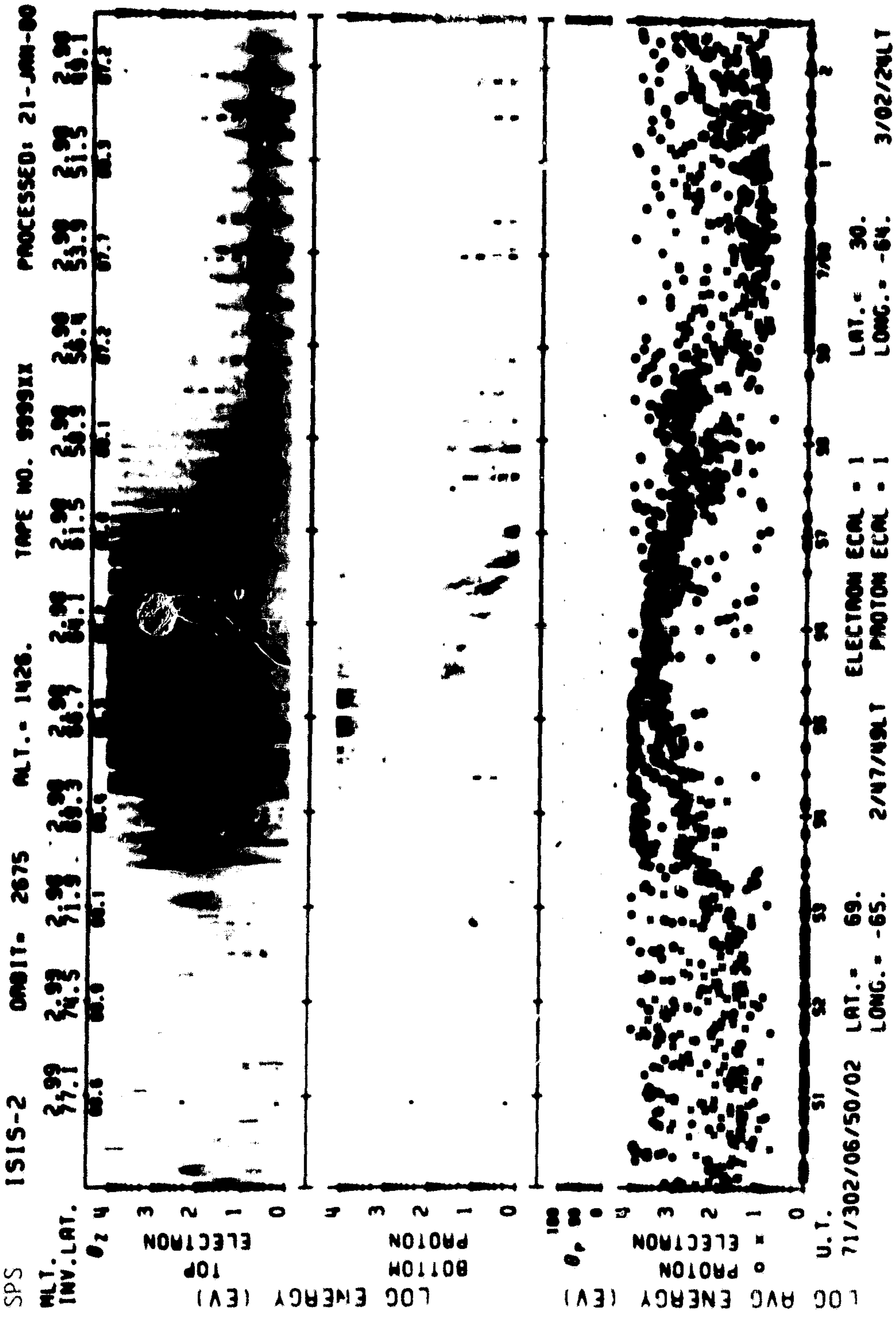

SET 13, FORMAT 6

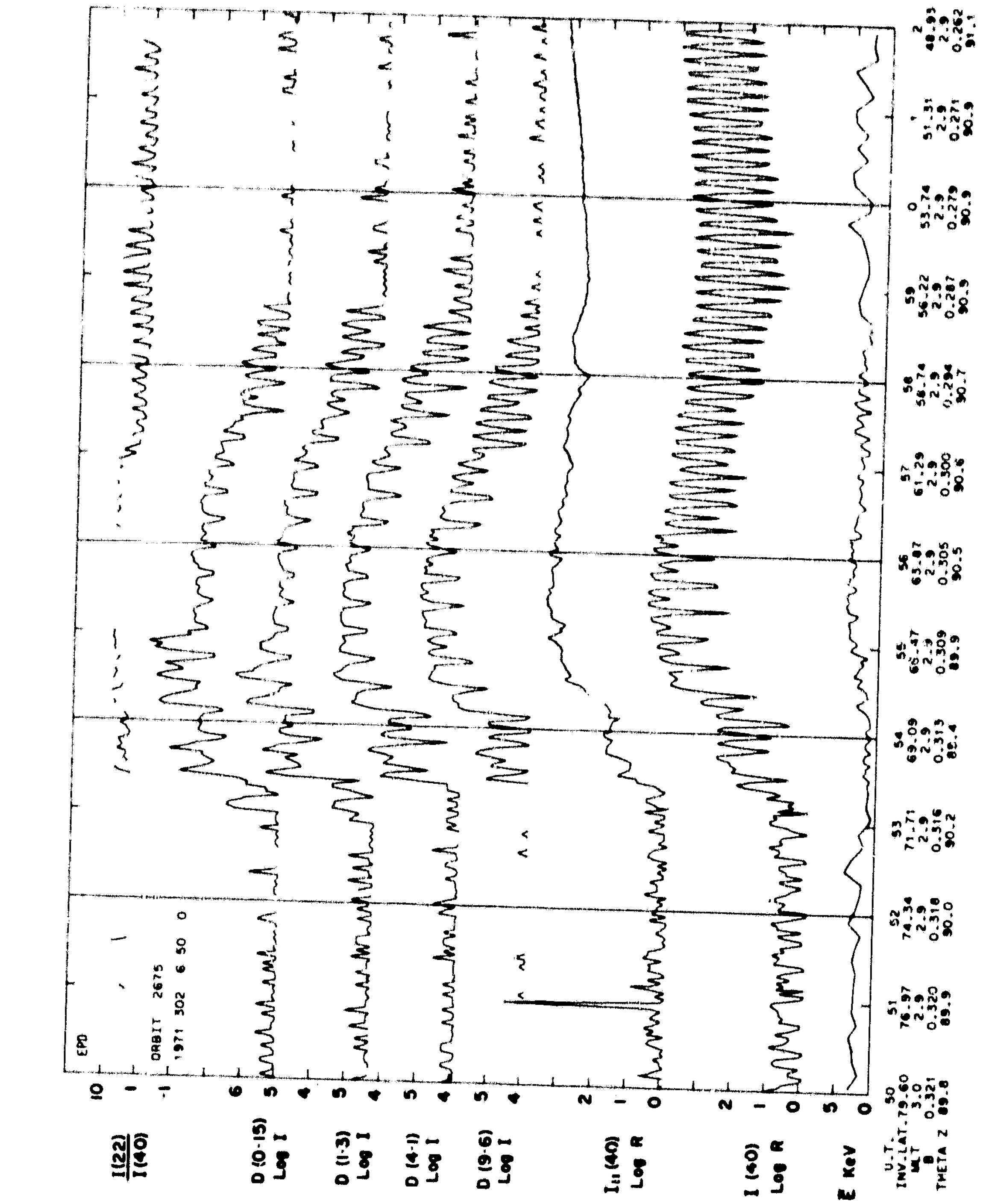

SET 13, FORMAT 3

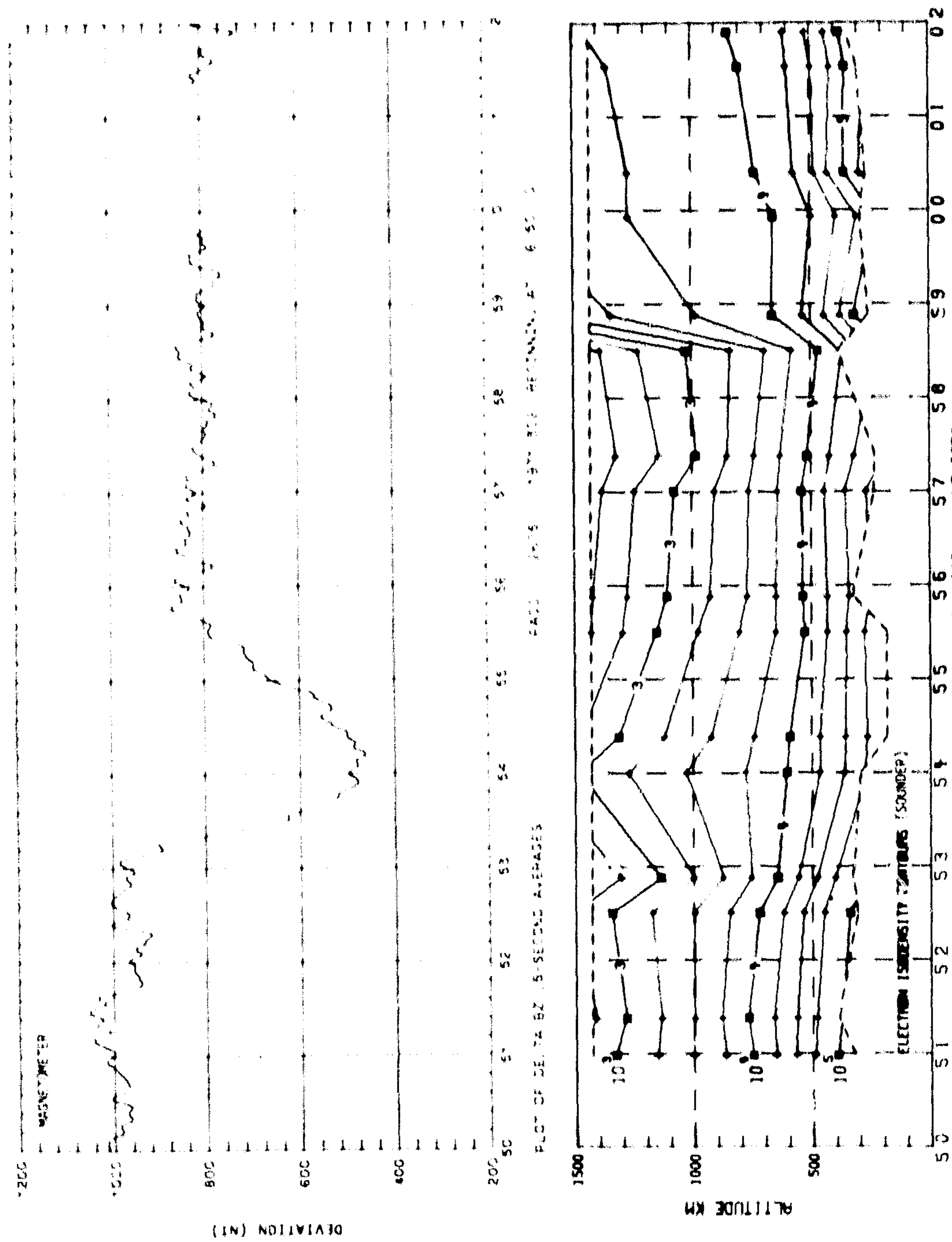

SET 13, FORMAT 2

ORBIT 2675
DATE 711029
DAY 302

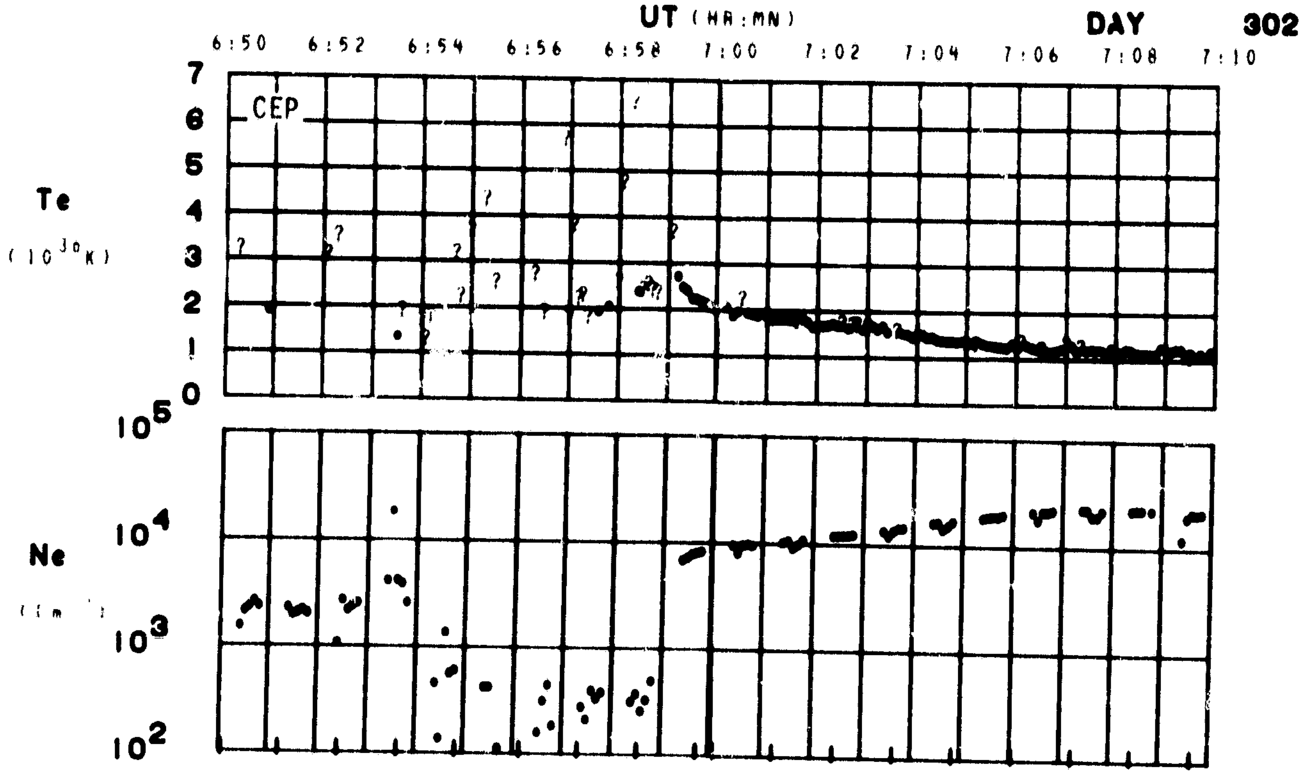

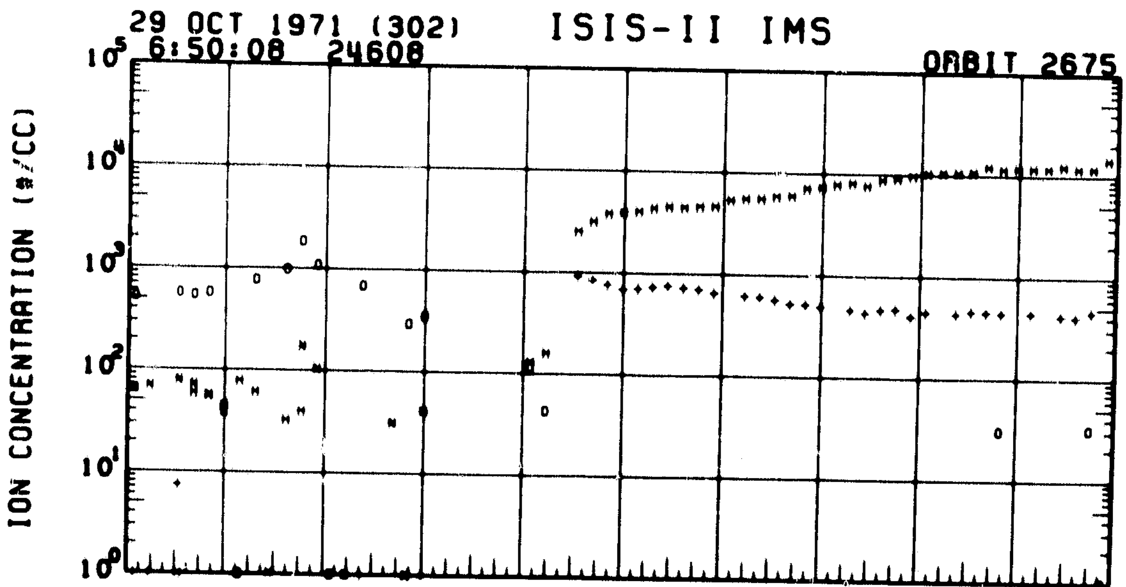

1 - M
4 - +
8 - Δ
14 - N
16 - O

UT	6:52	6:54	6:58	7:00	7:02	7:04	7:06	7:08
LAST	2:52	2:58	2:60	3:01	3:02	3:03	3:04	3:05
MLT	2:58	2:58	2:59	2:58	2:59	2:59	2:59	2:60
DLAT	73	67	55	48	42	36	30	24
INVL	74	69	58	54	49	44	40	36
GLAT	63	58	44	37	31	25	18	12
GLNG	-83	-83	-83	-83	-83	-83	-84	-84
SZEN	122	126	131	133	135	135	136	135
ALT	1427	1428	1428	1428	1428	1428	1428	1427

SET 13, FORMAT 4

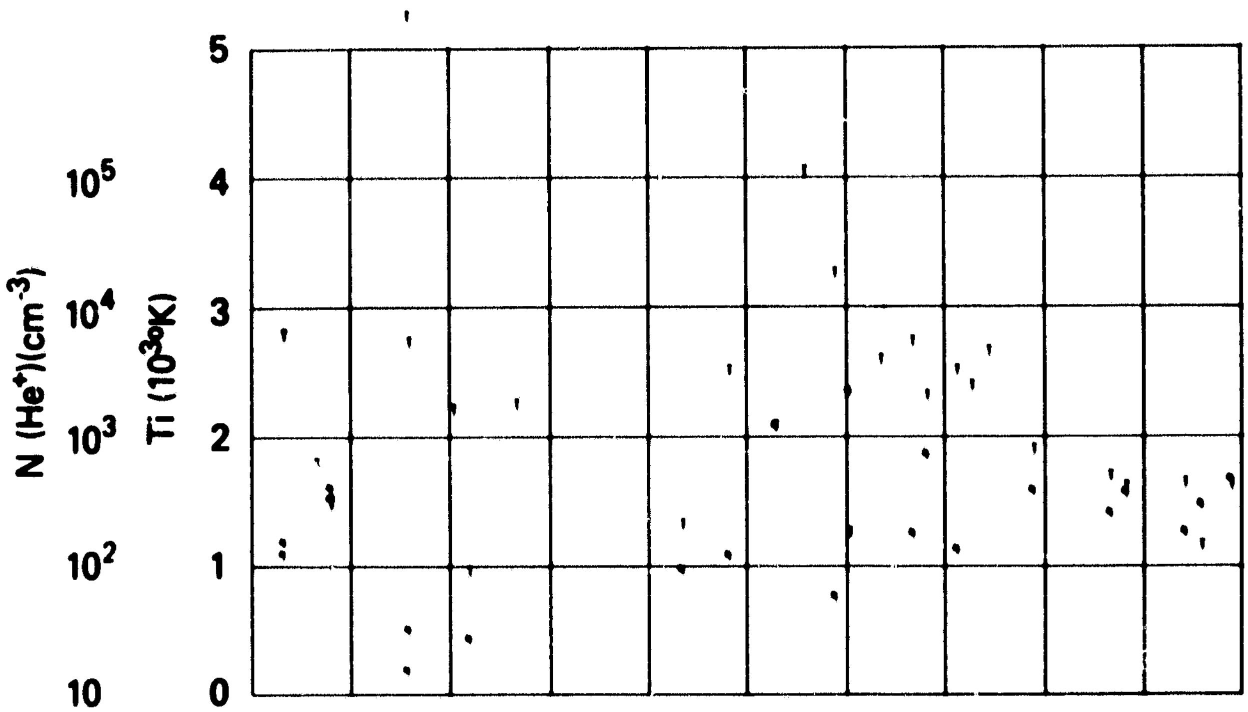

UT	6:52	6:54	6:58	7:00	7:02	7:04	7:06	7:08
LAST	2:52	2:58	2:60	3:01	3:02	3:03	3:04	3:05
ALT	2:59	2:59	2:59	2:59	2:59	2:59	2:59	2:60
DLAT	73	67	55	49	42	36	30	24
INVL	74	69	59	54	49	44	40	36
GLAT	63	56	44	37	31	25	19	12
GLNG	-63	-63	-53	-63	-63	-63	-64	-64
SZEN	122	126	131	133	135	135	136	135
ALT	1427	1428	1429	1429	1429	1428	1428	1427

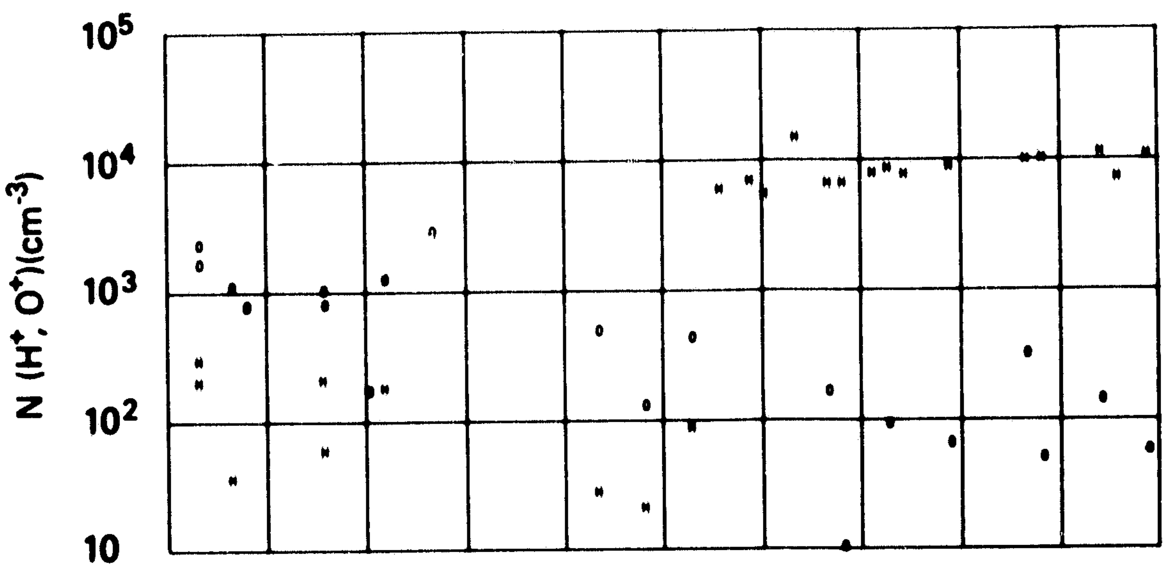

SET 13, FORMAT 5

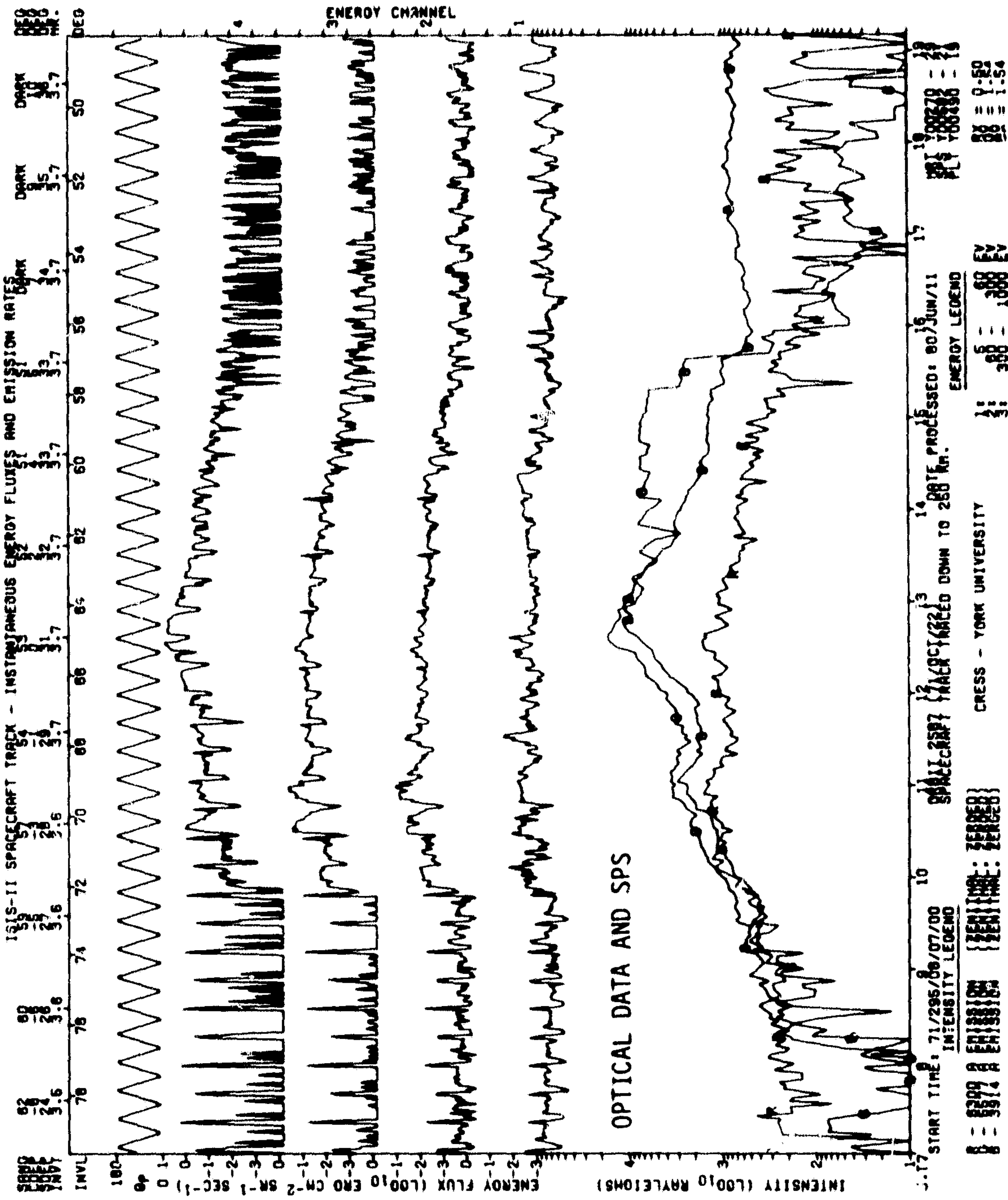

SET 14, FORMAT 1

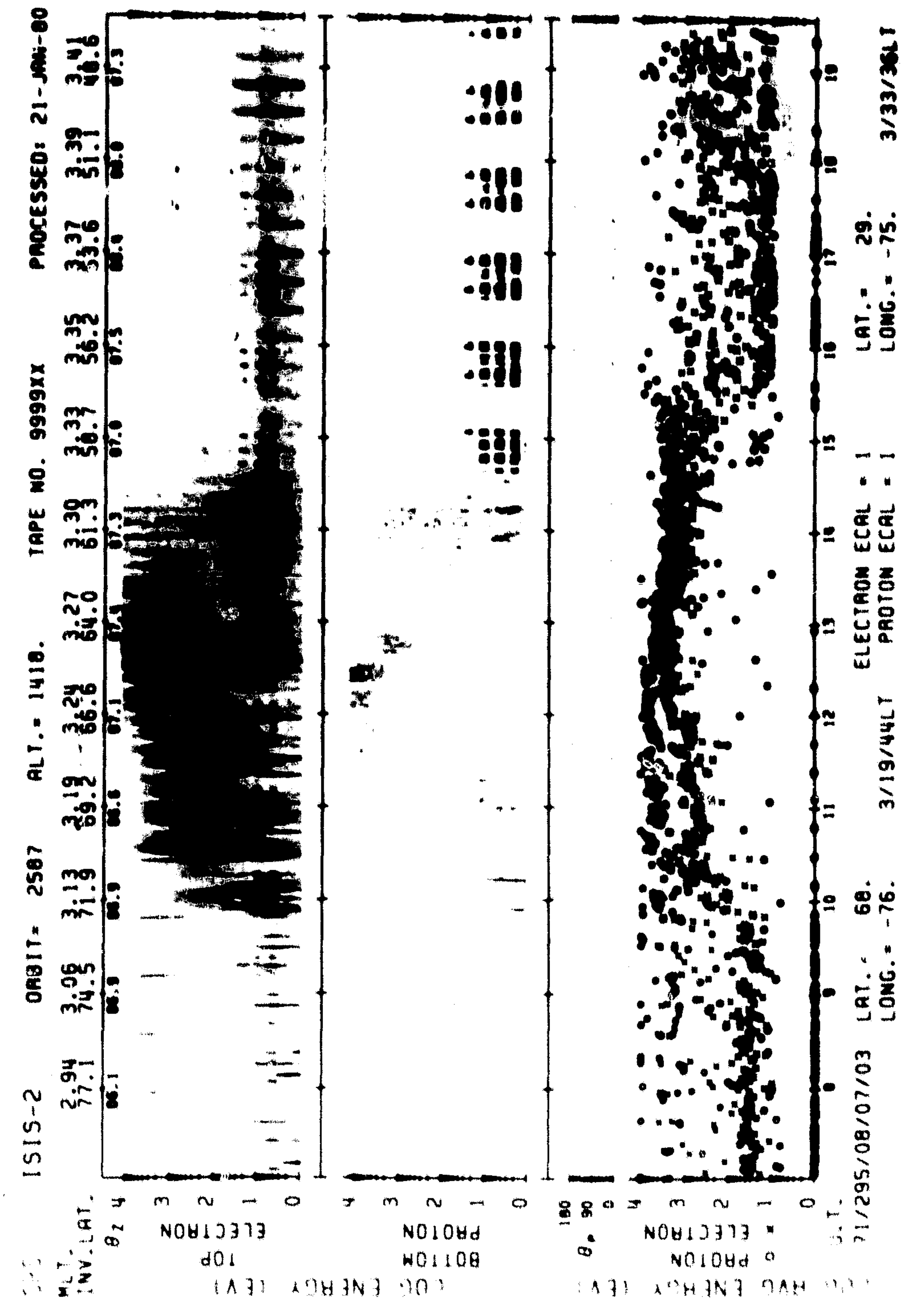

SET 14, FORMAT 6

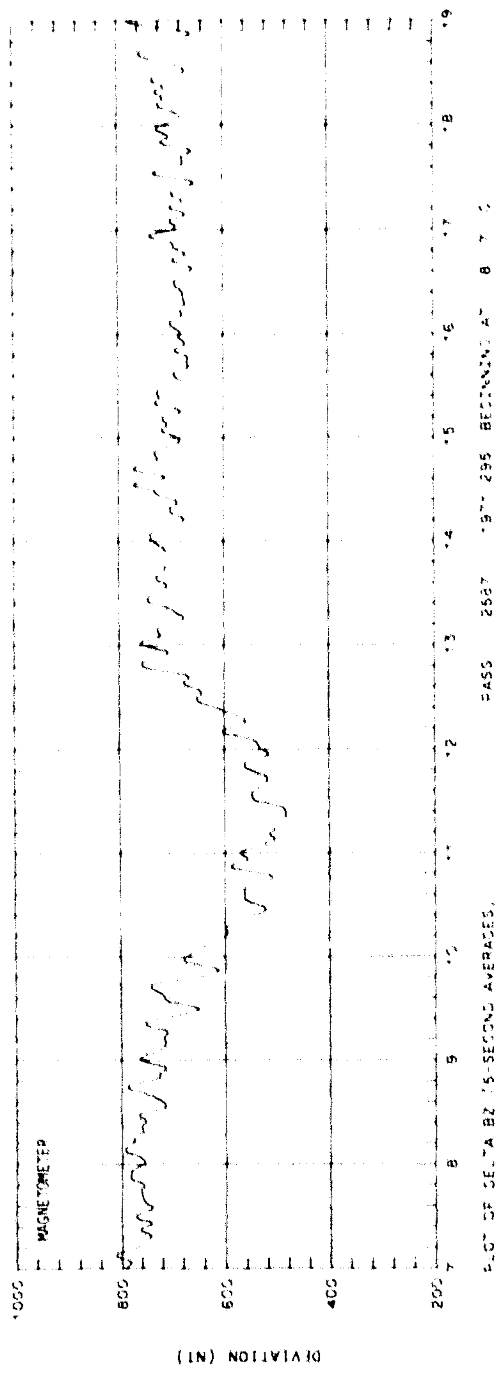

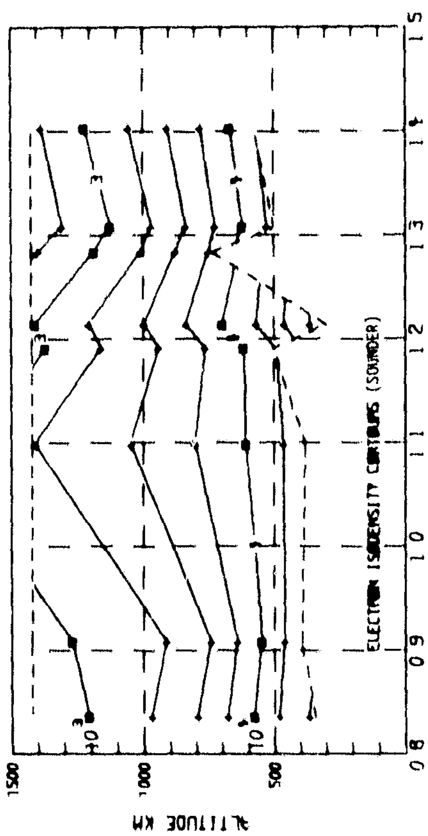

SET 14, FORMAT 2

ORBIT 2587
DATE 711022
DAY 295

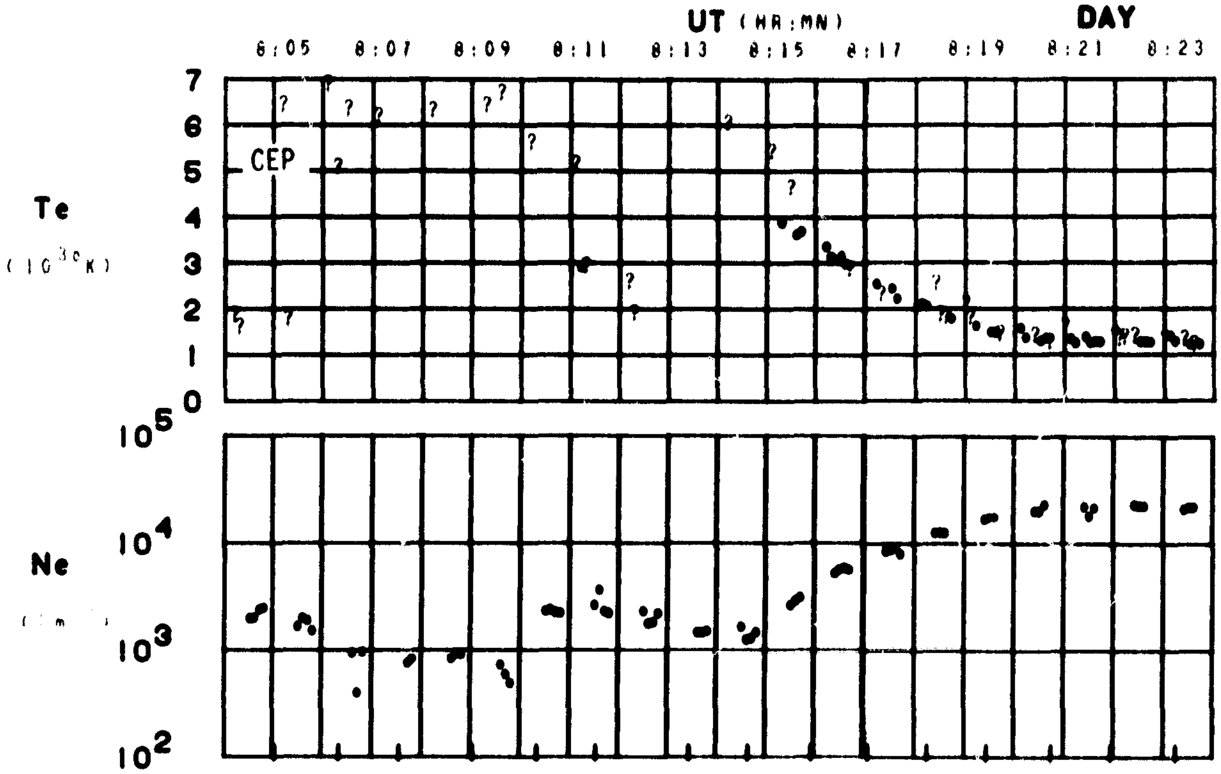

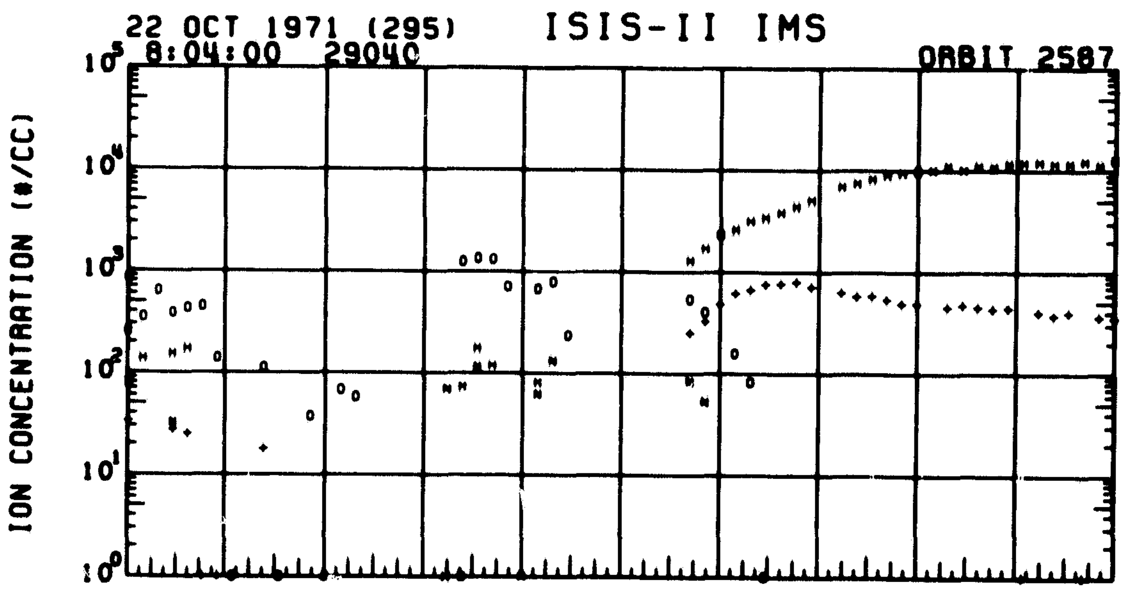

1 - H
4 - +
8 - Δ
14 - N
16 - O

UT	8:06	8:08	8:10	8:12	8:16	8:18	8:20	8:22
LAST	3:16	3:22	3:26	3:28	3:32	3:33	3:34	3:35
MLT	2:28	2:57	3:08	3:14	3:21	3:24	3:25	3:27
DLAT	82	77	72	66	53	46	40	33
INVL	82	77	72	66	56	51	46	41
GLAT	71	65	58	52	40	33	27	21
GLNG	-75	-74	-74	-74	-74	-74	-74	-75
SZEN	113	116	118	121	125	127	127	128
ALT	1416	1418	1421	1422	1424	1425	1426	1427

SET 14, FORMAT 4

RPA

711022

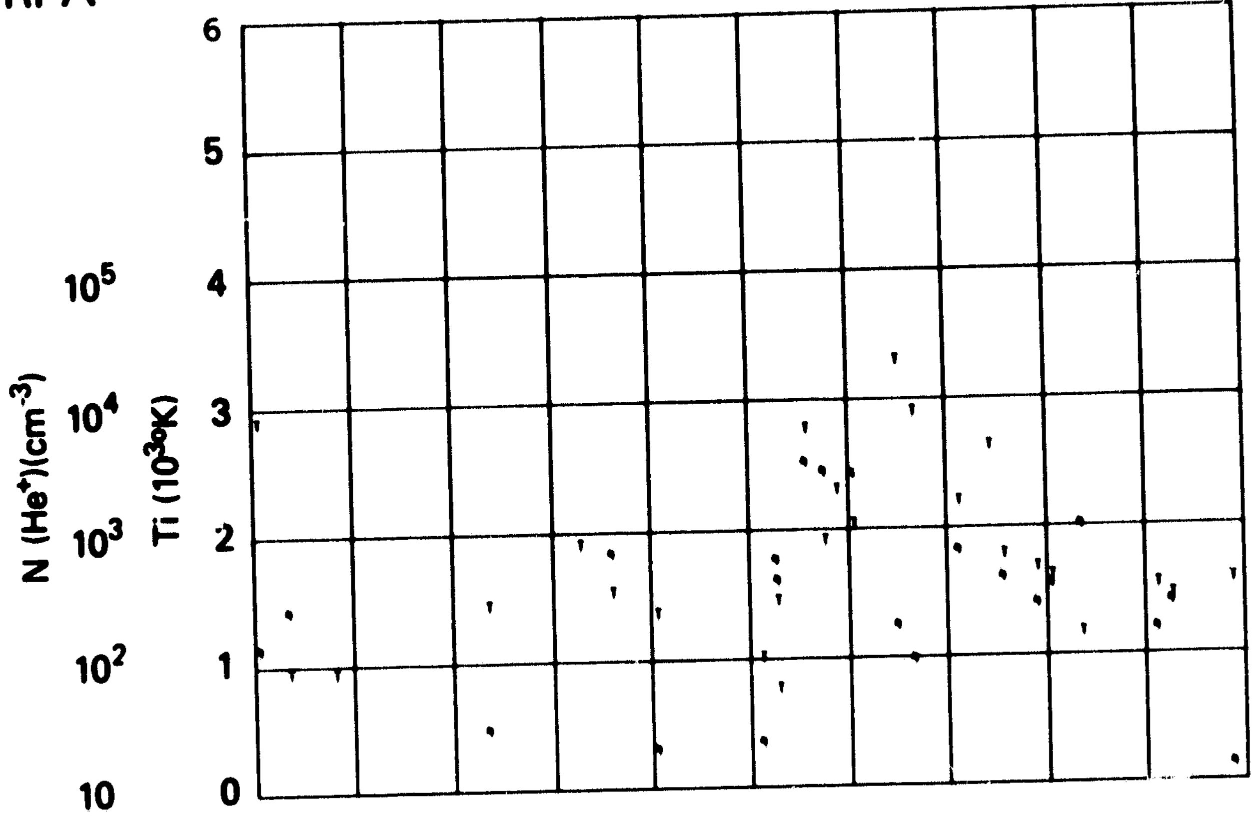

UT	8:06	8:08	8:10	8:12	8:16	8:18	8:20	8:22
LAST	3:16	3:22	3:26	3:28	3:32	3:33	3:34	3:35
MLT	2:20	2:57	3:08	3:14	3:21	3:24	3:25	3:27
DLAT	82	77	72	66	53	46	40	33
INVL	82	77	72	66	56	51	46	41
GLAT	71	65	59	52	40	33	27	21
GLNG	-75	-74	-74	-74	-74	-74	-74	-75
SZEN	113	116	119	121	125	127	127	128
ALT	1416	1419	1421	1422	1424	1425	1428	1427

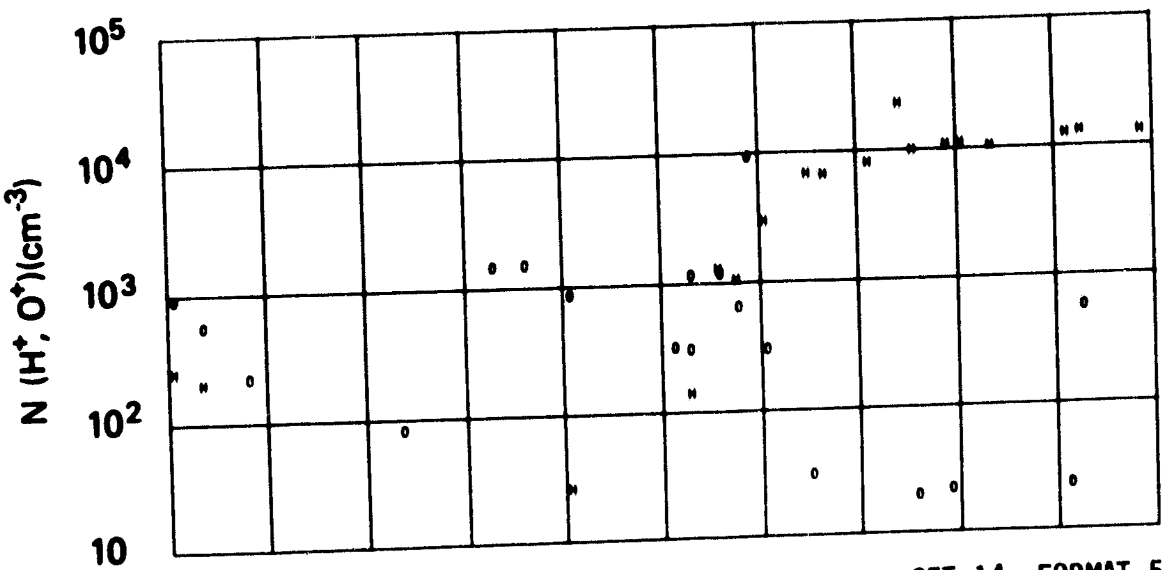

SET 14, FORMAT 5

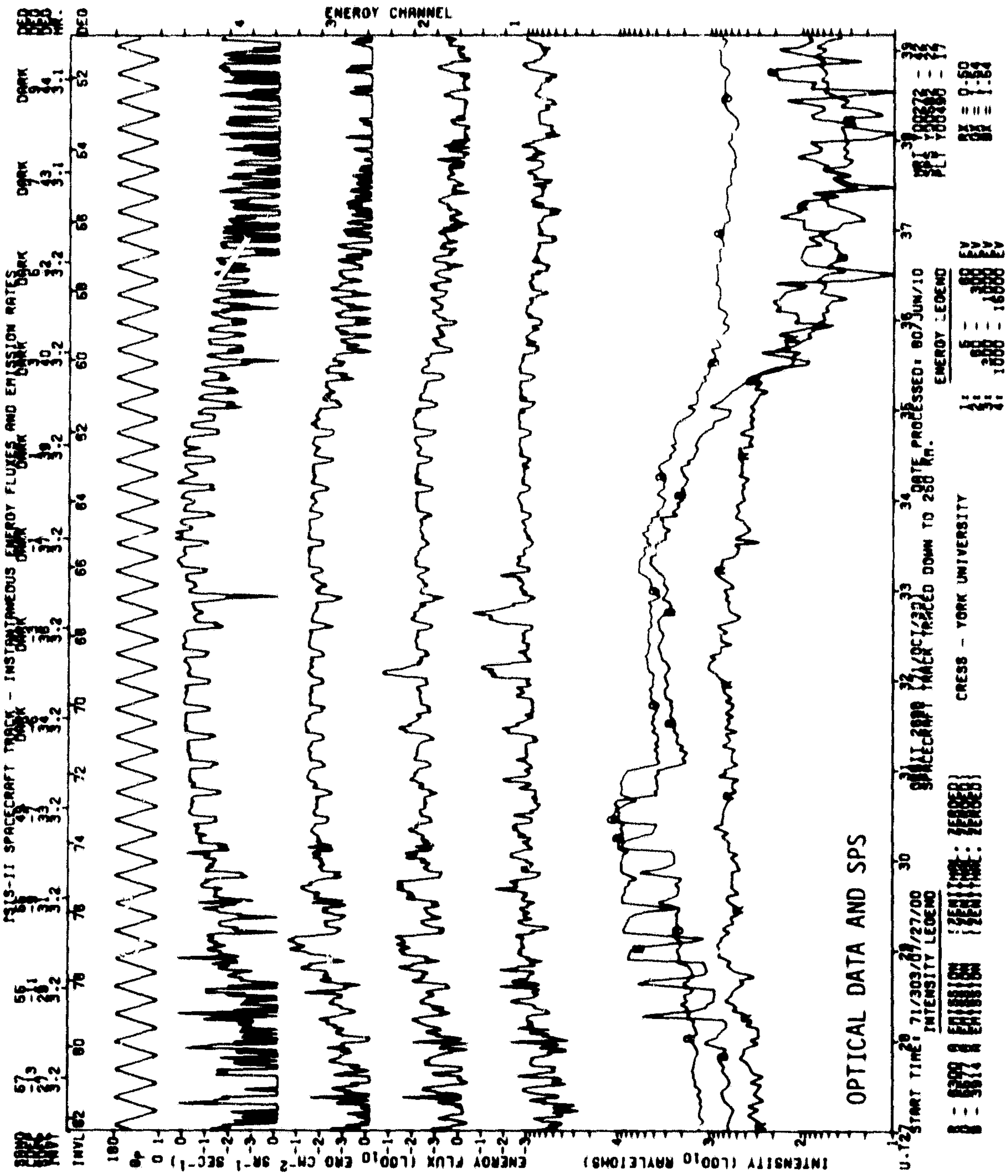

SET 15, FORMAT 1

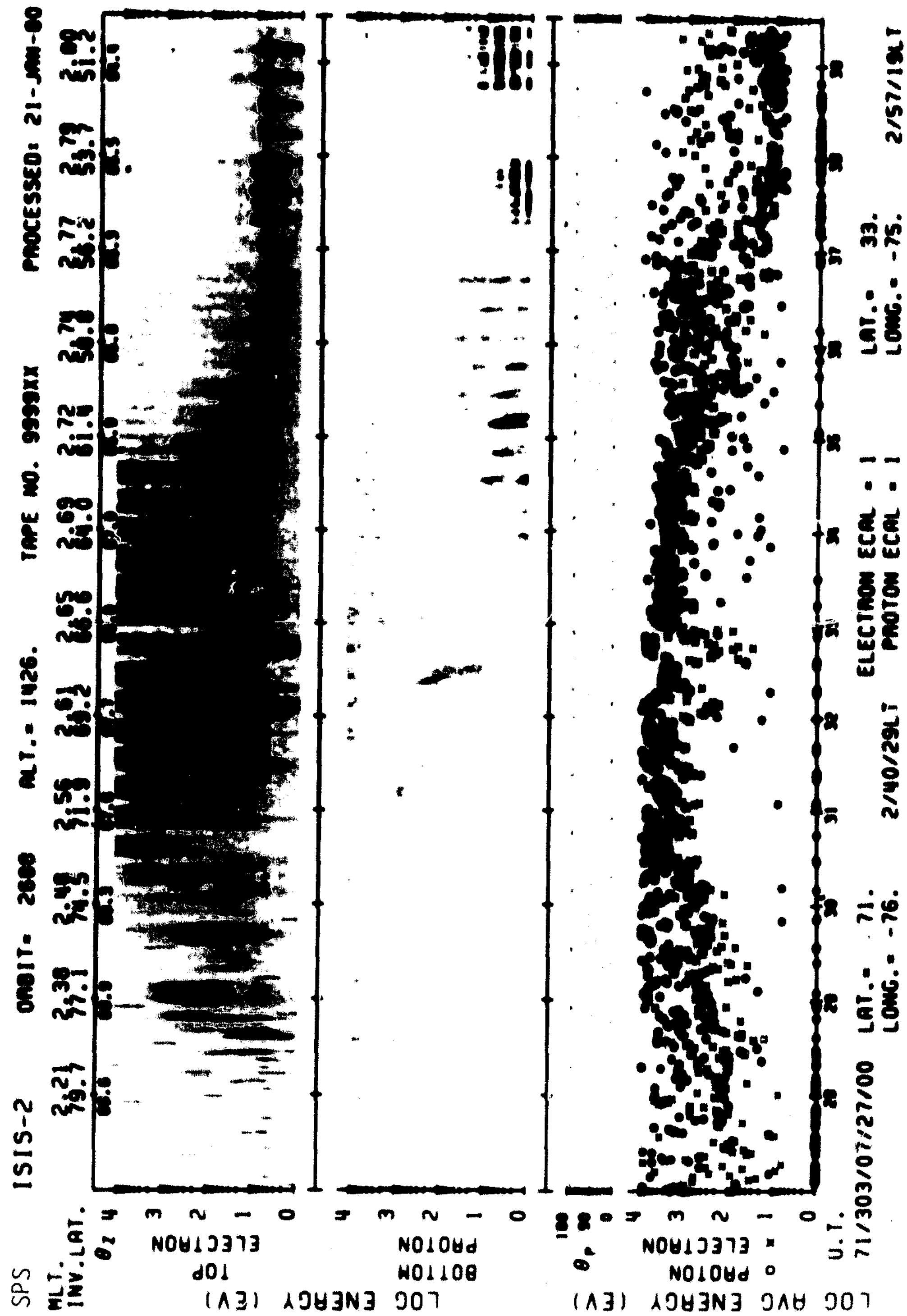

SET 15, FORMAT 6

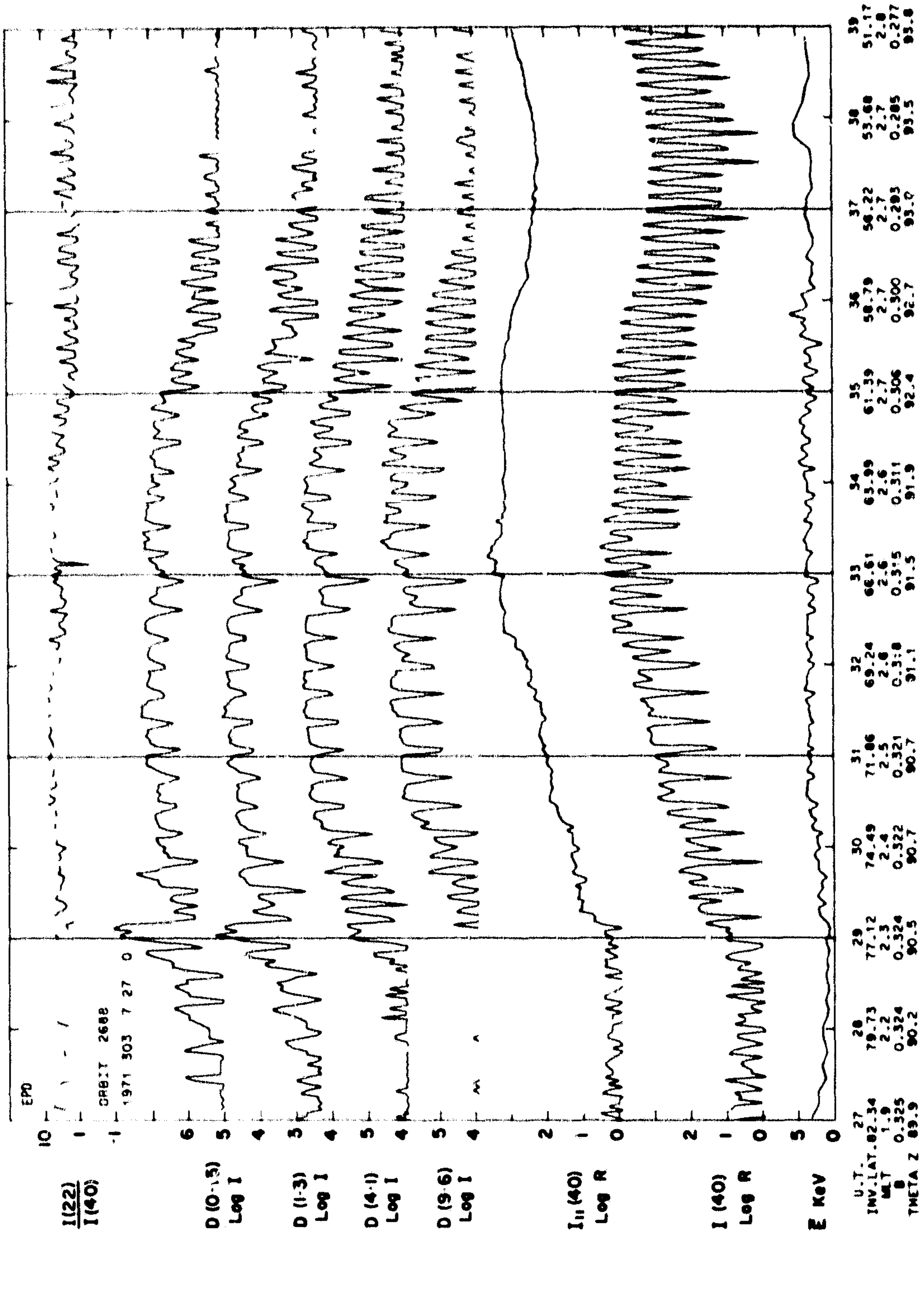

SET 15, FORMAT 3

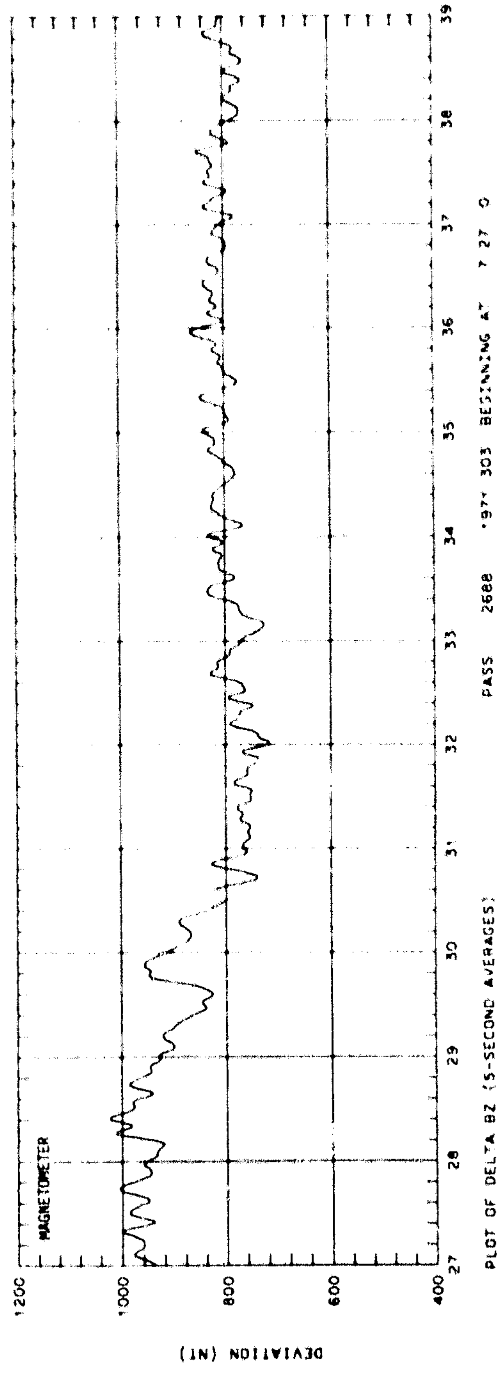

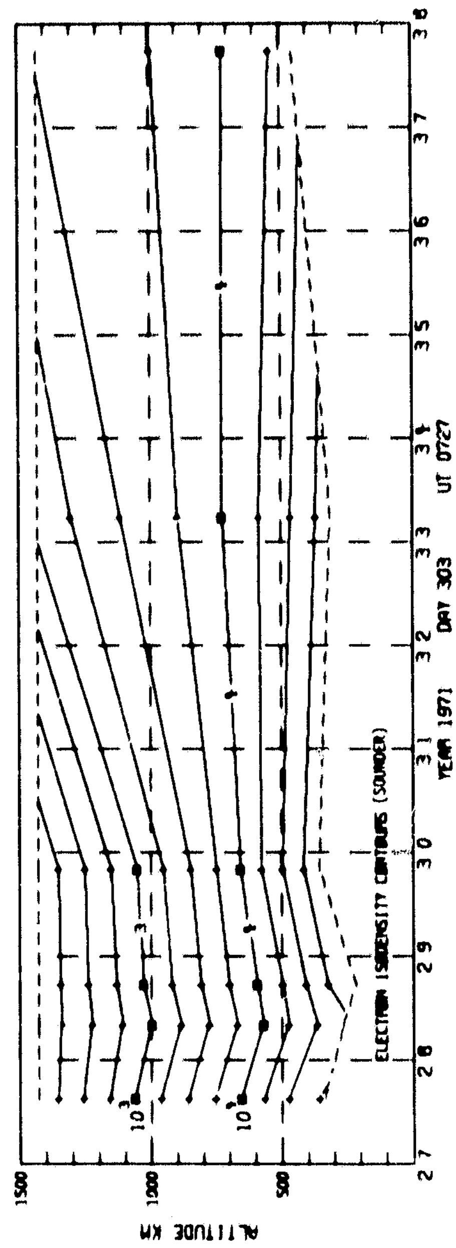

SET 15, FORMAT 2

ORBIT 2688
DATE 711030
DAY 303

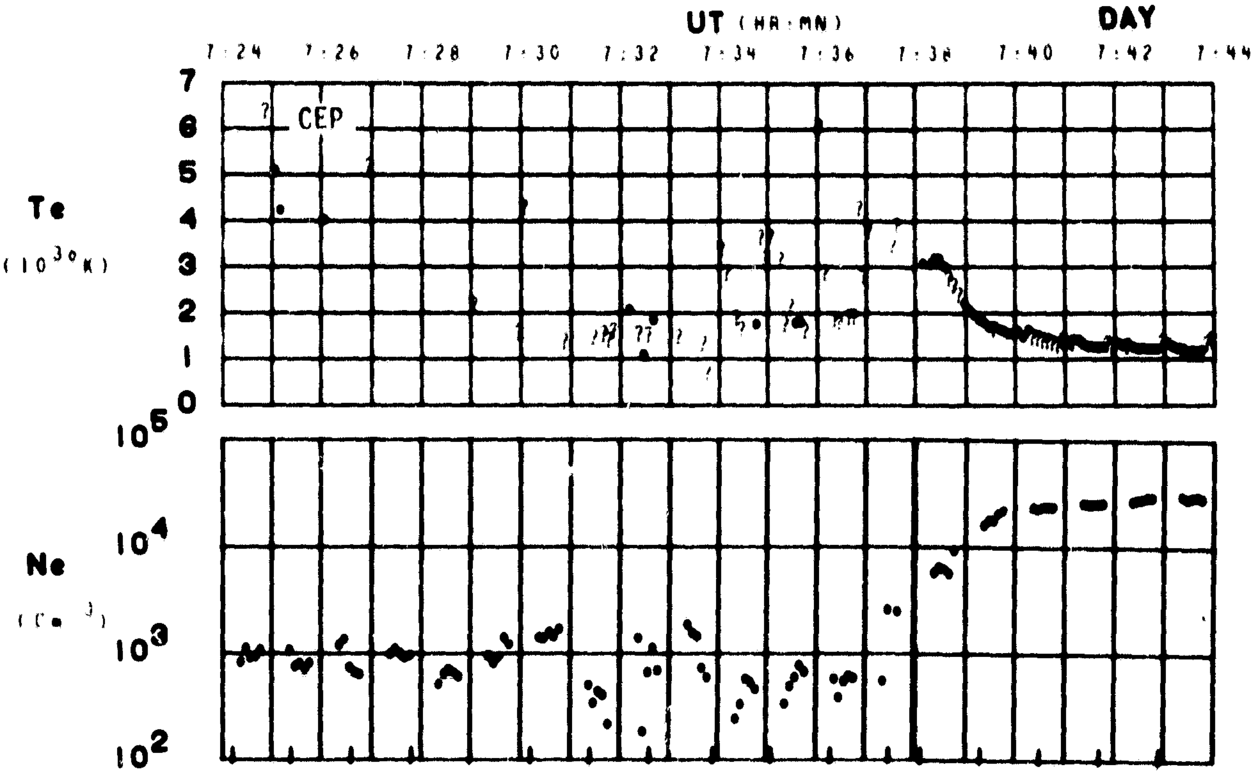

30 OCT 1971 (303) ISIS-II IMS
7:24:17 26657 ORBIT 2688

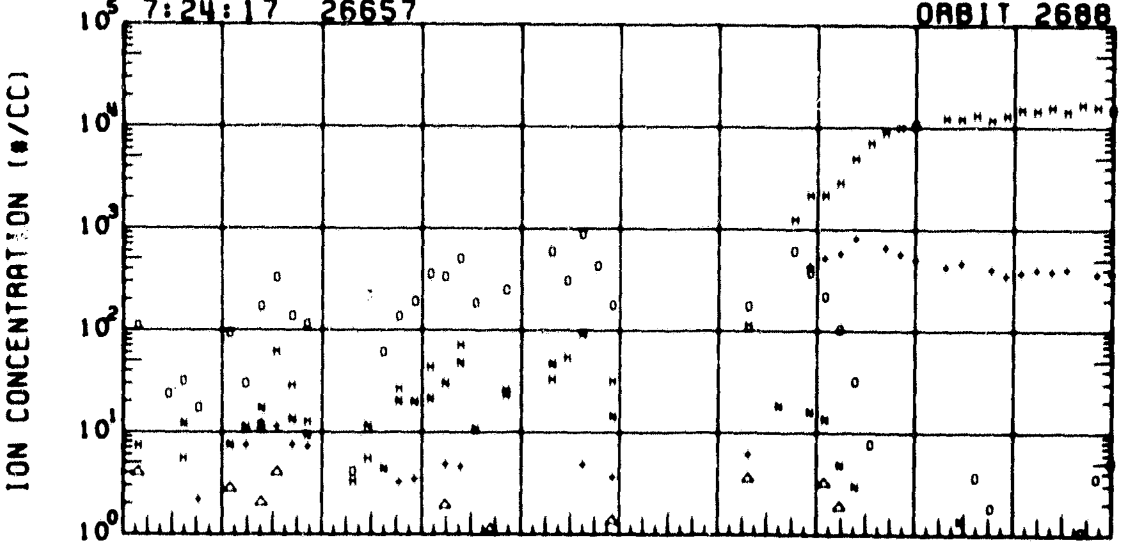

1	H	UT	7:26	7:28	7:30	7:32	7:36	7:38	7:40	7:42
4	+	LAST	2:36	2:44	2:48	2:51	2:55	2:57	2:58	2:59
8	△	MLT	1:09	2:12	2:28	2:31	2:45	2:47	2:48	2:51
14	N	DLAT	84	79	74	69	58	50	43	38
16	O	INVL	84	80	75	69	57	54	49	44
		GLAT	74	68	62	56	43	37	30	24
		GLNG	76	-74	-73	73	-73	-73	-74	-74
		SZEN	116	120	123	127	132	134	136	137
		ALT	1425	1427	1428	1429	1429	1429	1429	1428

SET 15, FORMAT 4

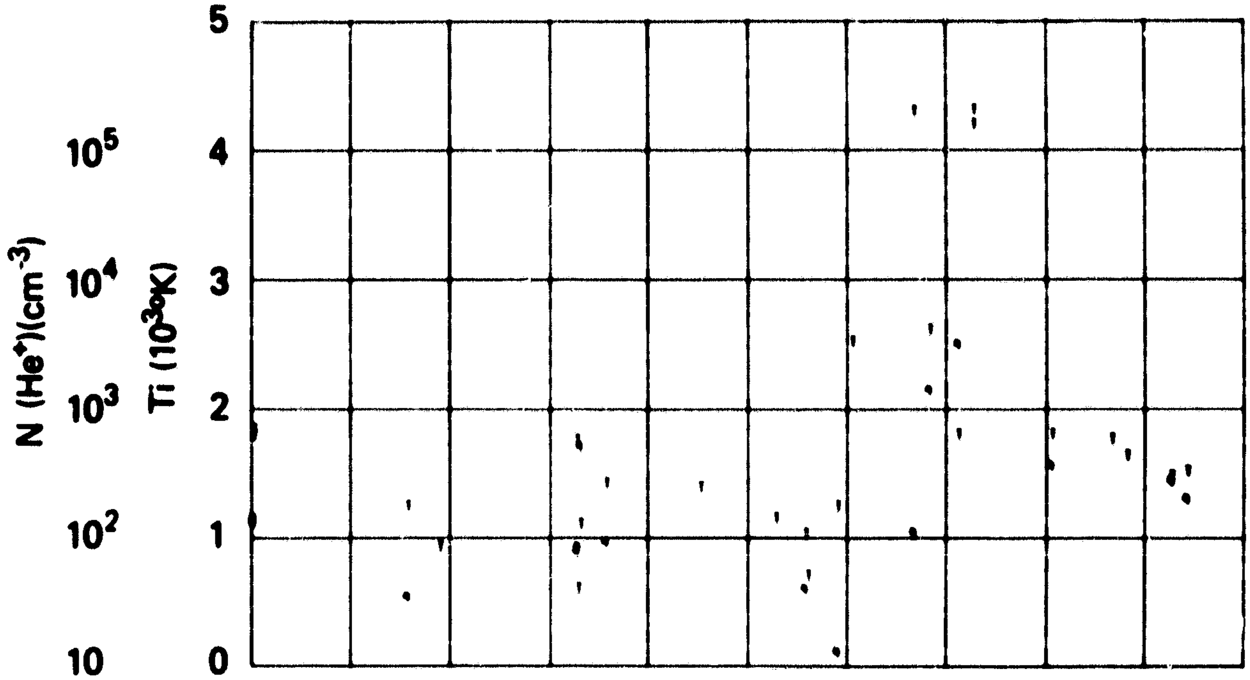

UT	7:26	7:28	7:30	7:32	7:36	7:38	7:40	7:42
LAST	21:36	21:44	21:48	21:51	21:55	21:57	21:58	21:59
MLT	11:09	21:12	21:29	21:37	21:45	21:47	21:49	21:51
DLAT	84	79	74	69	58	50	43	38
INVL	84	80	75	69	59	54	49	44
GLAT	74	68	62	56	43	37	30	24
GLNG	76	74	73	73	73	73	74	74
SZEN	116	120	123	127	132	134	136	137
ALT	1425	1427	1428	1429	1429	1429	1428	1428

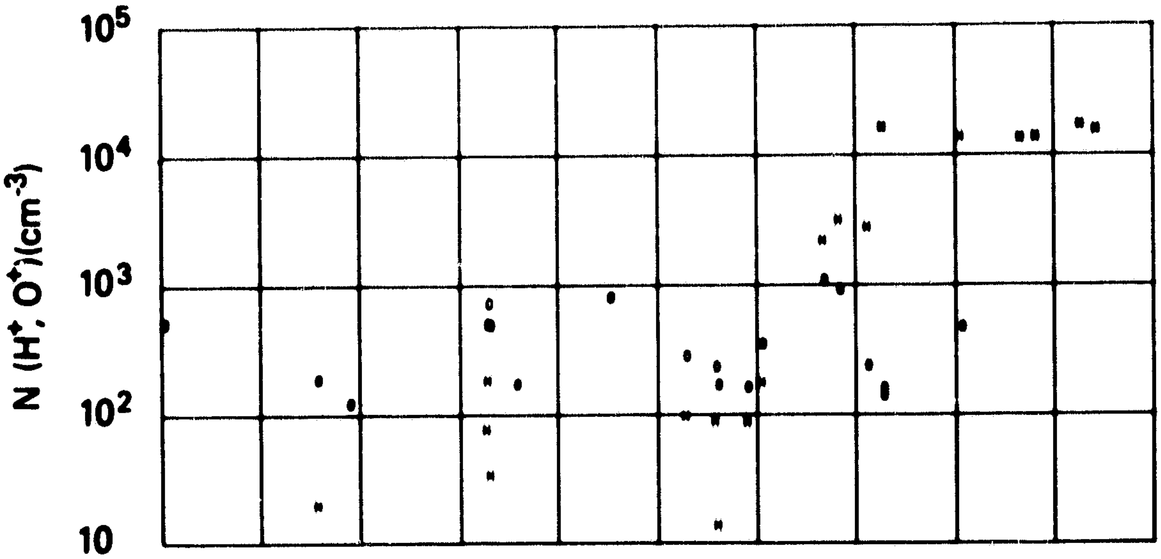

SET 15, FORMAT 5

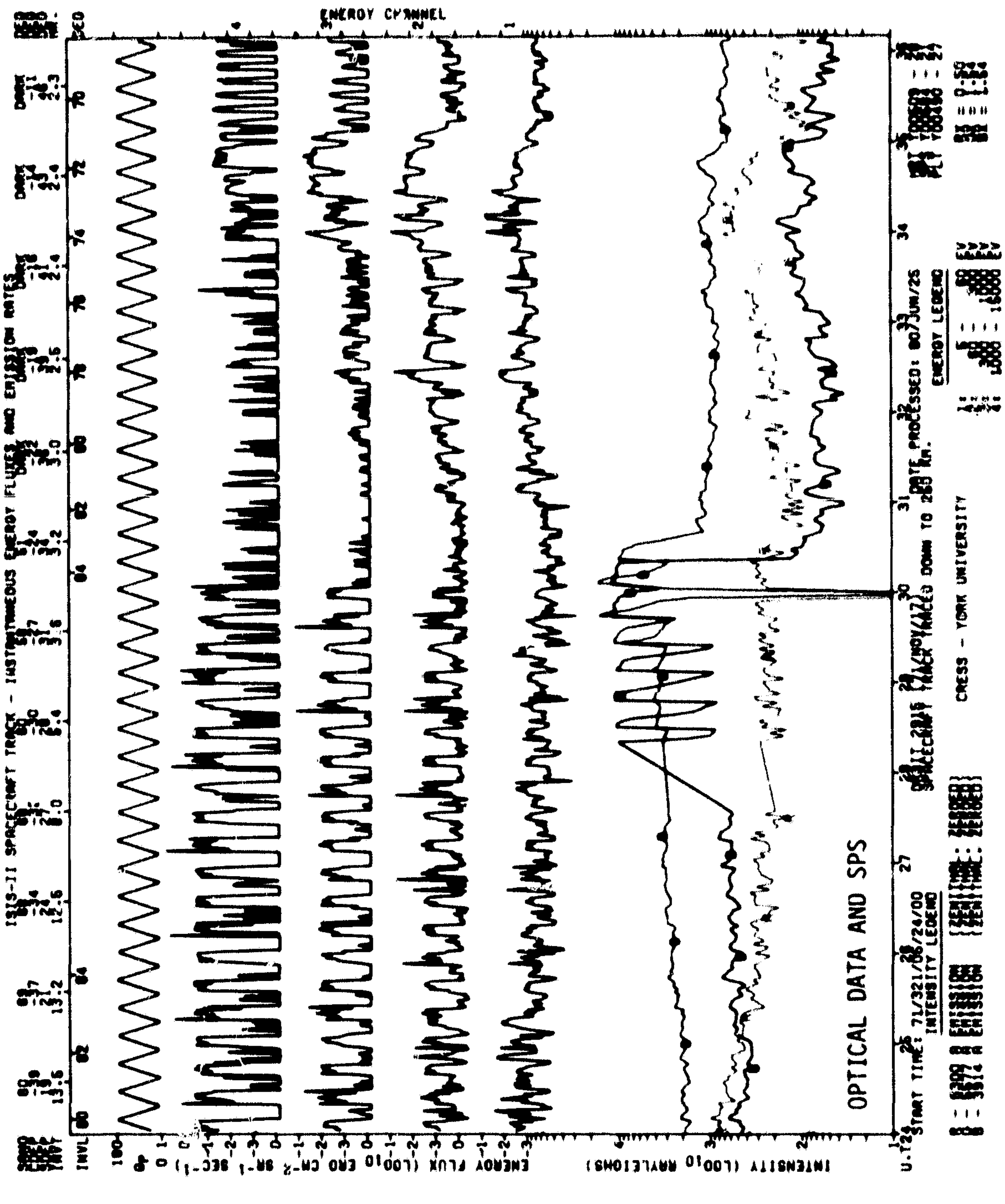

SET 16, FORMAT 1

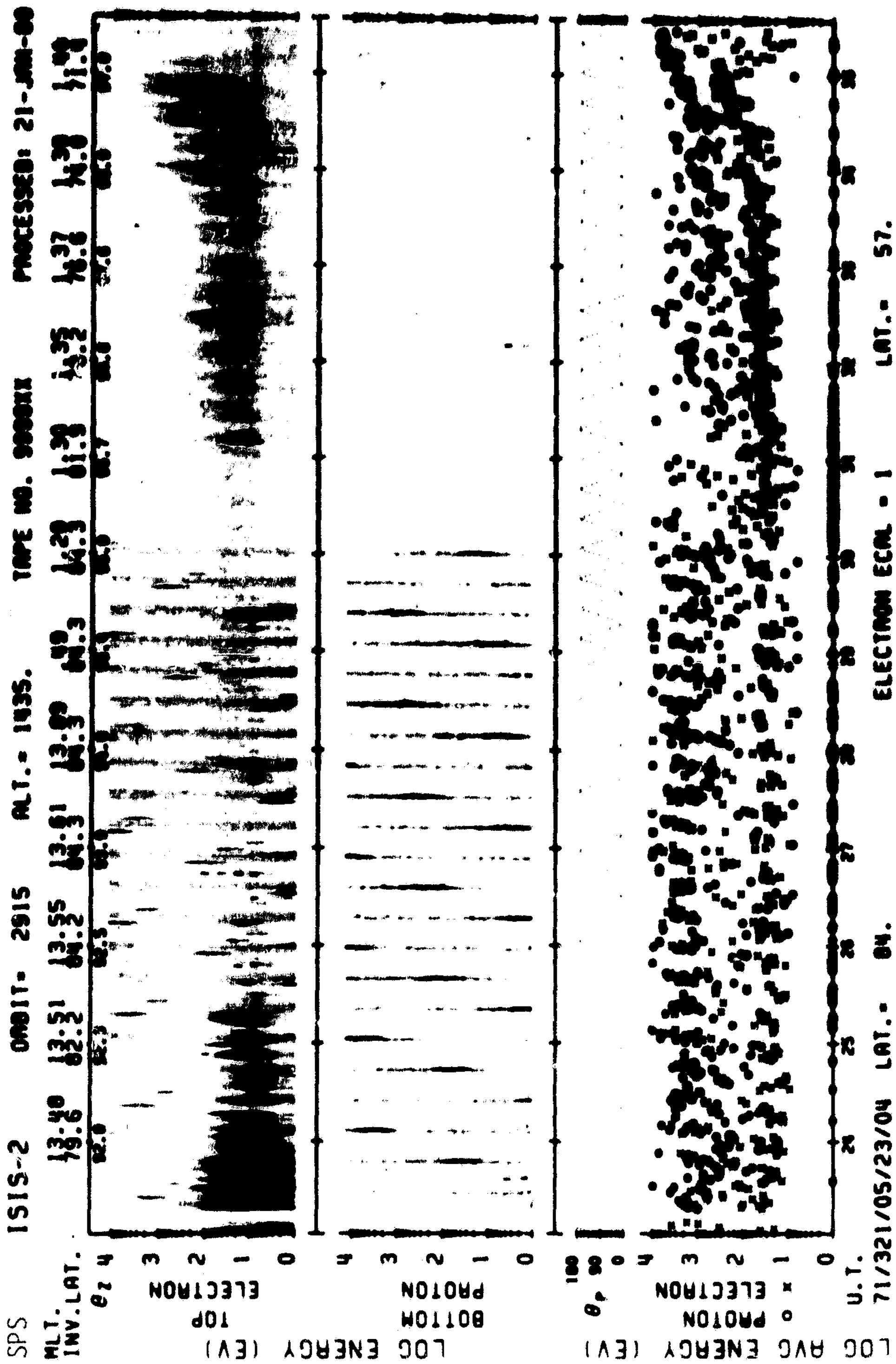

SET 16, FORMAT 6

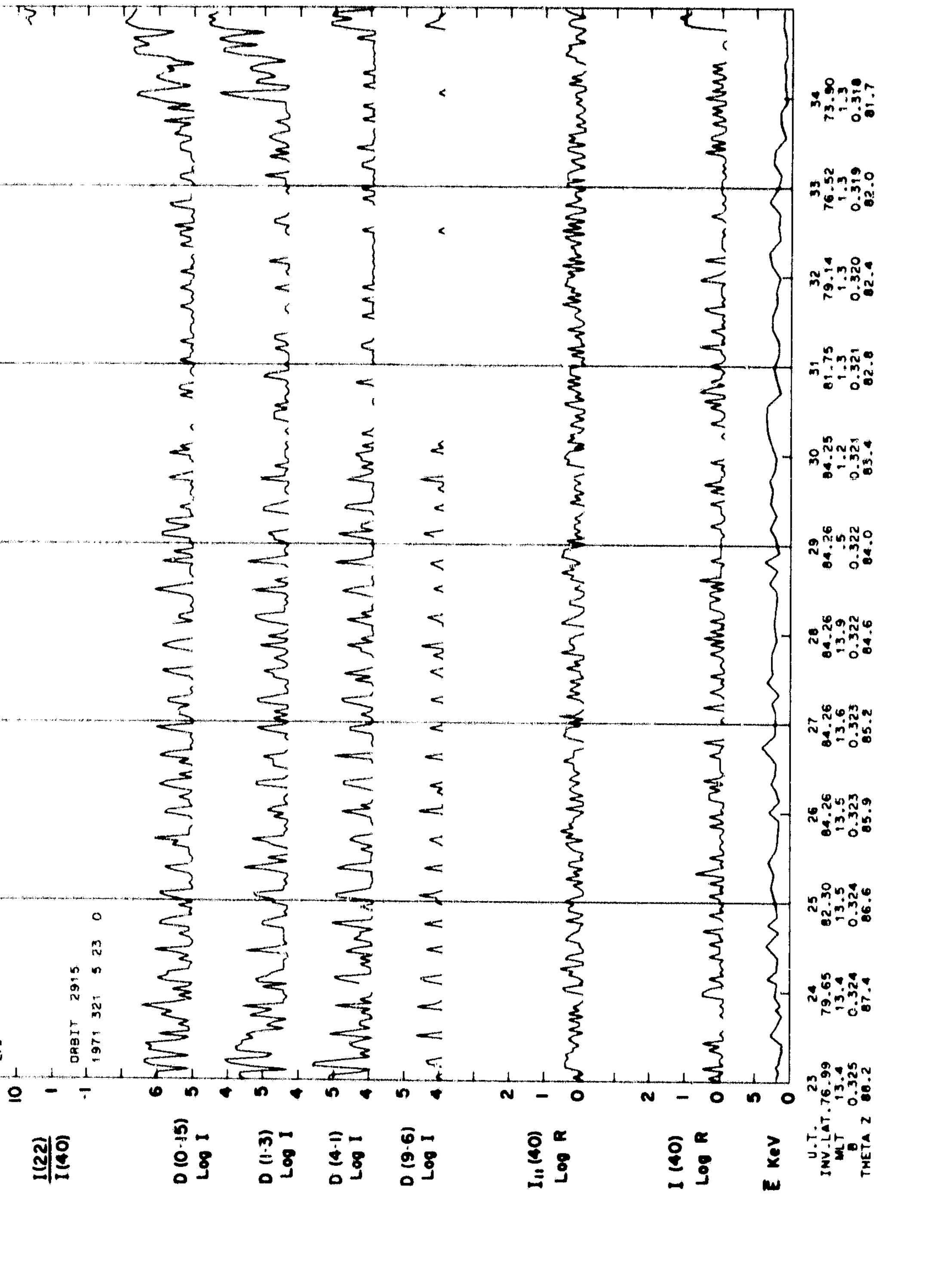

SET 16, FORMAT 3

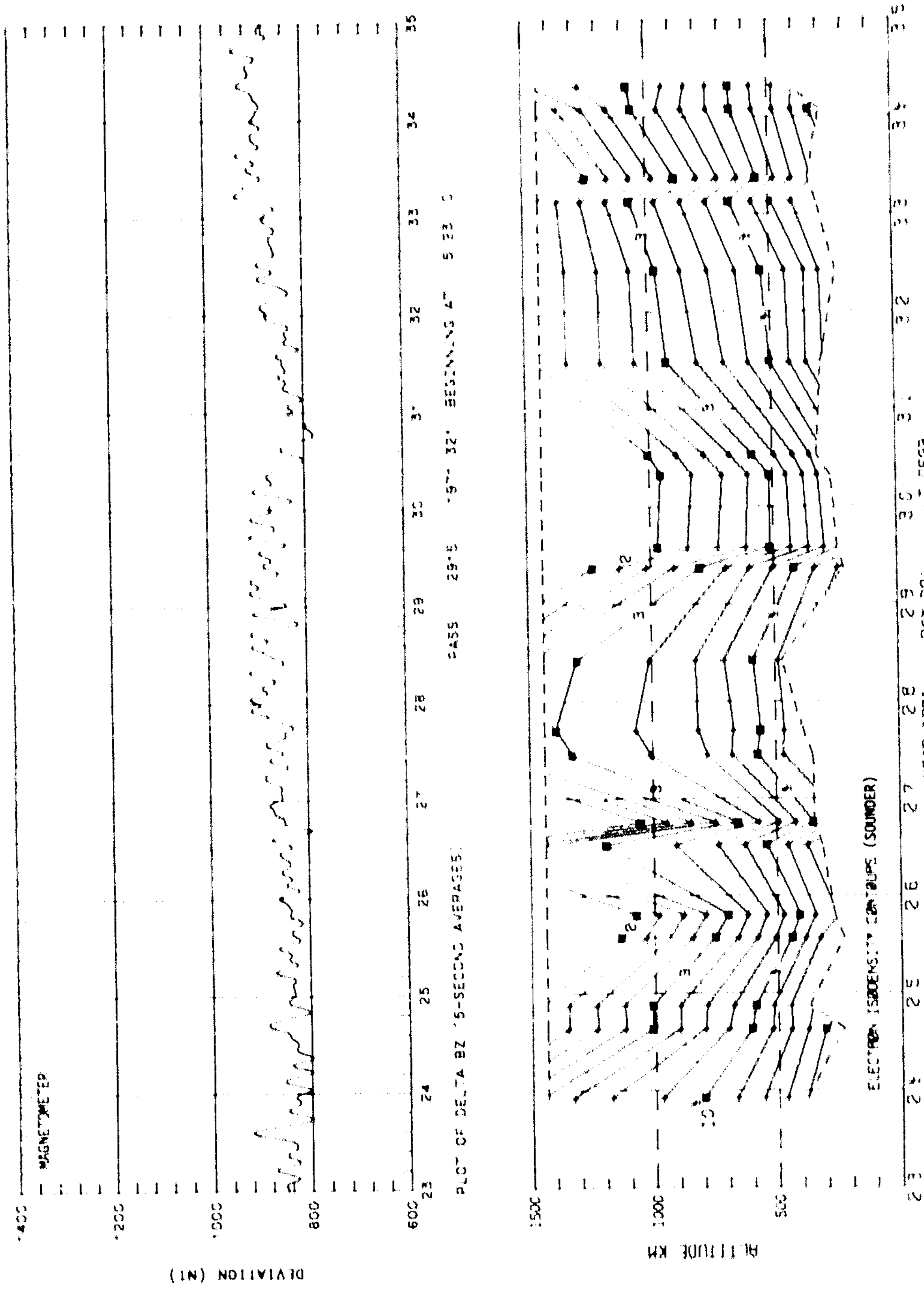

SET 16, FORMAT 2

ORBIT 2915
DATE 711117
DAY 321

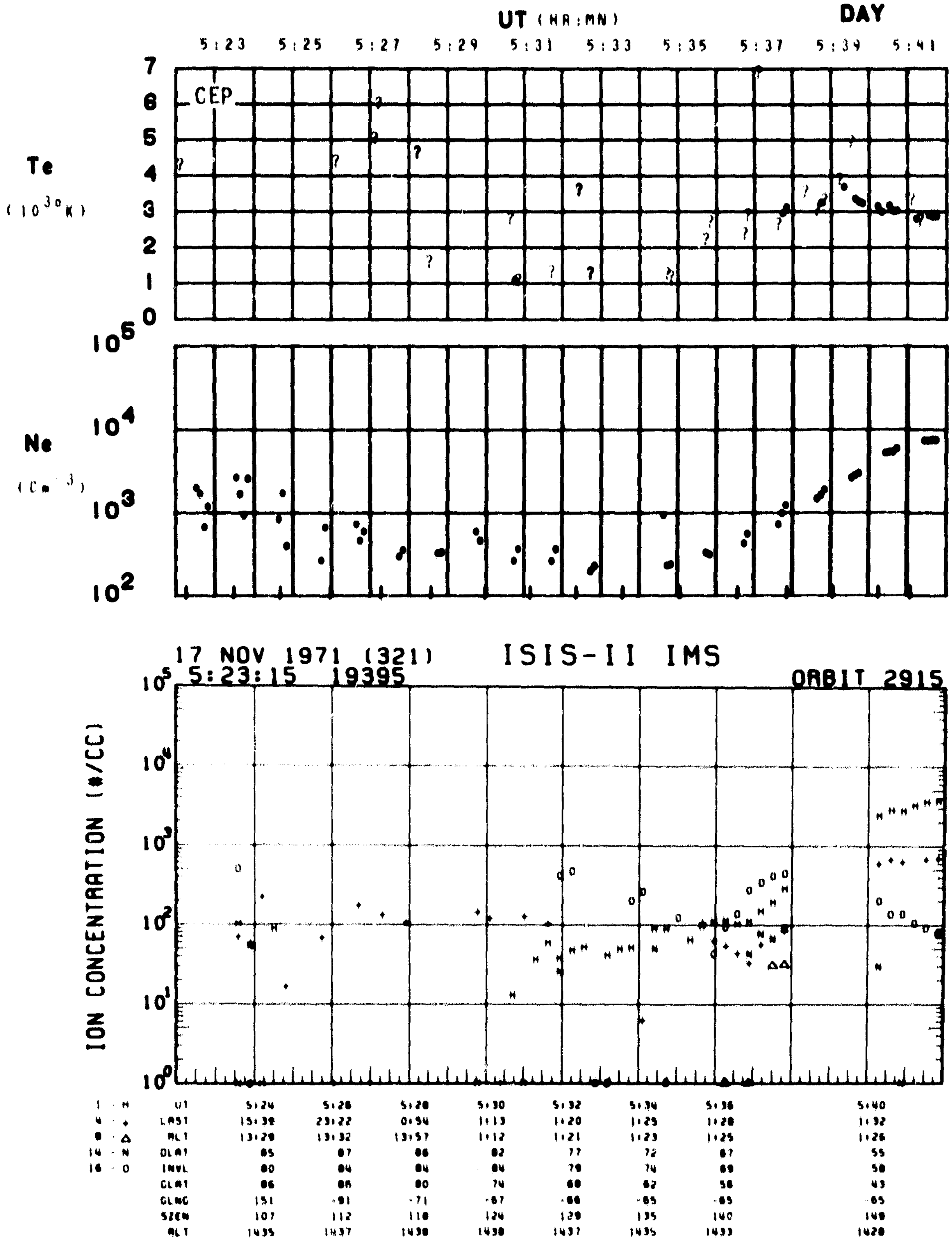

SET 16, FORMAT 4

Note different temperature scale

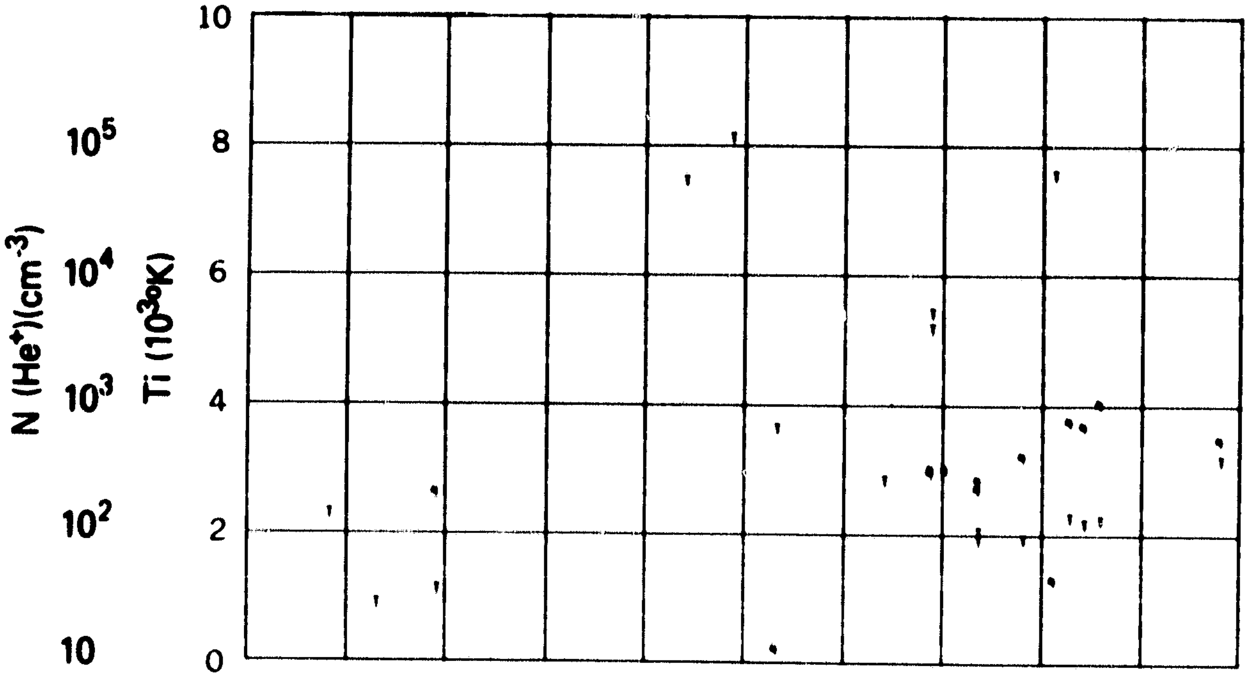

UT	5:24	5:26	5:28	5:30	5:32	5:34	5:36	5:40
LAST	15:38	23:22	0:54	1:13	1:20	1:25	1:28	1:32
MLT	13:28	13:32	13:57	1:12	1:21	1:23	1:25	1:26
DLAT	85	87	86	82	77	72	67	55
INVL	80	84	84	84	79	74	69	58
GLAT	86	86	80	74	68	62	56	43
GLNG	151	-91	-71	-67	-66	-65	-65	65
SZEN	107	112	118	124	129	135	140	149
ALT	1435	1437	1438	1438	1437	1435	1433	1428

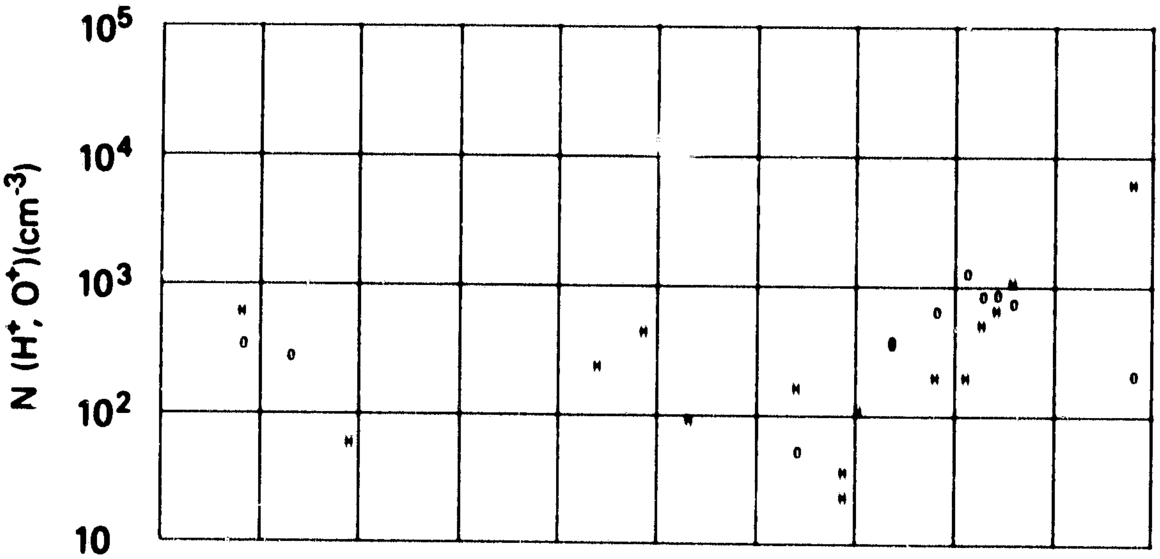

SET 16, FORMAT 5

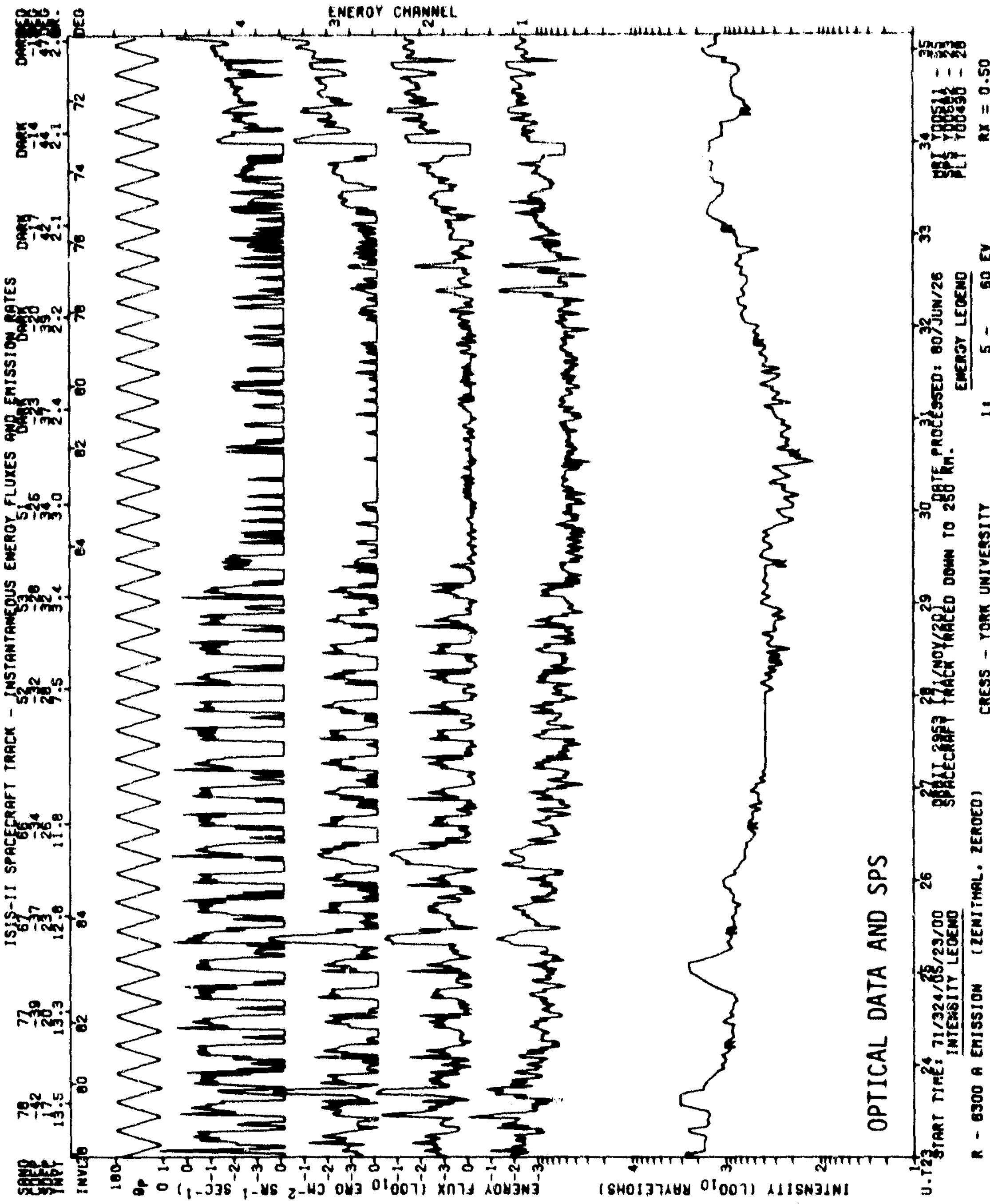

SET 17, FORMAT 1

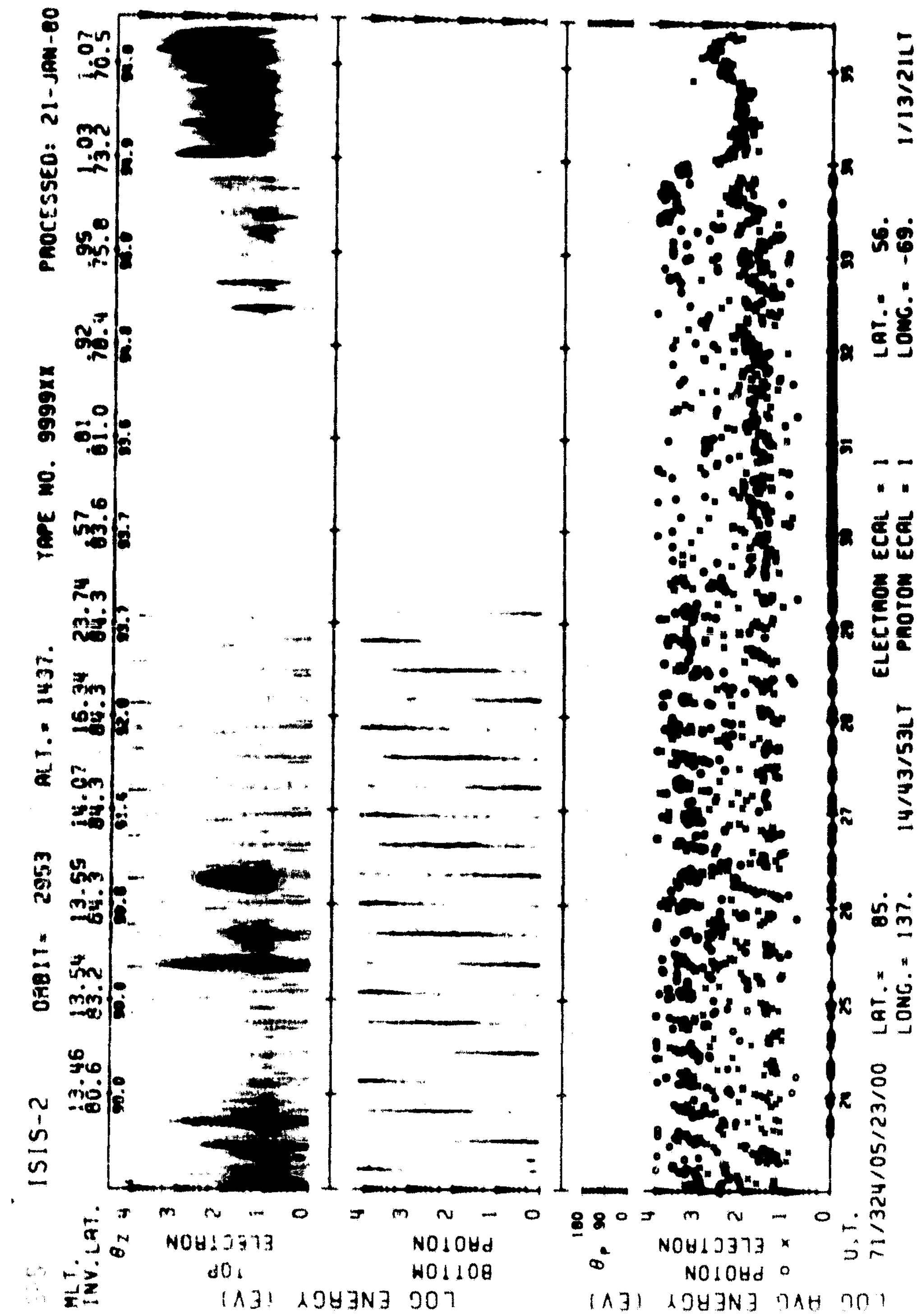

SET 17, FORMAT 6

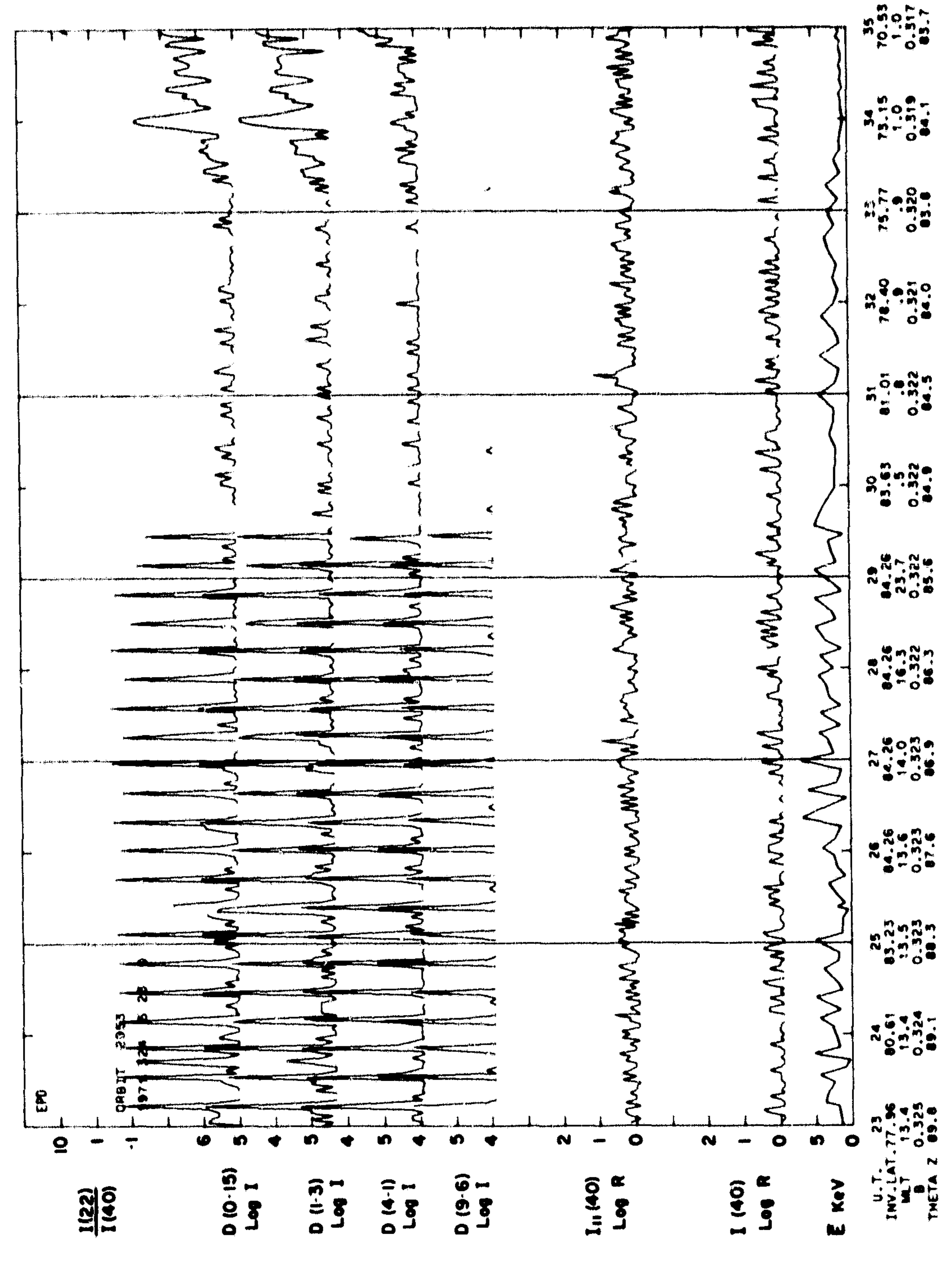

SET 17, FORMAT 3

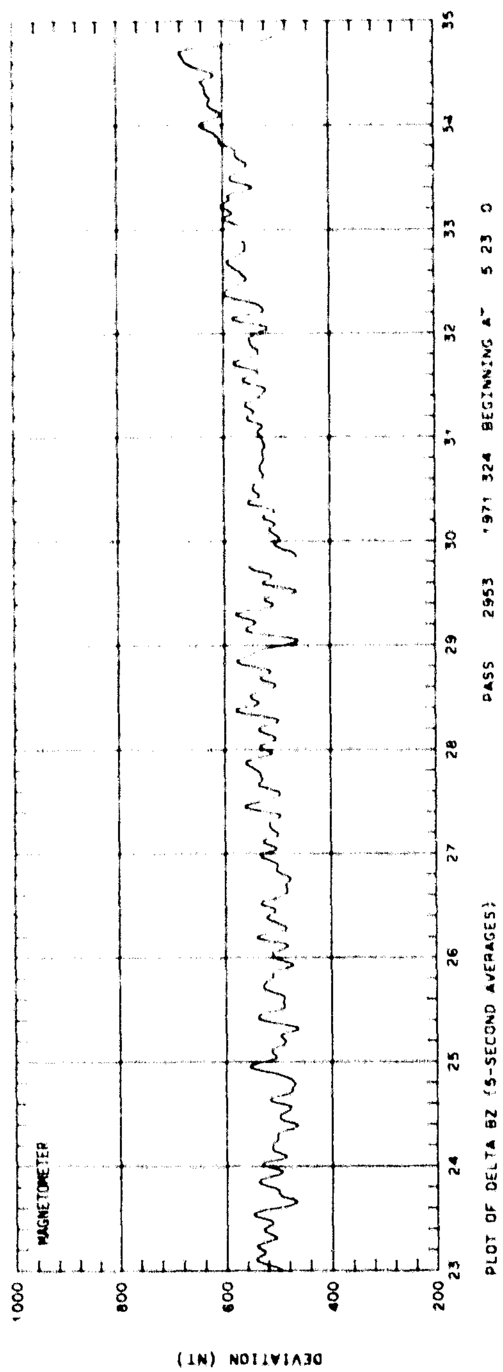

SET 17, FORMAT 2

ORBIT 2953
DATE 711120
DAY 324

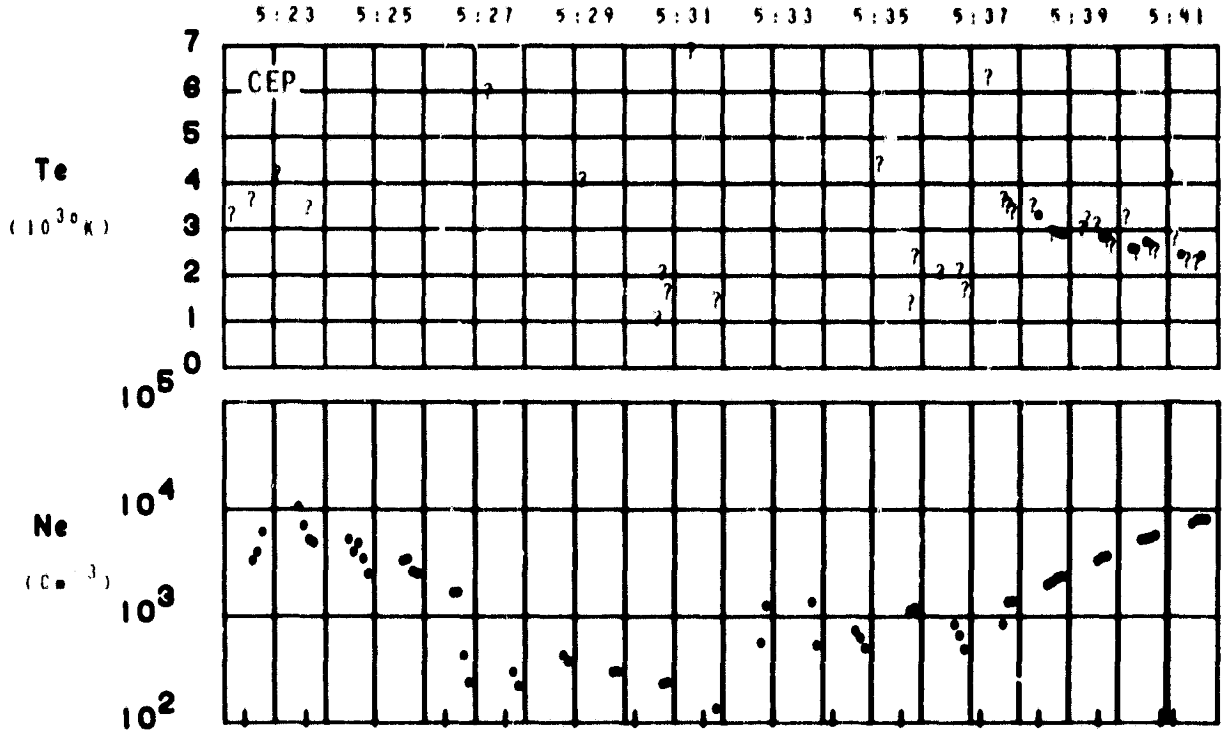

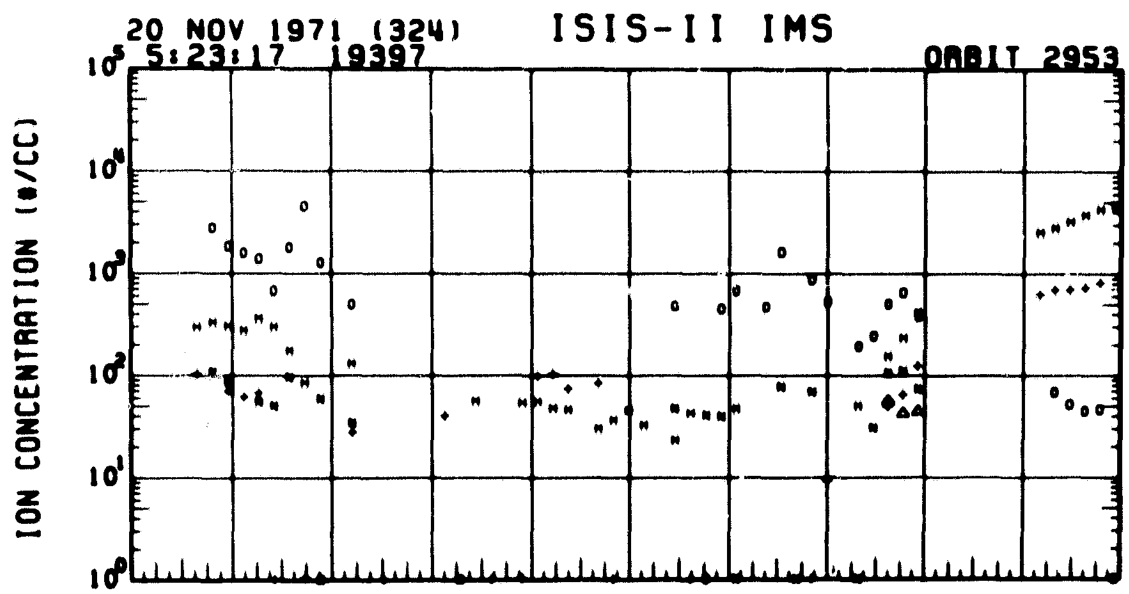

1 - H	UT	5:24	5:26	5:28	5:30	5:32	5:34	5:36	5:40
4 - +	LAST	18:17	23:47	0:45	1:00	1:07	1:11	1:14	1:10
8 - △	MLT	13:28	13:41	10:31	0:34	0:55	1:02	1:00	1:00
14 - N	OLAT	85	88	85	82	77	72	67	54
16 - O	INVL	91	84	84	84	78	73	68	58
	GLAT	87	85	79	73	67	61	54	42
	GLNG	140	-88	-73	-70	-68	-68	-68	-68
	SZEN	108	114	120	126	132	137	143	152
	ALT	1437	1438	1438	1438	1438	1434	1432	1428

SET 17, FORMAT 4

Note different temperature scale

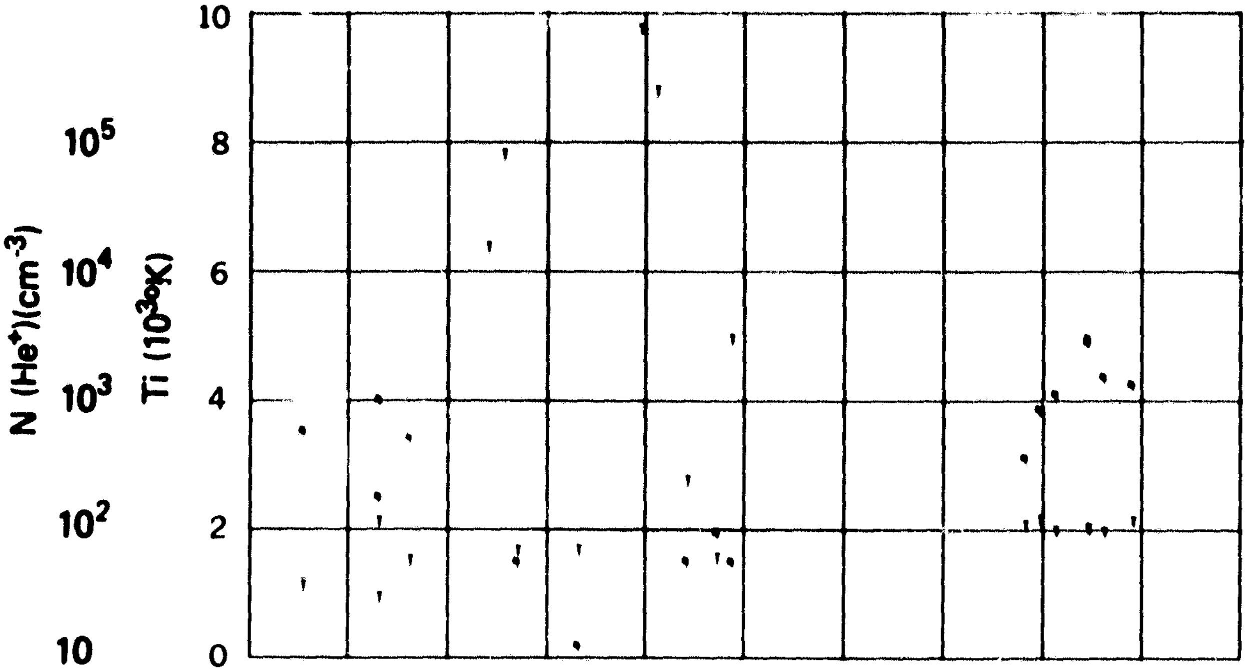

UT	5:24	5:26	5:28	5:30	5:32	5:34	5:36	5:40
LAST	16:17	23:47	0:45	1:00	1:07	1:11	1:14	1:18
MLT	13:20	13:41	16:31	0:34	0:55	1:02	1:06	1:09
DLAT	85	88	85	82	77	72	67	54
INVL	81	84	84	84	78	73	68	58
GLAT	87	85	79	73	67	61	54	42
GLNG	140	-88	-73	-70	-69	-68	-68	-68
SZEN	100	114	120	126	132	137	143	152
ALT	1437	1438	1438	1438	1438	1434	1432	1426

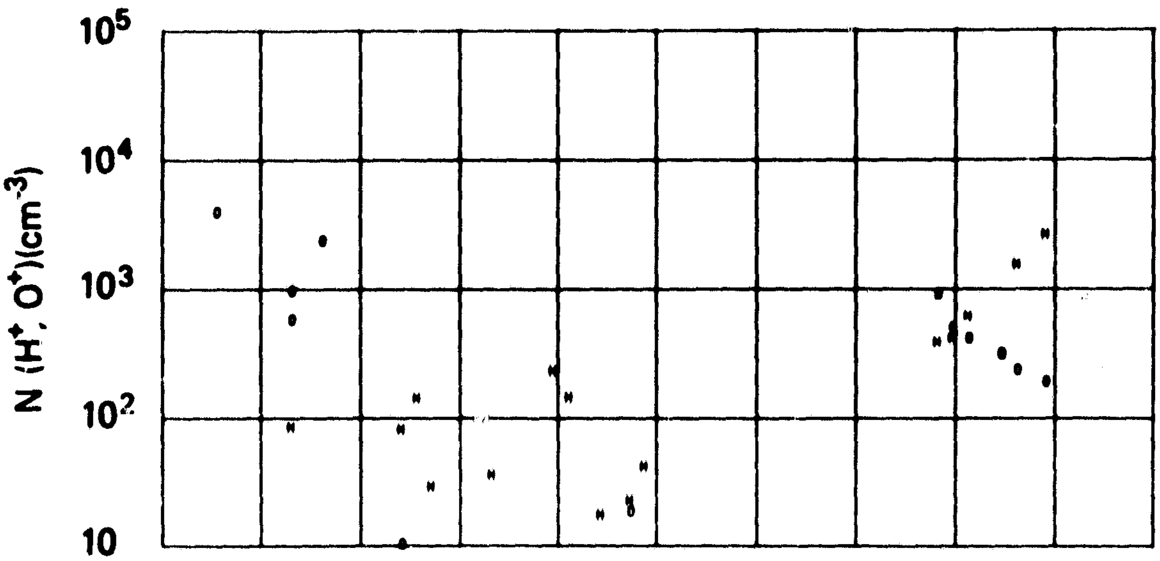

SET 17, FORMAT 5

71/324/0523

Excerpts of VLF Spectral film for the period 0523 - 0533

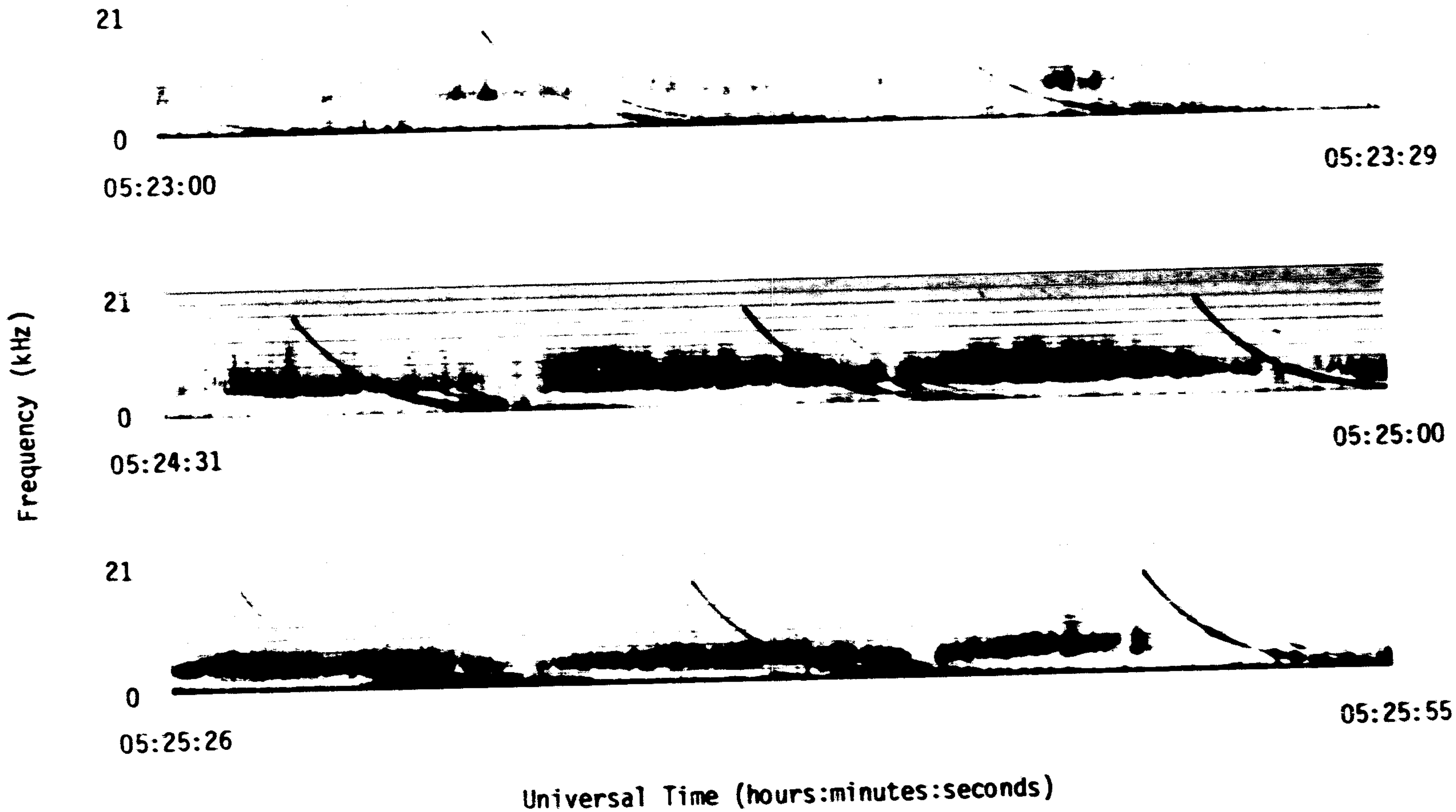

SET 17, FORMAT 11

71/324/0523

Excerpts of VLF Spectral film for the period 0523 - 0533

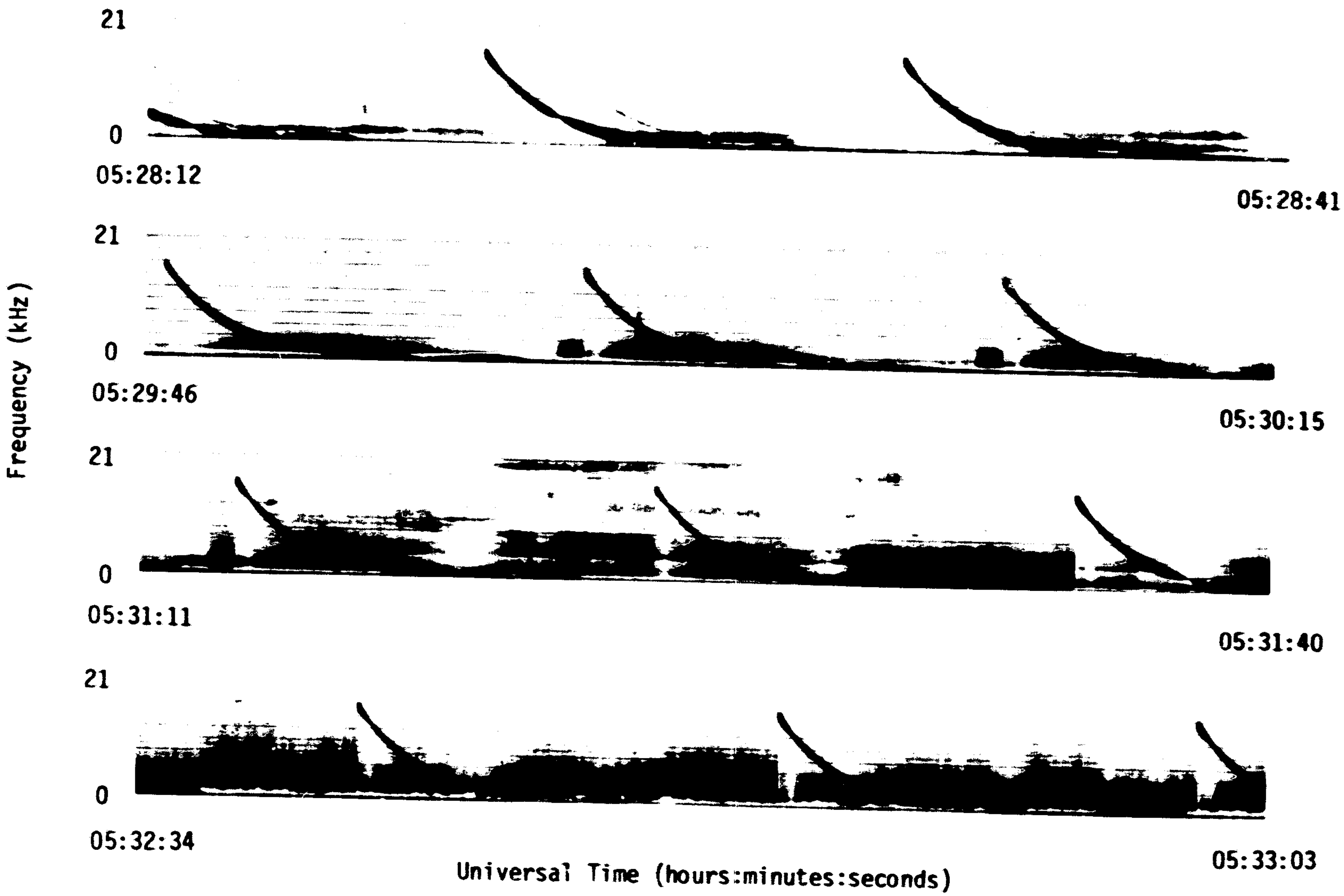

SET 17, FORMAT 11

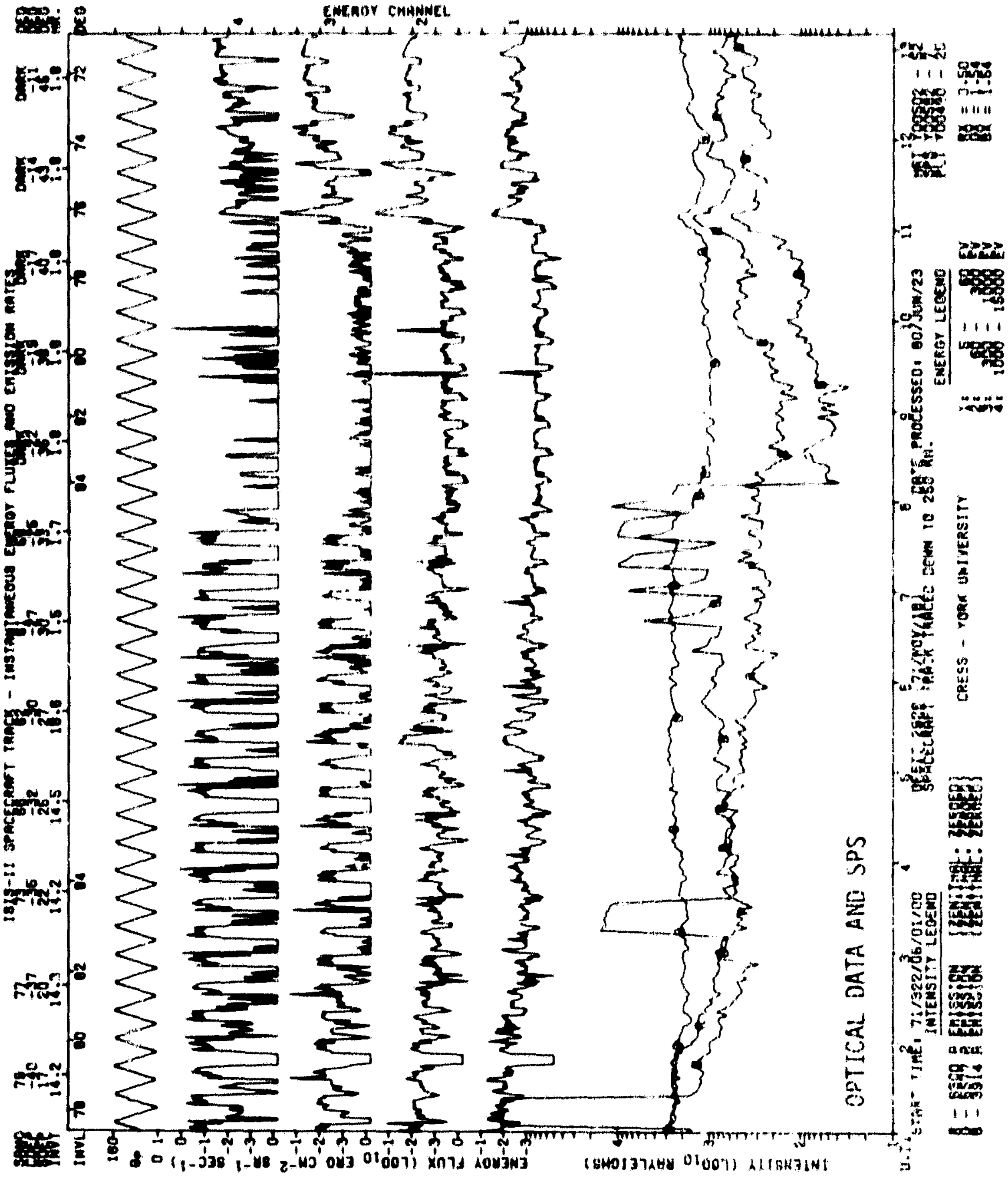

SET 18, FORMAT 1

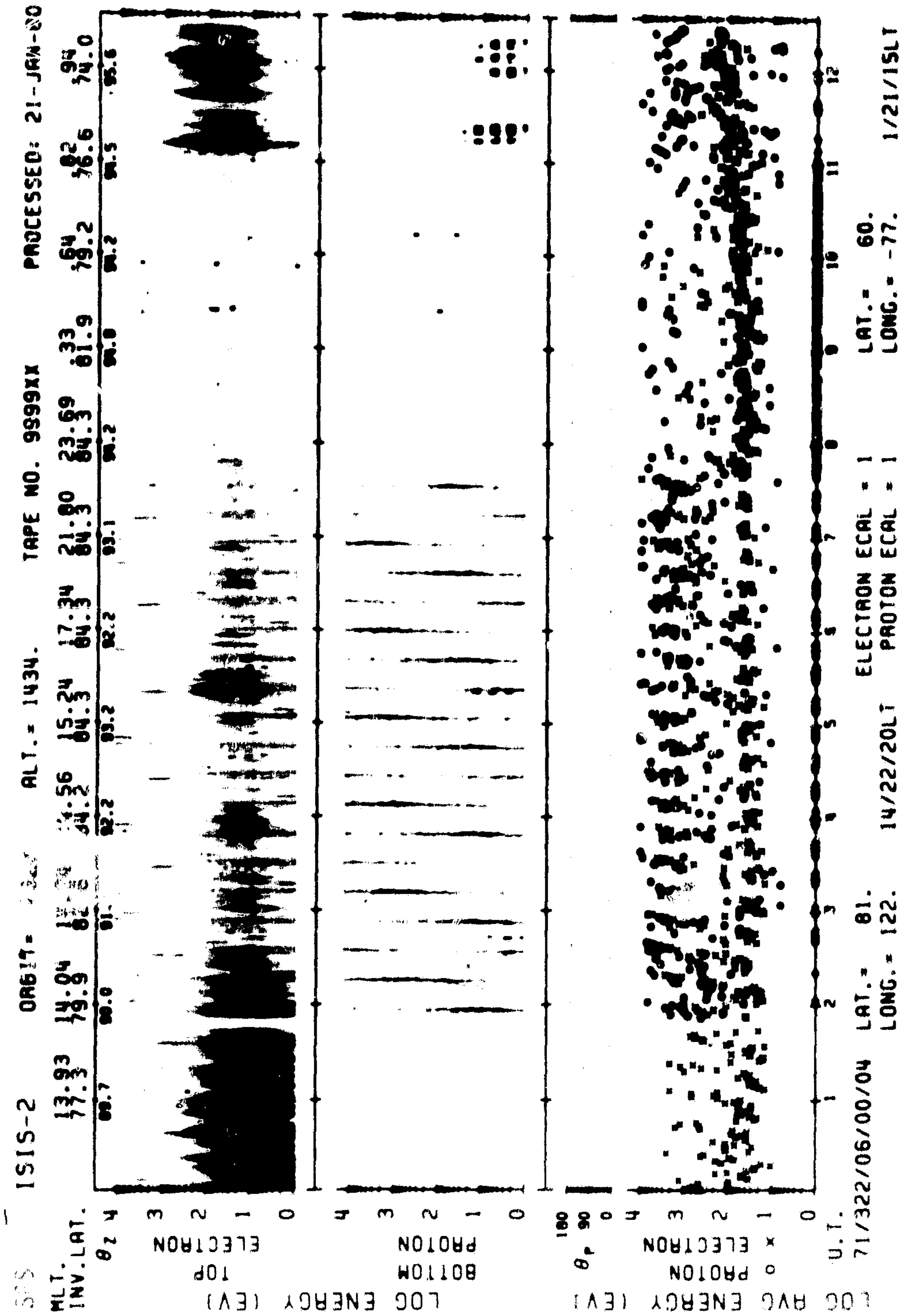

SET 18, FORMAT 6

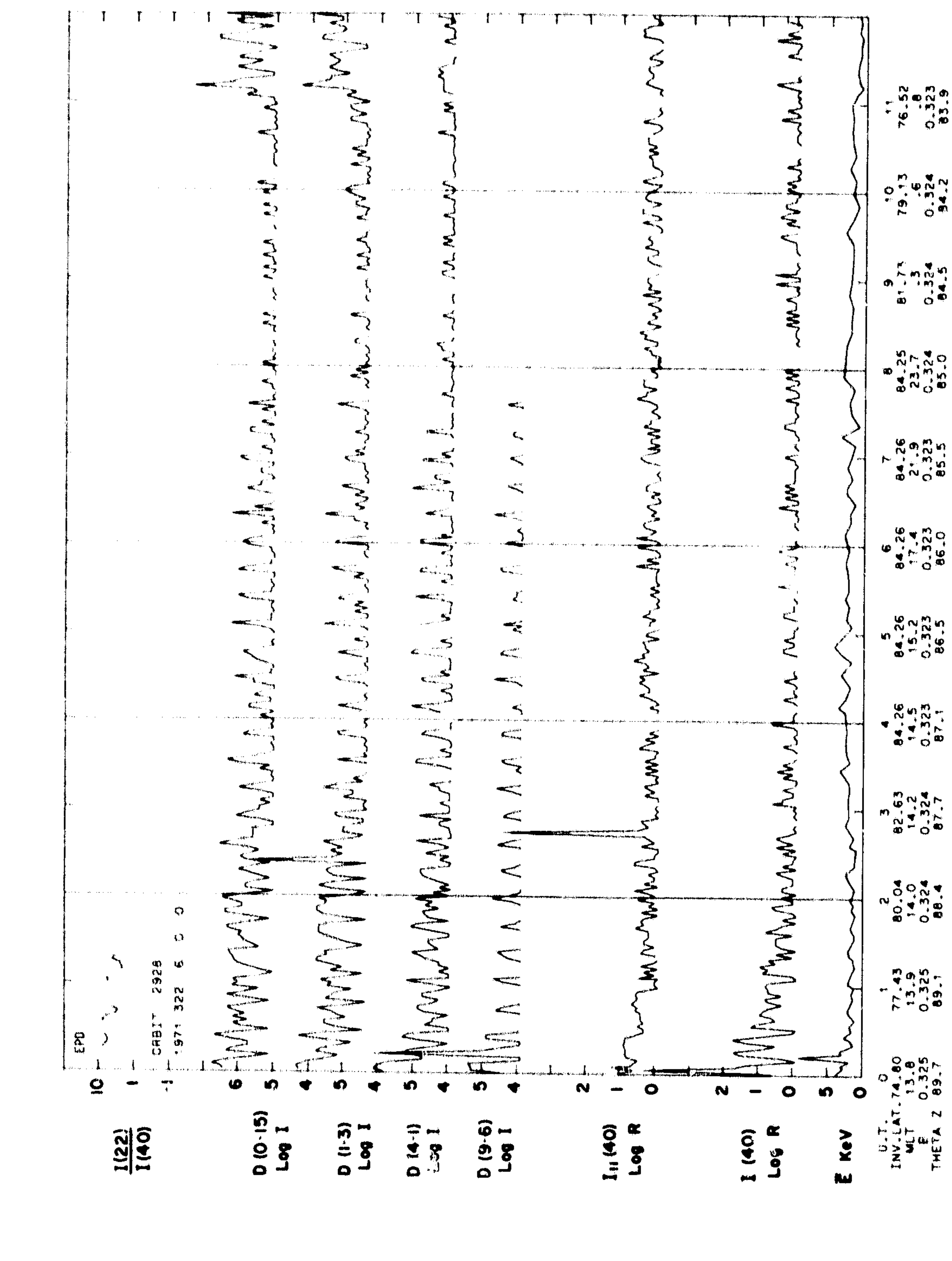

SET 18, FORMAT 3

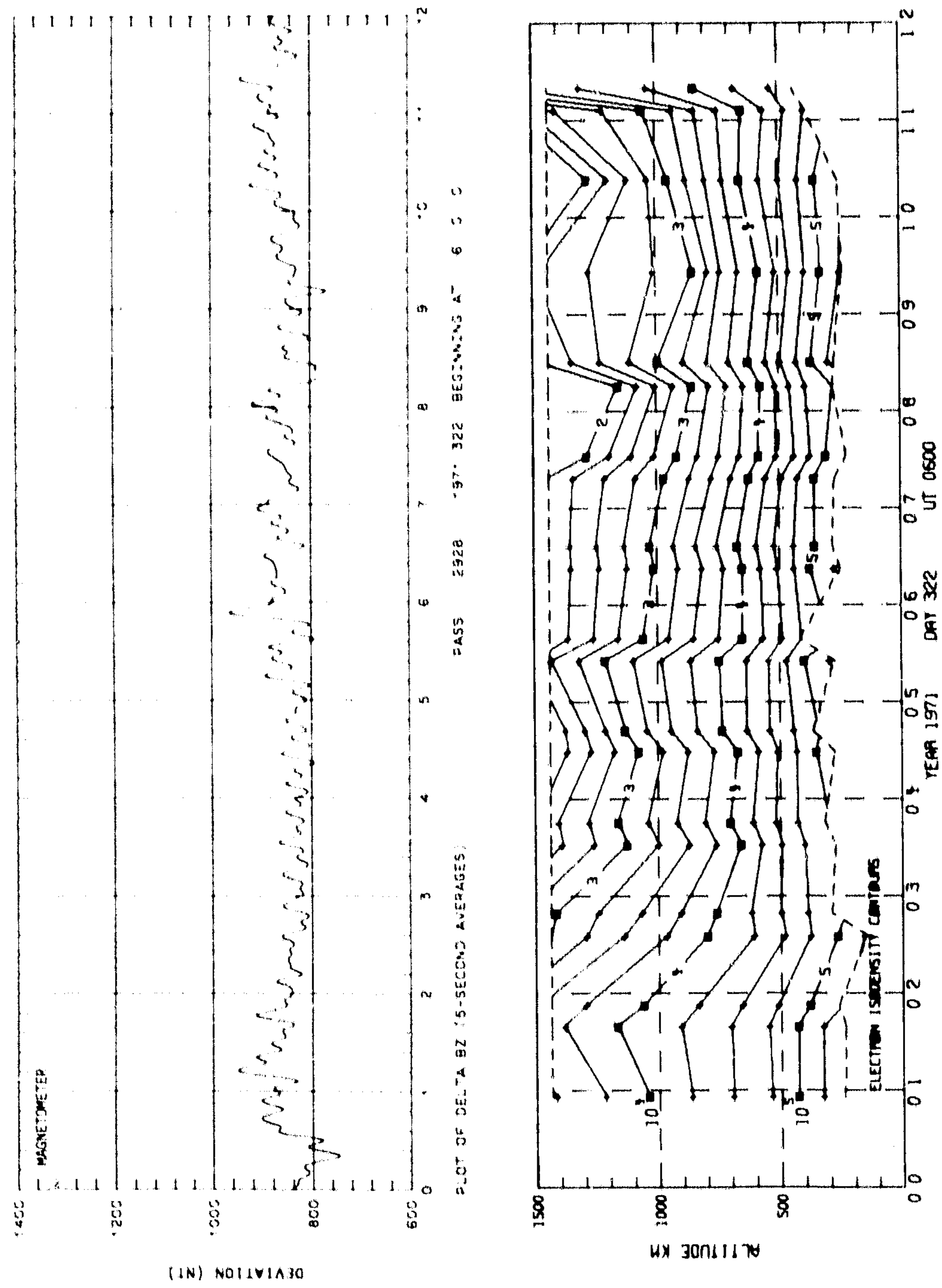

SET 18, FORMAT 2

ORBIT 2928
DATE 711118
DAY 322

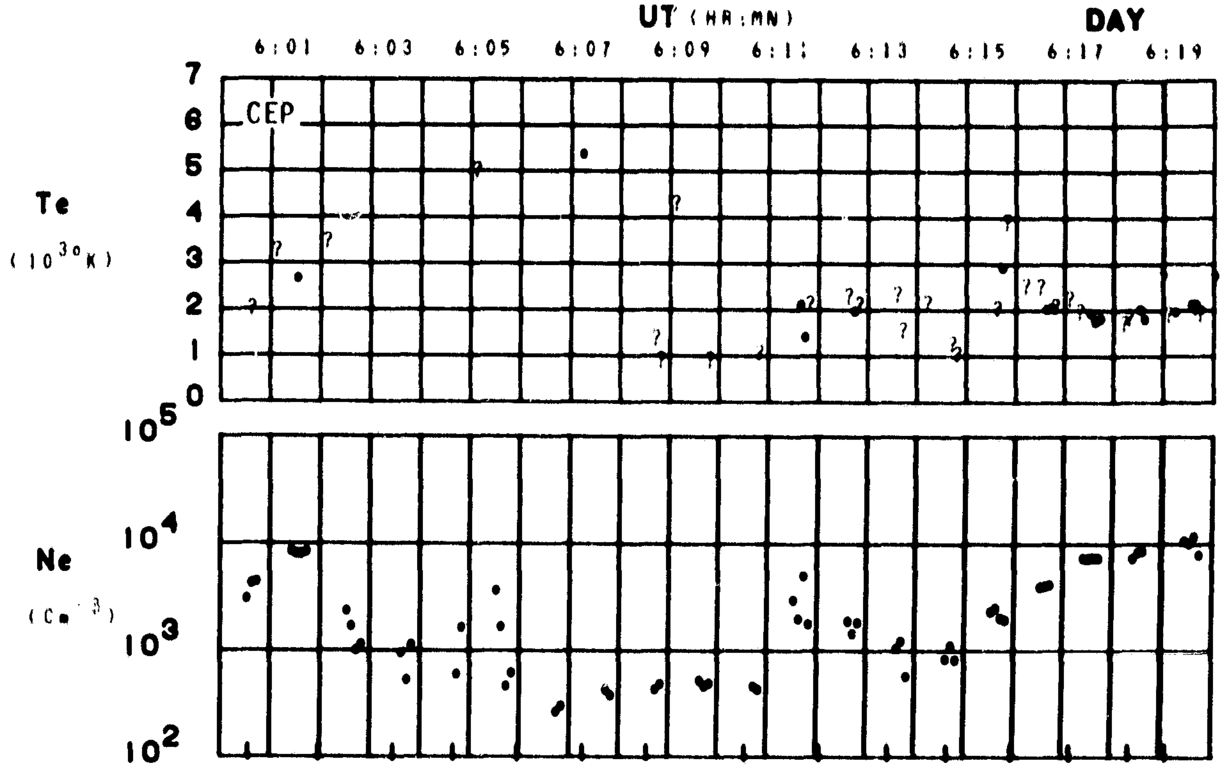

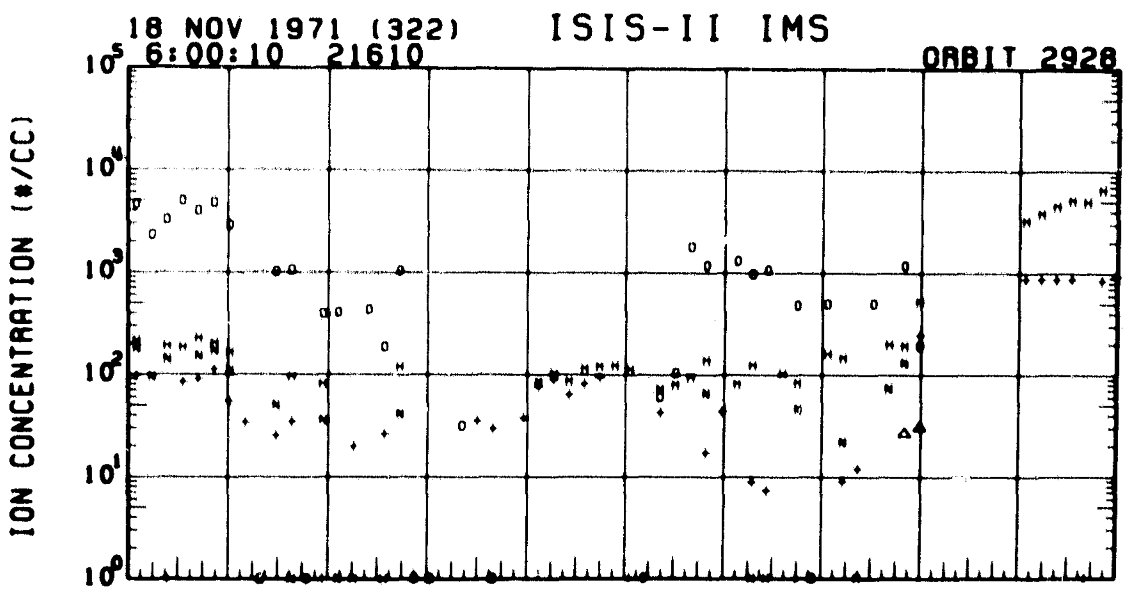

1 - H	UT	6:02	6:04	6:06	6:08	6:10	6:12	6:14	6:18
4 - <	LAST	15:53	15:37	0:52	1:09	1:18	1:21	1:23	1:27
8 - Δ	MLT	14:03	14:34	17:29	23:43	0:39	0:56	1:05	1:14
14 - N	DLAT	85	88	87	84	78	74	68	56
16 - O	INVL	80	84	84	84	79	74	69	58
	GLAT	87	86	80	74	67	61	55	42
	GLNG	147	-96	81	-77	-76	-76	-75	-75
	SZEN	108	113	119	125	130	136	141	150
	ALT	1436	1437	1438	1438	1437	1435	1433	1427

SET 18, FORMAT 4

RPA

711118

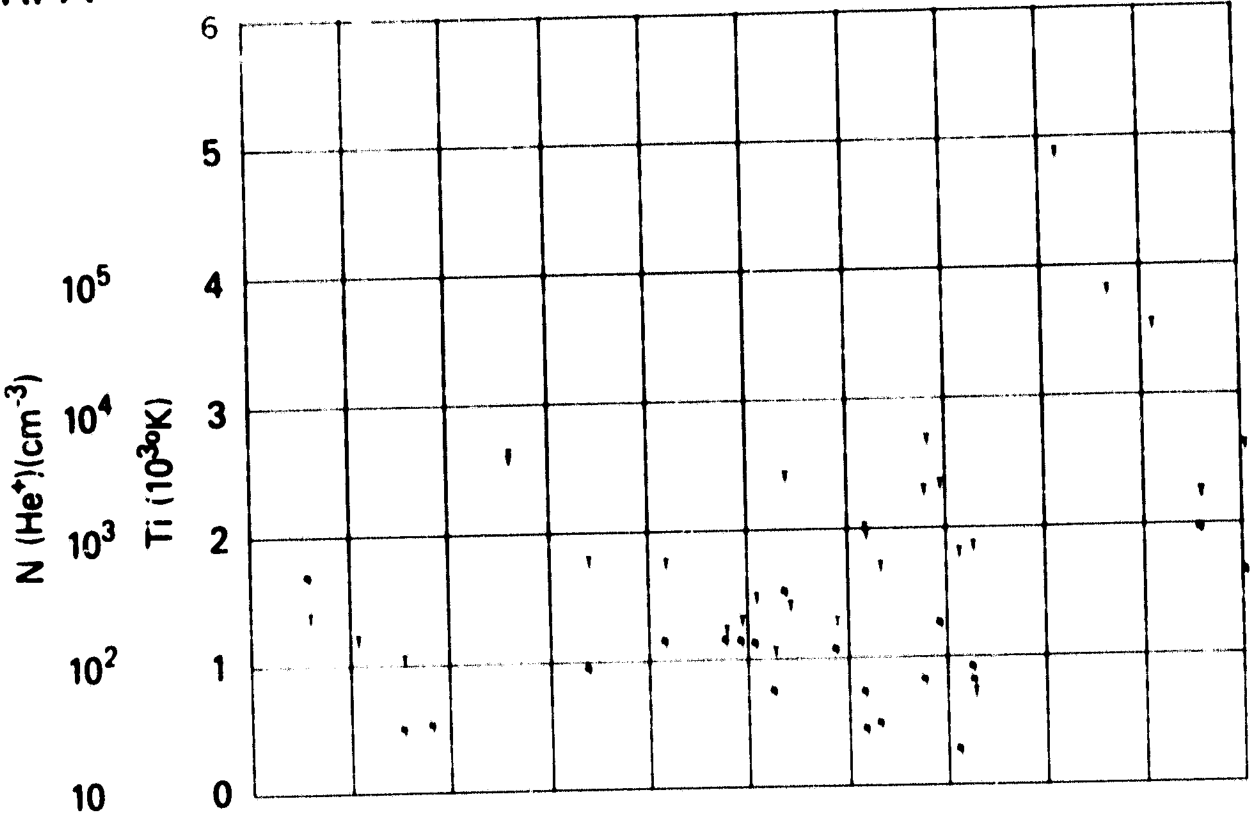

UT	6:02	6:04	6:06	6:08	6:10	6:12	6:14	6:18
LAST	15:53	15:37	0:52	1:09	1:18	1:21	1:23	1:27
MLT	14:03	14:34	17:29	23:43	0:39	0:56	1:05	1:14
DLAT	85	88	87	84	79	74	68	56
INVL	80	84	84	84	79	74	69	58
GLAT	87	86	80	74	67	61	55	42
GLNG	147	-96	81	77	-76	76	-75	-75
SZEN	108	113	119	125	130	136	141	150
ALT	1436	1437	1438	1438	1437	1435	1433	1427

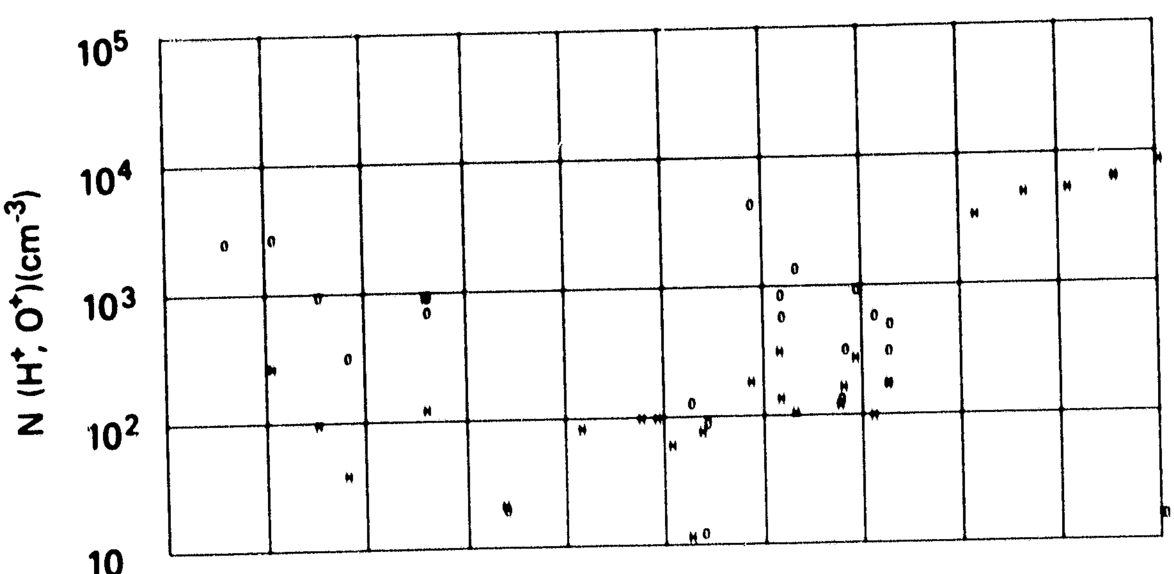

SET 18, FORMAT 5

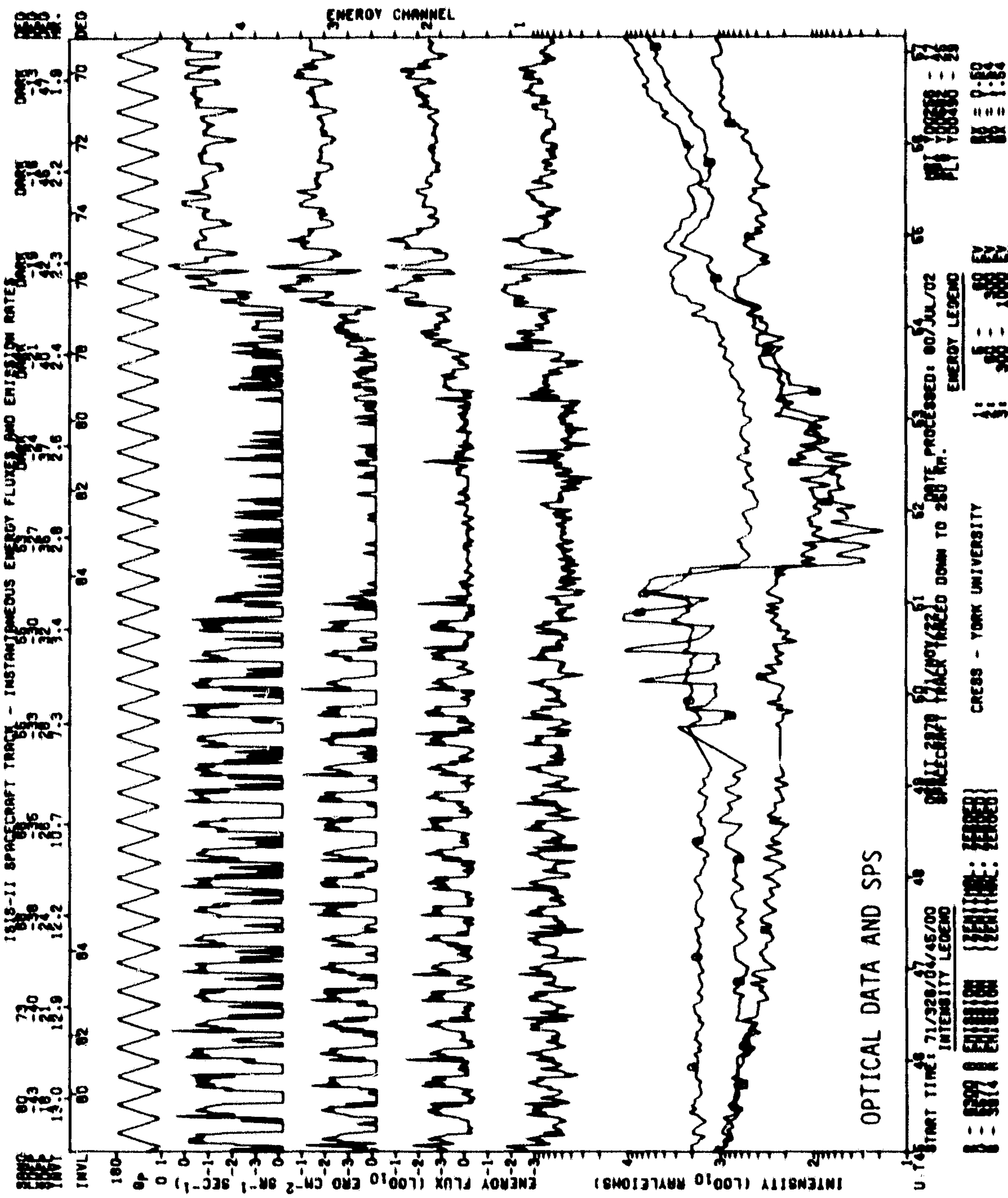

SET 19, FORMAT 1

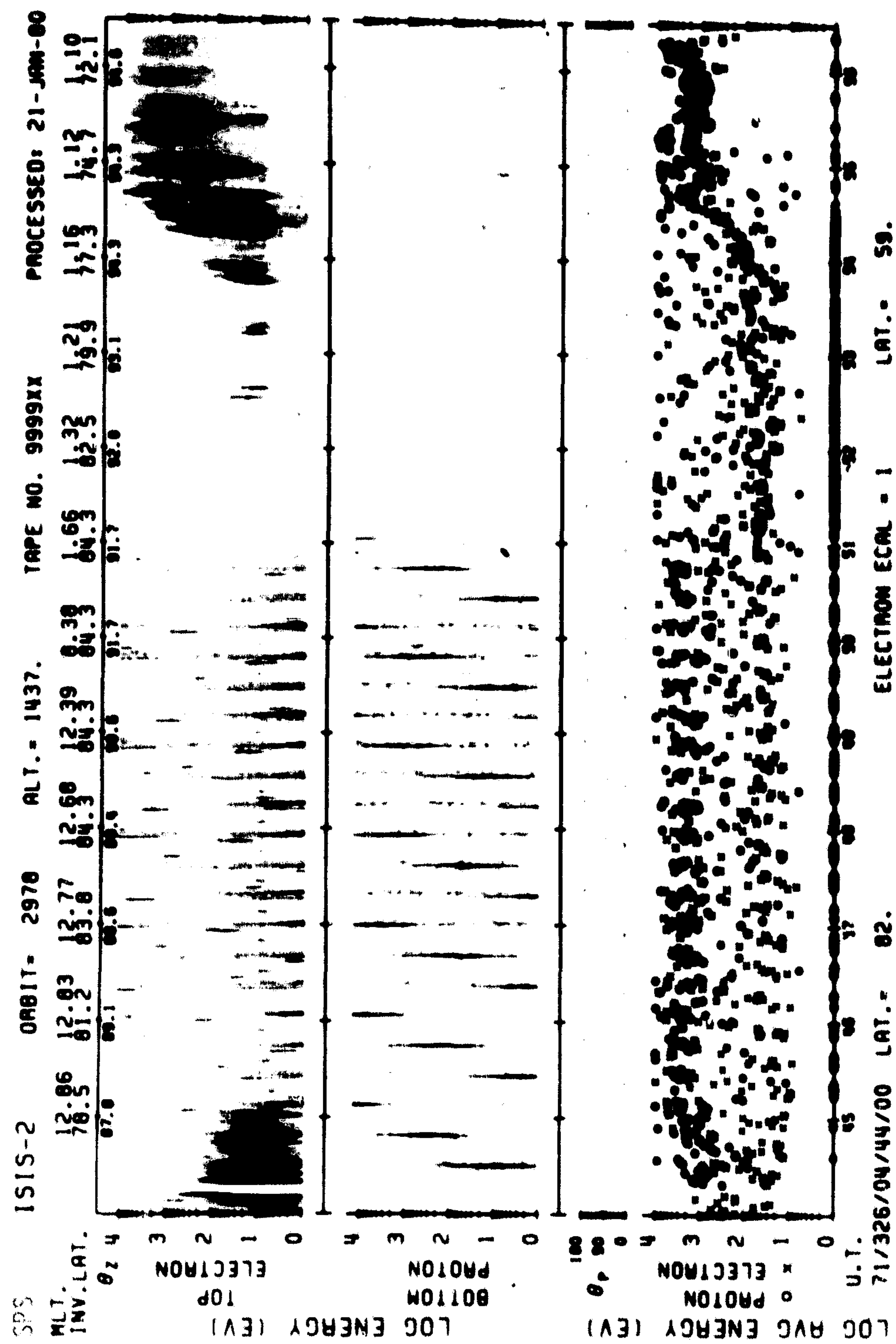

SET 19, FORMAT 6

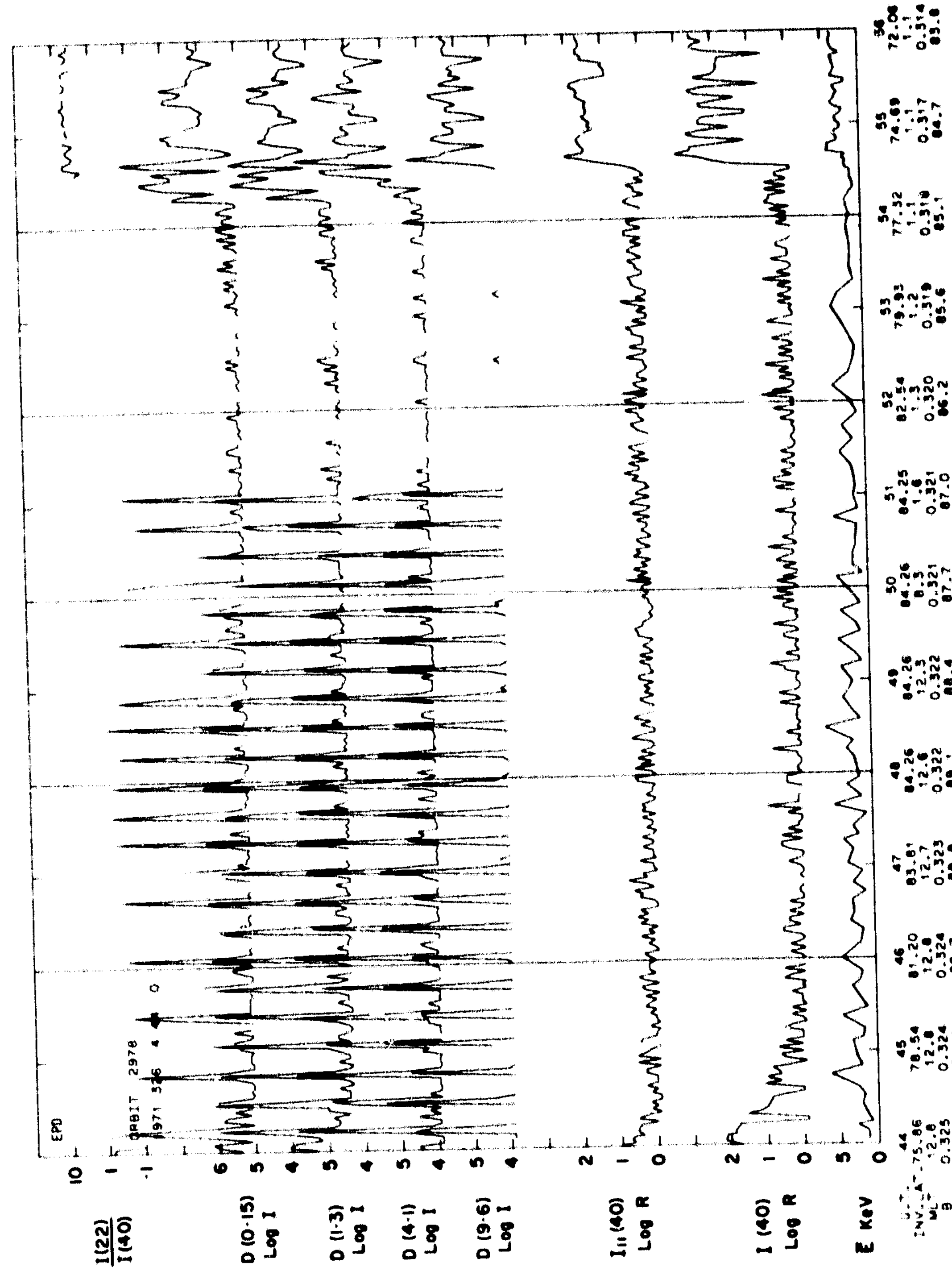

SET 19, FORMAT 3

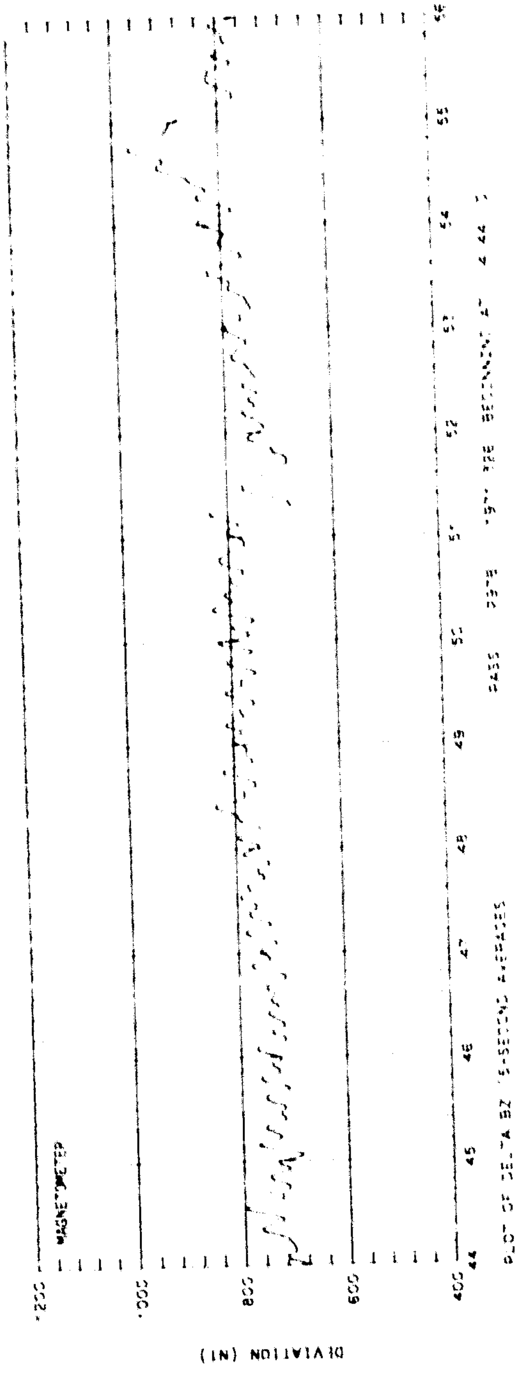

SET 19, FORMAT 2

ORBIT 2978
DATE 711122
DAY 326

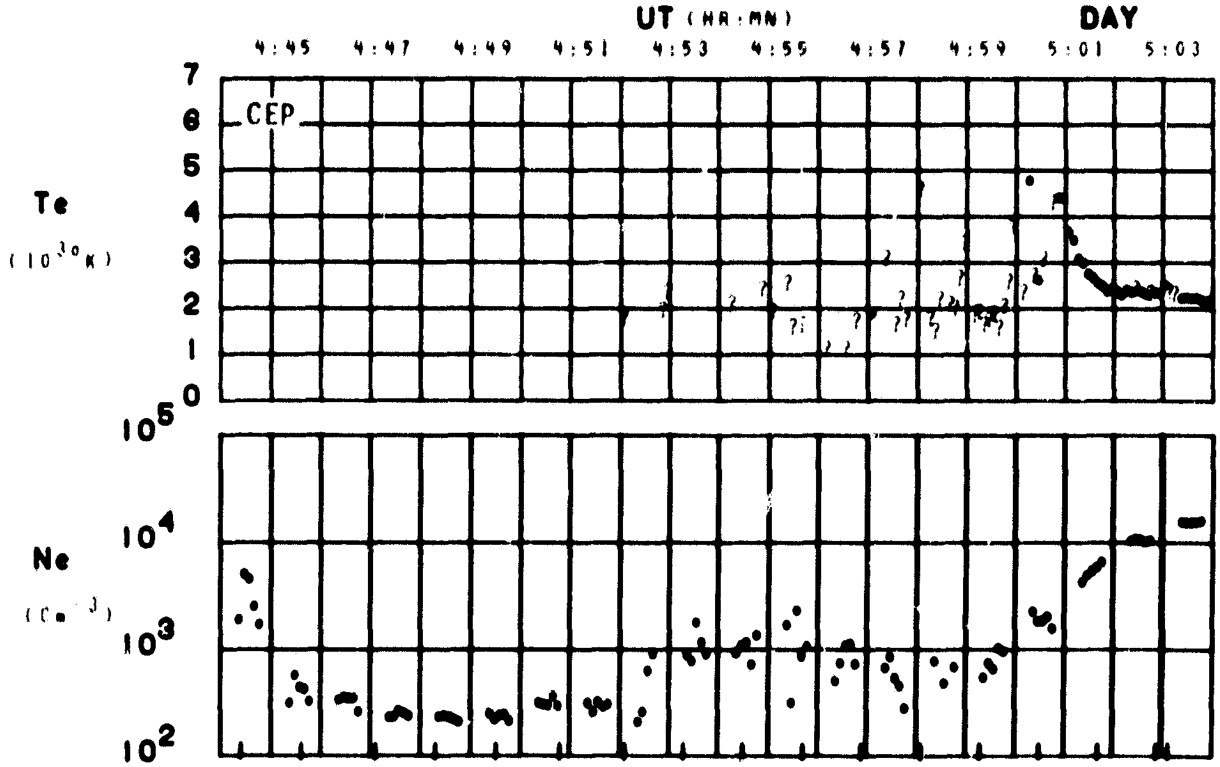

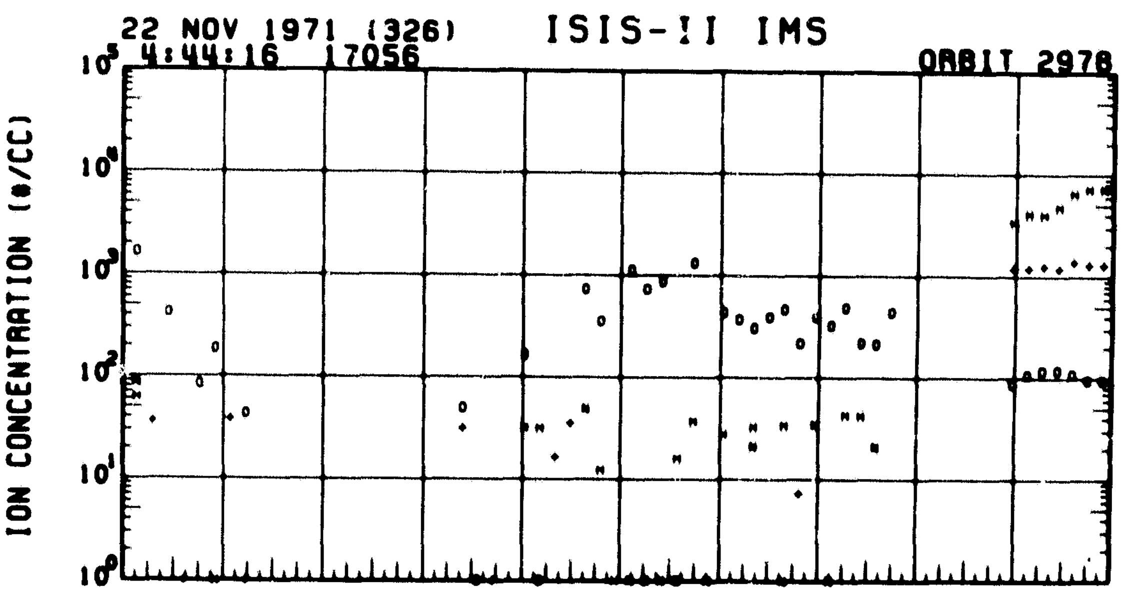

	UT	4:46	4:48	4:50	4:52	4:54	4:56	4:58	5:02
1 - H	LAST	10:35	23:51	0:37	0:51	0:58	1:02	1:05	1:00
4 - +	MLT	12:50	12:41	7:46	1:10	1:00	1:00	1:05	1:04
8 - △	DLAT	86	87	84	80	75	70	64	52
14 - N	INVL	81	84	84	83	77	72	67	57
16 - O	GLAT	88	85	78	73	66	60	54	41
	GLNG	-19	-77	-80	-83	-81	-81	-81	-81
	SZEN	108	115	121	127	133	138	144	154
	ALT	1438	1439	1438	1437	1436	1433	1430	1424

SET 19, FORMAT 4

RPA 711122

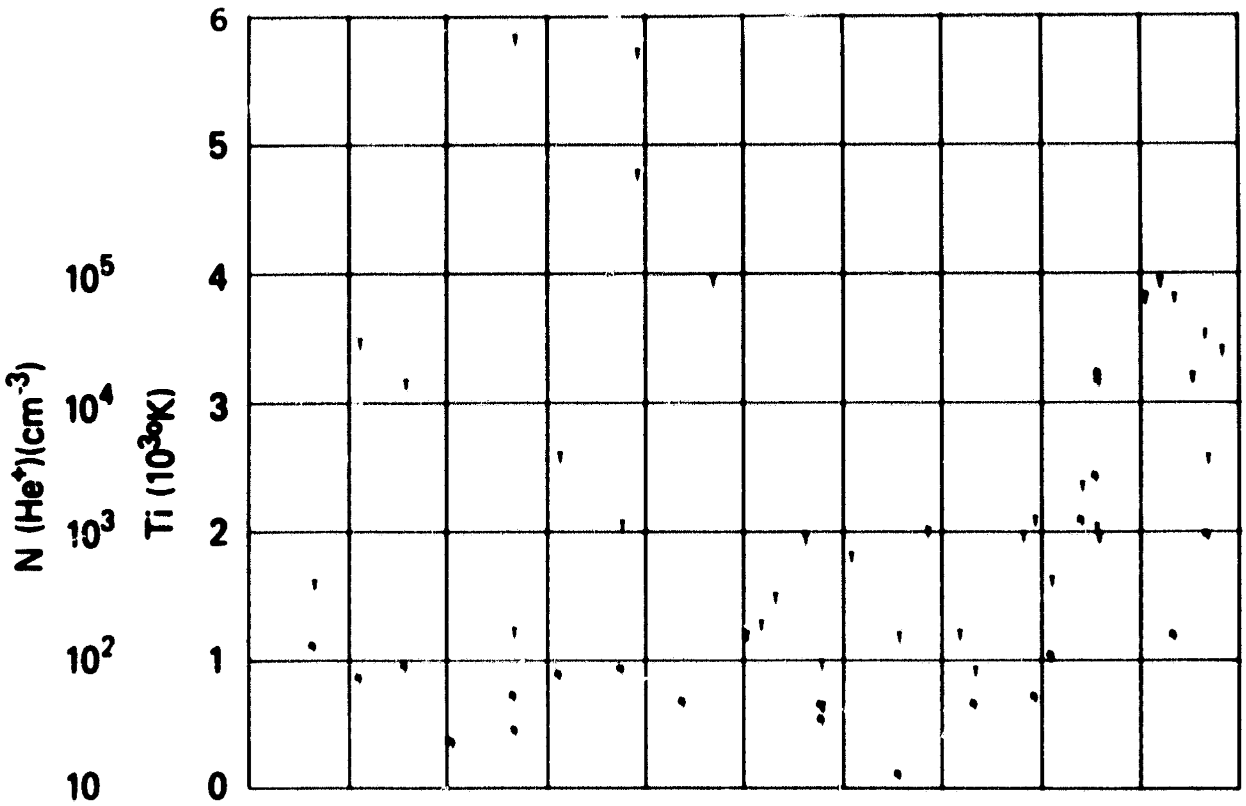

UT	4:46	4:48	4:50	4:52	4:54	4:56	4:58	5:02
LAST	18:35	23:51	0:37	0:51	0:58	1:02	1:05	1:08
MLT	12:50	12:41	7:56	1:19	1:09	1:06	1:05	1:04
DLAT	86	87	84	80	75	70	64	52
INVL	81	84	84	83	77	72	67	57
GLAT	88	85	78	73	66	60	54	41
GLNG	-19	-77	-66	-63	-61	-61	-61	-61
SZEN	109	115	121	127	133	139	144	154
ALT	1438	1439	1438	1437	1436	1433	1430	1424

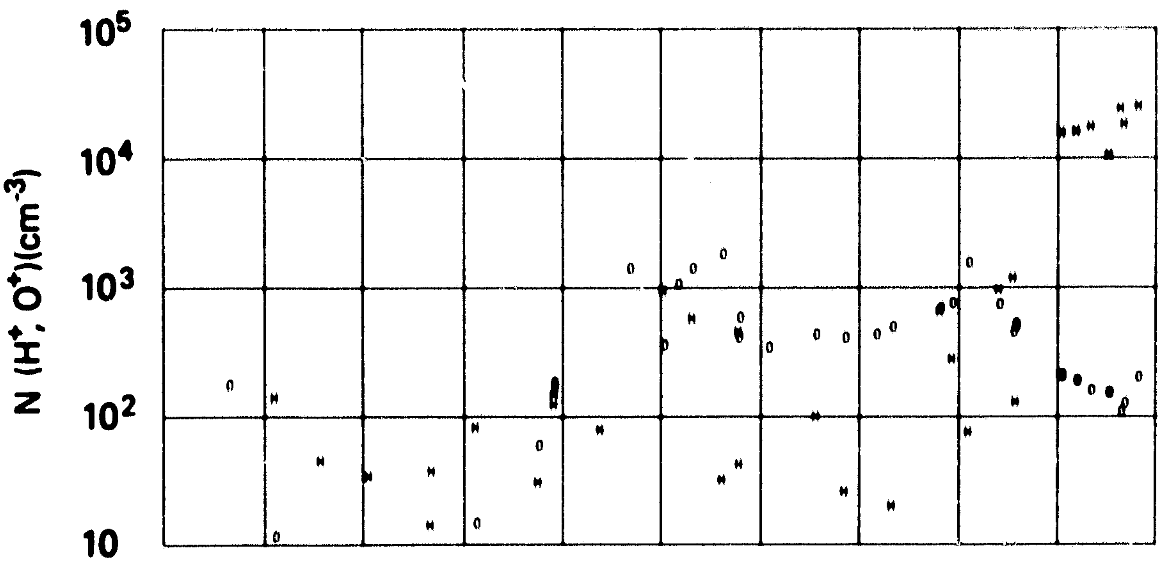

SET 19, FORMAT 5

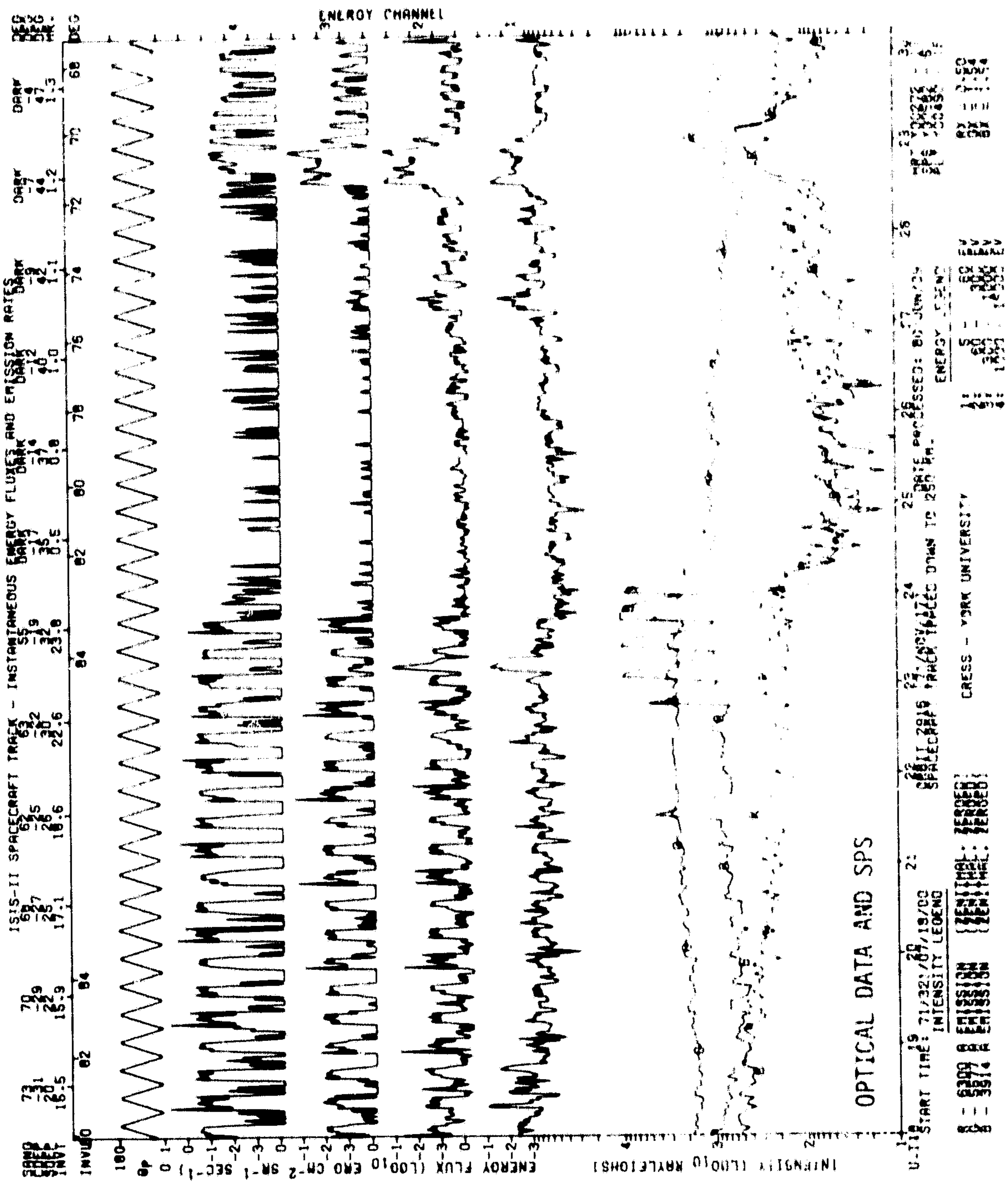

SET 20, FORMAT 1

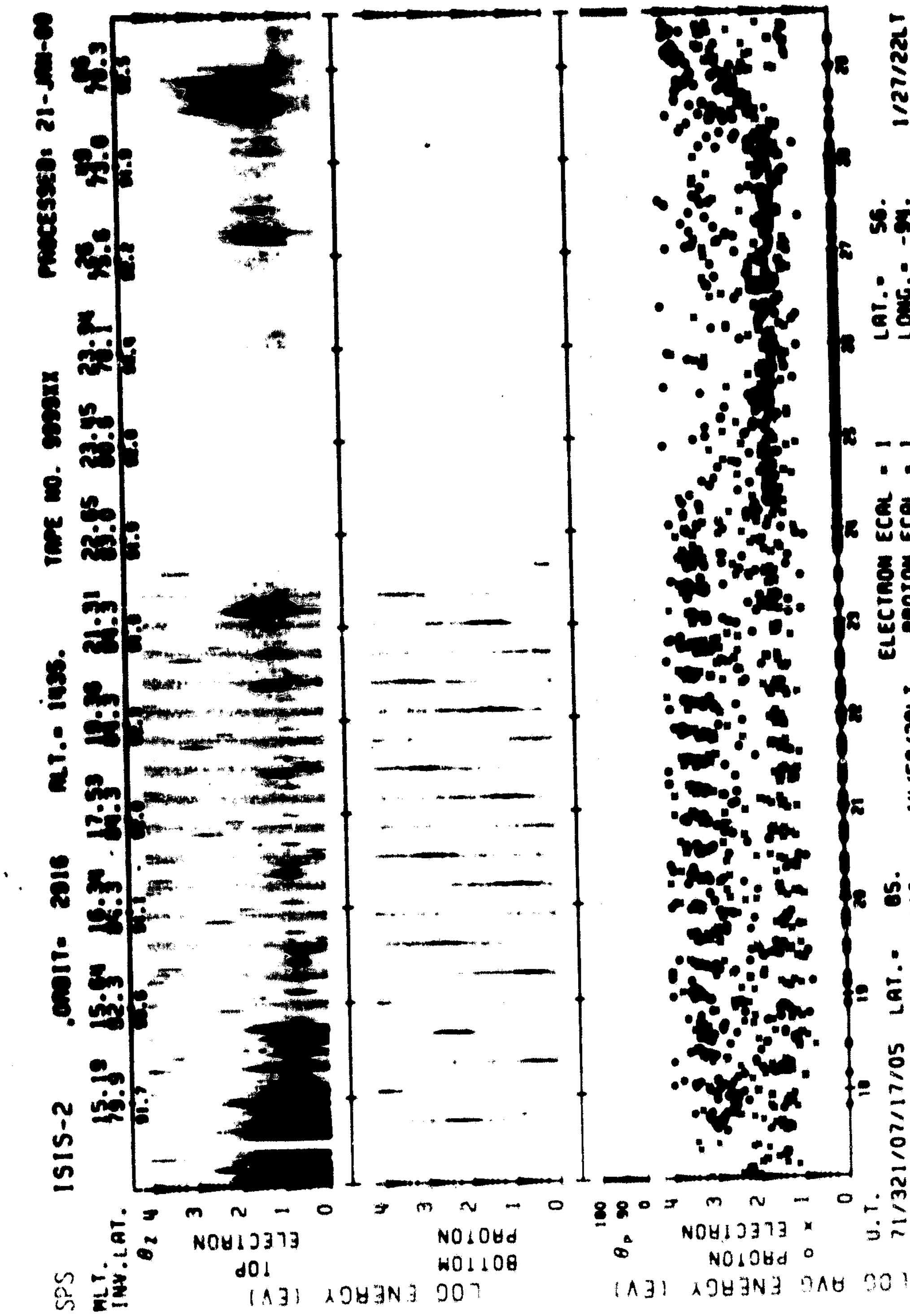

SET 20, FORMAT 6

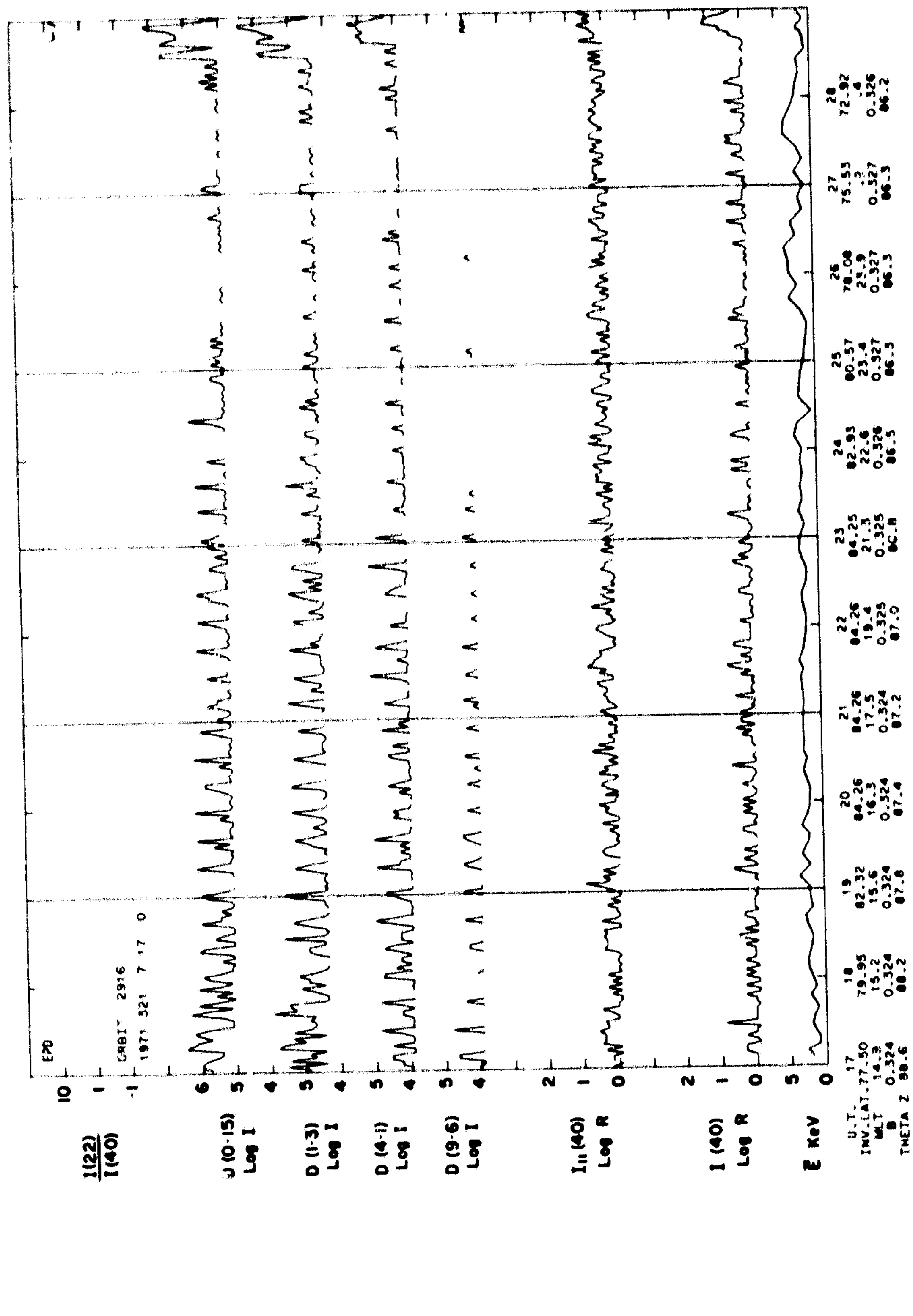

SET 20, FORMAT 3

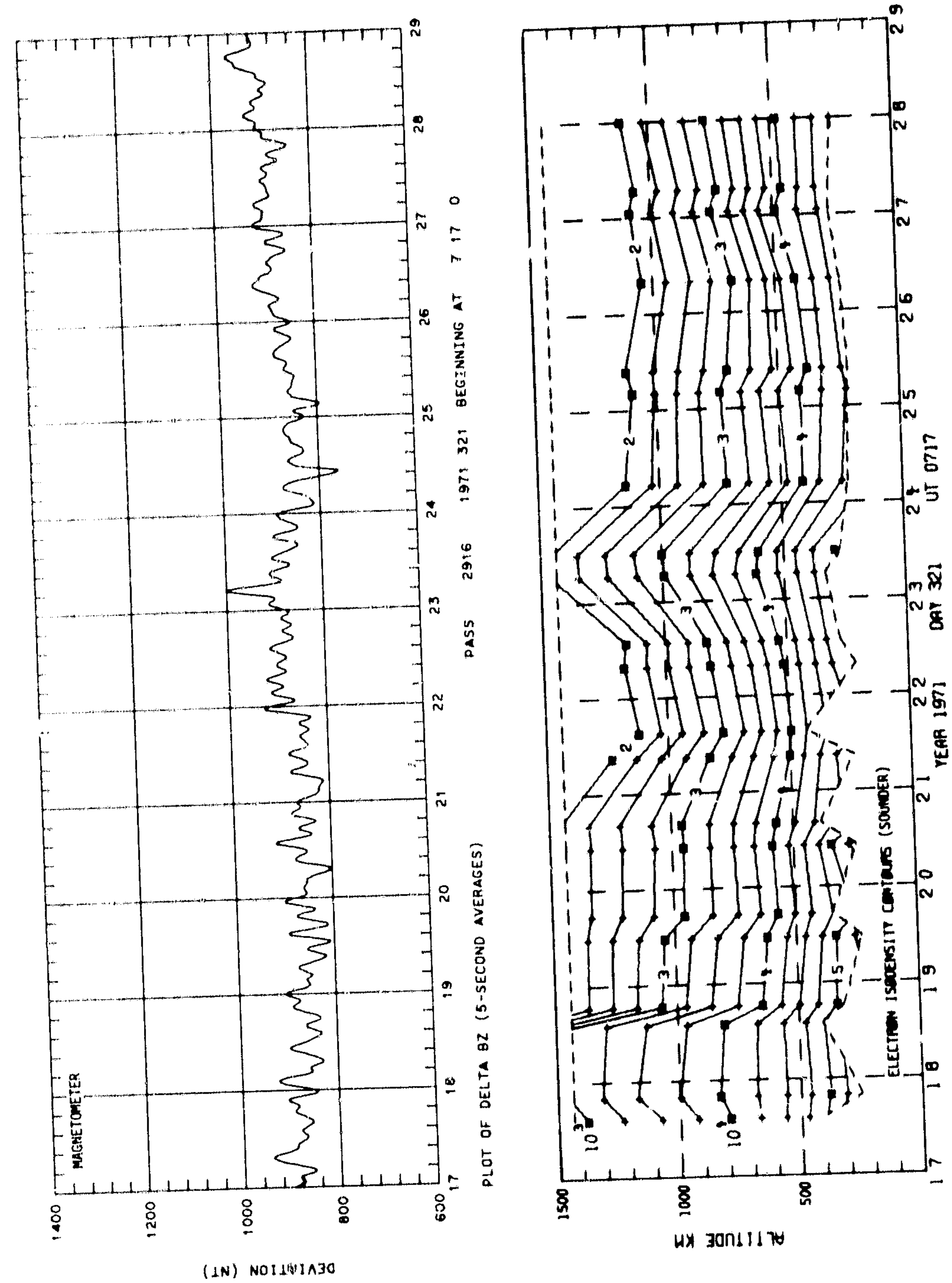

SET 20, FORMAT 2

ORBIT 2916
DATE 711117
DAY 321

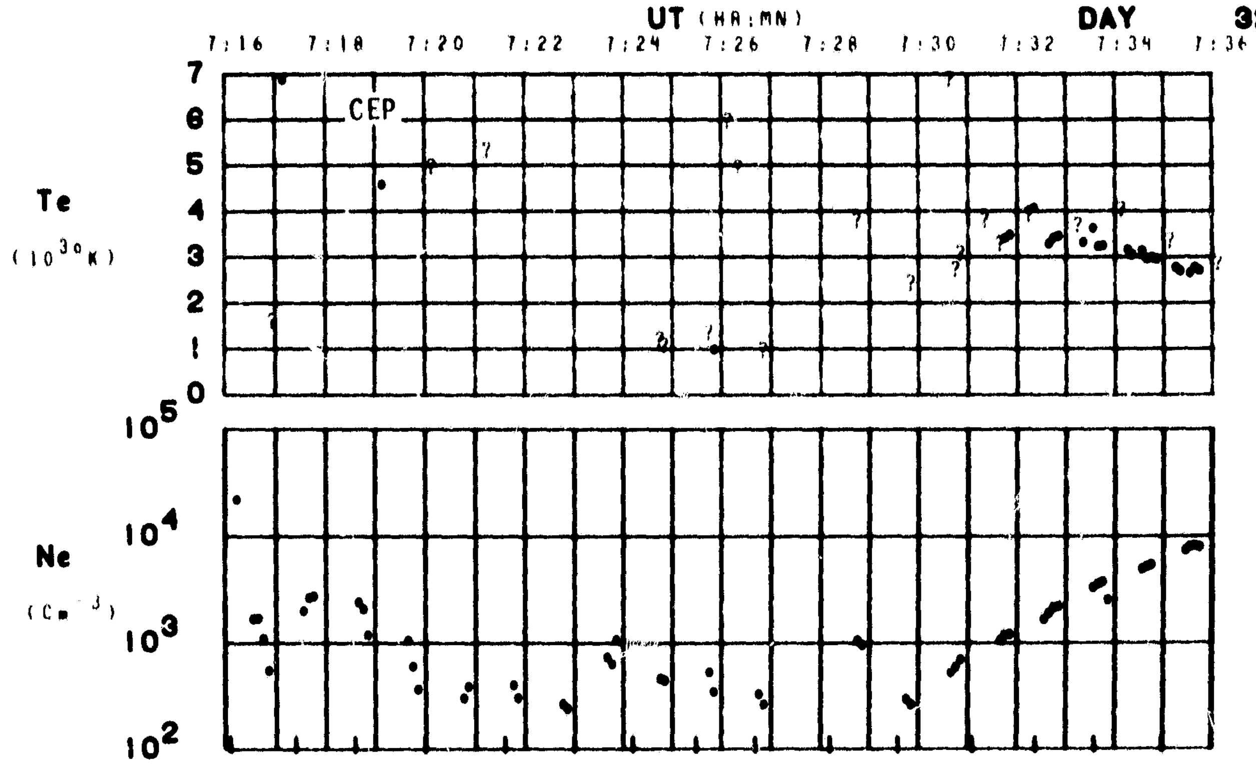

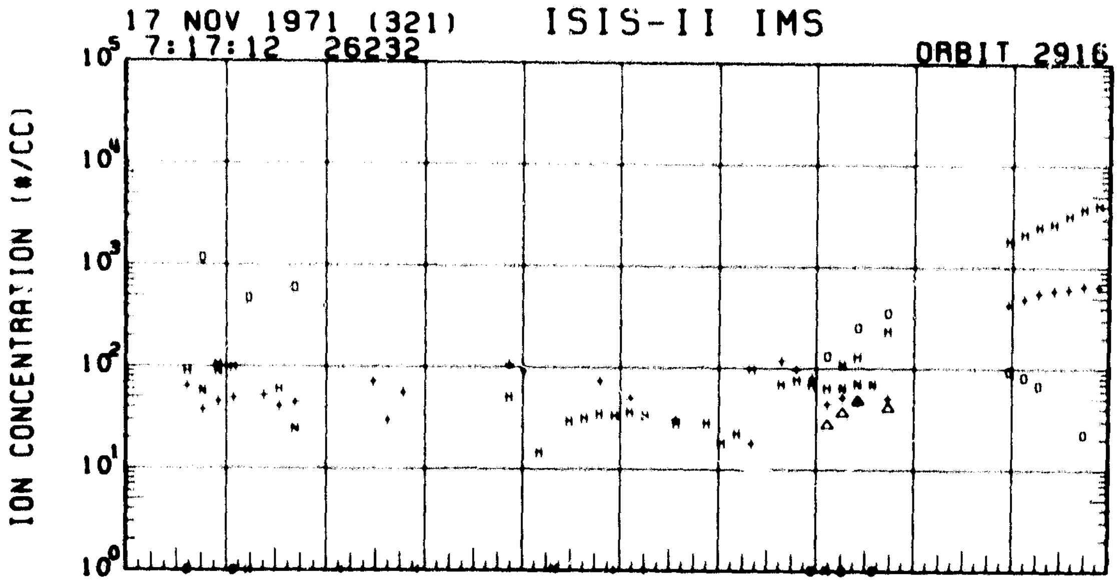

1 - H	UT	7:18	7:20	7:22	7:24	7:26	7:28	7:30	7:34
4 - +	LAST	16:14	0:13	0:58	1:14	1:21	1:25	1:28	1:32
8 - △	ALT	15:12	16:21	19:24	22:40	15:14	0:30	0:48	1:08
14 - N	DLAT	85	88	89	85	80	75	58	55
16 - O	INVL	80	84	84	83	78	73	68	57
	GLAT	87	85	79	73	67	61	54	42
	GLNG	133	-112	-99	-95	-94	-93	-93	-93
	SZEN	108	113	119	125	130	136	141	150
	ALT	1436	1437	1438	1437	1437	1435	1433	1428

SET 20, FORMAT 4

Note different temperature scale

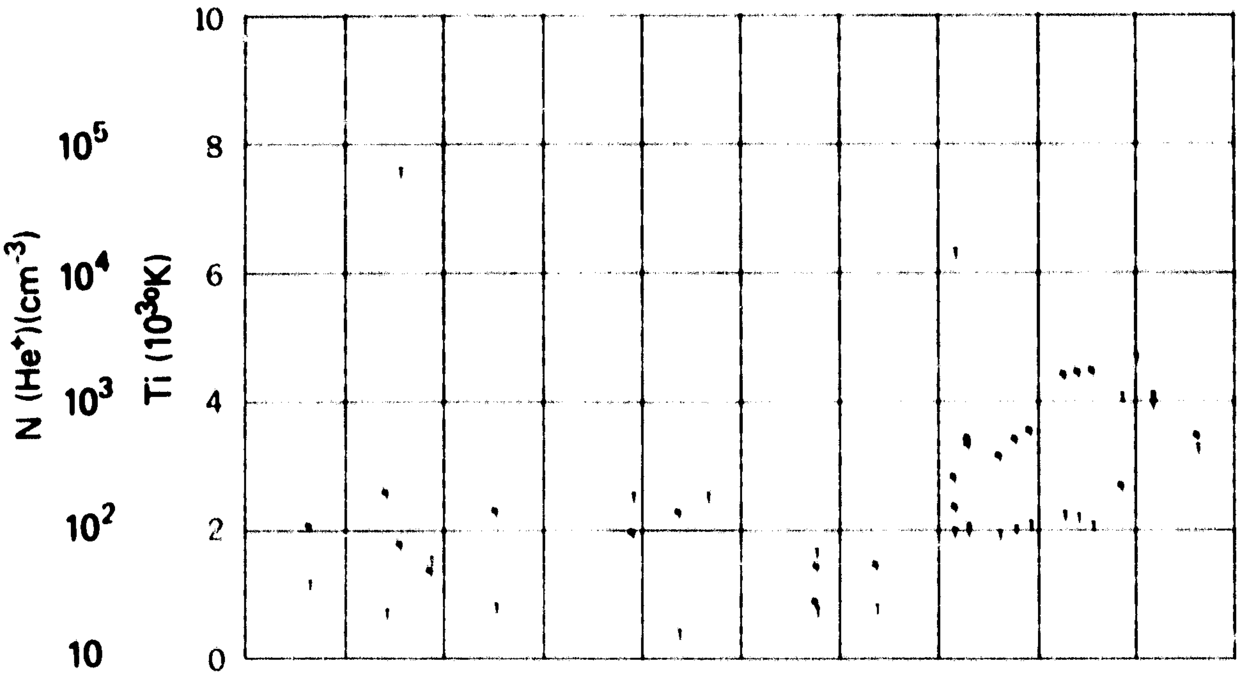

UT	7:18	7:20	7:22	7:24	7:26	7:28	7:30	7:34
LAST	18:14	0:13	0:50	1:14	1:21	1:25	1:28	1:32
MLT	15:12	16:21	19:24	22:40	15:14	0:30	0:40	1:08
DLAT	85	88	89	85	80	75	68	55
INVL	80	84	84	83	78	73	68	57
GLAT	87	85	79	73	67	61	54	42
GLNG	133	112	99	95	94	93	93	93
SZEN	108	113	119	125	130	136	141	150
ALT	1436	1437	1438	1437	1437	1435	1433	1428

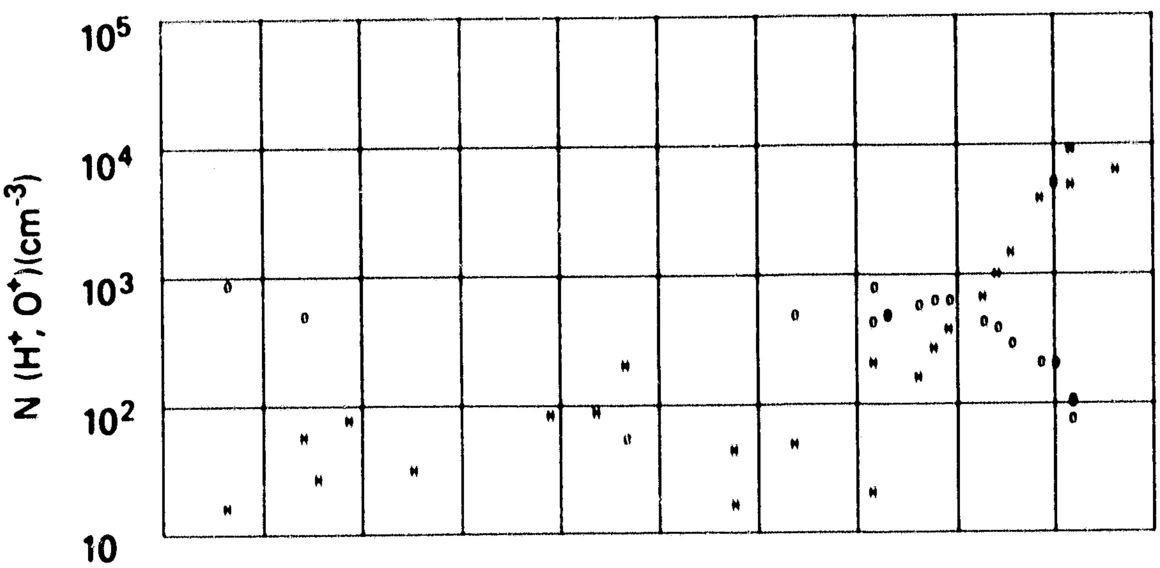

SET 20, FORMAT 5

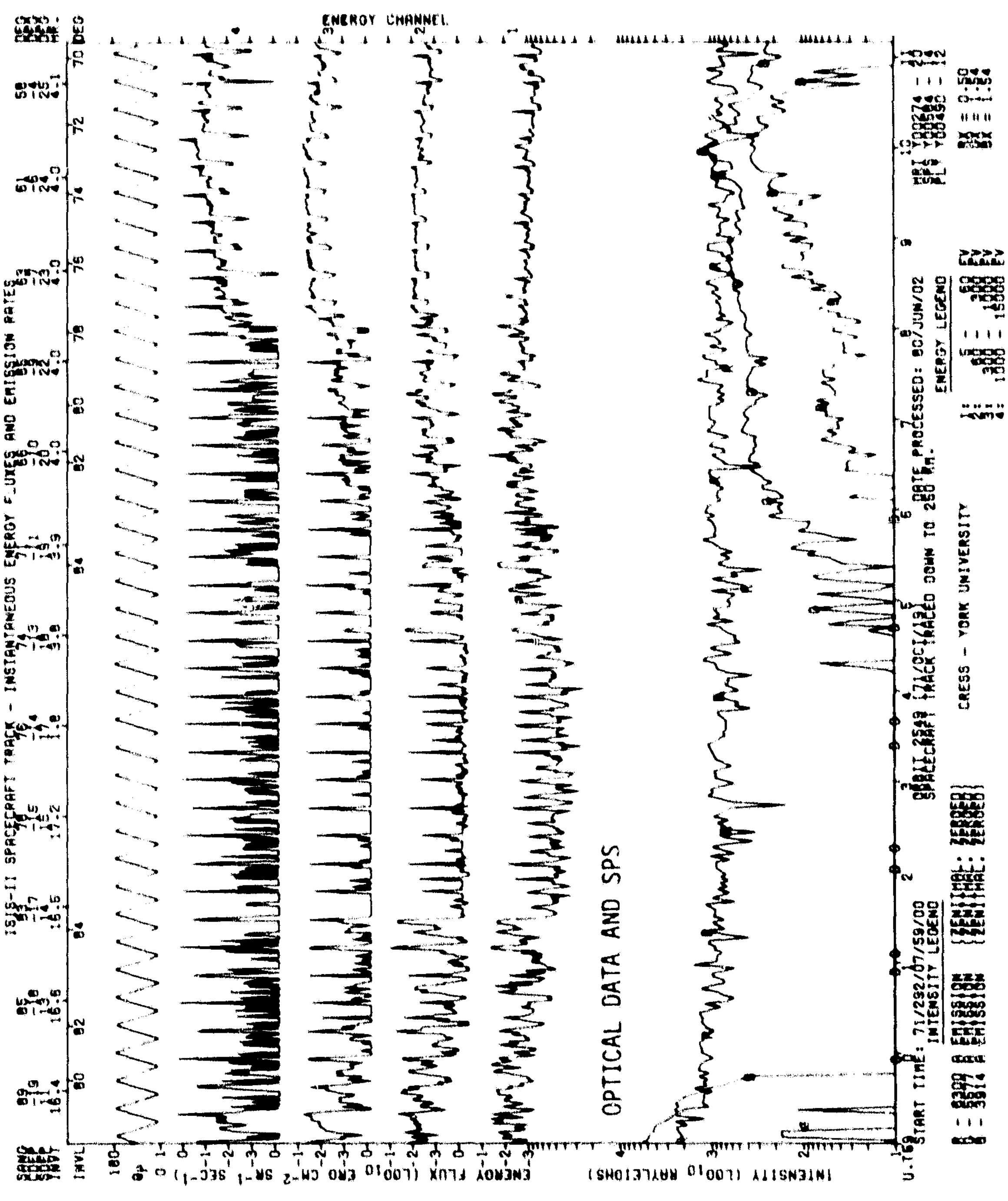

SET 21, FORMAT 1

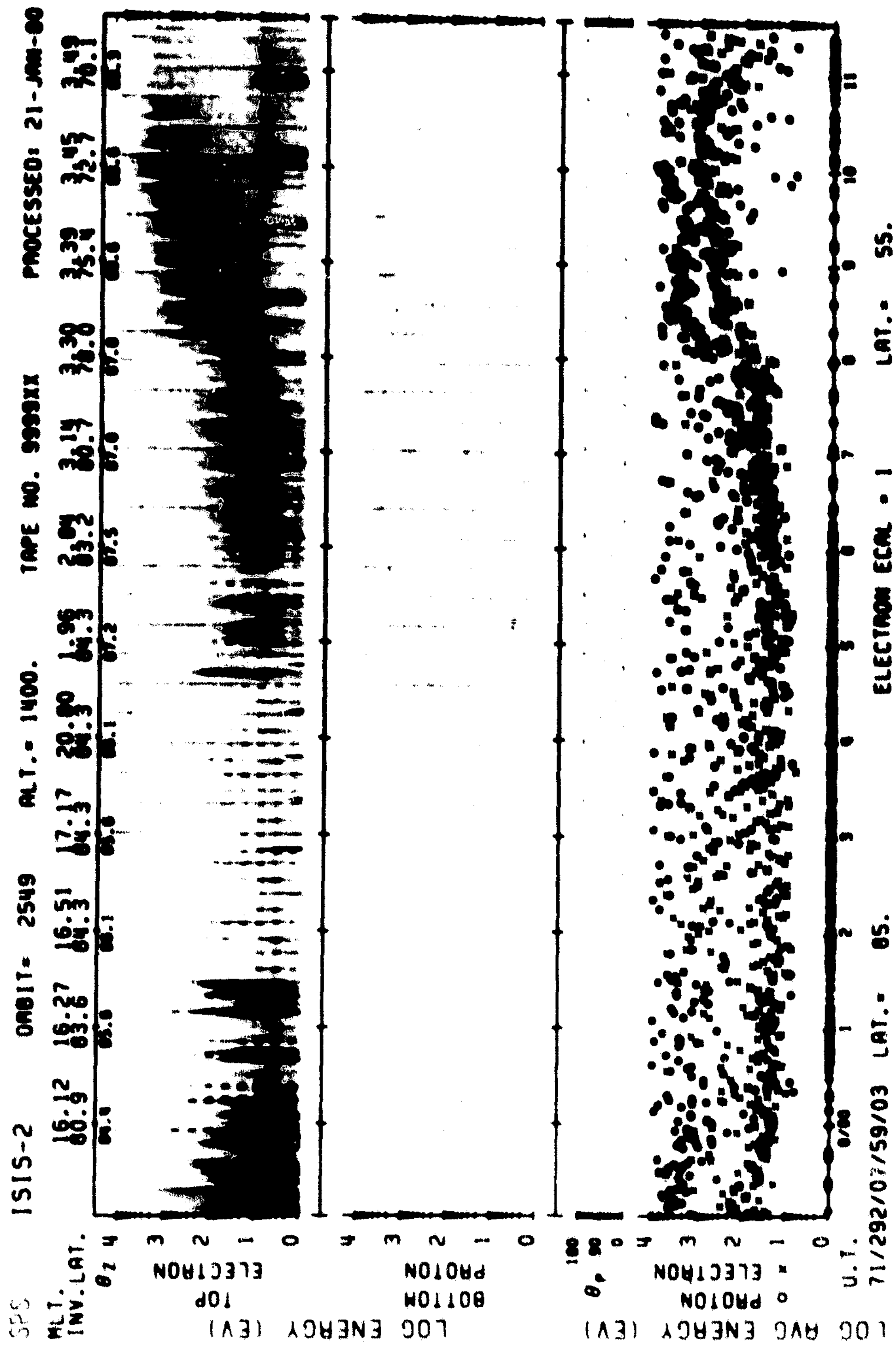

SET 21, FORMAT 6

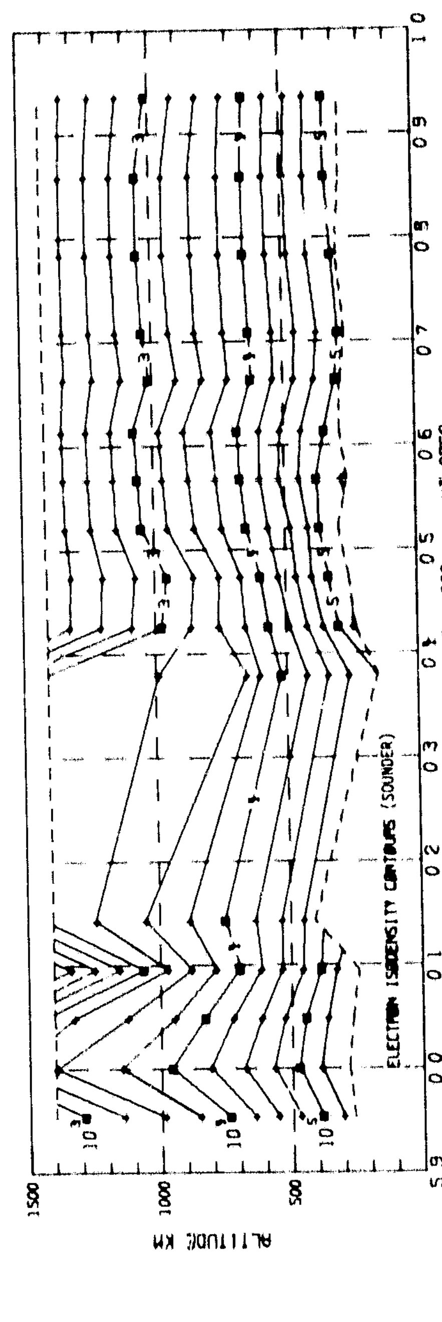

SET 21, FORMAT 2

ORBIT 2549
DATE 711019
DAY 292

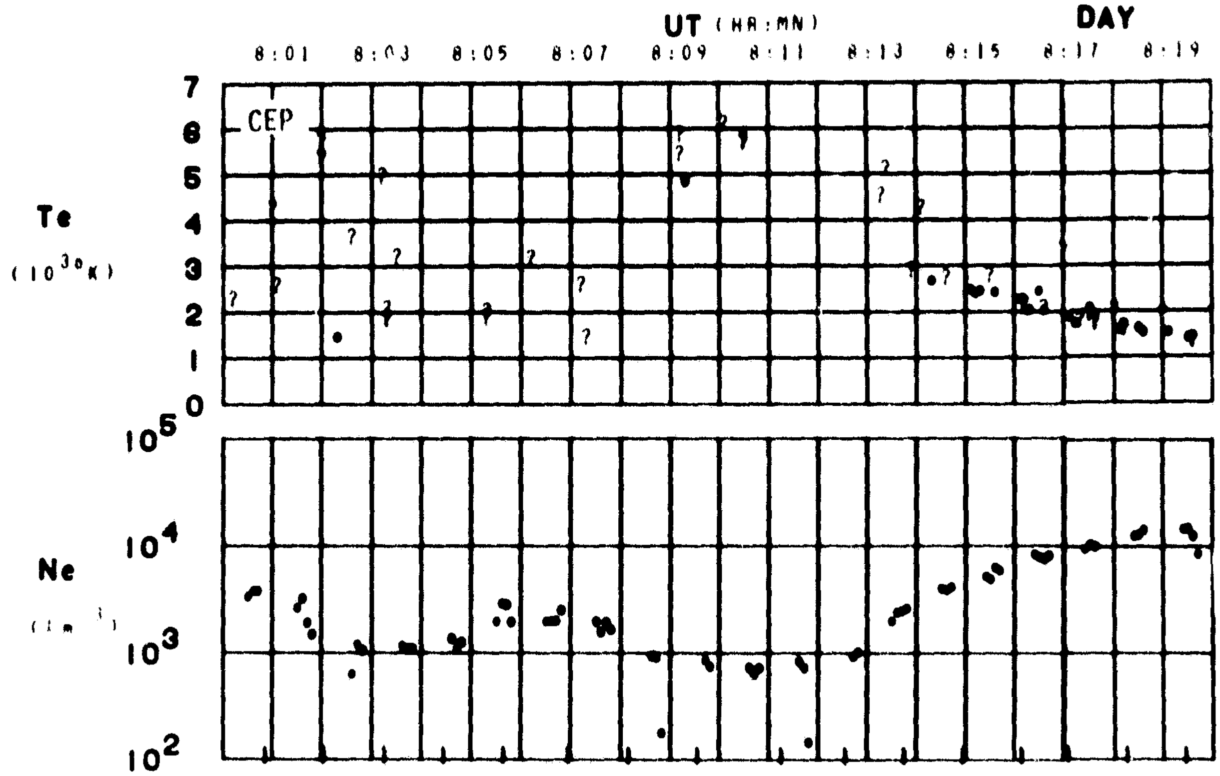

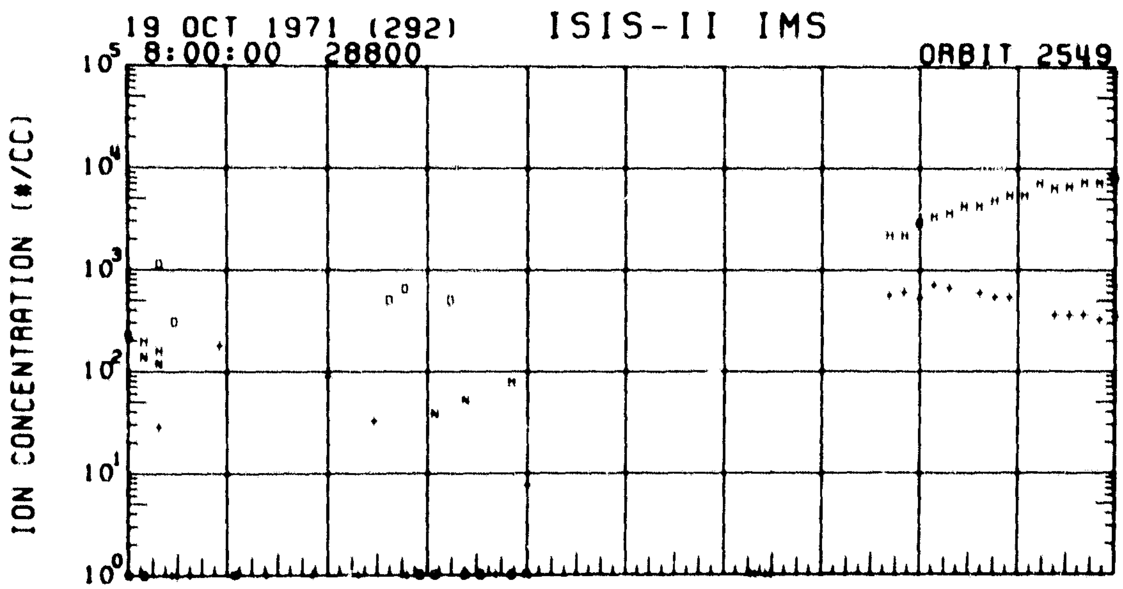

1	H
4	+
8	△
14	N
16	O

UT	8:02	8:04	8:06	8:08	8:10	8:12	8:16	8:18
LAST	2:26	3:14	3:27	3:34	3:38	3:41	3:45	3:46
MLT	16:32	21:12	2:52	3:18	3:27	3:32	3:37	3:38
DLAT	88	86	82	77	72	66	54	47
INVL	84	84	83	78	73	67	57	52
GLAT	85	79	72	66	60	53	41	35
GLNG	86	-75	-72	-71	71	-70	-71	-71
SZEN	104	107	110	113	116	118	122	123
ALT	1405	1409	1412	1414	1416	1418	142.	1423

SET 31, FORMAT 4

RPA

711019

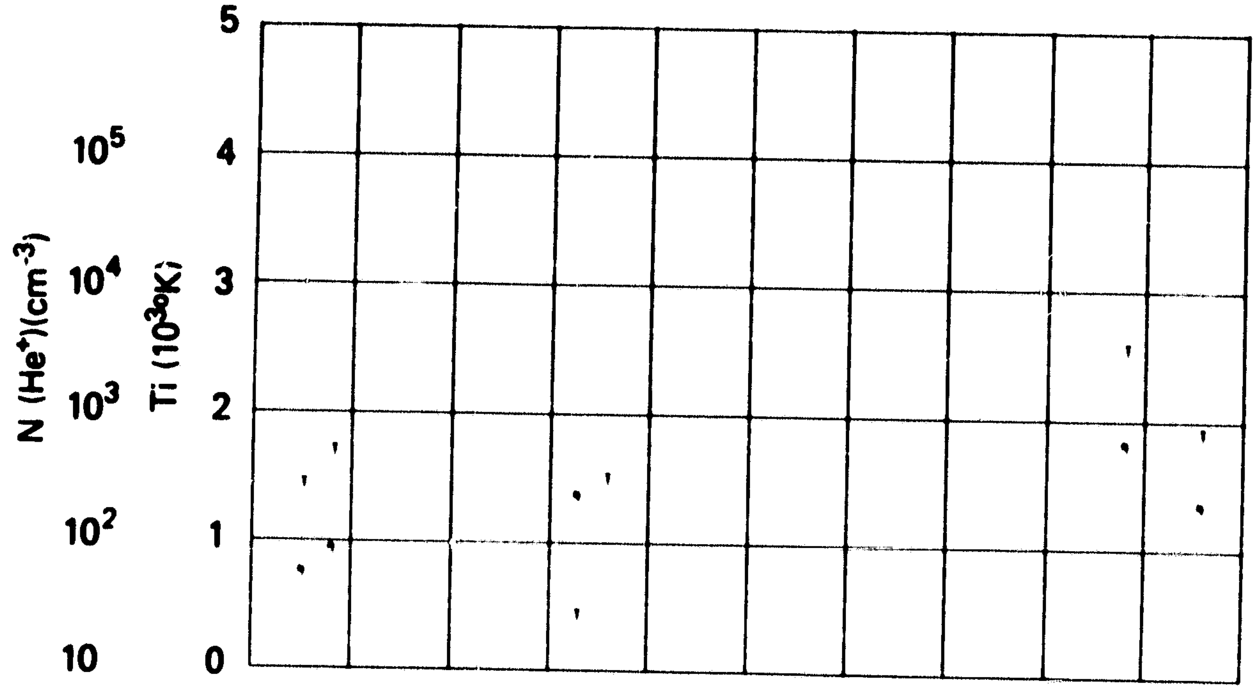

UT	8:02	8:04	8:06	8:08	8:10	8:12	8:16	8:18
LAST	2:26	3:14	3:27	3:34	3:38	3:41	3:45	3:46
MLT	16:32	21:12	2:52	3:18	3:27	3:32	3:37	3:39
DLAT	88	86	82	77	72	66	54	47
INVL	84	84	83	78	73	67	57	52
GLAT	85	79	72	66	60	53	41	35
GLNG	86	75	-72	71	71	70	-71	-71
SZEN	104	107	110	113	116	118	122	123
ALT	1405	1409	1412	1414	1416	1418	1421	1423

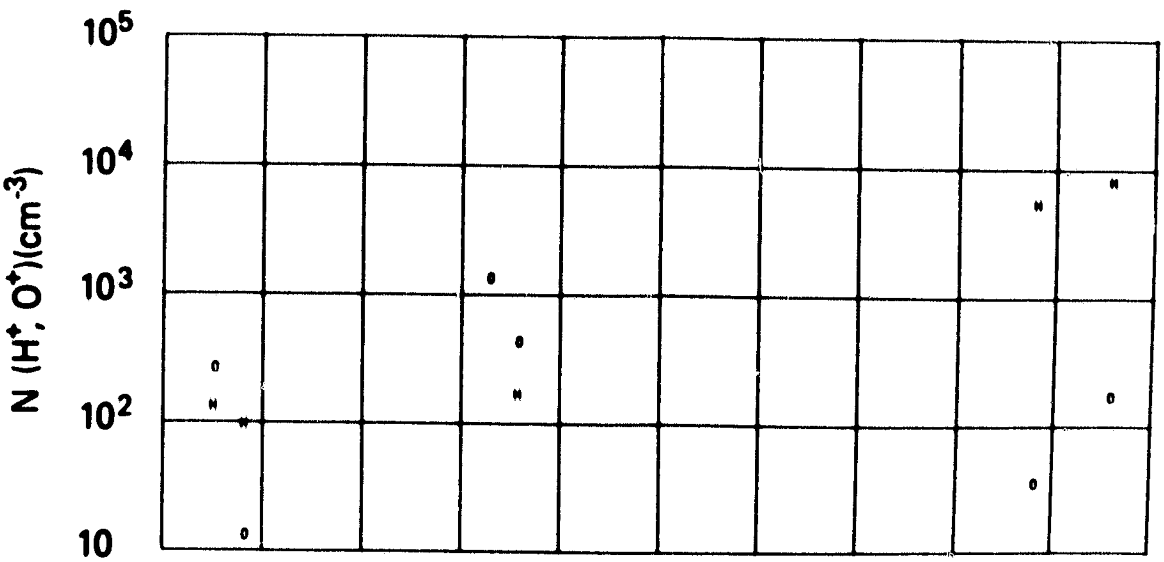

SET 21, FORMAT 5

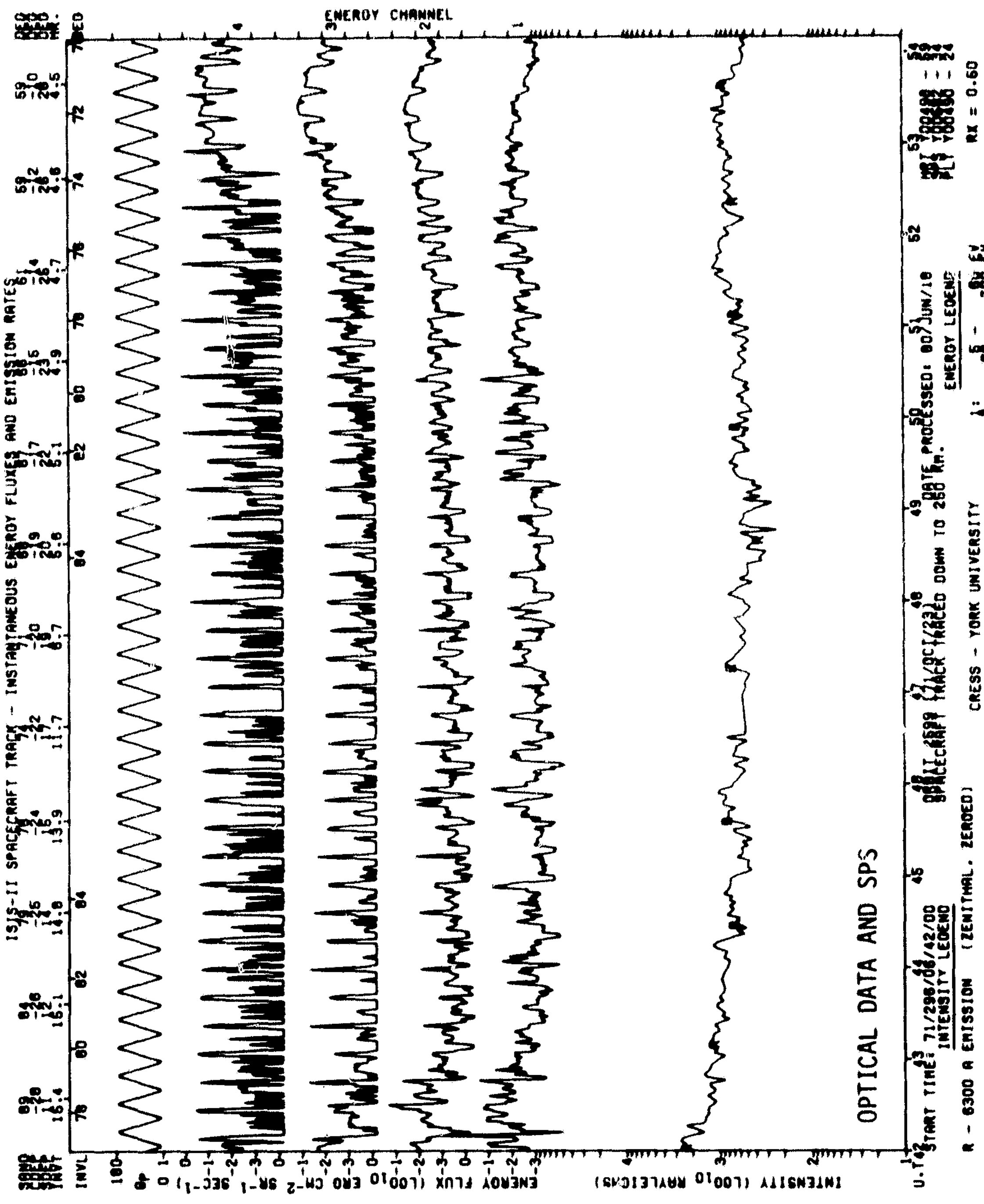

SET 22, FORMAT 1

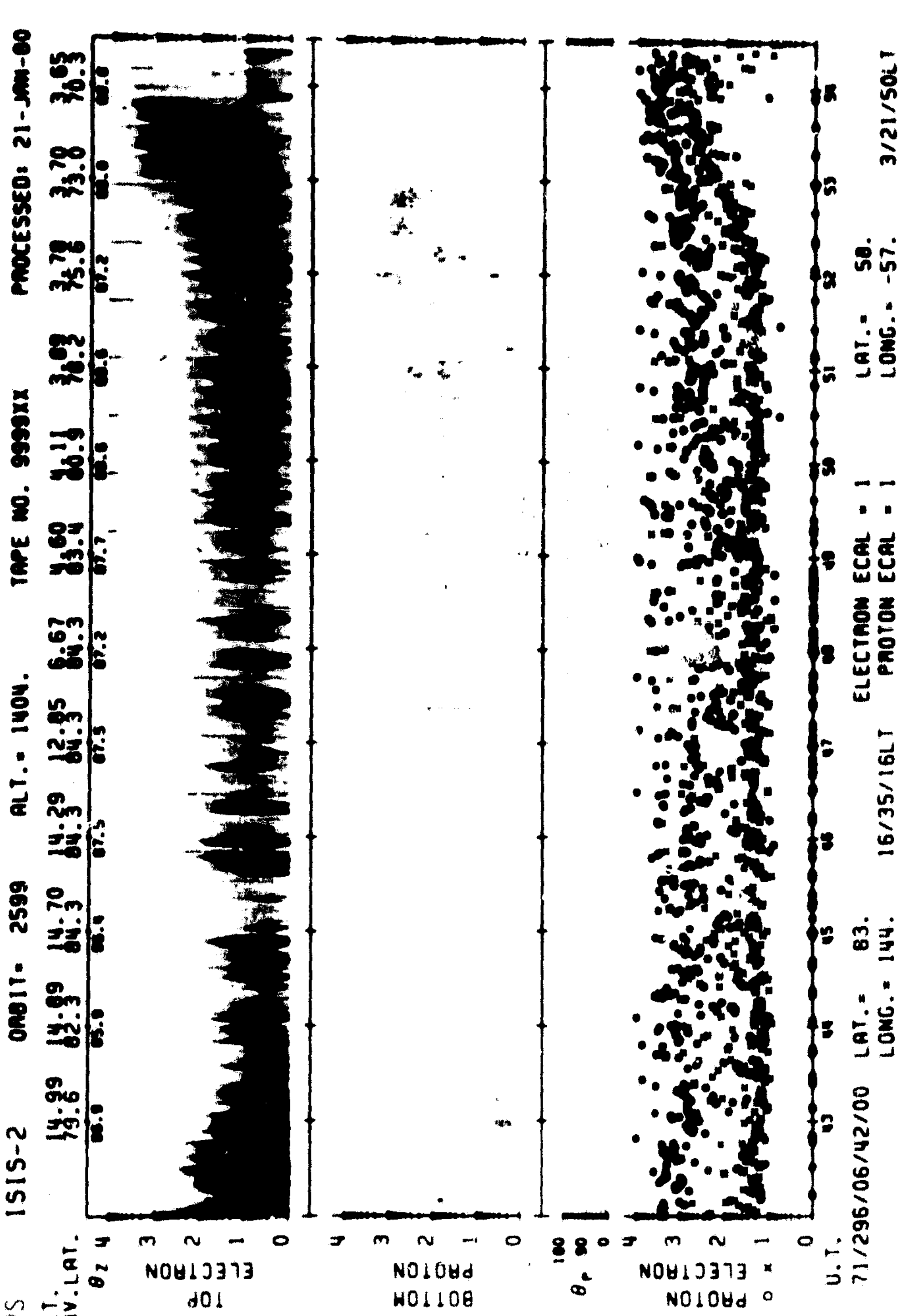

SET 22, FORMAT 6

ORBIT 2599
DATE 711023
DAY 296

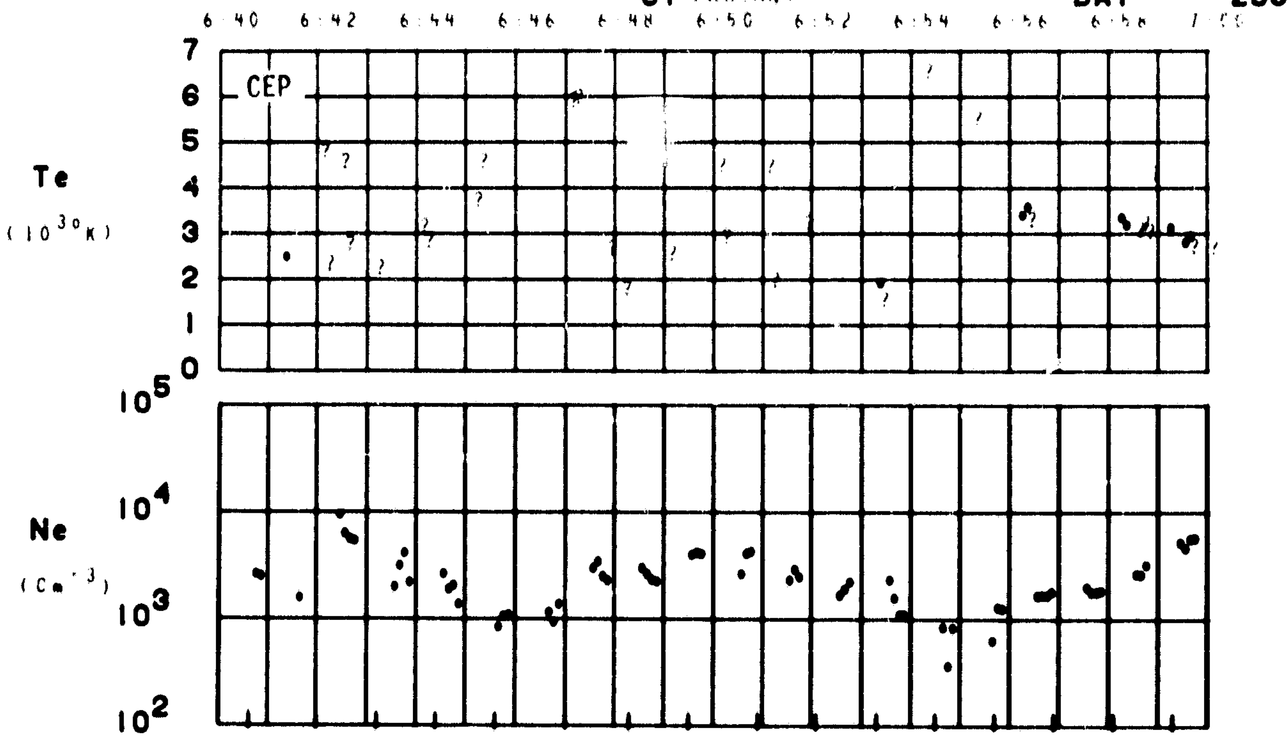

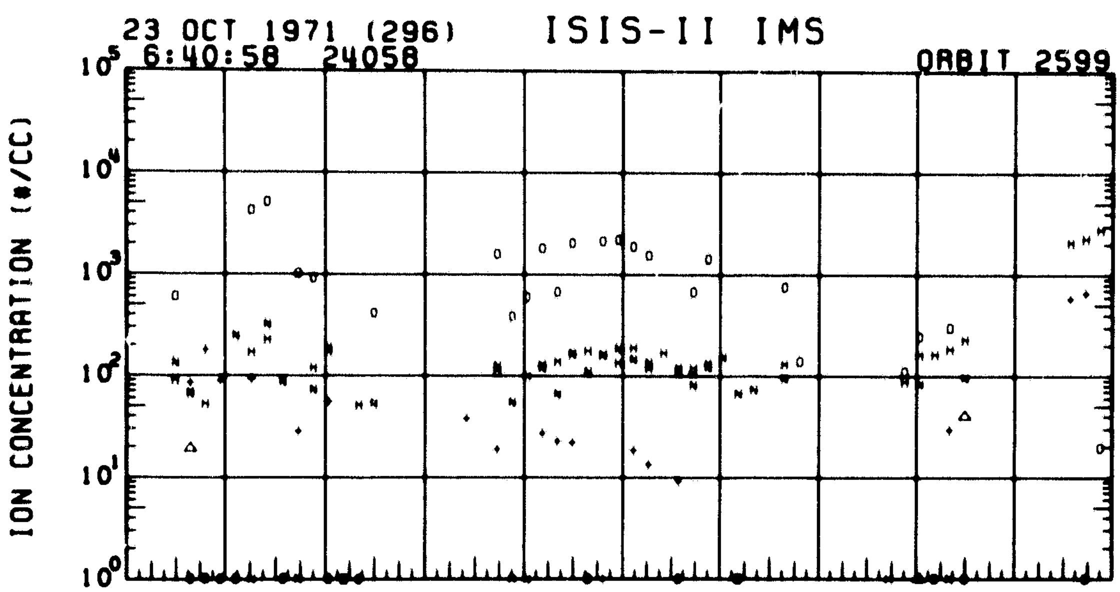

1 - H	UT	6:42	6:44	6:46	6:48	6:50	6:52	6:54	6:56
4 +	LAST	16:35	20:39	2:25	2:60	3:12	3:18	3:21	3:24
8 △	ALT	15:04	14:54	14:17	6:46	4:07	3:47	3:39	3:35
14 - N	DLAT	82	86	86	82	78	73	67	62
16 - O	INVL	77	82	84	84	81	76	70	65
	GLAT	83	88	84	78	71	65	59	52
	GLNG	144	-150	-68	-60	-57	-56	-56	-56
	SZEN	99	102	106	110	113	116	119	122
	ALT	1404	1408	1412	1415	1418	1420	1422	1423

SET 22, FORMAT 4

RPA

711023

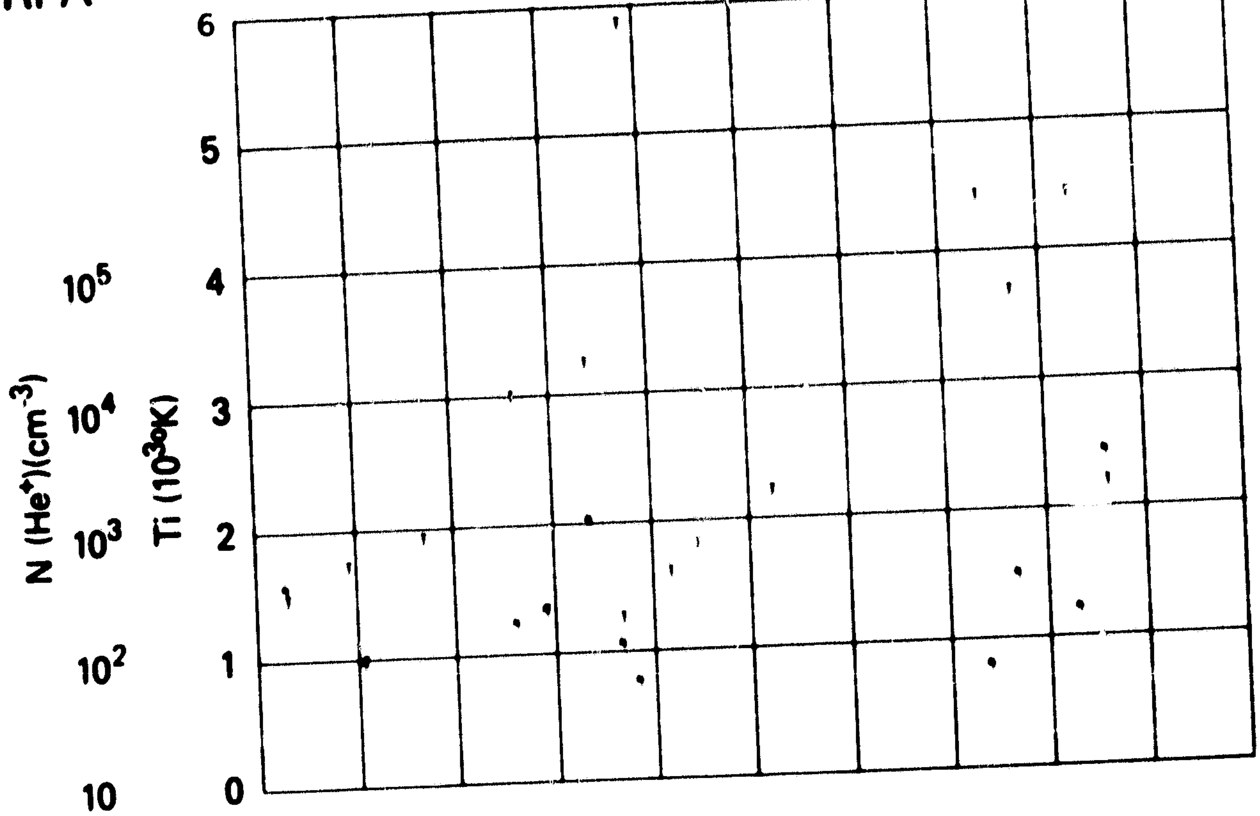

UT	6:42	6:44	6:46	6:48	6:50	6:52	6:54	6:56
LAST	16:35	20:38	2:25	2:00	3:12	3:18	3:21	3:24
MLT	15:04	14:54	14:17	6:46	4:07	3:47	3:38	3:35
DLAT	82	86	86	82	78	73	67	62
INV.	77	82	84	84	81	76	70	65
GLAT	83	88	84	78	71	65	58	52
GLNG	144	-150	-68	60	-57	-58	-58	-58
SZEN	99	102	106	110	113	116	118	122
ALT	1404	1408	1412	1415	1418	1420	1422	1423

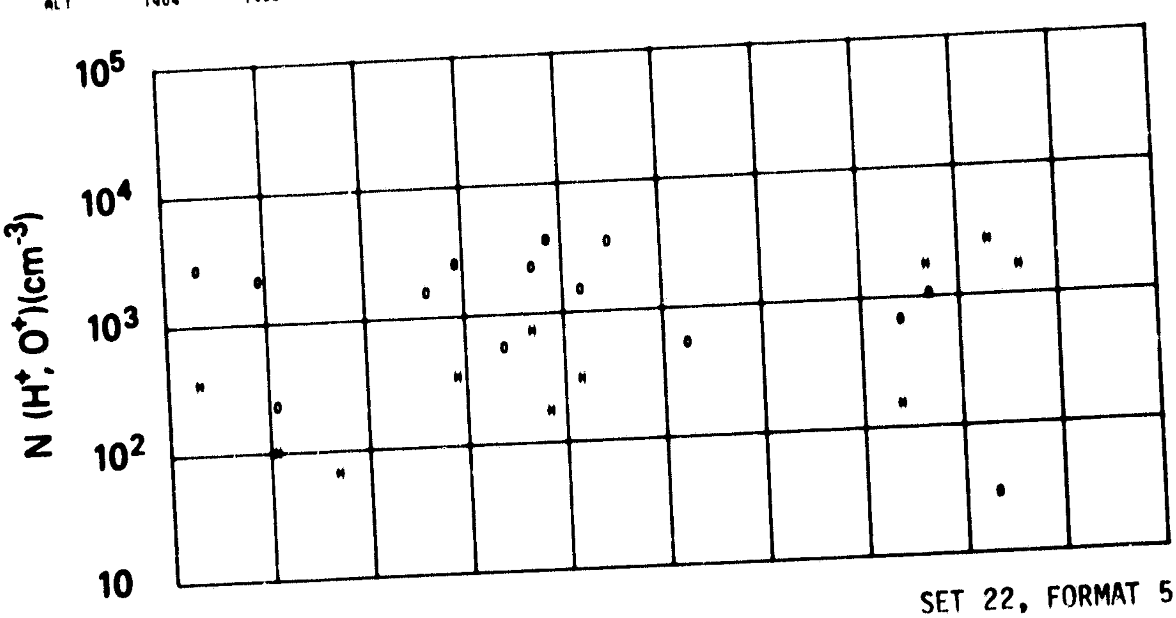

SET 22, FORMAT 5

71/296/0642

Excerpts of VLF Spectral film for the period 0642 - 0654

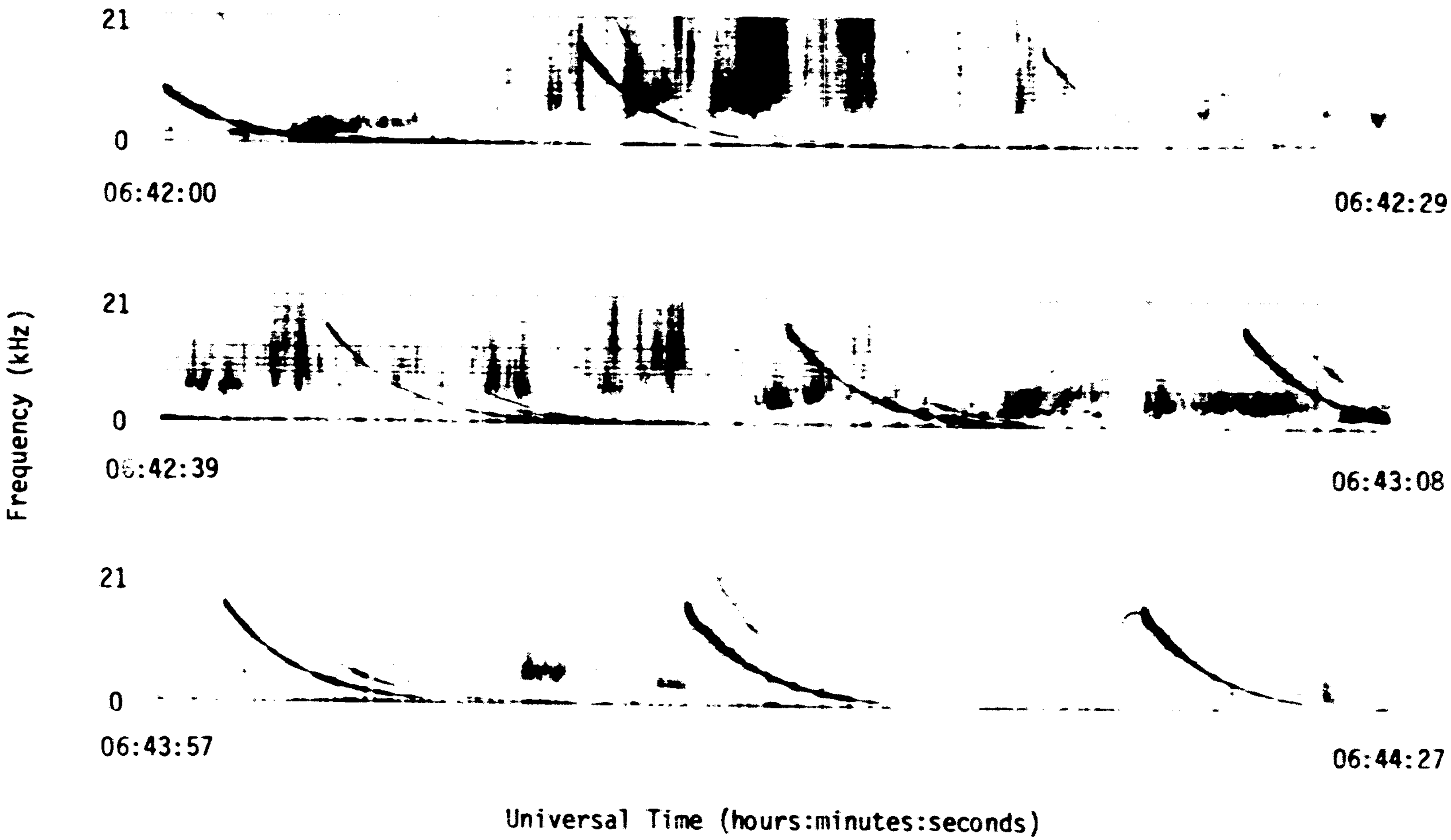

SET 22, FORMAT 11

71/296/0642

Excerpts of VLF Spectral film for the period 0642 - 0654

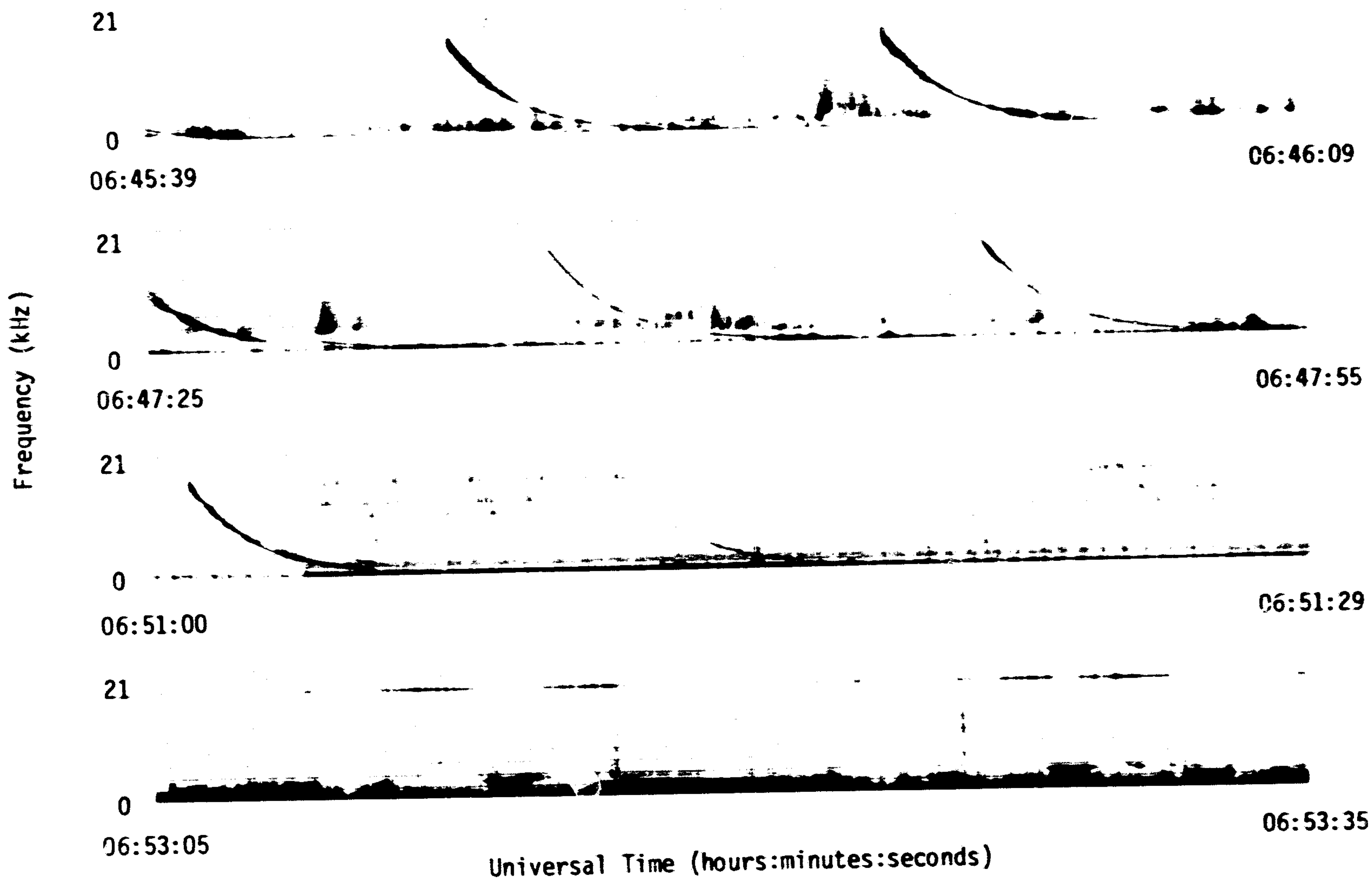

SET 22, FORMAT 11

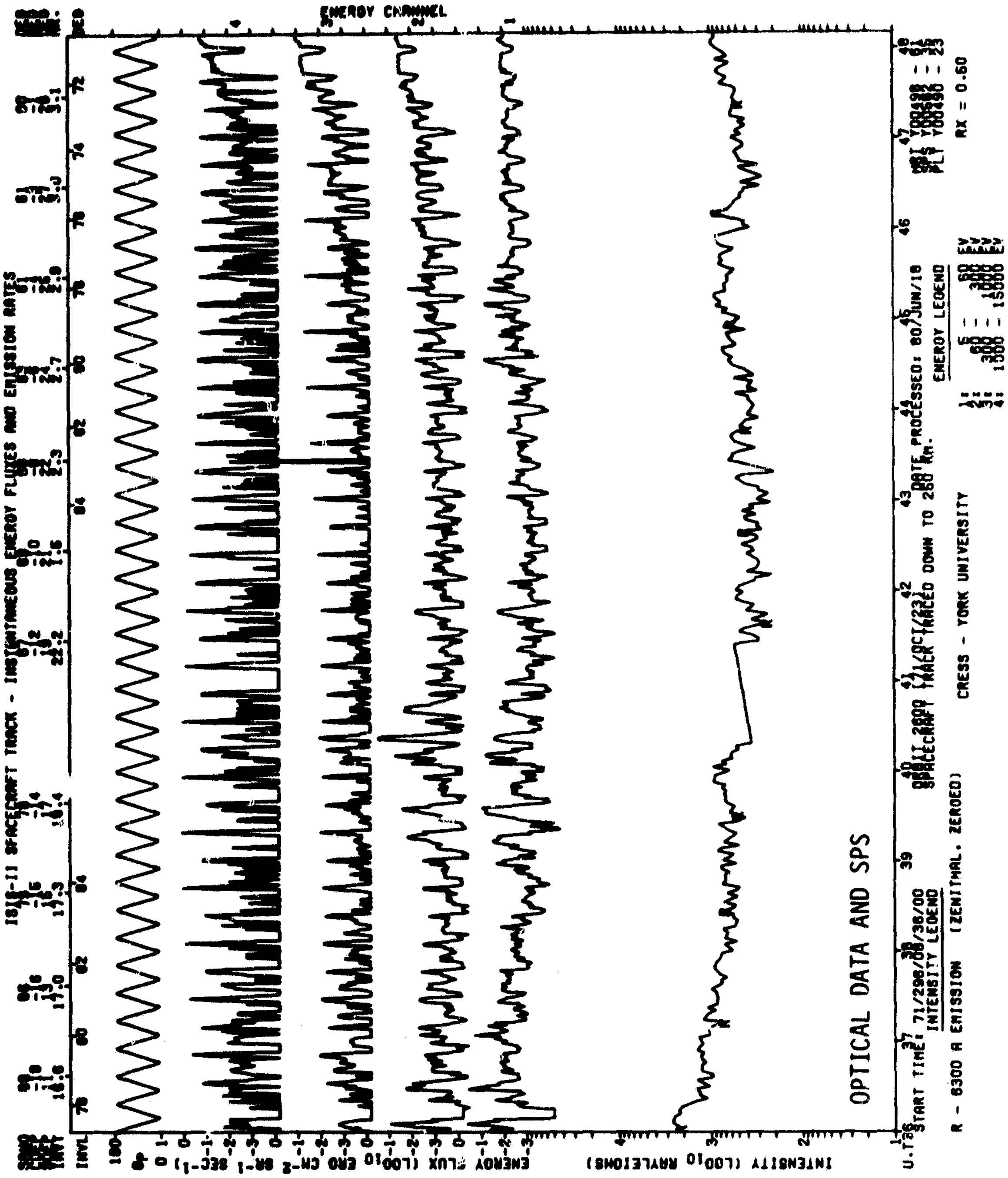

SET 23, FORMAT 1

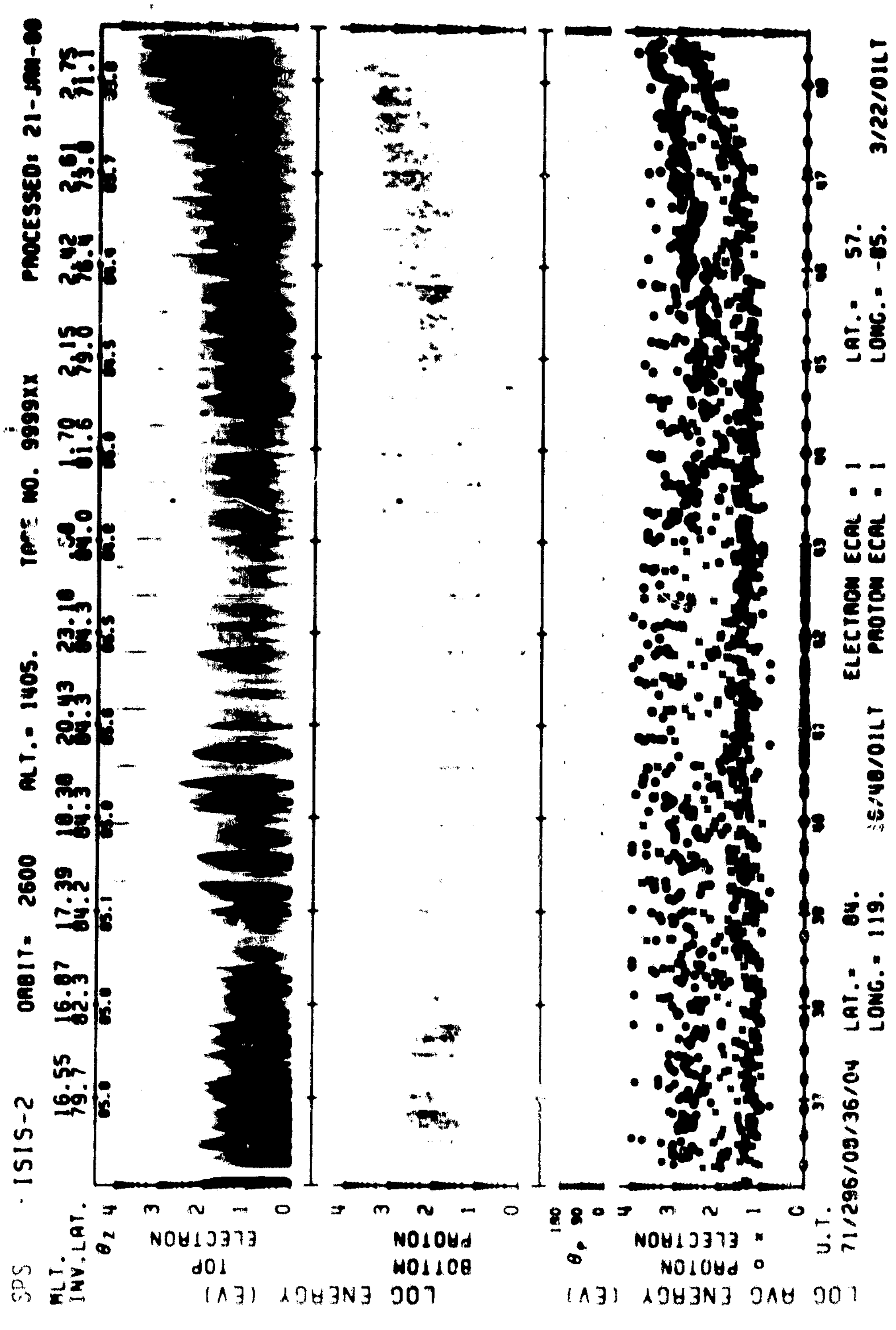

SET 23, FORMAT 6

ORBIT 2600
DATE 711023
DAY 296

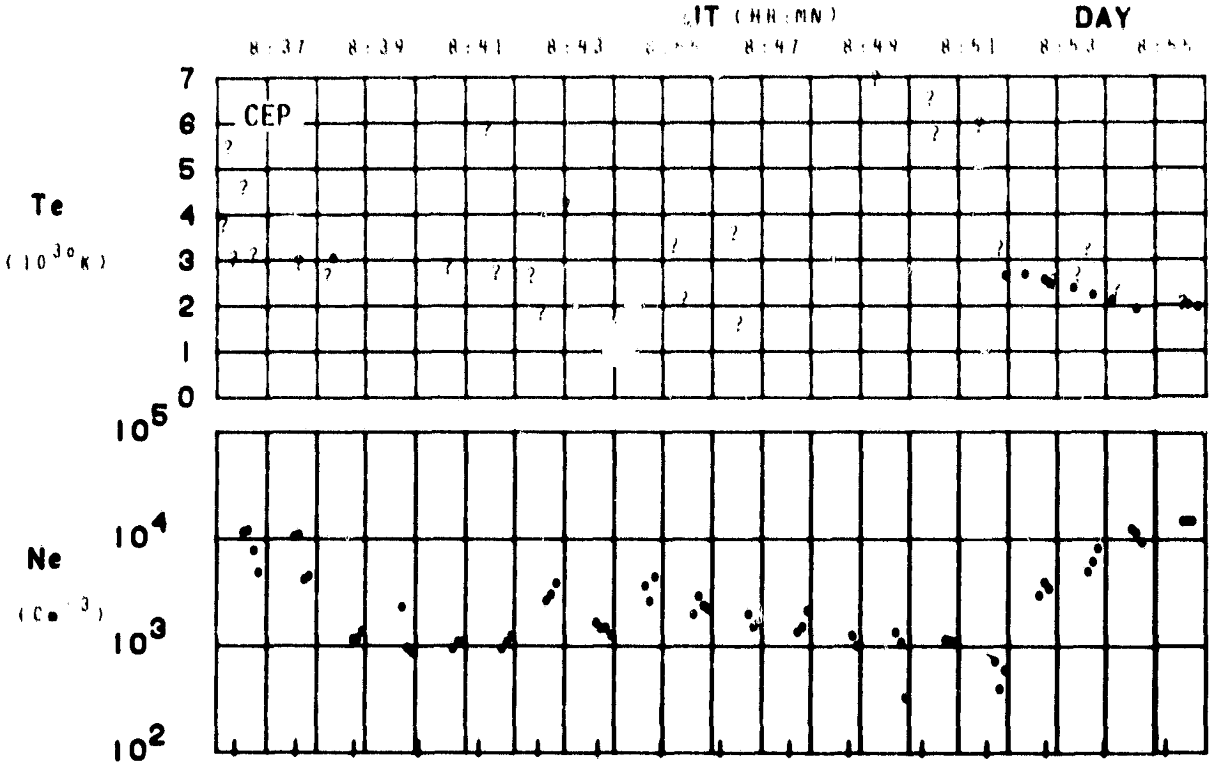

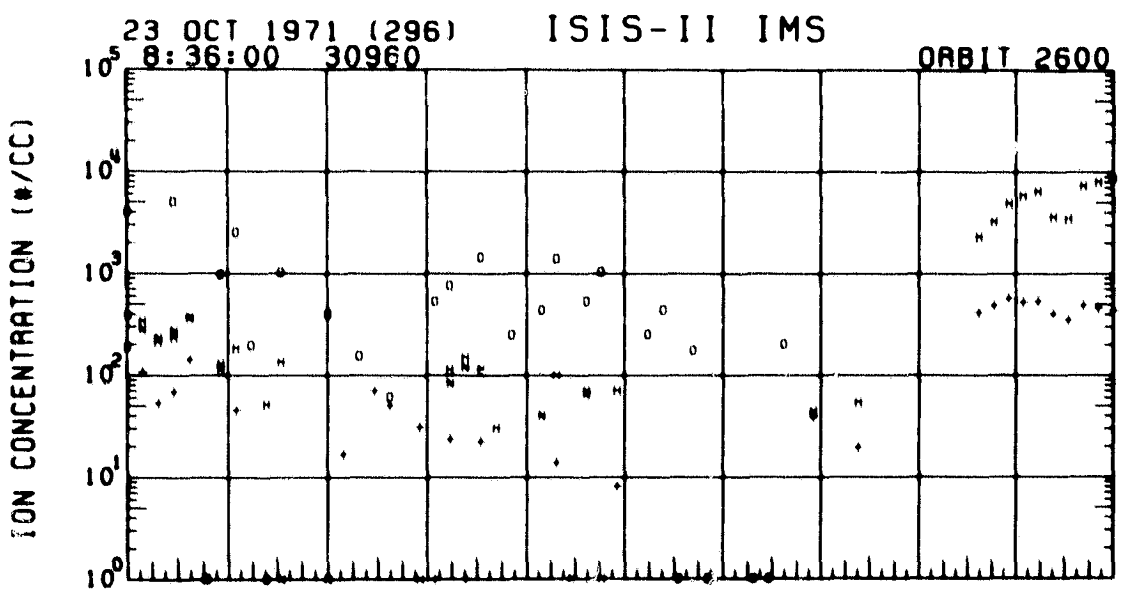

1 - H	UT	8:38	8:40	8:42	8:44	8:46	8:48	8:50	8:54
4 - +	LAST	22:34	2:34	3:02	3:13	3:18	3:22	3:24	3:27
8 - Δ	MLT	16:53	10:26	23:14	1:43	2:26	2:45	2:56	3:00
14 - N	DLAT	87	89	87	83	78	72	68	52
16 - O	INVL	82	84	84	81	76	71	66	55
	GLAT	88	83	77	70	64	58	51	39
	GLNG	-148	94	-88	-86	-85	-85	-84	-85
	SZEN	103	107	110	114	117	120	123	127
	ALT	1409	1412	1415	1418	1420	1422	1423	1425

SET 23, FORMAT 4

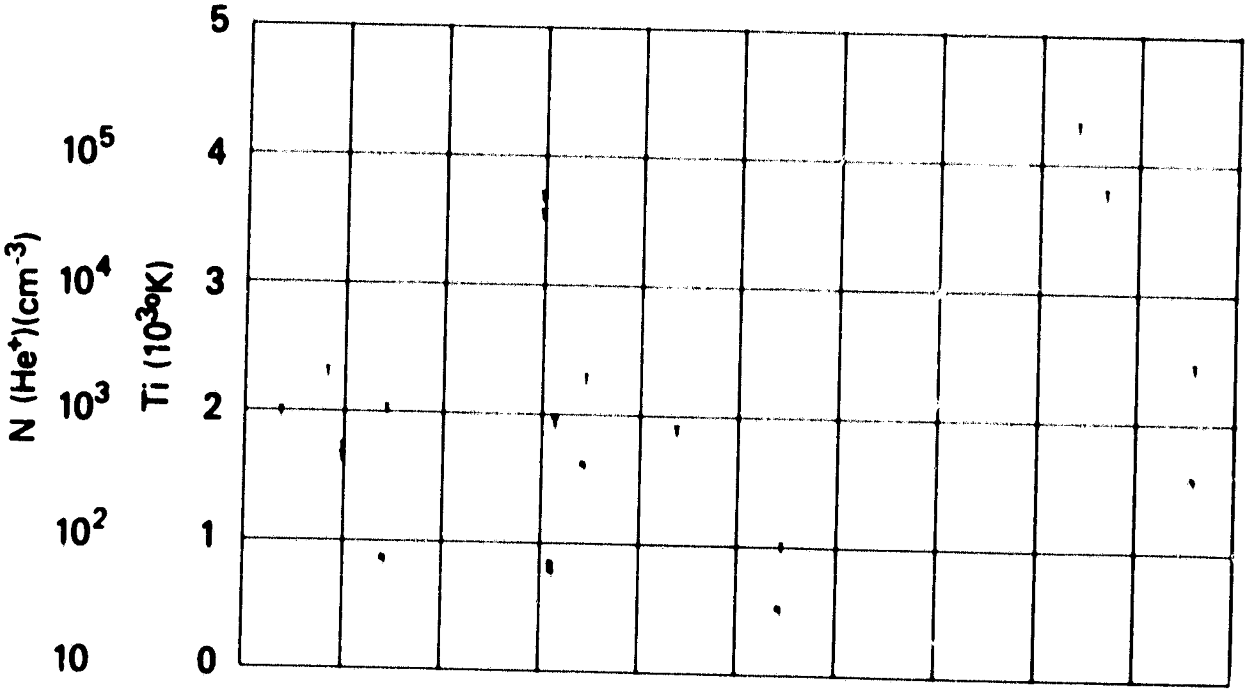

UT	8:38	8:40	8:42	8:44	8:46	8:48	8:50	8:54
LAST	22:34	2:34	3:02	3:13	3:18	3:22	3:24	3:27
MLT	16:53	18:26	23:14	1:43	2:26	2:45	2:56	3:08
DLAT	87	89	87	83	78	72	66	52
INVL	82	84	84	81	76	71	66	55
GLAT	88	83	77	70	64	58	51	38
GLNG	-148	-94	-88	-86	-85	-85	-84	-85
SZEN	103	107	110	114	117	120	123	127
ALT	1409	1412	1415	1418	1420	1422	1423	1425

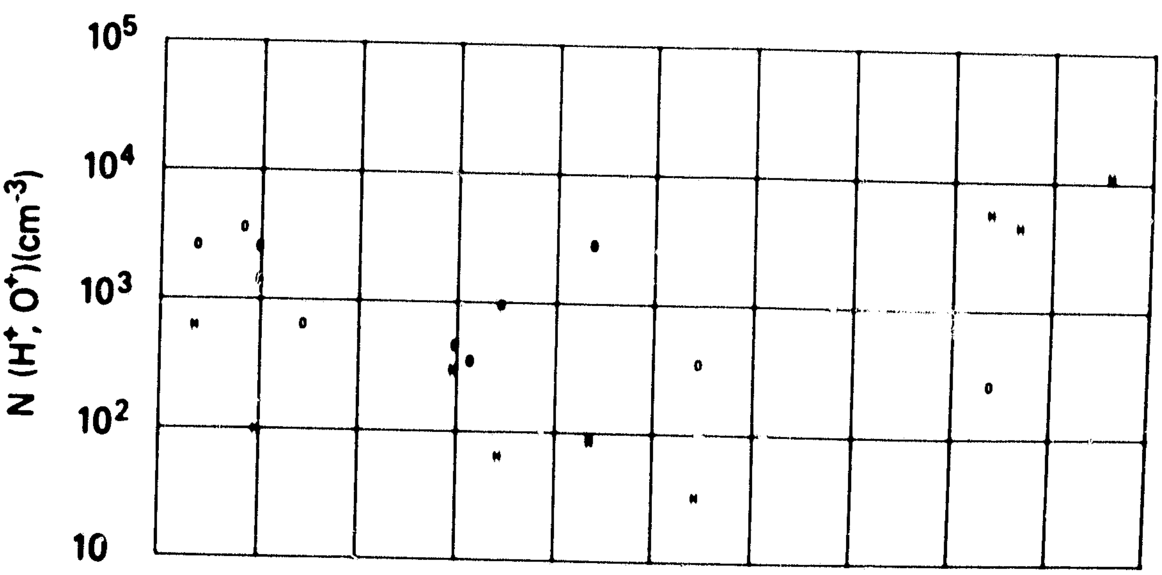

SET 23, FORMAT 5

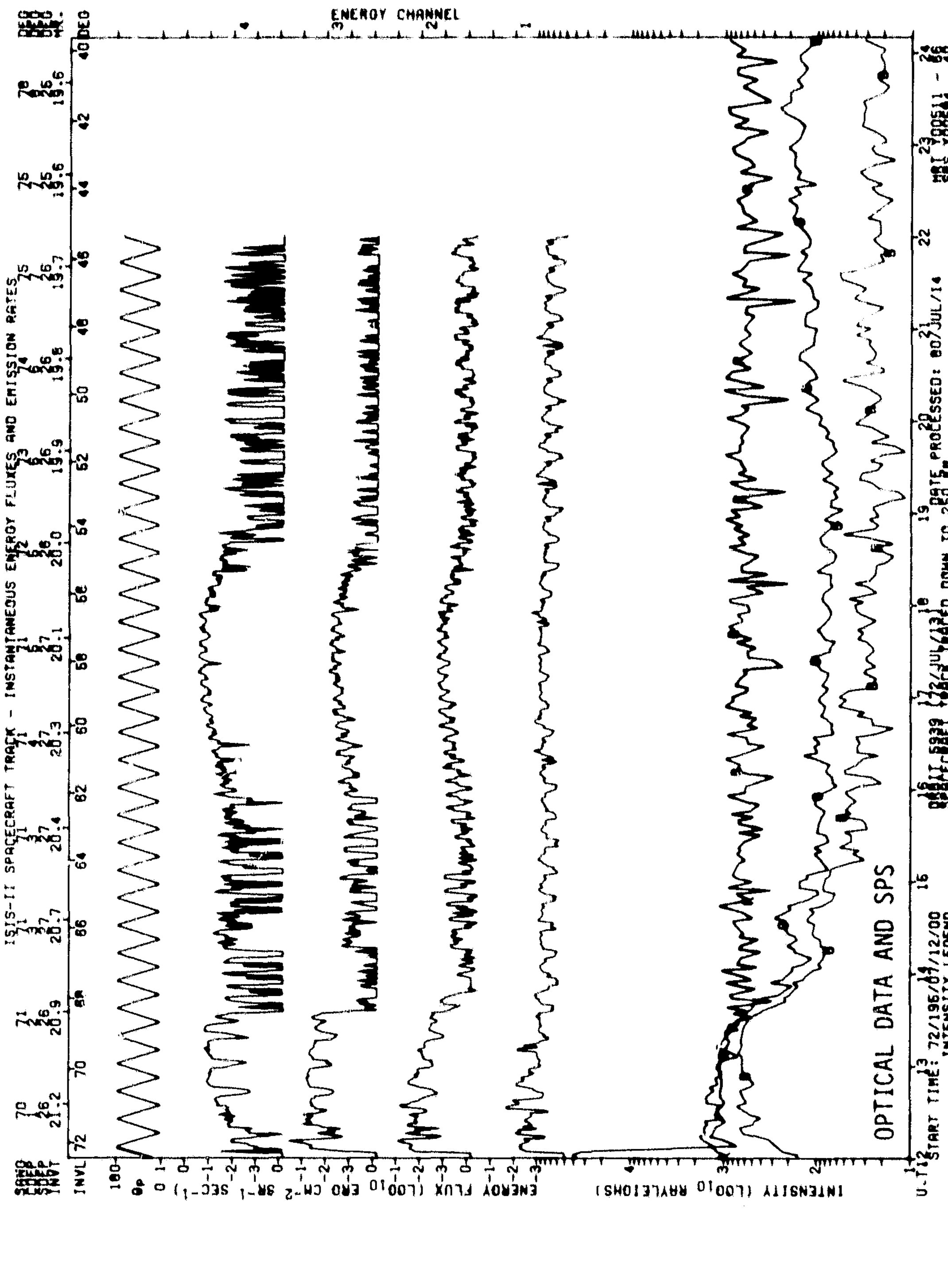

SET 24, FORMAT 1

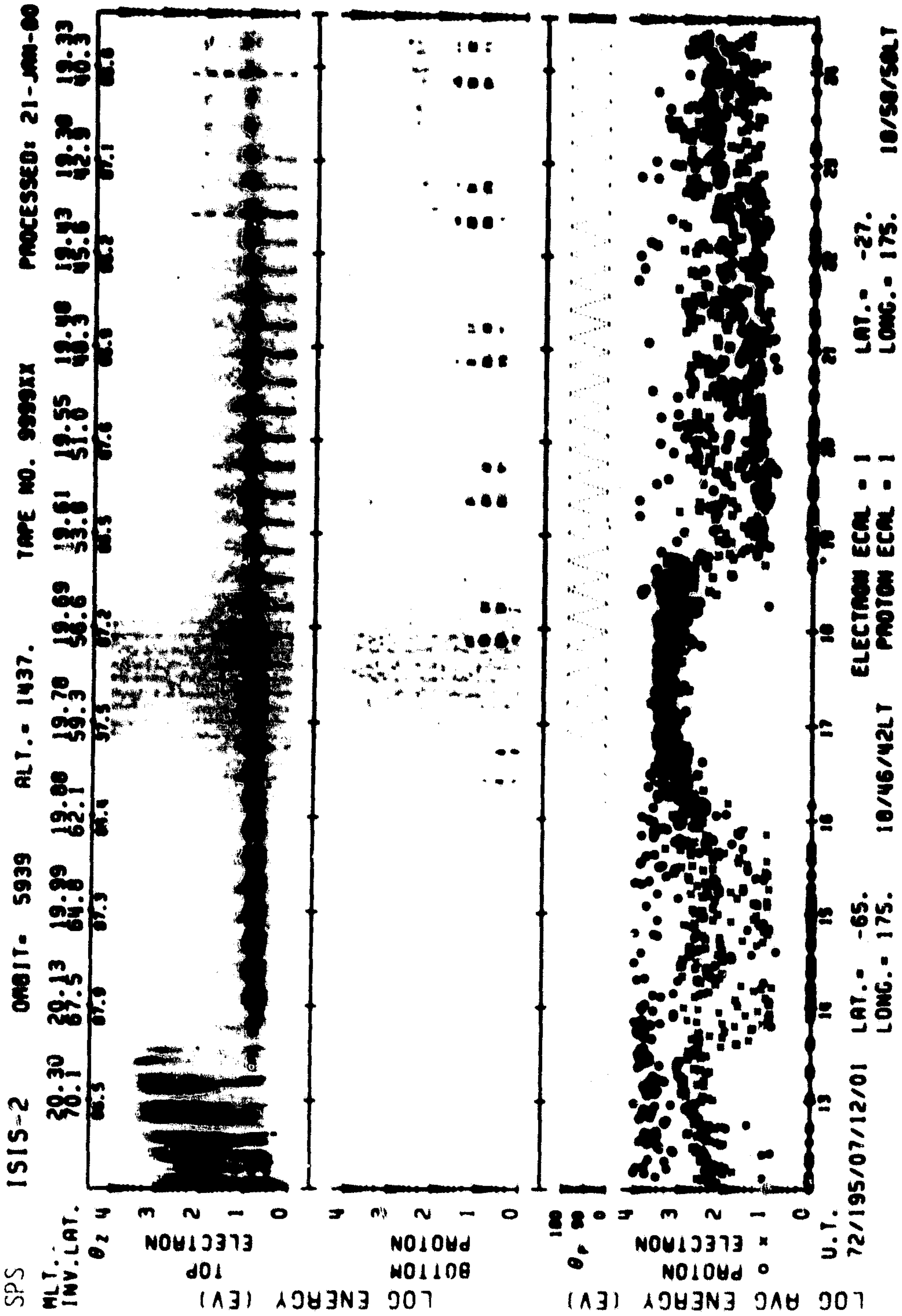

SET 24, FORMAT 6

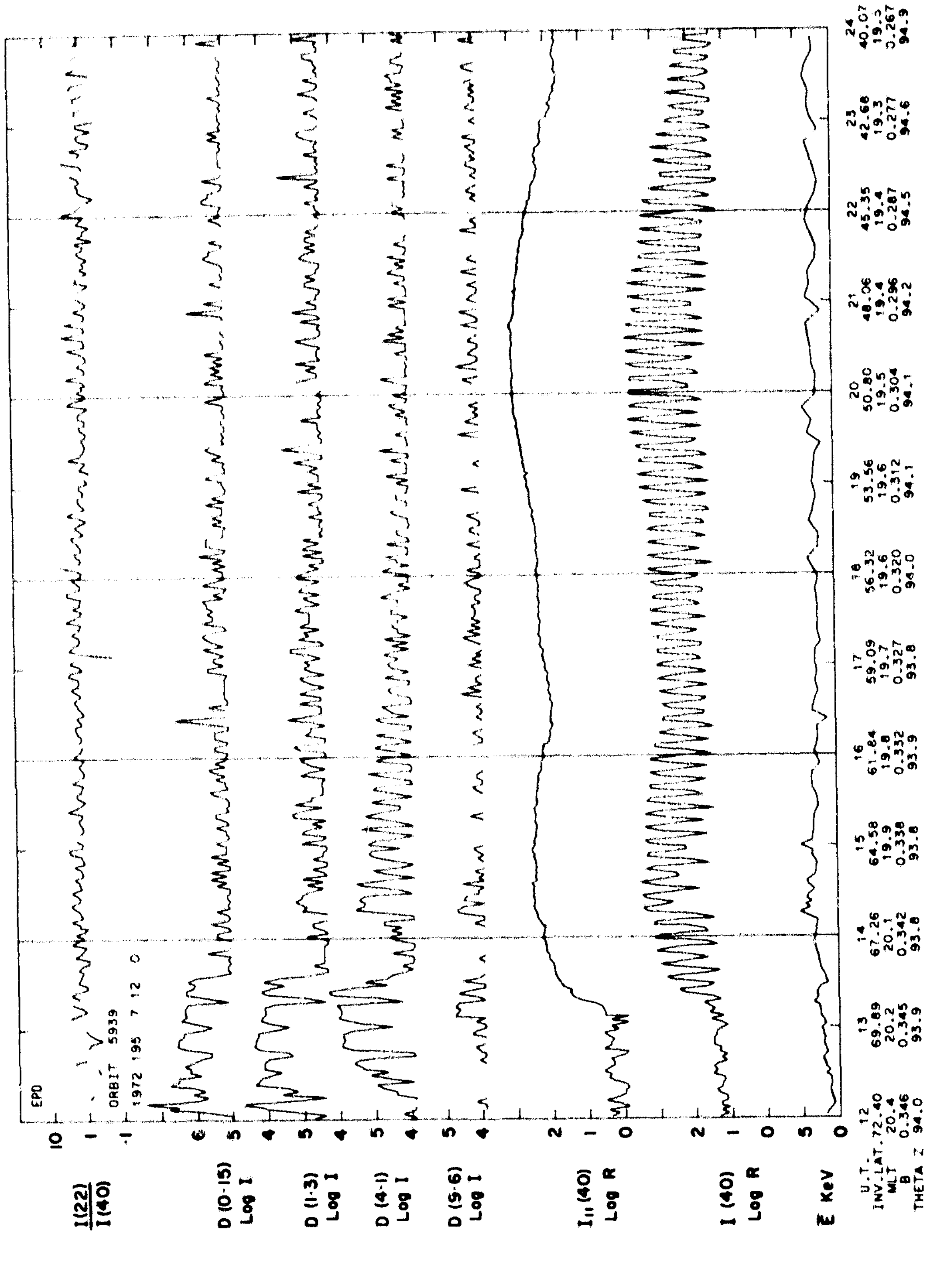

SET 24, FORMAT 3

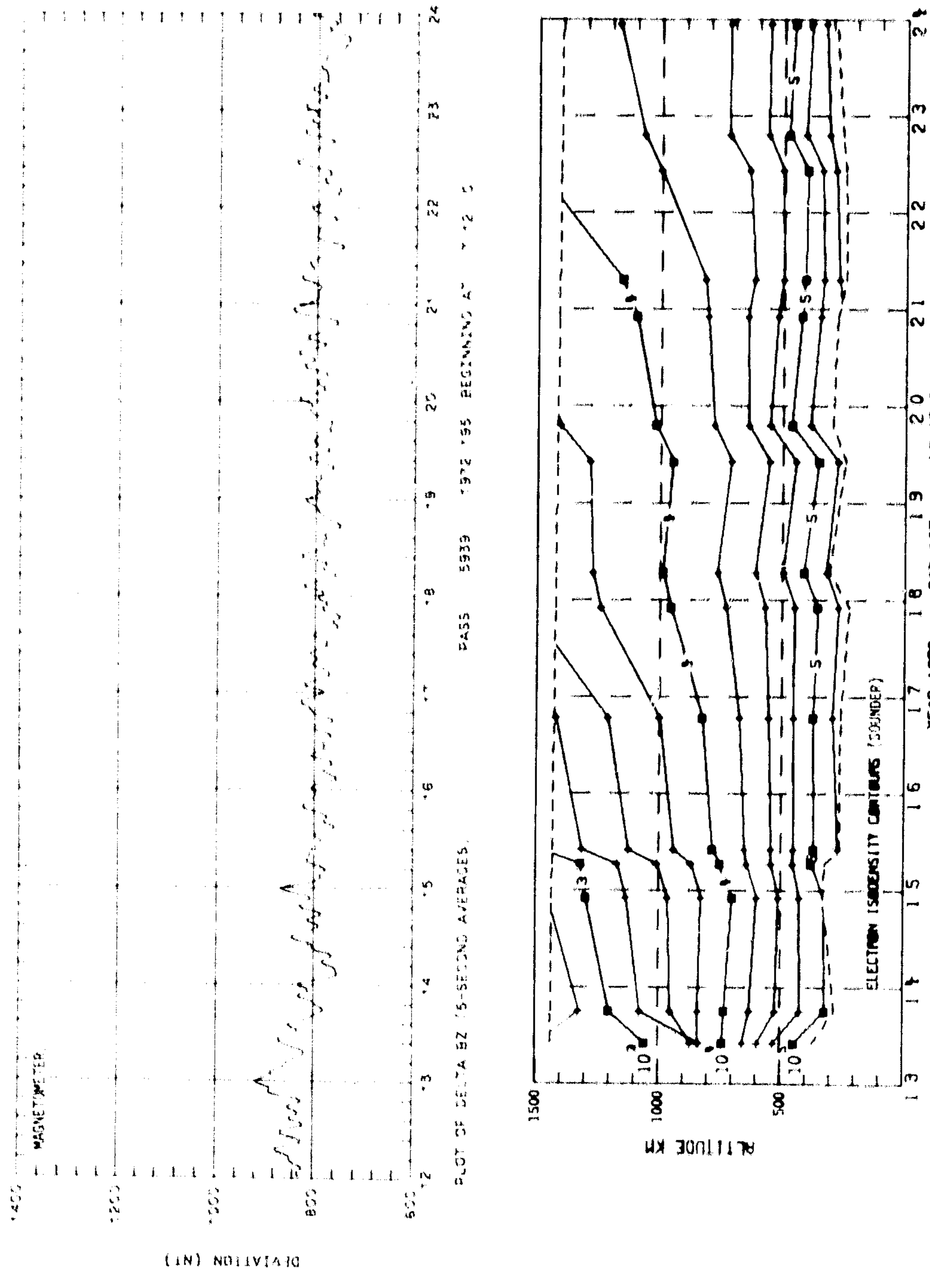

SET 24, FORMAT 2

ORBIT 5939
DATE 720713
DAY 195

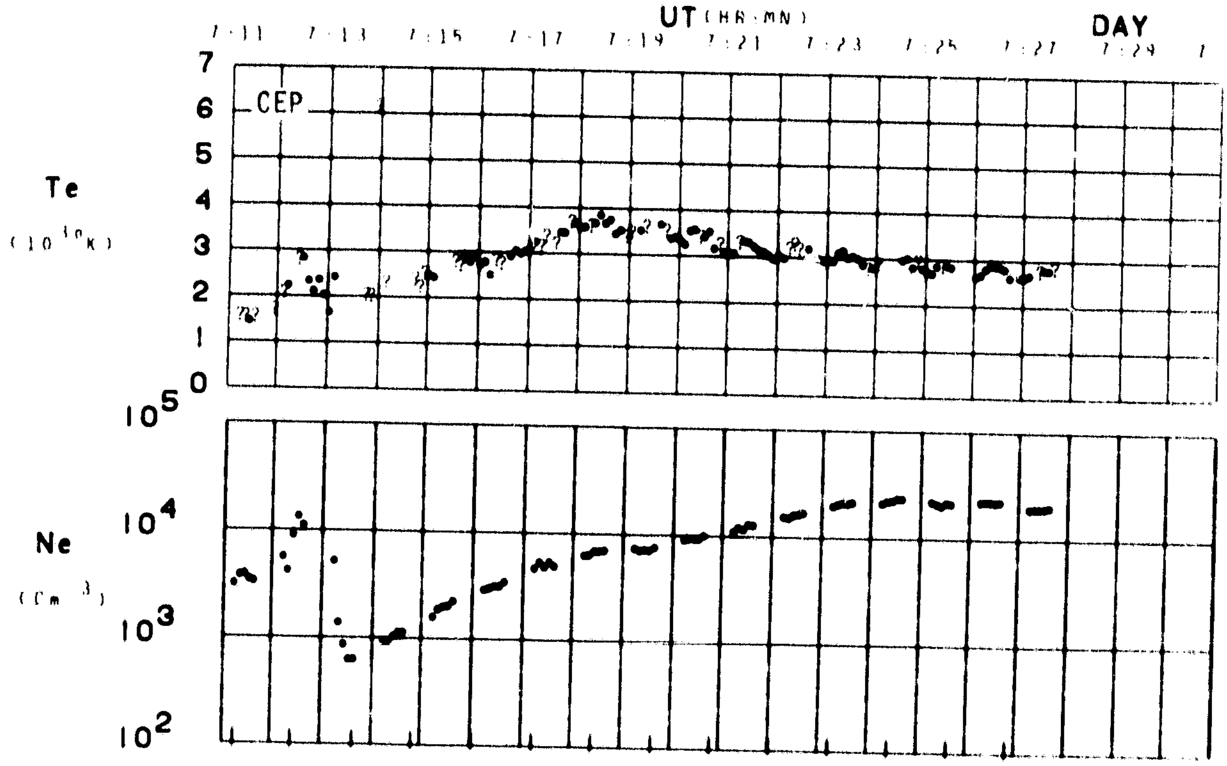

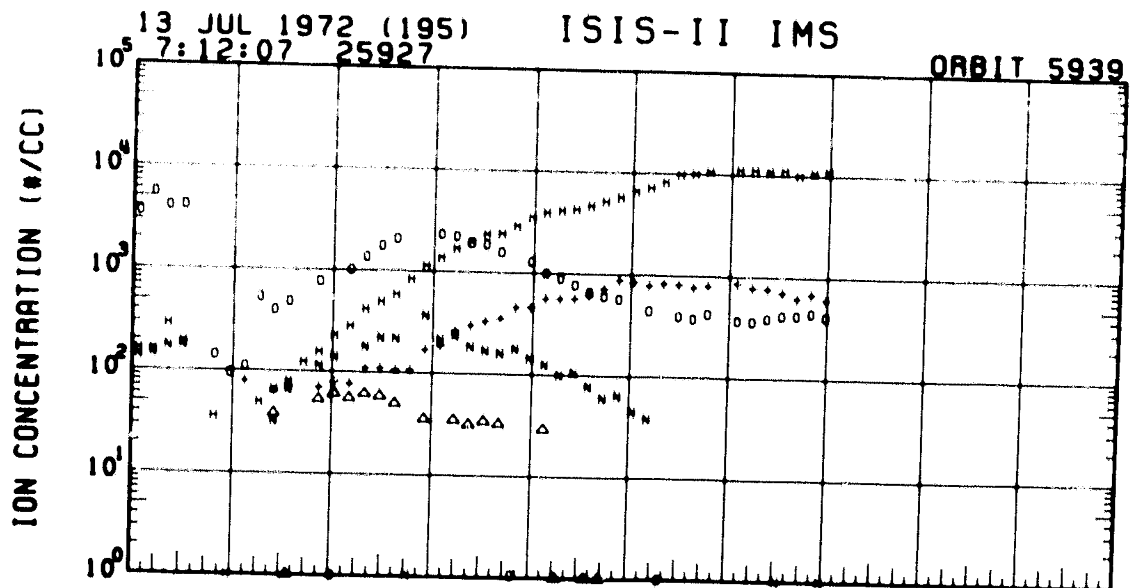

1 - H	UT	7:14	7:16	7:18	7:20	7:22	7:24
4 - +	LAST	18:50	18:53	18:55	18:56	18:58	18:59
8 - Δ	ALT	20:07	19:52	19:41	19:32	19:25	19:20
14 - N	DLAT	-67	-60	-54	-47	-40	-33
16 - O	INVL	67	62	56	51	45	40
	GLAT	-58	-52	-46	-39	-33	-27
	GLNG	176	176	176	176	175	175
	SZEN	115	115	115	114	114	112
	ALT	1432	1426	1420	1413	1407	1401

SET 24, FORMAT 4

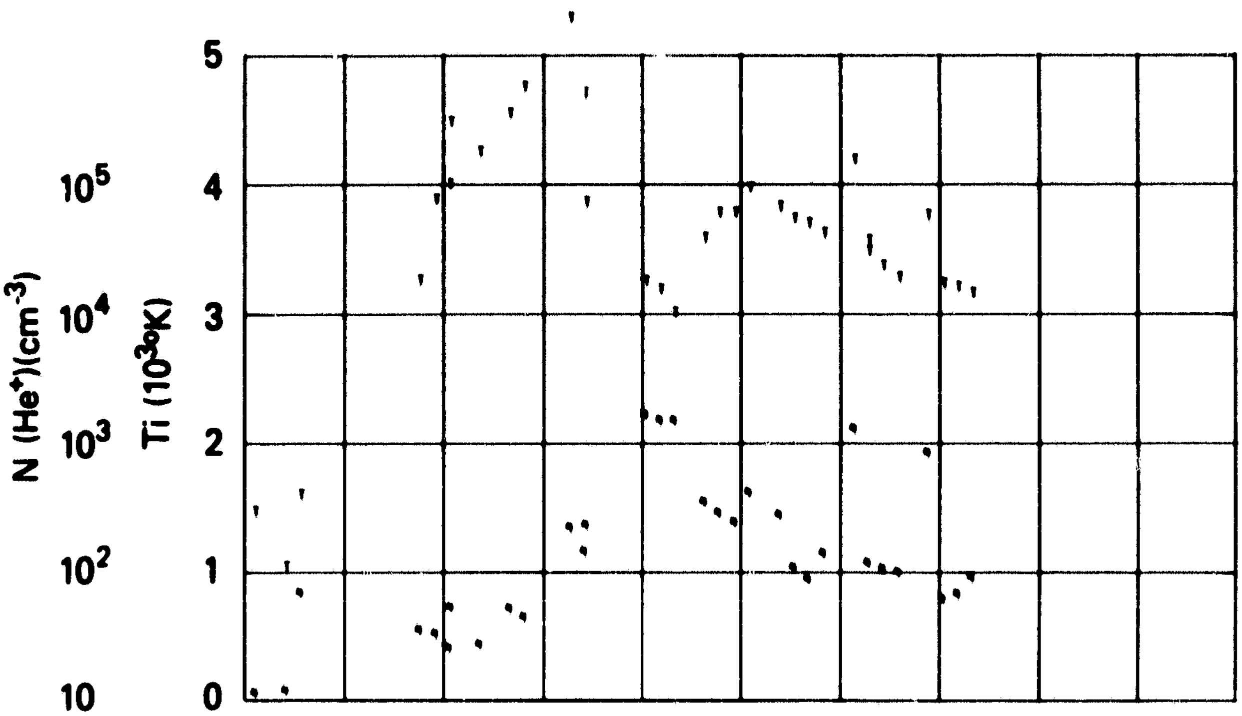

UT	7:14	7:16	7:18	7:20	7:22	7:24
LAST	10:50	10:53	10:55	10:56	10:58	10:59
MLT	20:07	19:52	19:41	19:32	19:25	19:20
DLAT	-57	-60	-54	-47	-40	-33
INVL	67	62	56	51	45	40
GLAT	-58	-52	-46	-39	-33	-27
GLNG	176	176	176	176	175	175
SZEN	115	115	115	114	114	112
ALT	1432	1426	1420	1413	1407	1401

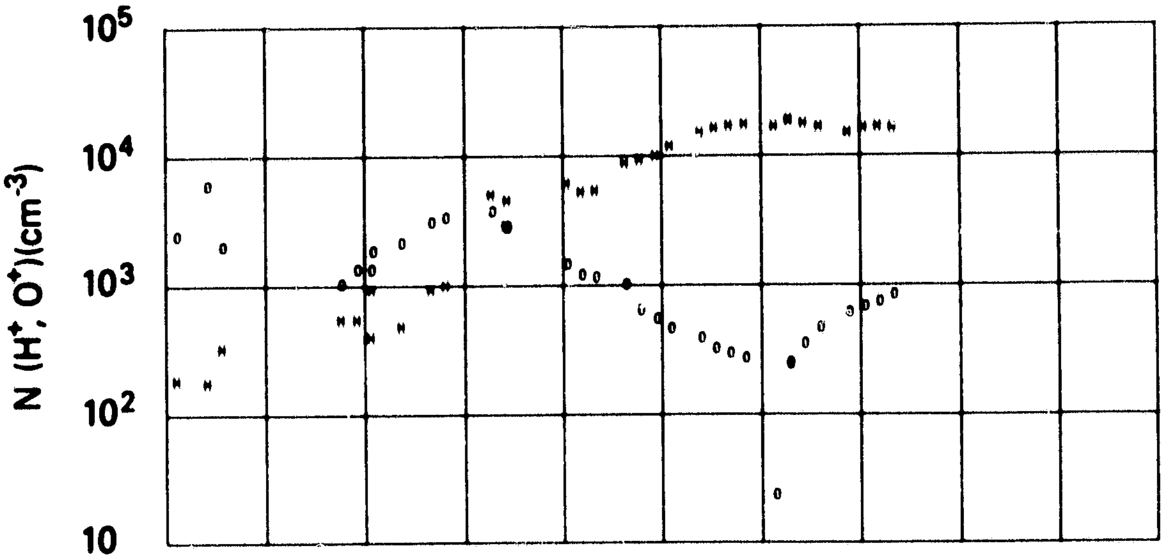

SET 24, FORMAT 5

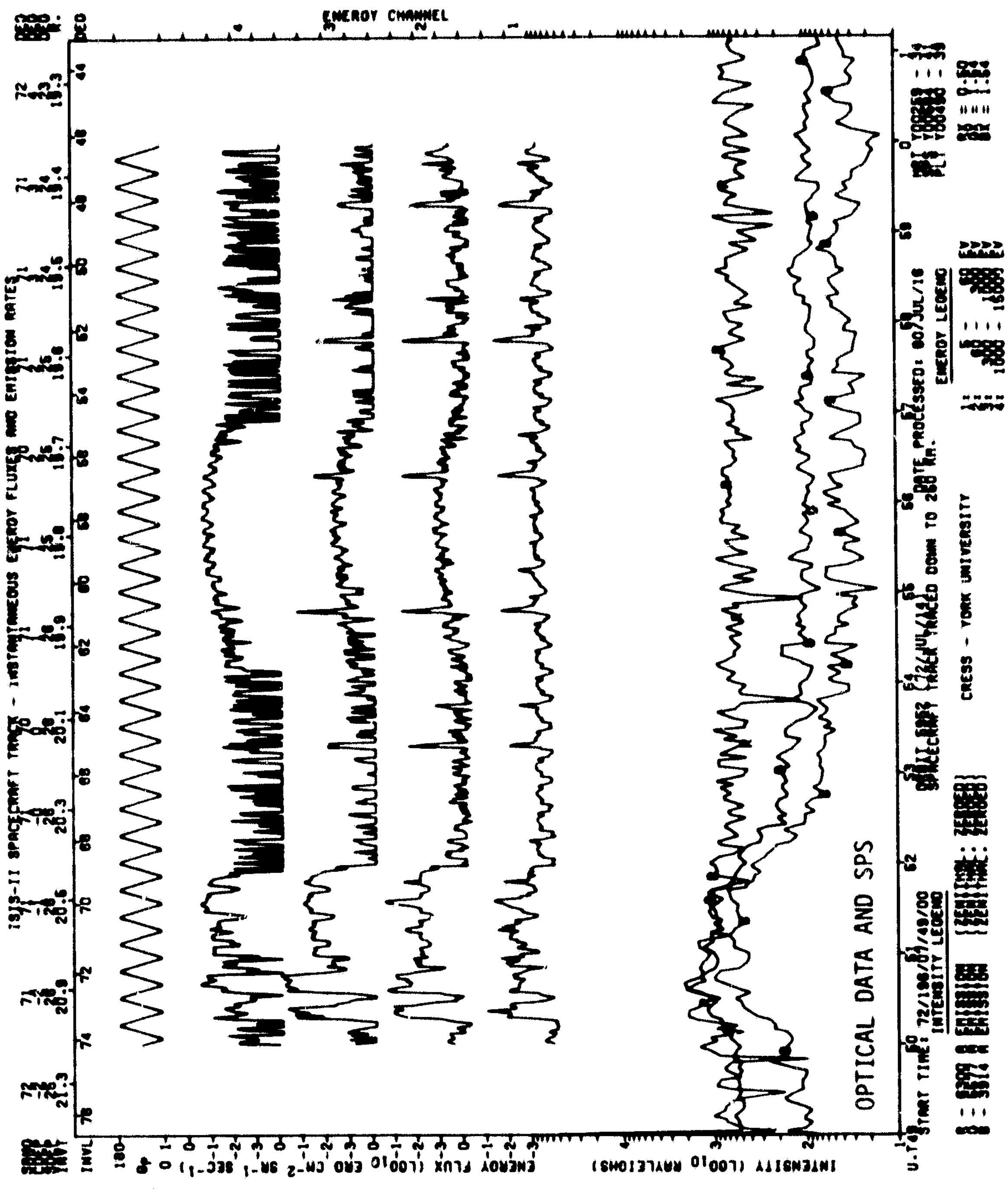

SET 25, FORMAT 1

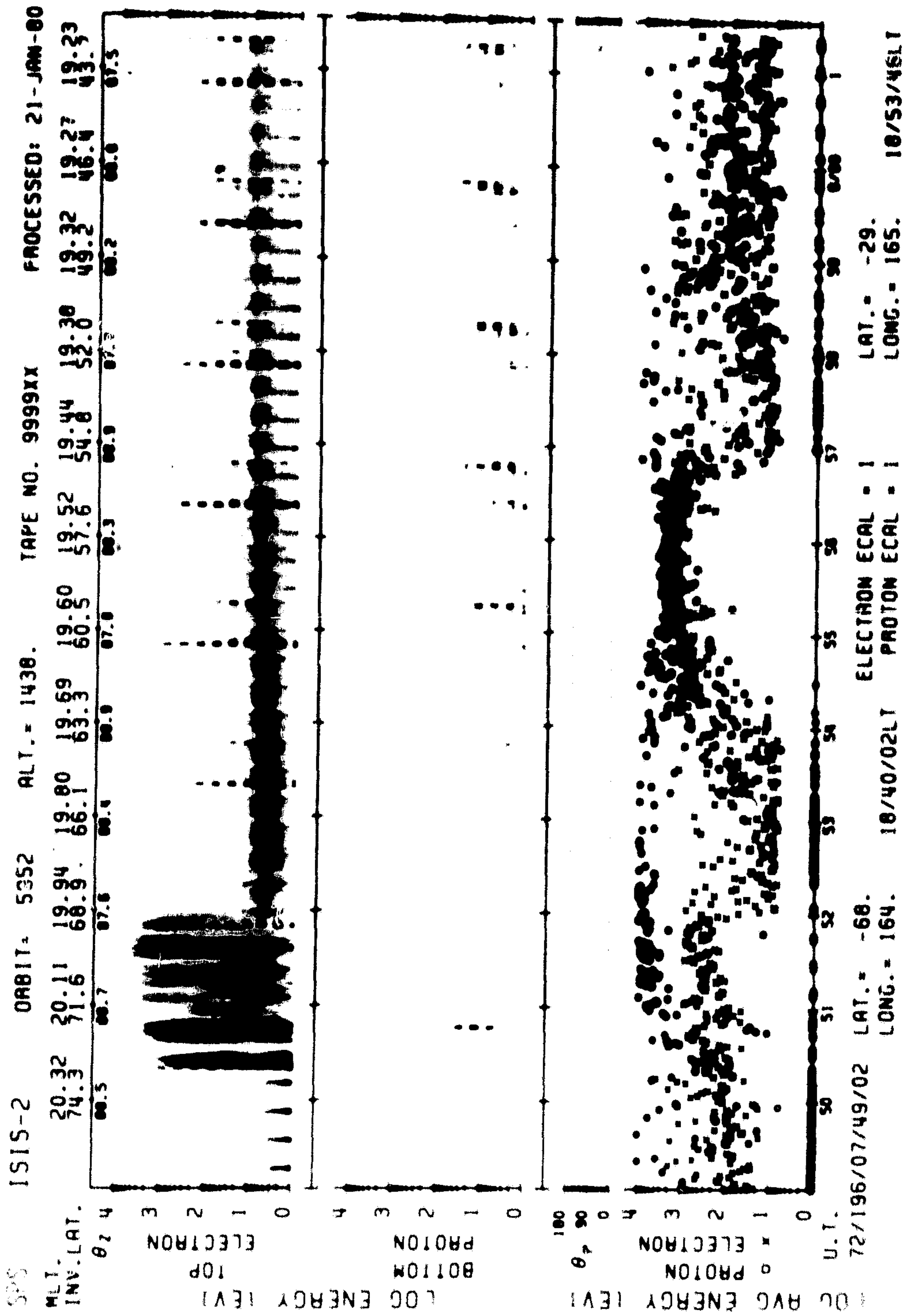

SET 25, FORMAT 6

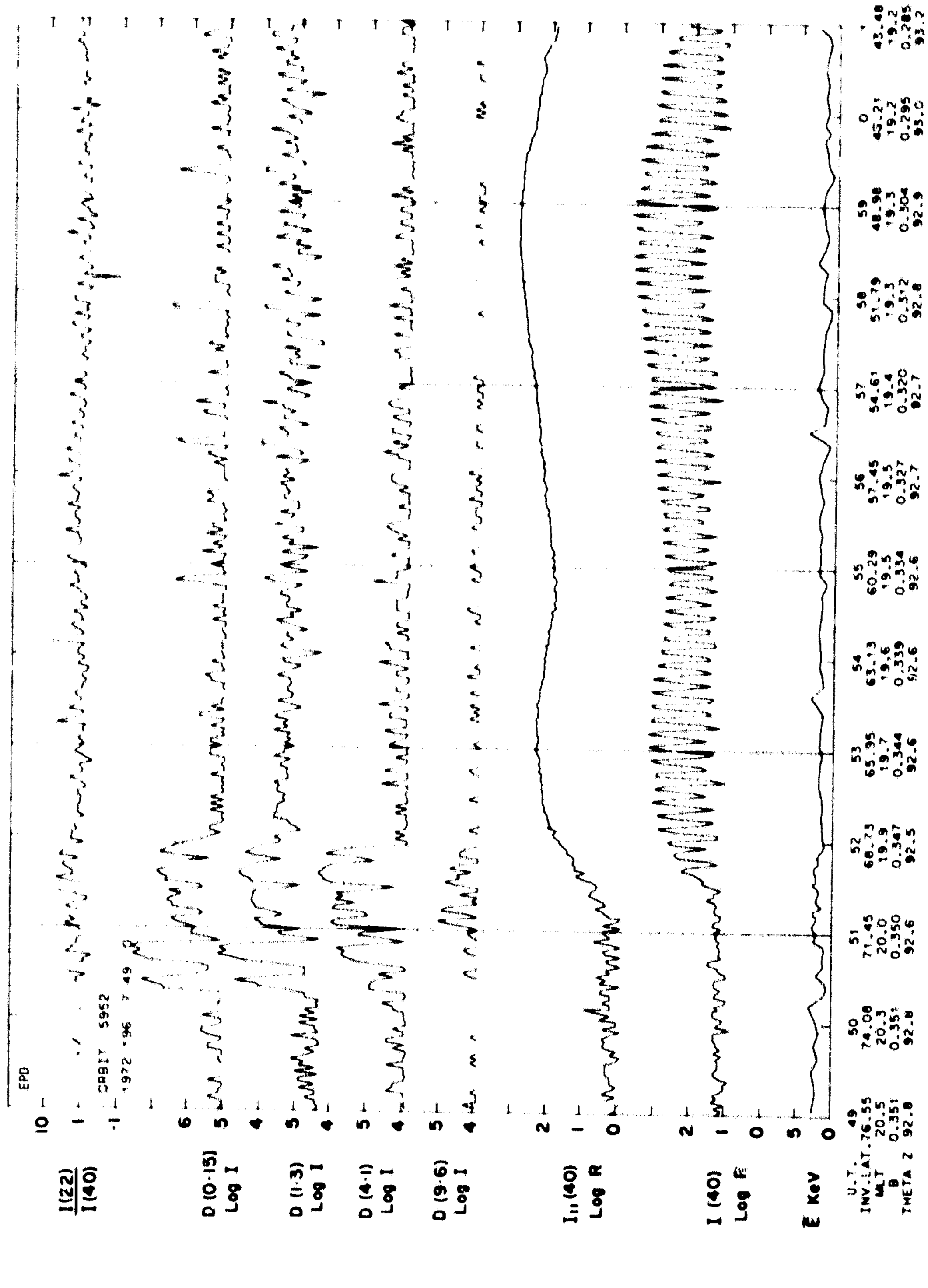

SET 25, FORMAT 3

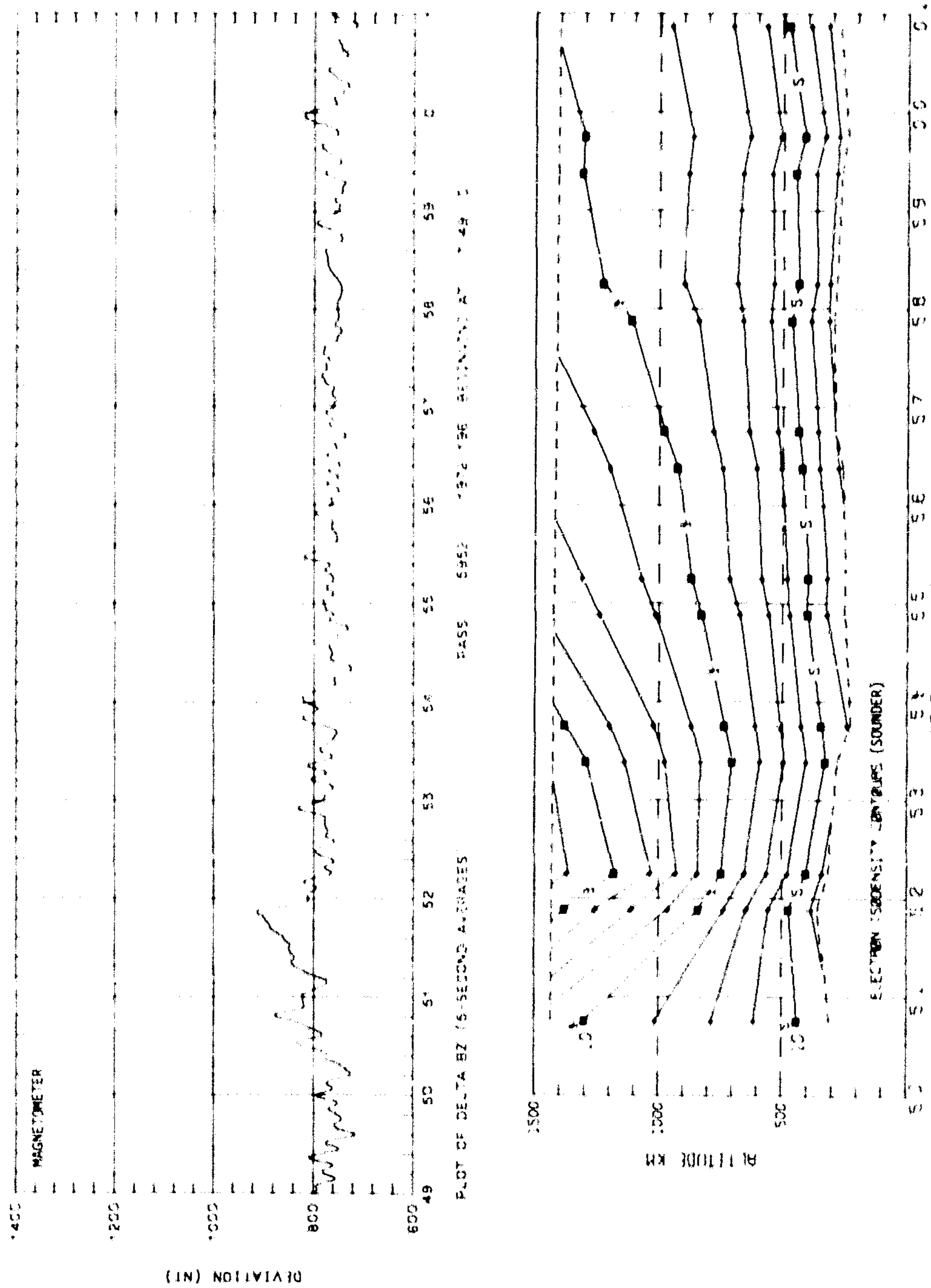

SET 25, FORMAT 2

ORBIT 5952
DATE 720714
DAY 196

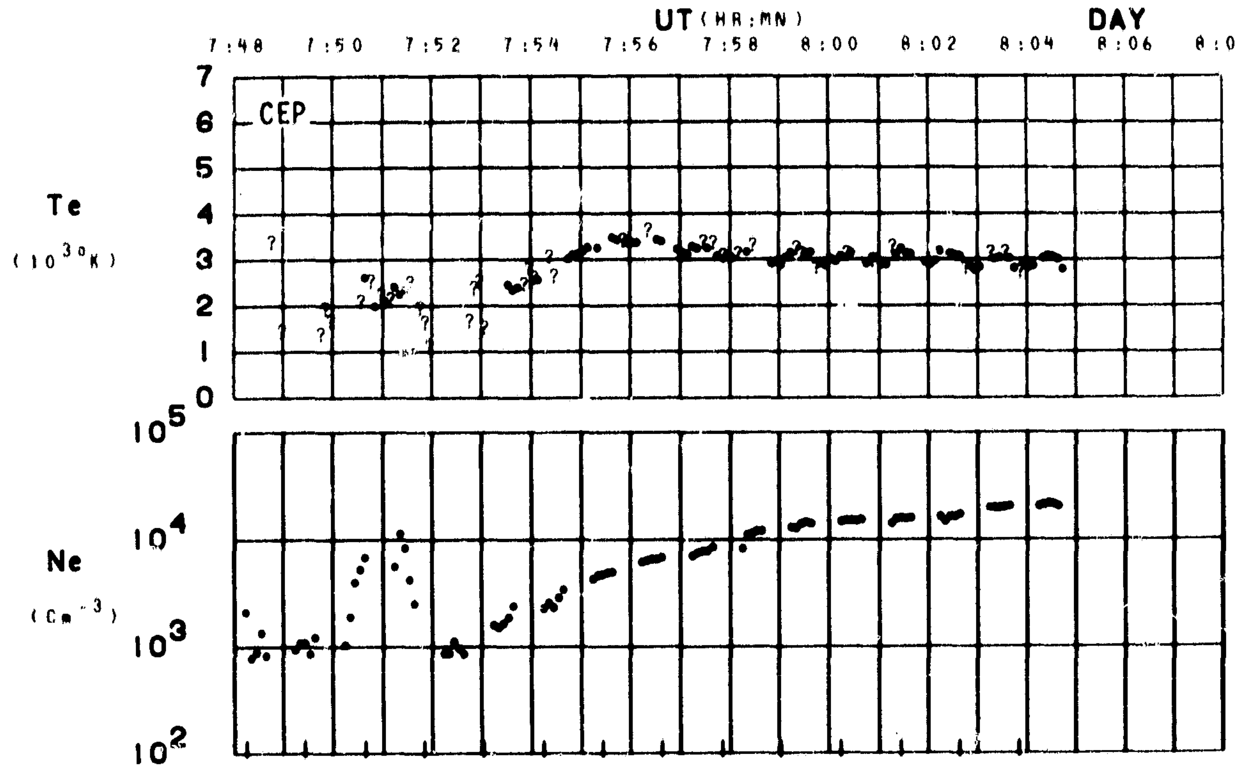

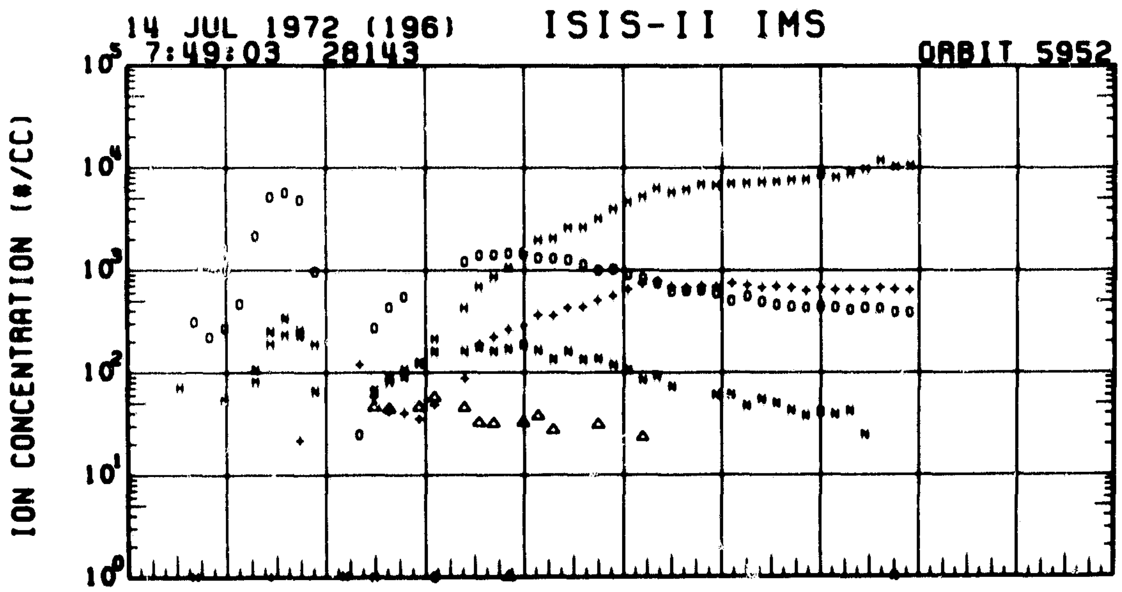

1 - H	UT	7:50	7:52	7:54	7:56	7:58	8:00	8:02
4 - +	LAST	18:42	18:46	18:48	18:50	18:52	18:53	18:54
8 - △	MLT	20:10	19:56	19:41	19:31	19:23	19:16	19:11
14 - N	DLAT	-76	-70	-63	-56	-48	-41	-34
16 - O	INVL	74	68	63	57	52	46	41
	GLAT	-64	-57	-51	-45	-38	-32	-26
	GLNG	185	185	185	185	185	185	184
	SZEN	114	114	114	114	113	112	111
	ALT	1435	1430	1424	1418	1411	1405	1398

SET 25, FORMAT 4

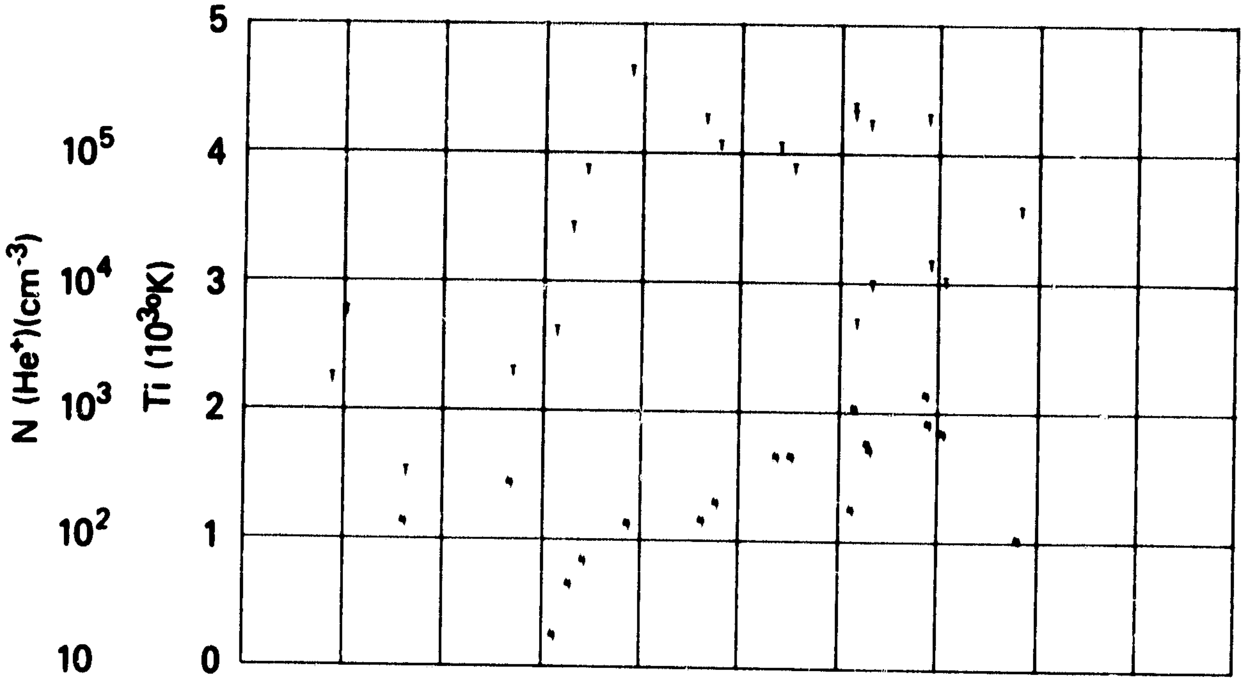

UT	7:50	7:52	7:54	7:56	7:58	8:00	8:02
LAST	18:42	18:46	18:48	18:50	18:52	18:53	18:54
MLT	20:18	19:56	19:41	19:31	19:23	19:16	19:11
DLAT	-76	-70	-63	-56	-48	-41	-34
INVL	74	69	63	57	52	46	41
GLAT	-64	-57	-51	-45	-39	-32	-26
GLNG	165	165	165	165	165	165	164
SZEN	114	114	114	114	113	112	111
ALT	1435	1430	1424	1418	1411	1405	1398

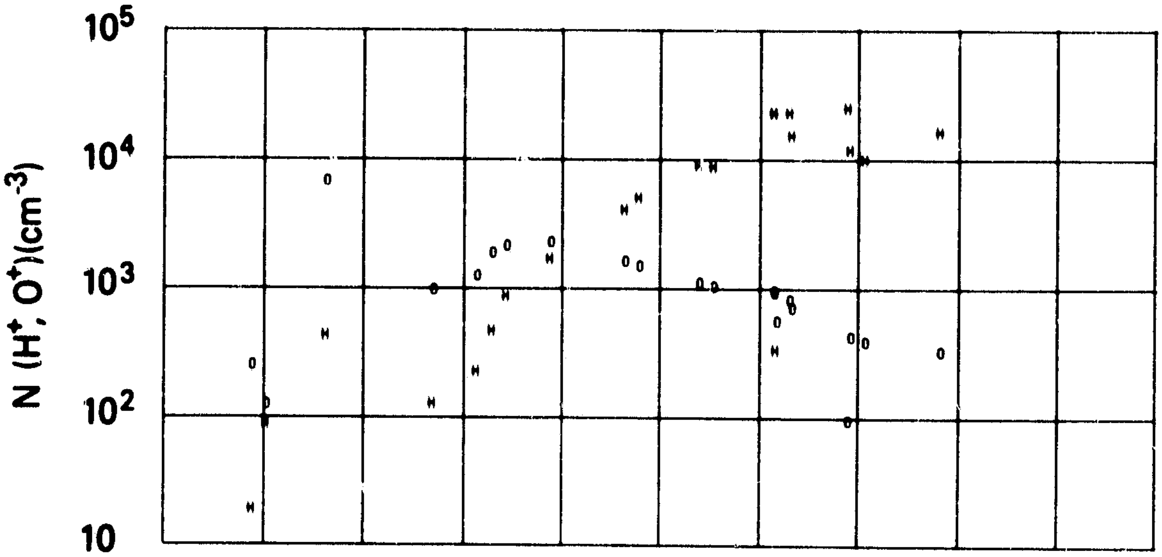

SET 25, FORMAT 5

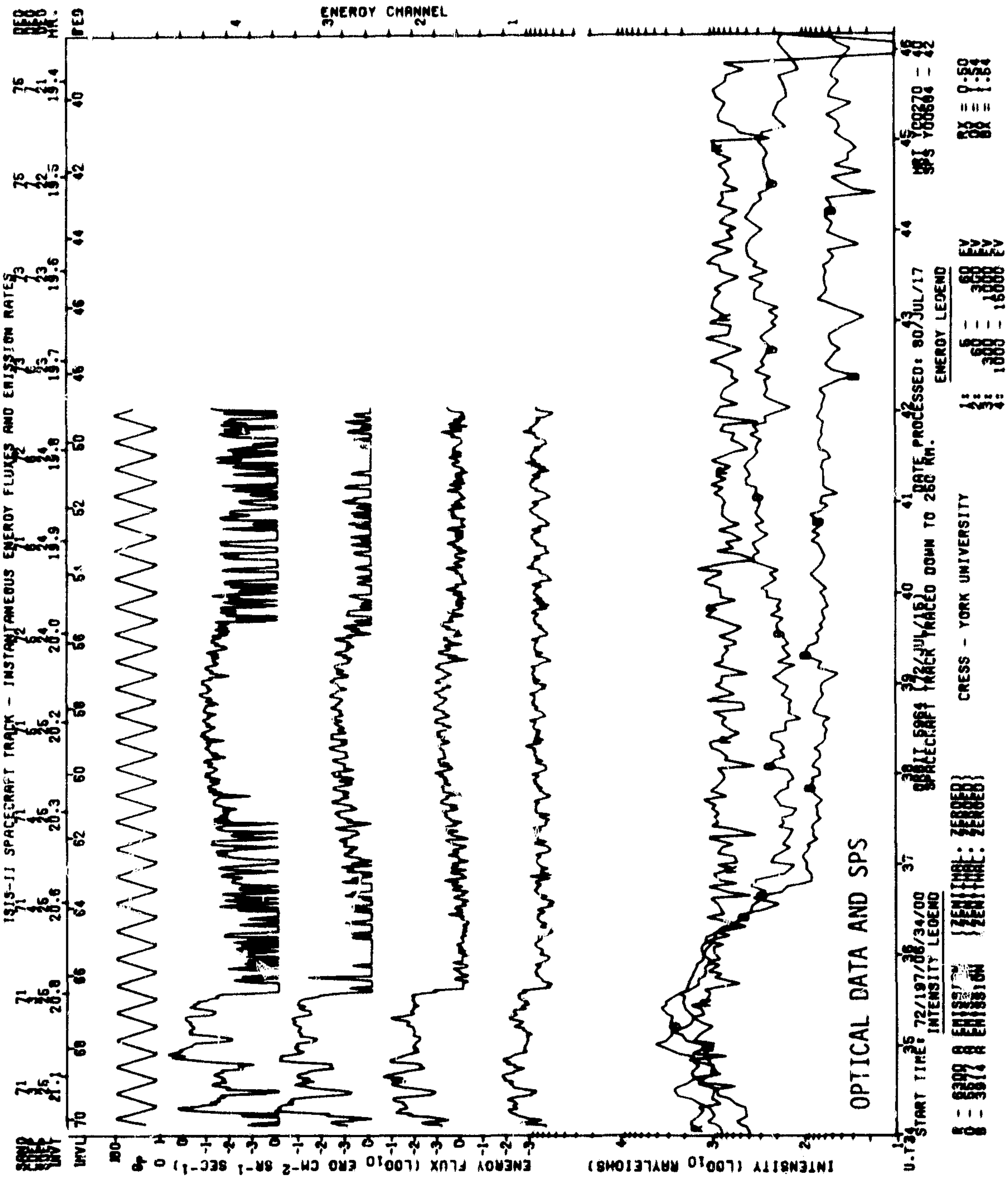

SET 26, FORMAT 1

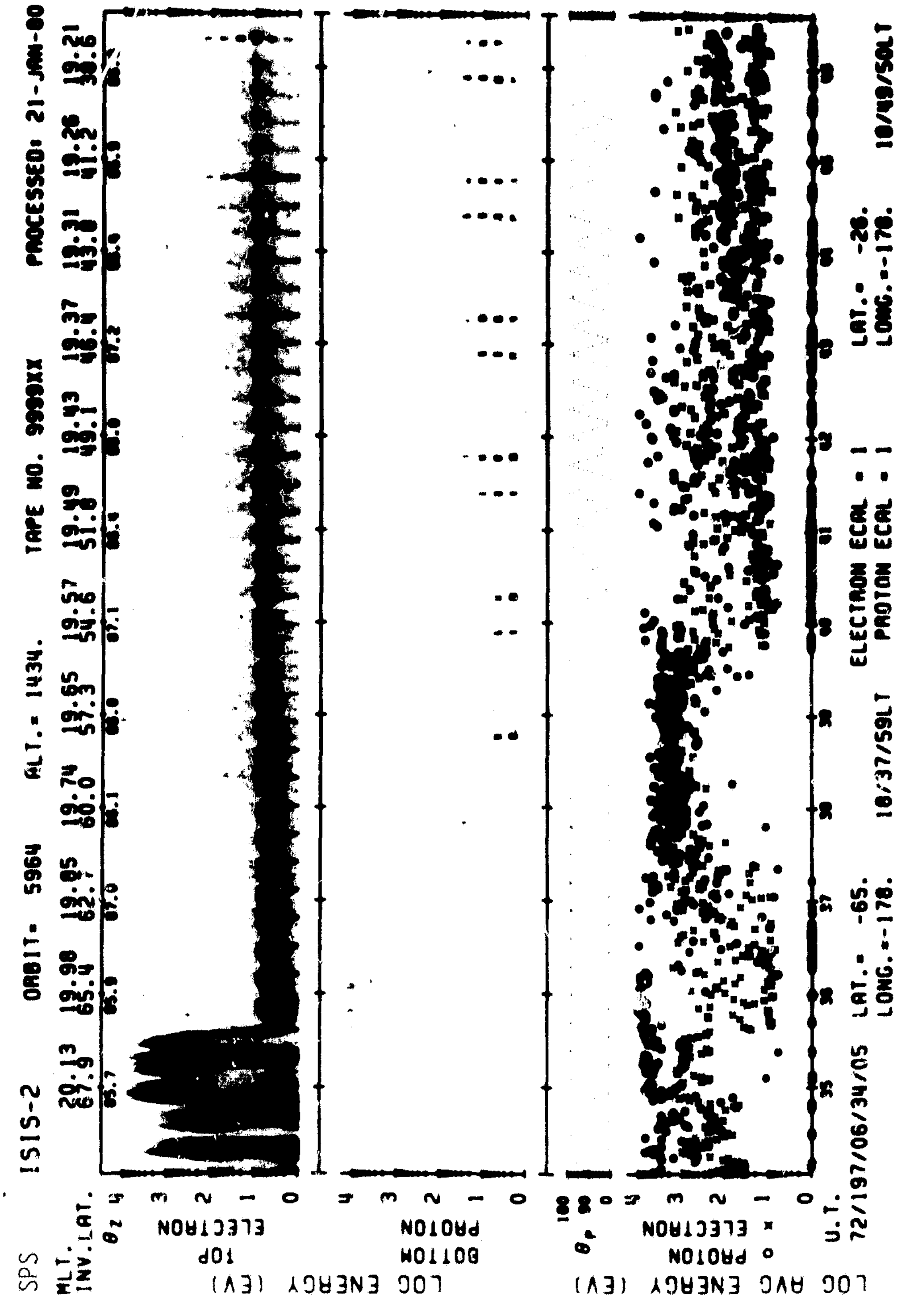

SET 26, FORMAT 6

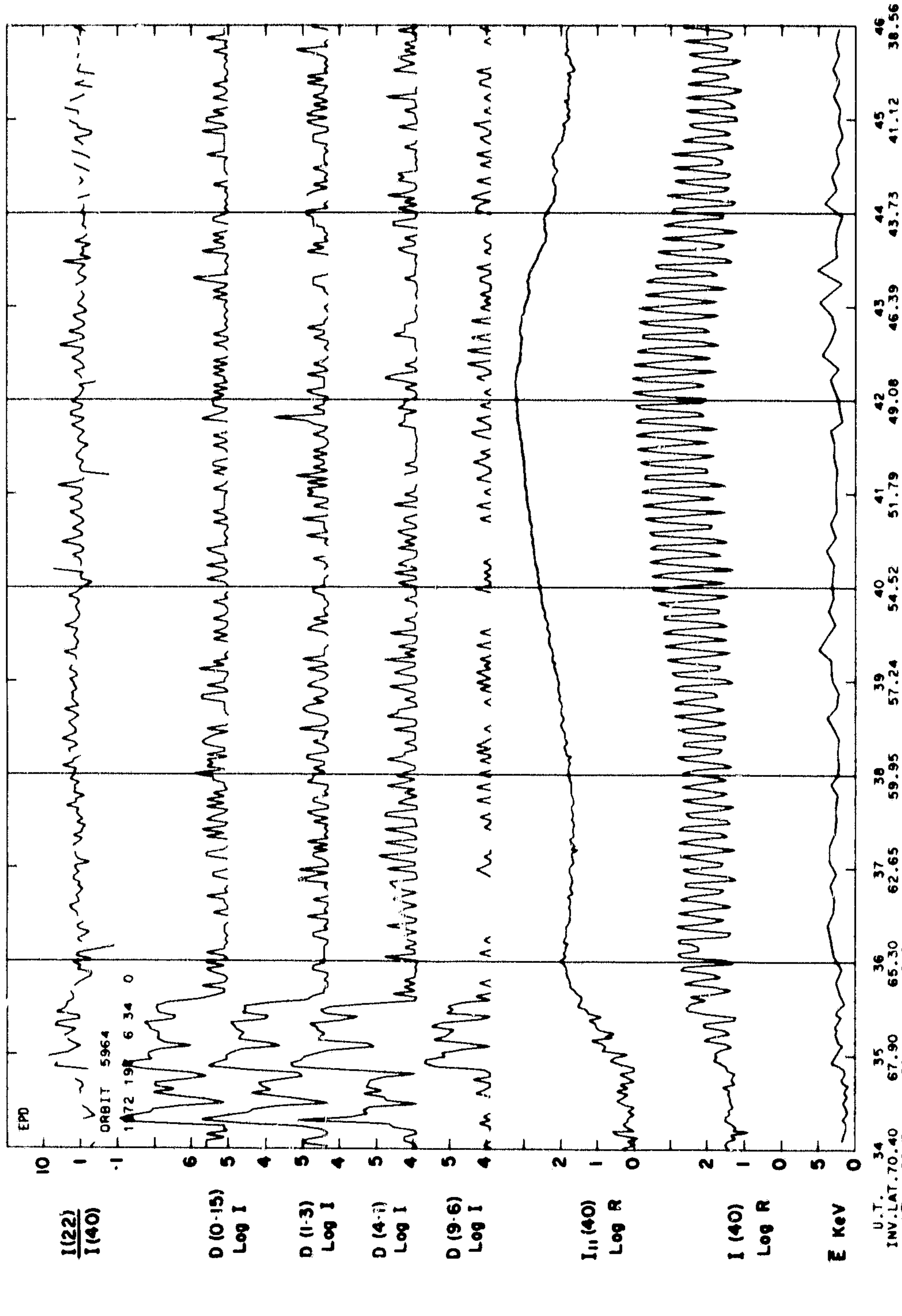

SET 26, FORMAT 3

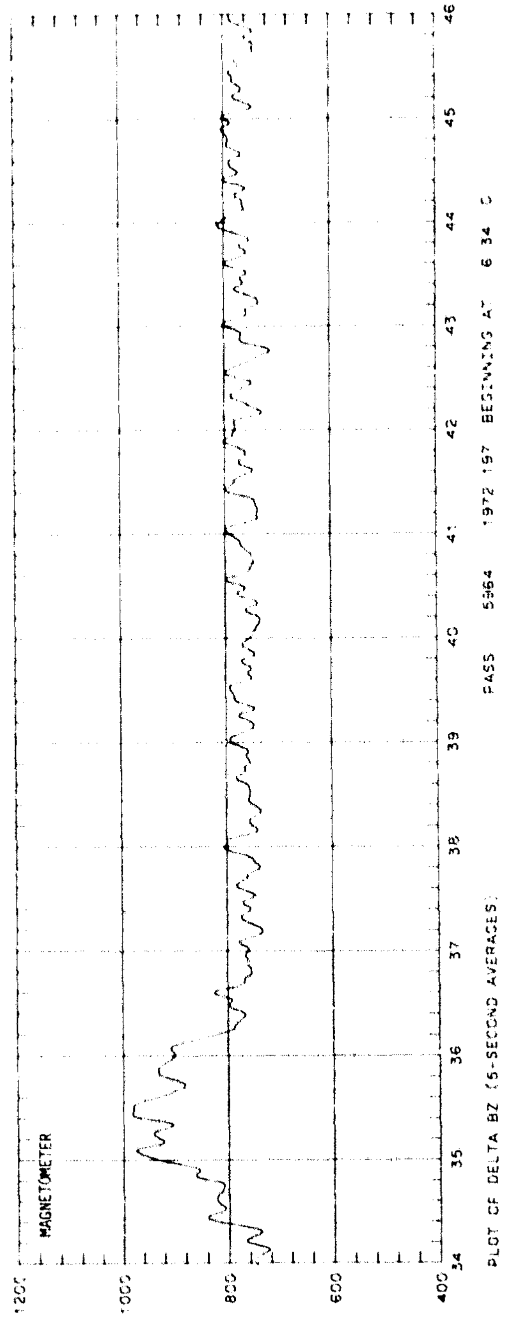

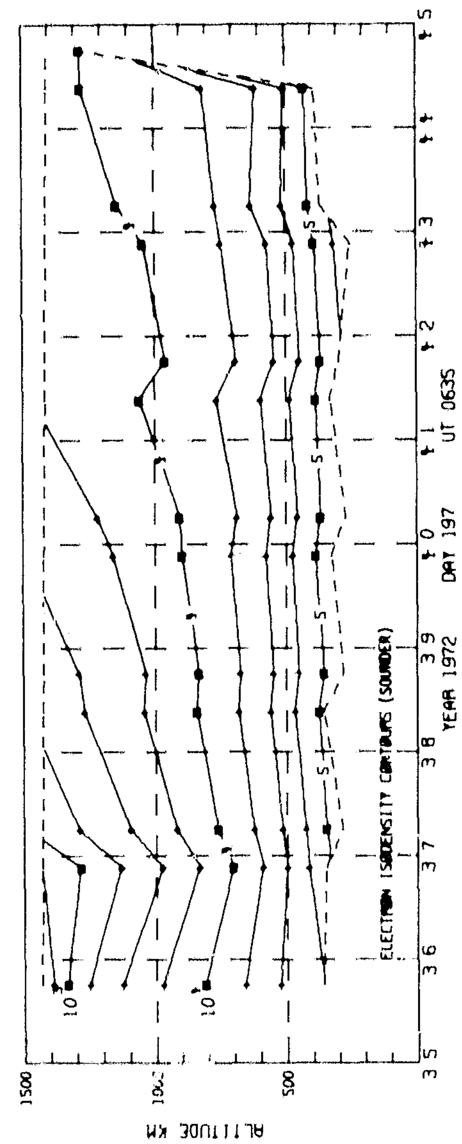

SET 26, FORMAT 2

ORBIT 5964
DATE 720715
DAY 197

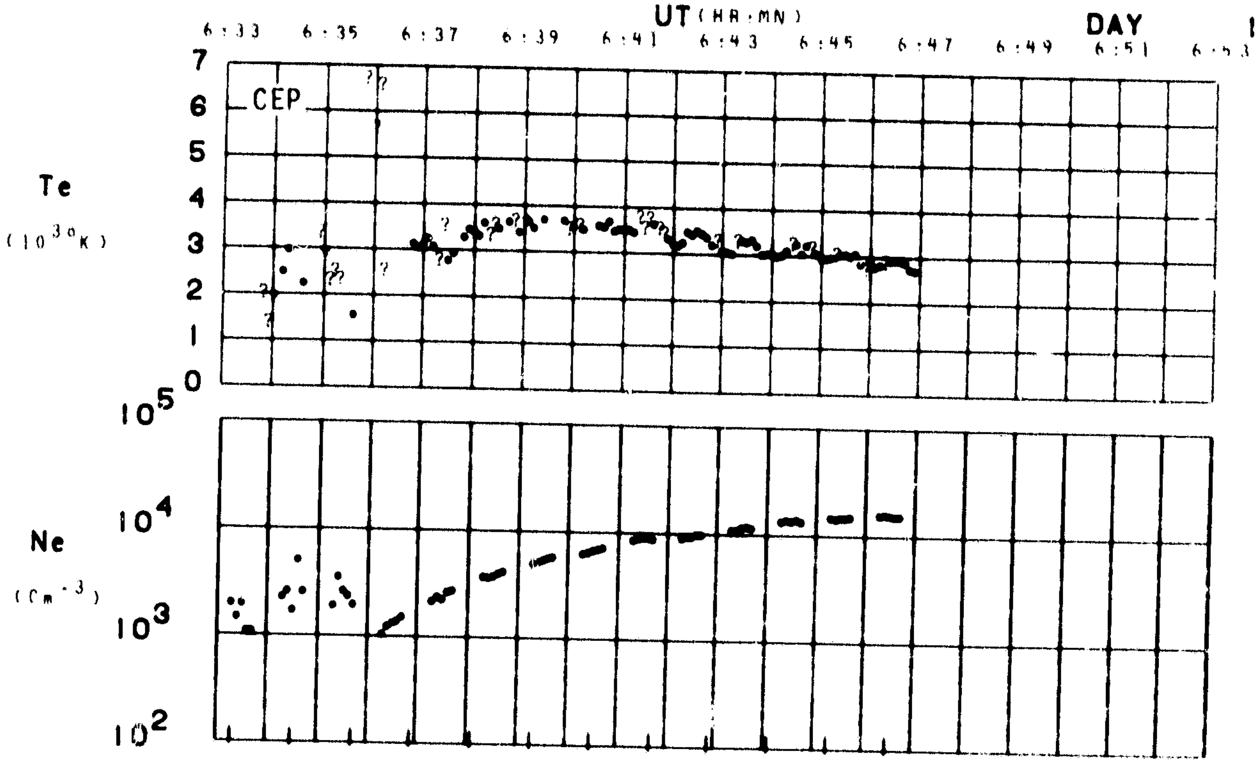

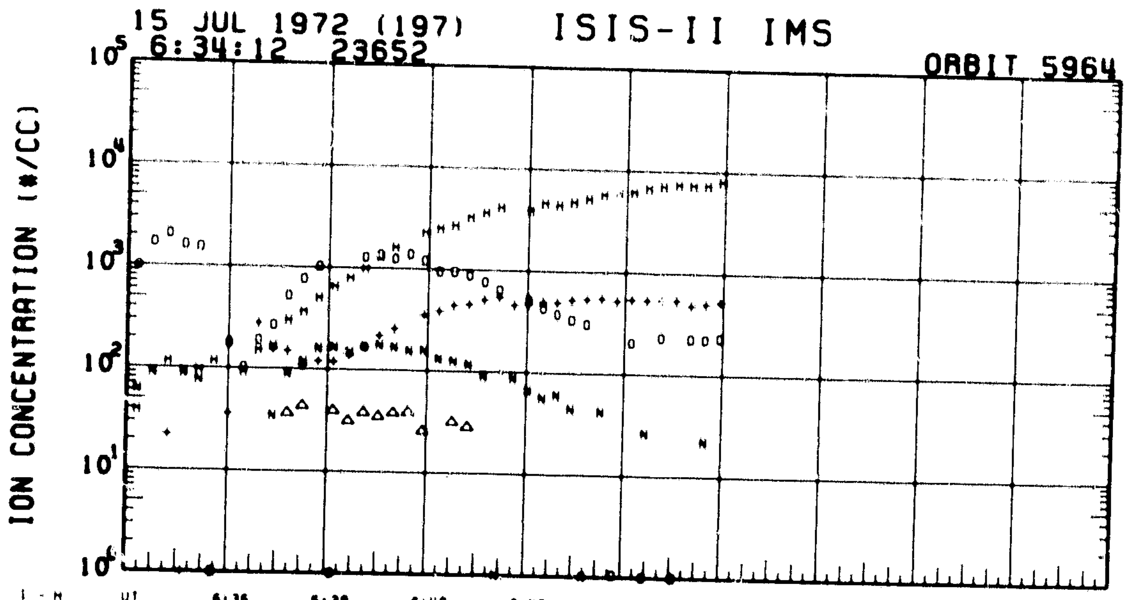

1 - H
4 - +
8 - Δ
14 - N
16 - O

UT	6:36	6:38	6:40	6:42	6:44
LAST	18:41	18:44	18:46	18:47	18:49
MLT	19:58	19:45	19:34	19:26	19:19
DLAT	-64	-58	-51	-44	-37
INVL	65	60	55	49	44
GLAT	-58	-51	-45	-38	-32
GLNG	-176	-176	-176	-176	-176
SZEN	114	[illegible]	113	112	111
ALT	1429	1423	1416	1410	1403

SET 26, FORMAT 4

RPA

720715

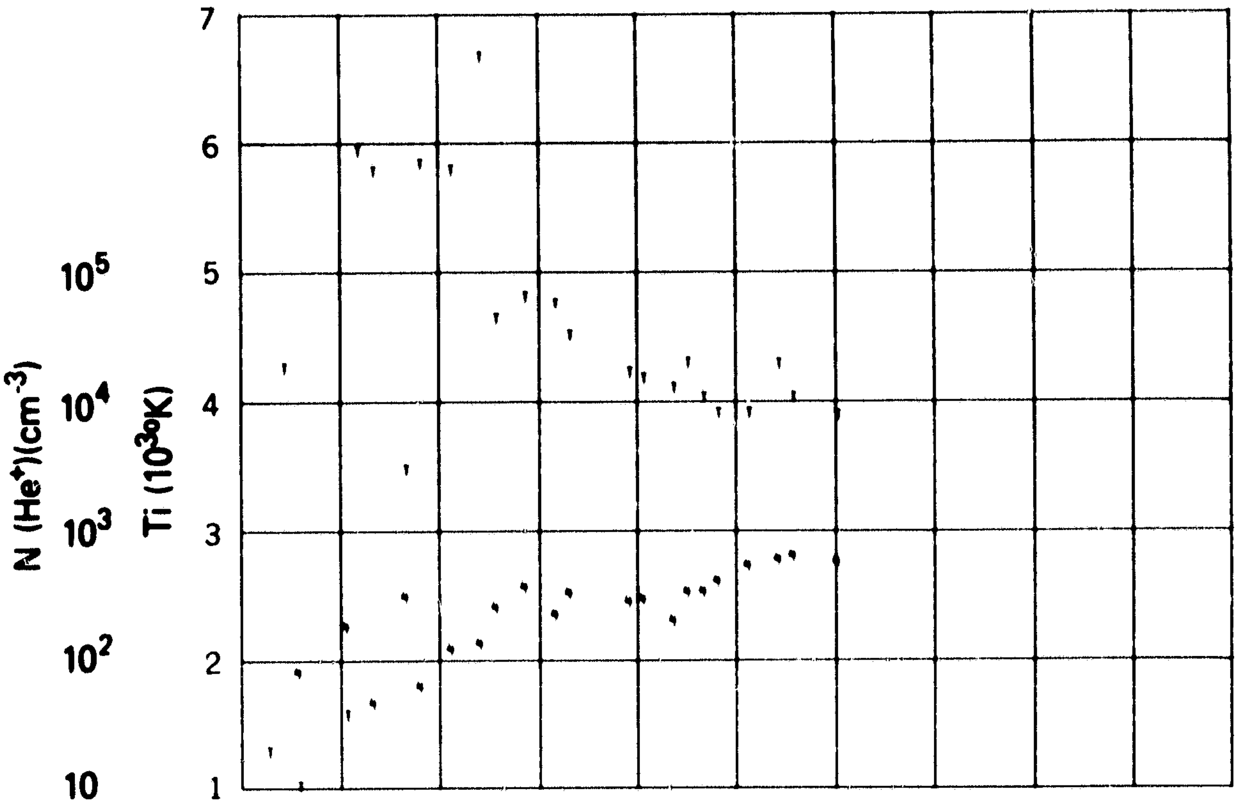

UT	6:36	6:38	6:40	6:42	6:44
LAST	10:41	10:44	10:46	10:47	10:49
MLT	19:59	19:45	19:34	19:26	19:19
DLAT	-64	-58	-51	-44	-37
INVL	65	60	55	49	44
GLAT	-58	-51	-45	-39	-32
GLNG	-176	-176	-176	-176	-176
SZEN	114	113	113	112	111
ALT	1429	1423	1416	1410	1403

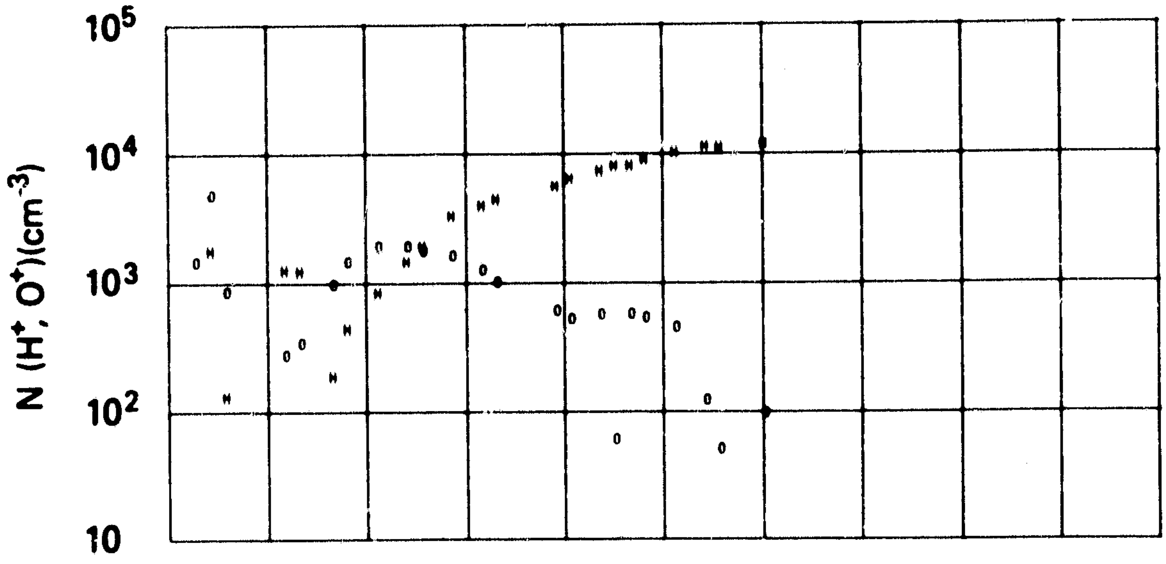

SET 26, FORMAT 5

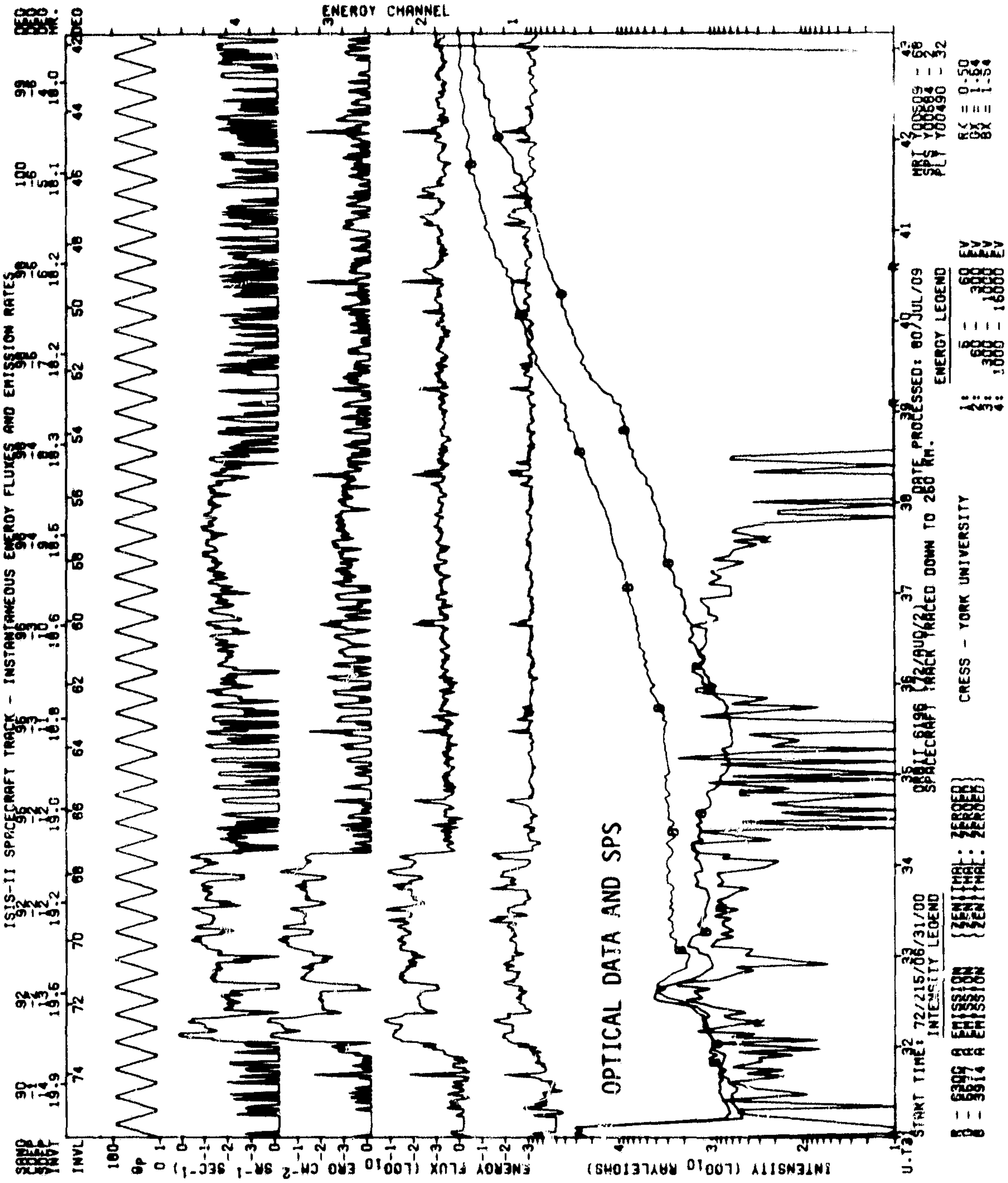

SET 27, FORMAT 1

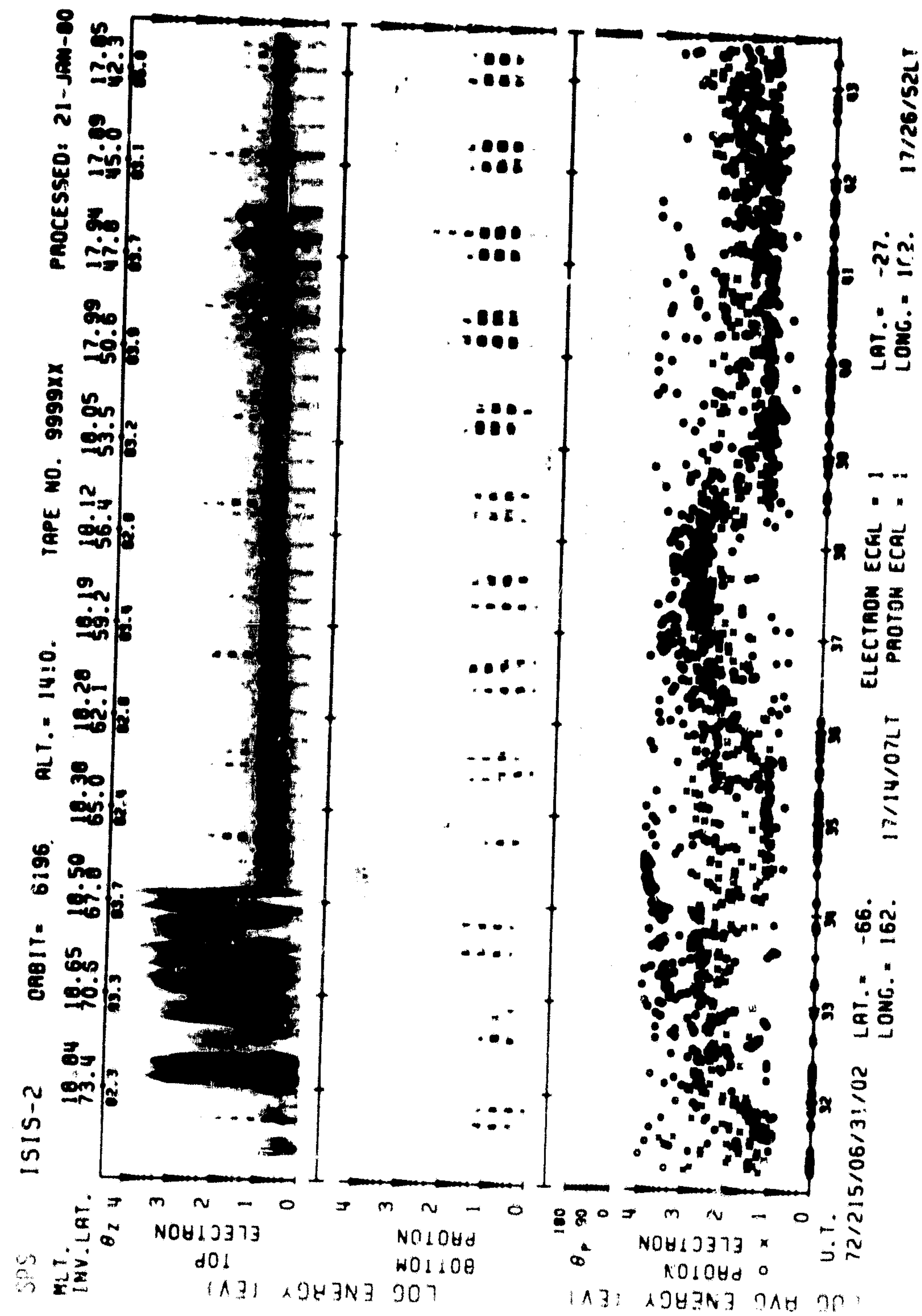

SET 27, FORMAT 6

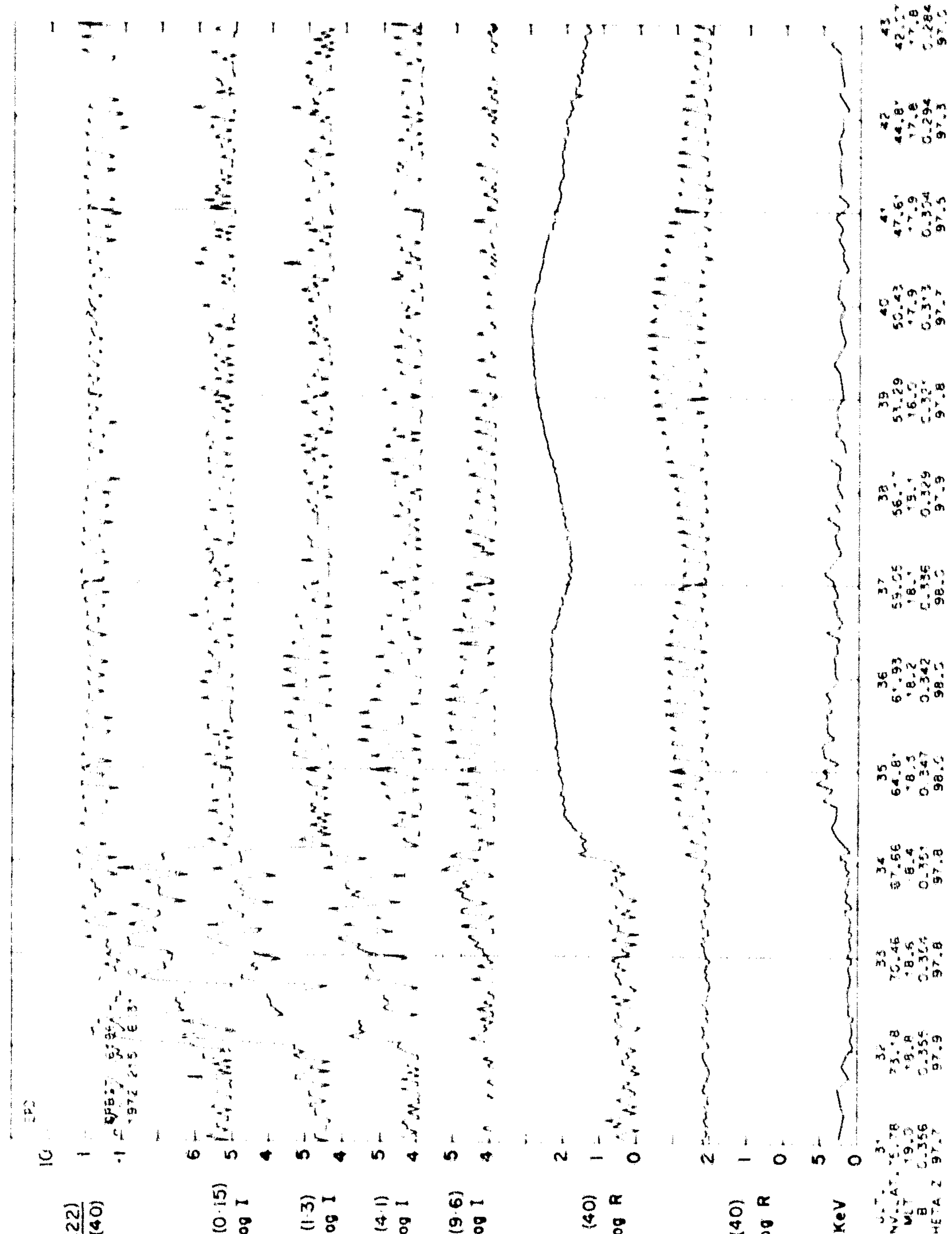

SET 27, FORMAT 3

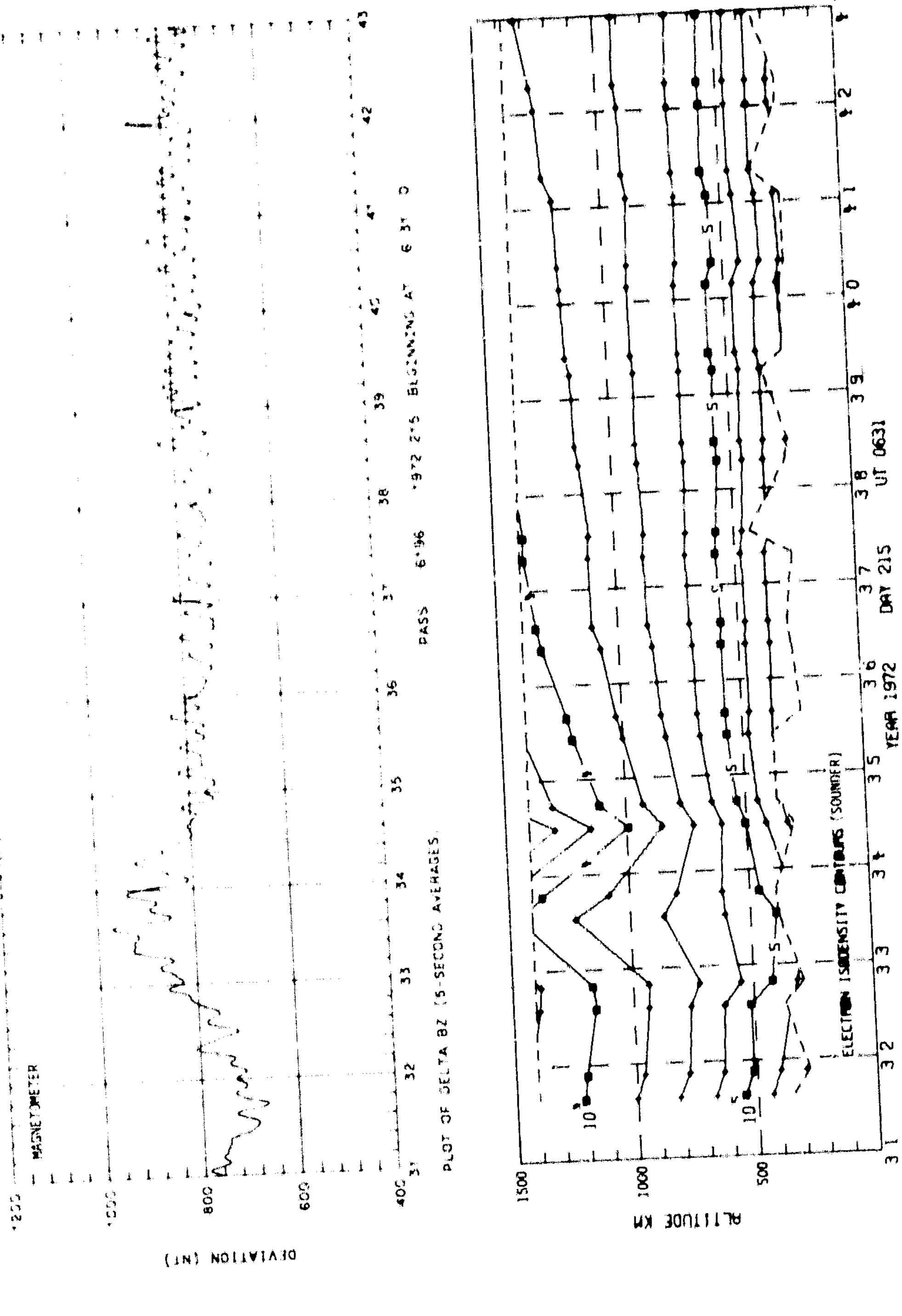

SET 27, FORMAT 2

ORBIT 6196
DATE 720802
DAY 215

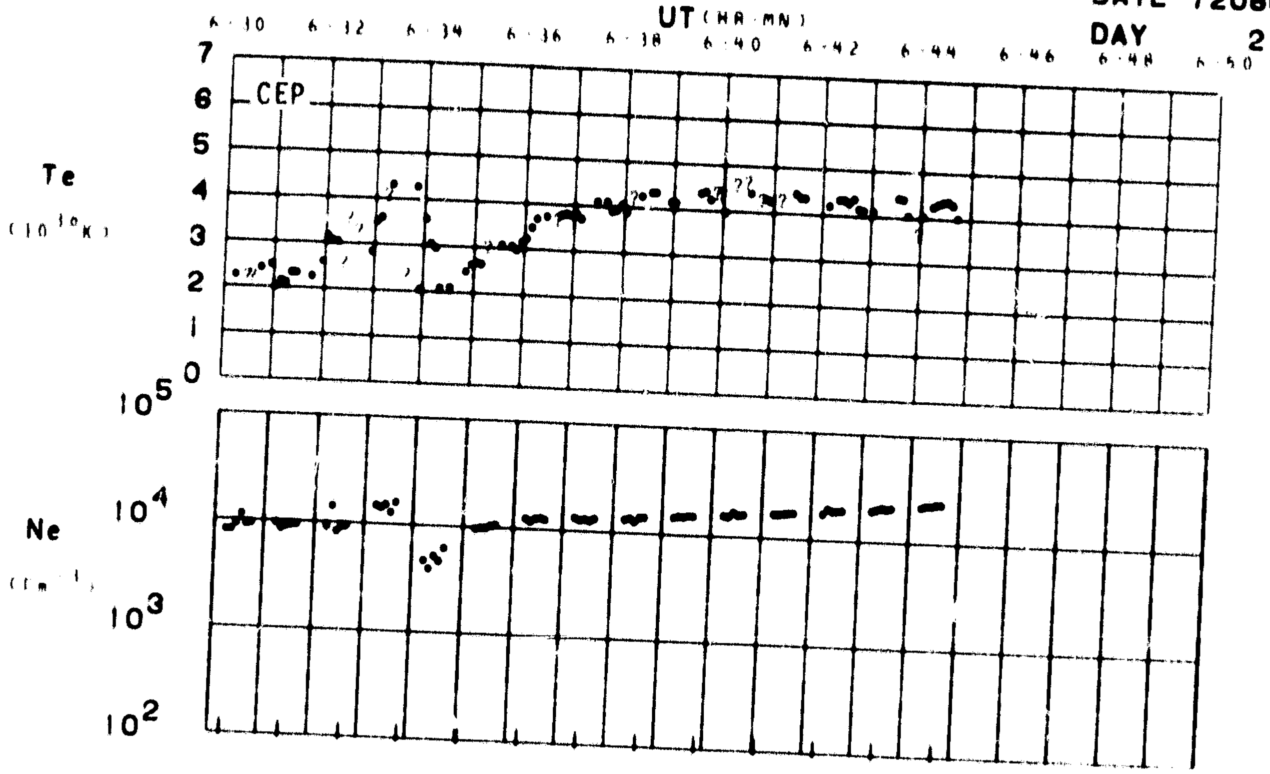

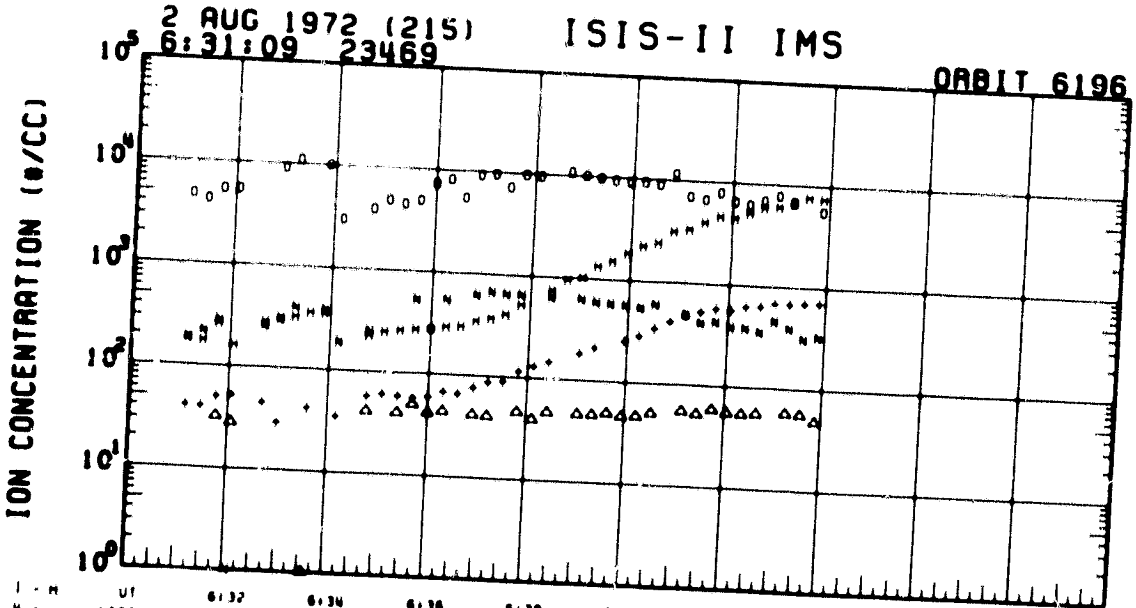

1 - H
4 - +
8 - Δ
14 - N
16

UT	6:32	6:34	6:36	6:38	6:40	6:42
LAST	17:16	17:19	17:22	17:24	17:25	17:28
MLT	10:50	10:30	10:16	10:07	17:59	17:53
DLAT	-75	-69	-61	-54	-47	-40
INVL	73	68	62	56	50	45
GLAT	-62	-56	-49	-43	-37	-30
GLNG	163	163	163	163	163	163
SZEN	101	99	98	96	94	92
ALT	1407	1401	1395	1389	1384	1378

SET 27, FORMAT 4

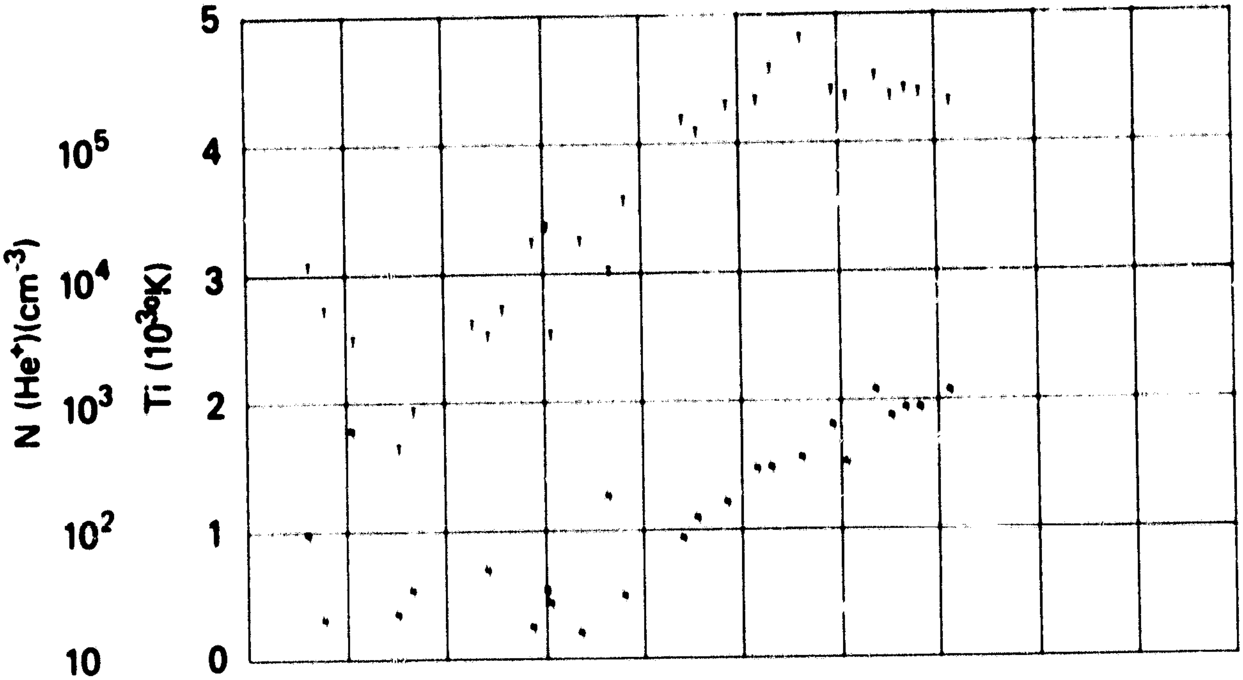

UT	6:32	6:34	6:36	6:38	6:40	6:42
LAST	17:16	17:19	17:22	17:24	17:25	17:28
MLT	10:50	10:30	10:16	10:07	17:58	17:53
DLAT	-75	-69	-61	-54	-47	-40
INVL	73	68	62	56	50	45
GLAT	62	-56	-49	-43	-37	-30
GLNG	163	163	163	163	163	163
SZEN	101	98	98	96	94	92
ALT	1407	1401	1395	1389	1384	1378

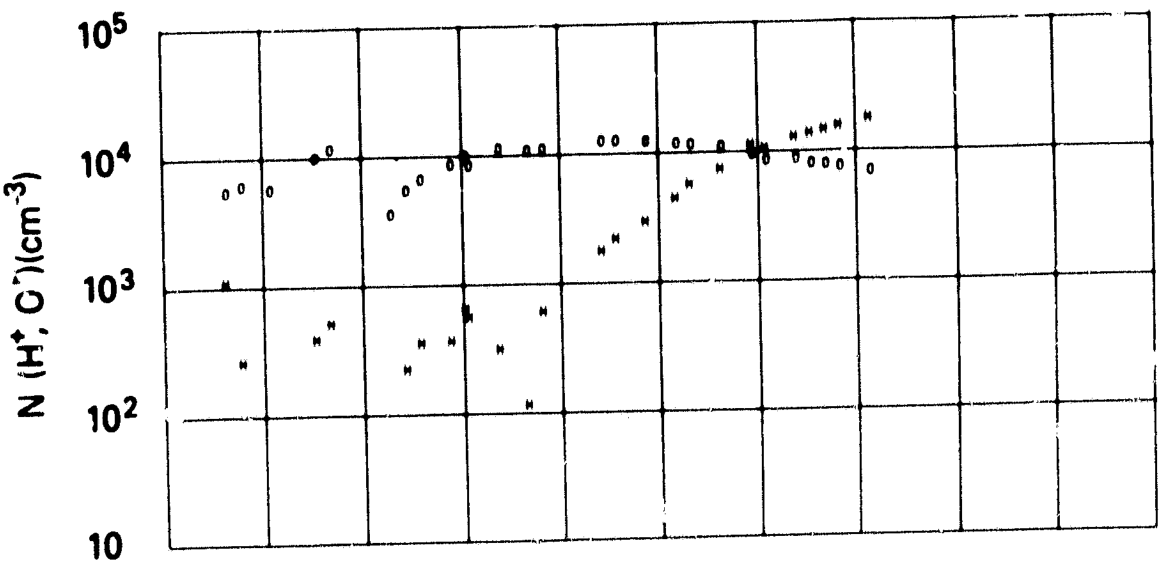

SET 27, FORMAT 5

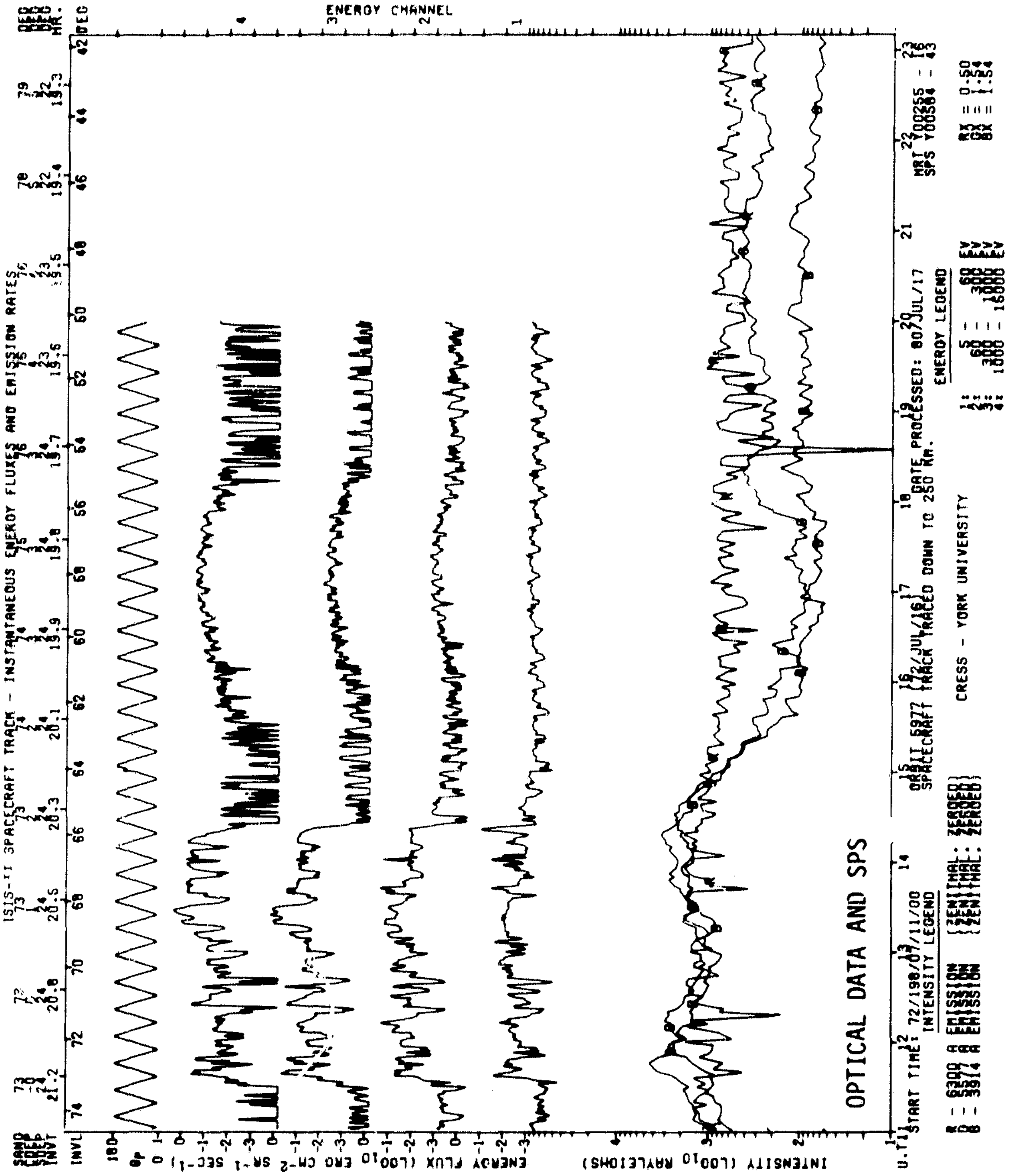

SET 28, FORMAT 1

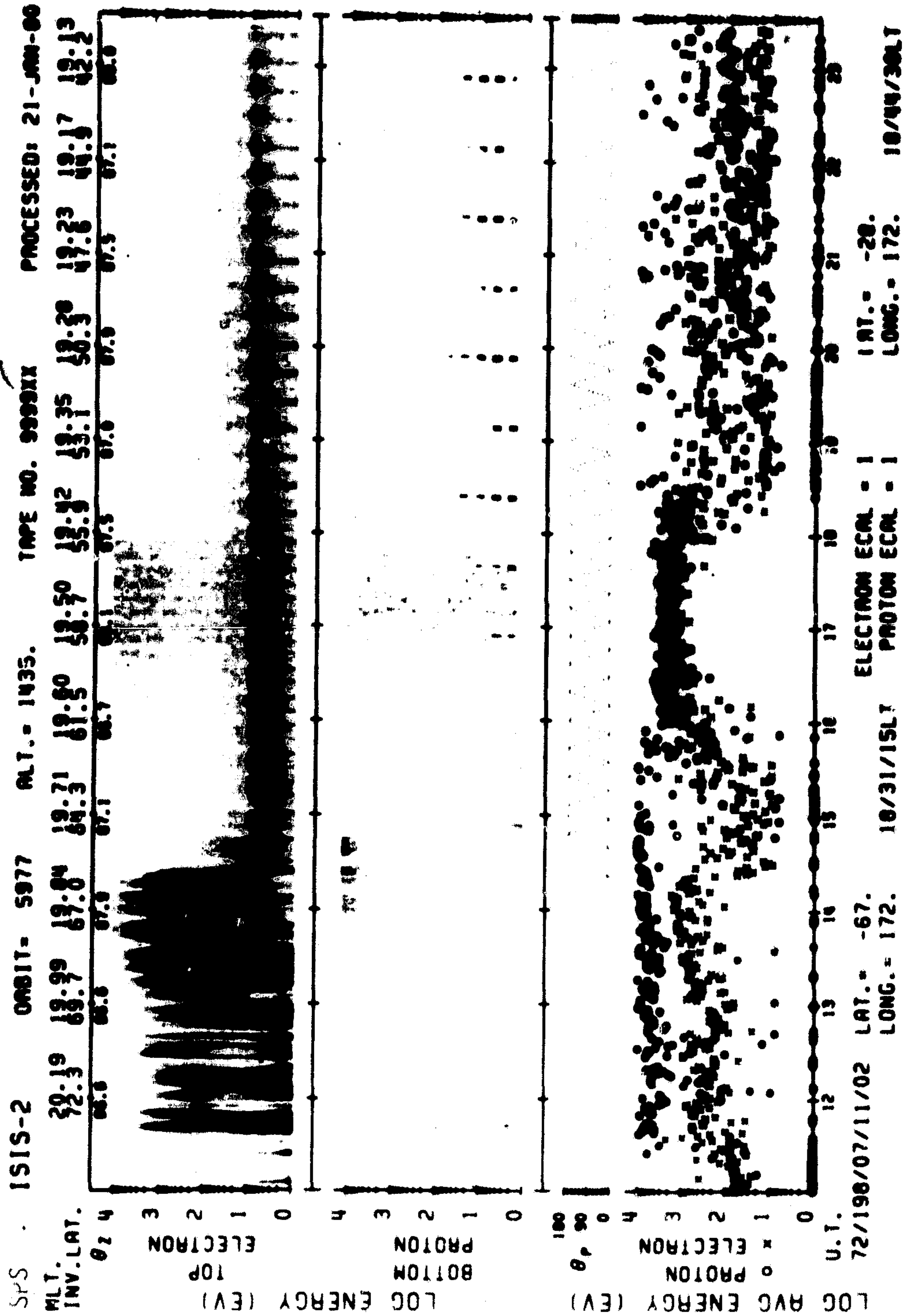

SET 28, FORMAT 6

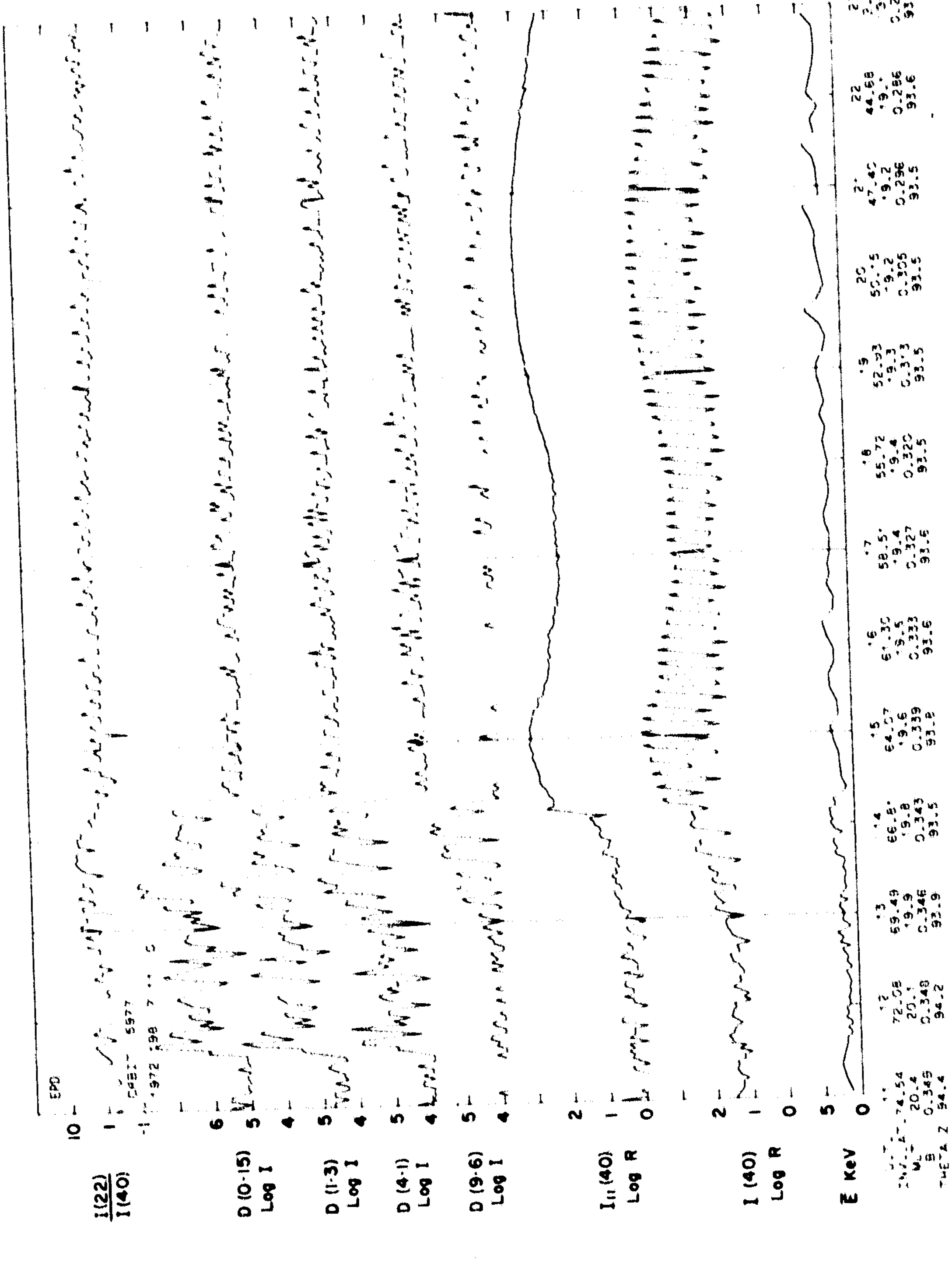

SET 28, FORMAT 3

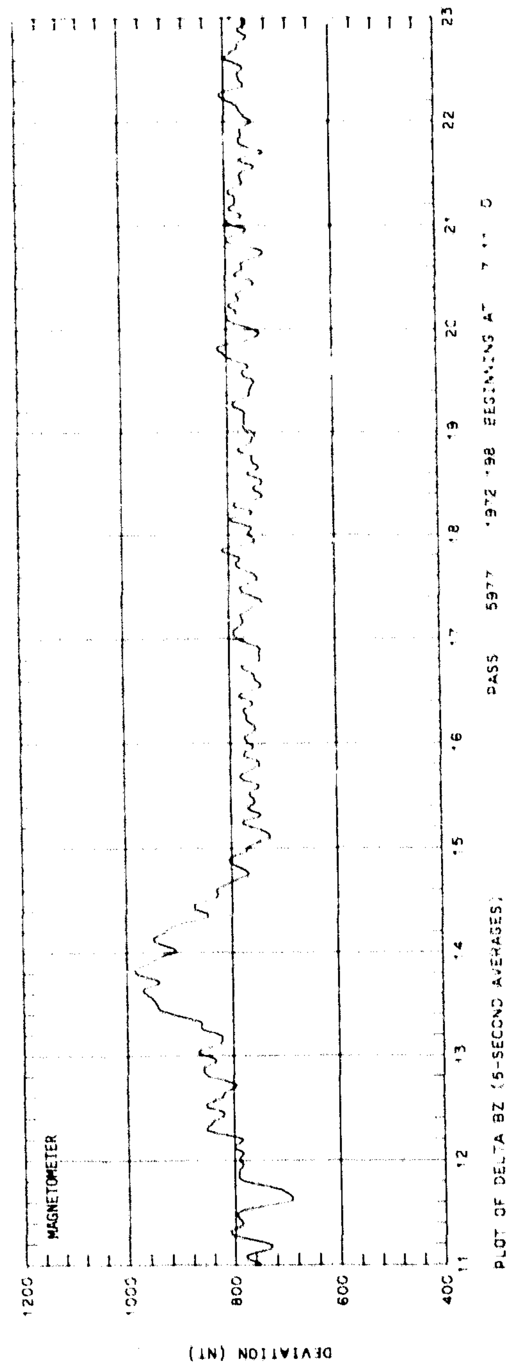

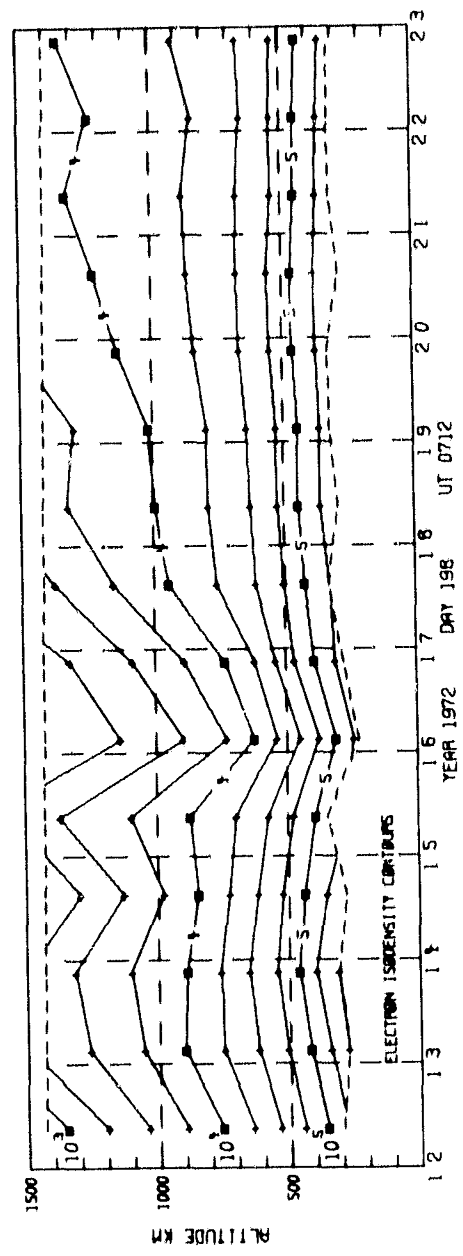

SET 28, FORMAT 2

ORBIT 5977
DATE 720716
DAY 198

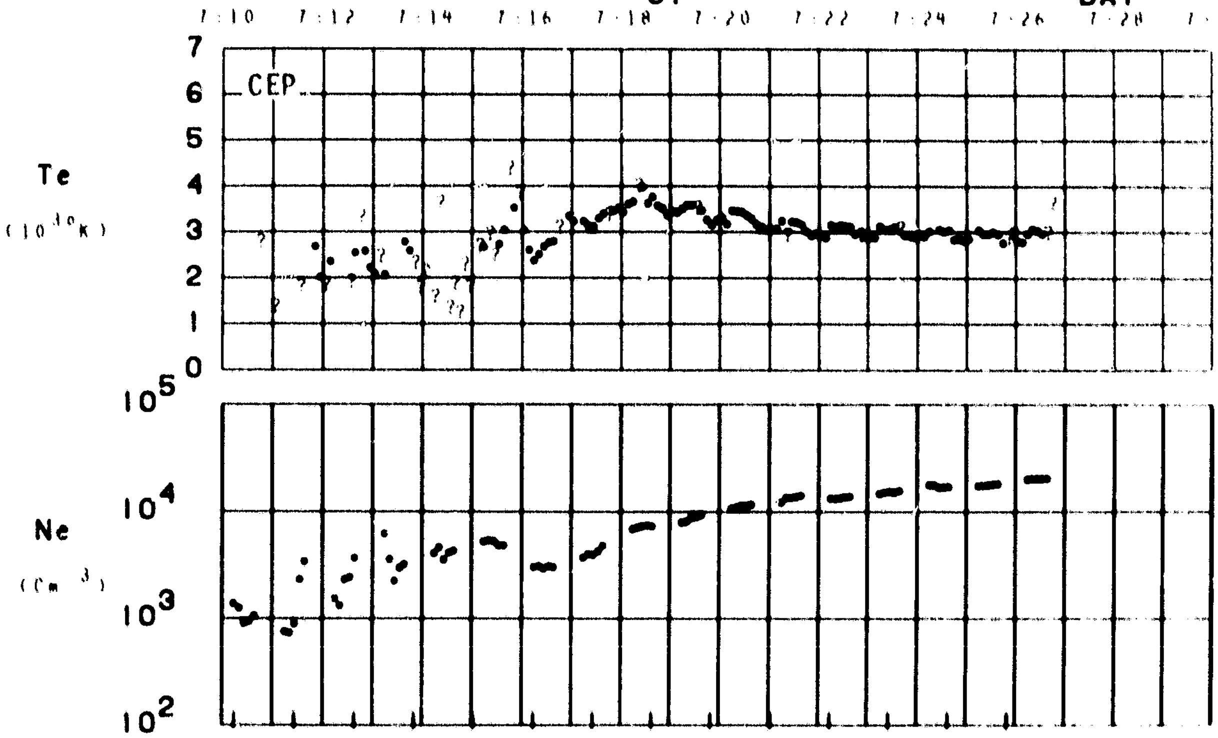

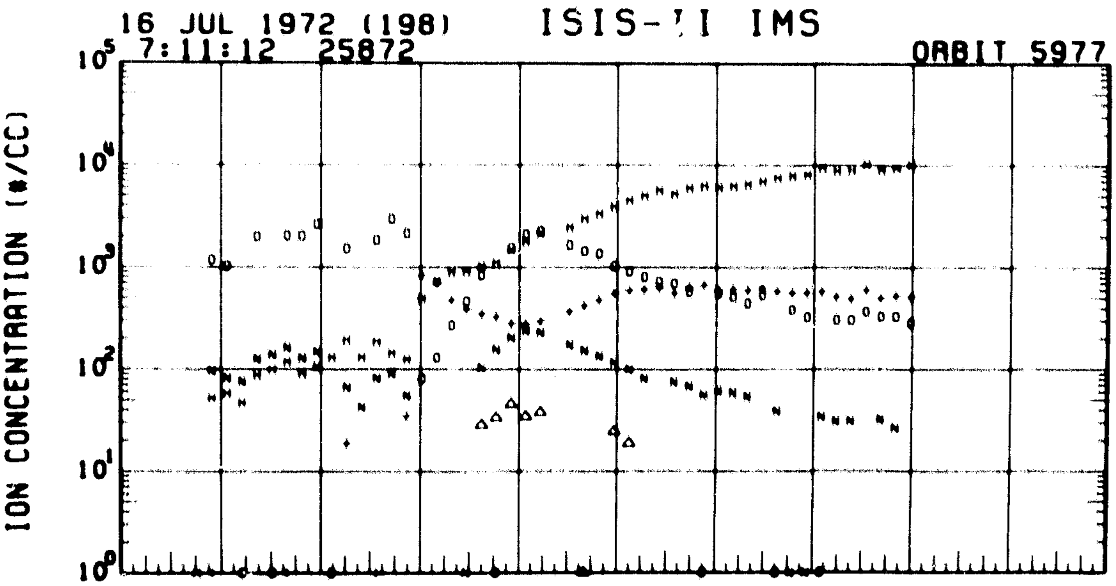

			7:12	7:14	7:16	7:18	7:20	7:22	7:24
1 - H		UT	7:12	7:14	7:16	7:18	7:20	7:22	7:24
4 - +		LAST	18:33	18:37	18:39	18:41	18:43	18:44	18:45
8 - Δ		ALT	20:10	19:50	19:35	19:25	19:17	19:10	19:05
14 - N		DLAT	-73	-67	-60	-53	-46	-38	-32
16 - O		INVL	72	67	61	56	50	45	39
		GLAT	-63	-57	-51	-44	-38	-32	-25
		GLNG	172	172	172	172	172	172	172
		SZEN	113	113	113	112	111	110	109
		ALT	1432	1427	1420	1414	1408	1401	1395

SET 28, FORMAT 4

RPA 720716

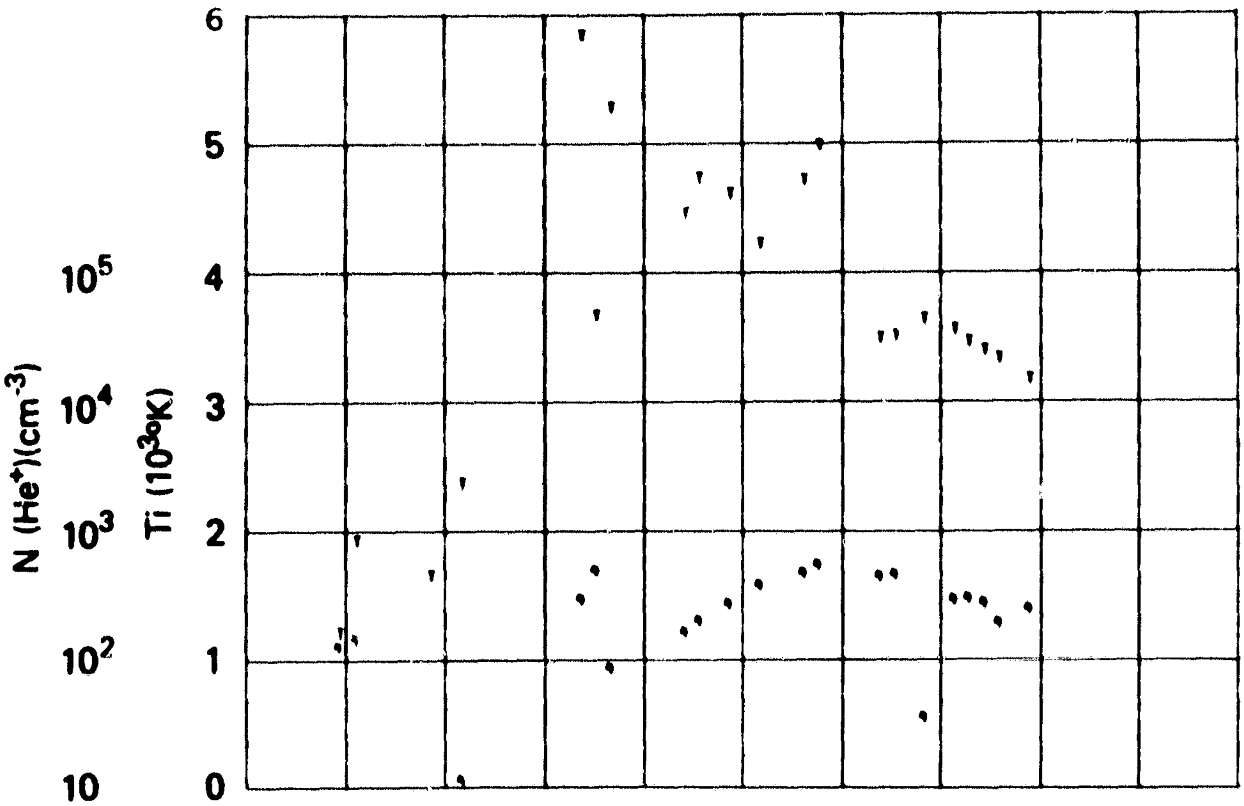

UT	7:12	7:14	7:16	7:18	7:20	7:22	7:24
LAST	10:33	10:37	10:38	10:41	10:43	10:44	10:45
MLT	20:10	19:50	19:35	19:25	19:17	19:10	19:05
DLAT	-73	-67	-60	-53	-46	-38	-32
INVL	72	67	61	56	50	45	38
GLAT	-63	-57	-51	-44	-38	-32	-25
GLNG	172	172	172	172	172	172	172
SZEN	113	113	113	112	111	110	108
ALT	1432	1427	1420	1414	1408	1401	1395

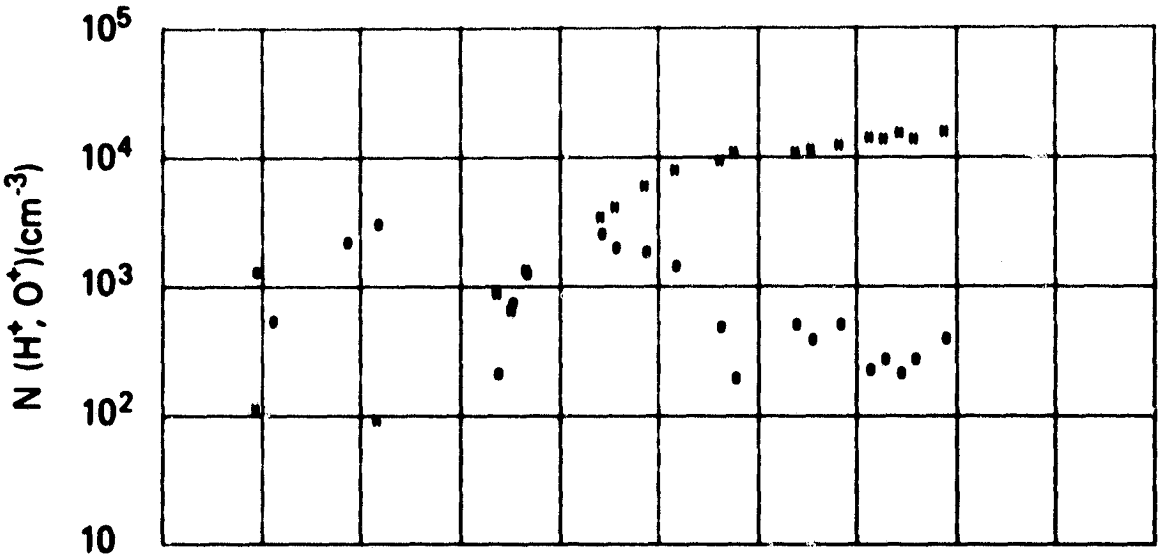

SET 28, FORMAT 5

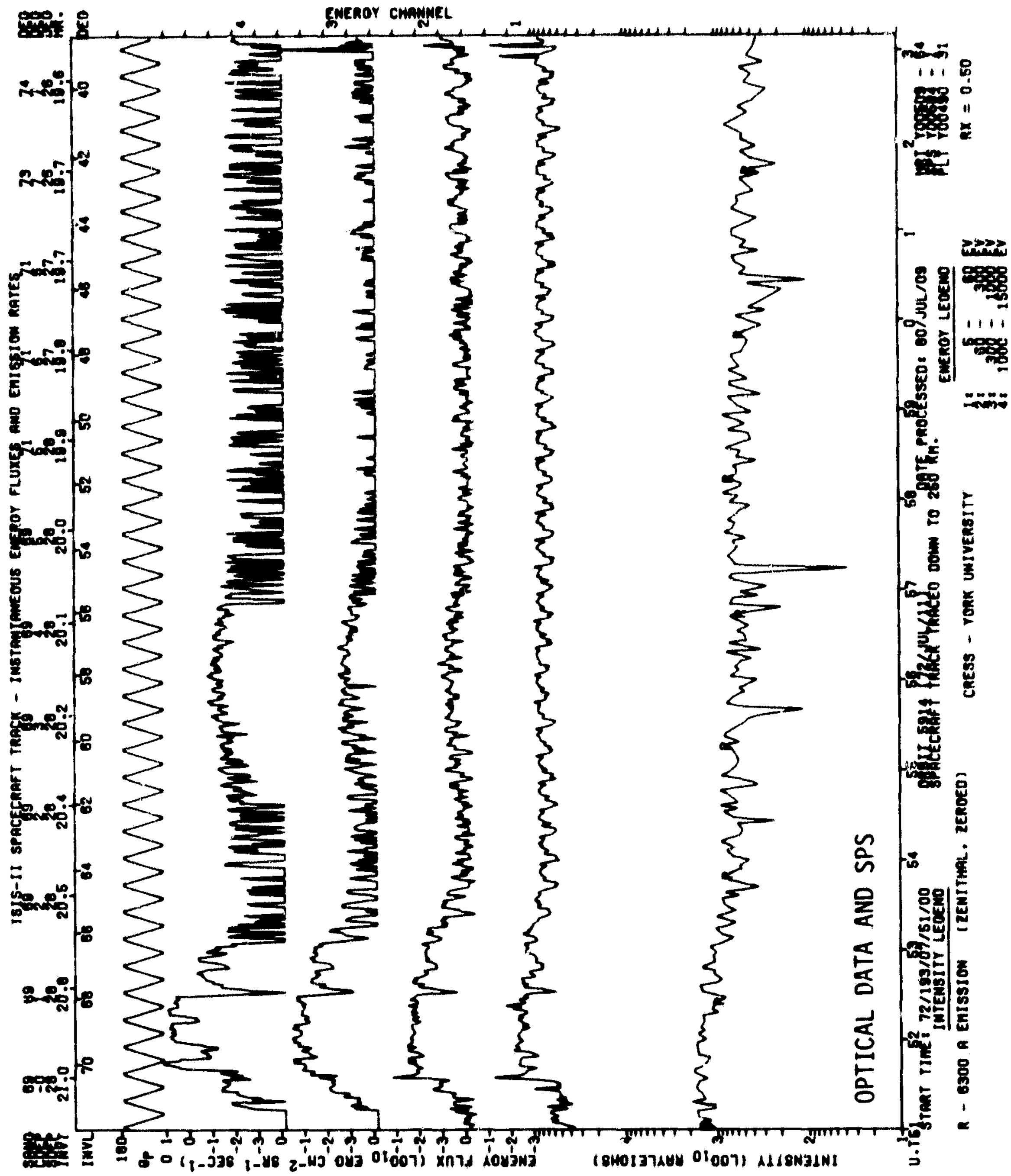

SET 29, FORMAT 1

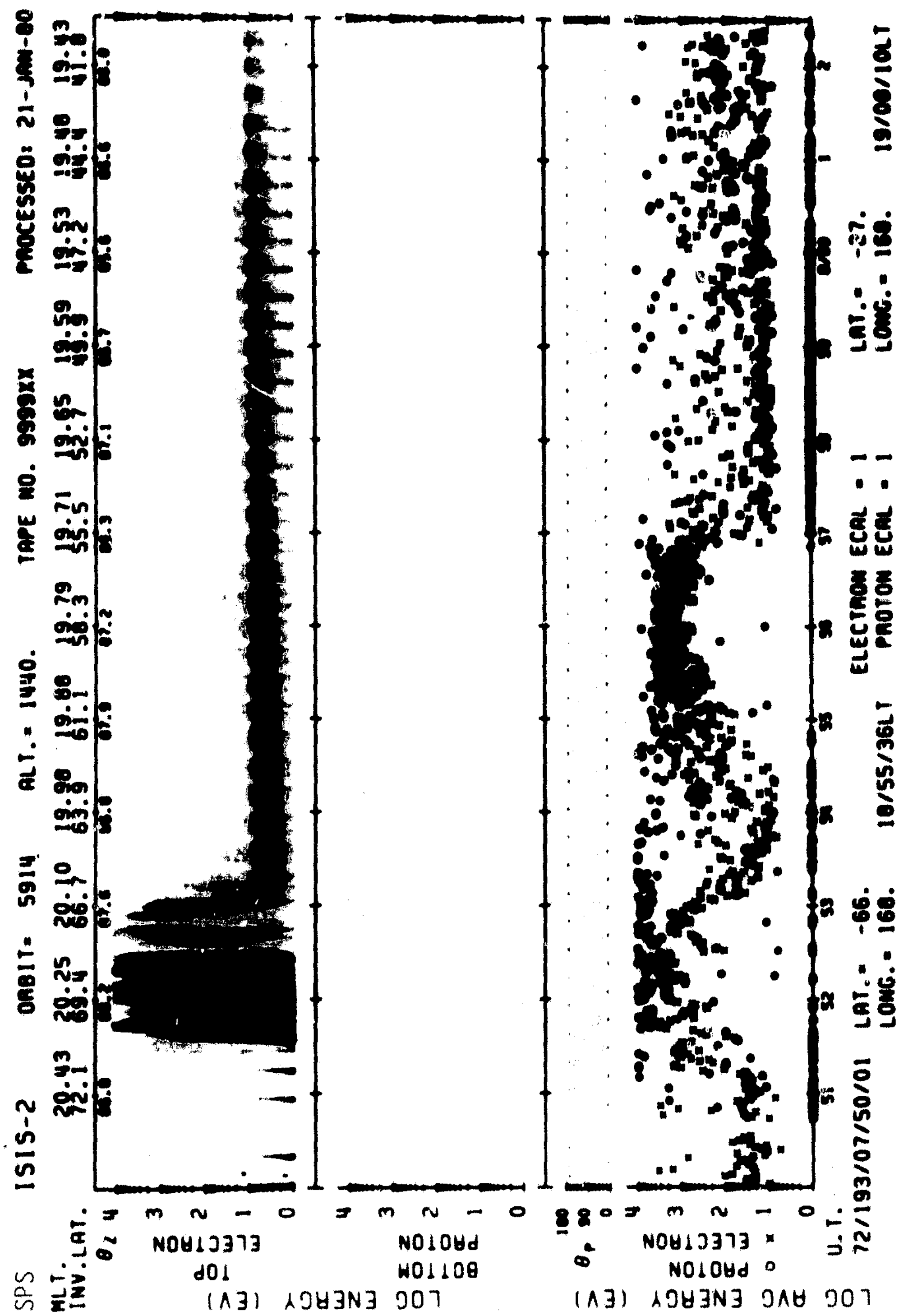

SET 29, FORMAT 6

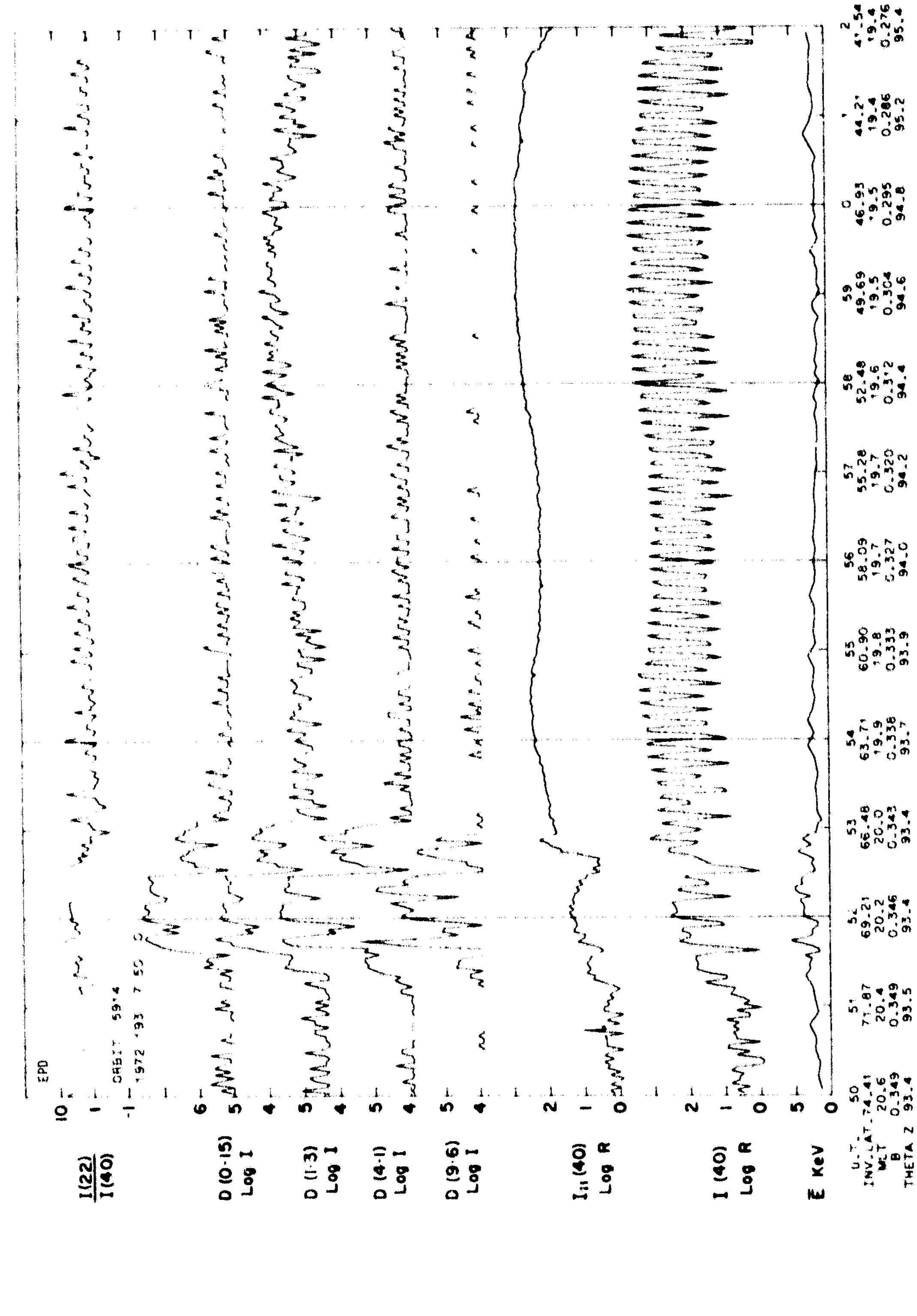

SET 29, FORMAT 3

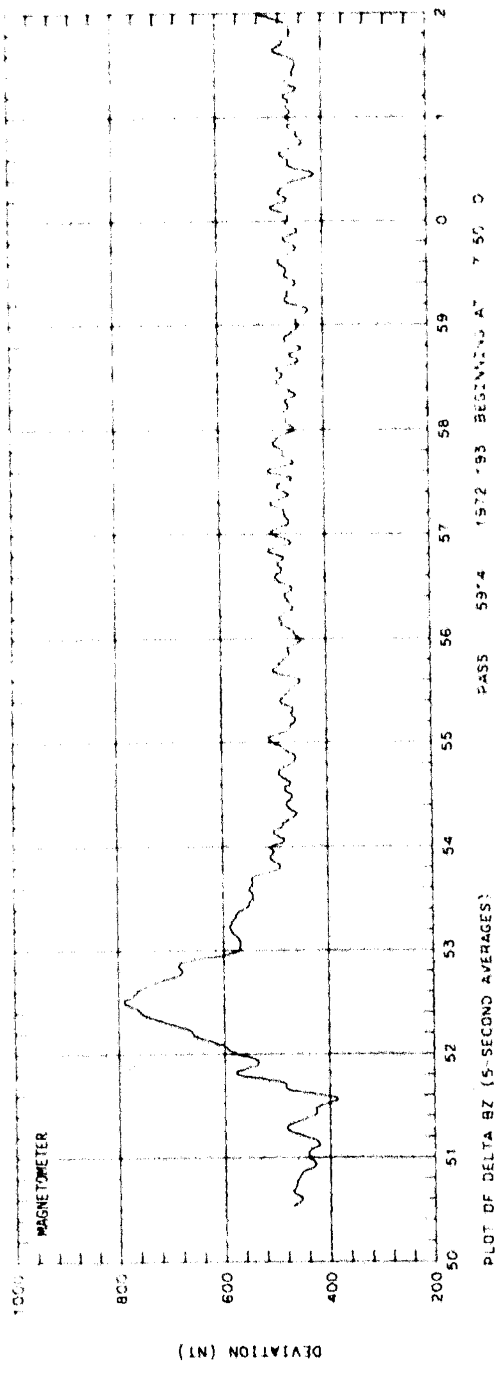

SET 29, FORMAT 2

ORBIT 5914
DATE 720711
DAY 193

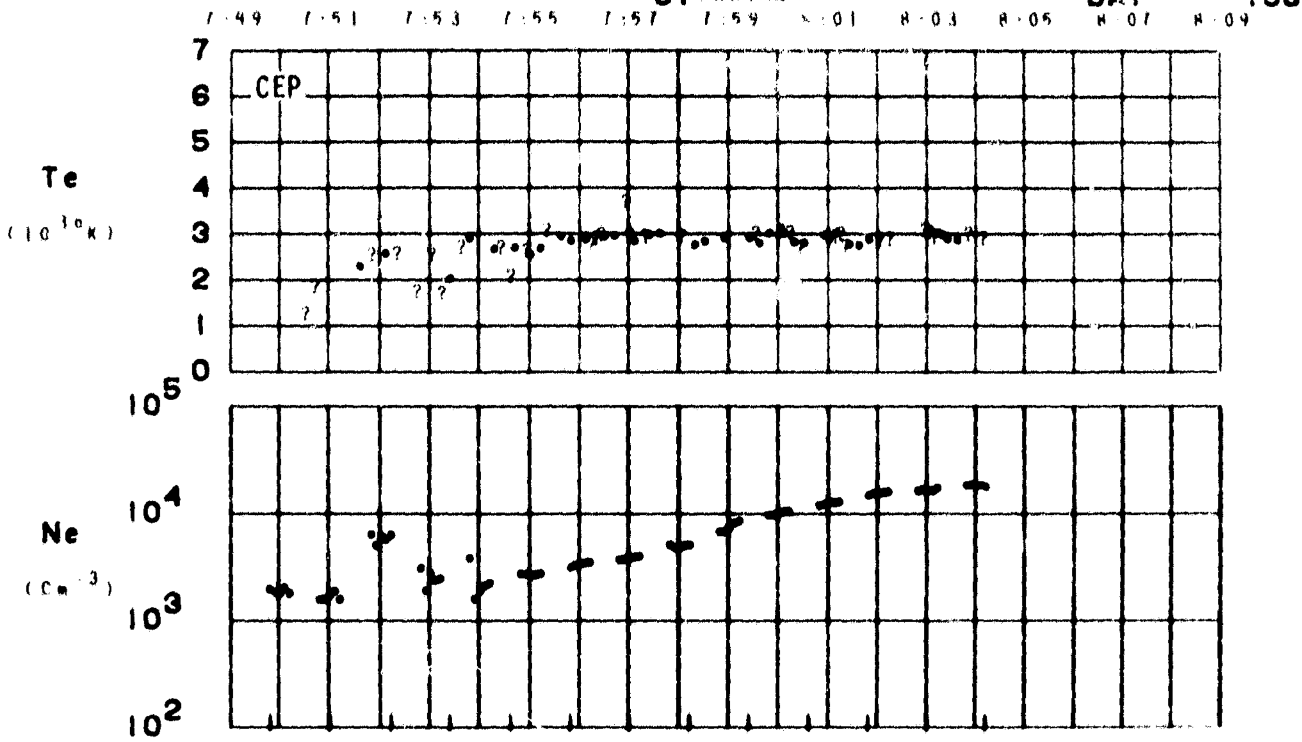

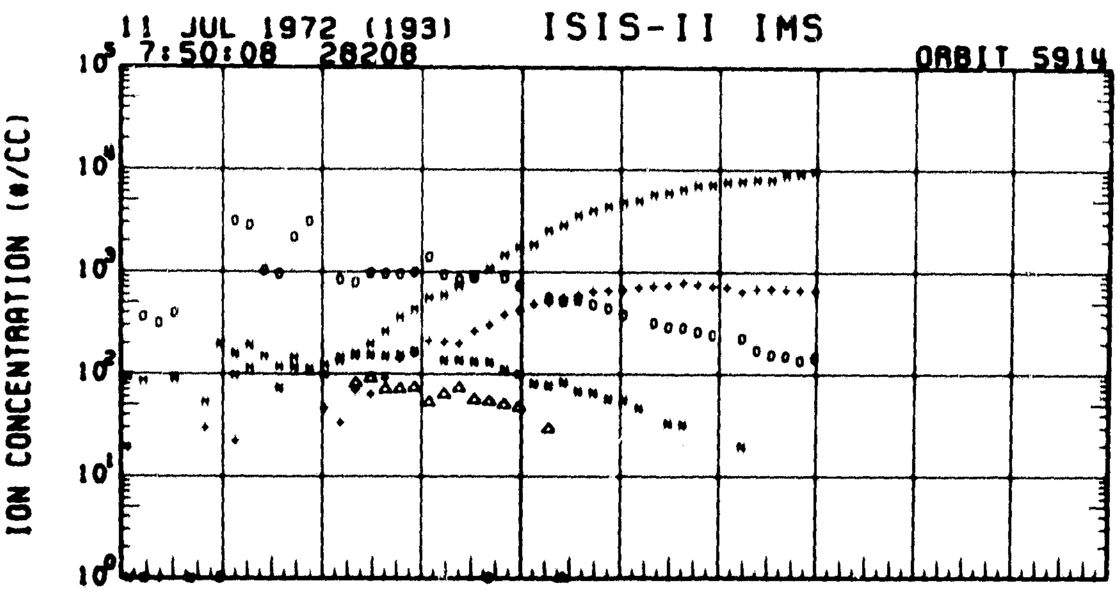

1 - H	UT	7:52	7:54	7:56	7:58	8:00	8:02
4 - +	LAST	18:59	19:02	19:04	19:06	19:07	19:09
8 - Δ	MLT	20:14	19:50	19:47	19:30	19:32	19:26
14 - N	DLAT	-70	-63	-56	-49	-42	-35
16 - O	INVL	69	64	58	52	47	42
	GLAT	-59	-52	-46	-40	-34	-27
	GLNG	188	188	188	188	188	188
	SZEN	116	117	117	116	116	115
	ALT	1435	1429	1423	1417	1411	1404

SET 29, FORMAT 4

RPA

720711

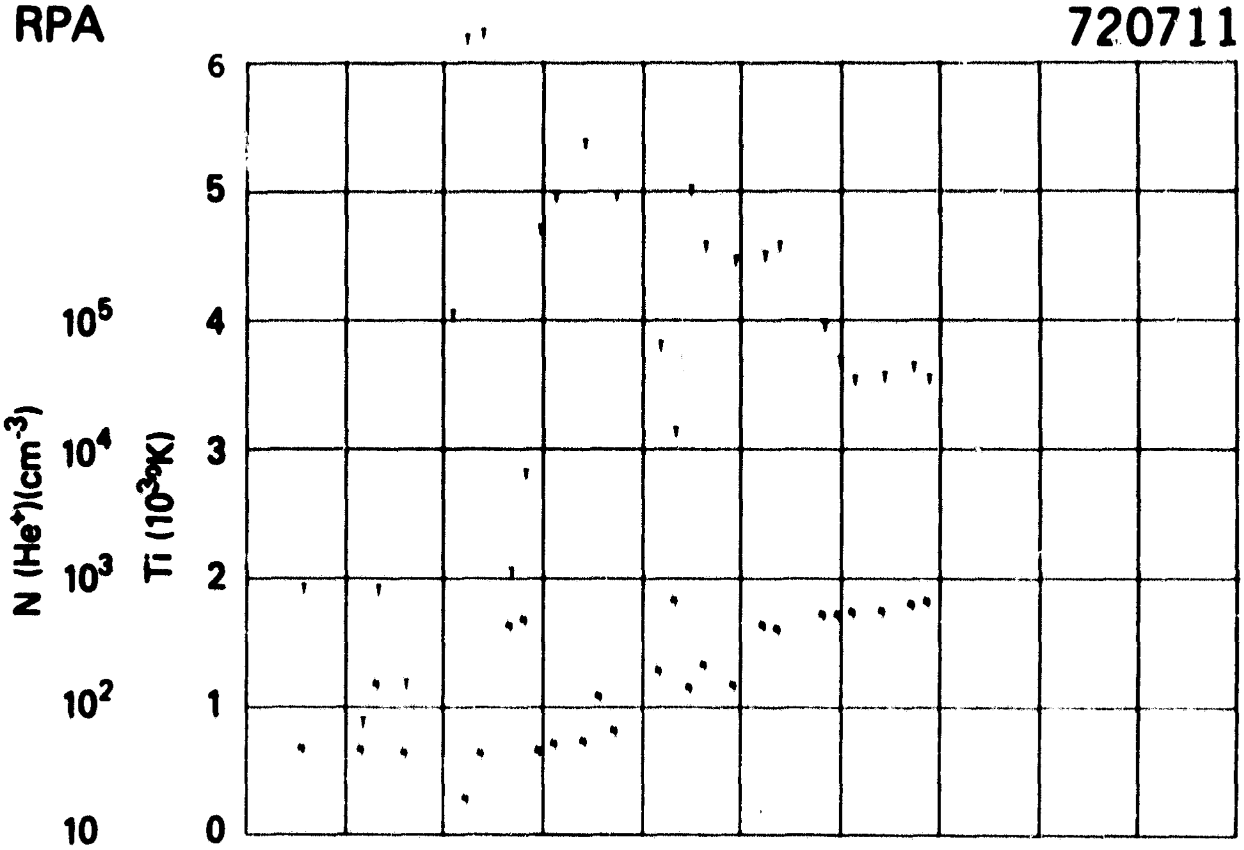

UT	7:52	7:54	7:56	7:58	8:00	8:02
LAST	18:58	19:02	19:04	19:06	19:07	19:08
MLT	20:14	19:58	19:47	19:38	19:32	19:26
DLAT	-70	-63	-56	-49	-42	-35
INVL	69	64	58	52	47	42
GLAT	-58	-52	-46	-40	-34	-27
GLNG	188	188	188	188	188	188
SZEN	116	117	117	116	116	115
ALT	1435	1429	1423	1417	1411	1404

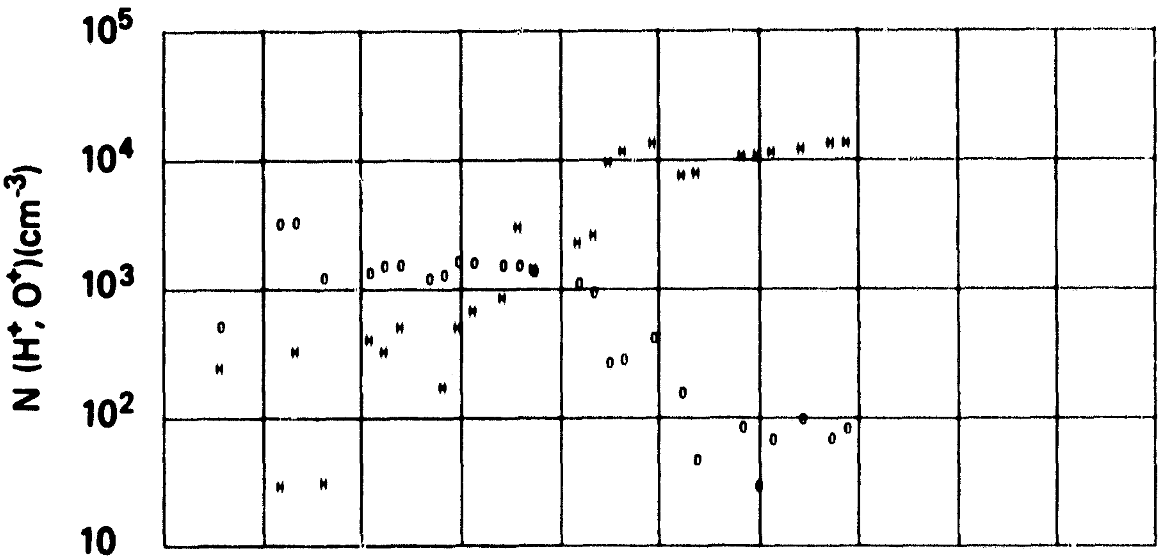

SET 29, FORMAT 5

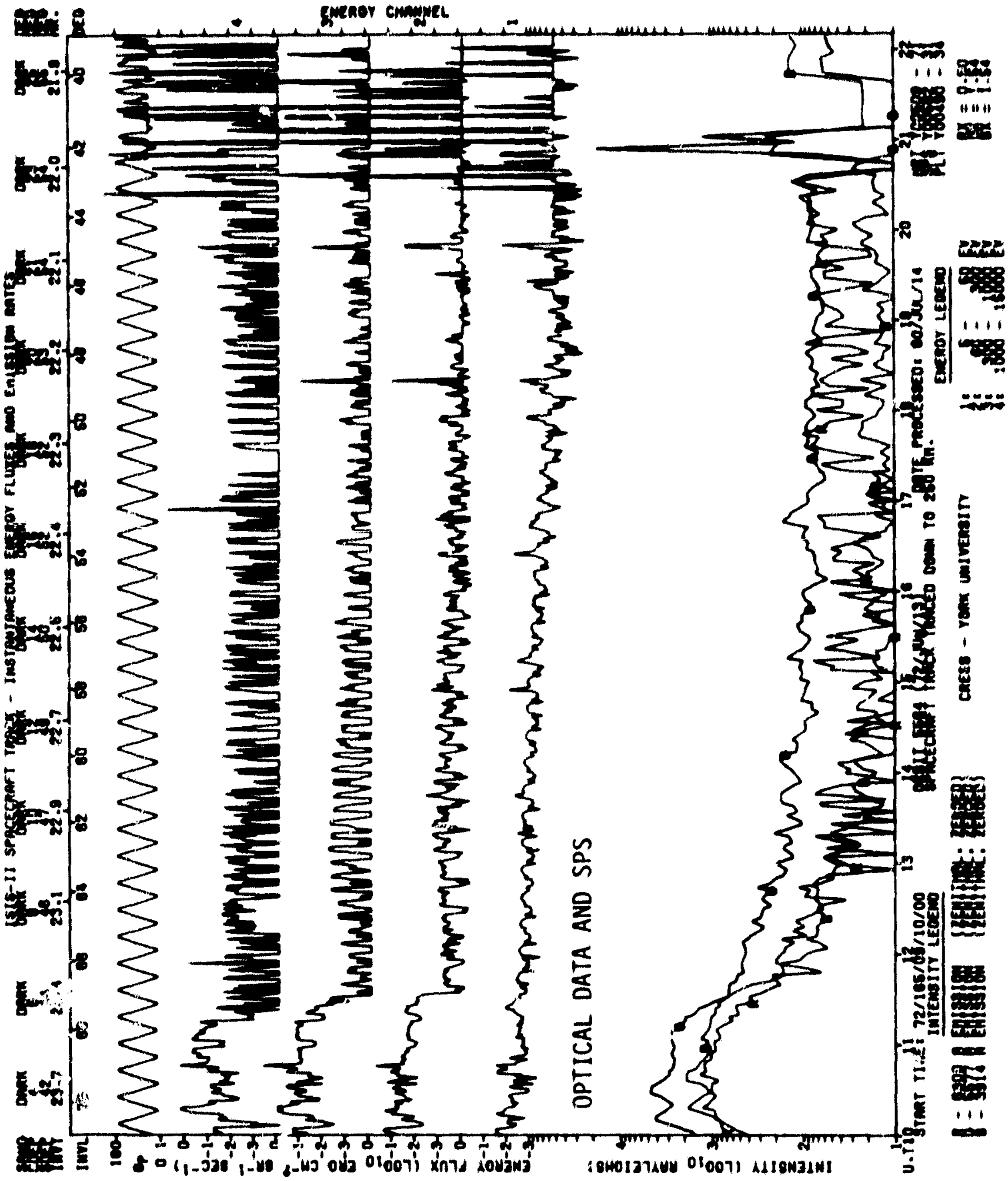

SET 30, FORMAT 1

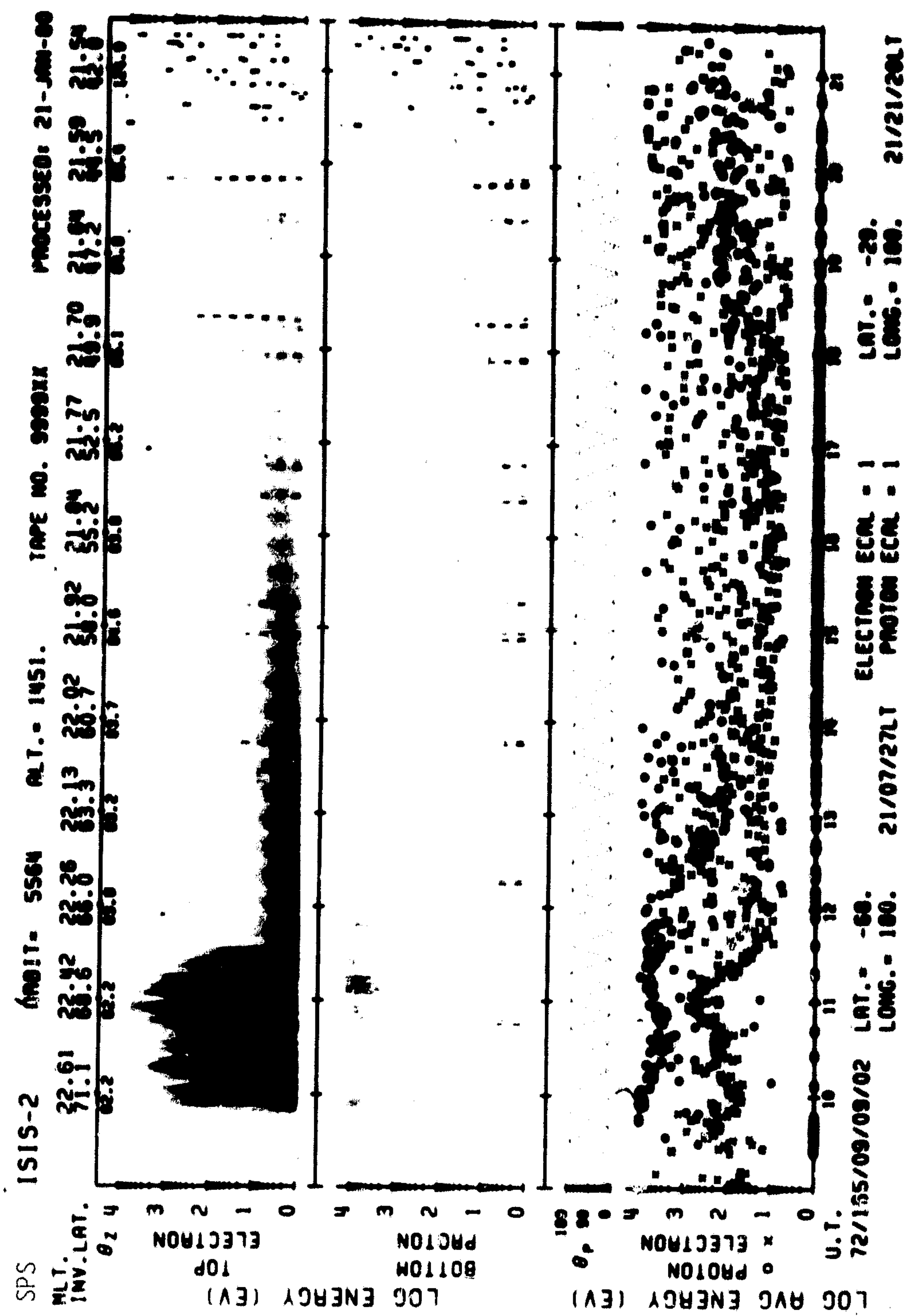

SET 30, FORMAT 6

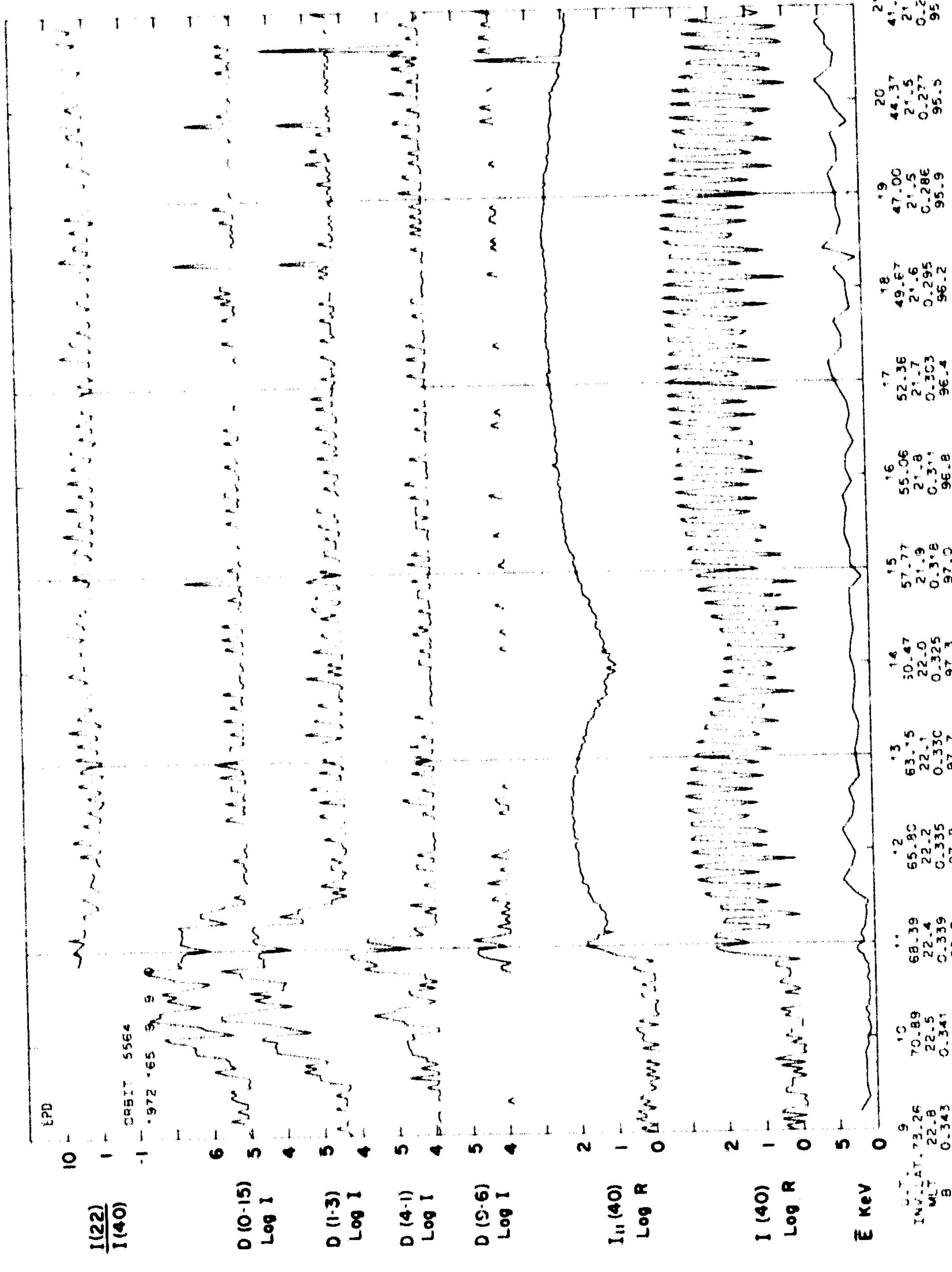

SET 30, FORMAT 3

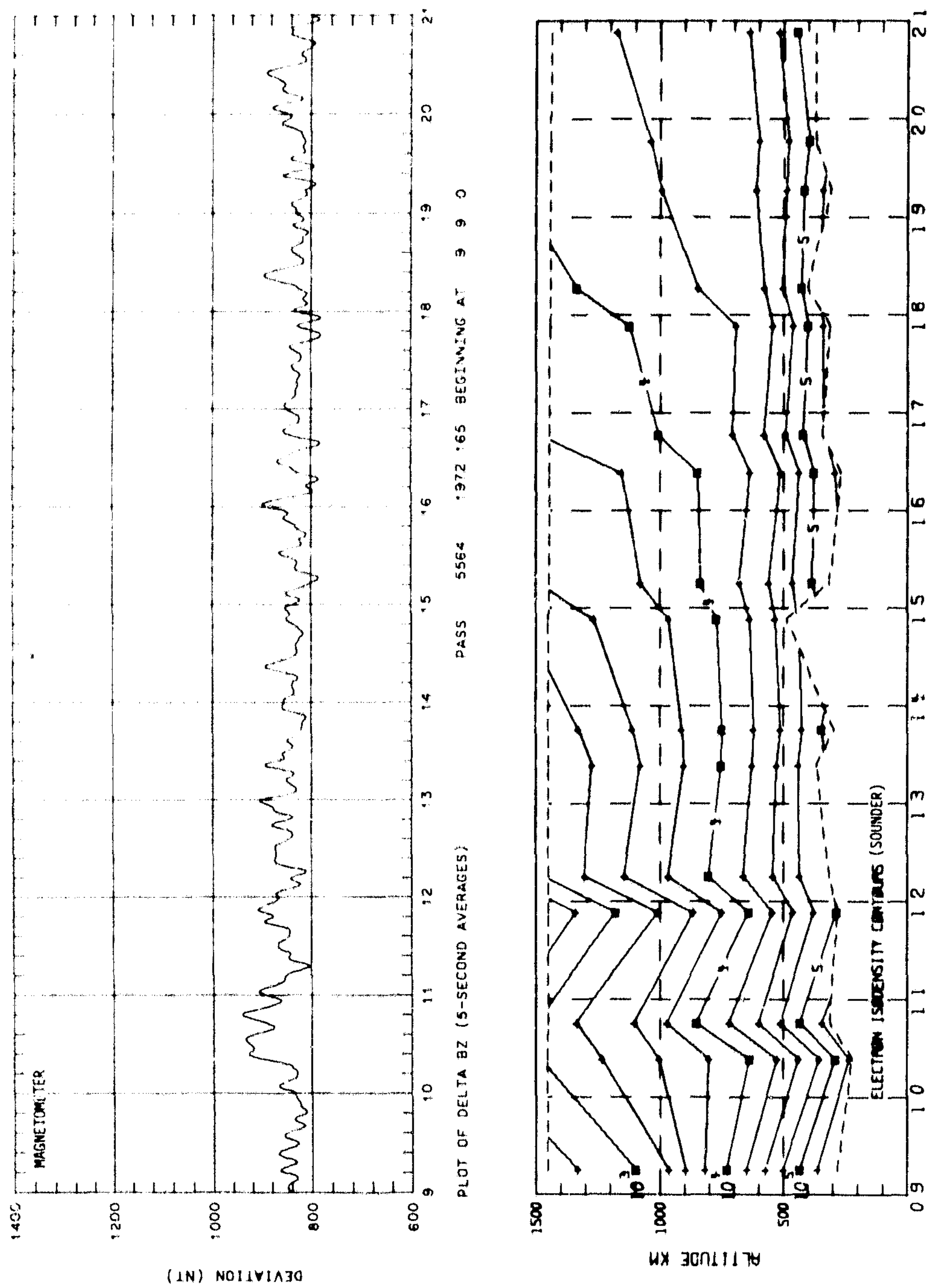

SET 30, FORMAT 2

ORBIT 5564
DATE 720613
DAY 165

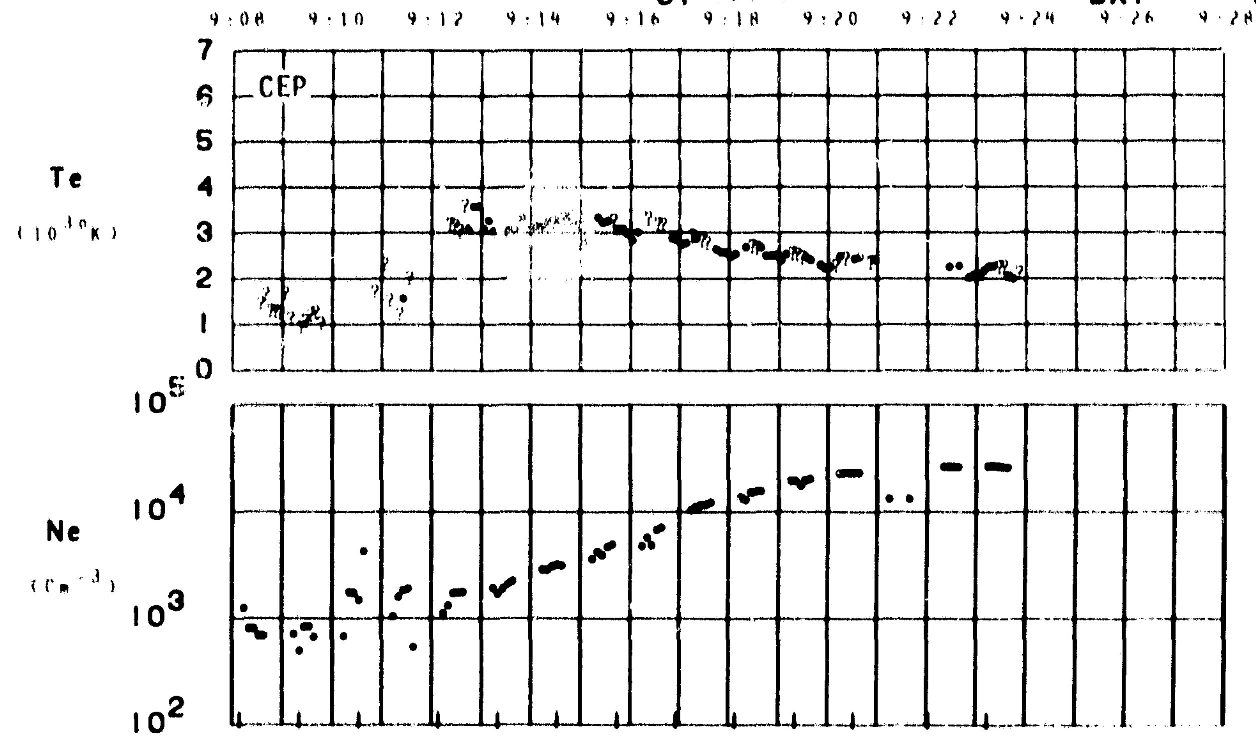

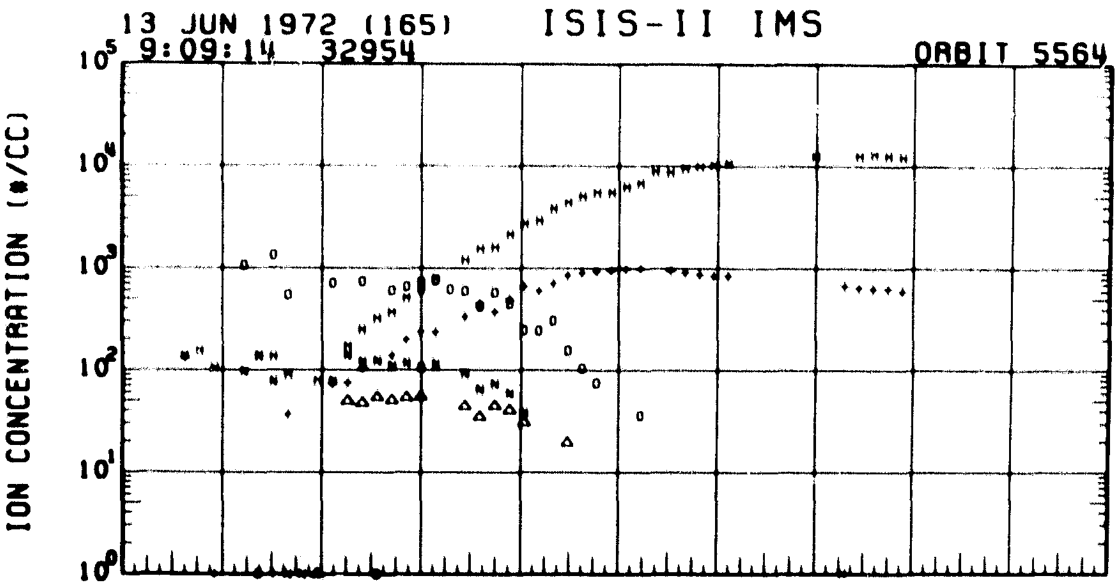

1 - H	UT	9:10	9:12	9:14	9:16	9:18	9:20	9:22
4 - +	LAST	21:10	21:13	21:16	21:18	21:19	21:21	21:22
8 - Δ	MLT	22:30	22:15	22:01	21:50	21:42	21:35	21:29
14 - N	DLAT	-71	-65	-58	-52	-45	-38	-31
16 - O	INVL	71	66	60	55	50	44	38
	GLAT	-64	-58	-51	-45	-38	-33	-26
	GLNG	180	-179	-179	-179	-179	-179	180
	SZEN	130	134	137	140	142	144	144
	ALT	1451	1448	1448	1445	1442	1439	1435

SET 30, FORMAT 4

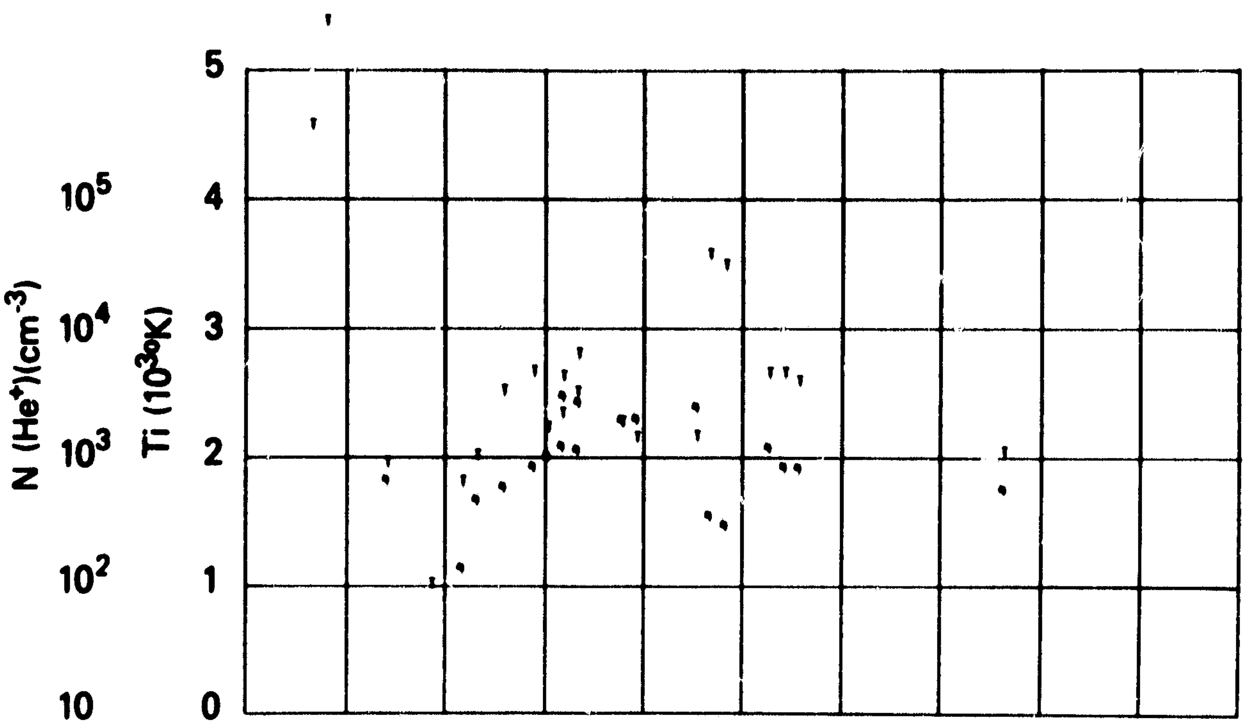

UT	9:10	9:12	9:14	9:16	9:18	9:20	9:22
LAST	21:10	21:13	21:16	21:18	21:19	21:21	21:22
MLT	22:38	22:15	22:01	21:50	21:42	21:35	21:28
DLAT	-71	-65	-58	-52	-45	-38	-31
INVL	71	66	60	55	50	44	38
GLAT	-64	-58	-51	-45	-38	-33	-26
GLNG	180	-179	-178	-179	-179	-178	180
SZEN	130	134	137	140	142	144	144
ALT	1451	1449	1448	1445	1442	1438	1435

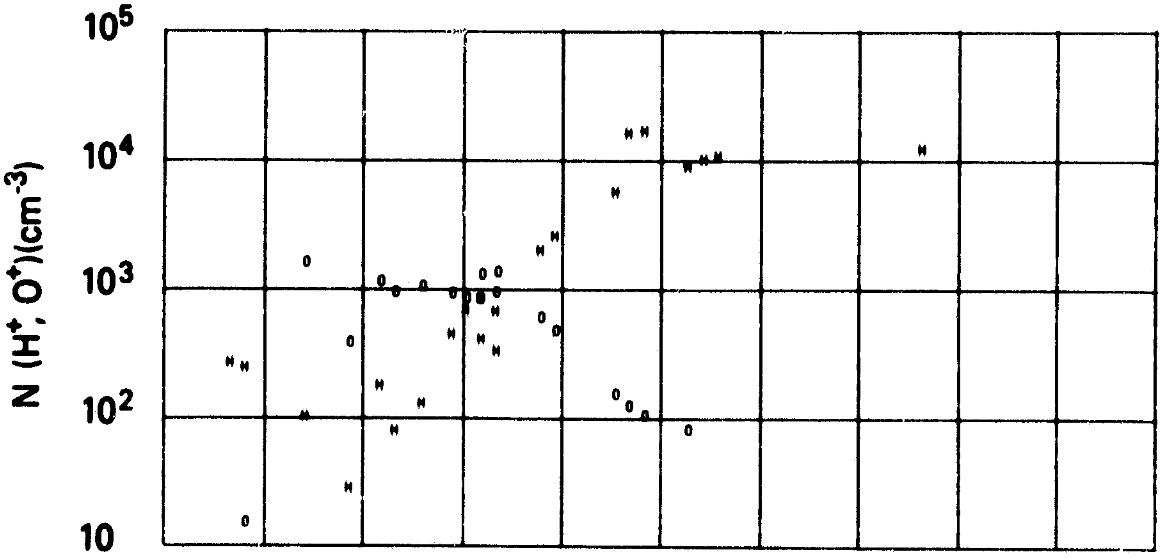

SET 30, FORMAT 5

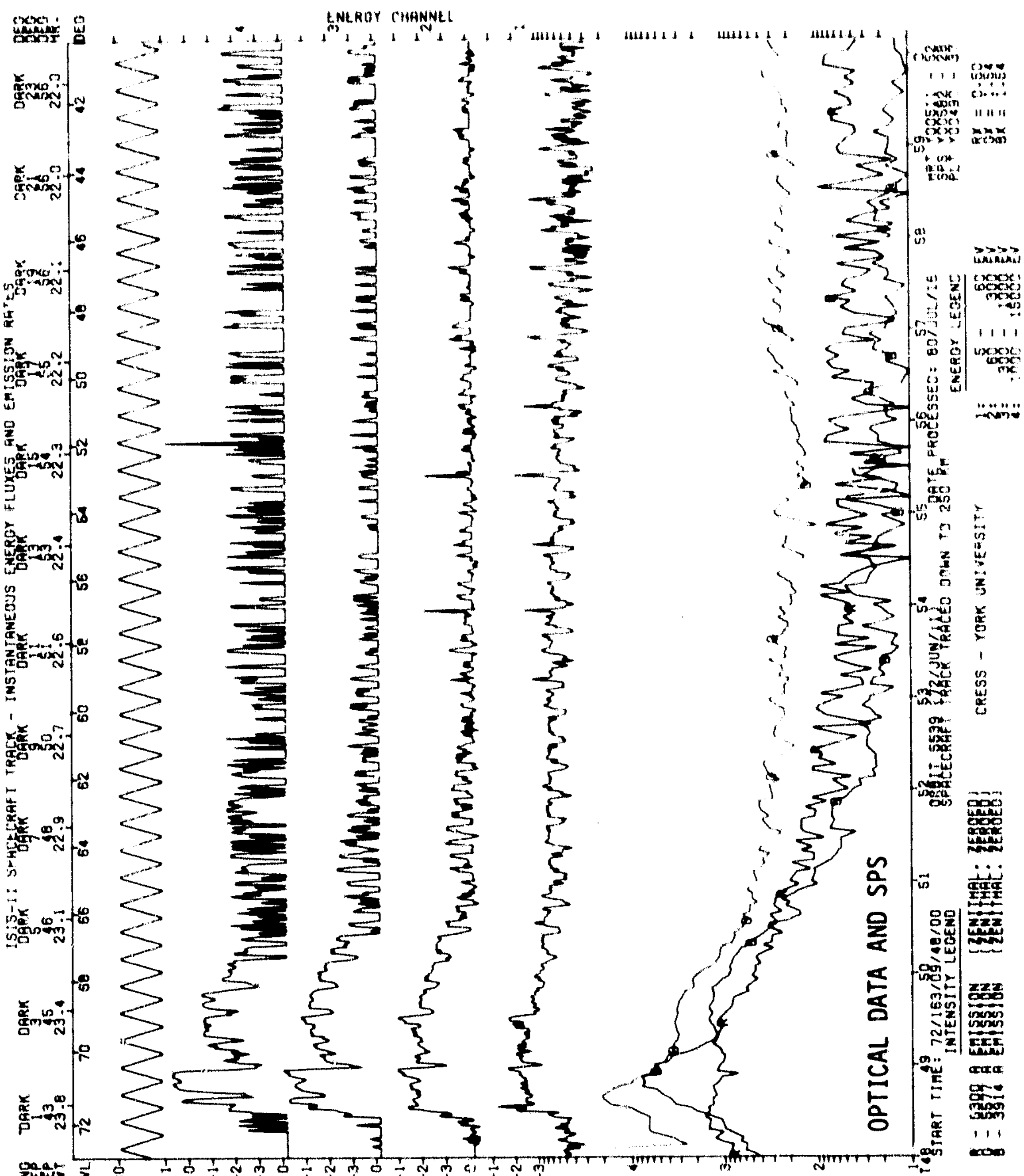

SET 31, FORMAT 1

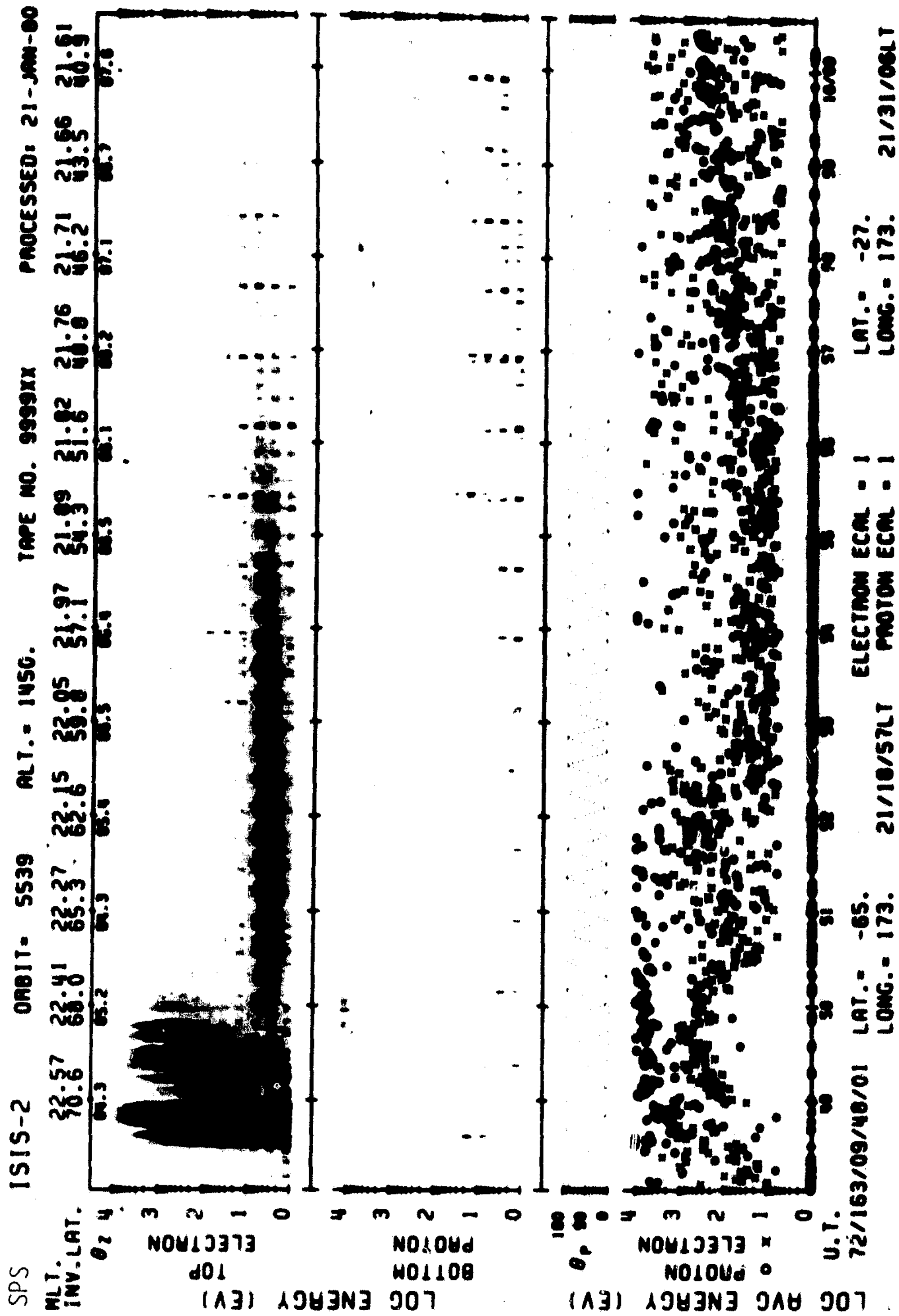

SET 31, FORMAT 6

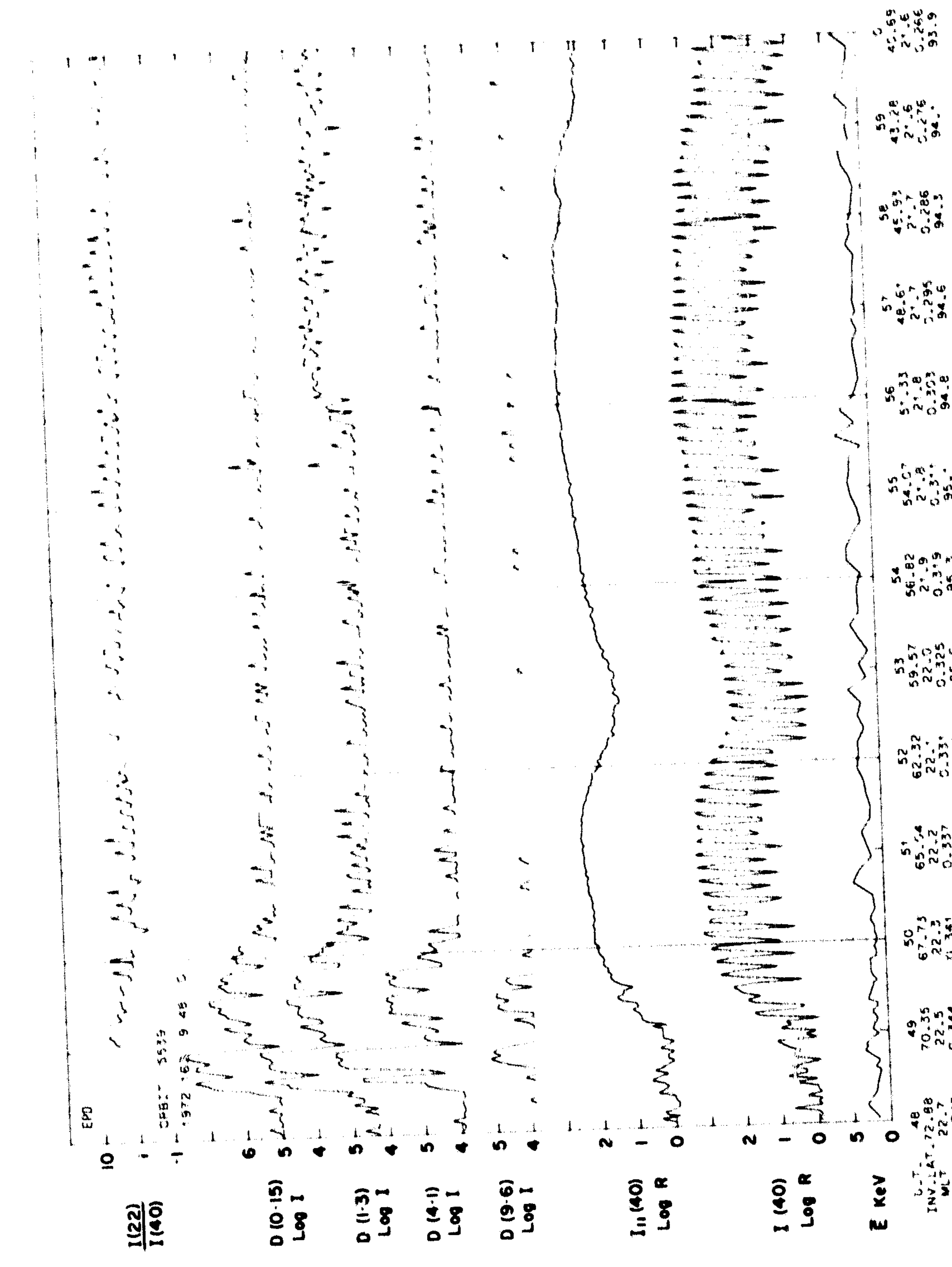

SET 31, FORMAT 3

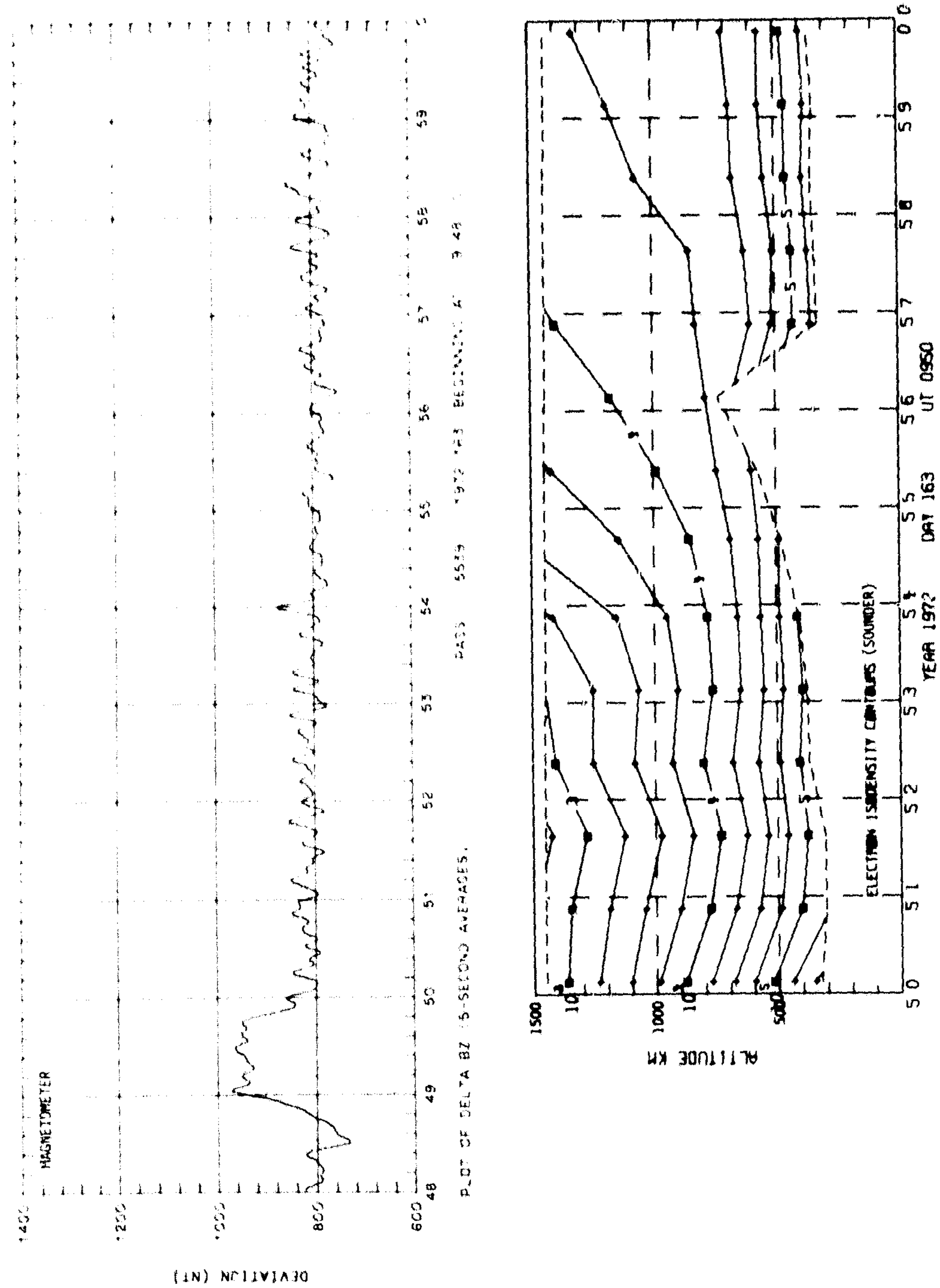

SET 31, FORMAT 2

ORBIT 5539
DATE 720611
DAY 163

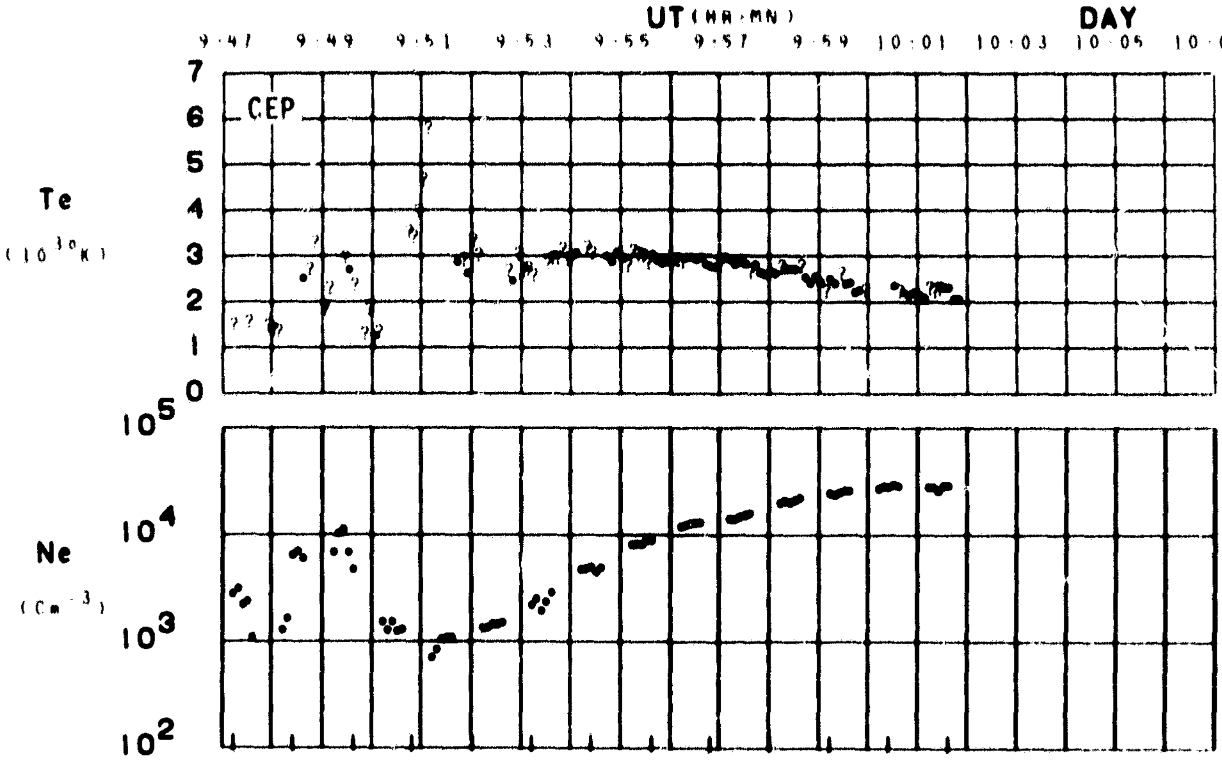

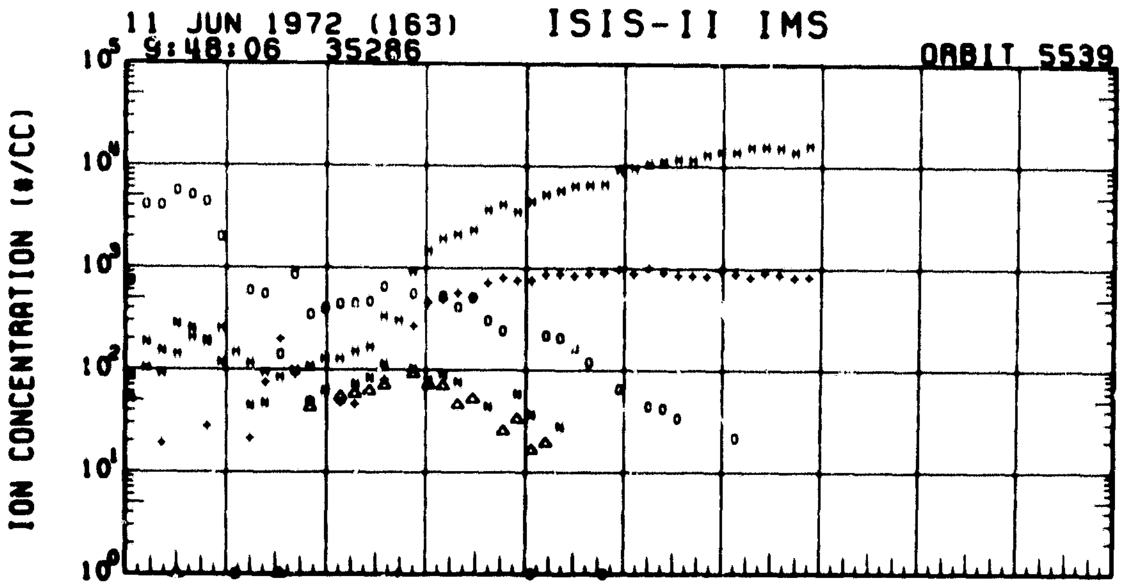

1 - H
4 - +
8 - Δ
14 - N
16 - O

UT	9:50	9:52	9:54	9:56	9:58	10:00
LAST	21:23	21:25	21:27	21:29	21:30	21:31
MLT	22:24	22:08	21:58	21:49	21:42	21:37
DLAT	-68	-61	-54	-47	-40	-34
INVL	68	62	57	51	46	41
GLAT	-58	-52	-46	-39	-33	-27
GLNG	173	173	173	173	173	173
SZEN	135	138	141	144	146	146
ALT	1448	1447	1445	1443	1440	1436

SET 31, FORMAT 4

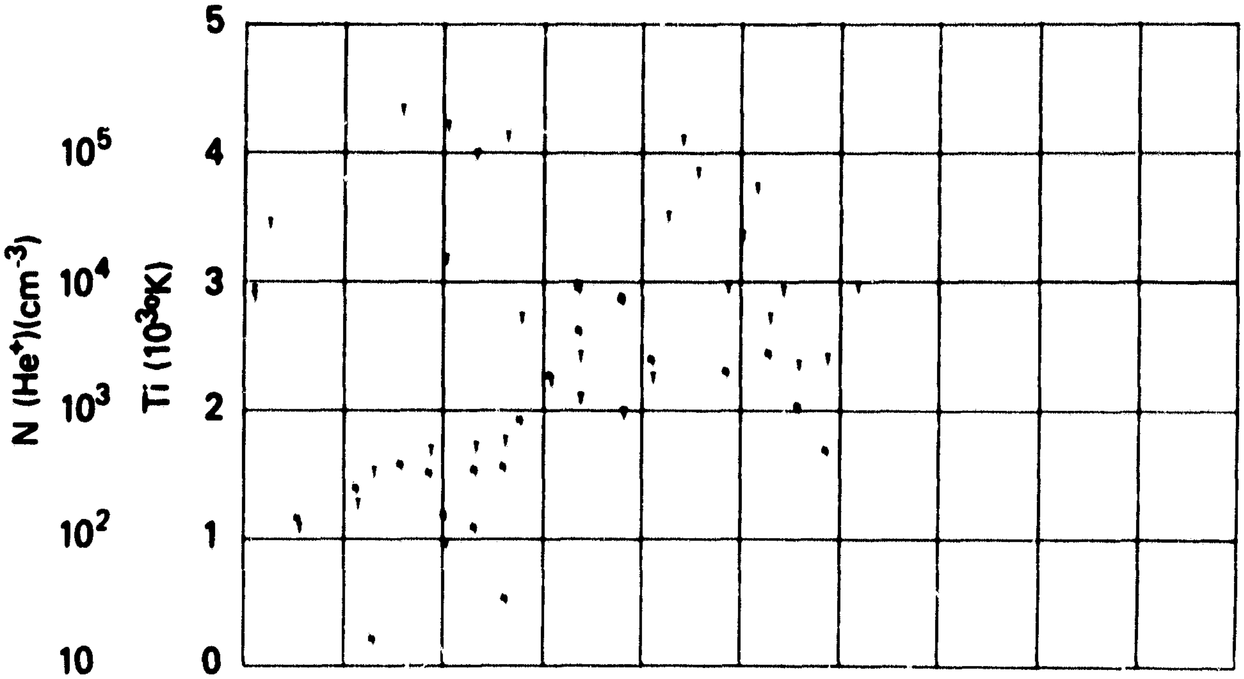

UT	9:50	9:52	9:54	9:56	9:58	10:00
LAST	21:23	21:25	21:27	21:28	21:30	21:31
MLT	22:24	22:08	21:58	21:49	21:42	21:37
DLAT	-68	-61	-54	-47	-40	-34
INVL	68	62	57	51	46	41
GLAT	-58	-52	-46	-39	-33	-27
GLNG	173	173	173	173	173	173
SZEN	135	138	141	144	146	146
ALT	1449	1447	1445	1443	1440	1436

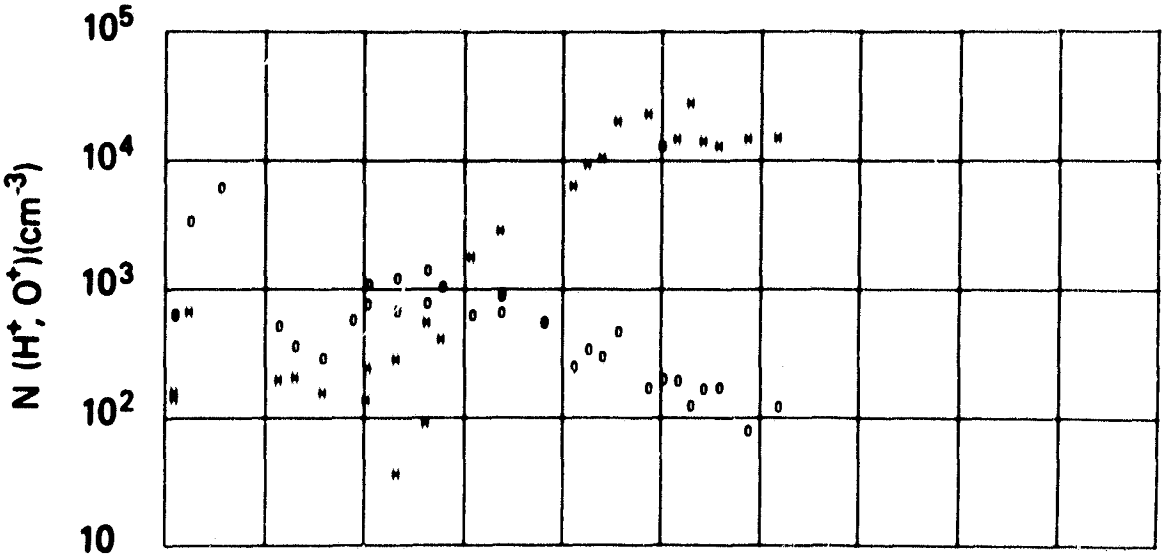

SET 31, FORMAT 5

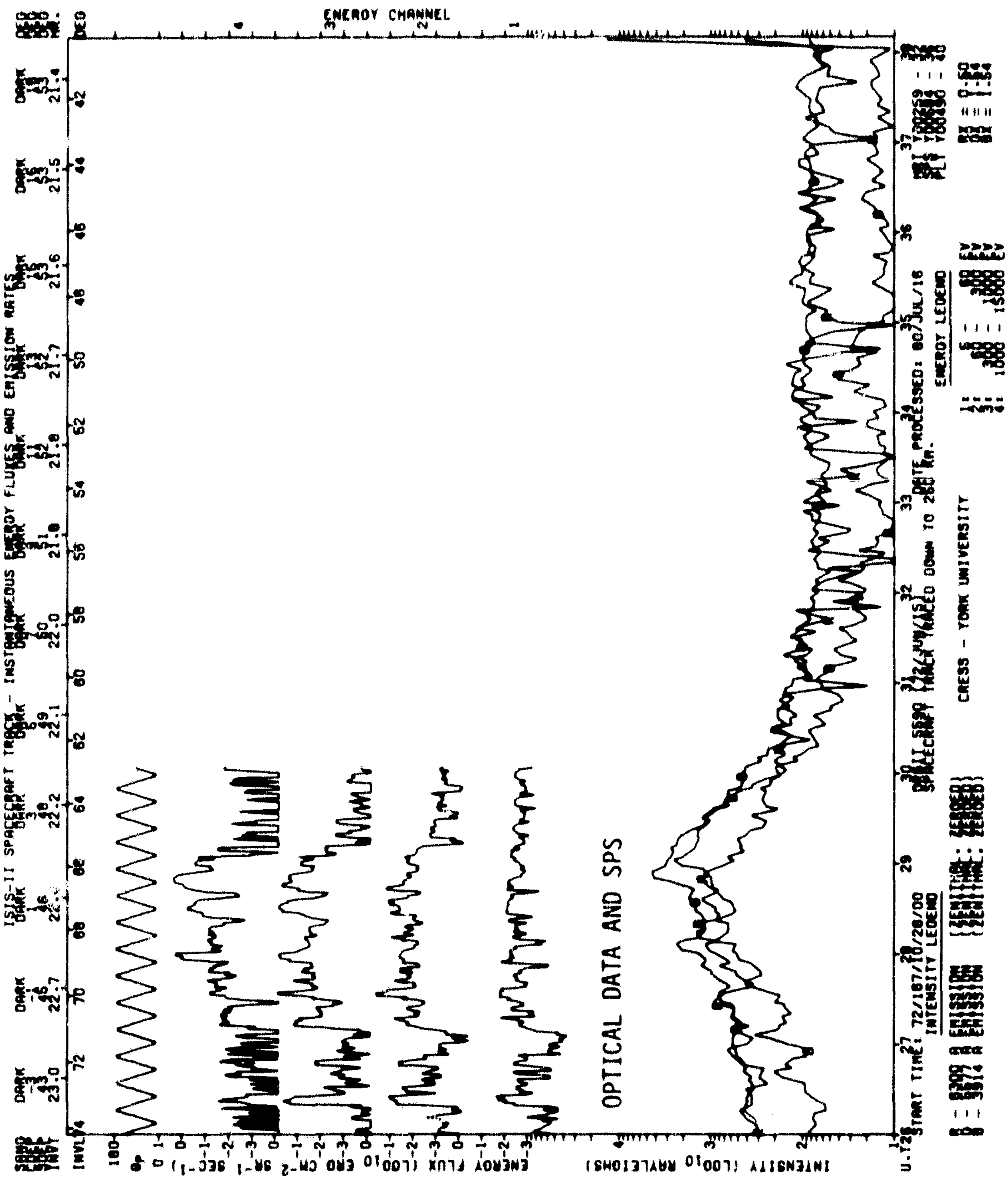

SET 32, FORMAT 1

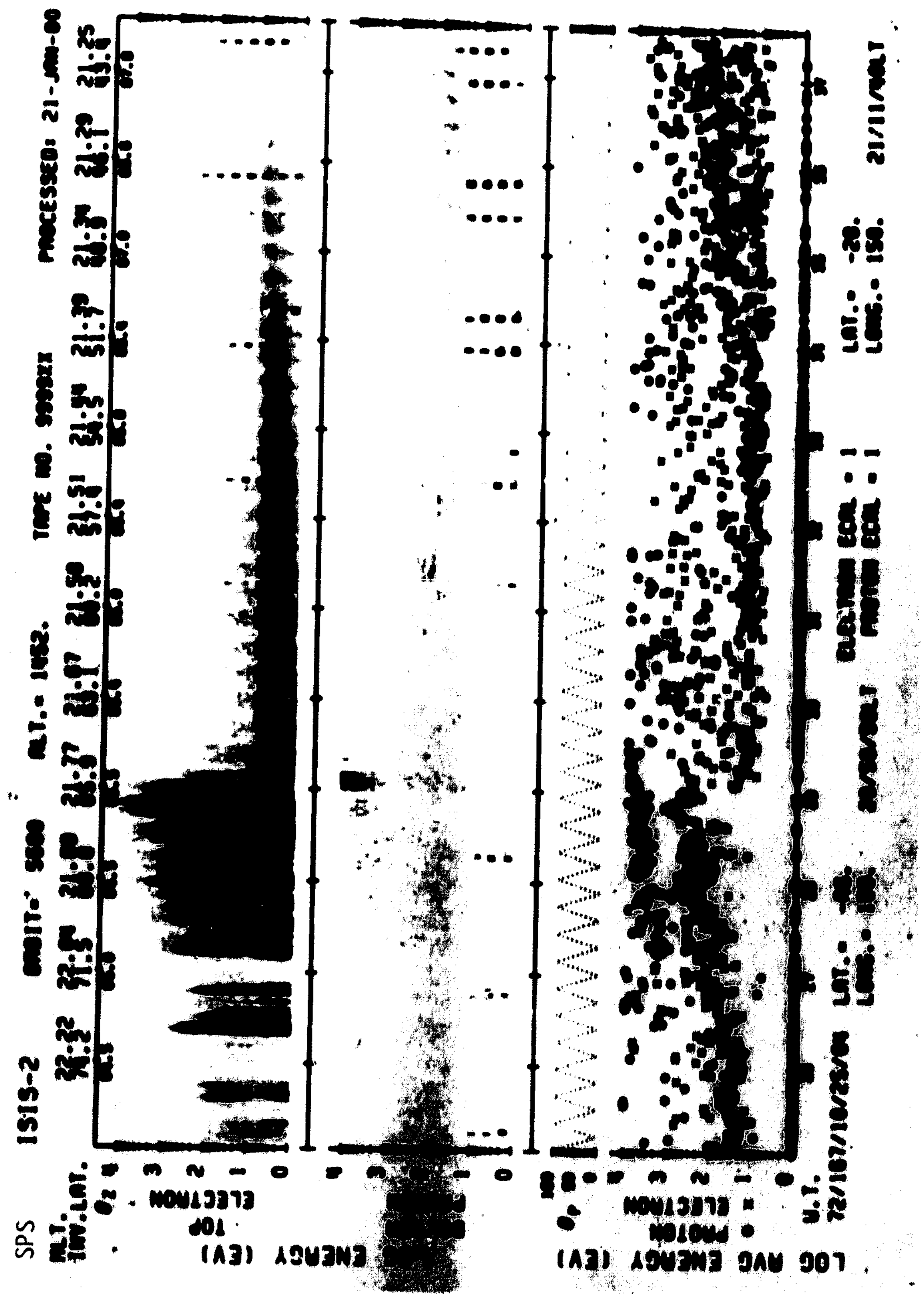

SET 32, FORMAT 6

ORIGINAL PAGE IS
OF POOR QUALITY

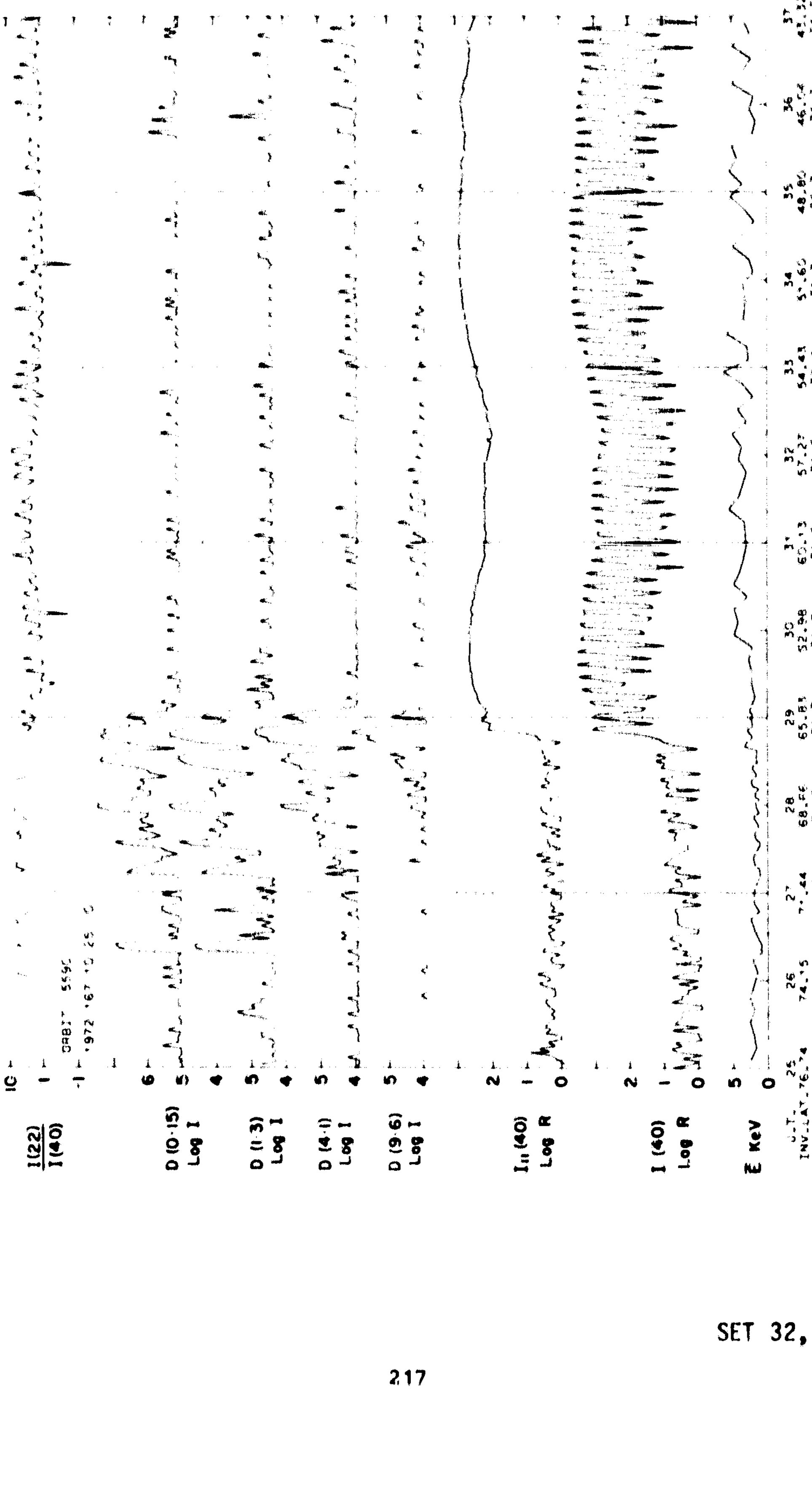

SET 32, FORMAT 3

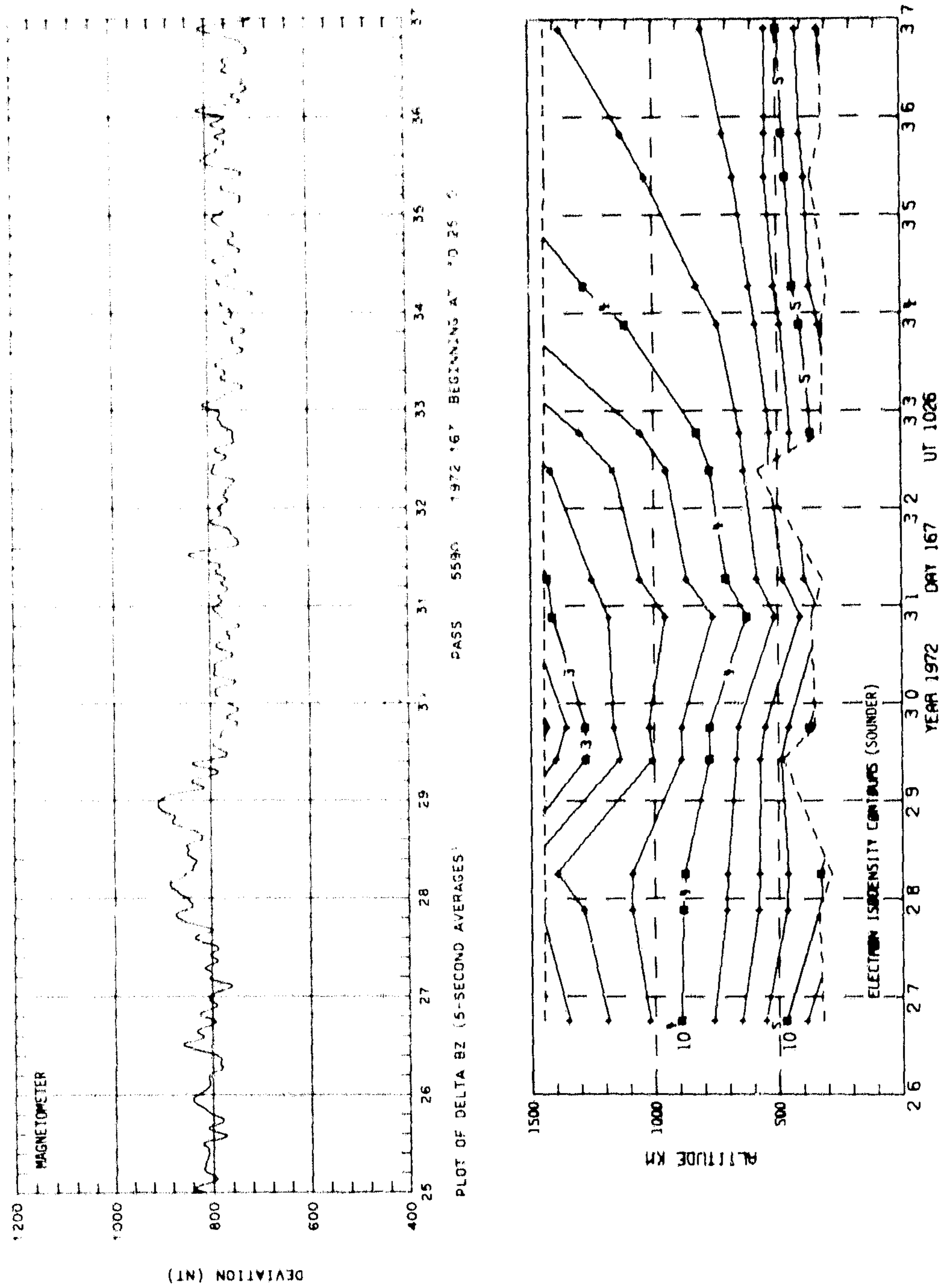

SET 32, FORMAT 2

ORBIT 5590
DATE 720615
DAY 167

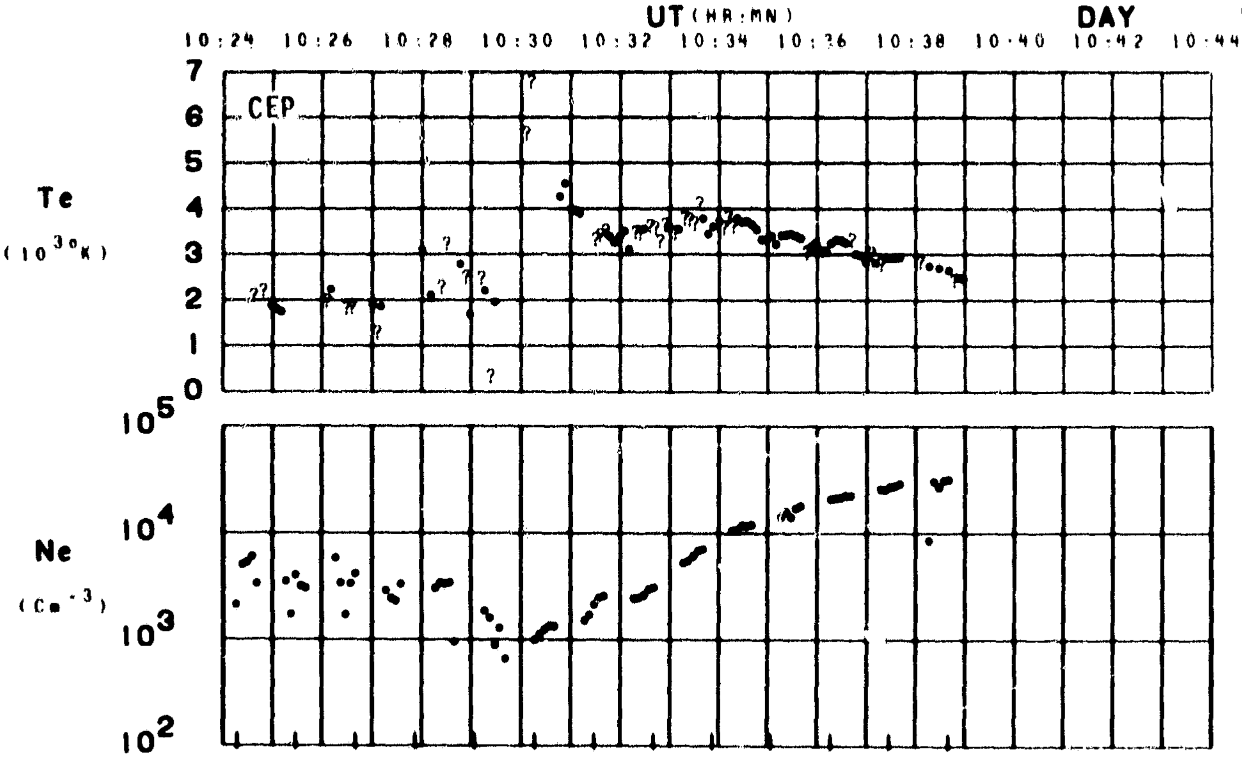

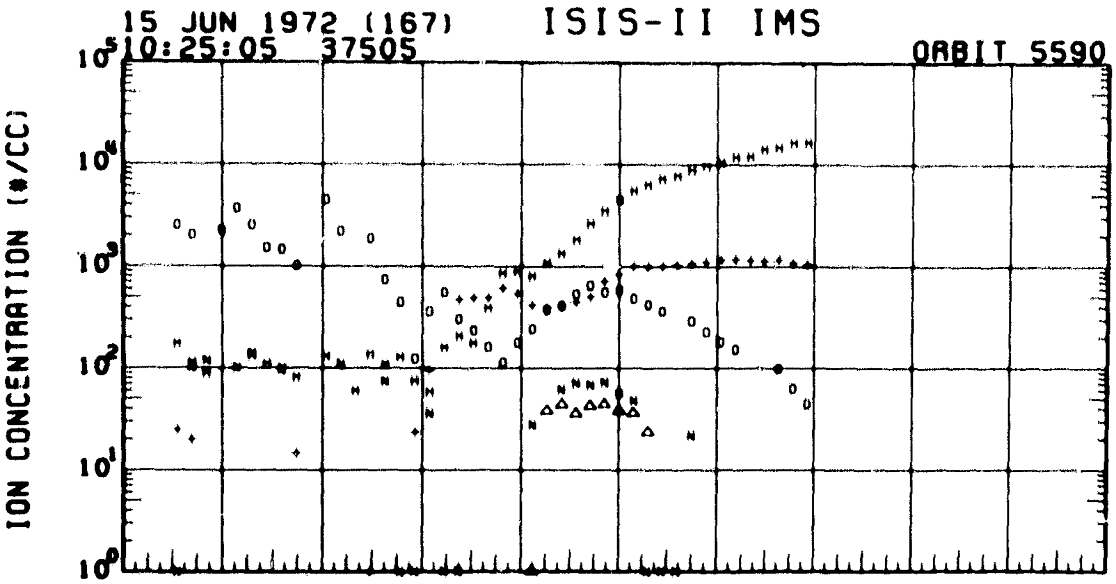

1 - H	UT	10:26	10:28	10:30	10:32	10:34	10:36
4 - +	LAST	21:01	21:04	21:07	21:08	21:10	21:11
8 - Δ	ALT	22:13	21:53	21:40	21:30	21:23	21:17
14 - N	DLAT	-77	-70	-63	-56	-48	-41
16 - O	INVL	74	68	63	57	52	46
	GLAT	-62	-56	-50	-44	-37	-31
	GLNG	159	159	159	159	159	158
	SZEN	130	134	137	139	141	142
	ALT	1451	1448	1447	1444	1441	1437

SET 32, FORMAT 4

RPA

720615

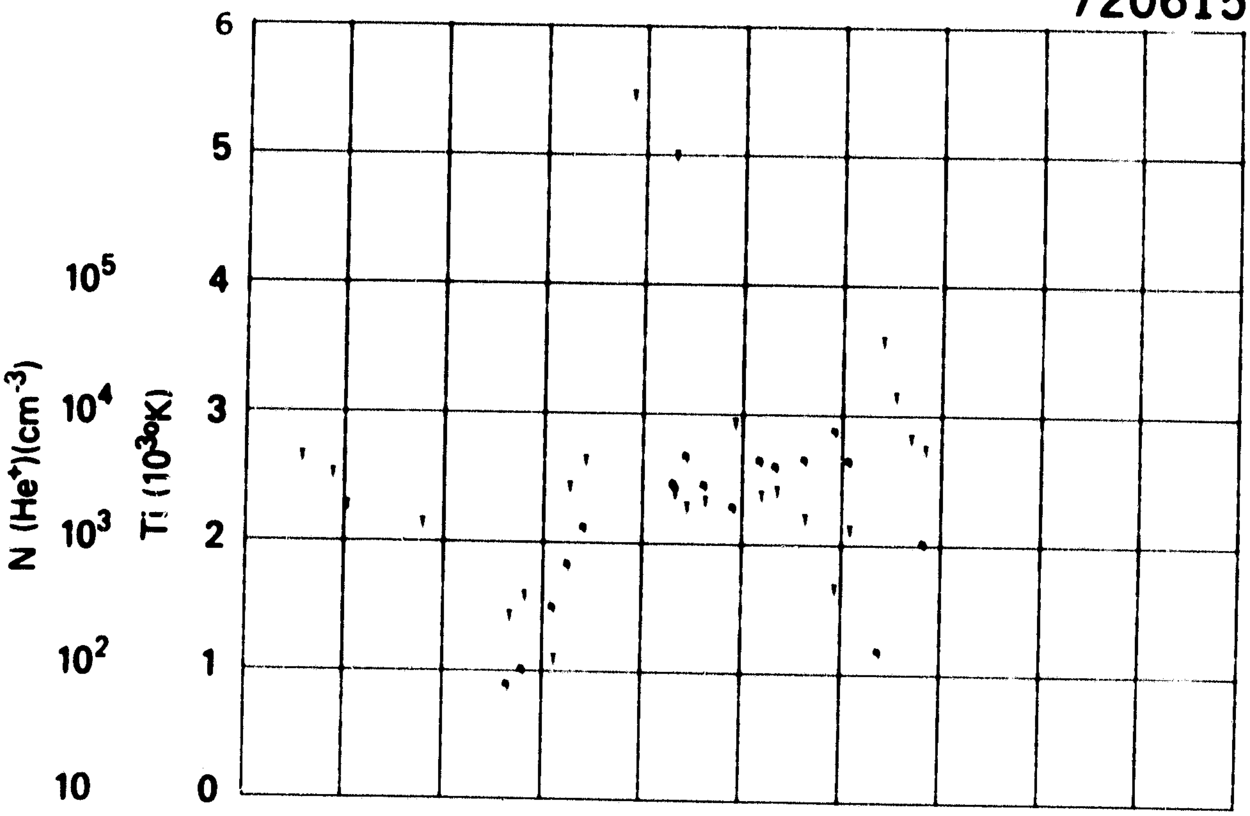

UT	10:26	10:28	10:30	10:32	10:34	10:36
LAST	21:01	21:04	21:07	21:08	21:10	21:11
MLT	22:13	21:53	21:40	21:30	21:23	21:17
DLAT	-77	-70	-63	-56	-48	-41
INV.	74	68	63	57	52	46
GLAT	-62	56	50	-44	-37	-31
GLNG	159	159	159	159	159	159
SZEN	130	134	137	139	141	142
ALT	1451	1449	1447	1444	1441	1437

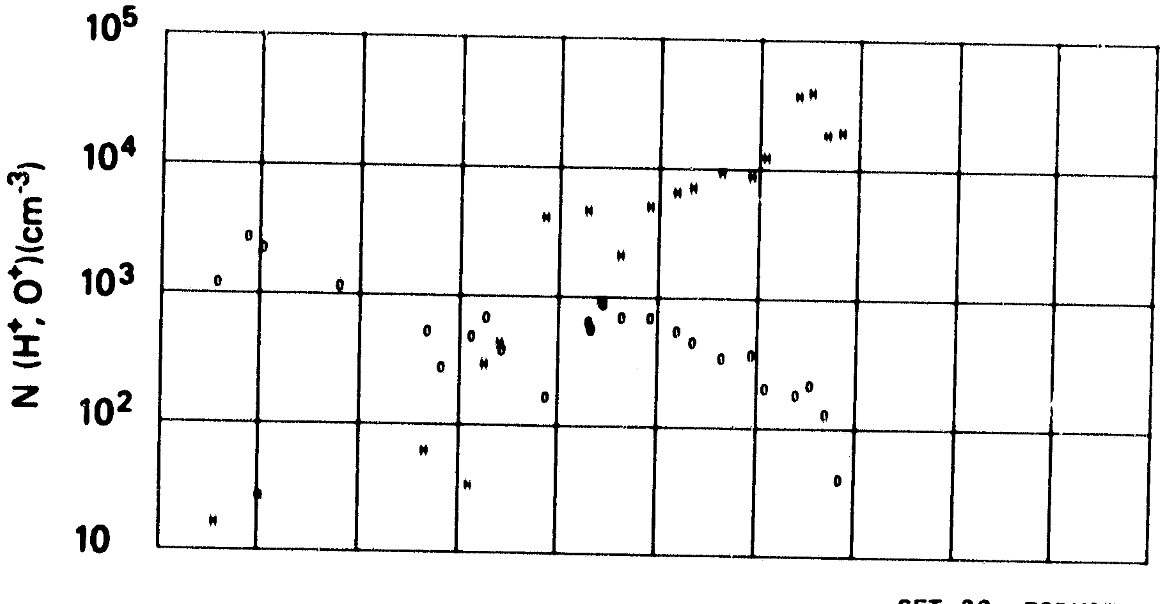

SET 32, FORMAT 5

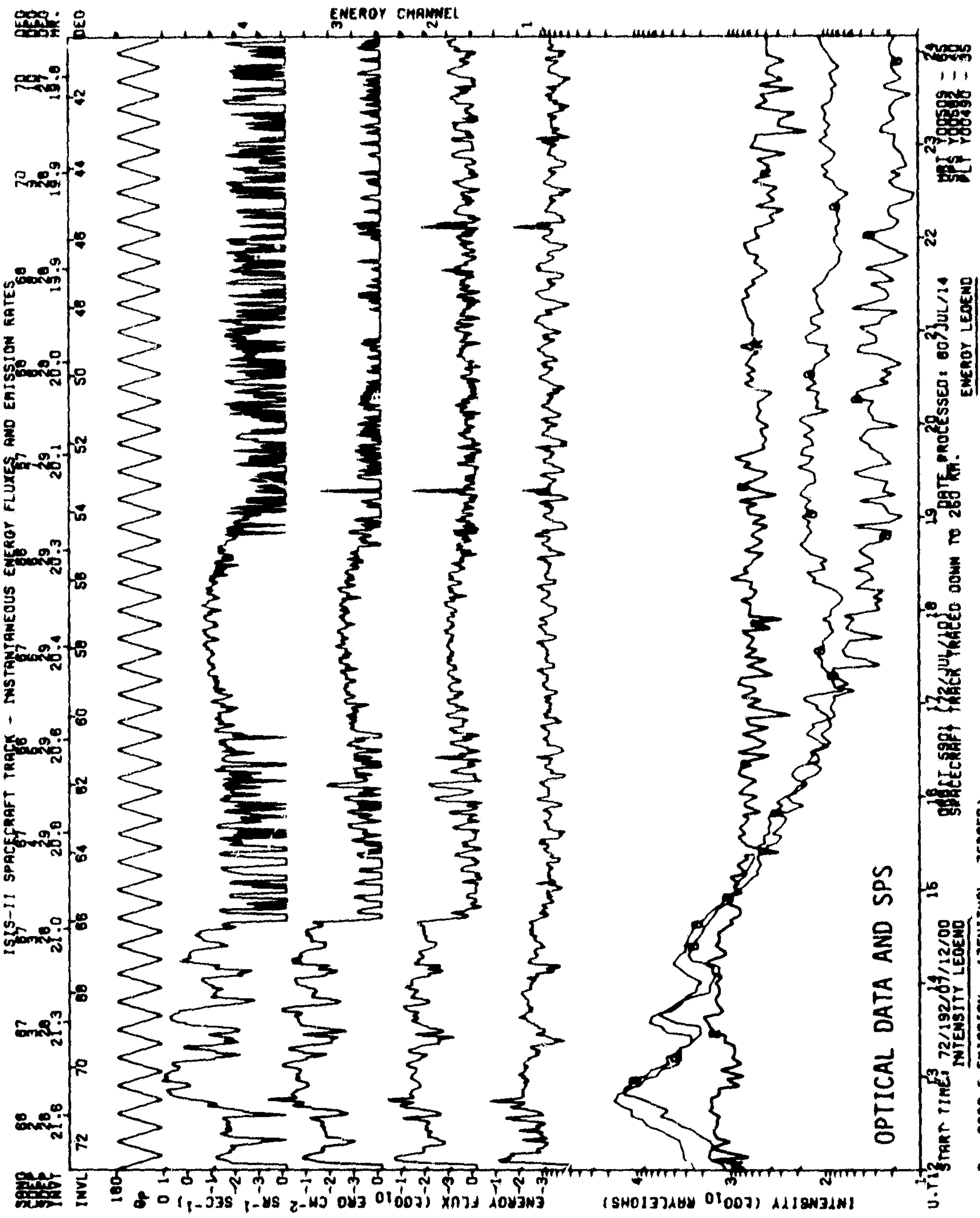

SET 33, FORMAT 1

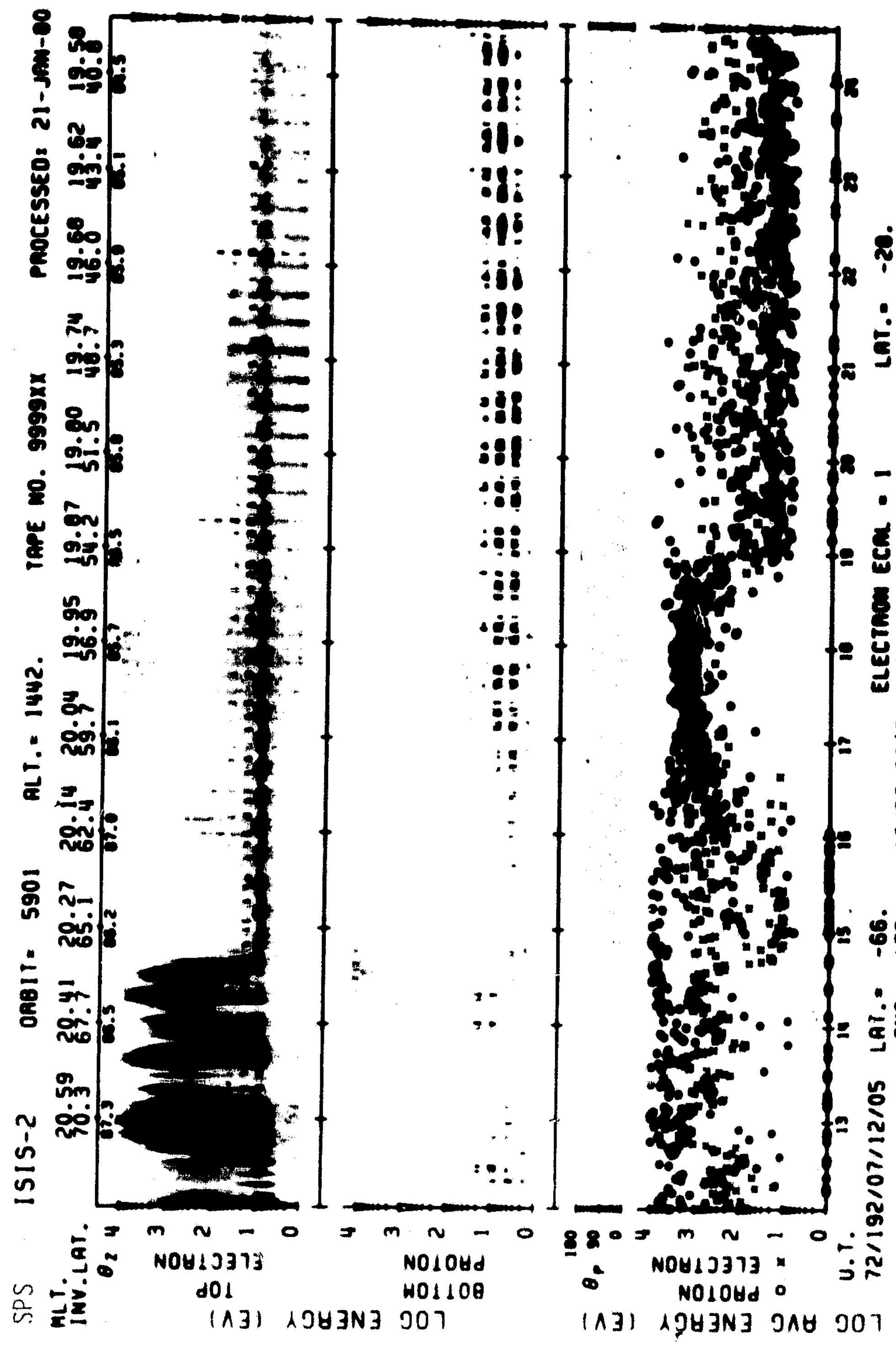

SET 33, FORMAT 6

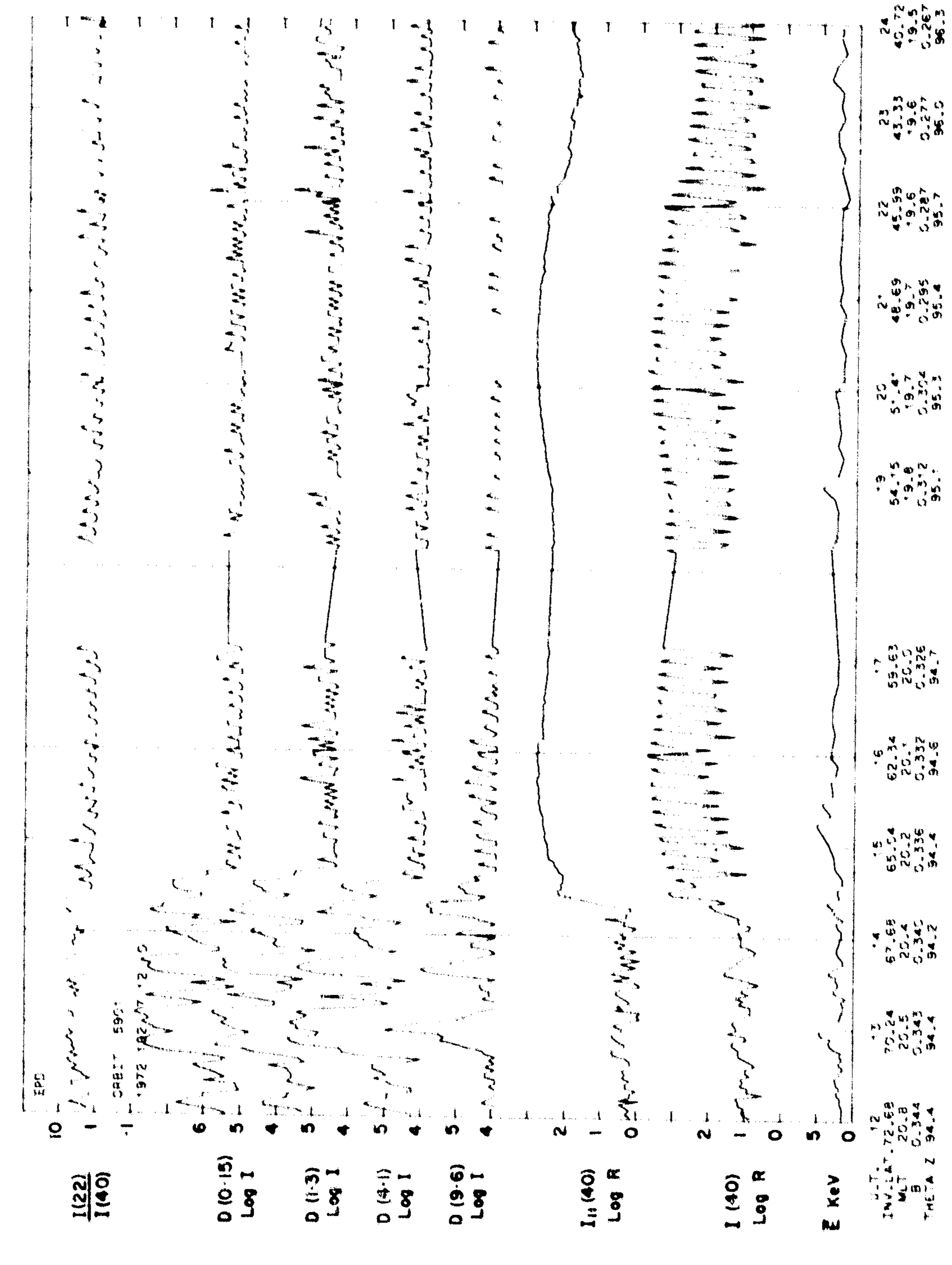

SET 33, FORMAT 3

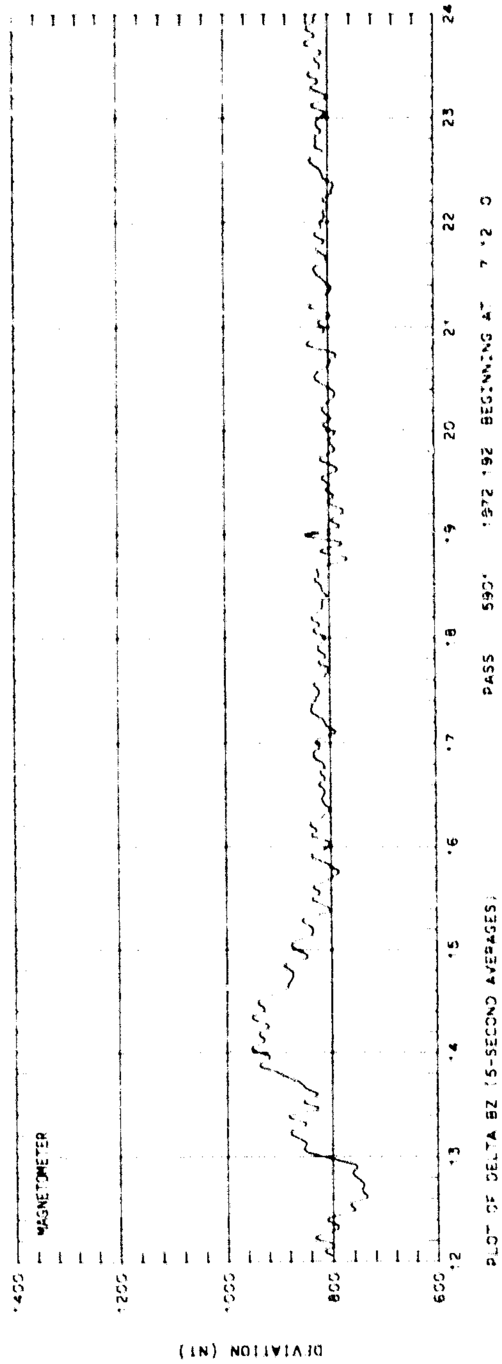

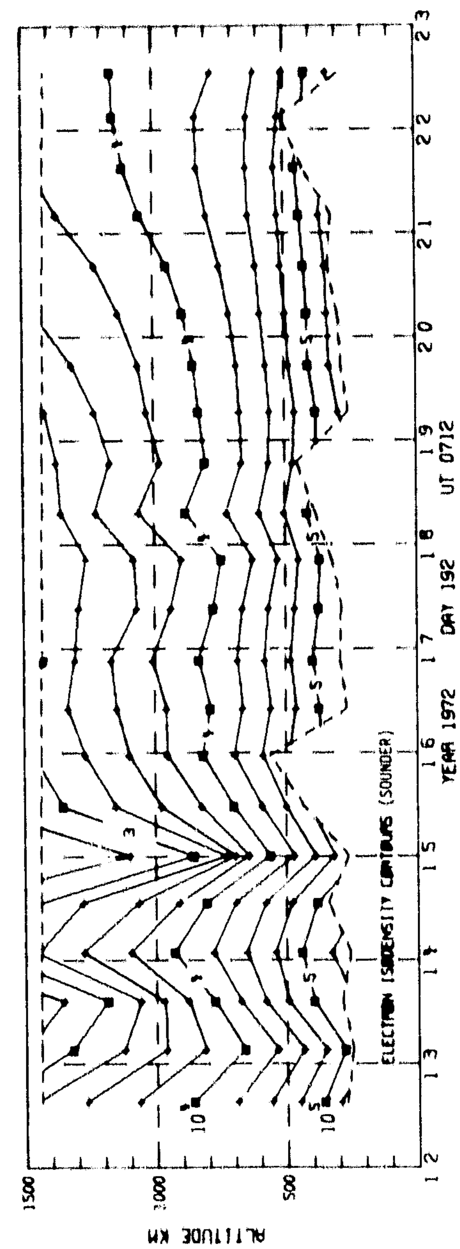

SET 33, FORMAT 2

ORBIT 5901
DATE 720710
DAY 192

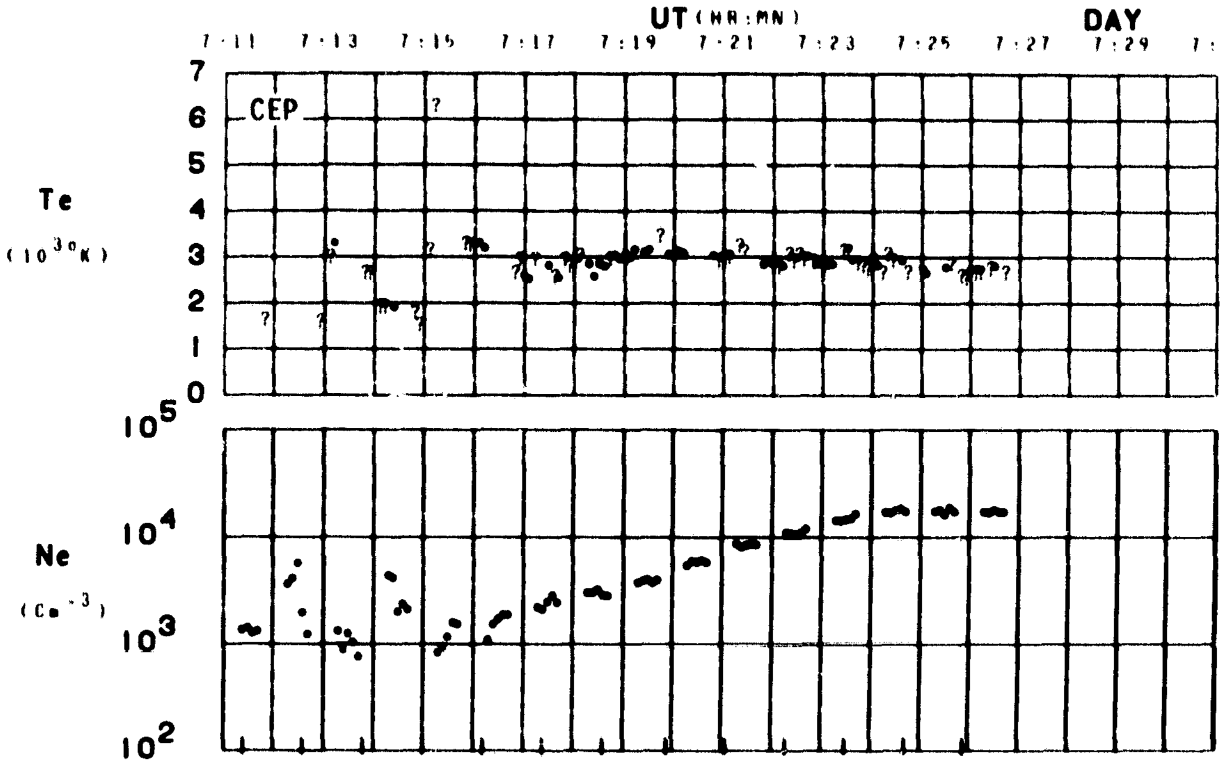

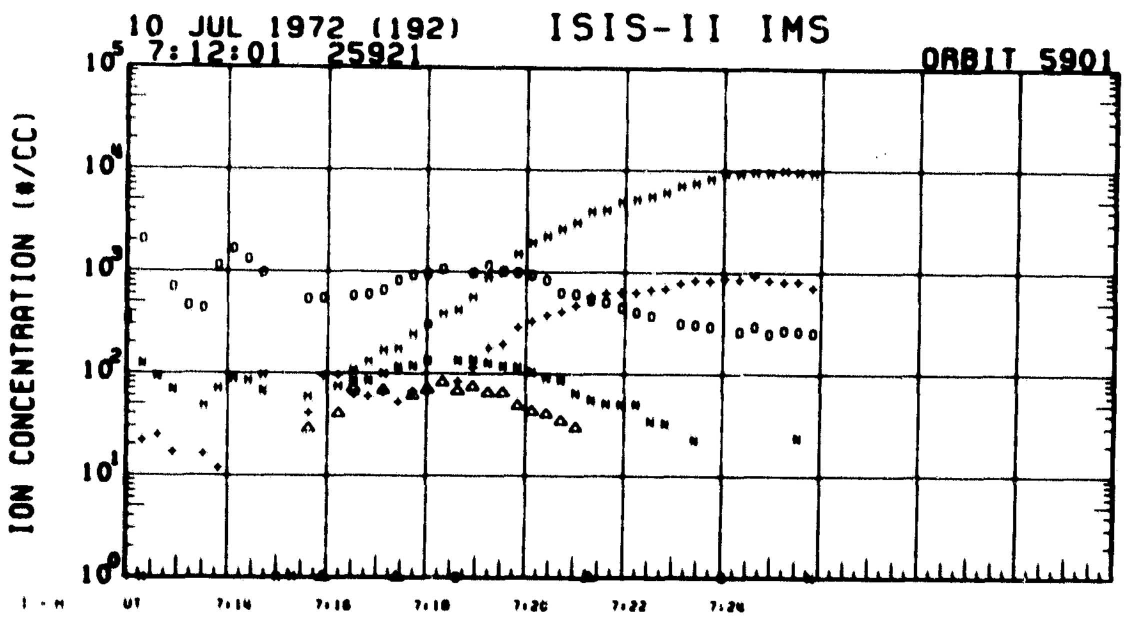

1 - H	UT	7:14	7:16	7:18	7:20	7:22	7:24
4 - +	LAST	19:04	19:07	19:09	19:10	19:12	19:13
8 - △	MLT	20:25	20:09	19:57	19:40	19:41	19:34
14 - N	DLAT	-67	-61	-54	-47	-40	-34
16 - O	INVL	68	62	57	51	46	41
	GLAT	-60	-53	-47	-41	-34	-28
	GLNG	179	179	179	179	179	179
	SZEN	117	118	118	117	117	116
	ALT	1437	1431	1425	1419	1413	1408

SET 33, FORMAT 4

Note different temperature scale

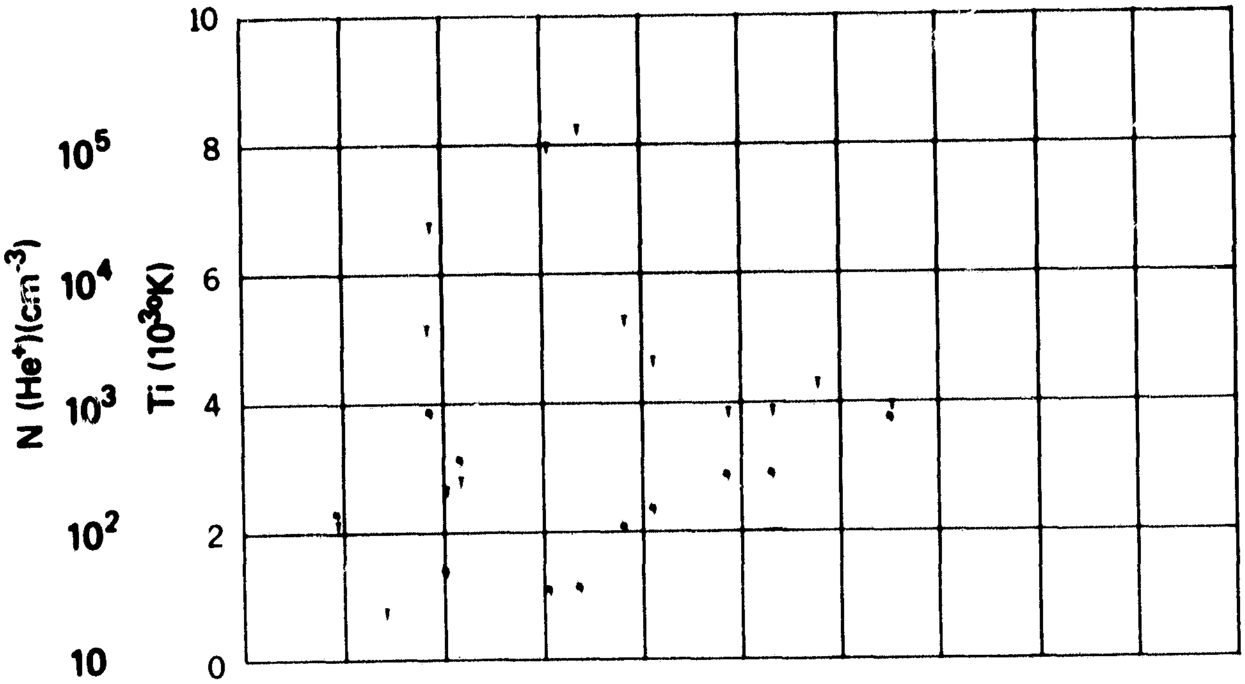

UT	7:14	7:16	7:18	7:20	7:22	7:24
LAST	19:04	19:07	19:09	19:10	19:12	19:13
MLT	20:25	20:09	19:57	19:48	19:41	19:34
DLAT	-67	-61	-54	-47	-40	-34
INVL	68	62	57	51	46	41
GLAT	-60	-53	-47	-41	-34	-28
GLNG	179	179	179	179	179	179
SZEN	117	118	118	117	117	116
ALT	1437	1431	1425	1419	1413	1408

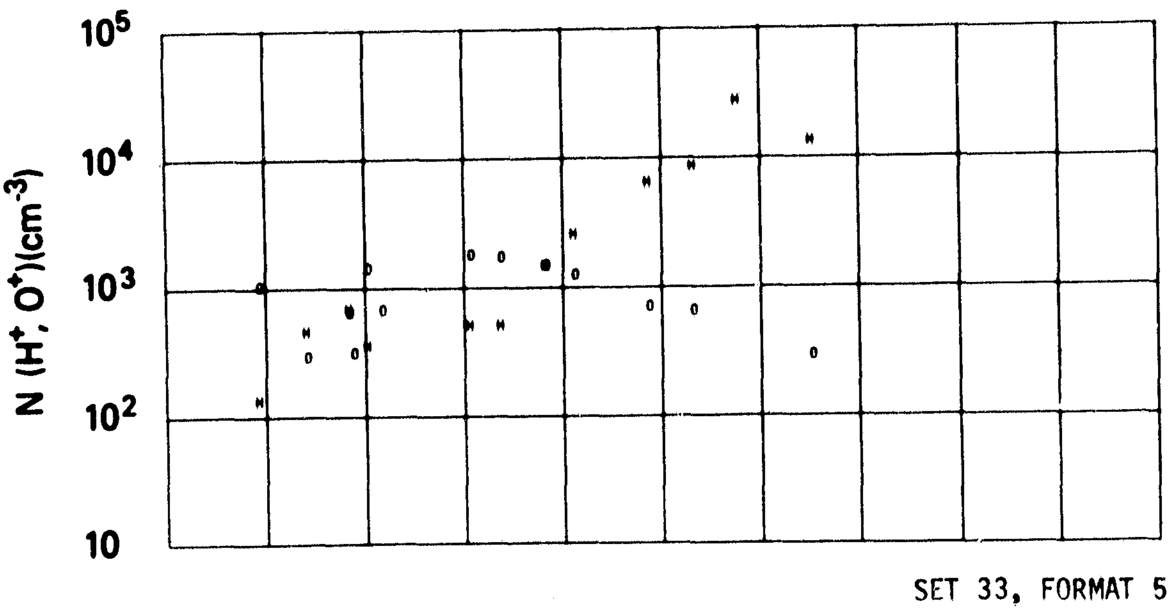

SET 33, FORMAT 5

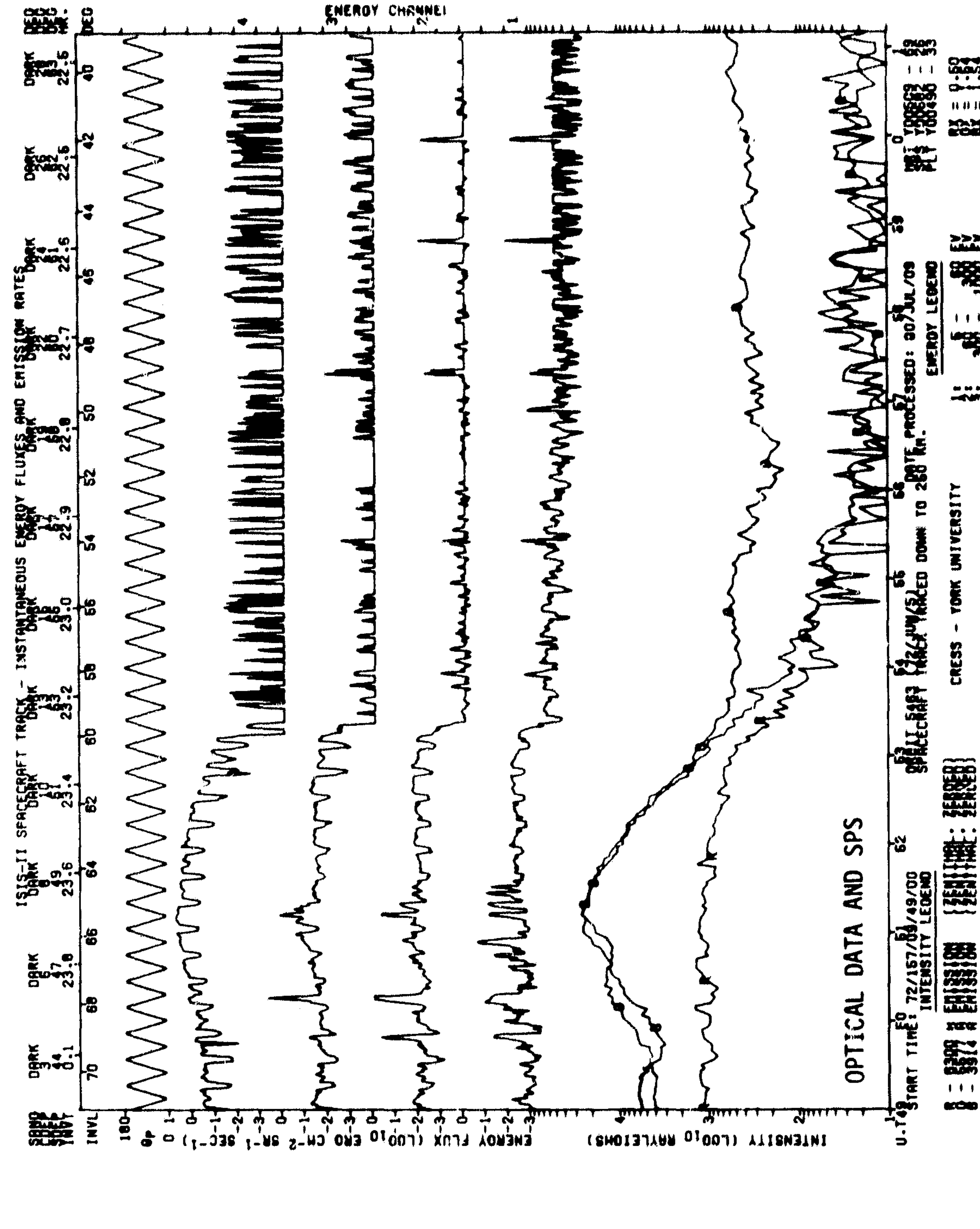

SET 34, FORMAT 1

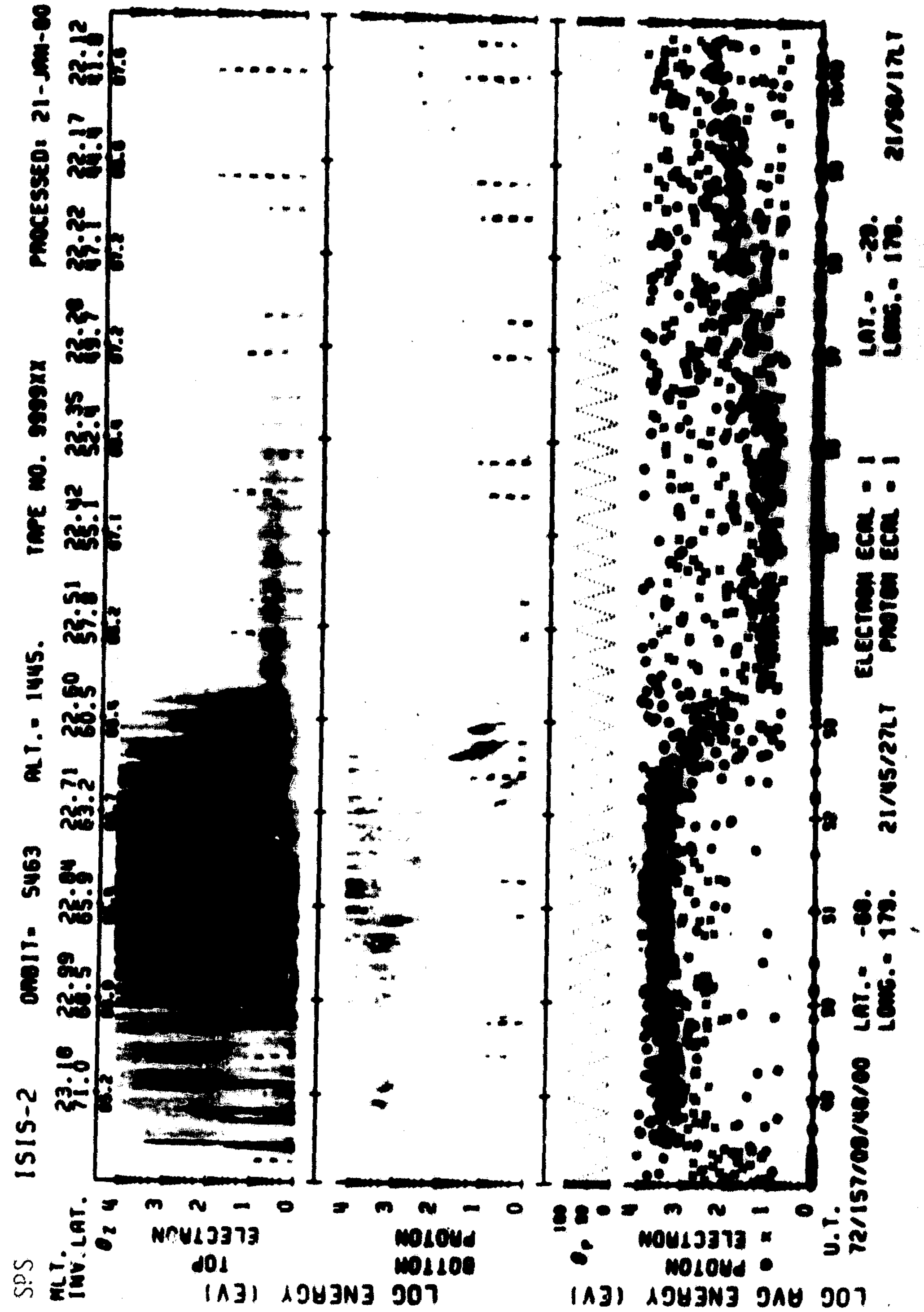

SET 34, FORMAT 6

ORIGINAL PAGE IS
OF POOR QUALITY

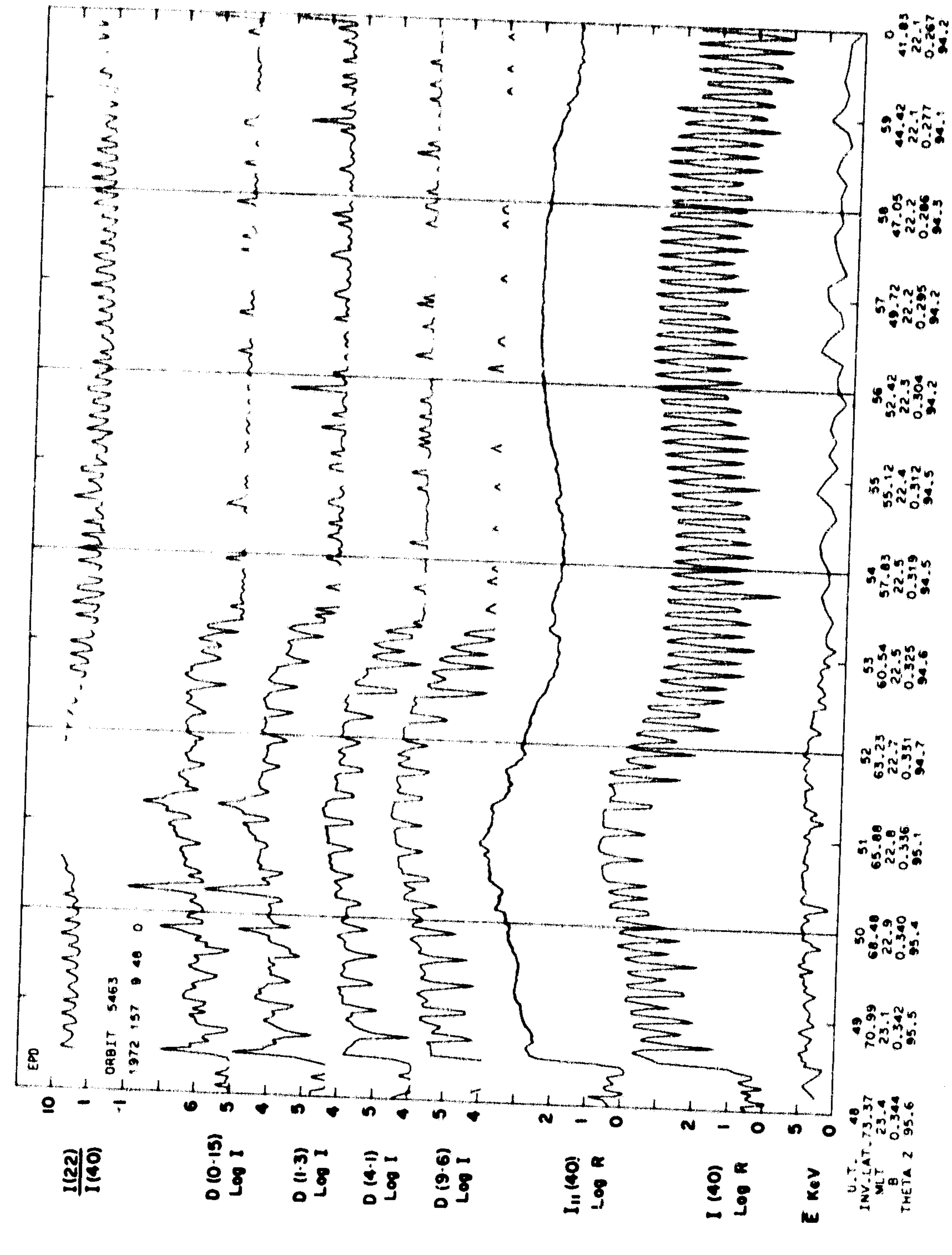

SET 34, FORMAT 3

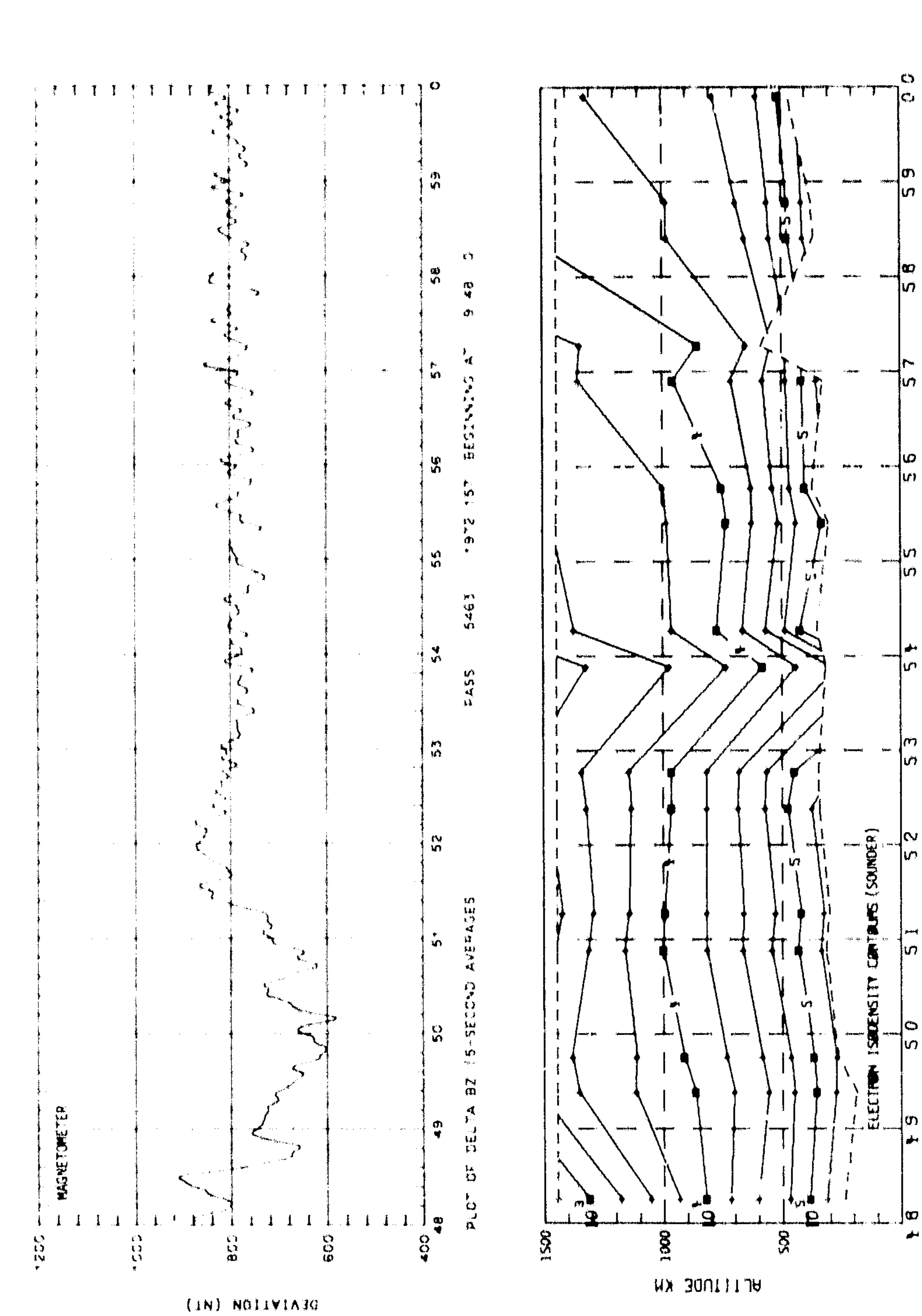

SET 34, FORMAT 2

ORBIT 5463
DATE 720605
DAY 157

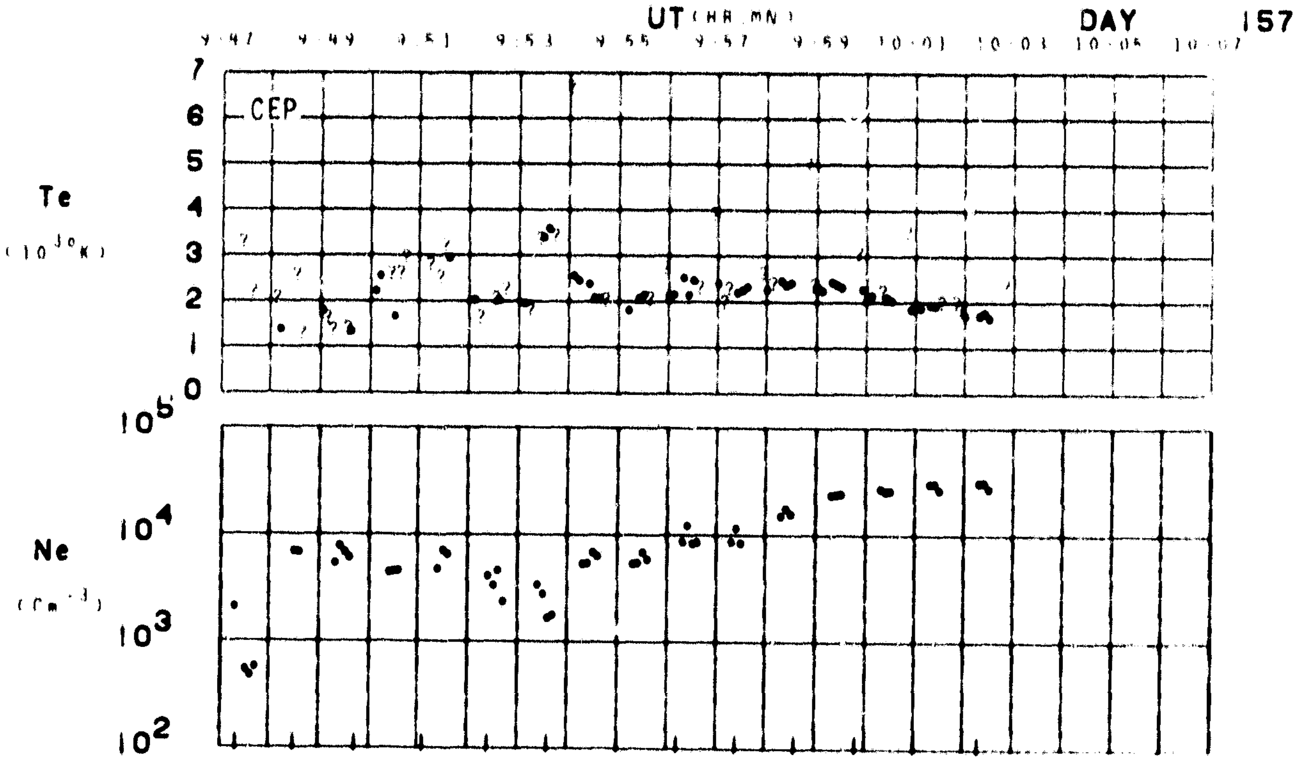

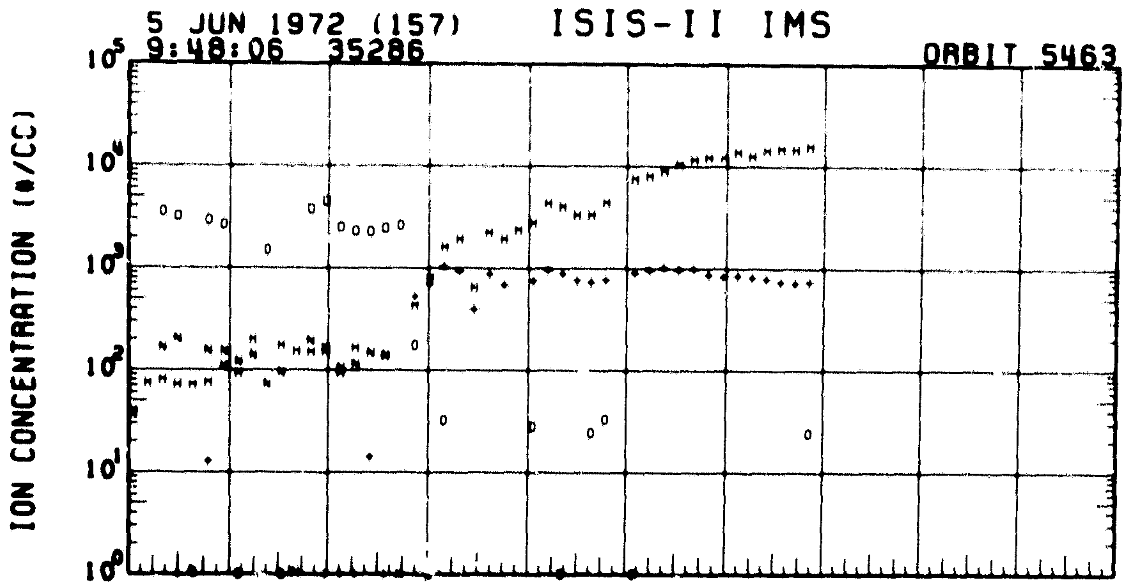

1 - H
4 - +
8 - △
14 - N
16 - O

UT	9:50	9:52	9:54	9:56	9:58	10:00
LAST	21:50	21:53	21:55	21:57	21:58	21:59
ALT	22:59	22:43	22:30	22:21	22:13	22:07
DLAT	-68	-62	-55	-48	-42	-35
INVL	68	63	58	52	47	42
GLAT	-61	-54	-48	-42	-36	-29
GLNG	180	180	180	180	180	179
SZEN	135	140	144	147	150	152
ALT	1445	1445	1444	1442	1440	1438

SET 34, FORMAT 4

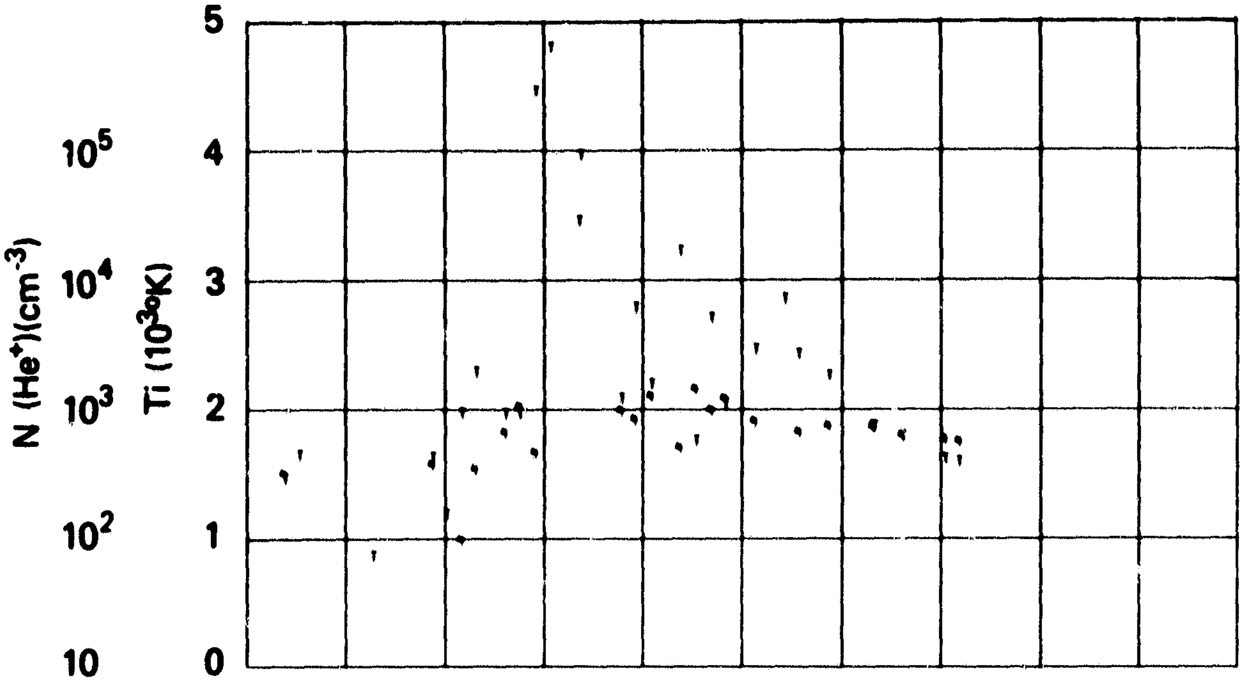

UT	9:50	9:52	9:54	9:56	9:58	10:00
LAST	21:50	21:53	21:55	21:57	21:58	21:58
MLT	22:59	22:43	22:30	22:21	22:13	22:07
DLAT	-60	-62	-55	-48	-42	-35
INVL	60	63	58	52	47	42
GLAT	-61	-54	-48	-42	-38	-28
GLNG	180	180	180	180	180	179
SZEN	135	140	144	147	150	152
ALT	1445	1445	1444	1442	1440	1438

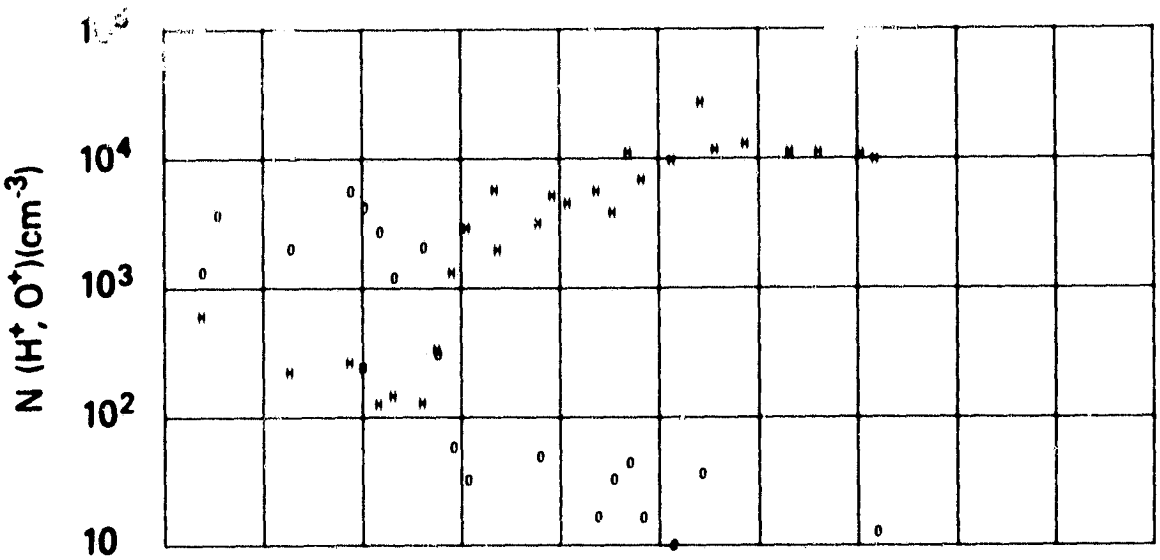

SET 34, FORMAT 5

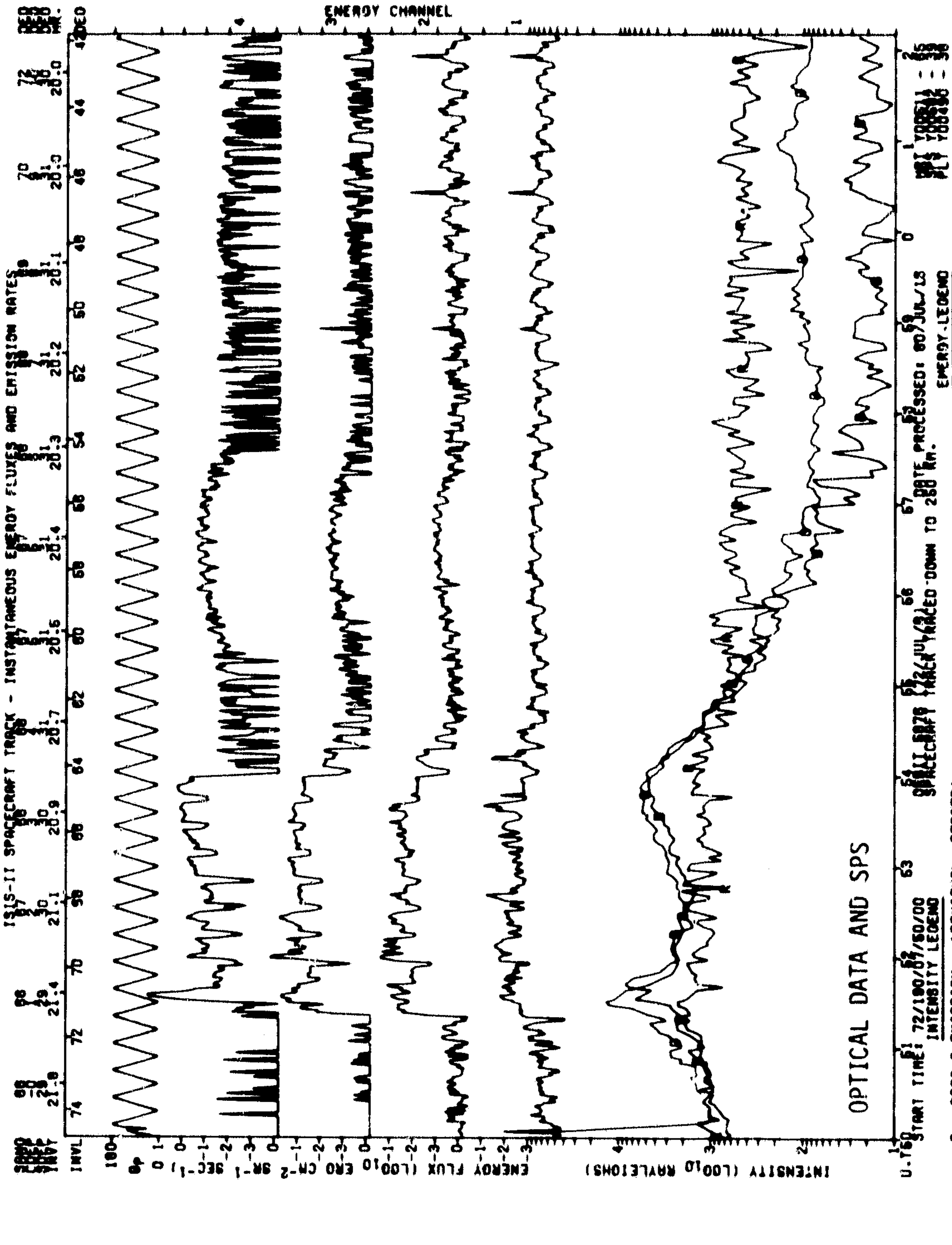

SET 35, FORMAT 1

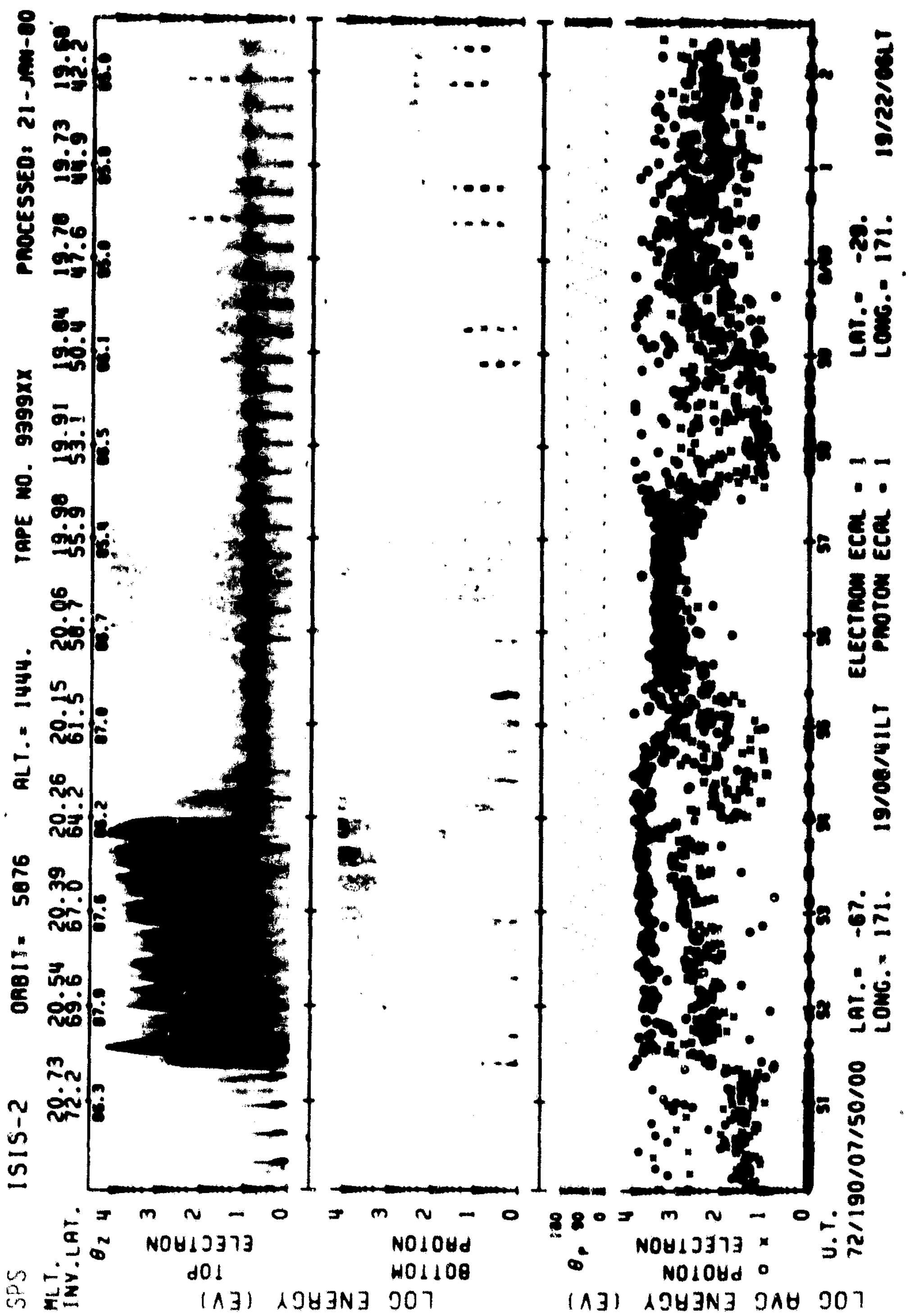

SET 35, FORMAT 6

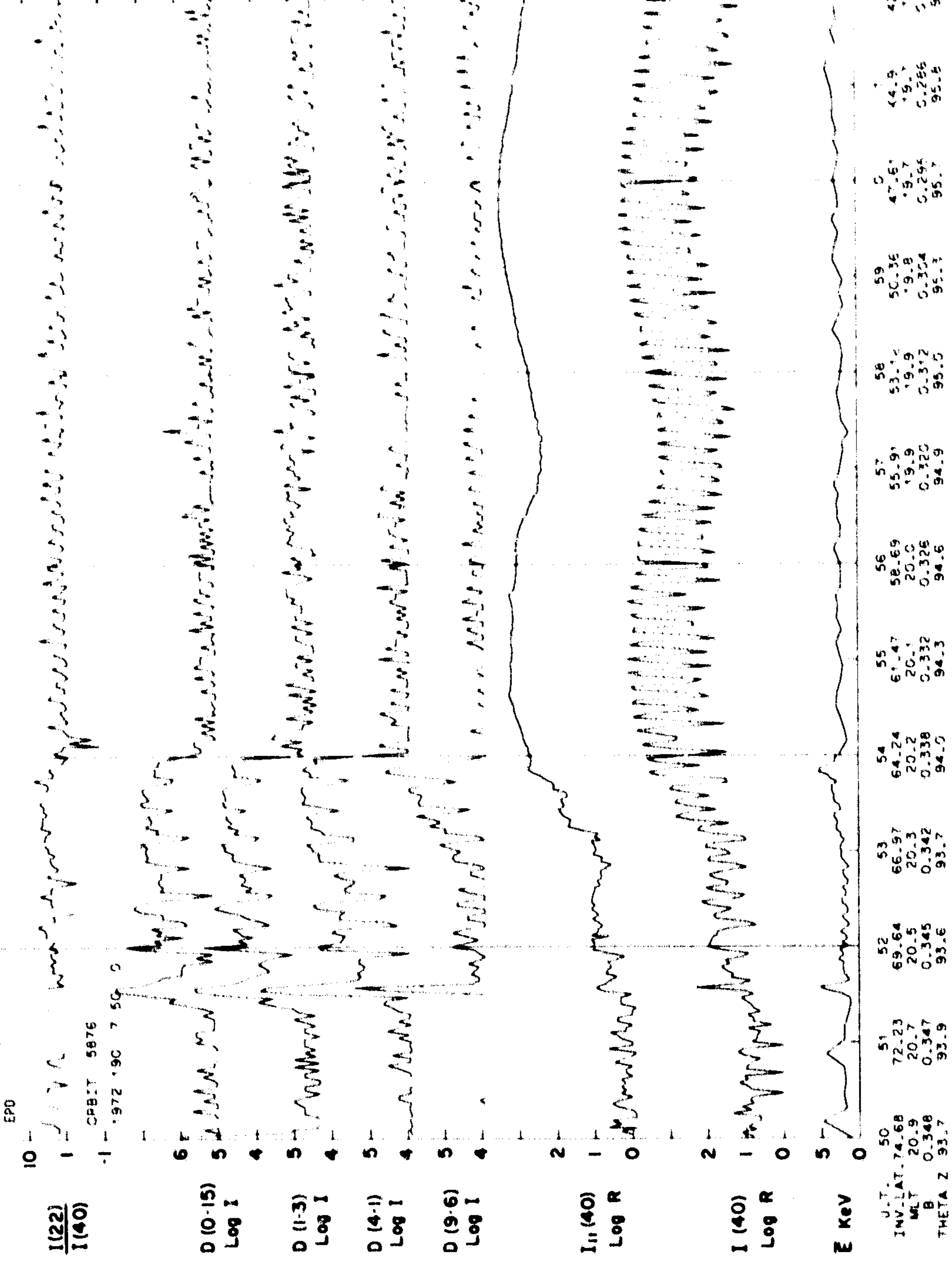

SET 35, FORMAT 3

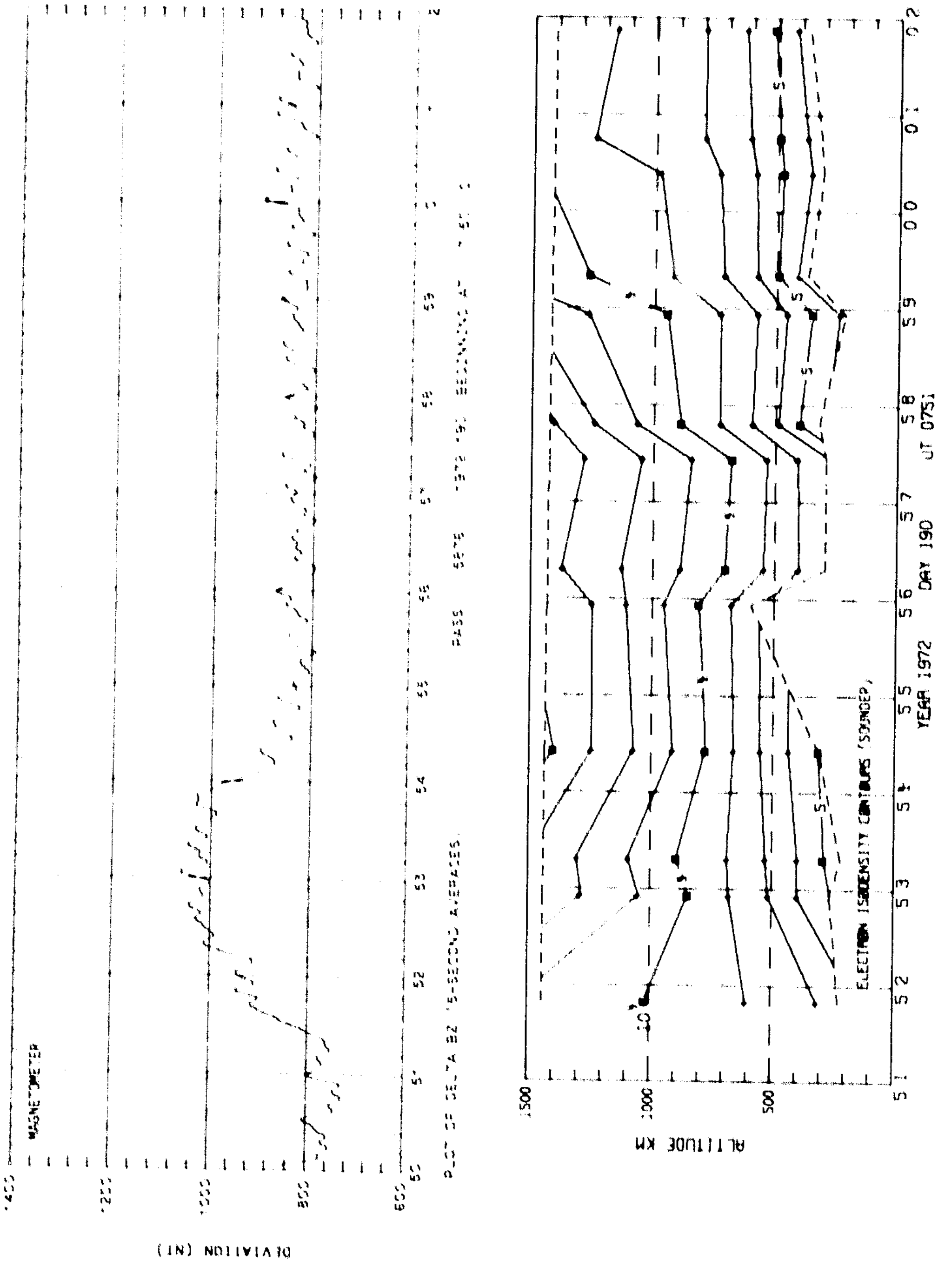

SET 35, FORMAT 2

ORBIT 5876
DATE 720708
DAY 190

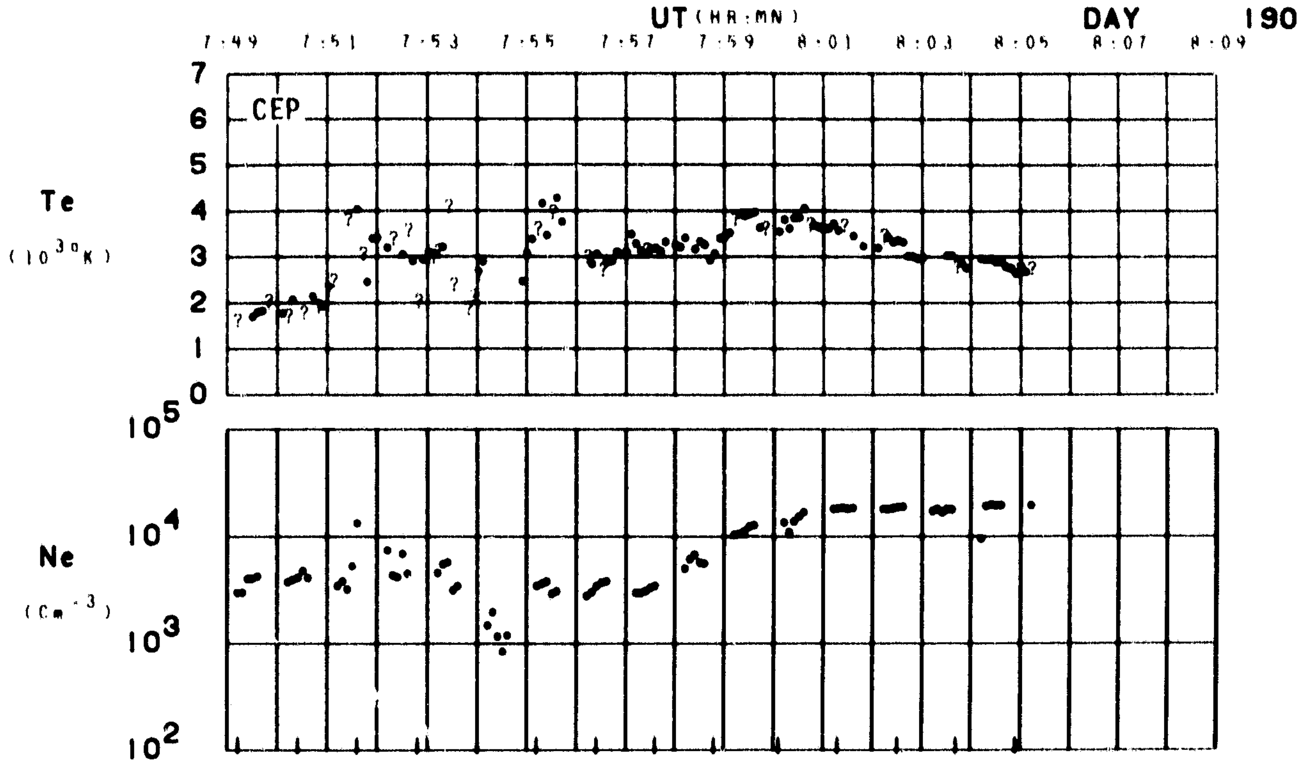

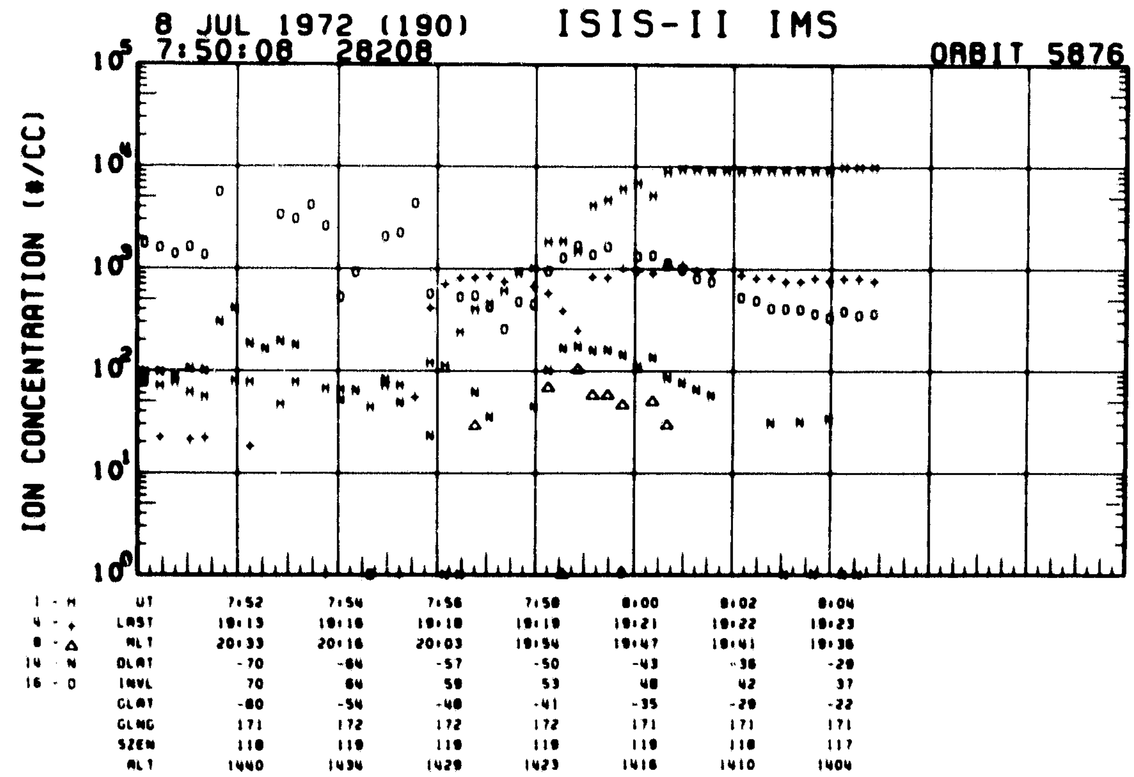

SET 35, FORMAT 4

RPA 720708

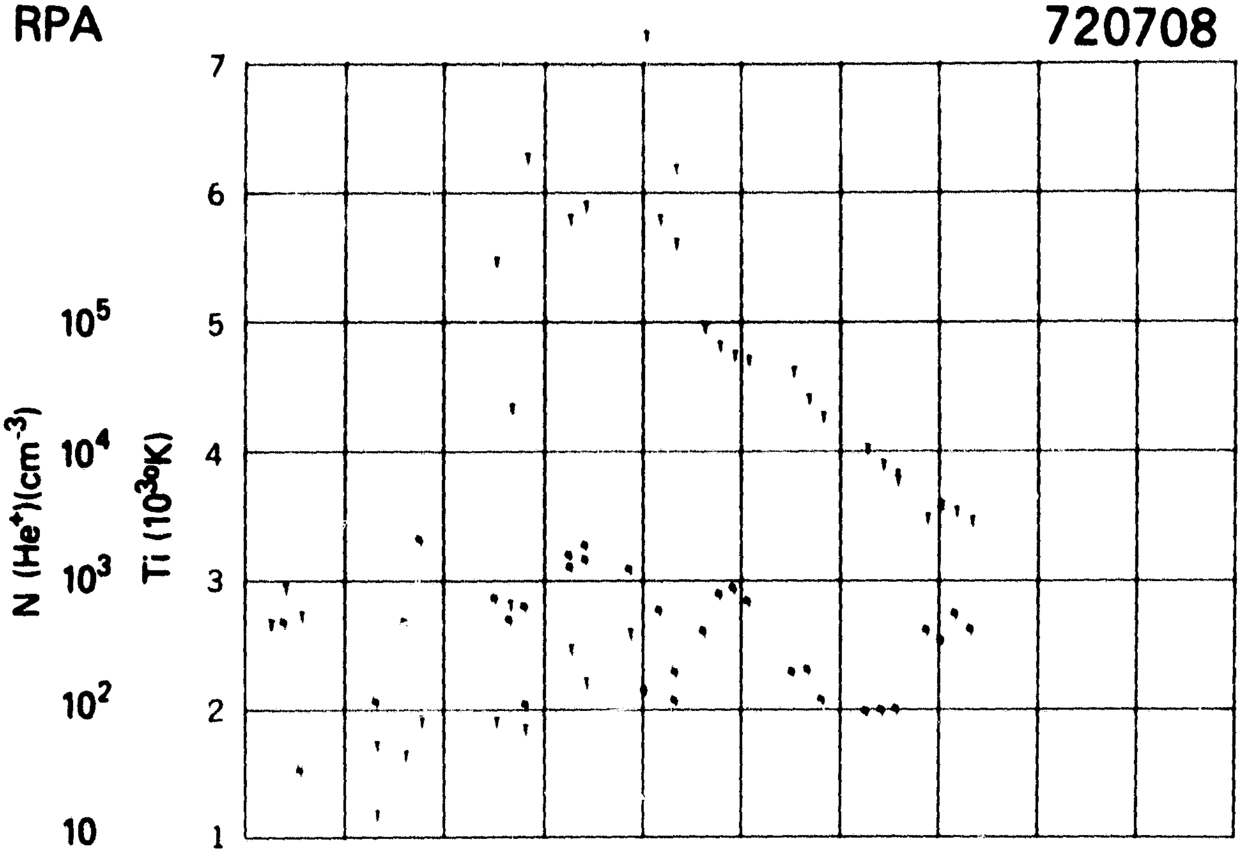

UT	7:52	7:54	7:56	7:58	8:00	8:02	8:04
LAST	19:13	19:16	19:18	19:19	19:21	19:22	19:23
MLT	20:33	20:16	20:03	19:54	19:47	19:41	19:38
DLAT	-70	-64	-57	-50	-43	-36	-29
INVL	70	64	59	53	48	42	37
GLAT	-60	-54	-48	-41	-35	-28	-22
GLNG	171	172	172	172	171	171	171
SZEN	118	119	119	118	119	118	117
ALT	1440	1434	1429	1423	1416	1410	1404

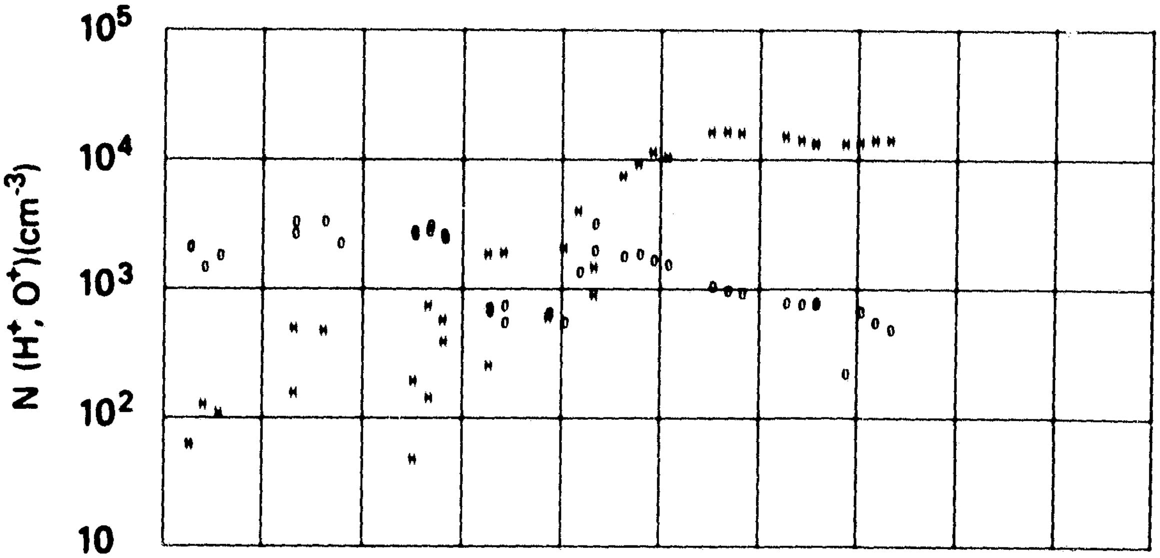

SET 35, FORMAT 5

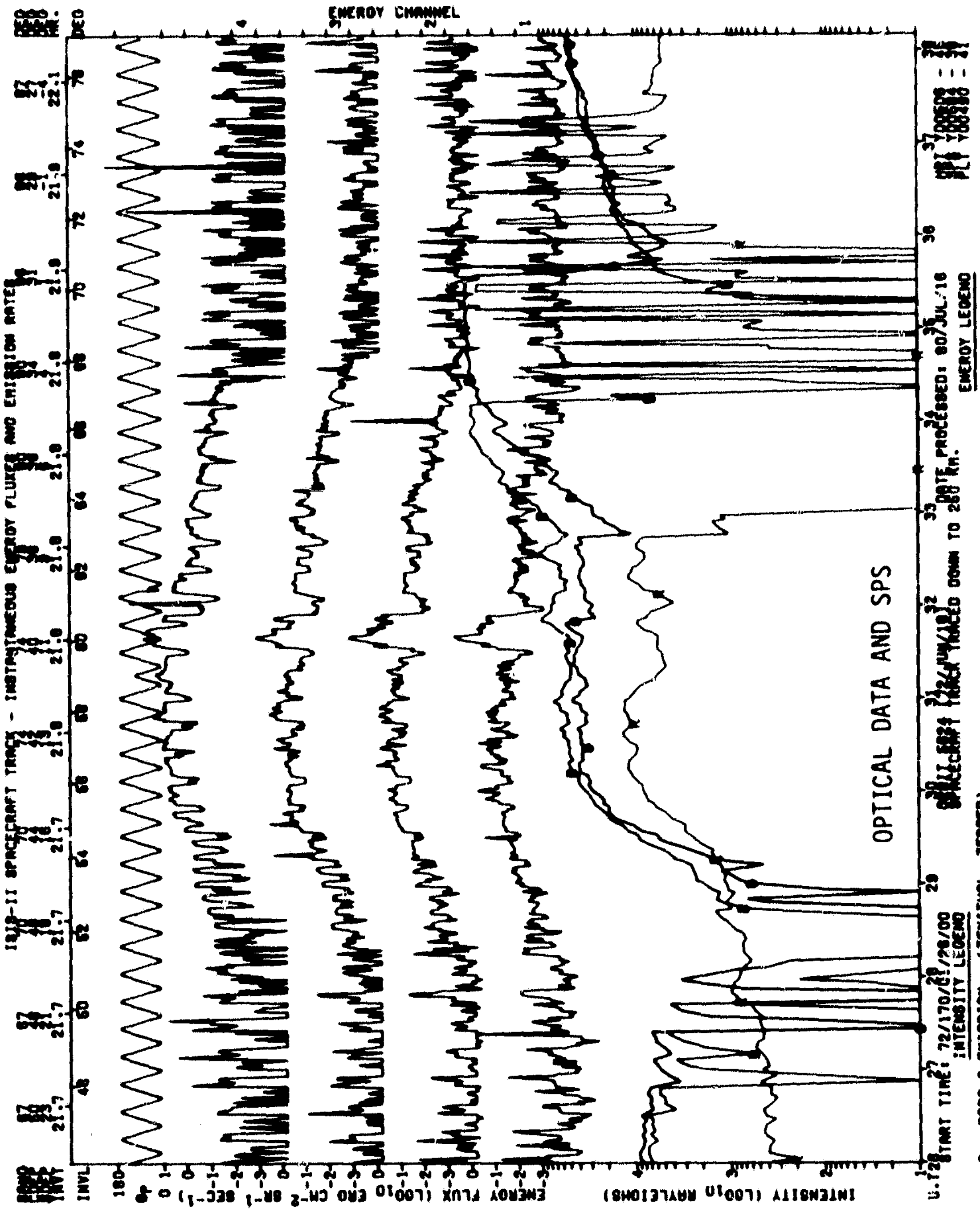

SET 36, FORMAT 1

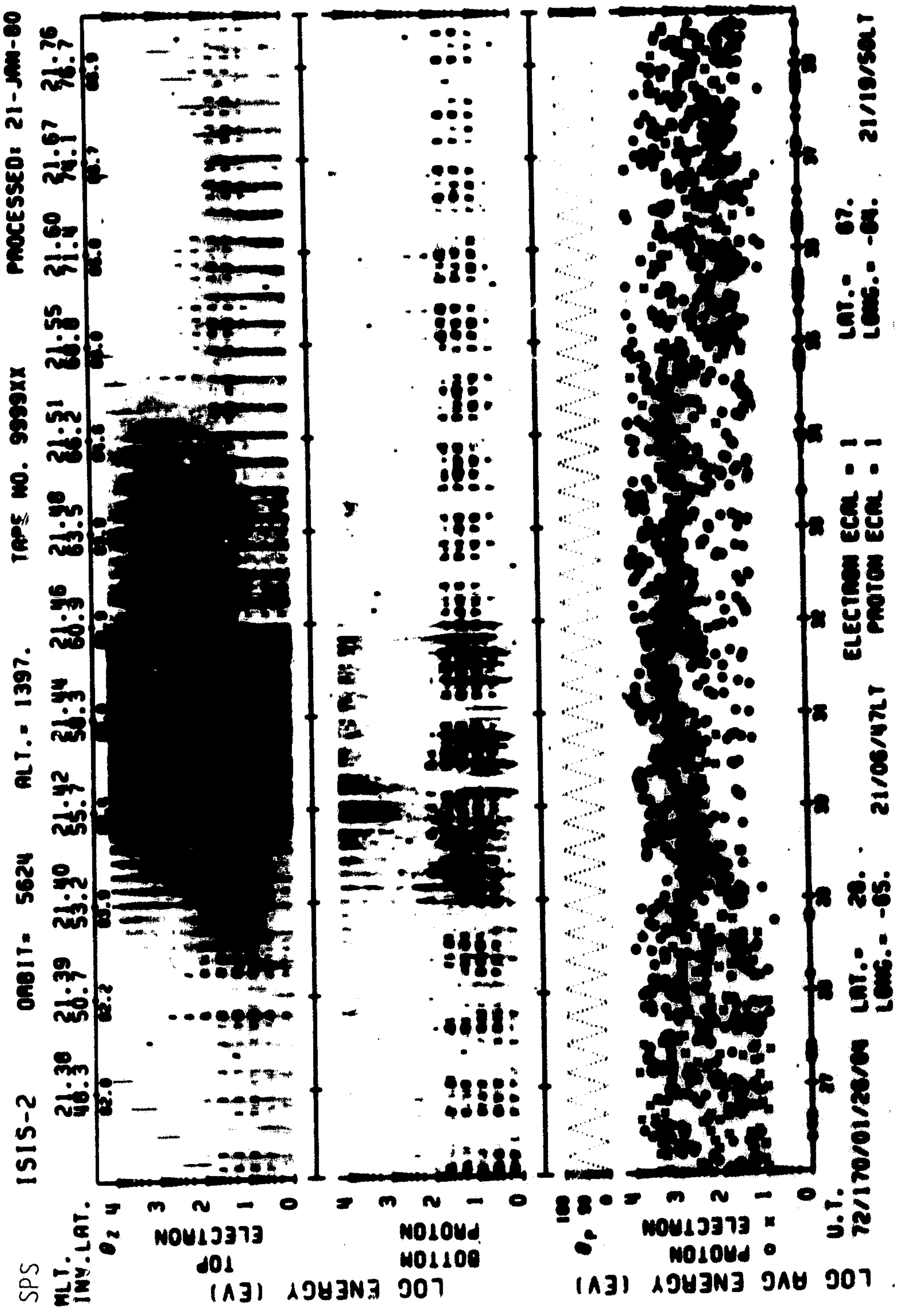

SET 36, FORMAT 6

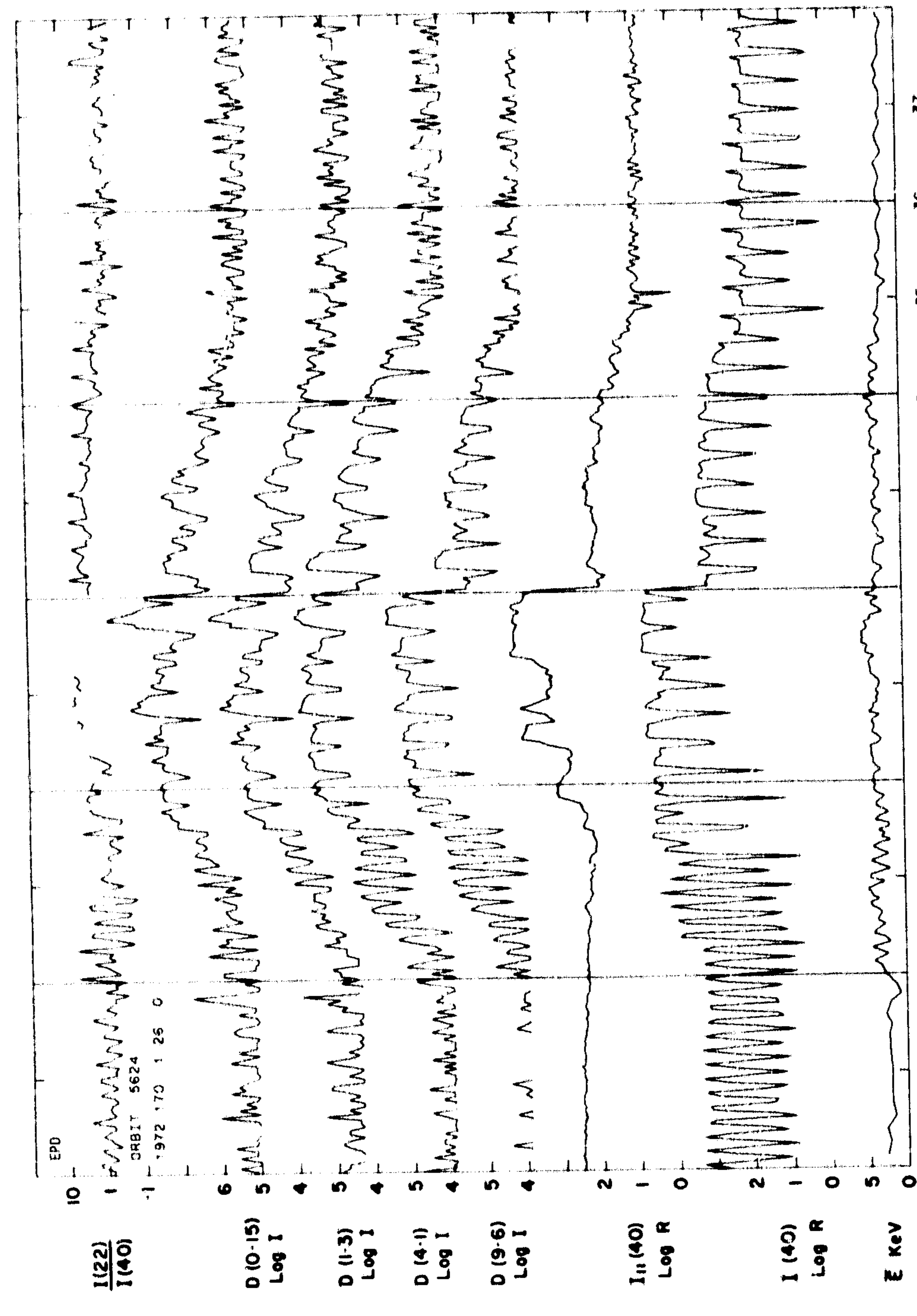

SET 36, FORMAT 3

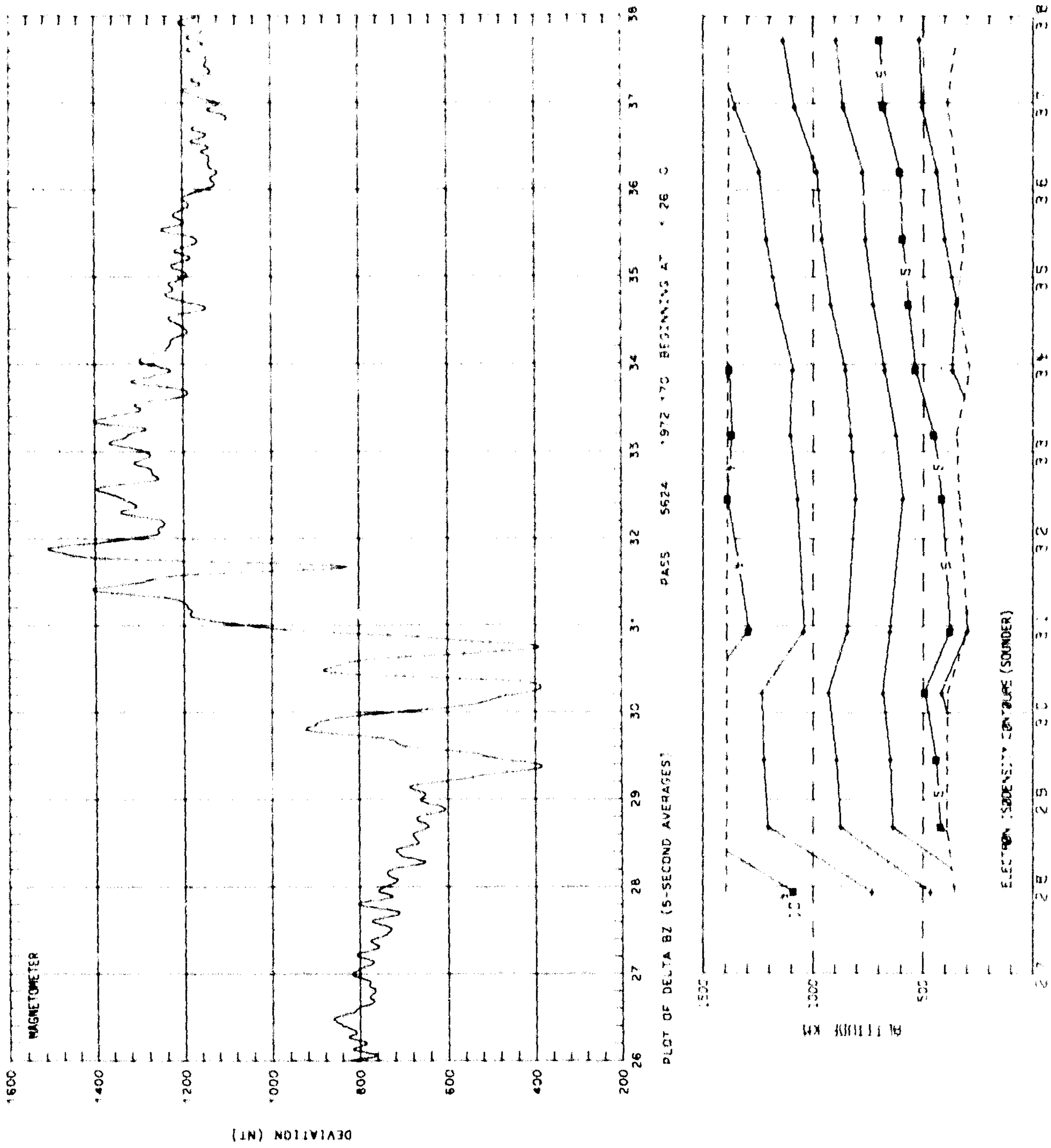

SET 36, FORMAT 2

ORBIT 5624
DATE 720618
DAY 170

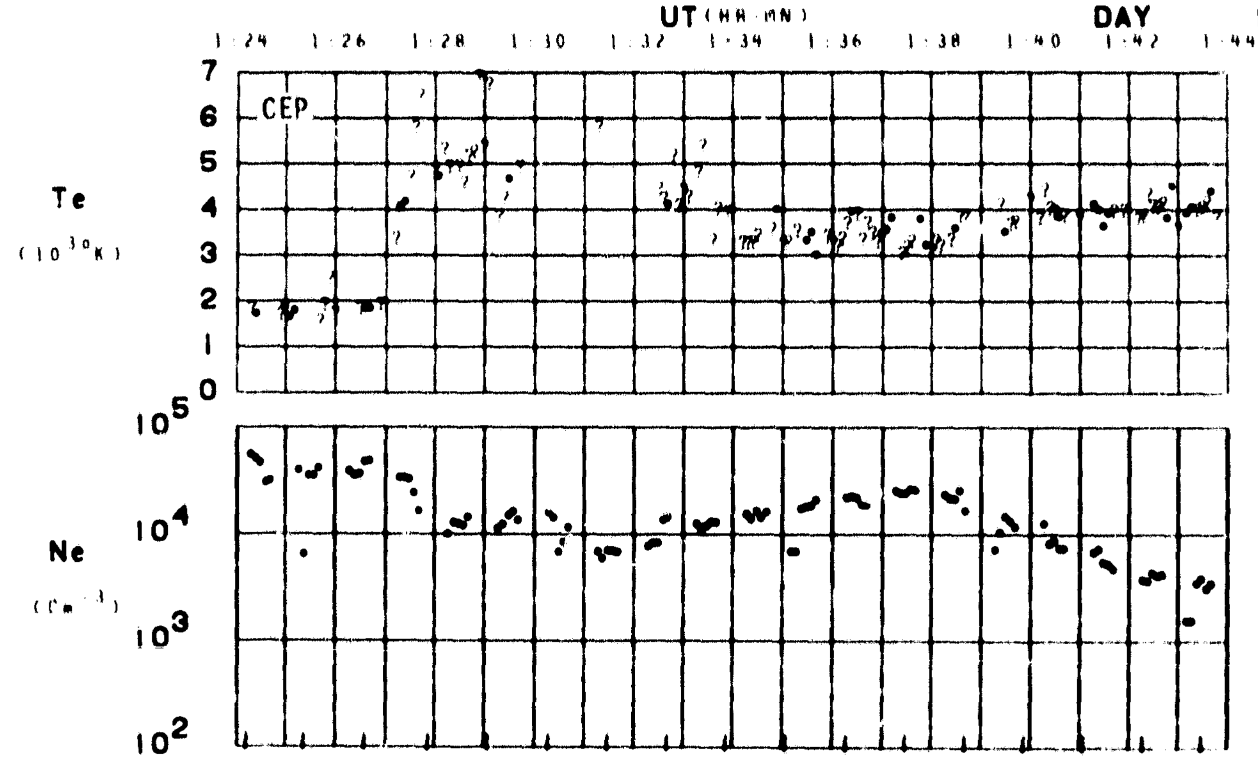

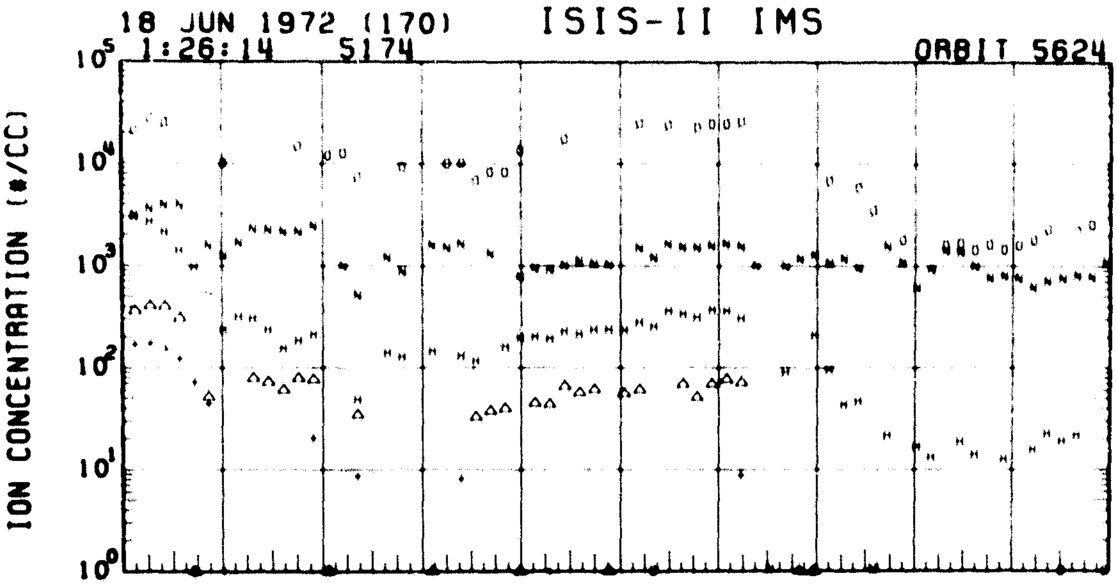

1 - H
4 - +
8 - Δ
14 - N
16 - O

UT	1:28	1:30	1:32	1:34	1:36	1:38	1:40	1:42	1:44
LAST	21:08	21:09	21:11	21:13	21:15	21:19	21:25	21:37	22:16
MLT	21:23	21:25	21:28	21:31	21:36	21:46	22:14	2:45	8:15
DLAT	45	52	58	64	70	75	79	82	84
INVL	51	56	61	66	72	77	82	84	84
GLAT	34	40	46	53	59	65	72	78	84
GLNG	64	64	64	64	64	64	62	60	50
SZEN	110	105	100	96	91	86	81	76	72
ALT	1394	1392	1389	1387	1385	1383	1381	1379	1377

SET 36, FORMAT 4

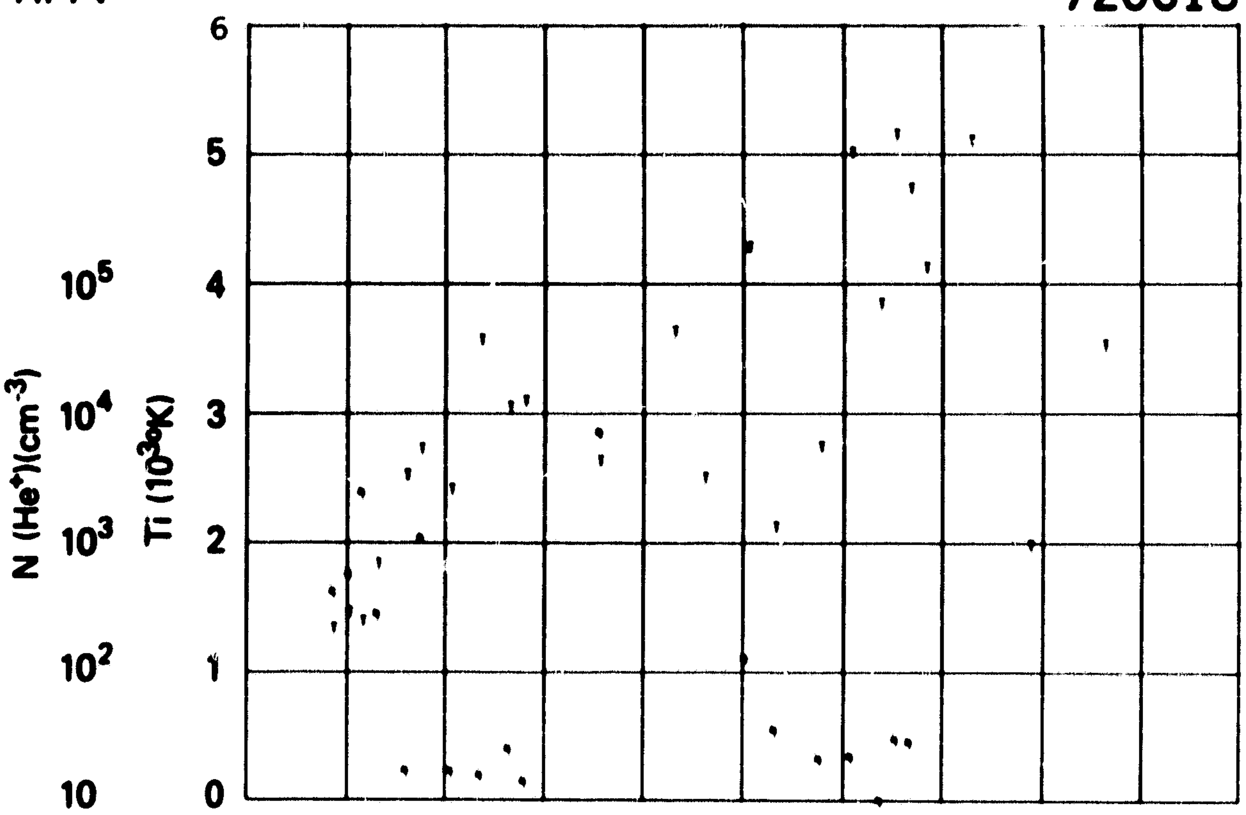

UT	1:28	1:30	1:32	1:34	1:36	1:38	1:40	1:42	1:44
LAST	21:08	21:09	21:11	21:13	21:15	21:18	21:25	21:37	22:18
MLT	21:23	21:25	21:28	21:31	21:36	21:48	22:14	2:45	0:15
DLAT	45	52	58	64	70	75	79	82	84
INVL	51	56	61	66	72	77	82	84	84
GLAT	34	40	46	53	59	65	72	78	84
GLNG	-84	-84	-84	-84	-84	-84	-82	-80	-50
SZEN	110	105	100	96	91	86	81	76	72
ALT	1394	1392	1389	1387	1385	1383	1381	1379	1377

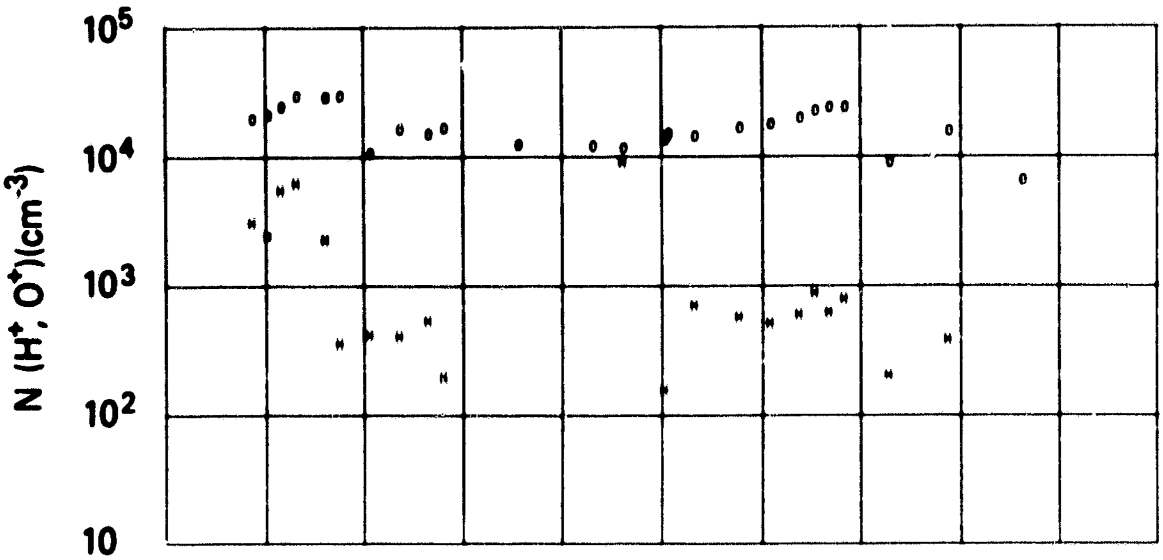

SET 36, FORMAT 5